RECENT ADVANCES IN BIOREMEDIATION/ BIODEGRADATION BY EXTREME MICROORGANISMS,
2nd Edition

EDITED BY: Edgardo Donati, Rajesh K. Sani, Kian Mau Goh and Kok Gan Chan
PUBLISHED IN: Frontiers in Microbiology

frontiers Research Topics

ISSN 1664-8714
ISBN 978-2-88971-167-3
DOI 10.3389/978-2-88971-167-3

About Frontiers

Frontiers is more than just an open-access publisher of scholarly articles: it is a pioneering approach to the world of academia, radically improving the way scholarly research is managed. The grand vision of Frontiers is a world where all people have an equal opportunity to seek, share and generate knowledge. Frontiers provides immediate and permanent online open access to all its publications, but this alone is not enough to realize our grand goals.

Frontiers Journal Series

The Frontiers Journal Series is a multi-tier and interdisciplinary set of open-access, online journals, promising a paradigm shift from the current review, selection and dissemination processes in academic publishing. All Frontiers journals are driven by researchers for researchers; therefore, they constitute a service to the scholarly community. At the same time, the Frontiers Journal Series operates on a revolutionary invention, the tiered publishing system, initially addressing specific communities of scholars, and gradually climbing up to broader public understanding, thus serving the interests of the lay society, too.

Dedication to Quality

Each Frontiers article is a landmark of the highest quality, thanks to genuinely collaborative interactions between authors and review editors, who include some of the world's best academicians. Research must be certified by peers before entering a stream of knowledge that may eventually reach the public - and shape society; therefore, Frontiers only applies the most rigorous and unbiased reviews.
Frontiers revolutionizes research publishing by freely delivering the most outstanding research, evaluated with no bias from both the academic and social point of view. By applying the most advanced information technologies, Frontiers is catapulting scholarly publishing into a new generation.

What are Frontiers Research Topics?

Frontiers Research Topics are very popular trademarks of the Frontiers Journals Series: they are collections of at least ten articles, all centered on a particular subject. With their unique mix of varied contributions from Original Research to Review Articles, Frontiers Research Topics unify the most influential researchers, the latest key findings and historical advances in a hot research area! Find out more on how to host your own Frontiers Research Topic or contribute to one as an author by contacting the Frontiers Editorial Office: frontiersin.org/about/contact

RECENT ADVANCES IN BIOREMEDIATION/ BIODEGRADATION BY EXTREME MICROORGANISMS,
2nd Edition

Topic Editors:
Edgardo Donati, National University of La Plata, Argentina
Rajesh K. Sani, South Dakota School of Mines and Technology, United States
Kian Mau Goh, University of Technology Malaysia, Malaysia
Kok Gan Chan, University of Malaya, Malaysia

Publisher's note: This is a 2nd edition due to an article retraction.

Citation: Donati, E., Sani, R. K., Goh, K. M., Chan, K. G., eds. (2021). Recent Advances in Bioremediation/Biodegradation by Extreme Microorganisms, 2nd Edition. Lausanne: Frontiers Media SA. doi: 10.3389/978-2-88971-167-3

Table of Contents

frontiers in Microbiology

EDITORIAL
published: 14 August 2019
doi: 10.3389/fmicb.2019.01851

Editorial: Recent Advances in Bioremediation/Biodegradation by Extreme Microorganisms

Edgardo Rubén Donati[1]*, *Rajesh Kumar Sani*[2], *Kian Mau Goh*[3] and *Kok-Gan Chan*[4,5]

[1] Facultad de Ciencias Exactas, CINDEFI (CCT, La Plata-CONICET, UNLP), Universidad Nacional de la Plata, La Plata, Argentina, [2] Department of Chemical and Biological Engineering, South Dakota School of Mines and Technology, Rapid City, SD, United States, [3] Faculty of Sciences, Universiti Teknologi Malaysia, Skudai, Malaysia, [4] Division of Genetics and Molecular Biology, Faculty of Science, Institute of Biological Sciences, University of Malaya, Kuala Lumpur, Malaysia, [5] International Genome Centre, Jiangsu University, Zhenjiang, China

Keywords: pollutants, bioremediation, biodegradation, biomineralization, extremophiles

Editorial on the Research Topic

Recent Advances in Bioremediation/Biodegradation by Extreme Microorganisms

OPEN ACCESS

Edited by:
Jean Armengaud, Commissariat à l'Energie Atomique et aux Energies Alternatives (CEA), France

Reviewed by:
Rafael Bosch, University of the Balearic Islands, Spain

***Correspondence:**
Edgardo Rubén Donati
donati@quimica.unlp.edu.ar

Specialty section:
This article was submitted to Microbiotechnology, Ecotoxicology and Bioremediation, a section of the journal Frontiers in Microbiology

Received: *26 June 2019*
Accepted: *26 July 2019*
Published: *14 August 2019*

Citation:
Donati ER, Sani RK, Goh KM and Chan K-G (2019) Editorial: Recent Advances in Bioremediation/Biodegradation by Extreme Microorganisms. Front. Microbiol. 10:1851. doi: 10.3389/fmicb.2019.01851

To remediate polluted sites, biological processes have many advantages from economic, environmental, and practical aspects. Adsorption and biodegradation of organic contaminants and the immobilization, mobilization, and/or transformation of metal(loid)s are the main remediation processes that can be mediated by the action of several microorganisms especially those extremophiles surviving in hostile environments with high concentrations of pollutants. The aim of this Research Topic of Frontiers in Microbiology is to provide an appropriate platform to publish the latest results on the bioremediation of various pollutants by extremophilic pure cultures or microbial consortia. This Research Topic consists of 4 reviews and 7 original articles.

Marques reviewed the theme of extremophiles as microfactories which are able to provide genetic or metabolic mechanisms as controlled services to the clean-up of environmental pollution. The review focuses on metal and radionuclides pollution, and includes a discussion about the use of synthetic biology to improve the bioremediation processes.

Two articles in this Research Topic are focused on heavy metal(loid)s contaminants. Figueroa et al. described that several microorganisms exhibited high resistance to 19 metal(loid)s. Most of those strains displayed metal or metalloid reducing activity, and have been successfully used for the biological synthesis of nanostructures containing metal(loid)s. Tellurium and gold nanostructures showed antibacterial properties, which inhibited *E. coli* and *L. monocytogenes* growth. Acid mine drainage (AMD) is considered a severe environmental problem provoked by the microbial oxidation of sulfidic minerals. Gupta et al. explored the abundance and role of indigenous microorganisms displaying sulfate- and metal(loid)- reducing activity in the natural attenuation of an AMD impacted soil (AIS). The addition of nutrients (e.g., cysteine and lactate) to AIS increased the activity of such microorganisms achieving an increase in pH from 3.5 to 6.6, and reduction of sulfate (95%), iron (50%), and other heavy metals. In this way, Gupta et al. demonstrated that addition of nutrients could biostimulated the growth of some members of phylum Firmicutes (e.g., sulfate- and iron- reducing microorganisms) and bioremediate AMD impacted sites.

Orellana et al. reviewed extensively the most recent research on polyextremophilic microorganisms isolated from a wide range of extreme environments including salars, geothermal springs, deserts, ice fields, and diverse zones in Chile such as Altiplano, Atacama Desert, Central Chile, Patagonia, and Antarctica. This review also discussed the molecular and physiological capabilities of many of these isolates which were beneficial for bioremediation processes.

Diverse anthropogenic activities, particularly the emission due to the burning of fossil fuels, have triggered an alarming rise of CO_2 in the environment. A description of the measures of greenhouse gases emission is reviewed by Bose and Satyanarayana. In this review, authors discussed the merits and demerits of various approaches with extensive bibliographical material. Finally, a deep description of the use of carbonic anhydrases (CA) for biomineralization of CO_2 was included. This methodology was proposed as one of the most economical methods to mitigate global warming.

The other six articles in this Research Topic are related to the bioremediation of organic pollutants. Park and Park described the strategies for alkane degradation under extreme conditions (e.g., low and high temperatures, high salt, and acidic and anaerobic conditions). Alkane degraders seem to possess exclusive metabolic pathways and survival strategies. The thermophilic sulfate-reducing archaeon *Archaeoglobus fulgidus* uses a novel alkylsuccinate synthase for long-chain alkane degradation, and the thermophilic *Candidatus Syntrophoarchaeum butanivorans* anaerobically oxidizes butane via alkyl-coenzyme M formation. In addition to alkane degradation, extremophiles produce energy via the glyoxylate shunt and the Pta-AckA pathway when grown on a diverse range of alkanes under stress conditions.

Blázquez et al. focused on the bioremediation of aromatic compounds such as toluene and xylenes. The degradation of such pollutants is relevant due to their carcinogenic and neurotoxic effects to humans. This article provided evidences that the *bss* and *bbs* genes are not only essential for anaerobic degradation of toluene but also for m-xylene oxidation in the beta-proteobacterium *Azoarcus* sp. The peripheral pathway for the anaerobic oxidation of toluene would consist of an initial activation catalyzed by a benzylsuccinate synthase and a subsequent modified oxidation of benzylsuccinate to benzoyl-CoA and succinyl-CoA (both pathways encoded by *bbs* genes). Su et al. determined the crystal structure of the dibenzothiophene (DBT) sulfone monooxygenase (*BdsA*) from *Bacillus subtilis* at the resolution of 2.2 Å. This is one of the key enzymes in the 4S desulfurization pathway catalyzing the oxidation of DBT sulfone to 2′-hydroxybiphenyl 2-sulfonic acid. The structure of the BdsA-FMN complex at 2.4 Å was also determined. Finally, Su et al. showed that mutations in the residues involved in catalysis or flavin substrate-binding, resulted in a significant loss of enzymatic activity.

Meier et al. studies the catabolism of hydroxylated aromatic acids in *A. adeninivorans* and showed that the genes encoding enzymes involved catabolic pathway of gallic acid are induced using aromatic acid substrates as inducers. Through the construction of gallic acid decarboxylase disruption mutants, the authors showed that gallic acid decarboxylase Agdc1p was the only enzyme responsible for the transformation of gallic acid. They suggest that this enzyme might have useful industrial applications not only in bioremediation processes but also in synthesis of chemicals.

Chandra et al. detected that effluents discharged from the pulp and paper industry contain various refractory and androgenic compounds, even after secondary treatment by activated processes. Most of these compounds are classified as endocrine-disrupting chemicals and are environmental toxicants. This study also assessed the degradability of such compounds by biostimulation. The results suggested that pulp and paper mill wastewater, after this secondary detoxification process, could be safe for disposal.

Lastly, Kirtzel et al. investigated the ability of *Schizophyllum commune* to degrade black slates (e.g., metamorphic rocks rich in sulfides, heavy metals and organic matters). *S. commune* is a filamentous basidiomycete possesses a broad range of enzymes including multicopper oxidases such as laccases and laccase-like oxidases. Both life forms (haploid monokaryotic and mated dikaryotic strains) were able to degrade the slate releasing metals at the same time.

This Research Topic of Frontiers in Microbiology shows how bioremediation by means of extremophiles is an active research theme.

AUTHOR CONTRIBUTIONS

All authors listed have made a substantial, direct and intellectual contribution to the work, and approved it for publication.

FUNDING

ED is Superior Researcher at CINDEFI (CONICET, Argentina) and acknowledges the financial support from ANPCYT (PICT 2015 0463 and PICT 2016 2535). This project was co-financially supported by Universiti Teknologi Malaysia RU grant (Grant number: 16H89) and (UK-SEA-NUOF) with project number 4B297. K-GC thanked University of Malaya for financial support (PPP grants: PG136-2016A, PG133-2016A, HIR grant: H50001-A-000027). RS acknowledges the support from National Science Foundation in the form of BuG ReMeDEE initiative (Award # 1736255).

Conflict of Interest Statement: The authors declare that the research was conducted in the absence of any commercial or financial relationships that could be construed as a potential conflict of interest.

frontiers in Microbiology

ORIGINAL RESEARCH
published: 11 December 2018
doi: 10.3389/fmicb.2018.02882

Low-Abundance Members of the *Firmicutes* Facilitate Bioremediation of Soil Impacted by Highly Acidic Mine Drainage From the Malanjkhand Copper Project, India

*Abhishek Gupta[1], Avishek Dutta[1,2], Jayeeta Sarkar[1], Mruganka Kumar Panigrahi[3] and Pinaki Sar[1]**

[1] *Environmental Microbiology and Genomics Laboratory, Department of Biotechnology, Indian Institute of Technology Kharagpur, Kharagpur, India,* [2] *School of Bioscience, Indian Institute of Technology Kharagpur, Kharagpur, India,* [3] *Department of Geology and Geophysics, Indian Institute of Technology Kharagpur, Kharagpur, India*

OPEN ACCESS

Edited by:
Rajesh K. Sani, South Dakota School of Mines and Technology, United States

Reviewed by:
Virginia Helena Albarracín, Center for Electron Microscopy (CIME), Argentina
Christopher Anthony Abin, University of Oklahoma, United States

***Correspondence:**
Pinaki Sar
sarpinaki@yahoo.com; psar@bt.iitkgp.ac.in

Specialty section:
This article was submitted to Microbiotechnology, Ecotoxicology and Bioremediation, a section of the journal Frontiers in Microbiology

Received: *31 December 2017*
Accepted: *12 November 2018*
Published: *11 December 2018*

Citation:
Gupta A, Dutta A, Sarkar J, Panigrahi MK and Sar P (2018) Low-Abundance Members of the Firmicutes Facilitate Bioremediation of Soil Impacted by Highly Acidic Mine Drainage From the Malanjkhand Copper Project, India. Front. Microbiol. 9:2882. doi: 10.3389/fmicb.2018.02882

Sulfate- and iron-reducing heterotrophic bacteria represented minor proportion of the indigenous microbial community of highly acidic, oligotrophic acid mine drainage (AMD), but they can be successfully stimulated for *in situ* bioremediation of an AMD impacted soil (AIS). These anaerobic microorganisms although played central role in sulfate- and metal-removal, they remained inactive in the AIS due to the paucity of organic carbon and extreme acidity of the local environment. The present study investigated the scope for increasing the abundance and activity of inhabitant sulfate- and iron-reducing bacterial populations of an AIS from Malanjkhand Copper Project. An AIS of pH 3.5, high soluble SO_4^{2-} (7838 mg/l) and Fe (179 mg/l) content was amended with nutrients (cysteine and lactate). Thorough geochemical analysis, 16S rRNA gene amplicon sequencing and qPCR highlighted the intrinsic metabolic abilities of native bacteria in AMD bioremediation. Following 180 days incubation, the nutrient amended AIS showed marked increase in pH (to 6.6) and reduction in soluble -SO_4^{2-} (95%), -Fe (50%) and other heavy metals. Concomitant to physicochemical changes a vivid shift in microbial community composition was observed. Members of the *Firmicutes* present as a minor group (1.5% of total community) in AIS emerged as the single most abundant taxon (∼56%) following nutrient amendments. Organisms affiliated to *Clostridiaceae, Peptococcaceae, Veillonellaceae, Christensenellaceae, Lachnospiraceae, Bacillaceae*, etc. known for their fermentative, iron and sulfate reducing abilities were prevailed in the amended samples. qPCR data corroborated with this change and further revealed an increase in abundance of dissimilatory sulfite reductase gene (*dsr*B) and specific bacterial taxa. Involvement of these enhanced populations in reductive processes was validated by further enrichments and growth in sulfate- and iron-reducing media. Amplicon sequencing of these enrichments confirmed growth of *Firmicutes* members

and proved their sulfate- and iron-reduction abilities. This study provided a better insight on ecological perspective of *Firmicutes* members within the AMD impacted sites, particularly their involvement in sulfate- and iron-reduction processes, *in situ* pH management and bioremediation.

Keywords: acid mine drainage, bioremediation, *Firmicutes,* biostimulation, quantitative PCR, metagenomics, dissimilatory sulfate reduction

INTRODUCTION

Acid mine drainage (AMD) is considered to be a global environmental problem faced by mining industries due to the biological oxidation of sulfidic minerals (Johnson and Hallberg, 2005; Neculita and Zagury, 2008; Qian et al., 2017). Owing to its highly toxic nature manifested through acidic pH, elevated levels of heavy metals and sulfate, AMD is not only a threat to aquatic and terrestrial ecosystems but considered to be a major contributor in long term degradation of environmental quality (Johnson and Hallberg, 2005; Chandra and Gerson, 2010; Hallberg, 2010). Despite its extreme nature, a diverse range of microorganisms inhabit AMD systems (Méndez-García et al., 2015; Chen et al., 2016; Huang et al., 2016). The most dominant bacterial populations residing in AMD are highly acidophilic, chemolithoautotrophic iron and sulfur oxidizers such as *Acidithiobacillus*, *Leptospirillum*, *Ferrithrix,* and *Ferritrophicum* etc. (Baker and Banfield, 2003; Chen et al., 2015, 2016; Méndez-García et al., 2015; Huang et al., 2016; Mesa et al., 2017; Teng et al., 2017). These acidophilic, autotrophic and Fe/S oxidizing microorganisms mainly contribute toward AMD generation and were studied extensively for their physiology, molecular mechanisms and ecological relevance (Denef et al., 2010; Kuang et al., 2013; Méndez-García et al., 2014; Chen et al., 2015; Goltsman et al., 2015; Chen et al., 2016), whereas the small heterotrophic populations thriving in the same niches could be of great significance in reducing AMD generation process and attenuating the overall hazard of these systems remain less explored.

Microbial sulfur- and iron-metabolisms through redox transformations coupled with or without energy generation constitute the major biochemical reactions within AMD (Baker and Banfield, 2003; Druschel et al., 2004). These transformation reactions facilitate generation of acidity and contribute toward raising the soluble -sulfate or -iron concentrations, while on the other hand could lead to reversal of such processes and aid to restoration of such environments. Sulfate- and iron-reductions are the two key reactions carried out by heterotrophic sulfate- or iron-reducing bacteria (SRBs or IRBs) that could reverse the AMD generation, metal precipitation and thus decrease the soluble metal concentrations and facilitate in raising the pH of AMD or AMD impacted ecosystems (Kaksonen et al., 2004; Church et al., 2007; Bijmans et al., 2009, 2010; Giloteaux et al., 2013). Bioremediation of AMD or AMD impacted ecosystems have been a subject of intense research in last decades (Kaksonen et al., 2004; Luptakova and Kusnierova, 2005; Church et al., 2007; Hiibel et al., 2008; Becerra et al., 2009; Bijmans et al., 2009; Hiibel et al., 2011; Burns et al., 2012; Moreau et al., 2013; Xingyu et al., 2013; Lefticariu et al., 2015; Sahinkaya et al., 2015; Deng et al., 2016; Zhang et al., 2016; Kefeni et al., 2017). In particular, enhancing the activities of indigenous microorganisms capable of sulfate- and/or iron-reduction and generation of alkalinity have gained interest for developing *in situ* bioremediation strategies (Neculita et al., 2007; Hiibel et al., 2008, 2011; Becerra et al., 2009; Bijmans et al., 2009; Burns et al., 2012; Xingyu et al., 2013; Lefticariu et al., 2015).

It is interesting to note that AMD or AMD impacted environment harbors SRBs and/or IRBs, but generally with low abundance and they remained metabolically less active at pH < 5.0 (Church et al., 2007; Sánchez-Andrea et al., 2011, 2012a; Giloteaux et al., 2013; Méndez-García et al., 2015). The limited presence and activities of these bacteria in AMD could be due to the presence of low organic carbon/other environmental variables and thermodynamic limitations as dissimilatory sulfate- and/or iron-reduction are energetically expensive (Church et al., 2007; Muyzer and Stams, 2008; Bird et al., 2011; Johnson, 2012; Giloteaux et al., 2013). Nevertheless, metabolic versatility of SRB has been exploited in bioremediation of AMD with different approaches, among which amendment of suitable carbon and electron sources, nitrogen, phosphorus compounds etc. are important (Kaksonen et al., 2004; Church et al., 2007; Neculita et al., 2007; Hiibel et al., 2008, 2011; Becerra et al., 2009; Bijmans et al., 2009; Burns et al., 2012; Xingyu et al., 2013; Zhang and Wang, 2014; Lefticariu et al., 2015; Zhang et al., 2017).

During the past decades, microbiology of AMD has been studied extensively, particularly the cultivation-independent deep sequencing studies have resolved the community composition and biogeochemical functions of previously unknown microorganisms (Bertin et al., 2011; Kuang et al., 2013; Méndez-García et al., 2014; Chen et al., 2015; Goltsman et al., 2015; Hua et al., 2015). In contrast, exploration of AMD communities with special reference to heterotrophic SRBs and IRBs or other metal reducing populations remained less explored (Giloteaux et al., 2013). *In situ* bioremediation of these hazardous wastes is limited due to paucity of knowledge on the diversity of SRBs/IRBs and factors that promote their activities.

In the present study we aimed to explore the abundance and role of indigenous sulfate- and/or metal-reducing bacterial populations in natural attenuation of an AMD impacted soil designated as AIS. Soil impacted with highly acidic, sulfate- and multiple heavy metal-rich AMD from Asia's largest open-cast copper mine of Malanjkhand Copper Project (MCP) was used in this study. Microcosm based approach was adopted to promote presence and activities of indigenous sulfate- and/or metal-reducing bacteria using cysteine and lactate as biostimulation agents. A thorough assessment of microbial populations involved

in sulfate/metal reduction and their characterization was done through 16S rRNA gene based amplicon sequencing coupled with qPCR and DGGE. The study was structured to answer the following questions: (i) How far it is possible to enhance the presence and activities of indigenous sulfate- and iron-reducing microbial populations present within an AMD impacted soil? (ii) What is the effect of such treatment(s) in the improvement of local physicochemical conditions, particularly the pH, concentrations of soluble -sulfate, -iron and -other heavy metals present therein? and (iii) Is it possible to enrich and cultivate the specific populations responsible for sulfate- and iron-reduction and management of the local physicochemical condition? The study demonstrates a comprehensive composition of microbial community residing in AIS and investigates the scope for *in situ* bioremediation.

MATERIALS AND METHODS

Sampling Site

The AMD impacted soil was collected in a sterile container from 5–10 cm below the top layer of a field flooded with AMD from a neighboring sump of Malanjkhand Copper Project (MCP), Balaghat district, Madhya Pradesh, India (N 21° 59.91′, E 080° 41.879′) in the year 2014. The soil is exposed to AMD for over 10 years. The AMD water is released (as overflow) from the adjacent sump which receives AMD continuously from the mine areas. Selected physicochemical parameters such as oxidation reduction potential (ORP), pH and conductivity were measured on-site using multiparameter (Orion Star A329 portable Multiparameter, Thermo Fisher Scientific). All samples were collected following aseptic techniques, stored immediately at 4°C, brought to the laboratory and stored at −80°C till further processing.

Microcosm Preparation

The microcosm setup was prepared with 5 g of AMD contaminated soil (AIS) using 20 ml filter sterilized distilled water in 30 ml glass vial. Three sets of microcosms were prepared. The first microcosm was amended with 0.1% (w/v) cysteine hydrochloride and designated as C. The second microcosm was amended with both 0.1% (w/v) cysteine hydrochloride and 0.1% (w/v) lactate (as sodium lactate), designated as C+L. The third microcosm was not amended with anything extra and designated as H (H stands for H_2O, since only filter sterilized distilled water was present with AIS). Killed control was prepared for each setup by adding 2% (w/v) $HgCl_2$ as biocide. The glass vials were sealed with gas-tight rubber stoppers and aluminum crimp seals. To mimic the natural environment nitrogen was not purged into the microcosm vials. The microcosms were incubated in dark for 180 days at 30°C. Each microcosm was set up in duplicate. Since the microcosms were of sacrificial type (i.e., the vial once opened was not reused in the same study) three experimental replicates were prepared: one for 4 months (120 days) incubation and marked as C_4M, C+L_4M, and H_4M; second for 5 months (150 days) incubation and marked as C_5M, C+L_5M, and H_5M and third for 6 months (180 days) incubation and marked as C_6M, C+L_6M, and H_6M. Physicochemical parameters were measured from each microcosm setups (at 120 and 180 days of incubation). Samples were withdrawn from each of the setup in triplicates and used for measuring the physicochemical parameters. The major physicochemical parameters such as pH and ORP of the slurry were measured by Orion Multi parameter (Orion Star A329 portable Multiparameter, Thermo Fisher Scientific). The slurry samples were taken out from the microcosm setup and centrifuged at 4000 rpm to settle down the soil particles. SO_4^{2-} estimation was performed with the supernatant through $BaCl_2$ turbidometric spectroscopy based method (Chesnin and Yien, 1951) while for Fe^{2+} estimation, samples were acidified to avoid any oxidation and Fe^{2+} concentration was measured by Ferrozine method (Viollier et al., 2000). The major elements such as Fe, Cu, As, Cr, Ni, and Zn were estimated from the slurry using atomic absorption spectroscopy (Perkin Elmer). In short, the slurry was centrifuged at 4000 rpm and supernatant was passed through 0.22 μm filter membrane and 2% HNO_3 was added to prevent any oxidation.

Metagenome Extraction, Library Preparation, and Sequencing

The microbial diversity analysis based on 16S rRNA gene amplicon targeted sequencing was performed with 6M setups (i.e., with 180 days incubation). Original AIS sample (0_Day) was also used for comparison. From the three microcosms and the 0_Day AIS, samples were withdrawn in triplicates and metagenome was extracted from each of the withdrawn samples using Power Soil DNA Isolation Kit (MoBio laboratories) according to the manufacturer's protocol. Metagenome from the replicate samples were pooled, mixed thoroughly and used for amplification of V4 region of 16S rRNA gene. V4 region of 16S rRNA gene was amplified with V4 specific primers (Bates et al., 2011). The following amplification conditions: 95°C for 5 min, 35 cycles of 95°C for 40 s, 50°C for 45 s and 72°C for 40 s with final extension at 72°C for 7 min were used for amplification of V4 region. Thereafter amplicons were purified using 2% E-gel (E-Gel SizeSelect II Agarose Gel, Thermo Fisher Scientific) and sequencing was performed with Ion S5™ System (Thermo Fischer Scientific). In order to understand the microbial diversity at 5M setups (i.e., with 150 days incubation), Denaturing gradient gel electrophoresis (DGGE) was performed with H_5M, C+L_5M, and C_5M samples. Metagenome was extracted in triplicates from these setups and were pooled together to amplify the V4 region using GC-clamp forward primer as described above. A DCode Universal Mutation Detection system (Bio-Rad, United States) was used to perform DGGE with similar protocol as described by Paul et al. (2015). The denaturing gradient from 35 to 70% was used for the present study. Twenty-three distinct bands in DGGE profile were excised and eluted by keeping it in 20 μl DNase free PCR water at 4°C for overnight. These gel eluted products were re-amplified by using without GC clamp 515F and 806R primers (V4 region) and were cloned into the pTZ57RT vector for sequencing. EzTaxon[1] and SILVA 119

[1]www.ezbiocloud.net

reference database[2] were used for the taxonomic assignment of the obtained sequences.

Quantification of Bacterial/Specific Taxa and *dsr*B Copy Number

Quantification of bacterial abundance and remarkably shifted taxa; *Firmicutes*, *Acidobacteria*, *Actinobacteria* as well as *dsr*B gene involved in sulfate reduction were performed for all the samples (0_Day, H_6M, C_6M, and C+L_6M). The bacterial abundance was quantified through bacterial specific 16S rRNA gene copy number. Similarly, abundance of *Actinobacteria*, *Acidobacteria,* and *Firmicutes* were quantified through specific 16S rRNA gene specific to these taxa. Copy numbers of functional gene *dsr*B were also quantified using qPCR based technique to estimate the sulfate-reducing populations. Real-time primers for bacterial 16S rRNA gene was taken from Muyzer et al. (1993), primers specific to *Actinobacteria* and *Firmicutes* was taken from Mühling et al. (2008), primer used for *Acidobacteria* as described by Lee and Cho (2011) and *dsr*B was taken from Purkamo et al. (2013). The qPCR was performed in Quant Studio 5 Real-Time PCR System (Thermo Fisher Scientific) with Power SYBR green PCR Mastermix (Invitrogen), with a total volume of 10 μl containing primer concentration of 5 picomoles and 2 μl of metagenomic DNA. All the reactions were set in triplicates. The following amplification conditions: 95°C for 10 min, 40 cycles of 95°C for 15 s, 55°C for 30 s and 72°C for 30 s was followed for bacterial and *ds*rB gene while 63°C, 59°C, and 57°C annealing temperature were used for *Actinobacteria, Acidobacteria,* and *Firmicutes*, respectively. Melting curve analysis was run after each assay to check PCR specificity. Bacterial 16S rRNA gene copy numbers were determined in each sample by comparing the amplification result to a standard dilution series ranging from 10^2 to 10^8 of plasmid DNA containing the 16S rRNA gene of *Achromobacter* sp. MTCC 12117. *Firmicutes* gene copy number was calculated from plasmid DNA containing 16S rRNA gene from *Bacillus*. Whereas 16S rRNA gene of *Actinobacteria* and *Acidobacteria* as well as *dsr*B gene were cloned from metagenome and different dilution series of plasmid DNA copy number were used to prepare the standard curve for comparing the amplification result. The efficiency of qPCR was calculated using formula $E = 10\,(-1/-Slope) - 1$. The standard curve was linear for all the taxa specific and *dsr*B gene. R^2 value was greater than 0.993 for all the standard curve while efficiency was ranges from 84 to 112% (**Supplementary Table S1**).

Enrichment of *Firmicutes* Specific Members and Their Potential Role in Fe^{3+} and SO_4^{2-} Reduction

Firmicutes specific populations were enriched in facultative anaerobic medium (Stieglmeier et al., 2009) and *Clostridium* specific medium containing following ingredients in g/L NaCl 2.0, K_2HPO_4 5.0, $MgCl_2$ 0.2, ferric citrate 0.2, yeast extract 1.0, lysine 0.5 and cellulose 7.0 at pH 7.0 in 50 ml glass serum vials. Both the media were purged with filtered N_2 gas for 15–20 min to remove the oxygen and cysteine HCl (0.025%) was added as a mild reducing agent. Serum bottles were sealed with rubber stoppers. Two ml slurry from both C_6M and C+L_6M was used as inoculum in both the media and incubated at 30°C for 2 weeks. The enrichment was sub-cultured three times in the same media before transferring into sulfate reducing medium (SRM) (modified from Postgate, 1963) and iron reducing medium (IRM) (containing ferric citrate 5 mM, NH_4Cl 1.50 g/L, NaH_2PO_4 0.60 g/L, KCl 0.10 g/L, sodium acetate 2.50 g/L and yeast extract 0.05 g/L). Nitrogen gas was flushed for 15–20 min and cysteine HCl (0.025%) was added as a mild reducing agent in both the media to make the environment anaerobic. The pH of these two media was set to 7.0 using 1N NaOH/1N HCl and incubated at 30°C for 2 weeks. Enriched population was sub-cultured thrice in same media after seeing the visual changes in the media (iron containing medium turned colorless, sulfate reducing medium turned black due to precipitation of iron sulfide). Remaining sulfate and increased iron (Fe^{2+}) concentrations were measured for assessing the reduction of sulfate and iron (Fe^{3+}) using $BaCl_2$ turbidometric method and Ferrozine method, respectively. Briefly, 2 ml samples were taken out and bacterial cells were pelleted down to use supernatant for estimation of SO_4^{2-} and Fe^{2+} concentration.

DNA Extraction From Enrichment

Total DNA from enriched populations was extracted from 4 ml of each enrichment. Equal volume of 0.5 M ammonium oxalate was added in iron enrichment to dissolve iron precipitates. The culture was pelleted at high speed for 5 min at room temperature. The cell pellet was dissolved in 500 μL TNE buffer (Tris HCl-10 mM, NaCl-2.0 M, EDTA-1 mM), 1/10 volume silica bead was added and vortexed for 15–20 min. 100 μL lysozyme (100 mg/ml) was added in the cell suspension, vortexed briefly to mix and incubated at 37°C for 2 h. 30 μL proteinase K (20 mg/ml) and 50 μL SDS (10%) were added and incubated at 37°C for 45 min. DNA was then extracted using chloroform:isoamyl alcohol (24:1). DNA pellet was washed twice with ice-cold 70% ethanol and the pellet was air dried. DNA was resuspended in PCR grade water. 16S rRNA gene amplicon from the DNA was prepared as described above for microcosm treatments (see section "Metagenome Extraction, Library Preparation, and Sequencing"). To understand the microbial diversity of these enrichments, amplicon based analysis was performed with *Clostridium* and facultative enrichments from both C_6M and C+L_6M setups but to identify the main iron and sulfate reducing populations, enrichments from C_6M was considered.

Diversity Analysis and Statistical Tool

Ion Torrent data analysis of V4 region of 16S rRNA gene was performed with QIIME 1.9.1 pipeline (Caporaso et al., 2010). Quality filtering of reads and bioinformatics were performed as described by Gupta et al., 2017. In brief, quality filtering was performed for raw reads to remove primers, sequences with homopolymers run of >6 bp and read length beyond the range of 230–300 bp. Only 3 primer mismatches

[2]www.arb-silva.de/documentation/release-119

were allowed due to degeneracy of primer set in this step. Denovo OTU picking was performed with uclust and SILVA 119 reference database[3] was used for taxonomy assignments of reads as mentioned in QIIME pipeline. The OTU level analysis was performed by sub-sampling the samples to the lowest number of reads obtained in any of the samples through QIIME 1.9.1 pipeline. Venn diagram was generated in InteractiVenn[4] (Heberle et al., 2015) for top 100 OTUs. Microbial metabolic pathways were estimated based on the 16S rRNA gene data from the closed OTU picking method using PICRUSt software package (Langille et al., 2013) on the web-based Galaxy server[5]. For PICRUSt analysis, Greengenes database[6] was used for taxonomy assignment. One-way ANOVA was performed to assess the changes in the microbial diversity between the treatments using PAST software version 3.20 (Hammer et al., 2001). Weighted pair group mean arithmetic (WPGA) based hierarchical clustering was performed with Bray–Curtis distance dissimilarity matrix. Ternary plot was generated using PAST software to assess difference in diversity pattern among the treatments. All the data represented for physicochemical parameters were mean of its triplicates with standard deviation.

Nucleotide Accession Number

Metagenomic sequences are available under the NCBI BioProject ID PRJNA416924. The SRR number for each samples are SRR6320797 (C+L_6M), SRR6320796 (C_6M), SRR6320800 (0_Day), SRR6320884 (H_6M), SRR6320885 (FA_C_6M), SRR6320921 (Clos_C_6M), SRR6320922 (Clos_IRM), SRR6320919 (FA_IRM), SRR6320923 (Clos_SRM), SRR6320920 (FA_SRM), SRR7865998 (FA_C+L) and SRR7865999 (Clos_C+L). Sequence of DGGE bands were submitted in Genbank under accession numbers MH938427-MH938447.

RESULTS

Change in Physicochemical Parameters After the End of Incubation

Nutrient amendments to AIS facilitated a considerable improvement of its physicochemical conditions (**Table 1**). At the onset of the study (0_Day), major physicochemical parameters of the soil slurry were measured. This sample was found to be of highly acidic (pH 3.51) nature; rich in soluble SO_4^{2-} (7838 mg/l) and Fe (179 mg/l). Following incubation with nutrients, significant increase in pH (up to pH 6.61) but decrease in ORP (up to 110 mV) were observed coupled with considerable changes in concentrations of SO_4^{2-}, Fe, Fe^{2+} and heavy metals. Control set (H_6M) with only water addition showed slight change with respect to the test physicochemical parameters while killed control did not show any shift at all. Incubation with only water (H_6M) could initiate reactions responsible for the observed shift in pH and ORP, presence of nutrients favored such reactions significantly. Following cysteine and cysteine + lactate amendment, soluble sulfate concentration was greatly reduced along with Fe (total Fe as well as Fe^{2+}), Cu, Zn and Ni. Compared to H_6M that showed nearly 50% decrease in SO_4^{2-} (to that of its initial level), cysteine + lactate addition could led to a 95% reduction. Microcosm amended with only cysteine showed only up to 76% lowering of SO_4^{2-} (compared to 0_Day). Soluble Fe level presented an interesting trend: concentrations of both total Fe and Fe^{2+} were enhanced in H_6M (2.3-fold for Fe and 2.5-fold Fe^{2+}) and C_6M (5.6-fold for Fe and 4.8-fold for Fe^{2+}), while the values decreased significantly (0.5-fold for Fe and 0.6-fold for Fe^{2+}) in C+L_6M. Although an overall enrichment experiment showed a strong role of the test nutrients in improving the local physicochemical condition of the AMD impacted soil, lactate + cysteine was identified as a better stimulant than cysteine alone.

Shift in Microbial Community Composition

16S rRNA gene amplicon sequencing and estimated diversity indices revealed an assessable shift in microbial community composition of AIS following incubation with nutrient amendments (**Table 2**). Both estimated Chao1 and observed OTUs were increased coupled with distinct shifts in microbial community composition (**Table 2**). The most abundant bacterial phyla within the AIS at 0_Day were *Proteobacteria* (42%), WD272 (20%), *Actinobacteria* (14%), *Acidobacteria* (11%), *Chloroflexi* (9%), and *Firmicutes* (1.5%) (**Figure 1**). Following incubation, a distinct shift in community composition with great enhancement of *Firmicutes* coupled with the striking decrease in abundance of *Proteobacteria*, *Acidobacteria*, and *Actinobacteria* were detected (**Figure 1**). Abundance of the members of *Firmicutes* affiliated to *Clostridia*, OPB54, *Negativicutes,* and *Bacilli* was increased in both C+L_6M and C_6M. The extent of enhancement of *Firmicutes* was up to 36.5-fold in C_6M and 35.4-fold in C+L_6M (**Figure 1**). *Proteobacteria* [*Gammaproteobacteria* (35%), *Alphaproteobacteria* (6%), *Betaproteobacteria* (1%), and *Deltaproteobacteria* (0.07%)] that constituted the major phylum at 0_Day was found to be considerably less prevalent within the communities enriched with various amendments (**Figure 1**). The noteworthy decrease in abundance of *Gammaproteobacteria* and *Alphaproteobacteria* was observed in all the setup whereas abundance of *Betaproteobacteria* and *Deltaproteobacteria* was increased in C_6M (**Figure 1**). Members of the phylum *Chloroflexi* (*Ktedonobacteria* and KD4-96) also showed a substantiate increase in their abundance in C_6M (19.0%) while it got reduced in C+L_6M (0.03%). The other major classes such as *Acidobacteria*, *Acidimicrobiia, Actinobacteria,* and *Thermoleophilia* showed decrease in their abundance in C_6M and C+L_6M (**Figure 1**).

Family level analysis within the 0_Day, H_6M, C_6M and C+L_6M microcosms showed increase in abundance of several families. The abundance of facultative and/or strict anaerobic members of *Clostridiales* (*Clostridiaceae 1*, Family XIII,

[3]www.arb-silva.de/documentation/release-119

[4]http://www.interactivenn.net

[5]https://huttenhower.sph.harvard.edu/galaxy

[6]http://greengenes.secondgenome.com

TABLE 1 | Details of physicochemical parameters of the microcosm setup.

Parameters	0_Day	H_4M	H_6M	C_4M	C_6M	C+L_4M	C+L_6M
pH	3.51 ± 0.01	3.60 ± 0.01	4.01 ± 0.01	5.86 ± 0.02	6.37 ± 0.01	6.12 ± 0.01	6.61 ± 0.01
ORP	200.51 ± 0.95	165.7 ± 1.0	140.61 ± 1.55	130.02 ± 1.09	120.23 ± 1.20	125.21 ± 1.15	110.02 ± 1.01
SO_4^{2-}	7838.20 ± 39.64	6780.78 ± 54.08	4005.88 ± 19.15	4282.33 ± 22.72	1860.21 ± 14.75	720.06 ± 11.31	365.58 ± 22.11
Fe^{2+}	130.89 ± 4.72	202.81 ± 3.57	336.64 ± 12.66	980.37 ± 6.45	628.83 ± 9.08	300.64 ± 4.77	79.29 ± 2.1
Fe	179.10 ± 1.55	300.81 ± 1.0	415.75 ± 1.75	1386.31 ± 1.11	735.13 ± 0.89	320.94 ± 1.10	90.01 ± 1.10
Cu	1.84 ± 0.07	0.31 ± 0.11	0.28 ± 0.08	0.13 ± 0.06	0.12 ± 0.07	0.18 ± 0.06	0.16 ± 0.05
Zn	1.79 ± 0.33	0.57 ± 0.21	0.46 ± 0.10	0.39 ± 0.10	0.16 ± 0.06	0.14 ± 0.04	0.13 ± 0.05
Ni	0.39 ± 0.11	0.32 ± 0.03	0.28 ± 0.06	0.16 ± 0.06	0.14 ± 0.07	0.16 ± 0.06	0.16 ± 0.07

All the units are represented in ppm except ORP (mV) and pH (SI unit). H, C and C+L denote unamended, cysteine amended and cysteine and lactate amended microcosms while 4M (120 days incubation) and 6M (180 days incubation) represent the time of incubation. The values are represented mean of three independent experiments with standard deviations.

TABLE 2 | Details of 16S rRNA gene reads and non-parametric diversity indices of microbial communities from microcosms and enrichments.

Sample name	Raw reads obtained	Quality filtered reads	Chao1	Observed OTUs	Simpson's index	Shannon's index	Goods Coverage
0_Day*	853984	516037	33511	17237	0.93	6.38	0.98
H_6M*	1613332	945208	59309	30274	0.97	7.45	0.98
C_6M*	1951074	1444246	51674	28392	0.93	6.36	0.99
C+L_6M*	1011838	590466	46528	23116	0.93	6.95	0.98
FA_C_6M	1299817	904305	16863	9003	0.51	2.72	0.99
FA_SRM**	1616369	1321436	33076	16041	0.41	2.71	0.99
FA_IRM**	1913139	1597931	32597	16545	0.36	2.44	0.99
Clos_C_6M	143284	95425	11341	5439	0.90	6.00	0.97
Clos_SRM**	1075968	846637	15109	8178	0.41	2.50	1.00
Clos__IRM**	299768	231499	14908	7311	0.60	4.23	0.98
FA_C+L_6M	703433	349793	4135	2725	0.48	2.71	0.99
Clos_C+L_6M	498707	381545	6810	4015	0.54	2.86	0.99

**Denotes the microcosm setup while rest denotes the enrichments. Enrichment was performed from both the setup (C_6M and C+L_6M) in facultative anaerobic and Clostridium specific media. FA, facultative anaerobic enrichment; FA_SRM, facultative anaerobic enrichment in sulfate reducing medium; FA_IRM, facultative anaerobic enrichment in iron reducing medium; Clos, Clostridium specific enrichment; Clos_SRM, Clostridium specific enrichment in sulfate reducing medium; and Clos_IRM, Clostridium specific enrichment in iron reducing medium. **Denotes the enrichment was performed for C_6M.*

Christensenellaceae, *Lachnospiraceae*, *Gracilibacteraceae*, *Peptococcaceae*, *Peptostreptococcaceae*, *Ruminococcaceae,* and VadinBB60), *Bacillales* (*Alicyclobacillaceae* and *Bacillaceae)*, *Veillonellaceae,* uncultured OPB54 and *Coriobacteriaceae* was increased in both C_6M and C+L_6M. Heat map analysis (**Figure 2**) of the distribution of major genera (also considering taxa classified up to family level) under *Clostridiales* indicated considerable enhancement in abundance of several taxa commonly attributed to sulfate- and iron-reduction following nutrient amendments. In contrast to this, only water amendment (control; H_6M) allowed enhancement of mostly known taxa involved in iron and sulfur oxidation [*Acidobacteriaceae* (Subgroup 1), *Gallionellaceae*, *Xanthomonadaceae*] and few other taxa such as OPB35 soil group, KD4-96, *Ktedonobacteria*_JG30-KF-AS9, BSV26 and *Cystobacteraceae.* Overall the successful enrichment of diverse fermentative and anaerobic populations was achieved, suppressing the growth of acidophilic members following creation of anoxic environment and supply of metabolizable C- and N-sources. A ternary plot was generated to understand the distribution of top 50 genera across 0_Day, C_6M and C+L_6M microcosm samples (**Figure 3**). The result showed that acidophilic genera such as *Ferrithrix, Metallibacterium, Acidobacterium*, uncultured *–Acidomicrobiales* and *-Acidobacteriaceae* Subgroup 1 etc. were more prevalent at 0_Day. In contrast, taxa affiliated to *Firmicutes*; *Desulfitobacterium, Clostridium Sensu Stricto 1, Desulfosporosinus, Desulfurispora*, uncultured *-Christensenellaceae*, -OPB54, *-Clostridiales* Family XVII, *-Ruminococcaceae,* -Lachnospiraceae, *-Peptococcaceae* etc. capable of sulfate- and iron-reduction dominated in C_6M and C+L_6M. One-way ANOVA analysis confirmed that microbial diversity among the treatments was significantly different ($P < 0.05$).

Microbial Shift at OTUs Level

In order to understand the dynamics of microbial community composition beyond the taxonomic level, most abundant OTUs (top 100 OTUs) from each of the microcosms were analyzed (**Figures 4A–D**). Top 100 OTUs from each microcosm contributed 79–85% of the total reads of the respective samples. The interesting finding was that when considering top 100 OTUs of one treatment, the same OTUs in another treatment

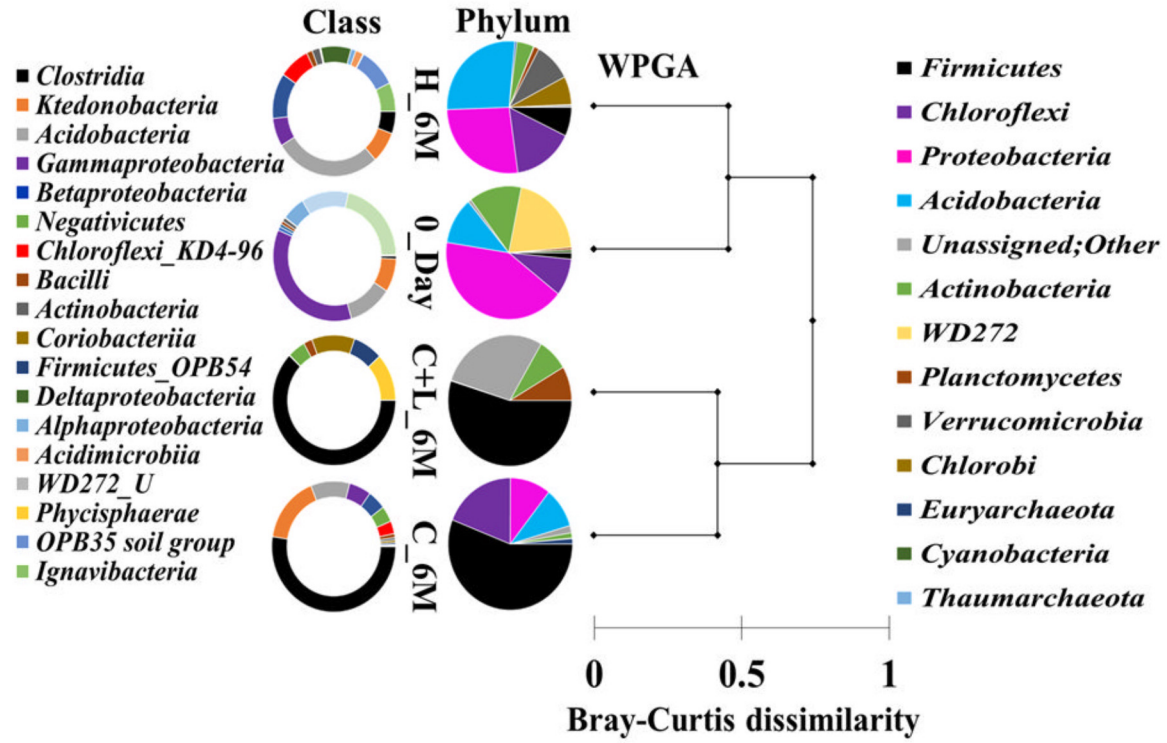

FIGURE 1 | Distribution of relative abundance of 16S rRNA gene sequences detected in microcosm setup (amended and unamended) at phylum-level (cumulative abundance > 0.1%) and class-level (top 18) taxonomic resolution. WPGA based agglomerative hierarchical clustering of treatments on the basis of abundance of phylum using Bray–Curtis dissimilatory matrix is represented. U denotes uncultured member.

contributed less percentage of the total reads, clearly indicating the effect of treatments (**Figures 4E–H**). Venn diagram depicted the pattern of sharing of OTUs among the treatments (**Figure 4I**) and signified that how the abundance of OTUs was significantly changed during the treatments. Taxonomic identities of these OTUs were determined to find their affiliation to 32 different taxa (**Figure 5**). Out of 100 OTUs from each of the microcosms, OTUs affiliated to *Firmicutes* were dominant in C+L_6M (80 OTUs) and C_6M (64 OTUs) while OTUs assigned to *Proteobacteria* were high in 0_Day (40 OTUs) and H_6M (33 OTUs) (**Figure 5**). These results were perfectly in line with our taxonomy based observation of increasing abundance of *Clostridia* in C+L_6M and C_6M. Total 26 OTUs (out of top 100 OTUs) were found to be shared between 0_Day and H_6M (**Figure 6A**). These common OTUs were affiliated mostly to acidophilic taxa. Among the C_6M and C+L_6M communities 24 shared OTUs were detected and these were affiliated to iron/sulfate reducing, fermentative and anaerobic *Firmicutes* taxa (**Figure 6B**).

qPCR Based Quantification of Bacterial/Specific Taxa and *dsr*B Gene

Quantitative estimation of the major taxa (*Firmicutes*, *Acidobacteria*, and *Actinobacteria*) as well as *dsr*B gene (involved in dissimilatory sulfate reduction) was performed for 0_Day, C_6M, C+L_6M and H_6M communities using qPCR based approach. Total bacterial 16S rRNA gene copies indicated a marginal reduction in bacterial abundance following microcosm amendments (**Figure 7**). The estimation of 16S rRNA gene copies for *Actinobacteria*, *Acidobacteria*, and *Firmicutes* corroborated with the amplicon based community data suggesting the decrease in abundance of *Actinobacteria* and *Acidobacteria* but increase in *Firmicutes* following nutrient amendment (**Figure 7**). The involvement of sulfate reducing bacteria in nutrient amended microcosms was highlighted by a remarkable increase in *dsr*B gene copy number from 7.8×10^4 to 3.9×10^5–1.0×10^6 (**Figure 7**).

PICRUSt Based Functional Prediction of the Community

Metabolic functions of the microbial communities were established through PICRUSt analysis. Using the genome-wide analysis tools integrated in PICRUSt, we could look into the genomic inventories related to sulfate and cysteine metabolism and other major biogeochemical processes of the enriched communities (**Supplementary Figure S1**). The result showed abundance of genes involved in dissimilatory sulfate metabolism (*apr*AB and *dsr*AB), cysteine metabolism (cysteine desulfhydrase, cysteine synthase, cystathionine synthase and cystathionine lyase) along with hydrogenases, metal tolerance/transporter gene for As, Fe, Cu, Zn, Co, etc., nitrogen metabolism and other major categories of metabolic functions. Considerable change in the abundance of *dsr*AB (involved in dissimilatory sulfate reduction)

FIGURE 2 | Heat map based relative abundance of distribution of top 50 *Clostridiales* members in all the microcosm setup. U and O denote uncultured member and others, respectively.

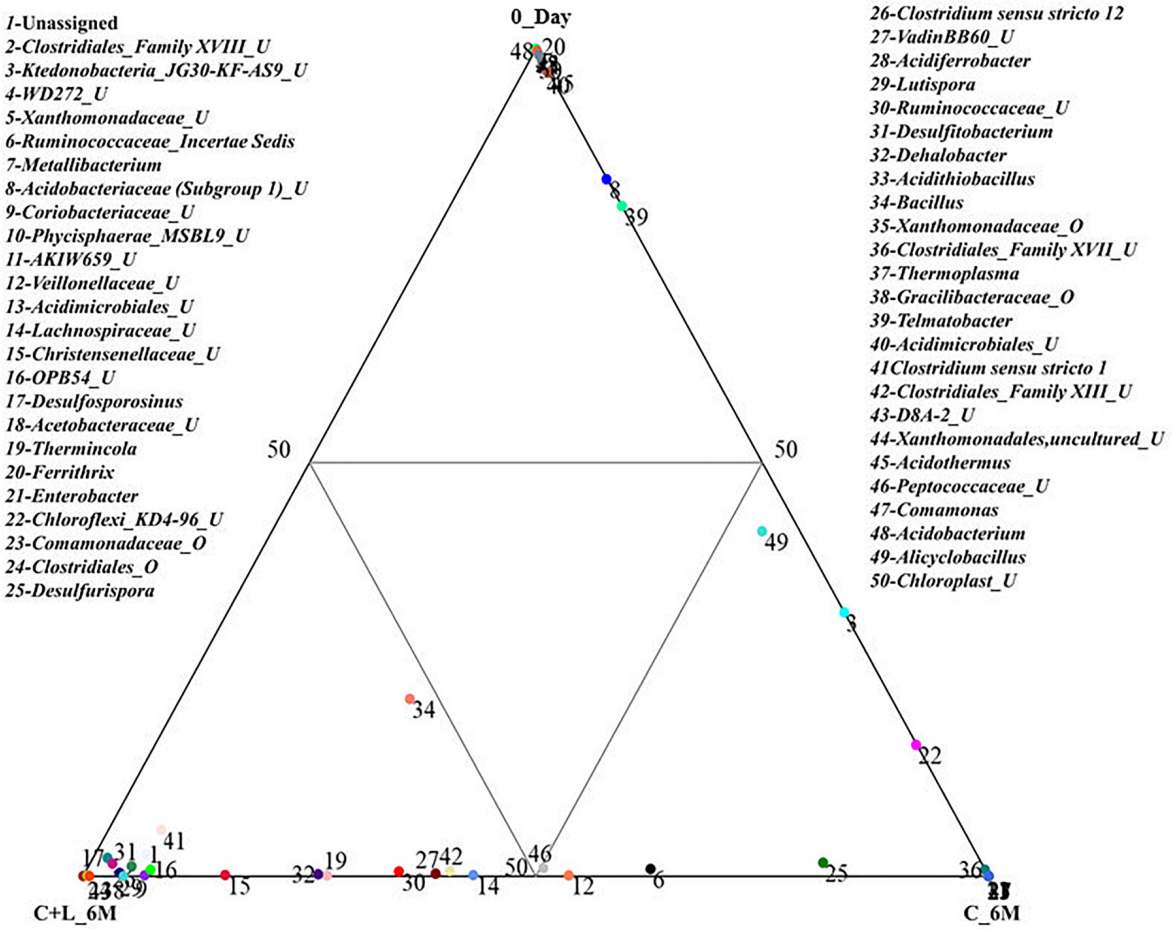

FIGURE 3 | Distribution of taxonomic groups at genera level in 0_Day, C_6M and C+L_6M. The 50 most abundant genera (cumulative abundance > 0.2%) associated with each sample is visualized in ternary plots. The position in the triangle indicates the relative abundance of each taxon among the three samples. U and O denote uncultured member and others, respectively.

and cysteine desulfhydrase (involved in cysteine utilization) was observed in nutrient amended microcosms. The analysis clearly indicated that enriched microbial populations were genetically equipped for dissimilatory sulfate reduction following cysteine amendment.

Enrichment of *Firmicutes* Members Using Specific Medium From Microcosm Setup

The 16S rRNA gene based investigation indicated that following cysteine amendment abundance of members of *Firmicutes* were enriched considerably. Most of these taxa were known for their role in anaerobic sulfate- and iron-reduction. Although the qPCR and PICRUSt supported the role of these members in the observed physicochemical changes within our AIS microcosms, final validation of their biogeochemical role was done by enrichment of the *Firmicutes* members under specific culture conditions. Cultures from both C_6M and C+L_6M microcosms were sub-cultured in two specific media: *Clostridium* specific and facultative anaerobic. Following three repeated sub-culturing in the respective media, taxonomic identities of the enriched populations were established by 16S rRNA gene based amplicon sequencing (**Figure 8A**). The results indicated that our culture conditions were highly supportive for the enrichment of *Firmicutes* members in both the *Clostridium* specific and facultative anaerobic media. Members of this phylum contributed 95.33–99.85% while *Proteobacteria*, *Actinobacteria,* and *Bacteroidetes* constituted very small populations (**Figure 8A**). The most dominant genera detected in the *Clostridium* specific enrichment belonged to *Clostridiales* and *Bacillales* members such as *Clostridium sensu stricto 1, Lysinibacillus, Ruminococcaceae_incertae sedis, Clostridium sensu stricto 10, Clostridium sensu stricto 12, Paenibacillus, Clostridiales*_Family XIII, uncultured *Planococcaceae* and uncultured *Veillonellaceae* members (**Figure 8B**). In the facultative anaerobic medium sub cultured from C_6M microcosm, *Bacillus* was the most dominant genera (75.70%) followed by *Clostridium sensu stricto 1* (20.63%), *Clostridium sensu stricto 12* (1.01%) and *Sporolactobacillus* (0.68%) (**Figure 8B**). In contrast, *Clostridium sensu stricto 12* and

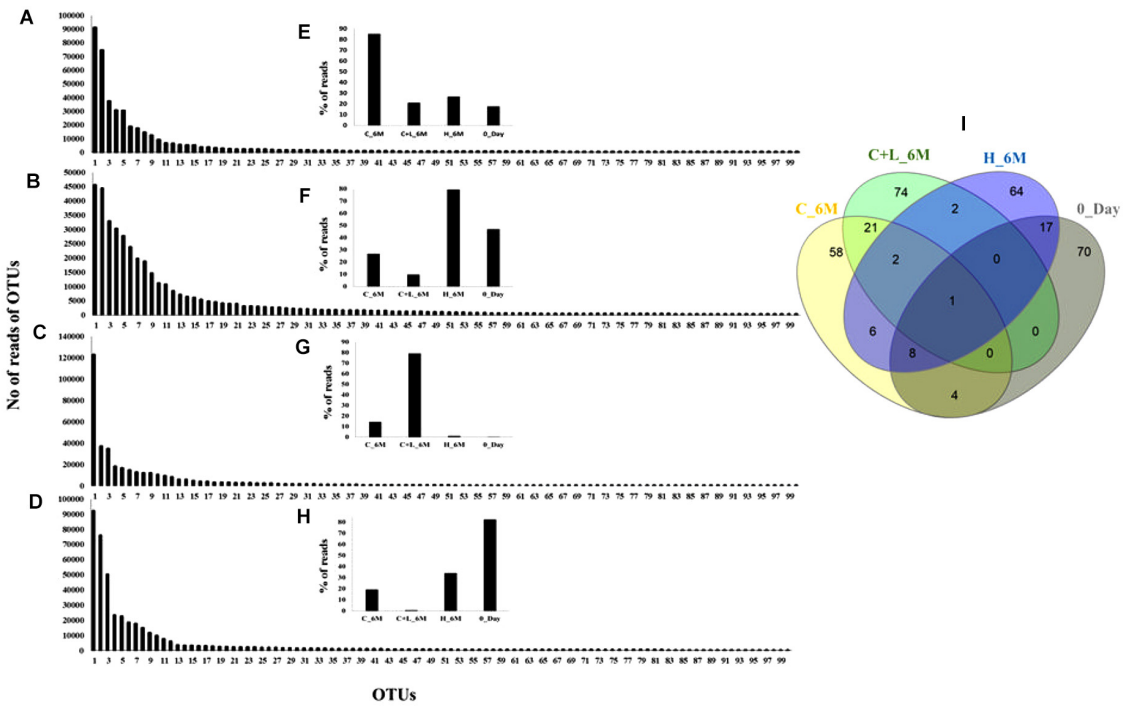

FIGURE 4 | Rank abundance based analysis of top 100 OTUs in the microcosm setup. Rank abundance profile of top 100 OTUs from each sample is depicted **(A)** C_6M, **(B)** H_6M, **(C)** C+L_6M, and **(D)** 0_Day. **(E–H)** represent the percent distribution of top 100 OTUs across the samples. (I) Venn diagram shows the shared and unique OTUs across the samples (considering top 100 OTUs from each sample). Detail taxonomic affiliations of 100 OTUs are presented in **Supplementary Table S2**

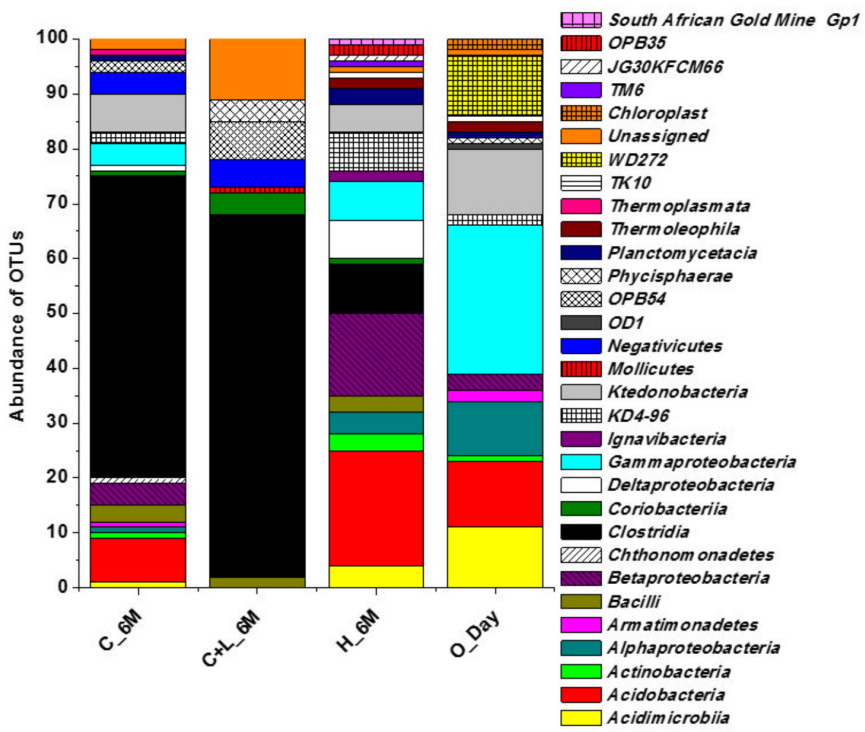

FIGURE 5 | Taxonomic distribution pattern (at class-level) of top 100 OTUs in each setup.

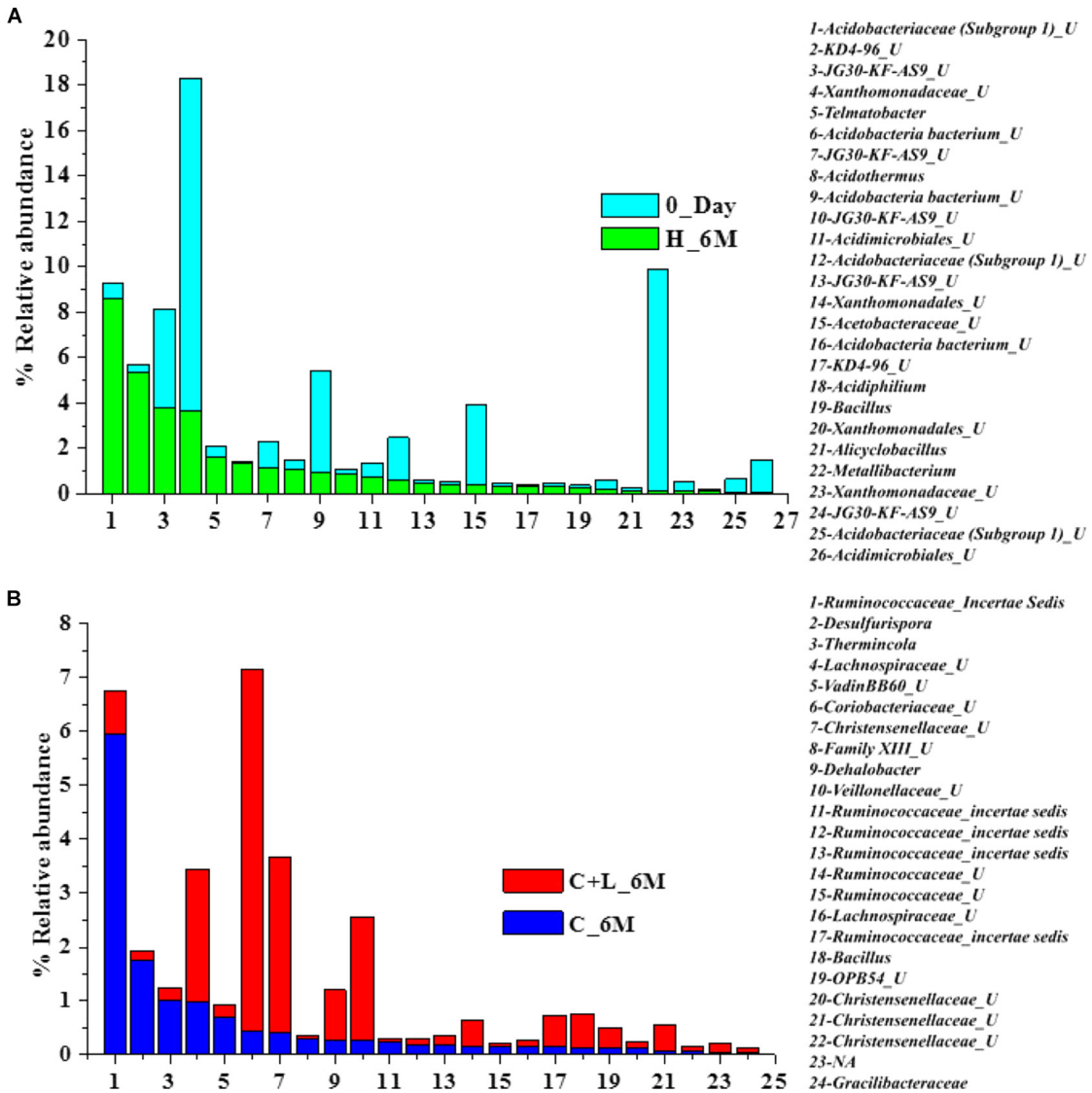

FIGURE 6 | Distribution of shared OTUs (from top 100 OTUs) between the samples **(A)** 0_Day and H_6M and **(B)** C+L_6M and C_6M. U denotes uncultured member.

Clostridium sensu stricto 11 accounted for more than 95% of the community grown in the same medium but subcultured from C+L_6M (**Figure 8B**).

Sulfate- and Iron-Reduction Potential of the Microorganisms Enriched in *Clostridium* Specific and Facultative Anaerobic Media

Bacterial cultures enriched in *Clostridium* specific and facultative anaerobic media were further inoculated in sulfate reducing and iron reducing media (designated as SRM and IRM) for assessing their potential toward sulfate- and iron-reduction. Following three repeated sub-culturing, 16S rRNA gene amplicon sequencing was done for all the four sets derived originally from C_6M microcosm. The amplicon sequencing result of *Clostridium* specific enrichment grown in SRM showed that uncultured *Veillonellaceae* members, *Ruminococcaceae incertae sedis* and *Clostridium sensu stricto 12* accounted for 92.25% (**Figure 8C**). The same enrichment culture grown in IRM showed the abundance of *Lysinibacillus* (80.43%) along with *Bacillus*, uncultured *Planococcaceae* member, *Clostridium sensu stricto 12* and *Clostridium sensu stricto 10* (**Figure 8C**). Similar study performed with facultative anaerobic enrichment indicated proliferation (cumulative abundance of 98%) of *Bacillus*, *Brevibacillus*, *Clostridium sensu stricto 10, Fictibacillus, Anoxybacillus,* and *Clostridium sensu stricto 1* in SRM (**Figure 8C**) while *Bacillus, Paenibacillus*, *Clostridium sensu stricto 10* and *Fictibacillus* accounted for 97.71% of the IRM culture (**Figure 8C**). Metabolic abilities of the enriched

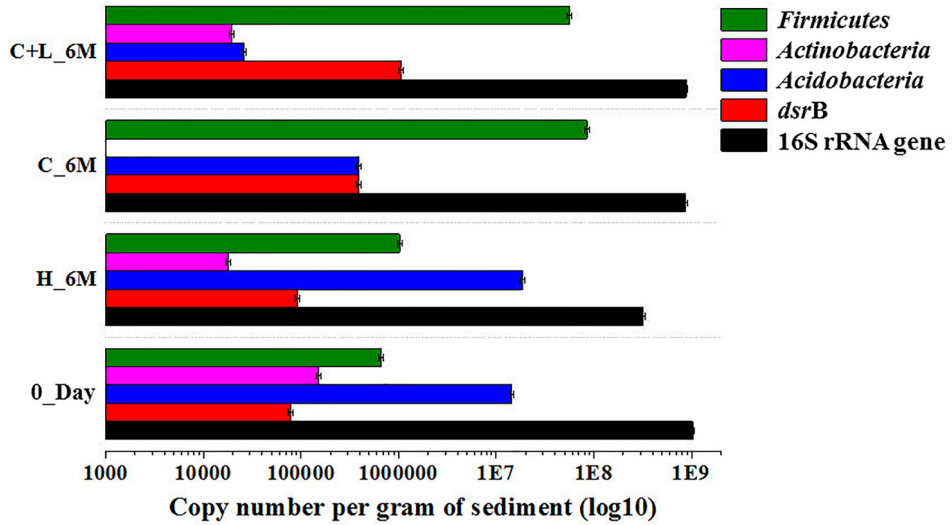

FIGURE 7 | Quantitative PCR based analysis of gene copy number of bacteria/specific taxa and *dsr*B gene among the microcosm setup.

populations derived from microcosms C_6M and C+L_6M microcosms toward sulfate- and iron-reduction were confirmed by quantitative estimation of SO_4^{2-} and Fe^{2+} ions. Nearly complete reduction of SO_4^{2-} (15 mM) and Fe^{3+} (5 mM) were noticed following 10–14 days of incubation, confirming their abilities for reduction of these terminal electron acceptors. The formation of black precipitates of iron sulfide in SRM and change in color of the IRM from yellow to light green or colorless with precipitation of Fe (Ferric citrate as redox indicator) (Pan et al., 2017) was also noted (**Supplementary Figure S2**). In order to confirm the presence of these SRB and IRB after 4 months of incubation where a decline in soluble iron concentration (Fe^{2+}) was observed due to precipitation with sulfide produced by sulfate reducing activity in the treatments, DGGE based microbial community analysis was performed with 5 months incubated microcosms (H_5M, C_5M, and C+L_5M). The banding pattern obtained for C_5M and C+L_5M communities showed enrichment of almost similar types of microbial populations (**Figure 9**). The enrichment of *Clostridium* sp., *Themincola* sp., *Bacillus* sp., *Steroidobacter* sp., as well as members of *Acidobacteriaceae*, *Ruminococcaceae*, and *Coriobacteriaceae* in these treatments clearly indicated their potential toward both iron- and sulfate-reduction (**Figure 9**). These groups were also detected in the same treatments through amplicon based sequencing after 6 months of incubation. These known iron and sulfate reducing populations were also detected in both iron and sulfate reducing media hence confirmed their involvement in reduction of iron and sulfate during 5 months of incubated setups.

DISCUSSION

Geomicrobiology of AMD including the nature of microorganisms and biogeochemical functions of various acidophilic microorganisms is well established. In contrast to that, the broader ecological roles of AMD organisms in terms of the attenuation of the hazardous nature of such acidic environment remain less explored. Our study demonstrated that it is possible to enhance the activities of indigenous sulfate- and iron-reducing bacteria of an AIS to achieve improvement of its major physicochemical parameters desirable for bioremediation. With respect to the major questions we posed during this study, our results proved that (a) it is possible to enhance the abundance and activities of autochthonous sulfate- and iron-reducing bacteria of an AIS and (b) this altered microbial community could lead toward changing the physicochemical conditions favorably, thus decreasing the hazardous nature of the studied sample considerably.

There are reports highlighting the presence of heterotrophic sulfate- and iron-reducing bacteria (*Clostridiaceae*, *Peptococcaceae*, and *Bacillaceae* members) within highly acidic AMD systems (Sánchez-Andrea et al., 2012a,b). Our biostimulation based approach was successful in enhancing the abundance of *Firmicutes* members capable of anaerobic sulfate-/iron-reduction. In the native AIS, these bacterial taxa constituted only 1.5% which (low abundance of heterotrophic reducing taxa) corroborated the earlier reports on different AMD environments (Chen L.X. et al., 2013; Kuang et al., 2013). Increase in abundance of these anaerobic/facultative anaerobic populations surpassing the acid producing-, sulfur- and metal-oxidizing microorganisms with nutrient amendments was impressive. All these members of the phylum *Firmicutes* were well known for their facultative to strict anaerobic metabolism, but not so much for sulfate- and iron-reduction except few taxa such as *Clostridium*, *Desulfosporosinus*, *Desulfotomaculum* etc. (Chockalingam and Subramanian, 2006; Church et al., 2007; Sánchez-Andrea et al., 2012b; Pan et al., 2017). The increased abundance of gene encoding dissimilatory sulfite reductase (*dsr*B) and *Firmicutes* specific 16S rRNA gene detected in

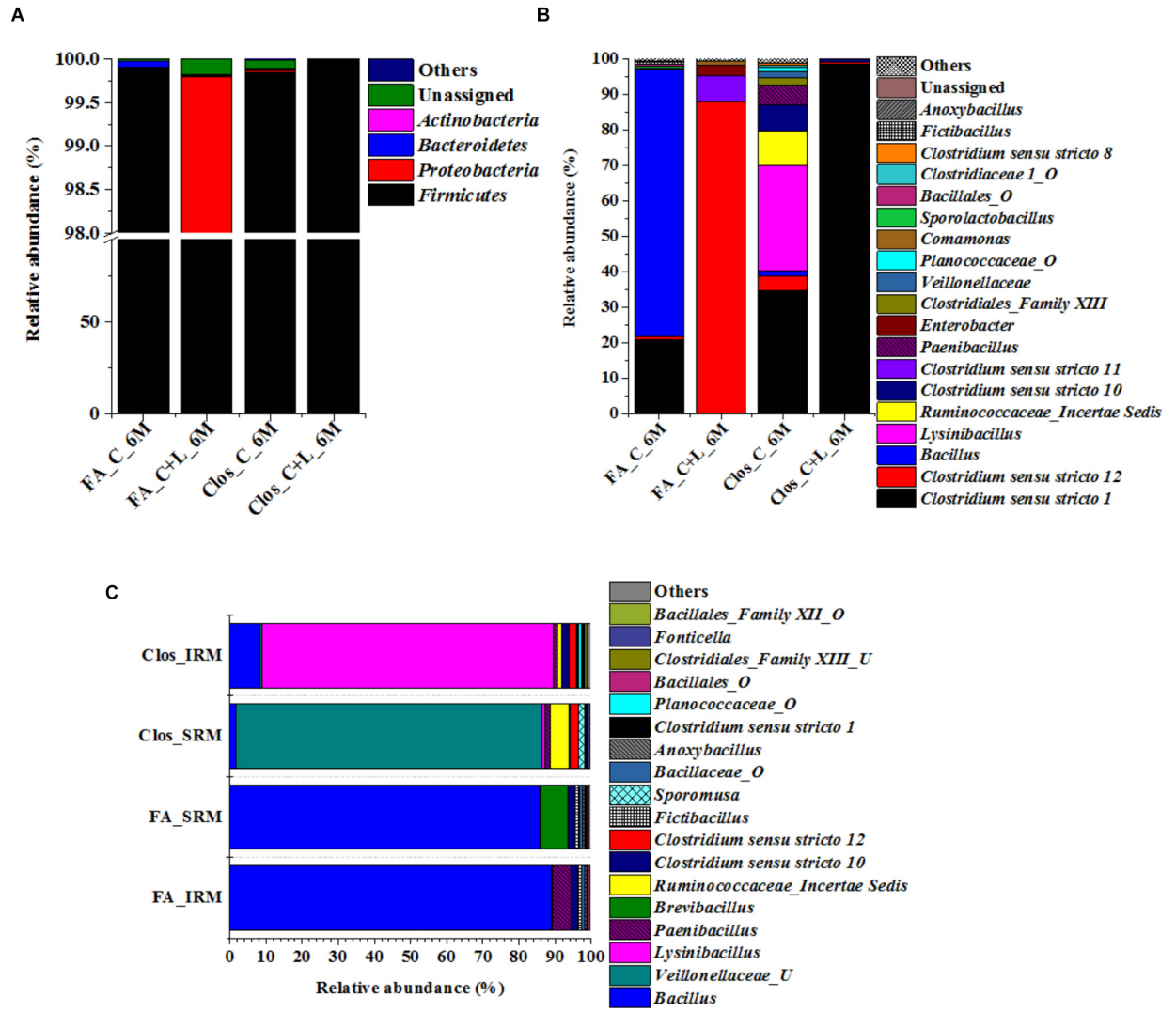

FIGURE 8 | Taxonomic distribution of enrichment setups from C_6M and C+L_6M. **(A)** Phylum-level distribution of enriched populations in *Clostridium* specific (Clos) and Facultative anaerobic (FA) enrichment. **(B)** Distribution of genera in *Clostridium* specific enrichment and Facultative anaerobic enrichment. **(C)** Shift in microbial diversity (represented at genera-level) when enriched population of Clos_C_6M and FA_C_6M were subjected to iron and sulfate reducing medium. Clos_IRM: distribution pattern of *Clostridium* specific enrichment in iron reducing medium; Clos_SRM: distribution pattern of *Clostridium* specific enrichment in sulfate reducing medium; FA_IRM: distribution pattern of Facultative anaerobic enrichment in iron reducing medium and FA_SRM: distribution pattern of Facultative anaerobic enrichment in iron reducing medium. U and O denote uncultured member and others, respectively.

qPCR, reduction of -sulfate/-iron and rise in pH were all in strong agreement. Our results demonstrated that a number of sulfate- and iron-reducing bacterial taxa present in AMD impacted environment can be proliferated and implicated with the desirable reductive processes successfully. The PICRUSt analysis confirmed that the enriched bacterial populations were genetically equipped for dissimilatory sulfate reduction processes.

The effect of cysteine (alone or along with lactate) as successful proxy to provide required metabolic resources and thus biostimulate the target groups of microorganisms could be attributed to its dual characteristics. Cysteine could be used by the microbes as a carbon and nitrogen source, and also might act as a reducing agent (that helps in scavenging the dissolved oxygen) to facilitate reduction of iron and sulfate. Microbes catabolize cysteine for their fermentative mode of metabolism through two enzymes (i) cysteine desulfhydrase which produces NH_3, pyruvate and H_2S and (ii) cystathionine-γ-lyase which utilizes an oxidized form of cysteine (Morra and Dick, 1991). Microbe mediated H_2S production was possible from selective enrichment of soil amended with cysteine through cysteine desulfhydrase enzyme. Wang et al. (2000) demonstrated that the genes encoding cysteine desulfhydrase and serine acetyltransferase may be used to develop a metabolically engineered *Escherichia coli* that can carry out aerobic sulfate reduction. Suitability of carbon sources rich in amino acids, but low in lignin in promoting sulfate

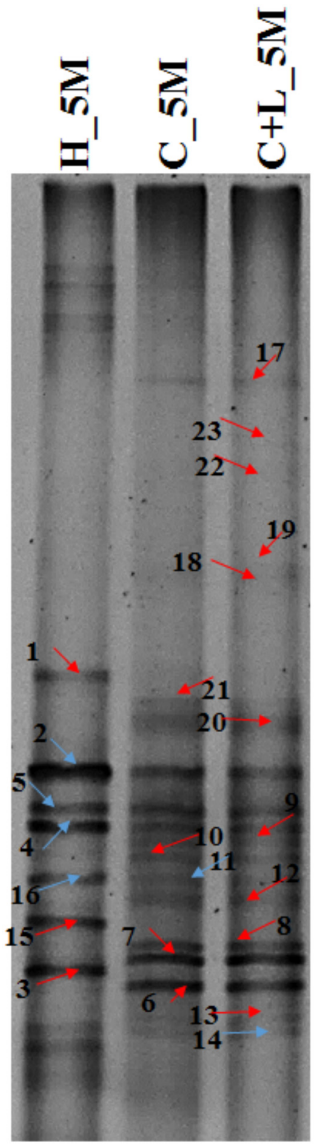

Band ID	EzTaxon/Silva_119 database
1	*Steroidobacter/Xanthomonadales*
2	*Steroidobacter/Xanthomonadales*
3	*Steroidobacter/Xanthomonadales*
4	*Paceibacter/Unassigned*
5	*Occallatibacter/Acidobacteriaceae_Subgroup 1*
6	*Acidobacteriaceae/Acidobacteriaceae_Subgroup 1*
7	**Clostridium/Clostridium sensu stricto 10*
8	* *Bacillus/Bacillus*
9	**Clostridum_g13/Ruminococcaceae*
10	*Solibacteraceae/Acidobacteria_subgoup3*
11	**Clostridium puniceum/Clostridium sensu stricto 1*
12	*Occallatibacter/Acidobacteriaceae_Subgroup 1*
13	*Solibacter/Candidatus Solibacter*
14	**Coriobacteriaceae/Coriobacteriaceae*
15	*Cyanobacteria/WD272*
16	*Acidobacteriaceae/Acidobacteriaceae_Subgroup 1*
17	* *Thermincola/Thermincola*
18	**Thermincola/Thermincola*
19	**Clostridium/Clostridium sensu stricto 1*
20	*Steroidobacter/Xanthomonadales*
21	*Steroidobacter/Xanthomonadales*
22	**Clostridium/Clostridium sensu stricto 1*
23	**Clostridium/Clostridium sensu stricto 1*

FIGURE 9 | Denaturing gradient gel electrophoresis (DGGE) profile of treatments (H_5M, C_5M, and C+L_5M) at 150 days of incubation. Red arrow indicates distinct band while blue represents common bands. *Represents the organisms detected in both treatment and enrichment of C_6M and C+L_6M.

reduction was also reported (Coetser et al., 2006). Recently, Zhang et al. (2017) established the role of tryptone and yeast extract in the remediation of mine tailings by promoting the growth of SRB.

Microbial taxa enriched during this study were reported to be of facultative- or strict-anaerobic nature, involved in anaerobic hydrolytic fermentation, cysteine utilization, acetate- and H_2S-production and metal reduction (Petrie et al., 2003; Church et al., 2007; Finke and Jørgensen, 2008; Kosaka et al., 2008; Li et al., 2011; Bertel et al., 2012; AlAbbas et al., 2013; Hausmann et al., 2016; Peng et al., 2016; Pan et al., 2017). The major genera identified in this study such as *Clostridium, Clostridium sensu stricto* members, *Lutispora, Sporobacter, Acetanaerobacterium, Caldicoprobacter, Gracilibacter, Oxobacter, Fonticella, Papillibacter*, as well as unclassified members of *Ruminococcaceae*, *Lachnospiraceae*, and *Christensenellaceae* were all reported as anaerobic, fermentative, cellulose- and cysteine-metabolizing, acetogenic, and iron reducing members (Grech-Mora et al., 1996; Defnoun et al., 2000; Chen and Dong, 2004; Lee et al., 2006; Shiratori et al., 2008; Bouanane-Darenfed et al., 2011; Chen M. et al., 2013; Fraj et al., 2013; Peng et al., 2016). Presence of these organisms was reported from diverse sulfur-rich environments including hot spring (Zavarzina et al., 2007; Bouanane-Darenfed et al., 2011; Fraj et al., 2013), mine tailings/drainage/soil (Sánchez-Andrea et al., 2011; Gupta et al., 2017), constructed wetland (Lee et al., 2006) and AMD treatments sites (Clarke et al., 2004; Kaksonen et al., 2004; Pruden et al., 2007; Bijmans et al., 2009; Hiibel et al., 2011;

Lu et al., 2011; Martins et al., 2011; Sánchez-Andrea et al., 2014; Deng et al., 2016). Considering the known metabolic characteristics of these taxa and their ecological relevance, we could attribute their abundance to the observed sulfate- and iron-reduction. In accordance with previous reports, the other known strict anaerobic sulfate reducing taxa such as *Desulfurispora*, *Desulfotomaculum*, *Desulfosporosinus,* and *Desulfitobacterium* was also enriched during our study (Kaksonen et al., 2004; Church et al., 2007; Hiibel et al., 2008, 2011; Bijmans et al., 2010). The enhanced abundance of facultative anaerobic fermentative and strictly anaerobic sulfate reducing populations following cysteine amendments highlights the synergistic role of these metabolically dependent organisms confirming the fermentation coupled with sulfate reduction phenomenon (Finke and Jørgensen, 2008). We hypothesize that in the presence of cysteine, fermentative organisms become activated, producing metabolites and deplete the dissolved oxygen rapidly and thereby creating more anoxic niches. Within these anoxic micro-niches strict anaerobic populations proliferate, making use of the sulfate as preferred terminal electron acceptor thus facilitates sulfate reduction and rise in pH (Church et al., 2007). Our attempt to confirm the physiological abilities of the enriched populations toward sulfate- and iron-reduction by using culture media specific for *Clostridium* and facultative anaerobic bacteria supported the above hypothesis. We were successful in identifying the facultative and strict anaerobic sulfate- and iron-reducing populations with conformity through specific enrichment and deep sequencing.

The potential involvement of individual members of the enriched populations toward reductive processes was validated by a third level of enrichment wherein sulfate- and iron-reducing populations were grown more selectively in two specific media. These sulfate- and iron-reducing bacteria specific enrichments were meant to segregate and identify the organisms responsible for individual terminal electron acceptor utilization (iron as Fe^{3+} and sulfate as SO_4^{2}). 16S rRNA gene sequencing of metagenomes retrieved from these enrichments revealed that members of the families *Clostridiaceae*, as well as *Bacillaceae* (genera *Lysinibacillus, Bacillus and Paenibacillus* etc.), *Veillonellaceae* and *Ruminococcaceae* etc. specifically contributed toward sulfate- or iron-reduction. Presence of these members in both C_5M and C+L_5M microcosms through DGGE further confirmed their potential of sulfate and iron reduction. *Clostridiaceae* and *Bacillaceae* members were previously reported in different AMD bioremediation studies or in sulfate-/iron-reducing enrichments/AMD environment (Clarke et al., 2004; Scala et al., 2006; Hiibel et al., 2008, 2011; Sánchez-Andrea et al., 2011; Yi et al., 2012; Giloteaux et al., 2013; Zhang and Wang, 2016; Zhang et al., 2016). The predominance of metal reducing *Pelosinus* (member of *Veillonellaceae*) on lactate amendment was reported by Mosher et al. (2012). Metal reduction and fermentative mode of metabolism of *Veillonellaceae* members were reported by earlier investigators including the whole genome sequence analysis of uncultured *Veillonellaceae* strain RU4 that confirmed presence of genes for sulfate reduction as well as polysulfide reduction (Brown et al., 2012; Shah, 2013; Kwon et al., 2016). Zhao et al. (2010) reported the role of *Ruminococcus* spp. (member of *Ruminococcaceae*) in sulfate reduction. Thus in our study, these enriched members confirmed their involvement in iron and sulfate reduction.

CONCLUSION

An acidic, sulfate-, iron- and other heavy metal-rich AMD impacted soil harbored low proportion of heterotrophic, sulfate- and iron-reducing anaerobic bacterial populations. These redox active members can be successfully stimulated by cysteine and lactate amendment. These enriched microbial groups can facilitate dramatic change in physiochemical condition. The microorganisms which got enriched with nutrient amendment belonged to the fermentative and strict anaerobic sulfate- and iron-reducing populations affiliated to *Clostridiaceae*, *Veillonellaceae, Bacillaceae*, *Ruminococcaceae* etc. Increased abundance of these organisms as evident from 16S rRNA amplicon sequencing and taxon-specific qPCR; enhancement of *dsr*B gene, change in genomic composition suitable for carrying out the required catabolic function corroborated with reduction in soluble sulfate- and iron-reduction and pH management. This study enabled us to gain a better insight on ecological perspective of the members of phylum *Firmicutes* indigenous to AMD impacted sites and more importantly, their involvement in sulfate- and, iron-reduction processes. The study also demonstrated the suitability of amino acid/protein rich natural substances as potent biostimulation agent for bioremediation of AMD/AMD impacted sites and provided us the specific microbial populations capable of anaerobic sulfate-, and/or iron-reduction which could be used as a potent bioaugmentation agent for future bioremediation applications.

AUTHOR CONTRIBUTIONS

PS conceived and designed the experiments and arranged funds. AG performed the major experiments. PS and AG were responsible for manuscript preparation. MP, PS, and AG arranged sampling from MCP. AG and JS performed the qPCR. AG and AD performed the bioinformatics analysis for deciphering microbial diversity. AG and AD performed the 16S rRNA gene amplicon sequencing in Ion S5 sequencer.

FUNDING

The authors are grateful to Department of Biotechnology, Government of India for funding the project (BT/PR 7533/BCE/8/959/2013, Dated 10/12/2013). The authors are thankful to IIT Kharagpur for providing the NGS facility (Ion S5 sequencer) through SGBSI challenge grant (IIT/SRIC/BT/ODM/2015-16/141). AG thanks the Department of Biotechnology, Government of India for providing fellowship under DBT-JRF category (DBT/2014/IITKH/113). Financial support to AD (IIT/ACAD (PGS&R)/F.II/2/14/BS/91R01) and JS (IIT/ACAD(PGS&R)/F.II/2/13/BT/91P01) from IIT Kharagpur and institutional fellowship was acknowledged.

ACKNOWLEDGMENTS

The generous help from Malanjkhand Copper Project, Hindustan Copper Limited authority for sample collections was acknowledged.

SUPPLEMENTARY MATERIAL

The Supplementary Material for this article can be found online at: https://www.frontiersin.org/articles/10.3389/fmicb.2018.02882/full#supplementary-material

REFERENCES

AlAbbas, F. M., Bhola, S. M., Spear, J. R., Olson, D. L., and Mishra, B. (2013). The shielding effect of wild type iron reducing bacterial flora on the corrosion of linepipe steel. *Eng. Fail. Anal.* 33, 222–235. doi: 10.1016/j.engfailanal.2013.05.020

Baker, B. J., and Banfield, J. F. (2003). Microbial communities in acid mine drainage. *FEMS Microbiol. Ecol.* 44, 139–152. doi: 10.1016/S0168-6496(03)00028-X

Bates, S. T., Berg-Lyons, D., Caporaso, J. G., Walters, W. A., Knight, R., and Fierer, N. (2011). Examining the global distribution of dominant archaeal populations in soil. *ISME J.* 5, 908–917. doi: 10.1038/ismej.2010.171

Becerra, C. A., López-Luna, E. L., Ergas, S. J., and Nüsslein, K. (2009). Microcosm-based study of the attenuation of an acid mine drainage-impacted site through biological sulfate and iron reduction. *Geomicrobiol. J.* 26, 9–20. doi: 10.1080/01490450802599 2

Bertel, D., Peck, J., Quick, T. J., and Senko, J. M. (2012). Iron transformations induced by an acid-tolerant *Desulfosporosinus* species. *Appl. Environ. Microbiol.* 78, 81–88. doi: 10.1128/AEM.06337-11

Bertin, P. N., Heinrich-Salmeron, A., Pelletier, E., Goulhen-Chollet, F., Arsène-Ploetze, F., Gallien, S., et al. (2011). Metabolic diversity among main microorganisms inside an arsenic-rich ecosystem revealed by meta-and proteogenomics. *ISME J.* 5, 1735–1747. doi: 10.1038/ismej.2011.51

Bijmans, M. F., De Vries, E., Yang, C. H., Buisman, N., Cees, J., Lens, P. N., et al. (2010). Sulfate reduction at pH 4.0 for treatment of process and wastewaters. *Biotechnol. Prog.* 26, 1029–1037. doi: 10.1002/btpr.400

Bijmans, M. F., Dopson, M., Peeters, T. W., Lens, P. N., and Buisman, C. J. (2009). Sulfate reduction at pH 5 in a high-rate membrane bioreactor: reactor performance and microbial community analyses. *J. Microbiol. Biotechnol.* 19, 698–708. doi: 10.4014/jmb.0809.502

Bird, L. J., Bonnefoy, V., and Newman, D. K. (2011). Bioenergetic challenges of microbial iron metabolisms. *Trends Microbiol.* 19, 330–340. doi: 10.1016/j.tim.2011.05.001

Bouanane-Darenfed, A., Fardeau, M. L., Grégoire, P., Joseph, M., Kebbouche-Gana, S., Benayad, T., et al. (2011). Caldicoprobacteralgeriensis sp. nov. A new thermophilic anaerobic, xylanolytic bacterium isolated from an Algerian hot spring. *Curr. Microbiol.* 62, 826–832. doi: 10.1007/s00284-010-9798-9

Brown, S. D., Podar, M., Klingeman, D. M., Johnson, C. M., Yang, Z. K., Utturkar, S. M., et al. (2012). Draft genome sequences for two metal-reducing *Pelosinus fermentans* strains isolated from a Cr (VI)-contaminated site and for type strain R7. *J. Bacteriol.* 194, 5147–5148. doi: 10.1128/JB.01174-12

Burns, A. S., Pugh, C. W., Segid, Y. T., Behum, P. T., Lefticariu, L., and Bender, K. S. (2012). Performance and microbial community dynamics of a sulfate-reducing bioreactor treating coal generated acid mine drainage. *Biodegradation* 23, 415–429. doi: 10.1007/s10532-011-9520-y

Caporaso, J. G., Kuczynski, J., Stombaugh, J., Bittinger, K., Bushman, F. D., Costello, E. K., et al. (2010). QIIME allows analysis of high-throughput community sequencing data. *Nat. Methods* 7, 335–336. doi: 10.1038/nmeth.f.303

Chandra, A. P., and Gerson, A. R. (2010). The mechanisms of pyrite oxidation and leaching: a fundamental perspective. *Surf. Sci. Rep.* 65, 293–315. doi: 10.1016/j.surfrep.2010.08.003

Chen, L. X., Hu, M., Huang, L. N., Hua, Z. S., Kuang, J. L., Li, S. J., et al. (2015). Comparative metagenomic and metatranscriptomic analyses of microbial communities in acid mine drainage. *ISME J.* 9, 1579–1592. doi: 10.1038/ismej.2013.242

Chen, L. X., Huang, L. N., Méndez-García, C., Kuang, J. L., Hua, Z. S., Liu, J., et al. (2016). Microbial communities, processes and functions in acid mine drainage ecosystems. *Curr. Opin. Biotechnol.* 38, 150–158. doi: 10.1016/j.copbio.2016.01.013

Chen, L. X., Li, J. T., Chen, Y. T., Huang, L. N., Hua, Z. S., Hu, M., et al. (2013). Shifts in microbial community composition and function in the acidification of a lead/zinc mine tailings. *Environ. Microbiol.* 15, 2431–2444. doi: 10.1111/1462-2920.12114

Chen, M., Cao, F., Li, F., Liu, C., Tong, H., Wu, W., et al. (2013). Anaerobic transformation of DDT related to iron (III) reduction and microbial community structure in paddy soils. *J. Agric. Food Chem.* 61, 2224–2233. doi: 10.1021/jf305029p

Chen, S., and Dong, X. (2004). *Acetanaerobacterium elongatum* gen. nov., sp. nov., from paper mill waste water. *Int. J. Syst. Evol. Microbiol.* 54, 2257–2262. doi: 10.1099/ijs.0.63212-0

Chesnin, L., and Yien, C. H. (1951). Turbidimetric determination of available sulfates. *Soil Sci. Soc. Am. J.* 15, 149–151. doi: 10.2136/sssaj1951.036159500150000C0032x

Chockalingam, E., and Subramanian, S. (2006). Studies on removal of metal ions and sulphate reduction using rice husk and *Desulfotomaculum nigrificans* with reference to remediation of acid mine drainage. *Chemosphere* 62, 699–708. doi: 10.1016/j.chemosphere.2005.05.013

Church, C. D., Wilkin, R. T., Alpers, C. N., Rye, R. O., and McCleskey, R. B. (2007). Microbial sulfate reduction and metal attenuation in pH 4 acid mine water. *Geochem. Trans.* 8:10. doi: 10.1186/1467-4866-8-10

Clarke, A. M., Kirby, R., and Rose, P. D. (2004). Molecular microbial ecology of lignocellulose mobilisation as a carbon source in mine drainage wastewater treatment. *Water* 30, 658–661.

Coetser, S. E., Pulles, W., Heath, R. G. M., and Cloete, T. E. (2006). Chemical characterisation of organic electron donors for sulfate reduction for potential use in acid mine drainage treatment. *Biodegradation* 17, 67–77. doi: 10.1007/s10532-005-7567-3

Defnoun, S., Labat, M., Ambrosio, M., Garcia, J. L., and Patel, B. K. (2000). *Papillibacter cinnamivorans* gen. nov., sp. nov., a cinnamate-transforming bacterium from a shea cake digester. *Int. J. Syst. Evol. Microbiol.* 50, 1221–1228. doi: 10.1099/00207713-50-3-1221

Denef, V. J., Mueller, R. S., and Banfield, J. F. (2010). AMD biofilms: using model communities to study microbial evolution and ecological complexity in nature. *ISME J.* 4, 599–610. doi: 10.1038/ismej.2009.158

Deng, D., Weidhaas, J. L., and Lin, L. S. (2016). Kinetics and microbial ecology of batch sulfidogenic bioreactors for co-treatment of municipal wastewater and acid mine drainage. *J. Hazard. Mater.* 305, 200–208. doi: 10.1016/j.jhazmat.2015.11.041

Druschel, G. K., Baker, B. J., Gihring, T. M., and Banfield, J. F. (2004). Acid mine drainage biogeochemistry at Iron Mountain, California. *Geochem. Trans.* 5:13. doi: 10.1185/1467-4866-5-13

Finke, N., and Jørgensen, B. B. (2008). Response of fermentation and sulfate reduction to experimental temperature changes in temperate and Arctic marine sediments. *ISME J.* 2, 815–829. doi: 10.1038/ISMEJ.2008.2

Fraj, B., Hania, W. B., Postec, A., Hamdi, M., Ollivier, B., and Fardeau, M. L. (2013). *Fonticella tunisiensis* gen. nov., sp. nov., isolated from a hot spring. *Int. J. Syst. Evol. Microbiol.* 63, 1947–1950. doi: 10.1099/ijs.0.041947-0

Giloteaux, L., Duran, R., Casiot, C., Bruneel, O., Elbaz-Poulichet, F., and Goñi-Urriza, M. (2013). Three-year survey of sulfate-reducing bacteria community structure in Carnoules acid mine drainage (France), highly contaminated by arsenic. *FEMS Microbiol. Ecol.* 83, 724–737. doi: 10.1111/1574-6941.12028

Goltsman, D. S. A., Comolli, L. R., Thomas, B. C., and Banfield, J. F. (2015). Community transcriptomics reveals unexpected high microbial diversity in acidophilic biofilm communities. *ISME J.* 9, 1014–1023. doi: 10.1038/ismej.2014.200

Grech-Mora, I., Fardeau, M. L., Patel, B. K. C., Ollivier, B., Rimbault, A., Prensier, G., et al. (1996). Isolation and characterization of *Sporobacter termitidis* gen. nov., sp. nov., from the digestive tract of the wood-feeding termite *Nasutitermes lujae*. *Int. J. Syst. Evol. Microbiol.* 46, 512–518. doi: 10.1099/00207713-46-2-512

Gupta, A., Dutta, A., Sarkar, J., Paul, D., Panigrahi, M. K., and Sar, P. (2017). Metagenomic exploration of microbial community in mine tailings of Malanjkhand copper project, India. *Genom. Data* 12, 11–13. doi: 10.1016/j.gdata.2017.02.004

Hallberg, K. B. (2010). New perspectives in acid mine drainage microbiology. *Hydrometallurgy* 104, 448–453. doi: 10.1016/j.hydromet.2009.12.013

Hammer, Ø., Harper, D. A. T., and Ryan, P. D. (2001). PAST: paleontological statistics software package for education and data analysis. *Palaeontol. Electronica* 4, 1–9.

Hausmann, B., Knorr, K. H., Schreck, K., Tringe, S. G., del Rio, T. G., Loy, A., et al. (2016). Consortia of low-abundance bacteria drive sulfate reduction-dependent degradation of fermentation products in peat soil microcosms. *ISME J.* 10, 2365–2375. doi: 10.1038/ismej.2016.42

Heberle, H., Meirelles, G. V., da Silva, F. R., Telles, G. P., and Minghim, R. (2015). InteractiVenn: a web-based tool for the analysis of sets through Venn diagrams. *BMC Bioinformatics* 16:169. doi: 10.1186/s12859-015-0611-3

Hiibel, S. R., Pereyra, L. P., Breazeal, M. V. R., Reisman, D. J., Reardon, K. F., and Pruden, A. (2011). Effect of organic substrate on the microbial community structure in pilot-scale sulfate-reducing biochemical reactors treating mine drainage. *Environ. Eng. Sci.* 28, 563–572. doi: 10.1089/ees.2010.0237

Hiibel, S. R., Pereyra, L. P., Inman, L. Y., Tischer, A., Reisman, D. J., Reardon, K. F., et al. (2008). Microbial community analysis of two field-scale sulfate-reducing bioreactors treating mine drainage. *Environ. Microbiol.* 10, 2087–2097. doi: 10.1111/j.1462-2920.2008.01630.x

Hua, Z. S., Han, Y. J., Chen, L. X., Liu, J., Hu, M., Li, S. J., et al. (2015). Ecological roles of dominant and rare prokaryotes in acid mine drainage revealed by metagenomics and metatranscriptomics. *ISME J.* 9, 1280–1294. doi: 10.1038/ismej.2014.212

Huang, L. N., Kuang, J. L., and Shu, W. S. (2016). Microbial ecology and evolution in the acid mine drainage model system. *Trends Microbiol.* 24, 581–593. doi: 10.1016/j.tim.2016.03.004

Johnson, D. B. (2012). Geomicrobiology of extremely acidic subsurface environments. *FEMS Microbiol. Ecol.* 81, 2–12. doi: 10.1111/j.1574-6941.2011.01293

Johnson, D. B., and Hallberg, K. B. (2005). Acid mine drainage remediation options: a review. *Sci. Total Environ.* 338, 3–14. doi: 10.1016/j.scitotenv.2004.09.002

Kaksonen, A. H., Plumb, J. J., Robertson, W. J., Franzmann, P. D., Gibson, J. A., and Puhakka, J. A. (2004). Culturable diversity and community fatty acid profiling of sulfate-reducing fluidized-bed reactors treating acidic, metal-containing wastewater. *Geomicrobiol. J.* 21, 469–480. doi: 10.1080/01490450490505455

Kefeni, K. K., Msagati, T. A., and Mamba, B. B. (2017). Acid mine drainage: prevention, treatment options, and resource recovery: a review. *J. Clean. Prod.* 151, 475–493. doi: 10.1016/j.jclepro.2017.03.082

Kosaka, T., Kato, S., Shimoyama, T., Ishii, S., Abe, T., and Watanabe, K. (2008). The genome of *Pelotomaculum thermopropionicum* reveals niche-associated evolution in anaerobic microbiota. *Genome Res.* 18, 442–448. doi: 10.1101/gr.7136508

Kuang, J. L., Huang, L. N., Chen, L. X., Hua, Z. S., Li, S. J., Hu, M., et al. (2013). Contemporary environmental variation determines microbial diversity patterns in acid mine drainage. *ISME J.* 7, 1038–1050. doi: 10.1038/ismej.2012.139

Kwon, M. J., O'Loughlin, E. J., Boyanov, M. I., Brulc, J. M., Johnston, E. R., Kemner, K. M., et al. (2016). Impact of organic carbon electron donors on microbial community development under iron-and sulfate-reducing conditions. *PLoS One* 11:e0146689. doi: 10.1371/journal.pone.0146689

Langille, M. G., Zaneveld, J., Caporaso, J. G., McDonald, D., Knights, D., Reyes, J. A., et al. (2013). Predictive functional profiling of microbial communities using 16S rRNA marker gene sequences. *Nat. Biotechnol.* 31, 814–821. doi: 10.1038/nbt.2676

Lee, S. H., and Cho, J. C. (2011). Group-specific PCR primers for the phylum Acidobacteria designed based on the comparative analysis of 16S rRNA gene sequences. *J. Microbiol. Methods* 86, 195–203. doi: 10.1016/j.mimet.2011.05.003

Lee, Y. J., Romanek, C. S., Mills, G. L., Davis, R. C., Whitman, W. B., and Wiegel, J. (2006). *Gracilibacter thermotolerans* gen. nov., sp. nov., an anaerobic, thermotolerant bacterium from a constructed wetland receiving acid sulfate water. *Int. J. Syst. Evol. Microbiol.* 56, 2089–2093. doi: 10.1099/ijs.0.64040-0

Lefticariu, L., Walters, E. R., Pugh, C. W., and Bender, K. S. (2015). Sulfate reducing bioreactor dependence on organic substrates for remediation of coal-generated acid mine drainage: field experiments. *Appl. Geochem.* 63, 70–82. doi: 10.1016/j.apgeochem.2015.08.002

Li, H., Peng, J., Weber, K. A., and Zhu, Y. (2011). Phylogenetic diversity of Fe (III)-reducing microorganisms in rice paddy soil: enrichment cultures with different short-chain fatty acids as electron donors. *J. Soils Sediments* 11:1234. doi: 10.1007/s11368-011-0371-2

Lu, J., Chen, T., Wu, J., Wilson, P. C., Hao, X., and Qian, J. (2011). Acid tolerance of an acid mine drainage bioremediation system based on biological sulfate reduction. *Bioresour. Technol.* 102, 10401–10406. doi: 10.1016/j.biortech.2011.09.046

Luptakova, A., and Kusnierova, M. (2005). Bioremediation of acid mine drainage contaminated by SRB. *Hydrometallurgy* 77, 97–102. doi: 10.1016/j.hydromet.2004.10.019

Martins, M., Santos, E. S., Faleiro, M. L., Chaves, S., Tenreiro, R., Barros, R. J., et al. (2011). Performance and bacterial community shifts during bioremediation of acid mine drainage from two Portuguese mines. *Int. Biodeterior. Biodegradation* 65, 972–981. doi: 10.1016/j.ibiod.2011.07.006

Méndez-García, C., Mesa, V., Sprenger, R. R., Richter, M., Diez, M. S., Solano, J., et al. (2014). Microbial stratification in low pH oxic and suboxic macroscopic growths along an acid mine drainage. *ISME J.* 8, 1259–1274. doi: 10.1038/ismej.2013.242

Méndez-García, C., Peláez, A. I., Mesa, V., Sánchez, J., Golyshina, O. V., and Ferrer, M. (2015). Microbial diversity and metabolic networks in acid mine drainage habitats. *Front. Microbiol.* 6:475. doi: 10.3389/fmicb.2015.00475

Mesa, V., Gallego, J. L., González-Gil, R., Lauga, B., Sánchez, J., Méndez-García, C., et al. (2017). Bacterial, archaeal, and eukaryotic diversity across distinct microhabitats in an acid mine drainage. *Front. Microbiol.* 8:1756. doi: 10.3389/fmicb.2017.01756

Moreau, J. W., Fournelle, J. H., and Banfield, J. F. (2013). Quantifying heavy metals sequestration by sulfate-reducing bacteria in an Acid mine drainage-contaminated natural wetland. *Front. Microbiol.* 4:43. doi: 10.3389/fmicb.2013.00043

Morra, M. J., and Dick, W. A. (1991). Mechanisms of H2S production from cysteine and cystine by microorganisms isolated from soil by selective enrichment. *Appl. Environ. Microbiol.* 57, 1413–1417.

Mosher, J. J., Phelps, T. J., Podar, M., Hurt, R. A., Campbell, J. H., Drake, M. M., et al. (2012). Microbial community succession during lactate amendment and electron acceptor limitation reveals a predominance of metal-reducing *Pelosinus* spp. *Appl. Environ. Microbiol.* 78, 2082–2091. doi: 10.1128/AEM.07165-11

Mühling, M., Woolven-Allen, J., Murrell, J. C., and Joint, I. (2008). Improved group-specific PCR primers for denaturing gradient gel electrophoresis analysis of the genetic diversity of complex microbial communities. *ISME J.* 2, 379–392. doi: 10.1038/ismej.2007.97

Muyzer, G., De Waal, E. C., and Uitterlinden, A. G. (1993). Profiling of complex microbial populations by denaturing gradient gel electrophoresis analysis of polymerase chain reaction-amplified genes coding for 16S rRNA. *Appl. Environ. Microbiol.* 59, 695–700.

Muyzer, G., and Stams, A. J. (2008). The ecology and biotechnology of sulphate-reducing bacteria. *Nat. Rev. Microbiol.* 6, 441–454. doi: 10.1038/nrmicro1892

Neculita, C. M., and Zagury, G. J. (2008). Biological treatment of highly contaminated acid mine drainage in batch reactors: long-term treatment and reactive mixture characterization. *J. Hazard. Mater.* 157, 358–366. doi: 10.1016/j.jhazmat.2008.01.002

Neculita, C. M., Zagury, G. J., and Bussière, B. (2007). Passive treatment of acid mine drainage in bioreactors using sulfate-reducing bacteria. *J. Environ. Qual.* 36, 1–16. doi: 10.2134/jeq2006.0066

Pan, Y., Yang, X., Xu, M., and Sun, G. (2017). The role of enriched microbial consortium on iron-reducing bioaugmentation in sediments. *Front. Microbiol.* 8:462. doi: 10.3389/fmicb.2017.00462

Paul, D., Kazy, S. K., Gupta, A. K., Pal, T., and Sar, P. (2015). Diversity, metabolic properties and arsenic mobilization potential of indigenous bacteria in arsenic contaminated groundwater of West Bengal, India. *PLoS One* 10:e0118735. doi: 10.1371/journal.pone.0118735

Peng, Q. A., Shaaban, M., Wu, Y., Hu, R., Wang, B., and Wang, J. (2016). The diversity of iron reducing bacteria communities in subtropical paddy soils of China. *Appl. Soil Ecol.* 101, 20–27. doi: 10.1016/j.apsoil.2016.01.012

Petrie, L., North, N. N., Dollhopf, S. L., Balkwill, D. L., and Kostka, J. E. (2003). Enumeration and characterization of iron (III)-reducing microbial communities from acidic subsurface sediments contaminated with uranium (VI). *Appl. Environ. Microbiol.* 69, 7467–7479. doi: 10.1128/AEM.69.12.7467-7479.2003

Postgate, J. R. (1963). Versatile medium for the enumeration of sulfate-reducing bacteria. *Appl. Microbiol.* 11, 265–267.

Pruden, A., Messner, N., Pereyra, L., Hanson, R. E., Hiibel, S. R., and Reardon, K. F. (2007). The effect of inoculum on the performance of sulfate-reducing columns treating heavy metal contaminated water. *Water Res.* 41, 904–914. doi: 10.1016/j.watres.2006.11.025

Purkamo, L., Bomberg, M., Nyyssönen, M., Kukkonen, I., Ahonen, L., Kietäväinen, R., et al. (2013). Dissecting the deep biosphere: retrieving authentic microbial communities from packer-isolated deep crystalline bedrock fracture zones. *FEMS Microbiol. Ecol.* 85, 324–337. doi: 10.1111/1574-6941.12126

Qian, G., Schumann, R. C., Li, J., Short, M. D., Fan, R., Li, Y., et al. (2017). Strategies for reduced acid and metalliferous drainage by pyrite surface passivation. *Minerals* 7:42. doi: 10.3390/min7030042

Sahinkaya, E., Yurtsever, A., Toker, Y., Elcik, H., Cakmaci, M., and Kaksonen, A. H. (2015). Biotreatment of As-containing simulated acid mine drainage using laboratory scale sulfate reducing upflow anaerobic sludge blanket reactor. *Miner. Eng.* 75, 133–139. doi: 10.1016/j.mineng.2014.08.012

Sánchez-Andrea, I., Knittel, K., Amann, R., Amils, R., and Sanz, J. L. (2012a). Quantification of Tinto River sediment microbial communities: importance of sulfate-reducing bacteria and their role in attenuating acid mine drainage. *Appl. Environ. Microbial.* 78, 4638–4645. doi: 10.1128/AEM.00848-12

Sánchez-Andrea, I., Rojas-Ojeda, P., Amils, R., and Sanz, J. L. (2012b). Screening of anaerobic activities in sediments of an acidic environment: Tinto River. *Extremophiles* 16, 829–839. doi: 10.1007/s00792-012-0478-4

Sánchez-Andrea, I., Rodríguez, N., Amils, R., and Sanz, J. L. (2011). Microbial diversity in anaerobic sediments at Rio Tinto, a naturally acidic environment with a high heavy metal content. *Appl. Environ. Microbiol.* 77, 6085–6093. doi: 10.1128/AEM.00654-11

Sánchez-Andrea, I., Sanz, J. L., Bijmans, M. F., and Stams, A. J. (2014). Sulfate reduction at low pH to remediate acid mine drainage. *J. Hazard. Mater.* 269, 98–109. doi: 10.1016/j.jhazmat.2013.12.032

Scala, D. J., Hacherl, E. L., Cowan, R., Young, L. Y., and Kosson, D. S. (2006). Characterization of Fe (III)-reducing enrichment cultures and isolation of Fe (III)-reducing bacteria from the Savannah River site, South Carolina. *Res. Microbiol.* 157, 772–783. doi: 10.1016/j.resmic.2006.04.001

Shah, M. (2013). *Iron Oxide Reduction by a Clostridial Consortium: Insights from Physiological and Genome Analyses*. New Brunswick, NJ: Rutgers University–New Brunswick.

Shiratori, H., Ohiwa, H., Ikeno, H., Ayame, S., Kataoka, N., Miya, A., et al. (2008). *Lutispora thermophila* gen. nov., sp. nov., a thermophilic, spore-forming bacterium isolated from a thermophilic methanogenic bioreactor digesting municipal solid wastes. *Int. J. Syst. Evol. Microbiol.* 58, 964–969. doi: 10.1099/ijs.0.65490-0

Stieglmeier, M., Wirth, R., Kminek, G., and Moissl-Eichinger, C. (2009). Cultivation of anaerobic and facultatively anaerobic bacteria from spacecraft-associated clean rooms. *Appl. Environ. Microbiol.* 75, 3484–3491. doi: 10.1128/AEM.02565-08

Teng, W., Kuang, J., Luo, Z., and Shu, W. (2017). Microbial diversity and community assembly across environmental gradients in acid mine drainage. *Minerals* 7:106. doi: 10.3390/min7060106

Viollier, E., Inglett, P. W., Hunter, K., Roychoudhury, A. N., and Van Cappellen, P. (2000). The ferrozine method revisited: Fe (II)/Fe (III) determination in natural waters. *Appl. Geochem.* 15, 785–790. doi: 10.1016/S0883-2927(99)00097-9

Wang, C. L., Maratukulam, P. D., Lum, A. M., Clark, D. S., and Keasling, J. D. (2000). Metabolic engineering of an aerobic sulfate reduction pathway and its application to precipitation of cadmium on the cell surface. *Appl. Environ. Microbiol.* 66, 4497–4502. doi: 10.1128/AEM.66.10.4497-4502.2000

Xingyu, L., Zou, G., Wang, X., Zou, L., Wen, J., Ruan, R., et al. (2013). A novel low pH sulfidogenic bioreactor using activated sludge as carbon source to treat acid mine drainage (AMD) and recovery metal sulfides: pilot scale study. *Miner. Eng.* 48, 51–55. doi: 10.1016/j.mineng.2012.11.004

Yi, W., Wang, B., and Qu, D. (2012). Diversity of isolates performing Fe (III) reduction from paddy soil fed by different organic carbon sources. *Afr. J. Biotechnol.* 11, 4407–4417. doi: 10.5897/AJB11.1216

Zavarzina, D. G., Sokolova, T. G., Tourova, T. P., Chernyh, N. A., Kostrikina, N. A., and Bonch-Osmolovskaya, E. A. (2007). *Thermincola ferriacetica* sp. nov., a new anaerobic, thermophilic, facultatively chemolithoautotrophic bacterium capable of dissimilatory Fe (III) reduction. *Extremophiles* 11, 1–7. doi: 10.1007/s00792-006-0004-7

Zhang, M., Liu, X., Li, Y., Wang, G., Wang, Z., and Wen, J. (2017). Microbial community and metabolic pathway succession driven by changed nutrient inputs in tailings: effects of different nutrients on tailing remediation. *Sci. Rep.* 7:474. doi: 10.1038/s41598-017-00580-3

Zhang, M., and Wang, H. (2014). Organic wastes as carbon sources to promote sulfate reducing bacterial activity for biological remediation of acid mine drainage. *Miner. Eng.* 69, 81–90. doi: 10.1016/j.mineng.2014.07.010

Zhang, M., and Wang, H. (2016). Preparation of immobilized sulfate reducing bacteria (SRB) granules for effective bioremediation of acid mine drainage and bacterial community analysis. *Miner. Eng.* 92, 63–71. doi: 10.1016/j.mineng.2016.02.008

Zhang, M., Wang, H., and Han, X. (2016). Preparation of metal-resistant immobilized sulfate reducing bacteria beads for acid mine drainage treatment. *Chemosphere* 154, 215–223. doi: 10.1016/j.chemosphere.2016.03.103

Zhao, Y. G., Wang, A. J., and Ren, N. Q. (2010). Effect of carbon sources on sulfidogenic bacterial communities during the starting-up of acidogenic sulfate-reducing bioreactors. *Bioresour. Technol.* 101, 2952–2959. doi: 10.1016/j.biortech.2009.11.098

Conflict of Interest Statement: The authors declare that the research was conducted in the absence of any commercial or financial relationships that could be construed as a potential conflict of interest.

frontiers in Microbiology

REVIEW
published: 30 October 2018
doi: 10.3389/fmicb.2018.02309

Living at the Frontiers of Life: Extremophiles in Chile and Their Potential for Bioremediation

*Roberto Orellana[1,2], Constanza Macaya[1], Guillermo Bravo[1], Flavia Dorochesi[1], Andrés Cumsille[1], Ricardo Valencia[1], Claudia Rojas[1] and Michael Seeger[1]**

[1] Laboratorio de Microbiología Molecular y Biotecnología Ambiental, Departamento de Química and Centro de Biotecnología Daniel Alkalay Lowitt, Universidad Técnica Federico Santa María, Valparaíso, Chile, [2] Departamento de Biología, Facultad de Ciencias Naturales y Exactas, Universidad de Playa Ancha, Valparaíso, Chile

Extremophiles are organisms capable of adjust, survive or thrive in hostile habitats that were previously thought to be adverse or lethal for life. Chile gathers a wide range of extreme environments: salars, geothermal springs, and geysers located at Altiplano and Atacama Desert, salars and cold mountains in Central Chile, and ice fields, cold lakes and fjords, and geothermal sites in Patagonia and Antarctica. The aims of this review are to describe extremophiles that inhabit main extreme biotopes in Chile, and their molecular and physiological capabilities that may be advantageous for bioremediation processes. After briefly describing the main ecological niches of extremophiles along Chilean territory, this review is focused on the microbial diversity and composition of these biotopes microbiomes. Extremophiles have been isolated in diverse zones in Chile that possess extreme conditions such as Altiplano, Atacama Desert, Central Chile, Patagonia, and Antarctica. Interesting extremophiles from Chile with potential biotechnological applications include thermophiles (e.g., *Methanofollis tationis* from Tatio Geyser), acidophiles (e.g., *Acidithiobacillus ferrooxidans, Leptospirillum ferriphilum* from Atacama Desert and Central Chile copper ores), halophiles (e.g., *Shewanella* sp. Asc-3 from Altiplano, *Streptomyces* sp. HKF-8 from Patagonia), alkaliphiles (*Exiguobacterium* sp. SH31 from Altiplano), xerotolerant bacteria (*S. atacamensis* from Atacama Desert), UV- and Gamma-resistant bacteria (*Deinococcus peraridilitoris* from Atacama Desert) and psychrophiles (e.g., *Pseudomonas putida* ATH-43 from Antarctica). The molecular and physiological properties of diverse extremophiles from Chile and their application in bioremediation or waste treatments are further discussed. Interestingly, the remarkable adaptative capabilities of extremophiles convert them into an attractive source of catalysts for bioremediation and industrial processes.

Keywords: extremophile, Chile, Atacama Desert, Altiplano, Patagonia, Antarctica, bioremediation

OPEN ACCESS

Edited by:
Jean Armengaud, Commissariat à l'Energie Atomique et aux Energies Alternatives (CEA), France

Reviewed by:
Camila Fernandez, UMR7621 Laboratoire d'Océanographie Microbienne (LOMIC), France
Karima Hezbri, National Institute of Applied Science and Technology, Tunisia

***Correspondence:**
Michael Seeger
michael.seeger@usm.cl

Specialty section:
This article was submitted to Microbiotechnology, Ecotoxicology and Bioremediation, a section of the journal Frontiers in Microbiology

Received: *30 April 2018*
Accepted: *10 September 2018*
Published: *30 October 2018*

Citation:
Orellana R, Macaya C, Bravo G, Dorochesi F, Cumsille A, Valencia R, Rojas C and Seeger M (2018) Living at the Frontiers of Life: Extremophiles in Chile and Their Potential for Bioremediation. Front. Microbiol. 9:2309. doi: 10.3389/fmicb.2018.02309

INTRODUCTION

Most the well-described forms of life are mainly adapted to face environments with "physiological conditions," a term described in literature as moderate temperature (10–37°C), pH ∼ 7, salinity ranging from 0.15 to 0.5 M NaCl, pressure 1 atm and enough water availability (Aguilar et al., 1998; Antranikian et al., 2005). However, there is still a large under-examined group of organisms, known as extremophiles, that are capable of adjust,

survive or thrive in hostile habitats that were previously thought to be inhospitable or even lethal for life (Rampelotto, 2013). In general, extremophiles are divided in two categories: extremophiles, which require one or more extreme conditions to grow, and extremotolerant organisms, which can tolerate extreme and/or toxic conditions, although they grow optimally at "physiological" conditions (Canganella and Wiegel, 2011). The study of extremophiles is a rather difficult field, mainly constrained by the complexity of reaching their ecological niches and isolating these microbes. Most extremophiles are still part of the microbial dark matter that has not been discovered yet (Bernard et al., 2018). Hunting microbes in extreme environment is a huge challenge for microbiologists worldwide, which could provide microorganisms, enzymes and biomolecules for diverse applications in biotechnology, biomedicine and industrial processes. The knowledge of the adaptation mechanisms of microbes to extreme environments provides metabolic networks, regulation circuits and pieces for systems biology and synthetic biology (Chen and Jiang, 2018). Extreme conditions drive the evolution of their inhabitants, highlighting the role of extremophiles as models for the study of the evolution of biological entities.

Newly developed technologies have allowed research on extreme environments to gain knowledge on microorganisms and provide significant insights about the origin of life on Earth. Recent studies have uncovered that the first terrestrial life form, known as LUCA (Last Universal Common Ancestor), was a thermophilic anaerobe capable of gaining energy from geochemical sources (Weiss et al., 2016). Basic research has provided valuable insights on how extremophiles can survive such challenging environments. However, the presence of highly sophisticated mechanisms of adaptation together with the availability of a sweet of novel biochemical pathways sustaining peculiar physiological metabolic capabilities converts extremophiles into a current focus of applied research to exploit their biotechnological potential (Rampelotto, 2013). Further attention has also been devoted to identification, isolation and characterization of biomolecules, most of them enzymes named as extremozymes, which are well adapted to be active also at extreme conditions (Rampelotto, 2013).

Extremophiles, can be classified according to the conditions in which they grow: thermophiles and hyperthermophiles (organisms growing at temperatures of 45–80°C and >80°C, respectively) (Madigan et al., 2000; Berenguer, 2011), psychrophiles (organisms that grow at <10°C) (Siddiqui et al., 2013), acidophiles and alkaliphiles (organisms optimally adapted to pH < 5 and pH > 9, respectively), halophiles (organisms that require NaCl for growth, in concentration of 200–5,900 mM) (Edbeib et al., 2016), microorganisms that survive in dry environments (water activity < 0.75) (Connon et al., 2007) and radiotolerant (UV resistant) extremophiles that are resistant to the permanent exposure to damaging solar radiation (Gabani et al., 2014) (**Table 1**). Additionally, it is worth mentioning that extremophiles are usually defined by one extreme condition, nevertheless, many natural environments possess two or more extreme conditions. The microbiota living on those ecosystems, also known as polyextremophiles, is adapted to an additional extreme condition to the one condition that characterizes them, such as temperature, pH, salinity (Urbieta et al., 2015b).

Chile occupies a long strip of territory in the south west of South America and with other countries shared part of the Antarctica. It has been referred to be a "biogeographic island" (Scherson et al., 2017), due to a series of geological events that have formed the current natural barriers Altiplano, Atacama Desert, Los Andes Mountains, Pacific Ocean, Patagonia, and Antarctica (Villagrán and Hinojosa, 1997; Villagrán and Armesto, 2005). Due to its extremely diverse geography and singular geochemical and climatic conditions, Chile gathers many extreme environments, which may result intolerably hostile or even lethal for most life forms, except for extremophiles (Rampelotto, 2013). In order to enable growth under these harsh conditions, extremophiles have been subjected to several adaptations, which have been only partially characterized to date. Altiplano, Atacama Desert, Central Chile, Patagonia, and Antarctica correspond to main geographical areas in Chile that harbor multiple extreme biotopes (**Figure 1**). Specific extreme biotopes of Chile are attractive scenarios to study the evolution of microorganisms under extreme conditions, which resemble the islands of the Galapagos Archipelago that provide Darwin inspiring ideas to build up the Theory of Evolution by Natural Selection of macroorganisms based on the divergence of species of birds, especially the Galapagos finches.

The preservation of the natural ecosystems and the restauration of polluted sites are crucial for a sustainable

TABLE 1 | General description of extremophiles present in diverse extreme environments of Chile.

Environmental parameter	Extremophile	Definition	Example	Reference
Temperature	Hyperthermophile	Growth > 80°C	*Pyrococcus* sp. M24D13	Dennett and Blamey, 2016
	Thermophile	Growth 45–80°C	*Methanofollis tationis*	Zabel et al., 1984
	Psychrophile	≤10°	*Pseudomonas* sp. ATH-43	Rodriguez-Rojas et al., 2016a
pH	Acidophile	pH < 5	*Acidithiobacillus ferrooxidans*	Demergasso et al., 2010
	Alkaliphile	pH ≥ 9	*Halomonas alkaliphila*	Quiroz et al., 2015
Salinity	Halophile	2,000–5,000 mM NaCl	*Haloferax* sp. CL47	Bonfá et al., 2011
UV radiation	Radioresistant	Radiation tolerant (40–400 nm)	*Deinococcus peraridilitoris*	Rainey et al., 2007
Water availability	Dehydration tolerant	Growth water activity < 0.75	*Streptomyces bulli*	Santhanam et al., 2013

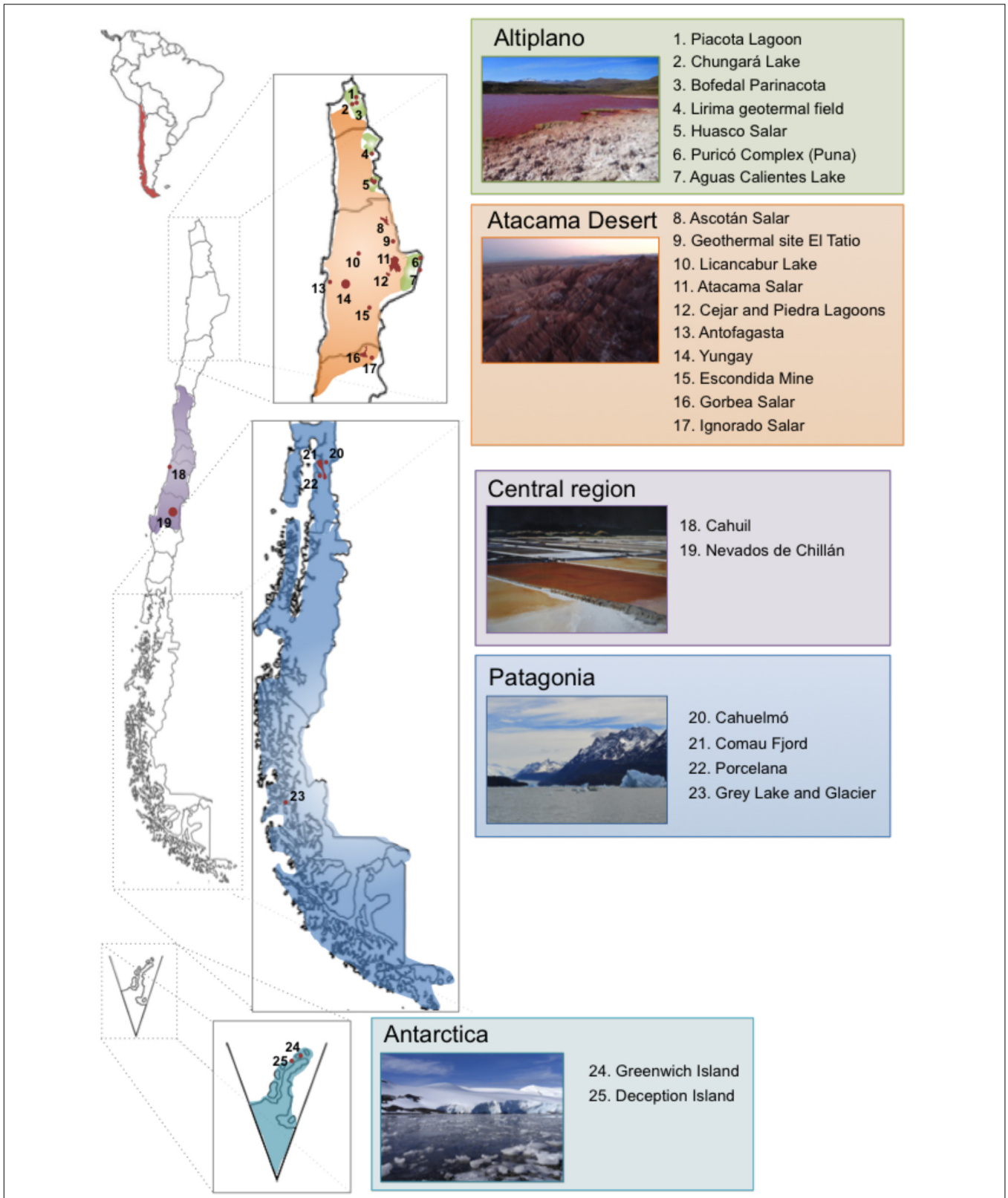

FIGURE 1 | Distribution of different extreme ecosystems harboring extremophiles in five main biotopes throughout Chile. Altiplano (photography: Red Lagoon, Amuyo, Camarones, Parinacota Region), Atacama Desert (photography: Moon Valley, San Pedro de Atacama, Antofagasta Region), Central Region (photography: Cahuil Saltern, Nilahue, O'Higgins Region), Patagonia (photography: Grey Lake and Glacier, Magallanes Region), and Antarctica (photography: Arturo Prat Station, Greenwich Island).

development. Bioremediation is an important technology for the clean up of environments contaminated with persistent organic pollutants [e.g., pesticides, polychlorobiphenyls (PCBs), petroleum hydrocarbons] and heavy metals (e.g., Hg, Cd) (Morgante et al., 2010; Saavedra et al., 2010; Rojas et al., 2011; Fuentes et al., 2014; Bravo, 2017). Mining of valuable metals such as copper, gold and silver is historically one the most relevant economic activities in Chile, mainly in the Northern and Central regions. Copper mining is the main activity in Chile, contributing with one third of the world's production. Unfortunately, this mining activity has been associated with heavy metal pollution in diverse sites. Microorganisms are main biocatalysts for bioremediation of polluted environments and waste treatment processes (Hernández et al., 2008a,b; Saavedra et al., 2010; Rojas et al., 2011; Fuentes et al., 2016; Méndez et al., 2017) and extremophilic microbes are required as catalysts for the bioremediation of polluted extreme environments. The aims of this review are to describe extremophiles that inhabit the main extreme biotopes in Chile, and their molecular and physiological capabilities that may be advantageous for the design and development of bioremediation processes.

BIOTOPES AND ECOLOGICAL NICHES

Chilean territory is spanned within a long altitudinal and latitude range that contributes to the origin of a suite of landscapes and geological features that are extreme habitats for microorganisms. Some of these ecosystems will be described briefly.

Atacama Desert

The Atacama Desert is located along the western border of South America and is the driest and oldest desert on Earth's, exhibiting similar conditions described for Mars. This ecosystem provides a unique collection of habitats, ideal for studying microbial dynamics in several extreme conditions, such as alkaline or acidic pH, high temperature, water stress, and UV radiation (**Figure 1**). Its distinctive climate is the result of the confluence of a subtropical high-pressure zone, the cold Humboldt Current on the coast, offshore winds, as well as the Andean rain-shadow effect and latitudinal position of the region (Houston and Hartley, 2003).

Altiplanic Ecosystems

The Andean Altiplano occupies part of Peruvian, Bolivian, and Chilean territory with a mean altitude of 3,700 m above sea level and covers an area that is 300 km wide and 1,500 km long (Muñoz and Charrier, 1996). The Altiplano is surrounded by volcanoes and mountains rising up to 6,700 m and represents one of the largest *plateaus* in the world. The Altiplano possess several extremes environments, such as thermal waters and geysers, some basins, salars, large lakes in the north and salt flats in the south. Some of the more characteristic Altiplano ecosystems are described below.

Parinacota Region

The paleolakes Chungará Lake, Parinacota Wetland, and Piacota Lagoon are located 4,300–4,500 m above sea level. The microbial community composition is highly variable between the different wetlands, but also between water and sediment samples (Dorador, 2007). Each of these environments supported a unique community of Bacteria and Archaea, revealing a differentiation between high altitude lakes, freshwater wetlands, and saline wetlands.

Geothermal Springs and Geysers

The extreme conditions (high temperature and pressure) are characteristic of hot springs and geysers located in the Northern region and is the result of the permanent interaction of groundwater with magma and hot igneous materials stemming from near the rather abundant volcanic areas (Jones and Renaut, 1997; Fernandez-Turiel et al., 2005; Rafferty, 2010).

The Geothermal site El Tatio (Kunza language, meaning "crying grandfather") is the largest geyser field in the Southern hemisphere and one of highest geysers around the world (∼4,200 m.a.s.l.) (Glennon and Pfaff, 2003). Located on the Andean Altiplano, it harbors over 100 erupting springs and is surrounded by high volcanoes. The water discharged by the Tatio Geyser is very rich in silica, with the highest concentrations reported for a natural surface water, of both arsenic (∼0.5 mM) and antimony (∼0.02 mM) at a nearly neutral pH (Landrum et al., 2009). These properties differ from other well-studies geothermal sites, such as basins in Yellowstone National Park, United States, and Dallol Volcano, Ethiopia, for which their waters can reach extreme pH values (Rowe et al., 1973; Barbieri and Cavalazzi, 2014). Therefore, El Tatio in an environment with unique physico-chemical characteristics.

The North regions of Chile harbor many hydrothermal fields that remained less explored than El Tatio. For instance, the Surire hydrothermal system, at 4,000 m.a.s.l., is located in the south part of Surire Salar (Procesi, 2014). The water discharges are characterized by higher concentration of sulfate. Analogous situation occurs with Lirima Geothermal field that is located at an altitude of 3,900 m.a.s.l., 25 km southwest of the Sillajhuay volcanic chain. The Lirima area contains bubbling pools with temperatures between 38°C and 80°C (Tassi et al., 2010; Procesi, 2014).

Salars

Chile harbors a huge diversity of salars along its territory. Saline ecosystems are located in Altiplano, Atacama Desert, Central Chile, and Patagonia. Specific salars that has been subjected to microbial studies will be described.

Athalassohaline Ecosystem: Huasco Salar

Athalassohaline systems are saline ecosystems with a non-marine origin but originated from evaporation of fresh water in a system dominated by calcium, magnesium and sulfate, in contrast with sodium and chloride that are prevalent in the ocean (Grant, 2006). At 3,800 m above sea level, Huasco Salar is a good example of an athalassohaline system (Dorador et al., 2010). These systems exhibit extreme conditions such as low temperatures

and atmospheric pressure, high solar radiation, negative water balance, and a wide range of salt concentrations (Castro-Severyn et al., 2017).

Acidic Salars: Ignorado Salar and Gorbea Salar

Two acidic salars in Chile are located in the Andes Mountains (Risacher et al., 2003). Gorbea Salar is located in a basin with extreme acidic brines, with pH ranging from 2 to 4 and NaCl concentrations from 0.03 to 1.3 M (Quatrini et al., 2017). Ignorado Salar is an acid saline lake, with surface waters with pH ranging from 3.3 to 4.1 and a total dissolved solids concentration from 0.5 to 3% (Karmanocky and Benison, 2016).

Borderline Salar: Atacama Salar

Salar de Atacama is located between the Atacama Desert and the westernmost margin of the Altiplano at 2,300 m above sea level (Zúñiga et al., 1991). It is the largest and oldest evaporating basin in Chile, and the largest Quaternary halite deposit worldwide (Warren, 2010; Lara et al., 2012). Salar de Atacama has some shallow lakes with high salt concentration (Zúñiga et al., 1991) and with distinct geological features compared to the Altiplano basins (Demergasso et al., 2010).

Central and Southern Salars

Other saline ecosystems are also located in the Central Region and the Southern Patagonia (De Los Rios-Escalante and Gajardo, 2010; Plominsky et al., 2014). Cáhuil Lagoon is a saline ecosystem located at the coast close to Pichilemu in Central Chile (**Figure 1**).

Patagonia

Patagonia is comprised by an extensive structure of cold fjords (e.g., Comau Fjord) and channels, and by oligotrophic cold lakes in Southern Chile, characterized by low temperatures, low nutrient concentration and low dissolved organic carbon (Gutiérrez et al., 2015; Aguayo et al., 2017). Cold lakes in Patagonia (e.g., Grey Lake, **Figure 1**) are affected by seasonal temperature variations, ranging from 4°C in winter to 20°C in summer (Aguayo et al., 2017).

Volcanic activity has been also reported with a high eruption frequency (Carrillo et al., 2018), which has formed numerous hydrothermal fields including Porcelana Hot Spring and Geyser, and Cahuelmo Hot Spring. Cahuelmo Hot Spring is a geothermal site located at the sea level coast of Cahuelmo Fjord, that contains waters rich in metallic minerals and elements such as pyrite, polonium, magnetite, and chalcopyrite (Mackenzie et al., 2013). On the other hand, Porcelana hot spring is located ∼100 m above sea level in Northern Patagonia. Porcelana is a pristine spring characterized by a rather extensive thermal gradient (∼38–69°C) and neutral pH (Alcamán et al., 2015).

Antarctica

Antarctica displays extreme climates and environmental conditions above and below the water surface. This environment is dominated by strong gradients in temperature (−10°C to −2°C), salinity (35–150%), and irradiation (<0.1% to 1–5% UV radiation), properties highly variable and ultimately governed by air temperature and snow cover (Cirés et al., 2017). The search of new pigments, antibiotics, and enzymes has become a main research focus in the Antarctic continent (Loperena et al., 2012; Órdenes-Aenishanslins et al., 2016; Lavin et al., 2017). In spite of been the coldest continent on Earth, surprisingly, Antarctica harbors many geothermal sites.

THERMOPHILES

Early life in Earth was initially dominated by thermophilic anaerobes that had chemoheterotrophic or chemolithoautotrophic metabolism capable of been sustained by hydrothermal energy sources (Woese et al., 1990; Konhauser et al., 2003; Weiss et al., 2016). Thermophiles are organisms, mainly prokaryotes, whose optimum growth temperatures are >44°C (Madigan et al., 2000). Hyperthermophiles are thermophiles that grow at temperatures >80°C (Berenguer, 2011) (**Table 1**). Thermophiles and hyperthermophiles are present in several natural ecosystems such as geothermal waters (**Figure 2**), hot springs, mud pots, fumaroles, geysers, deep-sea hydrothermal vents, volcanoes, and also in engineered environments, such as compost facilities and anaerobic reactors (Ahring, 1995; Rastogi et al., 2010; Urbieta et al., 2015b).

A general mechanism of thermophiles to safeguard their cellular components at high temperature is the adaption of thermophilic proteins through amino acid changes in their primary structure, increasing their thermal stabilities (Xu et al., 2018). Thermophilic proteins possess a larger fraction of amino acid residues in α-helices and have shorter amino acid length (Urbieta et al., 2015a; Xu et al., 2018). A main mechanism in thermophiles is the role of heat shock proteins (HSPs) including the chaperones DnaK, GroEL, and GroES to assist protein folding (**Figure 3**). DNA-repair systems (e.g., SOS system) are also active to respond to DNA damage. For the stabilization of the membranes, thermophiles use branched chain fatty acids and polyamines (e.g., spermidine). Another mechanism of thermophiles is the use of compatible solutes to stabilize cell components (Urbieta et al., 2015a). In addition, upregulated glycolysis pathway (e.g., pyruvate dehydrogenase complex) proteins provide immediate energy to cope with heat stress (Wang et al., 2015).

An increase in the use of (hyper)thermophilic microorganisms has been observed, especially for the need of the industry to couple biological solutions at high-temperature industrial processes (Urbieta et al., 2015a). Industrial waste reactors containing living microorganisms required to be pre-cooled down due to the fact that several industrial processes are carried out at temperatures >100°C (Gavrilescu, 2010). Therefore, (hyper)thermophiles offer a suitable solution due to their capabilities to grow at such high-temperature and also resist and metabolize several pollutants from contaminated industrial wastewaters (Vieille and Zeikus, 1996). Previous studies have demonstrated the high potential of (hyper)thermophilic pure cultures and consortia for bioremediation of heavy

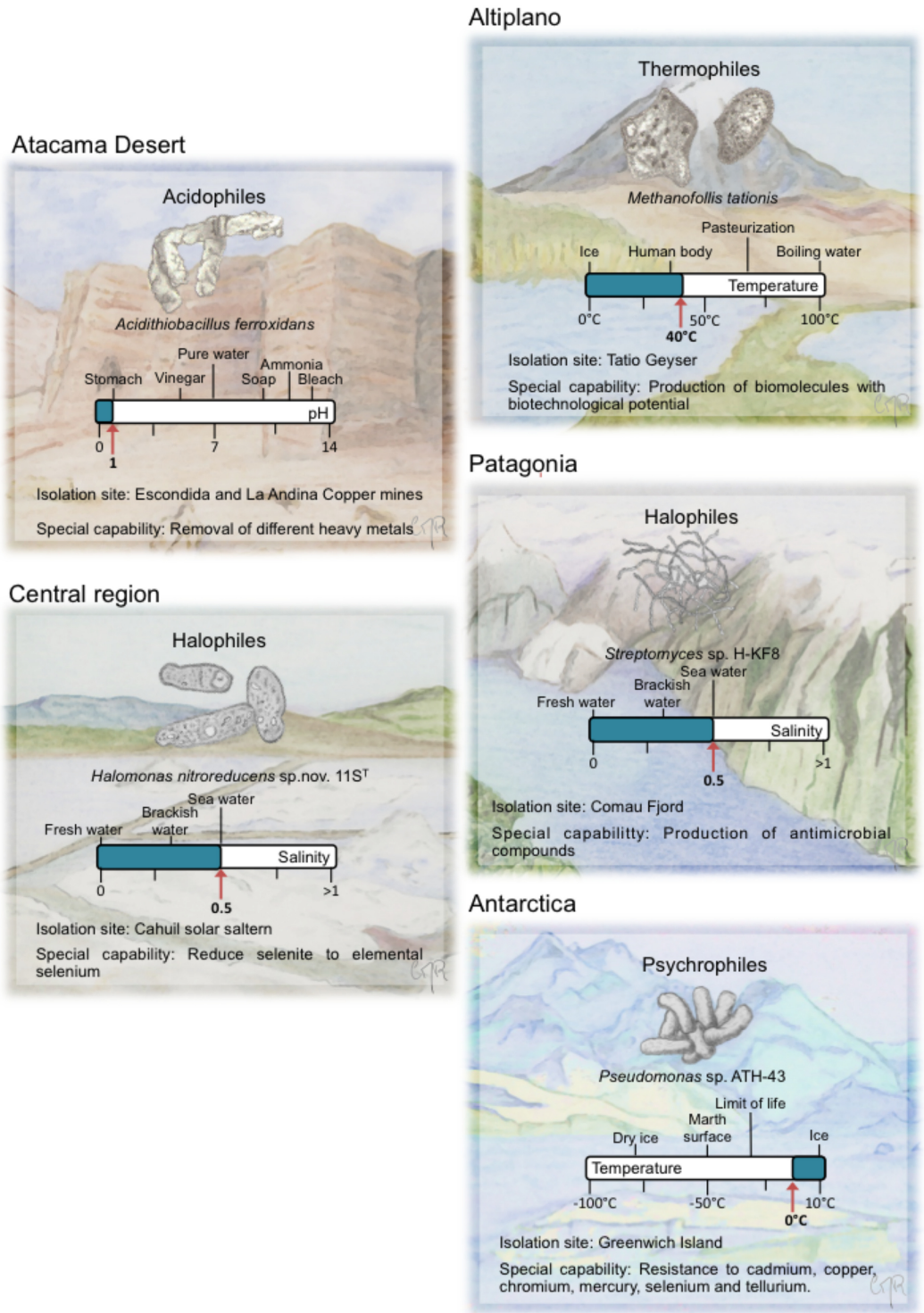

FIGURE 2 | Representative extremophiles from five main biotopes in Chile. For each extremophile, a special capability is described and its ecosystem is drawn. A bar with well-known values and the isolation value for each of the extreme environmental variables is depicted.

metal-contaminated surface and groundwaters, including biosorption and immobilization of radionuclides and heavy metals (Chatterjee et al., 2010; Sar et al., 2013), removal of heavy metals (Ilyas et al., 2014) and for degradation of persistent organic compounds such as aliphatic and (poly)aromatic hydrocarbons (Mnif et al., 2014; Zhou et al., 2018), and synthetic

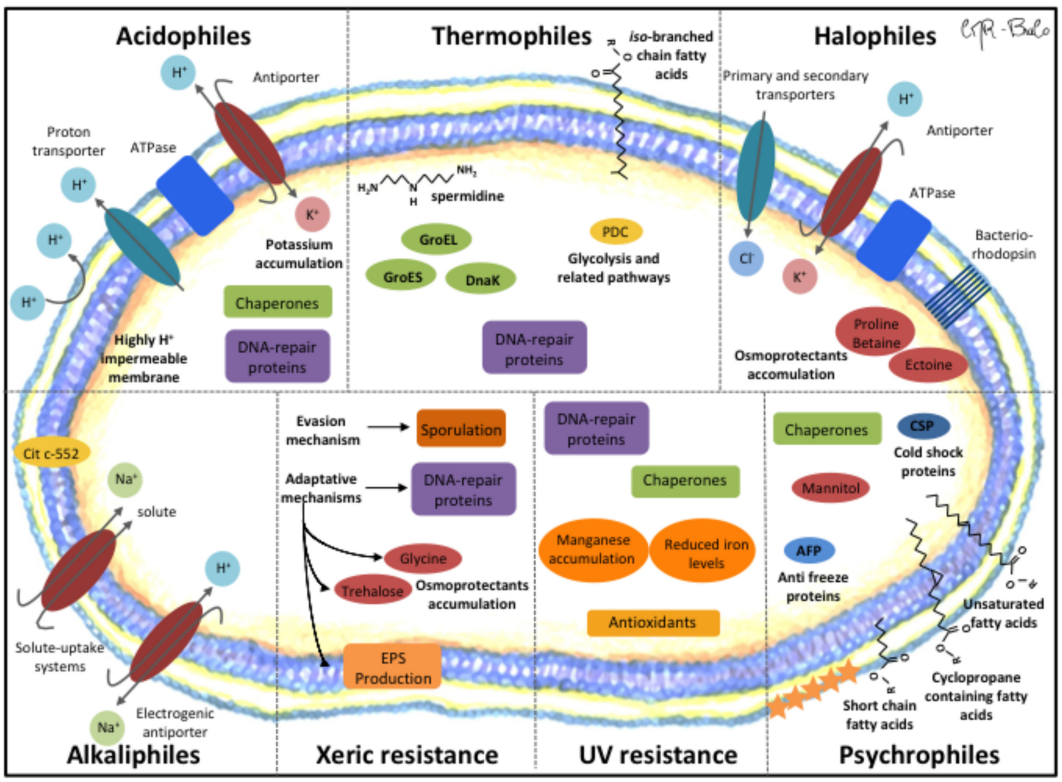

FIGURE 3 | Molecular mechanisms of extremophiles for their adaptation to extreme environmental conditions. Acidophiles. (i) Potassium antiporter releases protons towards the extracellular medium, (ii) ATP synthase, (iii) membrane highly impermeable to protons, (iv) Chaperones, and (v) DNA-repair proteins. Thermophiles. (i) Upregulated glycolysis proteins (e.g., pyruvate dehydrogenase complex (PDC)), (ii) Lipids with iso-branched chain fatty acids and long chain dicarboxylic fatty acids, (iii) polyamines (spermidine), and (iv) Chaperones. Halophiles. (I) High salt-in strategy: (i) chloride transporters (primary or secondary), (ii) potassium uptake into cells by concerted action of bacteriorhodopsin and ATP synthase. (II) Low-salt strategy: (i) *de novo* synthesis or uptake of osmoprotectants (proline-betaine, ectoine) that maintain osmotic balance and establish the proper turgor pressure under different salt concentration. Psychrophiles. (i) high degree of unsaturated, cyclopropane containing fatty acids and short chain fatty acids, (ii) Cold shock proteins (CSP) (iii) Chaperones, (iv) Anti-freeze proteins (AFP) restrict the ice growth on protein surfaces, (v) Mannitol and other compatible solutes accumulate in the cell cytoplasm as cryo-protectants to prevent protein aggregation, and (vi) Carotenoids (star symbols) support maintenance of membrane fluidity and prevent cell damage by UV radiation. UV resistance. (i) Manganese accumulation and reduced iron levels, (ii) Antioxidants (glutathione), (iii) Chaperones, and (iv) DNA-repair proteins. Xeric resistance. (I) Evasion mechanism: (i) bacteria sporulation. (II) Adaptation mechanism: (i) increased extracellular polymeric substances (EPS), (ii) DNA-repair proteins, and (iii) accumulation of osmoprotectants (glycine, trehalose). Alkaliphiles. (i) Electrochemical gradient of Na^+ and H^+ by electrogenic antiporters for proton accumulation, (ii) Na^+-solute uptake system, and (iii) Cytochrome c-552 enhance terminal oxidation function by electron and H^+ accumulation.

dyes (Deive et al., 2010). Increasing research is conducted into evaluating the applications of thermostable enzymes in waste treatment and remediation (Kataoka et al., 2014; Wang et al., 2015; Rigoldi et al., 2018).

A high portion of the Chilean territory is superimposed on the subducting Nazca plate, the largest tectonic relief, that drives displacement and rearrangements of geological structures and generates routinely megathrust earthquakes (Armijo et al., 2015). In those areas, the compression and decompression of magma may modulate volcanic activity on land, in the seafloor, and in the deep subsurface, generating abundant natural formations that are suitable for survival and growth of (hyper)thermophilic microbial life forms. Geothermal fields are usually main contributors of arsenic to both surface and subsurface water (Ballantyne and Moore, 1988; Smedley and Kinniburgh, 2002). The water influx is particularly important at the water discharged at the Tatio Geyser, which achieved in surface water a arsenic concentration of 45 mg L^{-1} (Landrum et al., 2009). The effluent discharges caused high arsenic levels (0.1–1.5 mgL^{-1}) throughout the basin of Loa River. Besides the potential human health risks (Yañez et al., 2005), those arsenic levels impact also the microbiota. *Pseudomonas fluorescens* and *Serratia odorifera* strains isolated from an arsenic-polluted river in the Atacama Desert showed tolerance to arsenic 800–1,000 mM (Campos et al., 2009; Escalante et al., 2009). Due to their physicochemical properties, the water discharged by the Tatio Geyser is an unique environment to study (hyper)thermophiles. A fraction of the water is very rich in silica, contains high antimony concentration (∼0.02 mM), low sulfite concentration (∼0.5 mM) at a nearly neutral pH (Landrum et al., 2009). Most of the worldwide studies efforts directed to the biotransformation of arsenic by (hyper)thermophiles have been restricted to sulfidic waters at extreme pH conditions, including high arsenic geothermal sites in Yellowstone National Park in United States and Dallol Volcano in Ethiopia (Rowe et al., 1973;

Barbieri and Cavalazzi, 2014). Research has been focused toward isolation and characterization of (hyper)thermophiles tolerant to As, or capable of playing a role on its biogeochemical cycle. The geothermal water discharges arsenite As(III), which is the most mobile and toxic form of arsenic that progressively oxidizes to arsenate As(V) downstream (Engel et al., 2013). Several prospections have shown that nearly all of the geyser features and streams at El Tatio are covered by biofilms and colorful microbial mats dominated by photosynthetic bacteria (*Chloroflexi* and cyanobacterial communities) (Fernandez-Turiel et al., 2005; Engel et al., 2013; Plenge et al., 2017). Microbial community analysis based on 16S rRNA gene of the geyser-discharge water revealed that *Chloroflexi*, *Deinococcus–Thermus*, *Aquificales*, and *Chlorobi* were the most prevalent microorganisms in the zones where arsenite reduction takes place (Engel et al., 2013). Indeed, the survey of functional genes revealed that most of the arsenite oxidase *aio*A-like gene found within the community showed high identity to genes belonging to strains of the thermophilic anoxygenic phototroph *Chloroflexus aurantiacus*. *Chloroflexi*-like *aioA* gene sequences obtained from the microbial community of El Tatio clustered on two separated clades likely representing additional diversity that could be associated with either novel groups of arsenic-resistant bacteria, or novel mechanisms of As resistance. It is also noteworthy to mention that *Chloroflexus aurantiacus* can either grow phototrophically under anaerobiosis or chemotrophically under aerobic and dark conditions, providing enough metabolic flexibility to function as a potential strain for bioremediation of As-contaminated environments, but also during carbon sequestration efforts (Tang et al., 2011).

Besides arsenic, the microbial communities associated to El Tatio cope with a wide variety of environmental stressors, such as the presence of other toxic metals (e.g., antimony) and the impact of extreme UV radiation. Living at such selective pressure has fostered the development and retention of a suite of metabolic and physiological adaptations that has enormous potential to be used for biotechnological applications. On one hand, multi-resistant microbial isolates may be useful in bioremediation. Furthermore, a second area of interest is the identification and characterization of the mechanisms of resistance to multiple stressors. Indeed, enzymes synthesized by (hyper)thermophiles display high levels of thermostability, converting them in candidates to explore potential novel applications for industrial processes. For example, the archaeon isolated from a solfataric pool located in El Tatio, *Methanofollis tationis* (**Figure 2**, first described as *Methanogenium tatii*) (Zabel et al., 1984; Zellner et al., 1999) produced its own particular pterin, a type of biomolecule involved in immune modulation, cellular signaling, metabolism and pigmentation. Two years after its isolation, the identification and structure of the novel pterin produced by *Methanofollis tationis*, named tatiopterin, were elucidated. Afterward, it has been shown that tatiopterin specifically enhances photostability of materials, preventing the bleaching of photosynthetic pigments due to irradiation (Elshahawi et al., 2015). More efforts in order to understand the role of such molecules under those conditions should be further explored. Specifically, one area of interest in this field is the increase of exploration efforts of novel thermozymes that can be applied for production of biofuels from starch and lignocellulosic waste materials. Due to their complex structure, lignocellulosic materials are degraded by physicochemical treatments to obtain cellulose, hemicellulose, and lignin, which can be further treated with hydrolytic enzymes (Urbieta et al., 2015a).

Previous prospections in the Surire Salar have described the presence of arsenic-precipitating bacteria, suggesting that may be also present in the Surire hydrothermal vents (Demergasso et al., 2007). The culturable mesophiles in Lirima wetland were reported, whereas the hot spring remain unexplored (Scott et al., 2015). Special attention should be devoted in this site due to the fact that water contain high chloride and boron concentrations, becoming a source of microorganisms capable of bioremediation of boron-polluted wastewaters. Microbes associated to the hydrothermal systems such as Puchuldiza-Tuja (4,100 m.a.s.l.), Colpitas (4,000 m.a.s.l.), Apacheta (4,500 m.a.s.l.) have not been explored yet.

Porcelana hot spring in Northern Patagonia is characterized by abundant and colorful microbial mats widespread along a rather extensive thermal gradient (∼38–69°C) (Alcamán et al., 2015). The microbial community associated to Porcelana hot spring is dominated by cyanobacteria, particularly of the diazotrophic *Mastigocladus* (Stigonematales) genus. Members of the same genus were also identified as part of biofilms in Copahue geothermal field at the North west corner of Neuquén province, Argentina (Urbieta et al., 2015b), indicating its cosmopolitan character (Miller, 2007). At Porcelana hot spring, *Mastigocladus* sp. strain CHP1 was the most dominant contributor of nitrogen through nitrogen fixation (∼87% of the *nifH* gene transcripts) (Alcamán et al., 2015). Physiological studies revealed that *Mastigocladus* isolates gather a broad range of metabolic plasticity regarding the nitrogen metabolism (Alcamán et al., 2017). *Mastigocladus* sp. strain CHP1 is capable to fix nitrogen at 60°C, the highest temperature reported for the activity of N_2-fixing filamentous cyanobacteria (Alcamán et al., 2015). Further studies should explore the metabolic versatility of *Mastigocladus* sp. strain CHP1 in the treatment of nitrate-contaminated industrial waters at high temperature.

Environments are so dynamic that surprise us. An iconographic example of such diversity is depicted by the fact that Antarctica, a continent well known as the coldest place on earth, also harbors many geothermal sites suited for the growth of (hyper)thermophile microorganisms (Flores et al., 2013). The uppermost temperatures of those sites range from 40 to 110°C, and has extremely low concentrations of nutrients, such as N and P, and high concentrations of heavy metals (Cu, Zn, Cd, Pb, and Hg) (Muñoz et al., 2011). Although environmental conditions seem to be harsh for microbial growth, recent studies have shown that the environment is suitable for thermophilic organisms. Bacteria from the *Geobacillus*, *Bacillus*, *Brevibacillus*, *Thermus* genera and uncultured sulfate reducing bacteria were abundant in a fumarole at 90–110°C from Deception Island, an active strato volcano located in the South Shetland Islands (Muñoz et al., 2011). Some of these microbes can carry metal redox interactions that have further implications for ore formation and might be capable to recover metals from ore-containing

materials. For instance, the thermophilic *Geobacillus* sp. strain ID17 is capable to synthesize gold nanoparticles when exposed to Au(III). The nanoparticles were found to be intracellularly accumulated raising the potential applications in bioremediation of gold-bearing wastes (Correa-Llantén et al., 2013). The synthesis of gold nanoparticles by bacteria can be useful for diverse biotechnological and medical applications (Montero-Silva et al., 2018). *Geobacillus* species are also capable to degrade organic pollutants. Indeed, members of the same clade including *Geobacillus thermoleovorans* T80 degrade hexadecane (70%) during bioremediation at ∼60°C. *Archaea* have also been isolated from soils extracted at Deception Island. Dennett and Blamey (2016) isolated the hyperthermophilic archaea *Pyrococcus* sp. M24D13, and characterized a novel thermostable cyanide-degrading nitrilase. This thermostable enzyme may be useful to remediate cyanide contaminated waste streams (Dennett and Blamey, 2016). (Hyper)thermophiles and their novel thermostable enzymes are of considerable biotechnological interest to find novel alternatives for bioremediation and other bioprocesses to be carried out at high temperatures.

ACIDOPHILES

Acidophiles are defined as organisms that grow at an optimum pH < 5 (Johnson, 2008). Extreme acidophiles are microorganisms that showed an optimum growth at pH 3 or less, whereas moderate acidophiles are those that grow with optimum pH between 3 and 5. Acid-tolerant microorganisms, have optimum pH > 5, but are still active in low pH environments (Johnson, 2007, 2008). Extreme acidophilic organisms are exclusively microbial and distributed in Archaea, Bacteria, and Eukarya domains (Sharma et al., 2016).

Acidophiles maintain the cytoplasmic pH close to neutrality to safeguard the acid-labile cellular constituents, which require the generation of a large pH gradient. Three main mechanisms are involved in the adaptation to an acidic environment (**Figure 3**). A first mechanism is an active pumping of protons to the maintenance of ΔpH, by proton flux systems. The role of proton efflux via transport pumps in the electron transport chain alongside the influx of protons through the F_0F_1-type ATP synthase has been described in *Bacillus acidocaldarius, Thermoplasma acidophilum,* and *Leptospirillum ferriphilum* (Michels and Bakker, 1985). Additional proton flux systems include primary proton pumps (symporter) and secondary proton pumps (e.g., cation/H^+ antiporter), and proton-consuming reactions. A carbonic anhydrase and amino acid decarboxylases that aid in pH homeostasis by consuming protons have been reported in *L. ferriphilum* (Christel et al., 2018). A second mechanism is a decreased permeability of the cell membrane to suppress the entry of protons into the cytoplasm. The influx of protons is inhibited by the inside positive membrane potential formed by K^+ ions (Christel et al., 2018). A wide *repertoire* of genes related to cell membrane biosynthesis that may be associated with acid tolerance was identified in *L. ferriphilum*. The presence of tetrapetric lipids in the cell membrane that provide tolerance to acidic pH has been reported in *Archaea Ferroplasma acidiphilum* and *Sulfolobus solfataricus*. A third mechanism is an improved protein and DNA-repair systems in acidophiles compared to neutrophils. An external pH shift from 3.5 to 1.5 induced proteins that are involved in the heat shock response such as chaperones in the acidophile *At. ferrooxidans* (Amaro et al., 1991).

Acidophilic microorganisms play an important role in biomining of metals from low grade sulfur minerals (Bustos et al., 1993; Seeger and Jerez, 1993; Seeger et al., 1996; Okibe et al., 2003; Demergasso et al., 2005, 2010; Acosta et al., 2017). Previous studies have demonstrated the role of acidophiles in bioremediation of polluted soils and waters, through (i) metal reductive processes (Kolmert and Johnson, 2001; Suzuki et al., 2003; Leigh et al., 2015), (ii) metal adsorption onto jarosites (Natarajan, 2008; Asta et al., 2009), (iii) metal biosorption (Liu et al., 2004; Chakravarty and Banerjee, 2012), and (iv) degradation of petroleum hydrocarbons (Stapleton et al., 1998; Margesin and Schinner, 2001; Christen et al., 2012; Arulazhagan et al., 2017). Additionally, enzymes from acidophilic microorganisms are explored due to their tolerance to low pH, which favors their industrial applications in starch, fruit juices, feed and baking industries (Matzke et al., 1997; Nakayama et al., 2000; Serour and Antranikian, 2002; Sharma et al., 2012). More recently novel applications of acidophiles including electric generation have been explored (Sulonen et al., 2015; Ni et al., 2016).

Acidophilic microorganisms are present in several natural habitats, such as solfataric fields and geothermal sulfur rich sites (Sharma et al., 2016). These sites are niches for a variety of acidophilic microorganisms with unique adaptations for survival in the hostile low pH environments such as *Sulfolobus solfataricus* and *Sulfolobus acidocaldarius* (Yellowstone National Park, United States) (Brock et al., 1972). Acidophilic microorganisms have also been reported in anthropogenic environments such as acidic mine drainage (AMD), which are associated with heavy metals and coal mining. The acidophilic microorganisms mobilize metals and generate AMD. AMD generates most of the extremely acidic niches on Earth and disseminates heavy metals in the environment (Panda et al., 2016).

In Chile, an important area where acidophiles have been studied is located in the Atacama Desert. The microbial solubilization of metals in acidic environments has been successfully used in bioleaching for the extraction of metals. In Escondida mine located 170 km south-east from Antofagasta, the analyses of the microbial community of a low-grade copper sulfide leach pile indicated the presence of *At. ferrooxidans* (**Figure 2**), *At. thiooxidans, L. ferriphilum,* and *F. acidiphilum* (Galleguillos et al., 2008; Remonsellez et al., 2009; Demergasso et al., 2010; Acosta et al., 2017). Prokaryotic acidophile microarray (PAM) analysis showed members of *Sulfobacillus* genus in samples from heap leaching (Remonsellez et al., 2009). 16S rRNA genes phylogenetic analysis, real time PCR and metagenomics analysis revealed in the heap leaching the bacteria *At. ferrooxidans, At. thiooxidans, At. caldus, At. ferrivorans, L. ferriphilum, S. acidophilus, S. thermosulfidooxidans,* and *Acidiphilium* spp., and the archaea *Ferroplasma acidiphilum, Ferroplasma acidarmanus,* and *Sulfolobus* spp.

(Demergasso et al., 2005, 2010; Soto et al., 2013; Acosta et al., 2017). *Acidithiobacillus*, *Leptospirillum*, and *Sulfobacillus* strains have also been reported in the copper tailings of La Andina mine in Central Chile (**Figure 2**). Molecular methods revealed the presence of heterotrophic acidophiles associated to *Acidobacterium capsulatum*, *Acidobacterium*-like bacterium and *Acidiphilum* sp. (Diaby et al., 2007). In Chile, solfataras throughout Andes Mountains (e.g., Purico Complex and Nevados de Chillán) that harbor acidophiles have been described. The moderate acidophile archaea *S. solfataricus* was isolated from a hot spring in Nevados de Chillán (Valdebenito-Rolack et al., 2017). To date, acidophilic microbes have been scarcely studied in diverse acidic environments in Chile including solfataras.

In the last decades, the bioremediation potential of acidophiles in acidic environments have been studied. Acidophiles capable to degrade phenol at low pH have been reported. The acidophile *S. solfataricus* degrades phenol (Christen et al., 2011). Zhou et al. (2016) reported the degradation by *S. acidophilus* of phenol, and methylphenols. Acidophilic bacteria able to grow in presence of alkanes have been described (Hamamura et al., 2005). Acidophiles including *Acidisphaera*, *Acidiphilium*, and *Acidithiobacillus* strains were capable to degrade 50% hexadecane in hydrocarbon-amended soil/sand mixtures. Acidophiles have been used for the treatment of petroleum-polluted wastewater under acidic condition (Arulazhagan et al., 2017). Acidophilic microorganisms such as *Acidithiobacillus* and *Sulfobacillus* strains may be useful for the remediation of hydrocarbon-polluted acidic sites (Ivanova et al., 2013).

The removal of heavy metals by acidophiles from Chile has been reported. *At. ferrooxidans* has been used for removal of different heavy metals at laboratory scale. The addition of *At. ferrooxidans* to an AMD increased precipitation kinetics of heavy metals and decreased water iron content, accelerating heavy metal removal (Darkwah et al., 2005). *At. ferrooxidans* has been used for the *ex situ* bioremediation of uranium (VI), removing up to 50% of uranium (100 mg L^{-1}) from polluted mine water (Romero-González et al., 2016). Takeuchi and Sugio (2006) reported that mercury was almost completely removed by volatilization in mercury-polluted soil by *At. ferrooxidans* strains SUG 2- 2 and MON-1. Also MON-1 cells immobilized in PVA resins efficiently volatilize mercury from mercury-polluted wastewater. Bioremediation by bioaugmentation with heavy metal-resistant bacteria of mercury-polluted waters has been reported (Rojas et al., 2011). This bioremediation process was scaled up (Bravo, 2017) and may be applied in mercury-polluted sites closed to metal mining activities. *At. ferrooxidans* and *Leptospirillum ferrooxidans* have been used for arsenite removal. Bioremoval occurs through the adsorption of arsenic (III) onto the jarosites generated during microbial growth (Natarajan, 2008). Furthermore, *At. ferrooxidans* and *At. thiooxidans* strains are able to reduce chromium (VI). The almost complete removal (93%) of chromium (VI) from electroplating waste by *A. thiooxidans* has been reported (Cabrera et al., 2007). *At. thiooxidans* is able to reduce uranium by polythionates that are synthesized during oxidative sulfur metabolism (Gargarello et al., 2010). *At. ferrooxidans* has been applied for removing sulfur from solids and gases and heavy metals from electric wastes and sludge (Zhang et al., 2018). In addition, the removal of Ni and Hg from port sediments through bioaugmentation with a consortium of iron-oxidizing acidophilic bacteria (*A. thiooxidans*, *A. ferrooxidans*, and *L. ferrooxidans*) in microcosm was observed (Beolchini et al., 2009).

Metal mining is a key player in the Chilean economy. Therefore, diverse acidophiles useful for bioleaching have been isolated, characterized and applied for bioleaching in Chile. Interestingly, some of these acidophilic microorganisms have been used at laboratory scale for the bioremediation of heavy metals and organic pollutants. However, the application of these acidophiles in bioremediation at industrial scale is still an important challenge. Acidophilic microbes from extreme environments are attractive biocatalysts for bioremediation processes under acidic conditions, especially for heavy metals.

HALOPHILIC MICROORGANISMS

Microorganisms belonging to the three domains of life are present over the whole range of salt concentrations in the environment (Oren, 1999). Halophiles are microorganisms that obligately require salt to grow (Margesin and Schinner, 2001). They are classified based on their optimal NaCl concentration for growth as slight halophiles (0.2 M), moderate halophiles (0.5–2.5 M), borderline extreme halophiles (>2.5–4.0 M) or extreme halophiles (>4.0–5.9 M) (Edbeib et al., 2016). Halophilic microorganisms are ubiquitous in salars, saline lakes, oceans, polar ice, and coastal areas (Edbeib et al., 2016). Halotolerants are microorganisms that grow in the presence and absence of NaCl, and those that grow in presence of >2.5 M NaCl are considered extremely halotolerant (Margesin and Schinner, 2001).

Halophilic and halotolerant microorganisms have adapted and evolved to survive in saline environments. They gather unique metabolic properties toward maintaining more water in the cytoplasm than in their surroundings, avoiding water losses. Halophilic or halotolerant microorganisms have evolved two main strategies (**Figure 3**). The first strategy is maintaining an intracellular salt concentration equivalent to the environment, and consequently, all intracellular systems have been adapted. This is achieved with chloride and potassium uptake into the cells by transporters (primary or secondary) and concerted action of bacteriorhodopsin and ATP synthase. The other strategy is maintaining low intracellular salt concentration, and therefore osmotic pressure is balanced by organic compatible solutes, such as betaine and ectoine. Due to its nature, the latter strategy does not require a global adaptation of the intracellular machinery (Oren, 1999; Margesin and Schinner, 2001).

Chile gathers several high saline environments. Most of them are concentrated in the Northern region, where 52 saline lakes and salt crusts are distributed alongside The Andes, spanning an area of over 200,000 km^2 of the Atacama Desert. The saline ecosystems found in the Northern region can be classified in (i) Borderline Salars, (ii) Athalassohaline ecosystems, which are located in the Altiplano, and (iii) Acidic Salars (Risacher et al., 2003; Risacher and Fritz, 2009). Particularly, in Lejía

Lake, an extreme saline lake nested at the base of Lascar Volcano in the Chilean Altiplano, two halotolerant bacteria closely related to *Halomonas alkaliantarctica* strain CRSS and capable to grow at 15% NaCl were isolated (Mandakovic et al., 2018). Other saline lakes are also located in Central region (Cáhuil Lagoon), and the Southern Patagonia (De Los Rios-Escalante and Gajardo, 2010; Plominsky et al., 2014). One third of bacterial isolates from different niches in the Atacama Salar were classified as moderate halophilic and halotolerant bacteria. These isolates belong to *Marinomonas*, *Vibrio*, *Alteromonas*, *Marinococcus*, *Acinetobacter*, *Micrococcus*, *Bacillus*, *Pseudomonas, Deleya*, *Staphylococcus* genera and also some Cyanobacteria, such as members of the *Cyanothece*, *Gloeocapsa*, and *Gloeobacter* genera (Zúñiga et al., 1991; Dorador, 2007). Saltern ecosystems are commonly dominated by Archaea, where members of the family *Halobacteriaceae* are the most common halophiles (Oren, 2002). Metagenomic studies performed on samples extracted from a salt crystallizer pond located in the Cáhuil Lagoon, revealed that 61% of the gene sequences belonged to Archaea, mainly from the *Halobacteriaceae* family, followed by 19% sequences from viruses and 16% from bacteria (Plominsky et al., 2014). Microbial communities in the Atacama Desert ecosystems, such as halites, saline soils and salt lakes, are also dominated by members of the *Halobacteriaceae* family (Robinson et al., 2015; Finstad et al., 2017).

Arsenic is a metalloid that is widely distributed at high concentrations along the Atacama Desert. The sources of arsenic are often associated with volcanic-hydrothermal springs, metal ores and anthropogenic activities. Microbial communities from Atacama Salar contributed to arsenic reduction (Lara et al., 2012), which is a process that has been widely studied in saline-alkaline systems (Oremland et al., 2004; Kulp et al., 2007). *Shewanella* sp. strains Asc-3 and CC-1 isolated from Ascotán low-pH salt flats (Demergasso et al., 2007; Lara et al., 2012) were capable of precipitating arsenic (**Table 2**). Surprisingly, arsenic-precipitating bacteria accounted for 50% of the bacterial communities, suggesting that arsenic-based processes in this ecosystem are significant in the formation of arsenic minerals (Demergasso et al., 2007).

Exiguobacterium sp. SH31 isolated from a moderate saline environment in Huasco Salar was able of grow in presence of As(III) 10 mM and As(V) 100 mM, highlighting its natural resistance to arsenic. *Exiguobacterium* strains capable of reducing arsenate and chromium have been reported. Interestingly, *Exiguobacterium* strains have been explored for bioremediation applications. An *E. aurantiacum* strain isolated from a lake in Southern Spain degrades pesticides (López et al., 2005). *Microbacterium* sp. CGR1 (**Table 2**) from the Atacama Desert tolerates NaCl 1.2 M, and possesses arsenic resistance (Mandakovic et al., 2015). An additional survey of metal resistance in halotolerant and halophilic isolates from the Atacama Desert showed that most of them were capable to cope with the presence of heavy metals such as Cd, Zn, Ni, Cu, and Co. For example, *Thalassobacillus devorans* showed high tolerance to cadmium and nickel (Moreno et al., 2012).

Other Chilean ecosystems such as Cahuil marine salterns are sources for strains capable to be used in bioremediation platforms. The extreme halophile *Haloferax* sp. CL47 that was isolated in Cahuil degrades several polyaromatic hydrocarbons (PAHs) such as naphthalene, anthracene, phenanthrene, pyrene and benzanthracene (Bonfá et al., 2011). In addition, *Haloferax* sp. CL47 has been used for petroleum degradation in wastewater. The extreme halophile *Halomonas nitroreducens* $11S^T$ (**Figure 2** and **Table 2**) showed the capability to reduce selenite to elemental selenium (González-Domenech et al., 2008).

Halotolerant strains belonging to the phylum *Actinobacteria* were isolated from marine sediment samples from the Comau Fjord in Northern Patagonia (Undabarrena et al., 2016). These strains showed tolerance to up to NaCl 1.7 M. *Streptomyces* sp. H-KF8 (**Figure 2**) tolerates different heavy metals, such as Ni (15 mM), Cu (0.75 mM), Co (6 mM), Zn (50 mM), Cd (1.5 mM), Hg (60 μM), Te (40 μM), Cr (20 mM), and As (100 mM). The genome sequencing of the *Streptomyces* sp. H-KF8 strain revealed the presence of 49 heavy metal resistance genes (Undabarrena et al., 2017).

Due to industrial activities or natural sources, saline environments frequently have a high concentration of organic compounds (Castillo-Carvajal et al., 2014; Edbeib et al., 2016). Industrial wastewaters frequently possess high salt concentration, and high levels of organic matter and pollutants, for which a wide variety of conventional biological treatments are not currently suitable (Bonfá et al., 2011). The presence of high levels of aromatic compounds in saline wastewater during crude

TABLE 2 | Halophiles isolated from diverse extreme environments in Chile and their bioremediation potential.

Strain	GenBank accession number	Isolation source	Salt tolerance (M)	Bioremediation potential	Reference
Haloferax sp. CL47	HQ438281	Cahuil Lagoon	3.4	Naphthalene, anthracene, phenanthrene, pyrene, and benzanthracene degradation	Bonfá et al., 2011
Halomonas nitroreducens $11S^T$	EF613113	Cahuil Lagoon	0.5–3.4	Selenite reduction	González-Domenech et al., 2008
Shewanella sp. Asc-3	EF157293	Ascotán salt flat	0–0.5	Arsenic precipitation	Demergasso et al., 2007
Shewanella sp. CC-1	EF157294				
Exiguobacterium sp. SH31	LYTG01000000	Huasco Salar	0.4	Arsenic resistance	Castro-Severyn et al., 2017
Microbacterium sp. CGR1	CP012299	Alto Andino, Atacama Desert	0–1.2	Arsenic resistance	Mandakovic et al., 2015

oil extraction has been described (Le Borgne et al., 2008). The biodegradation of hydrocarbon-derived pollutants in both soils and groundwater is impaired under elevated salt concentration (Lay et al., 2010). Thus, the application of halotolerant pollutant-degrading bacteria is essential for the bioremediation processes in saline environments.

Halophilic microorganisms capable of degrading hydrocarbons, lignocellulosic materials, chlorophenols, formaldehyde, nitroaromatic compounds have been reported (Oren et al., 1992; García et al., 2004). The halophile *Halomonas organivorans* degrades a wide range of aromatic compounds (García et al., 2004). *Halomonas* sp. KHS3 is capable to degrade diverse aromatic hydrocarbons and to produce extracellular rhamnolipids (Corti Monzón et al., 2018). Rhamnolipids are biosurfactants that are used for bioremediation and enhanced oil recovery (Rahman et al., 2003; Sachdev and Cameotra, 2013; Sekhon Randhawa and Rahman, 2014). Additionally, halophilic microorganisms capable of degrading lignocellulosic and nitroaromatic substrates, and chlorophenols have been reported (Oren et al., 1992). The applications of halotolerant bacteria for bioremediation of natural and industrial saline environments is an attractive challenge (Edbeib et al., 2016).

Climate change, chemical fertilizers and saline water used for irrigation are increasing salinity in agricultural soils (Valipour, 2014). Salt toxicity is a major restrictive factor in crop productivity and 20% of the cultivated land worldwide are seriously affected by salinity (Zhu, 2001; Farhangi-Abriz and Nikpour-Rashidabad, 2017). In response to salt stress, reactive oxygen species (ROS) are accumulated in plant tissues, damaging the photosynthetic apparatus and cellular membranes (Bose et al., 2014; Oukarroum et al., 2015). For preserving osmotic and ionic homeostasis under salt stress, plants accumulate osmolytes such a glycine betaine and proline (Farhangi-Abriz and Torabian, 2017). Halophilic and halotolerant microorganisms produce glycine betaine (Lamark et al., 1991) that may protect plants in saline soils. More recent studies have shown that other halotolerant bacterial mechanisms are also involved in plant protection: (i) increase production of extracellular hydrolytic enzymes (Rohban et al., 2009), (ii) increase activity of 1-aminocyclopropane-1-carboxylic acid (ACC) deaminase that reduced plant ethylene levels, which are typically increased by salt stress (Siddikee et al., 2010), (iii) increase indole-3-acetic acid (IAA) levels that enables plant to increase nutrient uptake under salt stress (Vacheron et al., 2013). These studies support the potential application of halotolerant plant growth promoting bacteria to protect crops in saline soils.

ALKALIPHILES

Alkaliphiles are organisms that grow on alkaline habitats (pH > 9), usually showing an optimal growth within pH ∼10 (Horikoshi, 1999). These extremophiles are classified in two main physiological groups: obligate and facultative alkaliphiles. Facultative alkaliphiles are capable of growing in the pH range of 7.0–9.5, whereas obligate alkaliphiles (e.g., *Bacillus krulwichiae*) showed an optimal growth between pH 10.0 and 12.0 (Krulwich and Guffanti, 1989). Alkaliphiles may coexist with neutrophilic microorganisms under mild basic pH conditions, and also live in specific extreme environments.

To cope with high pH, alkaliphile bacteria possess molecular mechanisms, which comprise the activation of both symporter and antiporter systems (**Figure 3**). Electrochemical gradient of Na^+ and H^+ is produced by electrogenic antiporters, and the symporter system allows the uptake of Na^+ and other solutes into the cells (Krulwich, 1995; Krulwich et al., 1998). The function of cytochrome *c*-552 in electron and H^+ accumulation enhances the function of terminal oxidation in respiratory system (Matsuno and Yumoto, 2015). These systems enable the influx of protons and solutes inside the cell due to the alteration in the distribution of ions (e.g., Na^+), maintaining the hydrosaline homeostasis and thermodynamic stability of the cell. The transporters are controlled, probably by signaling from a transmembrane pH sensor (Krulwich, 1995).

Diverse alkaliphilic microorganisms, including bacteria belonging to *Bacillus, Micrococcus*, *Pseudomonas*, and *Streptomyces* genera and eukaryotes, such as yeast and filamentous fungi, have been isolated from alkaline environments, including highly alkaline hyper-saline lakes (e.g., Lake Natron, Tanzania) and alkaline soda lakes (e.g., Lake Mono, CA, United States) (Duckworth et al., 1996; Groth et al., 1997; Horikoshi, 1999; Yakimov et al., 2001). Alkaliphiles are also present in highly alkaline enrichments generated by industrial activities (e.g., indigo dye plants) or soils with high alkalinity (e.g., estuaries with long periods of evaporation, clay particles with highly abundant alkaline crevices) (Grant, 2003; Sorokin et al., 2006).

Alkaliphilic microorganisms have been studied as novel sources for several biotechnological applications, including the treatment of highly toxic wastewater (e.g., dye-containing effluents). Textile effluents are characterized by the presence of high salt and alkaline pH along with the presence of toxic dyes (Maier et al., 2004; Khalid et al., 2012; Prasad and Rao, 2013). Several alkaliphiles have been isolated from these hostile environments and explored as biocatalysts for the treatment of dye-containing effluents (Hou et al., 2017). *Nesterenkonia lacusekhoensis* EMLA3 that was isolated from a highly alkaline textile effluent (pH ∼13) degrades the toxic azo dye methyl red in the presence of high salt concentration and heavy metals (Ni (II), Cr (VI), and Hg (II) (Bhattacharya et al., 2017). Alkaliphilic microorganisms have been applied to remove ammonia from N-rich saline wastewater, mainly produced by coke plants, fuel refining and fertilizer industries. Chemolithoautotrophic alkalophilic microorganisms have been applied to clean up ammonia pollution in effluents (Sheela et al., 2014; Cui et al., 2016). Complete ammonia oxidation into nitrate by bacteria could be useful for waste water treatment and to engineer ecosystems (Lawson and Lücker, 2018).

In Chile, alkaliphiles have been isolated mainly in the Northern Region, specifically along salt deposits from Atacama Desert and Altiplano. This region has aridic to semi-aridic climate regimes and comprises many different (hyper)saline deposits, including evaporitic basins, known as saltflats, and athalassohaline ponds (Chong, 1984; Demergasso

et al., 2004). Microorganisms in saltflats from Llamará Salar (Central Depression), Atacama Salar (Pre-Andean Depression), Ascotán Salar and Huasco Salar (Altiplano) have been reported (Demergasso et al., 2004; Dorador et al., 2008; Castro-Severyn et al., 2017), revealing insights of the special metabolic capabilities of these alkaliphiles and their responses to multiple stressors. Mandakovic et al. (2018) isolated from Lejía Lake in the Chilean Altiplano *Microbacterium sp*. CGR2, *Planococcus sp*. strains ALS7 and ALS8 that are tolerant to pH 12. However, the extremophiles from several alkaline ecosystems in Chile have not been explored. For example, Amarga Lake (Torres del Paine National Park, Patagonia) is a shallow cold lake with hypersaline water and an alkaline pH of 8.9 (Solari et al., 2004), which should harbor polyextremophile bacteria. However, to date in Amarga Lake only the presence of stromatolites has been reported.

Several heavy metal-resistant alkaliphiles have been isolated in Chile. The microbiota associated to the athalassohaline ecosystem Huasco Salar in the Atacama Desert showed resistance/tolerance to copper, tellurium, and arsenic (Castro-Severyn et al., 2017). *Exiguobacterium* isolates from this site carry a number of stress-related genetic determinants, including metal/metalloid resistance genes. For example, the arsenic resistant strain *Exiguobacterium* sp. SH31 has a set of genes encoding proteins required for arsenic resistance, including the arsenic efflux pump Acr3, growing in presence of arsenite (10 mM) and arsenate (100 mM) (Ordoñez et al., 2015; Castro-Severyn et al., 2017). Dorador et al. (2008) analyze ammonia-oxidizing bacteria (AOB) from four sites in Huasco Salar. A phylotype exhibited 98% sequence similarity to the extremely alkalitolerant ammonia-oxidizing *Nitrosomonas europaea/Nitrosococcus mobilis* (Squeo et al., 2006; Dorador et al., 2008). AOB play a key role in the nitrogen cycle. *Nitrosomonas* and *Nitrosococcus* genera belong to Nitrosobacteria that are AOB involved in the aerobic oxidation of ammonia into nitrite in agricultural soils (Hernández et al., 2011).

Alkaliphiles have been also found in unusual habitats. Quiroz et al. (2015) reported the presence of *Halomonas alkaliphila* in a brine shrimp *Artemia* that was collected from salty lagoons scattered in saltflats of the Atacama Desert (Browne, 1980; Abatzopoulos et al., 2002; Riddle et al., 2013; Quiroz et al., 2015). *Halomonas alkaliphila* is an alkaliphilic halotolerant bacterium that grows aerobically at pH 9, which has been previously isolated from a salt pool located in Montefredane, Italy (Romano et al., 2006). Recently, two *Halomonas* strains were isolated from Lejía Lake soil in Atacama Desert (Mandakovic et al., 2018). Due to its adaptation to a wide range of salt concentrations and alkaline pH, *Halomonas* may be useful for the clean up of polluted saline habitats (Berendes et al., 1996). Additional studies of novel alkaliphilic bacteria and archaea are required to understand their metabolism and physiology and to assess their bioremediation potential.

MICROBES IN DRY ENVIRONMENTS

An increase of dry environments in diverse regions due to low rainfall, high temperatures and drought has been associated to Climate change (Mukherjee et al., 2018). Water is essential for all living organisms (Robinson et al., 2015; Lebre et al., 2017). Arid environments like deserts are considered to be at the dry limit for life (Navarro-González et al., 2003; Bull and Asenjo, 2013). Extremophile xerotolerant organisms can survive in dry environments with water activity < 0.75 (Connon et al., 2007; Lebre et al., 2017). Water activity is calculated as the ratio of the vapor pressure in an environment relative to pure water, and it is considered to be the amount of water available to organisms in the environment (Lebre et al., 2017). Arid areas are biomes with a ratio of mean annual rainfall to mean annual evaporation of <0.05 mm year^{-1}, and <0.002 mm year^{-1} for extreme hyper-arid areas (Mohammadipanah and Wink, 2016). In addition to the low rainfall, other factors such as high and low temperatures, low water activity, high salinity, low concentrations of organic carbon and intense radiation intensify the xeric conditions, constraining the survival of microorganisms (Dose et al., 2001; Crits-Christoph et al., 2013).

Xerotolerant bacteria have developed two strategies to survive in dry environments: evasion of environmental stress and adaptative mechanisms (**Figure 3**). Evasion of dry environmental implies the conversion of cells into a state of non-replicative viability through the formation of spores (Crits-Christoph et al., 2013). Adaptative mechanisms are associated to preventing water loss and increasing water retention through the accumulation of osmoprotectants (trehalose, *L*-glutamate, glycine betaine), production of extracellular polymeric substances (EPS), modifications on the cell membrane to retain intracellular water, and synthesis of DNA-repair proteins (Dose et al., 2001; Lebre et al., 2017).

The Atacama Desert is the oldest desert on Earth with hyper-arid soils with mean rainfall <5 mm year^{-1} to 2.4 mm year^{-1} in the Yungay sector (Warren-Rhodes et al., 2006; Azua-Bustos et al., 2015). Nevertheless, microorganisms are capable to inhabit this extreme environment. Previous studies using culture-dependent methods have reported low numbers of bacteria in Atacama Desert soils, ranging from not detectable to 10^6 CFU per g of soil, with a high degree of spatial heterogeneity (Crits-Christoph et al., 2013). Analysis through culture-independent methods on the subsurface layers of the hyper-arid core showed limited abundance of microbial communities including *Proteobacteria, Actinobacteria, Cyanobacteria, Chloroflexi, Firmicutes, Gemmatimonadetes*, *Planctomycetes*, and *Thermomicrobia* phyla (Dong et al., 2007; Crits-Christoph et al., 2013; Azua-Bustos et al., 2015; Piubeli et al., 2015; Azua-Bustos et al., 2017).

Proteobacteria from Atacama Desert showed a high bioremediation potential. *Pseudomonas arsenicoxydans* strain VC-1 isolated from arsenic-polluted site is able to tolerate high concentration of As(III) (5 mM), and also capable of oxidizing As(III) to As(V) at high rates (Campos et al., 2010). *Actinobacteria* are the most abundant culturable phylum present in Atacama Desert soils, including strains from *Streptomyces, Nocardia, Microlunatus, Prauserella, Microcella, Arthrobacter, Cryobacterium, Frigobacterium, Dietzia, Nocardioides, Propionibacterium, Luteococcus, Kocuria*, and *Patulibacterium* genera (Bull and Asenjo, 2013). Actinobacteria plays a relevant ecological role including resistance to heavy

metals, recycling of substances, degradation of complex polymers and organic persistent pollutants, and synthesis of bioactive molecules (Claverías et al., 2015; Alvarez et al., 2017; Undabarrena et al., 2017), which may explain its capability to still predominate in such harsh environmental conditions. The extreme desiccating condition of deserts has been the main driving force in the evolution of several desert-derived Actinobacteria, which showed a wide range of biotechnological applications including the removal of organic and inorganic pollutants (Mohammadipanah and Wink, 2016; Alvarez et al., 2017). Chilean desert-Actinobacteria research has focused on obtaining microorganisms able to synthesize novel bioactive molecules (Bull and Asenjo, 2013; Azua-Bustos and González-Silva, 2014). Xerotolerant *Streptomyces bulli* and *S. atacamensis* synthesize ansamycin and 22-membered macrolactones with antibacterial and antitumor activities (Santhanam et al., 2013; Mohammadipanah and Wink, 2016). However, the potential of Atacama Desert-Actinobacteria toward bioremediation of pollutants and waste treatment remained underexplored.

As Atacama Desert conditions are too dry to support higher plants and most other photoautotrophic microorganisms, it gathers multiple features to ensure proliferation of primary producers. It has been shown that translucent rocks served as "refuge" for photosynthetic microbial communities, that are capable to colonize the underside of the rocks, where sufficient moisture depending of fog and dew is retained, and light intensities are not lethal. Indeed, hypolithic cyanobacteria are present in small spatially isolated islands on hyper arid Atacama Desert soil (Dong et al., 2007). These hypolithic *Cyanobacteria* communities are composed mainly of the *Chroococcidiopsis* genus, which is one of the most primitive representant of the phylum (Warren-Rhodes et al., 2006). *Chroococcidiopsis* strains are members of the hydrocarbon-degrading biofilms during bioremediation of hydrocarbon pollutants in aquatic environments (Al-Bader et al., 2013). Although Atacama *Cyanobacteria* has not been used in bioremediation processes, the use of xerotolerant bacteria of dry environments is an attractive strategy for bioremediation under hydric resource limitation.

Desertification and the demand for residential space in sites with water availability limitation have caused an increase of pollution in dry environments. Therefore, technologies for the bioremediation of polluted dry sites are required. Bioremediation of oils spills in desert soils has been reported (Godoy-Faúndez et al., 2008; Benyahia and Embaby, 2016). Strategies to alleviate the xeric stress are relevant to improve bioremediation processes in dry environments. Hereby, xerotolerant bacteria play a crucial role for bioremediation of soils in extreme dry conditions.

UV- AND GAMMA-RESISTANT MICROORGANISMS

Ultraviolet (UV) light is radiation with a wavelength between 40 and 400 nm. UV radiation is divided into five different ranges: (i) Vacuum UV (40–190 nm), (ii) Far UV (190–220 nm), (iii) Short-wavelength UVC (220–290 nm), (iv) Medium-wavelength UVB (290–320 nm), and (v) Relatively long-wavelength UVA (320–400 nm) (Marizcurrena et al., 2017). Life without an assured level of radiation is impossible (Pikuta et al., 2007). However, this type of radiation can be one of the most detrimental abiotic factors causing serious damages in organisms at community and cellular levels. On one hand, UV light constrains the microbial diversity and dynamics of ecosystems to only those UV-resistant (micro)organisms. On the other hand, UV radiation can affect cell survival, producing DNA damage and mutations, oxidative stress and protein denaturation (Marizcurrena et al., 2017; Pérez et al., 2017). UVB and UVC are the most harmful radiation to life (Paulino-Lima et al., 2016). UVB causes direct and indirect DNA damage. UVC may cause direct DNA damage by the formation of pyrimidine dimers and pyrimidine photoproducts (Marizcurrena et al., 2017). However, UVC is completely filtered by the atmosphere and does not reach the Earth's surface. UVB is mostly filtered by the atmosphere, but in places where the ozone layer is thinner, the protective filter activity of the atmosphere is progressively reduced, causing a higher penetration of UVB radiation (Yang et al., 2008).

In Chile, several places have exposure to extreme solar radiation levels and high doses of UVB due to the ozone layer hole (Cordero et al., 2016; Paulino-Lima et al., 2016; Pérez et al., 2017). Atacama Desert is characterized by its high altitude, prevalent cloudless conditions, extreme dryness, relatively low columns of ozone and water vapor and intense solar UV radiation (Cordero et al., 2016; Paulino-Lima et al., 2016), which converts this desert in a key region for international astrobiology studies. The microorganisms that are capable of living under these extreme conditions are known as UV resistant extremophiles (Gabani et al., 2014). The study of microorganisms living in these hostile environments is currently focused to gain understanding on the origin of life and early evolution on Earth, to develop models for predicting consequences of future Climate change and to exploit their potential for biotechnological applications (Pérez et al., 2017).

Ultraviolet resistant extremophiles have developed different strategies to resistant UV stress (**Figure 3**). These strategies are related to efficient machinery for DNA-repair, induction of chaperones and active defense against UV-induced oxidative stress (e.g., glutathione accumulation) (Pérez et al., 2017). The capability of these microorganisms to repair DNA damage has been associated to radiation resistance, since it has been suggested that radiotolerant bacteria accumulate high intracellular manganese and reduced iron levels (Pikuta et al., 2007), conferring them resistance to UV radiation (Paulino-Lima et al., 2016). These types of microorganisms are usually polyextremophiles, since it has been noticed that DNA damage that accumulates during desiccation is critical also for desiccation tolerance (Mattimore and Battista, 1996).

Novel species of the genus *Deinococcus* has been isolated, mainly from environments with high UV radiation, such as deserts and arctic zones (Hirsch et al., 2004; Rainey et al., 2005; Bruch et al., 2015; Guerra et al., 2015). Strains isolated from these environments have been proposed as biocatalysts for bioremediation of radioactive waste sites (Daly, 2000; Mrazek, 2002; Ghosal et al., 2005). UV resistant strains of the *Deinococcus* genus have been associated to

radiation resistance (Cox and Battista, 2005). *D. radiodurans* has been engineered for bioremediation of heavy metals and persistent organic pollutants (Daly, 2000; Cox and Battista, 2005). *Deinococcus peraridilitoris* strains KR-196, KR-198 and KR-200t (**Table 1**) were isolated from an arid desert soil collected in the north of Antofagasta, Chile. These isolates showed a high tolerance to ionizing radiation > 10 kGy, radiation even higher than reported for the model *Deinococcus radiodurans* strain R1 (10 kGy) (Cox and Battista, 2005; Rainey et al., 2007). *Deinococcus* sp. UDEC-P1 was isolated in Témpanos Lake, an oligotrophic lake in the Chilean Patagonia (Guerra et al., 2015). Due to their natural resistance to high levels of radiation, *Deinococcus* species isolated in Chile are potential candidates for bioremediation of radioactive wastes and environments.

High altitude lakes have the potential to be fertile niche for the isolation of novel UV-resistant microorganisms with potential for bioremediation processes. Escudero et al. (2007) have studied the diversity of microorganisms of high lakes Aguas Calientes (5,870 m above sea level) and Licancabur (5,916 m above sea level) located in the Northern Andes of Chile. These areas have high rates of UVB radiation (48.5 MW/cm^2). Analysis of sediments and brine of Aguas Calientes lake show that the microorganisms belong mainly to the phylum *Proteobacteria*, and 70% of the sequences could not be assigned to a phylogenetic group. Licancabur Lake showed a dominance of *Cytophaga–Flavobacteria–Bacteroidetes* and *Proteobacteria*. Plankton analysis of Licancabur Lake shows poor diversity and abundance in water samples, reporting *Cyanobacteria*, *Chrysophyceae*, *Euglenophyta*, and *Chlorophyceae* strains (Albarracín et al., 2015). In spite of these pioneering reports, the microbial communities and UV-resistant microorganisms of Chilean sites with extreme solar radiation levels such as high altitude deserts and lakes and Antarctica are still mainly unknown.

PSYCHROPHILES

Psychrophiles refer to microbes that are capable to grow at temperatures ranging from −20 to 20°C, with an optimal growth temperature of <15°C (Morita, 1975; Clarke et al., 2013). Psychrophilic bacteria possess diverse molecular mechanisms to survive at low temperatures (**Figure 3**). On one side, an increase of unsaturated fatty acids, cyclopropane-containing fatty acids and short chain fatty acids in membranes prevents the loss of membrane fluidity (Feller and Gerday, 2003; D'Amico et al., 2006). A second mechanisms is the high synthesis of cold-shock proteins (CSPs) and chaperones that protect the synthesis of RNA and proteins (Godin-Roulling et al., 2015). A third mechanism is the synthesis of anti-freeze proteins (AFPs) that binds to ice crystals and generates a state of thermal hysteresis (Kristiansen and Zachariassen, 2005; Muñoz et al., 2017). A fourth mechanism is the accumulation of mannitol and other compatible solutes as cryo-protectants to prevent cell damage by UV radiation. An additional mechanism is the transport of compatible solutes such as mannitol to stabilize the cytoplasmatic environment and prevent ice formation (Baraúna et al., 2017). Nevertheless, the most general mechanism is the adaptation of psychrophilic enzymes through inherent modifications of their primary structure. Some of these amino acid changes are minimal in comparison with mesophilic proteins, playing a role in catalytic regions or stabilization of the proteins (Feller and Gerday, 2003; D'Amico et al., 2006; Cavicchioli et al., 2011).

In Chile, psychrophiles have been isolated from several cold environments, such as the high mountains of Los Andes Mountain, vast ice regions, such as the Northern and Southern Ice Field, Southern extreme zones, such as the Patagonia, and the Antarctic continent. Antarctica became a subject of intense research in several fields, including the exploration of novel microbes and their pigments, antibiotics and enzymes. The development of special research programs that supports long-timed expedition logistics have facilitated the access of researchers and increase the research on the Antarctica (Loperena et al., 2012; Órdenes-Aenishanslins et al., 2016; Lavin et al., 2017). However, in-depth research conducted on psychrophiles in cold environments, such as a report in Alpine glacier (Ferrario et al., 2017), remain to be conducted.

Antarctica plays also a huge role in two mainstream research topics, global Climate change and global contamination assessment. The pollution in Antarctica is partly explained by the grasshopper effect: pollutants are moved across the globe in the atmosphere without suffering major changes and are later deposited in continuous-forming ice sheets across Antarctica surface. Other pollution source on Antarctica resides on human activity from military and scientific bases (ASOC, 2007). The detection of diverse organic and inorganic contaminants in Antarctic territory is of increasing concern. Since Antarctica is a region where the introduction of foreign microorganisms is forbidden, the only strategy for bioremediation processes is the application of native microbes (Poland et al., 2003; Gran-Scheuch et al., 2017).

Bacteria capable to degrade crude oil at low temperatures even below the freezing point have been reported (Gerdes et al., 2005; Bowman and Deming, 2014). Alkane hydroxylases are key enzymes for the degradation of alkanes, activating them through conversion into alcohols (van Beilen and Funhoff, 2007; Fuentes et al., 2014). A survey of alkane hydroxylases genes in psychrophilic bacteria reveals the adaptability of these proteins, giving valuable insights on the degradation of long chain hydrocarbons at low temperature. Mostly enzymes were related to the AlkB and cytochrome P450 alkane hydroxylases, but also LadA and AlmA enzymes involved in long-chain alkanes degradation were reported (Bowman and Deming, 2014). The primary structure of psychrophile enzymes differ from their mesophile homologs in the preferences for specific amino acids and increased flexibility on loops, bends, and α-helices. Notably, various novel genes were reported from *Psychrobacter, Octadecabacter, Glaciecola, Terriglobus and Photobacter* genera (Bowman and Deming, 2014). Obligated hydrocarbonoclastic microorganisms (i.e., microbes that use exclusively hydrocarbons as carbon sources) isolated near to Antarctic coast have been described. For example, *Oleispira antarctica*, whose genome

reveals a diversity of alkane degradation genes and a system of proteins that acts as cold barrier to circumvent low temperature effects that could stop hydroxylase reaction (Kube et al., 2013).

Studies performed in the Chilean Antarctic territory are mainly focused on Fildes Peninsula, where the human activity in scientific and military bases had caused several contamination events, including hydrocarbon spills. The estimation of the polluted area impacted is about 3.5 km^2, corresponding to 12% of the total area of the Peninsula (ASOC, 2007). However, bioremediation plans for these sites have not yet been reported. Remarkably, the hydrocarbon degradation potential of native microorganisms from the near Argentinian Carlini Station has been described. *Polaromonas naphthalenivorans*, a strain capable of naphthalene degradation and N_2 fixation, and strains belonging to *Nocardioides* genus were dominant in soils with higher hydrocarbon pollution (Vázquez et al., 2017). The hydrocarbonoclastic strains *Rhodococcus* sp. D32AFA, *Pseudomonas* sp. E43FB and *Sphingobium* sp. D43FB that degrade phenanthrene were isolated from diesel contaminated Antarctic soils (Gran-Scheuch et al., 2017). The Antarctic soil strain *Streptomyces* sp. So3.2 is able to produce a biosurfactant, which may be useful for hydrocarbon bioremediation (Lamilla et al., 2018).

Psychrophiles seem to be naturally adapted to cope with a wide-range of heavy metals in the environment (De Souza et al., 2006; Tomova et al., 2015; Gonzalez-Aravena et al., 2016). This adaptive trait may be explained by the presence of heavy metals in Antarctica's sediments. In addition a high occurrence of plasmids in Antarctic bacteria has been reported, which are probably related to the transfer of resistance/tolerance genes to heavy metals such as mercury, tellurium, cadmium, copper, chromium, and lead (Mangano et al., 2013; Gonzalez-Aravena et al., 2016; Rodriguez-Rojas et al., 2016a). Interestingly, a high proportion of these bacterial isolates are multiple heavy metal-resistant bacteria. Mercury- and tellurite-resistant strains were isolated from Greenwich Island (Rodriguez-Rojas et al., 2016b). *Pseudomonas putida* strain ATH-43 (**Figure 2** and **Table 2**) revealed high tolerance to cadmium, copper, chromium, and selenium, whereas *Psychrobacter* sp. ATH-62 is resistant to mercury and tellurite (Rodriguez-Rojas et al., 2016a). Heavy metal-resistant bacteria were also isolated from invertebrates from the Antarctic shores. Mercury-resistant *Pseudoalteromonas* sp. gw196 and *Colwellia* sp. gw172, and zinc and cadmium-resistant *Arthrobacter* and *Psychrobacter* strains were isolated from a marine sponge (Mangano et al., 2013). *Flavobacterium* and *Psychrobacter* strains with resistance to mercury and zinc were isolated from a sea urchin (Gonzalez-Aravena et al., 2016).

Antarctic bacteria have been also studied for additional biotechnological applications. An Antarctic psychrophilic *Pseudomonas* strain was able to produce quantum dots from Cd salts (Gallardo et al., 2014). A psychrophilic *Pseudomonas mandelli* able to produce alginate has also been reported (Bayat et al., 2015; Vasquez-Ponce et al., 2017). Alginate is useful to encapsulate microbes to improve the bioremediation of persistent organic pollutants such as pesticides in polluted soils (Morgante et al., 2010). Encapsulation of microbes in alginate beads may prevent stress or predation of the inocula (Morgante et al., 2010).

The diversity of bacteria from the Antarctica that showed wide range heavy metal resistance and hydrocarbon degradation capabilities revealed a complex community that include adapted cosmopolitan bacteria such as *Pseudomonas* and other native strains, which may be useful for bioremediation in cold environments.

CONCLUDING REMARKS AND FUTURE PERSPECTIVES

Chile has been referred to be a "biogeographic island" due to a succession of natural barriers, including Altiplano, Atacama Desert, Los Andes Mountains, South Pacific Ocean, Patagonia, and Antarctica. Geological processes and climatic conditions have driven the current geography of Chile into a set of diverse ecosystems that reassemble heaven for both extremophilic and polyextremophilic microorganisms. Those biotopes include a multiplicity of ecosystems with more than one extreme environmental condition, such a high salinity, low humidity, high UV radiation, high or low temperature, high or low pH, and high concentration of heavy metals. These extreme environmental conditions exert a strong pressure limiting the biodiversity of each niche, since every condition is associated with its own set of adaptations for stability on its environment. At specie-level, microbes that are capable to persist in such (multi) extreme conditions gather (multiple) metabolic capabilities that are not present in mesophilic microbes, and thus, represent a great potential for biotechnological and environmental applications (Liu et al., 2018). At an ecological level, it has been previously shown that microbial communities in extreme environments evolved at a faster rate than mesophiles living in benign environments, highlighting particularities of the evolutionary dynamic of such environments (Li et al., 2014). For these reasons, diverse research efforts have been initially focused on analyzing natural microbial communities of those sites and studying physiological and genomic characteristics of the microbial isolates.

Next generation sequencing (NGS) and next generation proteomics (NGPs) provide powerful techniques to gain insights about the molecular mechanisms involved in microbial adaptation to extreme conditions (Armengaud, 2016). These type of studies and methods will reveal the mechanisms and strategies used by microbes to adapt to extreme conditions and are useful to understand the evolution of microorganisms subjected to extreme conditions.

In recent years, there are significant advances in the field of extremophiles at the global level. Similar trend has also been reported by researchers from Chile, whose discoveries have made the field to flourish. This progress relied upon the advances of physico-chemical characterization of those biotopes together with the advent of high-throughput molecular tools to understand the complexity of microbial communities and improved tools and techniques for microbial isolation. Many of those studies have gained significant insights on the

molecular mechanisms involved in extremophiles' adaptations to extreme environments and their co-evolutionary processes, and also contributed to current biotechnological developments, such as Swissaustral, a company with headquarters in Chile, which performs functional enzymatic screening for industrial and biotechnological applications (Blamey et al., 2017). Additional research efforts must be invested into broadening the taxonomic breadth of extremophiles and expanding towards the study of extremolyes, metabolites utilized as biological defense mechanisms to combat extreme environmental stresses (such as ectoine).

The restoration of polluted environment is a crucial task for sustainable development. For the clean up of polluted sites, bioremediation is an attractive alternative to physico-chemical treatment processes. Microbes are main catalysts for the bioremediation of polluted environments. Extremophiles has been isolated in diverse zones in Chile that possess extreme conditions such as Altiplano, Atacama Desert, Central Chile, Patagonia, and Antarctica. Interestingly, the remarkable adaptative capabilities of extremophiles convert these organisms into an attractive source of catalysts for bioremediation and industrial processes.

Future research will carry out more detailed studies on extremophiles already described in order to deepen their knowledge and optimize their use in industrial processes including bioremediation. On the other side, a large number of extreme environments in Chile are still unexplored or underexplored. These habitats harbor microbial communities with metabolic capabilities useful for bioremediation processes and other applications. Therefore, future research should focus on the isolation, identification and characterization of a higher number of extremophiles from ecosystems with extreme conditions. Thereafter, studies should explore the metabolic potential of microbial isolates for application in biotechnology including the bioremediation of heavy metals and persistent organic pollutants. The basic research on extremophiles combined with the scale up of the biotechnological process including bioremediation and waste treatments will offer a bright future to Chilean economy and an increasing welfare to its inhabitants.

DEDICATION

This article is dedicated to the memory of Professor Dr. Burkhard Seeger Stein (1929–2016), who inspired the study of natural resources in Chile through his pioneering research and teaching.

AUTHOR CONTRIBUTIONS

RO, CM, GB, FD, AC, RV, CR, and MS wrote and discussed the article.

ACKNOWLEDGMENTS

The authors gratefully acknowledge Pedro Serrano, Alejandra Pemjean, Enrique Bialoskorski, Michael Seeger, and Sebastian Fuentes for the landscape photographies shown in **Figure 1**. The authors acknowledge Conicyt Ph.D. fellowships (CM, FD, and GB) and financial support of CONICYT Programa de Investigación Asociativa (PIA) Anillo ACT172128 GAMBIO (MS), FONDECYT 1151174 (http://www.fondecyt.cl) (MS), USM (http://www.usm.cl) (MS), CONICYT/PAI Concurso Nacional de Apoyo al Retorno de Investigadores desde el Extranjero 82140028 (http://www.conicyt.cl) (RO and MS), and Apoyo a la Formación de Redes Internacionales para Investigadores en Etapa Inicial 170600 (http://www.conicyt.cl) (RO and MS). The funders had no role in study design, data collection and analyses, decision to publish, or preparation of the manuscript.

REFERENCES

Abatzopoulos, T., Kappas, I., Beardmore, J., Clegg, J. S., and Sorgeloos, P. (2002). *Artemia: Basic and Applied Biology*. Dorcrecht: Kluwer Academic Publishers. doi: 10.1007/978-94-017-0791-6

Acosta, M., Galleguillos, P. A., Guajardo, M., and Demergasso, C. (2017). Microbial survey on industrial bioleaching heap by high-throughput 16S sequencing and metagenomics analysis. *Solid State Phenom*. 266, 219–223. doi: 10.4028/www.scientific.net/SSP.262.219

Aguayo, P., Gonzáles, P., Campos, V., Maugeri, T. L., Papale, M., Gugliandolo, C., et al. (2017). Comparison of prokaryotic diversity in cold, oligotrophic remote lakes of Chilean Patagonia. *Curr. Microbiol.* 74, 598–613. doi: 10.1007/s00284-017-1209-y

Aguilar, A., Ingemansson, T., and Magniea, E. (1998). Extremophile microorganisms as cell factories: support from the European Union. *Extremophiles* 2, 367–373. doi: 10.1007/s007920050080

Ahring, B. K. (1995). Methanogenesis in thermophilic biogas reactors. *Antonie Van Leeuwenhoek* 67, 91–102. doi: 10.1007/BF00872197

Al-Bader, D., Kansour, M. K., Rayan, R., and Radwan, S. S. (2013). Biofilm comprising phototrophic, diazotrophic, and hydrocarbon-utilizing bacteria: a promising consortium in the bioremediation of aquatic hydrocarbon pollutants. *Environ. Sci. Pollut. Res. Int.* 20, 3252–3262. doi: 10.1007/s11356-012-1251-z

Albarracín, V. H., Kurth, D., Ordoñez, O. F., Belfiore, C., Luccini, E., Salum, G. M., et al. (2015). High-Up: a remote reservoir of microbial extremophiles in Central Andean wetlands. *Front. Microbiol.* 6:1404. doi: 10.3389/fmicb.2015.01404

Alcamán, M. E., Alcorta, J., Bergman, B., Vásquez, M., Polz, M., and Díez, B. (2017). Physiological and gene expression responses to nitrogen regimes and temperatures in *Mastigocladus* sp. strain CHP1, a predominant thermotolerant cyanobacterium of hot springs. *Syst. Appl. Microbiol.* 40, 102–113. doi: 10.1016/j.syapm.2016.11.007

Alcamán, M. E., Fernández, C., Delgado, A., Bergman, B., and Díez, B. (2015). The cyanobacterium *Mastigocladus* fulfills the nitrogen demand of a terrestrial hot spring microbial mat. *ISME J.* 9. 2290–2303. doi: 10.1038/ismej.2015.63

Alvarez, A., Saez, J. M., Costa, J. S. D., Colin, V. L., Fuentes, M. S., Cuozzo, S. A., et al. (2017). Actinobacteria: current research and perspectives for bioremediation of pesticides and heavy metals. *Chemosphere* 166, 41–62. doi: 10.1016/j.chemosphere.2016.09.070

Amaro, A. M., Chamorro, D., Seeger, M., Arredondo, R., Peirano, I., and Jerez, C. A. (1991). Effect of external pH perturbations on in vivo protein synthesis by the acidophilic bacterium *Thiobacillus ferrooxidans*. *J. Bacteriol.* 173, 910–915. doi: 10.1128/jb.173.2.910-915.1991

Antranikian, G., Vorgias, C. E., and Bertoldo, C. (2005). Extreme environments as a resource for microorganisms and novel biocatalysts. *Adv. Biochem. Eng. Biotechnol.* 96, 219–262. doi: 10.1007/b135786

Armengaud, J. (2016). Next-generation proteomics faces new challenges in environmental biotechnology. *Curr. Opin. Biotechnol.* 38, 174–182. doi: 10.1016/j.copbio.2016.02.025

Armijo, R., Lacassin, R., Coundurier-Curveur, A., and Carrizo, D. (2015). Coupled tectonic evolution of Andean orogeny and global climate. *Earth Sci. Rev.* 143, 1–35. doi: 10.1016/j.earscirev.2015.01.005

Arulazhagan, P., Al-Shekri, K., Huda, Q., Godon, J. J., Basahi, J. M., and Jeyakumar, D. (2017). Biodegradation of polycyclic aromatic hydrocarbons by an acidophilic *Stenotrophomonas maltophilia* strain AJH1 isolated from a mineral mining site in Saudi Arabia. *Extremophiles* 21, 163–174. doi: 10.1007/s00792-016-0892-0

ASOC (2007). Implementation the Madrid Protocol: a case study of Fildes Peninsula, King George Island. *Paper Presented at the XXX Antarctic Treaty Consultative Meeting, 30 April – 11 May 2007*, New Delhi.

Asta, M. P., Cama, J., Martínez, M., and Giménez, J. (2009). Arsenic removal by goethite and jarosite in acidic conditions and its environmental implications. *J. Hazard. Mater.* 171, 965–972. doi: 10.1016/j.jhazmat.2009.06.097

Azua-Bustos, A., Caro-Lara, L., and Vicuña, R. (2015). Discovery and microbial content of the driest site of the hyperarid Atacama Desert, Chile. *Environ. Microbiol. Rep.* 7, 388–394. doi: 10.1111/1758-2229.12261

Azua-Bustos, A., and González-Silva, C. (2014). Biotechnological applications derived from microorganisms of the Atacama Desert. *Biomed. Res. Int.* 2014:909312. doi: 10.1155/2014/909312

Azua-Bustos, A., González-Silva, C., and Corsini, G. (2017). The hyperarid core of the Atacama Desert, an extremely dry and carbon deprived habitat of potential interest for the field of carbon science. *Front. Microbiol.* 8:993. doi: 10.3389/fmicb.2017.00993

Ballantyne, J. M., and Moore, J. N. (1988). Arsenic geochemistry in geothermal systems. *Geochim. Cosmochim. Acta* 52, 475–483. doi: 10.1016/0016-7037(88)90102-0

Baraúna, R. A., Freitas, D. Y., Pinheiro, J. C., Folador, A. R. C., and Silva, A. (2017). A proteomic perspective on the bacterial adaptation to cold: integrating OMICs data of the psychrotrophic bacterium *Exiguobacterium antarcticum* B7. *Proteomes* 5:E9. doi: 10.3390/proteomes5010009

Barbieri, R., and Cavalazzi, B. (2014). How do modern extreme hydrothermal environments inform the identification of martian habitability? The case of the El Tatio Geyser field. *Challenges* 5:430. doi: 10.3390/challe5020430

Bayat, Z., Hassanshahian, M., and Cappello, S. (2015). Immobilization of microbes for bioremediation of crude oil polluted environments: a mini review. *Open Microbiol. J.* 9, 48–54. doi: 10.2174/1874285801509010048

Benyahia, F., and Embaby, A. S. (2016). Bioremediation of crude oil contaminated desert soil: effect of biostimulation, bioaugmentation and bioavailability in biopile treatment systems. *Int. J. Environ. Res. Public Health* 13:219. doi: 10.3390/ijerph13020219

Beolchini, F., Dell'Anno, A., Rocchetti, L., Vegliò, F., and Danovaro, R. (2009). Biohydrometallurgy as a remediation strategy for marine sediments contaminated by heavy metals. *Adv. Mat. Res.* 71, 669–672. doi: 10.4028/www.scientific.net/AMR.71-73.669

Berendes, F., Gottschalk, G., Heine-Dobbernack, E., Moore, E. R. B., and Tindall, B. J. (1996). *Halomonas desiderata* sp.nov, a new alkaliphilic, halotolerant and denitrifying bacterium isolated from a municipal sewage works. *Microbiology* 19, 158–167. doi: 10.1016/S0723-2020(96)80041-5

Berenguer, J. (2011). "Thermophile," in *Encyclopedia of Astrobiology*, eds M. Gargaud, R. Amils, and J. C. Quintanilla. (Berlin: Springer), 1666–1667. doi: 10.1007/978-3-642-11274-4_1583

Bernard, G., Pathmanathan, J. S., Lannes, R., Lopez, P., and Bapteste, E. (2018). Microbial dark matter investigations: how microbial studies transform biological knowledge and empirically sketch a logic of scientific discovery. *Genome Biol. Evol.* 10, 707–715. doi: 10.1093/gbe/evy031

Bhattacharya, A., Goyal, N., and Gupta, A. (2017). Degradation of azo dye methyl red by alkaliphilic, halotolerant *Nesterenkonia lacusekhoensis* EMLA3: application in alkaline and salt-rich dyeing effluent treatment. *Extremophiles* 21, 479–490. doi: 10.1007/s00792-017-0918-2

Blamey, J. M., Fischer, F., Meyer, H. P., Sarmiento, F., and Zinn, M. (2017). "Chapter 14: enzymatic biocatalysis in chemical transformations: a promising and emerging field in green chemistry practice," in *Biotechnology of Microbial Enzymes* ed. G. Brahmachari (London: Elsevier Science).

Bonfá, M. R. L., Grossman, M. J., Mellado, E., and Durrant, L. R. (2011). Biodegradation of aromatic hydrocarbons by Haloarchaea and their use for the reduction of the chemical oxygen demand of hypersaline petroleum produced water. *Chemosphere* 84, 1671–1676. doi: 10.1016/j.chemosphere.2011.05.005

Bose, J., Rodrigo-Moreno, A., and Shabala, S. (2014). ROS homeostasis in halophytes in the context of salinity stress tolerance. *J. Exp. Bot.* 65, 1241–1257. doi: 10.1093/jxb/ert430

Bowman, J. S., and Deming, J. W. (2014). Alkane hydroxylase genes in psychrophile genomes and the potential for cold active catalysis. *BMC Genomics* 15:1120. doi: 10.1186/1471-2164-15-1120

Bravo, G. (2017). *Bioremediation of Mercury Polluted Agricultural Soils Using Cupriavidus Metallidurans MSR33 in a Rotary Drum Reactor and its Effects on Microorganisms Involved in the Nitrogen Cycle*. Ph.D. thesis, Universidad Técnica Federico Santa María, Pontificia Universidad Católica de Valparaíso, Valparaíso.

Brock, T. D., Brock, K. M., Belly, R. T., and Weiss, R. L. (1972). *Sulfolobus*: a new genus of sulfur-oxidizing bacteria living at low pH and high temperature. *Arch. Microbiol.* 84, 54–68. doi: 10.1007/BF00408082

Browne, R. A. (1980). Acute response versus reproductive performance in five strains of brine shrimp exposed to copper sulphate. *Mar. Environ. Res.* 3, 185–193. doi: 10.1016/0141-1136(80)90026-4

Bruch, E. M., De Groot, A., Un, S., and Tabares, L. C. (2015). The effect of gamma-ray irradiation on the Mn (II) speciation in *Deinococcus radiodurans* and the potential role of Mn (II)-orthophosphates. *Metallomics* 7, 908–916. doi: 10.1039/C5MT00009B

Bull, A. T., and Asenjo, J. A. (2013). Microbiology of hyper-arid environments: recent insights from the Atacama Desert, Chile. *Antonie Van Leeuwenhoek* 103, 1173–1179. doi: 10.1007/s10482-013-9911-7

Bustos, S., Castro, S., and Montealegre, R. (1993). The Sociedad Minera Pudahuel bacterial thin-layer leaching process at Lo Aguirre. *FEMS Microbiol. Rev.* 11, 231–235. doi: 10.1111/j.1574-6976.1993.tb00289.x

Cabrera, G., Viera, M., Gomez, J. M., Cantero, D., and Donati, E. (2007). Bacterial removal of chromium (VI) and (III) in a continuous system. *Biodegradation* 18, 505–513. doi: 10.1007/s10532-006-9083-5

Campos, V. L., Escalante, G., Yañez, J., Zaror, C. A., and Mondaca M. A. (2009). Isolation of arsenite-oxidizing bacteria from a natural biofilm associated to volcanic rocks of Atacama Desert, Chile. *J. Basic Microbiol.* 49, S93–S97. doi: 10.1002/jobm.200900028

Campos, V. L., Valenzuela, C., Yarza, P., Kämpfer, P., Vidal, R., Zaror, C., et al. (2010). *Pseudomonas arsenicoxydans* sp nov., an arsenite-oxidizing strain isolated from the Atacama desert. *Syst. Appl. Microbiol.* 33, 193–197. doi: 10.1016/j.syapm.2010.02.007

Canganella, F., and Wiegel, J. (2011). Extremophiles: from abyssal to terrestrial ecosystems and possibly beyond. *Naturwissenschaften* 98, 253–279. doi: 10.1007/s00114-011-0775-2

Carrillo, U., Díaz-Villanueva, V., and Modenutti, B. (2018). Sustained effects of volcanic ash on biofilm stoichiometry, enzyme activity and community composition in North-Patagonia streams. *Sci. Total Environ.* 621, 235–244. doi: 10.1016/j.scitotenv.2017.11270

Castillo-Carvajal, L. C., Sanz-Martín, J. L., and Barragán-Huerta, B. E. (2014). Biodegradation of organic pollutants in saline wastewater by halophilic microorganisms: a review. *Environ. Sci. Pollut. Res.* 21, 9578–9588. doi: 10.1007/s11356-014-3036-z

Castro-Severyn, J., Remonsellez, F., Valenzuela, S. L., Salinas, C., Fortt, J., Aguilar, P., et al. (2017). Comparative genomics analysis of a new *Exiguobacterium* strain from Salar de Huasco reveals a repertoire of stress-related genes and arsenic resistance. *Front. Microbiol.* 8:456. doi: 10.3389/fmicb.2017.00456

Cavicchioli, R., Charlton, T., Ertan, H., Omar, S. M., Siddiqui, K. S., and Williams, T. J. (2011). Biotechnological uses of enzymes from psychrophiles. *Microb. Biotechnol.* 4, 449–460. doi: 10.1111/j.1751-7915.2011.00258.x

Chakravarty, R., and Banerjee, P. C. (2012). Mechanism of cadmium binding on the cell wall of an acidophilic bacterium. *Bioresour. Technol.* 108, 176–183. doi: 10.1016/j.biortech.2011.12.100

Chatterjee, S. K., Bhattacharjee, I., and Chandra, G. (2010). Biosorption of heavy metals from industrial waste water by *Geobacillus thermodenitrificans*. *J. Hazard. Mater.* 175, 117–125. doi: 10.1016/j.jhazmat.2009.09.136

Chen, G. Q., and Jiang, X. R. (2018). Next generation industrial biotechnology based on extremophilic bacteria. *Curr. Opin. Biotechnol.* 50, 94–100. doi: 10.1016/j.copbio2017.11.016

Chong, G. (1984). Die Salatre in Nordchile – Geologie. *Struk. Geochim. Goetekt Forschung* 67:146.

Christel, S., Herold, M., Bellenberg, S., El Hajjami, M., Buetti-Dinh, A., Pivkin, I. V., et al. (2018). Multiomics reveals the lifestyle of the acidophilic, mineral-oxidizing model species *Leptospirillum ferriphilum* T. *Appl. Environ. Microbiol.* doi: 10.1128/AEM.02091-17 [Epub ahead of print].

Christen, P., Davidson, S., Combet-Blanc, Y., and Auria, R. (2011). Phenol biodegradation by the thermoacidophilic archaeon *Sulfolobus solfataricus* 98/2 in a fed-batch bioreactor. *Biodegradation* 22, 475–484. doi: 10.1007/s10532-010-9420-6

Christen, P., Vega, A., Casalot, L., Simon, G., and Auria, R. (2012). Kinetics of aerobic phenol biodegradation by the acidophilic and hyperthermophilic archaeon *Sulfolobus solfataricus* 98/2. *Biochem. Eng. J.* 62, 56–61. doi: 10.1016/j.bej.2011.12.012

Cirés, S., Casero, M. C., and Quesada, A. (2017). Toxicity at the edge of life: a review on cyanobacterial toxins from extreme environments. *Mar. Drugs* 15:233 doi: 10.3390/md15070233

Clarke, A., Morris, G. J., Fonseca, F., Murray, B. J., Acton, E., and Price, H. C. (2013). A low temperature limit for life on Earth. *PLoS One* 8:e66207. doi: 10.1371/journal.pone.0066207

Claverías, F. P., Undabarrena, A., González, M., Seeger, M., and Cámara, B. (2015). Culturable diversity and antimicrobial activity of Actinobacteria from marine sediments in Valparaíso bay, Chile. *Front. Microbiol.* 28:737. doi: 10.3389/fmicb.2015.00737

Connon, S. A., Lester, E. D., Shafaat, H. S., Obenhuber, D. C., and Ponce, A. (2007). Bacterial diversity in hyperarid Atacama Desert soils. *J. Geophys. Res. Biogeosci.* 112:G04S17. doi: 10.1029/2006JG000311

Cordero, R. R., Damiani, A., Seckmeyer, G., Jorquera, J., Caballero, M., Rowe, P., et al. (2016). The solar spectrum in the Atacama Desert. *Sci. Rep.* 6:22457. doi: 10.1038/srep22457

Correa-Llantén, D. N., Muñoz-Ibacache, S. A., Castro, M. E, Muñoz, P. A., and Blamey, J. M. (2013). Gold nanoparticles synthesized by *Geobacillus* sp. strain ID17 a thermophilic bacterium isolated from Deception Island, Antarctica. *Microb. Cell Fact.* 12:75. doi: 10.1186/1475-2859-12-75

Corti Monzón, G., Nisenbaum, M., Herrera Seitz, K., and Murialdo, S. E. (2018). New findings on aromatic compounds degradation and their metabolic pathways, the biosurfactant production and motility of the halophilic bacterium *Halomonas* sp. KHS3. *Curr. Microbiol.* 75, 1108–1118. doi: 10.1007/s00284-018-1497-x

Cox, M., and Battista, J. (2005). *Deinococcus radiodurans* - the consummate survivor. *Nat. Rev. Microbiol.* 3, 882–892. doi: 10.1038/nrmicro1264

Crits-Christoph, A., Robinson, C. K., Barnum, T., Fricke, W. F., Davila, A. F., Jedynak, B., et al. (2013). Colonization patterns of soil microbial communities in the Atacama Desert. *Microbiome* 1:28. doi: 10.1016/j.syapm.2010.02.007

Cui, Y. W., Zhang, H. Y., Ding, J. R., and Peng, Y. Z. (2016). The effect of salinity on nitrification using halophilic nitrifiers in a sequencing batch reactor treating hypersaline wastewater. *Sci. Rep.* 6:24825. doi: 10.1038/srep24825

Daly, J. M. (2000). Engineering radiation-resistant bacteria for environmental biotechnology. *Curr. Opin. Biotechnol.* 11, 280–285. doi: 10.1016/S0958-1669(00)00096-3

D'Amico, S., Collins, T., Marx, J. C., Feller, G., and Gerday, C. (2006). Psychrophilic microorganisms: challenges for life. *EMBO Rep.* 7, 385–389. doi: 10.1038/sj.embor.7400662

Darkwah, L., Rowson, N. A., and Hewitt, C. J. (2005). Laboratory scale bioremediation of acid mine water drainage from a disused tin mine. *Biotechnol. Lett.* 27, 1251–1257. doi: 10.1007/s10529-005-3201-z

De Los Rios-Escalante, P., and Gajardo, G. (2010). Potential heterogeneity in crustacean zooplankton assemblages in southern Chilean saline lakes. *Braz. J. Biol.* 70, 1031–1032. doi: 10.1590/S1519-69842010000500016

De Souza, M. J., Nair, S., Loka Bharathi, P. A., and Chandramohan, D. (2006). Metal and antibiotic-resistance in psychrotrophic bacteria from Antarctic Marine waters. *Ecotoxicology* 15, 379–384. doi: 10.1007/s10646-006-0068-2

Deive, F. J., Domínguez, A., Barrio, T., Mosocoso, F., Morán, P., Longo, M. A., et al. (2010). Decolorization of dye reactive black 5 by newly isolated thermophilic microorganisms from geothermal sites in Galicia (Spain). *J. Hazard. Mater.* 182, 735–742. doi: 10.1016/j.jhazmat.2010.06.096

Demergasso, C., Casamayor, E. O., Chong, G., Galleguillos, P., Escudero, L., and Pedrós-Alío, C. (2004). Distribution of prokaryotic genetic diversity in athalassohaline lakes of the Atacama Desert, Northern Chile. *FEMS Microbiol. Ecol.* 48, 57–69. doi: 10.1016/j.femsec.2003.12.013

Demergasso, C., Galleguillos, F., Soto, P., Serón, M., and Iturriaga, V. (2010). Microbial succession during a heap bioleaching cycle of low grade copper sulfides: does this knowledge mean a real input for industrial process design and control? *Hydrometallurgy* 104, 382–390. doi: 10.1016/j.hydromet.2010.04.016

Demergasso, C. S., Castillo, D., and Casamayor, E. O. (2005). Molecular characterization of microbial populations in a low-grade copper ore bioleaching test heap. *Hydrometallurgy* 80, 241–253. doi: 10.1016/j.hydromet.2005.07.013

Demergasso, C. S., Chong, D. G., Escudero, G. L., Mur, J. J. P., and Pedrós-Alió, C. (2007). Microbial precipitation of arsenic sulfides in Andean salt flats. *Geomicrobiol. J.* 24, 111–123. doi: 10.1080/01490450701266605

Dennett, G. V., and Blamey, J. M. (2016). A new thermophilic nitrilase from an antarctic hyperthermophilic microorganism. *Front. Bioeng. Biotechnol.* 4:5. doi: 10.3389/fbioe.2016.00005

Diaby, N., Dold, B., Pfeifer, H. R., Holliger, C., Johnson, D. B., and Hallberg, K. B. (2007). Microbial communities in a porphyry copper tailings impoundment and their impact on the geochemical dynamics of the mine waste. *Environ. Microbiol.* 9, 298–307. doi: 10.1111/j.1462-2920.2006.01138.x

Dong, H., Rech, J. A., Jiang, H., Sun, H., and Buck, B. J. (2007). Endolithic cyanobacteria in soil gypsum: occurrences in Atacama (Chile), Mojave (United States), and Al-Jafr Basin (Jordan) Deserts. *J. Geophys. Res.* 112:G02030. doi: 10.1029/2006JG000385

Dorador, C., Vila, I., Remonsellez, F., Imhoff, J. F., and Witzel, K. P. (2010). Unique clusters of archea in Salar de Huasco, an athalassohaline evaporitic basin of the Chilean Altiplano. *FEMS Microbiol. Ecol.* 73, 291–302. doi: 10.1111/j.1574-6941.2010.00891.x

Dorador, C. I. (2007). *Microbial Communities in High Altitude Altiplanic Wetlands in Northern Chile: Phylogeny, Diversity and Function*. Ph.D. thesis, Christian-Albrechts-Universität, Kiel.

Dorador, C., Busekow, A., Vila, I., Imhoff, J., and Witzel, K. P. (2008). Molecular analysis of enrichment cultures of ammonia oxidizers from the Salar de Huasco, a high altitude saline wetland in northern Chile. *Extremophiles* 12, 405–414. doi: 10.1007/s00792-008-0146-x

Dose, K., Bieger-Dose, A., Ernst, B., Feister, U., Gómez-Silva, B., Klein, A., et al. (2001). Survival of microorganisms under the extreme conditions of the Atacama Desert. *Orig. Life Evol. Biosph.* 31, 287–303. doi: 10.1023/A:1010788829265

Duckworth, A. W., Grant, W. D., Jones, B. E., and Vansteenbergen, R. (1996). Phylogenetic diversity of soda lake alkaliphiles. *FEMS Microbiol. Ecol.* 19, 181–191. ?doi: 10.1016/0168-6496(96)00003-7

Edbeib, M. F., Wahab, R. A., and Huyop, F. (2016). Halophiles: biology, adaptation, and their role in decontamination of hypersaline environments. *World J. Microbiol. Biotechnol.* 32:135. doi: 10.1007/s11274-016-2081-9

Elshahawi, S. I., Shaaban, K. A., Kharel, M. K., and Thorson, J. S. (2015). A comprehensive review of glycosylated bacterial natural products. *Chem. Soc. Rev.* 44, 7591–7697. doi: 10.1039/c4cs00426d

Engel, A. S., Johnson, L. R., and Porter, M. L. (2013). Arsenite oxidase gene diversity among chloroflexi and proteobacteria from El tatio geyser field, Chile. *FEMS Microbiol. Ecol.* 83, 745–756. doi: 10.1111/1574-6941.12030

Escalante, G., Campos, V. L., Valenzuela, C., Yañez, J., Zaror, C., and Mondaca, M. A. (2009). Arsenic resistant bacteria isolated from arsenic contaminated river in the Atacama Desert (Chile). *Bull. Environ. Contam. Toxicol.* 83, 657–661. doi: 10.1007/s00128-009-9868-4

Escudero, L., Chong, G., Demergasso, C., Farías, M. E., Cabrol, N. A., Grin, E., et al. (2007). Investigating microbial diversity and UV radiation impact at the high-altitude Lake Aguas Calientes, Chile. *Proc. SPIE Int. Soc. Opt. Eng.* 6694:66940Z. doi: 10.1117/12.736970

Farhangi-Abriz, S., and Nikpour-Rashidabad, N. (2017). Effect of lignite on alleviation of salt toxicity in soybean (*Glycine max* L.) plants. *Plant Physiol. Biochem.* 120, 186–193. doi: 10.1016/j.plaphy.2017.10.007

Farhangi-Abriz, S., and Torabian, S. (2017). Antioxidant enzyme and osmotic adjustment changes in bean seedlings as affected by biochar under salt stress. *Ecotoxicol. Environ. Saf.* 137, 64–70. doi: 10.1016/j.ecoenv.2016.11.029

Feller, G., and Gerday, C. (2003). Psychrophilic enzymes: hot topics in cold adaptation. *Nat. Rev. Microbiol.* 1, 200–208. doi: 10.1038/nrmicro773

Fernandez-Turiel, J. L., Garcia-Valles, M., Gimeno-Torrente, D., Saavedra-Alonso, J., and Martinez-Manent, S. (2005). The hot spring and geyser sinters of El Tatio, Northern Chile. *Sediment. Geol.* 180, 125–147. doi: 10.1016/j.sedgeo.2005.07.005

Ferrario, C., Pittino, F., Tagliaferri, I., Gandolfi, I., Bestetti, G., Azzoni, R. S., et al. (2017). Bacteria contribute to pesticide degradation in cryoconite holes in an Alpine glacier. *Environ. Pollut.* 230, 919–926. doi: 10.1016/j.envpol.2017.07.039

Finstad, K. M., Probst, A. J., Thomas, B. C., Andersen, G. L., Demergasso, C., Echeverría, A., et al. (2017). Microbial community structure and the persistence of cyanobacterial populations in salt crusts of the hyperarid Atacama Desert from genome-resolved Metagenomics. *Front. Microbiol.* 8:1435. doi: 10.3389/fmicb.2017.01435

Flores, P. A., Amenábar, M. J., and Blamey, J. M. (2013). "Hot environments from Antarctica: source of thermophiles and hyperthermophiles, with potential biotechnological applications," in *Thermophilic Microbes in Environmental and Industrial Biotechnology: Biotechnology of Thermophiles*, eds T. Satyanarayana, J. Littlechild, and Y. Kawarabayasi. (Dordrecht: Springer), 99–118.

Fuentes, S., Barra, B., Caporaso, J. G., and Seeger, M. (2016). From rare to dominant: a fine-tuned soil bacterial bloom during petroleum hydrocarbon bioremediation. *Appl. Environ. Microbiol.* 82, 888–896. doi: 10.1128/AEM.02625-15

Fuentes, S., Méndez, V., Aguila, P., and Seeger, M. (2014). Bioremediation of petroleum hydrocarbons: catabolic genes, microbial communities and applications. *Appl. Microbiol. Biotechnol.* 98, 4781–4794. doi: 10.1007/s00253-014-5684-9

Gabani, P., Prakash, D., and Singh, O. V. (2014). Bio-signature of ultraviolet-radiation-resistant extremophiles from elevated land. *Am. J. Microbiol. Res.* 2, 94–104. doi: 10.12691/ajmr-2-3-3

Gallardo, C., Monrás, J. P., Plaza, D. O., Collao, B., Saona, L. A., Durán-Toro, V., et al. (2014). Low-temperature biosynthesis of fluorescent semiconductor nanoparticles (CdS) by oxidative stress resistant Antarctic bacteria. *J. Biotechnol.* 187, 108–115. doi: 10.1016/j.jbiotec.2014.07.017

Galleguillos, P., Remonsellez, F., Galleguillos, F., Guiliani, N., Castillo, D., and Demergasso, C. (2008). Identification of differentially expressed genes in an industrial bioleaching heap processing low-grade copper sulphide ore elucidated by RNA arbitrarily primed polymerase chain reaction. *Hydrometallurgy* 94, 148–154. doi: 10.1016/j.hydromet.2008.05.031

García, M. T., Mellado, E., Ostos, J. C., and Ventosa, A. (2004). *Halomonas organivorans* sp. nov. a moderate halophile able to degrade oarmatic compound. *Int. Syst. Evol. Microbiol.* 54, 1723–1728. doi: 10.1099/ijs.0.63114-0

Gargarello, R. M., Di Gregorio, D., Huck, H., Fernandez Niello, J., and Curutchet, G. (2010). Reduction of uranium (VI) by *Acidithiobacillus thiooxidans* and *Acidithiobacillus ferrooxidans*. *Hydrometallurgy* 104, 529–532. doi: 10.1016/j.hydromet.2010.03.032

Gavrilescu, M. (2010). Environmental biotechnology: achievement, opportunities and challenges. *Dyn. Biochem. Process. Biotechnol. Mol. Biol.* 4, 1–36.

Gerdes, B., Brinkmeyer, R., Dieckmann, G., and Helmke, E. (2005). Influence of crude oil on changes of bacterial communities in Arctic sea-ice. *FEMS Microbiol. Ecol.* 53, 129–139. doi: 10.1016/j.femsec.2004.11.010

Ghosal, D., Omelchenko, M. V., Gaidamakova, E. K., Matrosova, V. Y., Vasilenko, A., Venkateswaran, A., et al. (2005). How radiation kills cells: survival of *Deinococcus radiodurans* and *Shewanella oneidensis* under oxidative stress. *FEMS Microbiol. Rev.* 29, 361–375. doi: 10.1016/j.femsre.2004.12.007

Glennon, A., and Pfaff, R. M. (2003). The extraordinary thermal activity of the El Tatio geysers, Antofagasta Province, Chile. *GOSA Trans.* 8, 31–78.

Godin-Roulling, A., Schmidpeter, P. A., Schmid, F. X., and Feller, G. (2015). Functional adaptations of the bacterial chaperone trigger factor to extreme environmental temperatures. *Environ. Microbiol.* 17, 2407–2420. doi: 10.1111/1462-2920.12707

Godoy-Faúndez, A., Antizar-Ladislao, B., Reyes-Bozo, L., Camano, A., and Sáez-Navarrete, C. (2008). Bioremediation of contaminated mixtures of desert mining soil and sawdust with fuel oil by aerated in-vessel composting in the Atacama Region (Chile). *J. Hazard. Mater.* 151, 649–657. doi: 10.1016/j.jhazmat.2007.06.038

Gonzalez-Aravena, M., Urtubia, R., Del Campo, K., Lavín, P., Wong, C. M. V., Cárdenas, C. A., et al. (2016). Antibiotic and metal resistance of cultivable bacteria in the Antarctic sea urchin. *Antarct. Sci.* 28, 261–268. doi: 10.1017/S0954102016000109

González-Domenech, C. M., Béjar, V., Martínez-Checa, F., and Quesada, E. (2008). *Halomonas nitroreducens* sp.nov., a novel nitrate- and nitrite-reducing species. *Int. J. Syst. Evol. Microbiol.* 58, 872–876. doi: 10.1099/ijs.0.65415-0

Gran-Scheuch, A., Fuentes, E., Bravo, D. M., Jiménez, J. C., and Pérez-Donoso, J. M. (2017). Isolation and characterization of phenanthrene degrading bacteria from diesel fuel-contaminated Antarctic soils. *Front. Microbiol.* 8:1634. doi: 10.3389/fmicb.2017.01634

Grant, W. D. (2003). "Alkaline environments and biodiversity," in *Extremophiles (Life Under Extreme External Conditions),* ed. C. Gerday (Eolss: Oxford).

Grant, W. D. (2006). "Alkaline environments and biodiversity, in extremophilies," in *Encyclopedia of Life Support Systems (EOLSS). Developed under the Auspices of the UNESCO,* eds G. Charles and G. Nicolas (Eolss: Oxford).

Groth, I., Schumann, P., Rainey, F. A., Martin, K., Schuetze, B., and Augsten, K. (1997). *Bogoriella caseilytica* gen. nov., sp. nov., a new alkaliphilic actinomycete from a soda lake in Africa. *Int. J. Syst. Bacteriol.* 47, 788–794. doi: 10.1099/00207713-47-3-788

Guerra, M., González, K., González, C., Parra, B., and Martínez, M. (2015). Dormancy in *Deinococcus* sp. UDEC-P1 as a survival strategy to escape from deleterious effects of carbon starvation and temperature. *Int. Microbiol.* 18, 189–194. doi: 10.2436/20.1501.01.249

Gutiérrez, M. H., Galand, P. E., Moffat, C., and Pantoja, S. (2015). Melting glacier impacts community structure of bacteria, archea and fungi in a Chilean Patagonia fjord. *Environ. Microbiol.* 17, 3882–3897. doi: 10.1111/1462-2920.12872

Hamamura, N., Olson, S. H., Ward, D. M., and Inskeeo, W. P. (2005). Diversity and functional analysis of bacterial communities associated with natural hydrocarbon seeps in acidic soils at Rainbow Springs, Yellowstone National Park. *Appl. Environ. Microbiol.* 71, 5943–5950. doi: 10.1128/AEM.71.10.5943-5950.2005

Hernández, M., Jia, Z., Conrad, R., and Seeger, M. (2011). Simazine application inhibits nitrification and changes the ammonia-oxidizing bacterial communities in a fertilized agricultural soil. *FEMS Microbiol. Ecol.* 78, 511–519. doi: 10.1111/j.1574-6941.2011.01180.x

Hernández, M., Morgante, V., Ávila, M., Villalobos, P., Miralles, P., González, M., and Seeger, M. (2008a). Novel s-triazine-degrading bacteria isolated from agricultural soils of central Chile for herbicide bioremediation. *Electron. J. Biotechnol.* 11, 1–7. doi: 10.2225/vol11-issue5-fulltext-4

Hernández, M., Villalobos, P., Morgante, V., González, M., Reiff, C., Moore E., and Seeger, M. (2008b). Isolation and characterization of a novel simazine-degrading bacterium from Chilean agricultural soils, *Pseudomonas* sp. MHP41. *FEMS Microbiol. Lett.* 286, 184–190. doi: 10.1111/j.1574-6968.2008.01274.x

Hirsch, P., Gallikowski, C. A., Siebert, J., Peissl, K., Kroppenstedt, R., Schumann, P., et al. (2004). *Deinococcus frigens* sp. nov., *Deinococcus saxicola* sp. nov., and *Deinococcus marmoris* sp. nov., low temperature and draught-tolerating, UV-resistant bacteria from continental Antarctica. *Syst. Appl. Microbiol.* 27, 636–645. doi: 10.1078/0723202042370008

Horikoshi, K. (1999). Alkaliphiles: some applications of their products for biotechnology. *Microbiol. Mol. Biol. Rev.* 63, 735–750.

Hou, Y., Zhang, R., Yu, Z., Huang, L., Liu, Y., and Zhou, Z. (2017). Accelerated azo dye degradation and concurrent hydrogen production in the single-chamber photocatalytic microbial electrolysis cell. *Bioresour. Technol.* 224, 63–68. doi: 10.1016/j.biortech.2016.10.069

Houston, J., and Hartley, A. J. (2003). The central Andean west-slope rainshadow and its potential contribution to the origin of hyper-aridity in the Atacama Desert. *Int. J. Climatol.* 23, 1453–1464. doi: 10.1002/joc.938

Ilyas, S., Lee, J. C., and Kim, B. (2014). Bioremoval of heavy metals from recycling industry electronic waste by a consortium of moderate thermophiles: process development and optimization. *J. Clean. Prod.* 70, 194–202. doi: 10.1016/j.jclepro.2014.02.019

Ivanova, A. E., Kizilova, A. K., Kanat'eva, A. Y., Kravchenko, I. K., Kurganov, A. A., and Belyaev, S. (2013). A hydrocarbon-oxidizing acidophilic thermotolerant bacterial association from sulfur blocks. *Microbiology* 82, 482–489. doi: 10.1134/S0026261713040048

Johnson, D. B. (2008). Biodiversity and interactions of acidophiles: key to understanding and optimizing microbial processing of ores and concentrates. *Trans. Nonferrous Met. Soc. China* 18, 1367–1373. doi: 10.1016/S1003-6326(09)60010-8

Johnson, D. B. (2007). "Physiology and ecology of acidophilic microorganisms,". in *Physiology and Biochemistry of Extremophiles*, eds G. Gerday and N. Glansdorff (Washington, DC: AMS press), 275–270. doi: 10.1128/9781555815813.ch20

Jones, B., and Renaut, R. W. (1997). Formation of silica oncoids around geysers and hot springs at El Tatio, Northern Chile. *Sedimentology* 44, 287–304. doi: 10.1111/j.1365-3091.1997.tb01525.x

Karmanocky, F. J. III, and Benison, K. C. (2016). A fluid inclusion record of magmatic/hydrothermal pulses in acid Salar Ignorado gypsum, northern Chile. *Geofluids* 16, 490–506. doi: 10.1111/gfl.12171

Kataoka, M., Yamaoka, A., Kawasaki, K., Shigeri, Y., and Watanabe, K. (2014). Extraordinary denaturant tolerance of keratinolytic protease complex assemblies produced by Meiothermus ruber H328. *Appl. Microbiol. Biotechnol.* 98, 2973–2980. doi: 10.1007/s00253-013-5155-8

Khalid, A., Kausar, F., Arshad, M., Mahmood, T., and Ahmed, I. (2012). Accelerated decolorization of reactive azo dyes under saline conditions by bacteria isolated from Arabian seawater sediment. *Appl. Microbiol. Biotechnol.* 96, 1599–1606. doi: 10.1007/s00253-012-3877-7

Kolmert, Å., and Johnson, D. B. (2001). Remediation of acidic waste waters using immobilised, acidophilic sulfate-reducing bacteria. *J. Chem. Technol. Biotechnol.* 76, 836–843. doi: 10.1002/jctb.453

Konhauser, K. O., Jones, B., Reysenbach, A. L., and Renaut, R. W. (2003). Hot spring sinters: keys to understanding Earth's earliest life forms. *Can. J. Earth Sci.* 40, 1713–1724. doi: 10.1139/e03-059

Kristiansen, E., and Zachariassen, K. E. (2005). The mechanism by which fish antifreeze proteins cause thermal hysteresis. *Cryobiology* 5, 262–280. doi: 10.1016/j.cryobiol.2005.07.007

Krulwich, T. A. (1995). Alkaliphiles:'basic'molecular problems of pH tolerance and bioenergetics. *Mol. Microbiol.* 15, 403–410. doi: 10.1111/j.1365-2958.1995.tb02253.x

Krulwich, T. A., and Guffanti, A. A. (1989). Alkalophilic bacteria. *Annu. Rev. Microbiol.* 43, 435–463. doi: 10.1146/annurev.mi.43.100189.002251

Krulwich, T. A., Ito, M., Hicks, D. B., Gilmour, R., and Guffanti, A. A. (1998). pH homeostasis and ATP synthesis: studies of two processes that necessitate inward proton translocation in extremely alkaliphilic *Bacillus* species. *Extremophiles* 2, 217–222. doi: 10.1007/s007920050063

Kube, M., Chernikova, T. N., Al-Ramahi, Y., Beloqui, A., Lopez-Cortez, N., Guazzaroni, M. E., et al. (2013). Genome sequence and functional genomic analysisof the oil-degrading bacterium *Oleispira antarctica*. *Nat. Commun.* 4:2156. doi: 10.1038/ncomms3156

Kulp, T. R., Han, S., Saltikov, C. W., Lanoil, B. D., Zargar, K., and Oremland, R. S. (2007). Effects of imposed salinity gradients on dissimilatory arsenate reduction, sulfate reduction, and other microbial processes in sediments from two California soda lakes. *Appl. Environ. Microbiol.* 73, 5130–5137. doi: 10.1128/AEM.00771-07

Lamark, T., Kaasen, I., Eshoo, M. W., Falkenberg, P., McDougall, J., and Strom, A. R. (1991). DNA sequence and analysis of the *bet* genes enconding the osmoregulatory choline-glycine betaine pathway of *Escherichia coli*. *Mol. Microbiol.* 5, 1049–1064. doi: 10.1111/j.1365-2958.1991.tb01877.x

Lamilla, C., Braga, D., Castro, R., Guimarães, C., de Castilho, L. V., Freire, D. M., et al. (2018). *Streptomyces luridus* So3. 2 from Antarctic soil as a novel producer of compounds with bioemulsification potential. *PLoS One* 13:e0196054. doi: 10.1371/journal.pone.0196054

Landrum, J. T., Bennett, P. C., Engel, A. S., Alsina, M. A., Pastén, P. A., and Milliken, K. (2009). Partitioning geochemistry of arsenic and antimony, El Tatio Geyser Field, Chile. *Appl. Geochem.* 24, 664–676. doi: 10.1016/j.apgeochem.2008.12.024

Lara, J., González, L. E., Ferrero, M., Díaz, G. C., Pedrós-Alió, C., and Demergasso, C. (2012). Enrichment of arsenic transforming and resistant heterotrophic bacteria from sediments of two salt lakes in Northern Chile. *Extremophiles* 16, 523–538. doi: 10.1007/s00792-012-0452-1

Lavin, P. L., Yong, S. T., Wong, C. M., and Gonzalez, A. R. (2017). The trade-off between antimicrobial production and growth of an Antartic psychrotroph *Streptomyces sp*. strain INACH3013. *Antarct. Sci*. 29, 427–428. doi: 10.1017/S0954102017000141

Lawson, C. E., and Lücker, S. (2018). Complete ammonia oxidation: an important control on nitrification in engineered ecosystems? *Curr. Opin. Biotechnol.* 50, 158–165. doi: 10.1016/j.copbio.2018.01.015

Lay, W. C. L., Liu, Y., and Fane, A. G. (2010). Impacts of salinity on the performance of high retention membrane bioreactors for water reclamation: a review. *Water Res.* 44, 21–40. doi: 10.1016/j.watres.2009.09.026

Le Borgne, S., Paniagua, D., and Vazquez-Duhalt, R. (2008). Biodegradation of organic pollutants by halophillic Bacteria and Archaea. *J. Mol. Microbiol. Biotechnol.* 15, 74–92. doi: 10.1159/000121323

Lebre, P. H., De Maayer, P., and Cowan, D. A. (2017). Xerotolerant bacteria: surviving through a dry spell. *Nat. Rev. Microbiol.* 15, 285–296. doi: 10.1038/nrmicro.2017.16

Leigh, M. B., Wu, W. M., Cardenas, E., Uhlik, O., Carroll, S., Gentry, T., et al. (2015). Microbial communities biostimulated by ethanol during uranium (VI) bioremediation in contaminated sediment as shown by stable isotope probing. *Front. Environ. Sci. Eng.* 9, 453–464. doi: 10.1007/s11783-014-0721-6

Li, S. J., Hua, Z. S., Huang, L. N., Li, J., Shi, S. H., and Chen, L. X., et al. (2014). Microbial communities evolve faster in extreme environments. *Sci. Rep.* 27:6205. doi: 10.1038/srep06205

Liu, H. L., Chen, B. Y., Lan, Y. W., and Cheng, Y. C. (2004). Biosorption of Zn (II) and Cu (II) by the indigenous *Thiobacillus thiooxidans*. *Chem. Eng. J.* 97, 195–201. doi: 10.1016/S1385-8947(03)00210-9

Liu, Z., Cichocki, N., Bonk, F., Günther, S., Schattenberg, F., Harms, H., Müller, S. (2018). Ecological stability properties of microbial communities assessed by flow cytometry. *mSphere* 3:e00564-17. doi: 10.1128/mSphere.00564-17

Loperena, L., Soria, V., Varela, H., Lupo, S., Bergalli, A., Guigou, M., et al. (2012). Extracellular enzymes produced by microorganisms isolated from maritime Antarctica. *World J. Microbiol. Biotechnol.* 28, 2249–2256. doi: 10.1007/s11274-012-1032-3

López, L., Pozo, C., Rodelas, B., Calvo, C., Juárez, B., Martínez-Toledo, M. V., et al. (2005). Identification of bacteria isolated from an oligotrophic lake with pesticide removal capacities. *Ecotoxicology* 14, 299–312. doi: 10.1007/s10646-003-6367-y

Mackenzie, R., Pedros-Alio, C., and Díez, B. (2013). Bacterial composition of microbial mats in hot springs in Northern Patagonia: variations with seasons and temperature. *Extremophiles* 17, 123–136. doi: 10.1007/s00792-018-1027-6

Madigan, M. T., Martinko, J. M., and Parker, J. (2000). *Brock Biology of Microorganisms*. New Jersey, NJ: Prentice Hall.

Maier, J., Kandelbauer, A., Erlacher, A., Cavaco-Paulo, A., and Gübitz, G. M. (2004). A new alkali-thermostable azoreductase from *Bacillus* sp. strain SF. *Appl. Environ. Microbiol.* 70, 837–844. doi: 10.1128/AEM.70.2.837-844.2004

Mandakovic, D., Cabrera, P., Pulgar, R., Maldonado, J., Aravena, P., Latorre, M., et al. (2015). Complete genome sequence of *Microbacterium* sp. CGR1, bacterium tolerant to wide abiotic conditions isolated from the Atacama Desert. *J. Biotechnol.* 216, 149–150. doi: 10.1016/j.jbiotec.2015.10.020

Mandakovic, D., Maldonado, J., Pulgar, R., Carrera, P., Gaete, A., Urtuvia, V., et al. (2018). Microbiome analysis and bacterial isolation from Lejía Lake soil in Atacama Desert. *Extremophiles* 22, 665–673. doi: 10.1007/s00792-018-1027-6

Mangano, S., Michaud, L., Caruso, C., and Lo Giudice, A. (2013). Metal and antibiotic resistance in psychrotrophic bacteria associated with the Antarctic sponge *Hemigellius pilosus* (Kirkpatrick, 1907). *Polar Biol.* 37, 227–235. doi: 10.1007/s00300-013-1426-1

Margesin, R., and Schinner, F. (2001). Bioremediation (natural attenuation and biostimulation) of diesel-oil-contaminated soil in an alpine glacier skiing area. *Appl. Environ. Microbiol.* 67, 3127–3133. doi: 10.1128/AEM.67.7.3127-3133.2001

Marizcurrena, J. J., Morel, M. A., Braña, V., Morales, D., Martinez-López, W., and Castro-Sowinski, S. (2017). Searching for novel photolyases in UVC-resistant Antarctic bacteria. *Extremophiles* 21, 409–418. doi: 10.1007/s00792-016-0914-y

Matsuno, T., and Yumoto, I. (2015). Bioenergetics and the role of soluble cytochromes c for alkaline adaptation in gram-negative alkaliphilic *Pseudomonas*. *Biomed. Res. Int*. 2015:847945. doi: 10.1155/2015/847945

Mattimore, V., and Battista, J. R. (1996). Radioresistance of *Deinococcus radiodurans*: functions necessary to survive ionizing radiation are also necessary to survive prolonged desiccation. *J. Bacteriol.* 178, 633–637. doi: 10.1128/jb.178.3.633-637.1996

Matzke, J., Schwermann, B., and Bakker, E. P. (1997). Acidostable and acidophilic proteins: the example of the α-amylase from *Alicyclobacillus acidocaldarius*. *Comp. Biochem. Physiol.* 118, 475–479. doi: 10.1016/S0300-9629(97)00008-X

Méndez, V., Fuentes, S., Morgante, V., Hernández, M., González, M., Moore, E., et al. (2017). Novel hydrocarbon-degrading and heavy metal-resistant *Acinetobacter*, *Kocuria* and *Pseudomonas* strains isolated from a crude oil-polluted soil in central Chile. *J. Soil Sci. Plant Nutr.* 17, 1074–1087. doi: 10.4067/S0718-95162017000400017

Michels, M., and Bakker, E. P. (1985). Generation of a large, protonophore-sensitive proton motive force and pH difference in the acidophilic bacteria *Thermoplsma acidophilum* and *Bacillus acidocaldarius*. *J. Bacteriol.* 161, 231–237.

Miller, S. R. (2007). "Diversity of the cosmopolitan thermophile *Mastigocladus laminosus* at global, regional and local scales", in *Algae and Cyanibacteria in Extreme Environments. Cellular Origin, Life in Extreme Habitats and Astrobiology*, ed. J. Seckbach (Dordrecht: Springer), 399–410. doi: 10.1007/978-1-4020-6112-7_21

Mnif, S., Sayadi, S., and Chamkha, M. (2014). Biodegradative potential and characterization of a novel aromatic-degrading bacterium isolated from a geothermal oil field under saline and thermophilic conditions. *Int. Biodeterior. Biodegradation* 86, 258–264. doi: 10.1016/j.ibiod.2013.09.015

Mohammadipanah, F., and Wink, J. (2016). Actinobacteria from arid and desert habitats: diversity and biological activity. *Front. Microbiol.* 6:1541. doi: 10.3389/fmicb.2015.01541

Montero-Silva, F., Durán, N., and Seeger, M. (2018). Synthesis of extracellular gold nanoparticles using *Cupriavidus metallidurans* CH34 cells. *IET Nanobiotechnol.* 12, 40–46. doi: 10.1049/iet-nbt.2017.0185

Moreno, M. L., Piubeli, F., Bonfá, M. R., García, M. T. L., Durrant, L. R., and Mellado, E. (2012). Analysis and characterization of cultivable extremophilic hydrolytic bacterial community in heavy-metal-contaminated soils from the atacama desert and their biotechnological potentials. *J. Appl. Microbiol.* 113, 550–559. doi: 10.1111/j.1365-2672.2012.05366.x

Morgante, V., López-López, A., Flores, C., González, M., González, B., Vásquez, M., et al. (2010). Bioaugmentation with *Pseudomonas* sp. strain MHP41 promotes simazine attenuation and bacterial community changes in agricultural soils. *FEMS Microbiol. Ecol.* 71, 114–126. doi: 10.1111/j.1574-6941.2009.00790.x

Morita, R. Y. (1975). Psychrophilic bacteria. *Bacteriol. Rev.* 39, 144–167.

Mrazek, J. (2002). New technology may reveal mechanisms of radiation resistance in *Deinococcus radiodurans*. *Proc. Natl. Acad. Sci. U.S.A.* 99, 10943–10944. doi: 10.1073/pnas.182429699

Mukherjee, S., Mishra, A., and Trenberth, K. E. (2018). Climate change and drought: a perspective on drought indices. *Curr. Clim. Change Rep.* 4, 145–163. doi: 10.1007/s40641-018-0098-x

Muñoz, N., and Charrier, R. (1996). Uplift of the western border of the Altiplano on west-vergent thrust system, Northern Chile. *J. South Am. Earth Sci.* 9, 171–181. doi: 10.1016/0895-9811(96)00004-1

Muñoz, P. A., Flores, P. A., Boehmwald, F. A., and Blamey, J. M. (2011). Thermophilic bacteria present in a sample from Fumarole Bay, Deception Island. *Antarct. Sci.* 23, 549–555. doi: 10.1017/S0954102011000393

Muñoz, P. A., Márquez, S. L., González-Nilo, F. D., Márquez-Miranda, V., and Blamey, J. M. (2017). Structure and application of antifreeze proteins from Antarctic bacteria. *Microb. Cell Fact.* 16:138. doi: 10.1186/s12934-017-0737-2

Nakayama, T., Tsuruoka, N., Akai, M., and Nishino, T. (2000). Thermostable collagenolytic activity of a novel thermophilic isolate, *Bacillus* sp. strain NTAP-1. *J. Biosci. Bioeng.* 89, 612–614. doi: 10.1016/S1389-1723(00)80067-5

Natarajan, K. A. (2008). Microbial aspects of acid mine drainage and its bioremediation. *Trans. Nonferrous Met. Soc. China* 18, 1352–1360. doi: 10.1016/S1003-6326(09)60008-X

Navarro-González, R., Rainey, F. A., Molina, P., Bagaley, D. R., Hollen, B. J., de la Rosa, J., et al. (2003). Mars-like soils in the Atacama Desert, Chile, and the dry limit of microbial life. *Science* 302, 1018–1021. doi: 10.1126/science.1089143

Ni, G., Christel, S., Roman, P., Wong, Z. L., Bijmans, M. F., and Dopson, M. (2016). Electricity generation from an inorganic sulfur compound containing mining wastewater by acidophilic microorganisms. *Res. Microbiol.* 167, 568–575. doi: 10.1016/j.resmic.2016.04.010

Okibe, N., Gericke, M., Hallberg, K. B., and Johnson, D. B. (2003). Enumeration and characterization of acidophilic microorganisms isolated from a pilot plant stirred-tank bioleaching operation. *Appl. Environ. Microbiol.* 69, 1936–1943. doi: 10.1128/AEM.69.4.1936-1943.2003

Órdenes-Aenishanslins, N., Anziani-Ostuni, G., Vargas-Reyes, M., Alarcón, J., Tello, A., and Pérez-Donoso, J. M. (2016). Pigments from UV-resistant Antarctic bacteria as photosensitizers in dye sensitized solar cells. *J. Photochem. Photobiol. B* 162, 707–714. doi: 10.1016/j.jphotobiol.2016.08.004

Ordoñez, O., Lanzarotti, E., Kurth, D., Cortez, N., Farias, M. E., and Turjanski, A. G. (2015). Genome comparison of two *Exiguobacterium* strains from high altitude Andean lakes with different arsenic resistance: identification and 3D modeling of the Acr3 efflux pump. *Front. Environ. Sci.* 3:50. doi: 10.3389/fenvs.2015.00050

Oremland, R. S., Stolz, J. F., and Hollibaugh, J. T. (2004). The microbial arsenic cycle in Mono Lake, California. *FEMS Microbiol. Ecol.* 48, 15–27. doi: 10.1016/j.femsec.2003.12.016

Oren, A. (1999). Bioenergetic aspects of halophilism. *Microbiol. Mol. Biol. Rev.* 63, 334–348. doi: 10.1016/j.jphotobiol.2016.08.004

Oren, A. (2002). Diversity of halophilic microorganisms: Environments, phylogeny, physiology, and applications. *J. Ind. Microbiol. Biotechnol.* 28, 56–63. doi: 10.1038/sj/jim/7000176

Oren, A., Gurevich, P., Azachi, M., and Henis, Y. (1992). Microbial degradation of pollutants at high salt concentrations. *Biodegradation* 3, 387–398. doi: 10.1007/BF00129095

Oukarroum, A., Bussotti, F., Goltsev, V., and Kalaji, H. M. (2015). Correlation between reactive oxygen species production and photochemistry of photosystem I and II in *Lemna gibba* L. plants uder salt stress. *Environ. Exp. Bot.* 109, 80–88. doi: 10.1016/j.envexpbot.2014.08.005

Panda, S., Mishra, S., and Akcil, A. (2016). Bioremediation of acidic mine effluents and the role of sulfidogenic biosystems: a mini-review. *Euro Mediterr. J. Environ. Integr.* 1:8. doi: 10.1007/s41207-016-0008-3

Paulino-Lima, I. G., Fujishima, K., Navarrete, J. U., Galante, D., Rodrigues, F., Azua-Bustos, A., et al. (2016). Extremely high UV-C radiation resistant microorganisms from desert environments with different manganese concentrations. *J. Photochem. Photobiol. B Biol.* 163, 327–336. doi: 10.1016/j.jphotobiol.2016.08.017

Pérez, V., Hengst, M., Kurte, L., Dorador, C., Jeffrey, W. H., Wattiez, R., et al. (2017). Bacterial survival under extreme UV radiation: a comparative proteomics study of *Rhodobacter* sp., isolated from high altitude wetlands in Chile. *Front. Microbiol.* 8:1173. doi: 10.3389/fmicb.2017.01173

Pikuta, E. V., Hoover, R. B., and Tang, J. (2007). Microbial extremophilesat the limits of life. *Crit. Rev. Microbiol.* 33, 183–209. doi: 10.1080/10408410701451948

Piubeli, F., Moreno, M., Kishi, T. L., Henrique-Silva, F., García, M. T., and Mellado, E. (2015). Phylogenetic profiling and diversity of bacterial communities in the Death Valley, an extreme habitat in the Atacama Desert. *Indian J. Microbiol.* 55, 392–399. doi: 10.1016/j.syapm.2010.02.007

Plenge, M. F., Engel, A. S., Omelon, C. R., and Bennett, P. (2017). Thermophilic archaeal diversity and methanogenesis from El Tatio geyser field, Chile. *Geomicrobiol. J.* 34, 220–230. doi: 10.1080/01490451.2016.1168496

Plominsky, A., Delherbe, N., Ugalde, J., Allen, E., Blanchet, M., Keda, P., et al. (2014). Metagenome sequencing of the microbial community of a solar saltern crystallizer pond at Cáhuil Lagoon, Chile. *Genome Announc.* 2:e01172-14. doi: 10.1128/genomeA.01172-14

Poland, J. S., Riddle, M. J., and Zeeb, B. A. (2003). Contaminants in the arctic and the antarctic: a comparison of sources, impacts, and remediation options. *Polar Rec.* 39, 369–383. doi: 10.1017/S0032247403002985

Prasad, A. S., and Rao, K. V. (2013). Aerobic biodegradation of Azo dye by *Bacillus cohnii* MTCC 3616; an obligately alkaliphilic bacterium and toxicity evaluation of metabolites by different bioassay systems. *Appl. Microbiol. Biotechnol.* 97, 7469–7481. doi: 10.1007/s00253-012-4492-3

Procesi, M. (2014). Geothermal potential evaluation for Northern Chile and suggestions for new energy plans. *Energies* 7, 5444–5459. doi: 10.3390/en7085444

Quatrini, R., Escudero, L. V., Moya-Beltrán, A., Galleguillos, P. A., Issottaa, F., Acosta, M., et al. (2017). Draft genome sequence of *Acidithiobacillus thiooxidans* CLST isolated from the acidic hypersaline Gorbea salt flat in northern Chile. *Stand. Genomic Sci.* 12:84. doi: 10.1186/s40793-017-0305-8

Quiroz, M., Triadó-Margarit, X., Casamayor, E. O., and Gajardo, G. (2015). Comparison of the Artemia bacteria associations in brines, laboratory cultures and the gut environment: a study based on Chilean hypersaline environments. *Extremophiles* 19, 135–147. doi: 10.1007/s00792-014-0694-1

Rafferty, J. P. (2010). *Plate Tectonics, Volcanoes, and Earthquakes*. New York, NY: Britannica Educational Publishing.

Rahman, K. S., Rahman, T. J., Kourkoutas, Y., Petsas, I., Marchatn, R., and Banat, I. M. (2003). Enhanced bioremediation of n-alkane in petroleum sludge using bacterial consortium amended with rhamnolipid and micronutirents. *Bioresour. Technol.* 90, 159–168. doi: 10.1016/S0960-8524(03)00114-7

Rainey, F. A., Ferreira, M., Nobre, M. F., Ray, K., Bagaley, D., Earl, A. M., et al. (2007). *Deinococcus peraridilitoris* sp. nov., isolated from a coastal desert. *Int. J. Syst. Evol. Microbiol.* 57, 1408–1412. doi: 10.1099/ijs.0.64956-0

Rainey, F. A., Ray, K., Ferreira, M., Gatz, B. Z., Nobre, F., and Bagaley, D., et al. (2005). Extensive diversity of ionizing-radiation-resistant bacteria recovered from Sonoran Desert soil and description of nine new species of the genus *Deinococcus* obtained from a single soil sample. *Appl. Environ. Microbiol.* 71, 5225–5235. doi: 10.1128/AEM.71.11.7630.2005

Rampelotto, P. H. (2013). Extremophiles and extreme environtments. *Life* 3, 482–485. doi: 10.3390/life3030482

Rastogi, G., Bhalla, A., Adhikari, A., Bischoff, K. M., Hughes, S. R., Christopher, L. P., et al. (2010). Characterization of thermostable cellulases produced by *Bacillus* and *Geobacillus* strains. *Bioresour. Technol.* 101, 8798–8806. doi: 10.1016/j.biortech.2010.06.001

Remonsellez, F., Galleguillos, F., Moreno-Paz, M., Parro, V., Acosta, M., and Demergasso, C. (2009). Dynamic of active microorganisms inhabiting a bioleaching industrial heap of low-grade copper sulfide ore monitored by real-time PCR and oligonucleotide prokaryotic acidophile microarray. *Microb. Biotechnol.* 2, 613–624. doi: 10.1111/j.1751-7915.2009.00112.x

Riddle, M. R., Baxter, B. K., and Avery, B. J. (2013). Molecular identification of microorganisms associated with the brine shrimp *Artemia franciscana*. *Aquat. Biosyst.* 9:7. doi: 10.1186/2046-9063-9-7

Rigoldi, F., Donini, S., Redaelli, A., Parisini, E., and Gautieri, A. (2018). Review: engineering of thermostable enzymes for industrial applications. *APL Bioeng.* 2:011501. doi: 10.1063/1.4997367

Risacher, F., Alonso, H., and Salazar, C. (2003). The origin of brines and salts in Chilean salars: a hydrochemical review. *Earth Sci. Rev.* 63, 249–293. doi: 10.1016/S0012-8252(03)00037-0

Risacher, F., and Fritz, B. (2009). Origin of salts and brine evolution of Bolivian and Chilean salars. *Aquat. Geochem.* 15, 123–157. doi: 10.1007/s10498-008-9056-x

Robinson, C. K., Wierzchos, J., Black, C., Crits-Christoph, A., Ma, B., Ravel, J., et al. (2015). Microbial diversity and the presence of algae in halite endolithic communities are correlated to atmospheric moisture in the hyper-arid zone of the Atacama Desert. *Environ. Microbiol.* 17, 299–315. doi: 10.1111/1462-2920.12364

Rodriguez-Rojas, F., Castro-Nallar, E., Undabarrena, A., Muñoz-Díaz, P., Arenas-Salinas, M., Díaz-Vásquez, W. et al. (2016a). Draft genome sequence of a multi-metal resistance bacterium *Pseudomonas* putida ATH-43 isolated from Greenwich Island, Antarctica. *Front. Microbiol.* 7:1777. doi: 10.3389/fmicb.2016.01777

Rodriguez-Rojas, F., Diaz-Vasquez, W., Undabarrena, A., Muñoz-Diaz, P., Arenas, F., and Vásquez, C. (2016b). Mercury-mediated cross-resistance to tellurite in *Pseudomonas* spp. isolated from the Chilean Antarctic territory. *Metallomics* 8, 108–117. doi: 10.1039/c5mt00256g

Rohban, R., Amoozegar, M. A., and Ventosa, A. (2009). Screening and isolation of halophilic bacteria producing extracellular hydrolyses from Howz Soltan Lake, Iran. *J. Ind. Microbiol. Biotechnol.* 36, 333–340. doi: 10.1007/s10295-008-0500-0

Rojas, L. A., Yañez, C., González, M., Lobos, S., Smalla, K., and Seeger, M. (2011). Characterization of the metabolically modified heavy metal-resistant *Cupriavidus metallidurans* strain MSR33 generated for mercury bioremediation. *PLoS One* 6:e17555. doi: 10.1371/journal.pone.0017555

Romano, I., Lama, L., Nicolaus, B., Poli, A., Gambacorta, A., and Giordano, A. (2006). *Halomonas alkiliphila* sp. nov., a novel halotolerant alkalphilic bacterium isolated from a salt pool in Campania (Italy). *J. Gen. Appl. Microbiol.* 52, 339–348. doi: 10.1016/j.syapm.2005.03.010

Romero-González, M., Nwaobi, B. C., Hufton, J. M., and Gilmour, D. J. (2016). *Ex-situ* bioremediation of U (VI) from contaminated mine water using *Acidithiobacillus ferrooxidans* strains. *Front. Environ. Sci.* 4:39. doi: 10.3389/fenvs.2016.00039

Rowe, J. J., Fournier, R. O., and Morey, G. W. (1973). Chemical analysis of thermal waters in Yellowstone National Park, Wyoming, 1960-65. *U.S. Geol. Surv. Bull.* 1303:31.

Saavedra, M., Acevedo, F., González, M., and Seeger, M. (2010). Mineralization of PCBs by the genetically modified strain *Cupriavidus necator* JMS34 and its application for bioremediation of PCBs in soil. *Appl. Microbiol. Biotechnol.* 87, 1543–1554. doi: 10.1007/s00253-010-2575-6

Sachdev, D. P., and Cameotra, S. S. (2013). Biosurfactants in agriculture. *Appl. Microbiol. Biotechnol.* 97, 1005–1016. doi: 10.1007/s00253-012-4641-8

Santhanam, R., Rong, X., Huang, Y., Andrews, B. A., Asenjo, J. A., and Goodfellow, M. (2013). *Streptomyces bullii* sp. nov., isolated from a hyper-arid Atacama Desert soil. *Antonie Van Leeuwenhoek* 103:367–373. doi: 10.1007/s10482-012-9816-x

Sar, P., Kazy, S. K., Paul, D., and Sarkar, A. (2013). "Metal bioremediation by thermophilic microorganisms," in *Thermophilic Microbes in Environmental and Industrial Biotechnology: Biotechnology of Thermophiles*, eds T. Satyanarayana, J. Littlechild, and Y. Kawarabayasi (Dordrecht: Springer), 171–201. doi: 10.1007/978-94-007-5899-5_6

Scherson, R. A., Thornhill, A. H., Urbina-Casanova, R., Freyman, W. A., Pliscoff, P. A., and Mishler, B. D. (2017). Spatial phylogenetics of the vascular flora of Chile. *Mol. Phylogenet. Evol.* 112, 88–95. doi: 10.1016/j.ympev.2017.04.021

Scott, S., Dorador, C., Oyanedel, J. P., Tobar, I., Hengst, M., Maya, G., et al. (2015). Microbial diversity and trophic components of two high altitude wetlands of the Chilean Altiplano. *Gayana* 79, 45–56. doi: 10.4067/S0717-65382015000100006

Seeger, M., and Jerez, C. A. (1993). Response of *Thiobacillus ferrooxidans* to phosphate limitation. *FEMS Microbiol. Rev.* 11:42. doi: 10.1111/j.1574-6976.1993.tb00264.x

Seeger, M., Osorio, G., and Jerez, C. A. (1996). Phosphorylation of GroEL and DnaK and other proteins from *Thiobacillus ferrooxidans* grown under different conditions. *FEMS Microbiol. Lett.* 138, 129–134. doi: 10.1111/j.1574-6968.1996.tb08145.x

Sekhon Randhawa, K. K., and Rahman, P. K. (2014). Rhamnolipid biosurfactants-past, present, and future scenario of global market. *Front. Microbiol.* 5:454. doi: 10.3389/fmicb.2014.00454

Serour, E., and Antranikian, G. (2002). Novel thermoactive glucoamylases from the thermoacidophilic Archaea *Thermoplasma acidophilum*, *Picrophilus torridus* and *Picrophilus oshimae*. *Antonie Van Leeuwenhoek* 81, 73–83. doi: 10.1023/A:1020525525490

Sharma, A., Kawarabayasi, Y., and Satyanarayana, T. (2012). Acidophilic bacteria and archaea: acid stable biocatalysts and their potential applications. *Extremophiles* 16, 1–19. doi: 10.1007/s00792-011-0402-3

Sharma, A., Parashar, D., and Satyanarayana, T. (2016). "Acidophilic microbes: biology and applications," in *Biotechnology of Extremophiles: Advances and Challenges*, ed. P.H. Rampelotto (Porto Alegre: Springer), 215–241.

Sheela, B., Khasim, S., and Rao, O. (2014). Bioremediation of ammonia using ammonia oxidizing bacteria isolated from Sewage. *Int. J. Environ. Bioremediat. Biodegrad.* 2, 146–150. doi: 10.12691/ijebb-2-4-1

Siddikee, M. A., Chauhan, P. S., Anandham, R., Han, G. H., and Sa, T. (2010). Isolation, characterization, and use for plant growth promotion under salt stress, of ACC deaminase-producing halotolerant bacteria derived from coastal soil. *J. Microbiol. Biotechnol.* 20, 1577–1584. doi: 10.4014/jmb.1007.07011

Siddiqui, K. S., Williams, T. J., Wilkins, D., Yau, S., Allen, M., Brown, M., et al. (2013). Psychrophiles. *Annu. Rev. Earth Planet. Sci.* 41, 87–115. doi: 10.1146/annurev-earth-040610-133514

Smedley, P. L., and Kinniburgh, D. G. (2002). A review of the source, behaviour and distribution of arsenic in natural waters. *Appl. Geochem.* 17, 517–568. doi: 10.1016/S0883-2927(02)00018-5

Solari, M. A., Herve, F., and Martinez, J. (2004). The presence of living stromatolites at Laguna Amarga, Torres del Paine National Park, southernmost Chile. *Abstr. Prog. Geol. Soc. Am.* 36:57.

Sorokin, D. Y., Zhilina, T. N., Lysenko, A. M., Tourova, T. P., and Spiridonova, E. M. (2006). Metabolic versatility of haloalkaliphilic bacteria from soda lakes belonging to the *Alkalispirillum-Alkalilimnicola* group. *Extremophiles* 10, 213–220. doi: 10.1007/s00792-005-0487-7

Soto, P., Acosta, M., Tapia, P., Contador, Y., Velásquez, A., Espoz, C., et al. (2013). From mesophilic to moderate thermophilic populations in an industrial heap bioleaching process. *Adv. Mat. Res*. 825, 376–379.

Squeo, F., Warner, B. R., Aravena, D., and Espinoza, D. (2006). Bofedales: high altitude peatlands of the central Andes. *Rev. Chil. Hist. Nat.* 79, 245–255. doi: 10.4067/S0716-078X2006000200010

Stapleton, R. D., Savage, D. C., Sayler, G. S., and Stacey, G. (1998). Biodegradation of aromatic hydrocarbons in an extremely acidic environment. *Appl. Environ. Microbiol.* 64, 4180–4184.

Sulonen, M. L., Kokko, M. E., Lakaniemi, A. M., and Puhakka, J. A. (2015). Electricity generation from tetrathionate in microbial fuel cells by acidophiles. *J. Hazard. Mater.* 284, 182–189. doi: 10.1016/j.jhazmat.2014.10.045

Suzuki, Y., Kelly, S. D., Kemner, K. M., and Banfield, J. F. (2003). Microbial populations stimulated for hexavalent uranium reduction in uranium mine sediment. *Appl. Environ. Microbiol.* 69, 1337–1346. doi: 10.1128/AEM.69.3.1337-1346.2003

Takeuchi, F., and Sugio, T. (2006). Volatilization and recovery of mercury from mercury-polluted soils and wastewaters using mercury-resistant *Acidithiobacillus ferrooxidans* strains SUG 2-2 and MON-1. *Environ. Sci.* 13, 305–316.

Tang, K. H., Barry, K., Dalin, E., Han, C. S., Hauser, L. J., Honchak, B. M., et al. (2011). Complete genome sequence of the filamentous anoxygenic phototrophic bacterium *Chloroflexus aurantiacus*. *BMC Genomics* 12:334. doi: 10.1186/1471-2164-12-334

Tassi, F., Aguilera, F., Darrah, T., Vaselli, O., Capaccioni, B., and Poreda, R. J. (2010). Fluid geochemistry of hydrothermal system in the Arica-Parinacota, Tarapacá and Antofagasta regions (northern Chile). *J. Volcanol. Geotherm. Res.* 192, 1–15. doi: 10.1016/j.volgeores.2010.02.006

Tomova, I., Stoilova-Disheva, M., Lazarkevich, I., and Vasileva-Tonkova, E. (2015). Antimicrobial activity and resistance to heavy metals and antibiotics of heterotrophic bacteria isolated from sediment and soil samples collected from two Antarctic islands. *Front. Life Sci.* 8, 348–357. doi: 10.1080/21553769.2015.104413

Undabarrena, A., Beltrametti, F., Claverías, F. P., González, M., Moore, E. R. B., Seeger, M., et al. (2016). Exploring the diversity and antimicrobial potential of marine actinobacteria from the Comau Fjord in Northern Patagonia, Chile. *Front. Microbiol.* 7:1135. doi: 10.3389/fmicb.2016.01135

Undabarrena, A., Ugalde, J. A., Seeger, M., and Cámara, B. (2017). Genomic data mining of the marine actinobacteria *Streptomyces* sp. H-KF8 unveils insights into multi-stress related genes and metabolic pathways involved in antimicrobial synthesis. *PeerJ* 5:e2912. doi: 10.7717/peerj.2912

Urbieta, M. S., Donati, E. R., Chan, K. G., Sin, L. L., and Goh, K. M. (2015a). Thermophiles in the genomic era: biodiversity, science, and applications. *Biotechnol. Adv.* 33, 633–647. doi: 10.1016/j.biotechadv.2015.04.007

Urbieta, M. S., Gonzalez-Toril, E., Bazán, A. A., Giaveno, M. A., and Donati, E. (2015b). Comparison of the microbial communities of hot springs waters and the microbial biofilms in the acidic geothermal area of Copahue (Neuquen, Argentina). *Extremophiles* 19, 437–450. doi: 10.1007/s00792-015-0729-2

Vacheron, J., Desbrosses, G., Bouffaud, M. L., Touraine, B., Moënne-Loccoz, Y., Muller, D., et al. (2013). Plant growth-promoting rhizobacteria and root system functioning. *Front. Plant Sci.* 4:356. doi: 10.3389/fpls.2013.00356

Valdebenito-Rolack, E., Ruiz-Tagle, N., Abarzúa, L., Aroca, G., and Urrutia, H. (2017). Characterization of a hyperthermophilic sulphur-oxidizing biofilm produced by archaea isolated from a hot spring. *Electron. J. Biotechnol.* 25, 58–63. doi: 10.1016/j.ejbt.2016.11.005

Valipour, M. (2014). Drainage, waterlogging, and salinity. *Arch. Agron. Soil Sci.* 60, 1625–1640. doi: 10.1080/03650340.2014.905676

van Beilen, J. B., and Funhoff, E. G. (2007). Alkane hydroxylases involved in microbial alkane degradation. *Appl. Microbiol. Biotechnol.* 74, 13–21. doi: 10.1007/s00253-006-0748-0

Vasquez-Ponce, F., Higuera-Llantén, S., Pavlov, M. S., Ramirez-Orellana, R., Marshall, S. H., and Olivares-Pacheco, J. (2017). Alginate overproduction and biofilm formation by psychrotolerant *Pseudomonas mandelii* dependent on temperatura in Antartic marine sediments. *Electronic J. Biotechnol.* 28, 27–34. doi: 10.1016/j.ejbt.2017.05.001

Vázquez, S., Monien, P., Minetti, R. P., Jürgens, J., Curtosi, A., Primitz, V. J., et al. (2017). Bacterial communities and chemical parameters in soils and coastal sediments in response to diesel spills at Carlini Station, Antarctica. *Sci. Total Environ.* 605–606, 26–37. doi: 10.1016/j.scitotenv.2017.06.129

Vieille, C., and Zeikus, J. G. (1996). Thermozymes: identifying molecular determinants of protein structural and functional stability. *Trends Biotechnol.* 14, 183–190. doi: 10.1016/0167-7799(96)10026-3

Villagrán, C., and Armesto, J. J. (2005). "Fitogeografía histórica de la cordilera de la costa de chile", in *Historia, biogeografía y ecología de los bosques costeros de Chile*, eds C. Smith-Ramírez, J. J. Armesto, and C. Valdovinos (Santiago: Editorial Universitaria), 99–115.

Villagrán, C., and Hinojosa, F. (1997). Historia de los bosques del sur de sudamérica, II: análisis fitogeográfico. *Rev. Chil. Hist. Nat.* 70, 241–267.

Wang, L., Cheng, G., Dai, Z., Zhao, Z. S., Liu, F., Li, S., et al. (2015). Degradation of intact chicken feathers by *Thermoactinomyces* sp. CDF and characterization of its keratinolytic protease. *Appl. Microbiol. Biotechnol.* 99, 3949–3959. doi: 10.1007/s00253-014-6207-4

Warren, J. K. (2010). Evaporites through time: tectonic, climatic and eustatic controls in marine and nonmarine deposits. *Earth Sci. Rev.* 98, 217–268. doi: 10.1016/j.earscirev.2009.11.004

Warren-Rhodes, K. A., Rhodes, K. L., Pointing, S. B., Ewing, S. A., Lacap, D. C., Gómez-Silva, B., et al. (2006). Hypolithic Cyanobacteria, dry limit of photosynthesis, and microbial ecology in the hyperarid Atacama Desert. *Microb. Ecol.* 52, 389–398. doi: 10.1007/s00248-006-9055-7

Weiss, M. C., Sousa, F. L., Mrnjavac, N., Neukirchen, S., Roettger, M., Nelson-Sathi, S., et al. (2016). The physiology and habitat of the last universal common ancestor. *Nat. Microbiol.* 1:16116. doi: 10.1038/nmicrobiol.2016.116

Woese, C. R., Kandler, O., and Wheelis, M. L. (1990). Towards a natural system of organisms: proposal for the domains archaea, bacteria, and eucarya. *Proc. Natl. Acad. Sci. U.S.A.* 87, 4576–4579. doi: 10.1073/pnas.87.12.4576

Xu, L., Wu, Y. H., Zhou, P., Cheng, H., Liu, Q., and Xu, X. W. (2018). Investigation of the thermophilic mechanism in the genus *Porphyrobacter* by comparative genomic analysis. *BMC Genomics* 19:385. doi: 10.1186/s12864-018-4789-4

Yakimov, M. M., Giuliano, L., Chernikova, T. N., Gentile, G., Abraham, W. R., Lünsdorf, H., et al. (2001). *Alcalilimnicola halodurans* gen. nov., sp. nov., an alkaliphilic, moderately halophilic and extremely halotolerant bacterium, isolated from sediments of soda-depositing Lake Natron, East Africa Rift Valley. *Int. J. Syst. Evol. Microbiol.* 51, 2133–2143. doi: 10.1099/00207713-51-6-2133

Yañez, J., Fierro, V., Mansilla, H. D., Figueroa, L., Cornejo, L., and Barnes, R. M. (2005). Arsenic speciation in human hair: a new perspective for epidemiological assessment in chronic arsenisism. *J. Environ. Monit.* 7, 1335–1341. doi: 10.1039/B506313B

Yang, Y., Itahashi, S., Yokobori, S., and Yamagishi, A. (2008). UV-resistant bacteria isolated from upper troposphere and lower stratosphere. *Biol. Sci. Space* 22, 18–25. doi: 10.2187/bss.22.18

Zabel, H. P., König, H., and Winter, J. (1984). Isolation and characterization of a new coccoid methanogen, *Methanogenium tatii* spec. nov. from a solfataric field on Mount Tatio. *Arch. Microbiol.* 137, 308–315. doi: 10.1007/BF00410727

Zellner, G., Boone, D. R., Keswani, J., Whitman, W. B., Woese, C. R., Hagelstein, A., et al. (1999). Reclassification of *Methanogenium tationis* and *Methanogenium liminatans* as *Methanofollis tationis* gen. nov., comb. nov. and *Methanofollis liminatans* comb. nov. and description of a new strain of *Methanofollis liminatans*. *Int. J. Syst. Bacteriol.* 49, 247–255. doi: 10.1099/00207713-49-1-247

Zhang, S., Yan, L., Xing, W., Chen, P., Zhang, Y., and Wang, W. (2018). *Acidithiobacillus ferroxidans* and its potential application. *Extremophiles* 22, 563–579. doi: 10.1007/s00792-018-1024-9

Zhou, J. F., Gao, P. K., Dai, X. H., Cui, X. Y., Tian, H. M., Xie, J. J., et al. (2018). Heavy hydrocarbon degradation of crude oil by a novel thermophilic

Geobacillus stearothermophilus strain A-2. *Int. Biodeterior. Biodegradation* 126, 224–230. doi: 10.1016/j.ibiod.2016.09.031

Zhou, W., Guo, W., Zhou, H., and Chen, X. (2016). Phenol degradation by *Sulfobacillus acidophilus* TPY via the meta-pathway. *Microbiol. Res.* 190, 37–45. doi: 10.1016/j.micres.2016.05.005

Zhu, J. K. (2001). Plant salt tolerance. *Trends Plant Sci.* 6, 66–71. doi: 10.1016/S1360-1385(00)01838-0

Zúñiga, L. R., Campos, V., Pinochet, H., and Prado, B. (1991). A limnological reconnaissance of Lake Tebenquiche, Salar de Atacama, Chile. *Hydrobiologia* 210, 19–24. doi: 10.1007/BF00014320

Conflict of Interest Statement: The authors declare that the research was conducted in the absence of any commercial or financial relationships that could be construed as a potential conflict of interest.

frontiers in Microbiology

ORIGINAL RESEARCH
published: 24 October 2018
doi: 10.3389/fmicb.2018.02545

Enzymatic Bioweathering and Metal Mobilization From Black Slate by the Basidiomycete *Schizophyllum commune*

*Julia Kirtzel[1], Soumya Madhavan[1], Natalie Wielsch[2], Alexander Blinne[3], Yvonne Hupfer[2], Jörg Linde[4], Katrin Krause[1], Aleš Svatoš[2] and Erika Kothe[1]**

[1] Microbial Communication, Institute of Microbiology, Friedrich Schiller University, Jena, Germany, [2] Research Group Mass Spectrometry/Proteomics, Max Planck Institute for Chemical Ecology, Jena, Germany, [3] Helmholtz Institute Jena, Jena, Germany, [4] Hans Knöll Institute, Jena, Germany

Schizophyllum commune is a filamentous basidiomycete causing white-rot in many wood species with the help of a broad range of enzymes including multicopper oxidases such as laccases and laccase-like oxidases. Since these enzymes exhibit a broad substrate range, their ability to oxidatively degrade black slate was investigated. Both haploid monokaryotic, and mated dikaryotic strains were able to grow on black slate rich in organic carbon as sole carbon source. On defined media, only the monokaryon showed growth promotion by addition of slate. At the same time, metals were released from the slate and, after reaching a threshold concentration, inhibited further growth of the fungus. The proteome during decomposition of the black slate showed induction of proteins potentially involved in rock degradation and stress resistance, and the gene for laccase-like oxidase *mco2* was up-regulated. Specifically in the dikaryon, the laccase gene *lcc1* was induced, while *lcc2* as well as *mco1, mco3,* and *mco4* expression levels remained similar. Spectrophotometric analysis revealed that both life forms were able to degrade the rock and produce smaller particles.

Keywords: *Schizophyllum commune*, bioweathering, proteome, laccases, multicopper oxidases, rock, black slate

OPEN ACCESS

Edited by:
Edgardo Donati, National University of La Plata, Argentina

Reviewed by:
Eric D. van Hullebusch, UMR7154 Institut de Physique du Globe de Paris (IPGP), France
John Stephen Horton, Union College, United States

***Correspondence:**
Erika Kothe
erika.kothe@uni-jena.de

Specialty section:
This article was submitted to Microbiotechnology, Ecotoxicology and Bioremediation, a section of the journal Frontiers in Microbiology

Received: *26 January 2018*
Accepted: *05 October 2018*
Published: *24 October 2018*

Citation:
Kirtzel J, Madhavan S, Wielsch N, Blinne A, Hupfer Y, Linde J, Krause K, Svatoš A and Kothe E (2018) Enzymatic Bioweathering and Metal Mobilization From Black Slate by the Basidiomycete Schizophyllum commune. Front. Microbiol. 9:2545. doi: 10.3389/fmicb.2018.02545

INTRODUCTION

In lignin degradation performed by white-rot fungi like *Schizophyllum commune,* peroxidases and multicopper oxidases are involved. The lignin degrading enzymes (FOLymes, Levasseur et al., 2008) can be identified from fungal genomes, and 16 FOLymes including two laccases and four other multicopper oxidases were identified for *S. commune* (Ohm et al., 2010). Compared to other white-rot fungi, *S. commune* lacks genes encoding peroxidases and thus features a slim FOLyme repertoire (Ohm et al., 2010).

Multicopper oxidases, including true laccases, show a wide range of substrate utilization and thus are involved in various degradative and biosynthesis processes. With two laccases (*lcc1* and *lcc2*) and four laccase-like multicopper oxidases (*mco1*, *mco2*, *mco3,* and *mco4*), each containing copper binding domains with the typical four laccase signature sequences (Madhavan et al., 2014), *S. commune* seems well equipped for acting on an array of organic carbon fractions occurring in nature including wood, but also bitumen or kerogen. Kerogen is the altered form of lignin present

in sedimentary rocks like shales and slates. Indeed, previous studies have confirmed the ability of *S. commune* to degrade black slate material resulting in a release of heavy metals and carbon as dissolved organic matter (Wengel et al., 2006; Kirtzel et al., 2017).

Black slates are low-grade metamorphic rocks rich in sulfides, heavy metals and high amounts of organic matter altered into kerogen. Black slates and shales are important to nature as they are a prominent reservoir of organic carbon and experience several changes when they are exposed to oxygen. Weathering of such organic matter is essential for the geochemical cycles of carbon and oxygen, and fungal involvement in this process may lead to fast weathering of the rock material (Fischer et al., 2007). Due to their metal contents, black slates have been mined for aluminum, copper or vitriol production, but also for production of uranium. In Thuringia, Germany, the former vitriol mines at Saalfeld and Morassina and the former uranium mine near Ronneburg are examples for black slate mining activities. The high sulfide contents, especially at the former Ronneburg mining site, has led to acid mine drainage representing a major environmental challenge. The weathering leading to metal release and acidification through sulfide (pyrite) oxidation is often linked to bacterial activity (Mustin et al., 1992; Uroz et al., 2009; Konhauser et al., 2011).

Nevertheless, the activity of fungi can largely contribute to such bacterial activities as fungi are able to secrete organic and inorganic acids, and widen cracks in the rock and thus expose fresh surfaces to bacterial activity (Burford et al., 2003; Hoffland et al., 2004). This will be specifically important in dense rock material like black slates. However, in order to exert a force on the rock, in addition to directional growth, the fungus requires enzymatic degradation of the rock material to induce surface roughness which in turn enables hyphal attachment (Willmann and Fakoussa, 1997; Burford et al., 2003).

The structure of kerogen in black slates has been suggested to be similar to lignin components, explaining the observed lytic activities (Catcheside and Mallett, 1991; Hofrichter et al., 1997a,b). In accordance with this observation, fungi have been identified to depolymerize or transform coal (Hofrichter et al., 1997a,b; Petsch et al., 2001; Wengel et al., 2006). Here, we focus on the differential expression and enzymes active in the degradation of black slate.

The life cycle of basidiomycetes involves germination and haploid, monokaryotic mycelial growth from sexually formed basidiospores. If two compatible mates fuse, a dikaryon with two parental nuclei per cell is formed (Freihorst et al., 2016). This dikaryon can then form fruiting bodies under optimal environmental conditions, in which haploid basidiospores are produced, which makes it a good model to study sexual development (Raper and Miles, 1958; Kothe, 1997). *S. commune* is able to complete this life cycle on water agar with black slate as the only carbon and nutrient source within 2–3 weeks (**Supplementary Figure S1**).

The significance of fungi in bioweathering of rocks and minerals gained considerable attention during the last decades. However, only very few investigations deal with basidiomycetes and their enzymatic biodegradation. In the present study, we investigated the ability of *S. commune* to degrade black slate and use it as a carbon source. The effect of black slate on mono- and dikaryotic strains was examined, as well as the influence of the rock material on fungal growth and metabolism. Since the two life stages show different enzyme expression patterns, we performed proteome analyses to identify secreted proteins participating in black slate degradation. To the best of our knowledge, these results provide a first insight into possible rock decay mechanisms for *S. commune*. Detected multicopper oxidases were further investigated *via* an enzymatic assay and differential expression analysis during growth of both *S. commune* life stages on black slate.

MATERIALS AND METHODS

Strains and Culture Conditions

Pre-cultures of *S. commune* monokaryon 4–39 and dikaryon 12–43 × 4–39 (Jena Microbial Resource Collection, Jena, Germany) were grown in liquid complex yeast extract medium (Raper and Hoffman, 1974). After 5 days, the mycelium was washed twice with water, homogenized and resuspended in 100 ml half diluted minimal medium (Raper and Hoffman, 1974). Of this, 7 ml were used to inoculate 200 ml half diluted minimal medium containing 3 g powdered black slate (0.5 g < 63 μm, 2.5 g 63 μm-1 mm fractions obtained by sieve analysis, collected from Schmiedefeld, a former alum mining area in Thuringia, Germany) and incubated at 28°C and 130 rpm. The specific surface area of black slate has been shown to vary between 10 and 20 m^2/g (Fischer and Gaupp, 2004, 2005).

Growth Rate

The effect of black slate on biomass production was determined for monokaryon and dikaryon in liquid medium using three biological replicates according to the above-mentioned culture conditions in presence and absence of black slate. Dry weight was determined over a period of 4 weeks and every black slate containing sample was normalized to the corresponding control containing no black slate. Fungal growth and the interaction with black slate were observed microscopically (Stemi 2000-C and LSM 780, Zeiss, Germany) 14 days after inoculation. At different points in time, mycelium and black slate were harvested by centrifugation at 11,000 rpm for 30 min and dried at 60°C. After subtracting the weight of black slate that had been added to the culture, the fungal biomass was calculated. To determine the effect of black slate for every replicate, the control biomass was subtracted from the appropriate biomass treated with black slate and the final change in growth was expressed in mg.

Metal Release

Black slate containing liquid culture medium was analyzed to examine fungal-induced metal release from the rock material. Black slate containing medium inoculated with *S. commune* monokaryon was sampled after different points in time. Samples were filtered (0.22 μm, Rotilabo, Roth, Germany), acidified using HNO_3 and analyzed by ICP-MS (X Series II, Thermo Fisher Scientific). Measurements were performed with three biological

and three technical replicates using non-inoculated samples for control.

Spectrophotometric Assay for Quantification of Black Slate Solubilization

Fungal solubilization of black slate was spectrophotometrically quantified by measuring organic substances such as (dissolved) humic substances released from black slate. Liquid cultures of monokaryon and dikaryon as well as controls without fungal biomass were incubated with and without powdered black slate and centrifuged for 5 min at 8000 rpm to allow settling of mycelium and large rock particles. The supernatant was transferred into cuvettes (Greiner Bio-One, Germany) and the absorbance was measured at 450 nm (Ultrospec 2100*pro*, Amersham Biosciences, Germany), the most suitable wavelength to determine dark-colored organic substances from black slate. Measurements were performed with three biological replicates and statistical analysis was achieved using paired, two-tailed *t*-test. Degraded black slate particles were microscopically examined (Axioplan 2 microscope, Zeiss, Germany) and their sizes were measured using SPOT advanced (Diagnostic Instruments, Germany).

Protein Extraction

For preparation of protein extracts, liquid culture medium of four biological replicates was separated from fungal cultures and, when added, supplemented black slate 7 days after inoculation by centrifugation and 50 ml of the supernatant were concentrated to 1.5 ml (Amicon Ultra-15 Centrifugal Filter Units, 3 kDa, Merck Millipore, Germany). The supernatant was centrifuged at 12,000 × *g* for 30 min to remove cell debris or insoluble compounds. Secreted proteins were precipitated by the addition of 10 % (w/v) trichloroacetic acid.

After centrifugation at 13,000 × g for 10 min at 4°C, the supernatant was discarded, the pellet washed twice in 90% acetone (−20°C) and subsequently dried at room temperature.

For shotgun analysis, the pellet was resuspended in 50 mM NH_4HCO_3 and prior trypsin (Roche) digestion the samples were reduced with 10 mM DTT at 56°C and alkylated with 55 mM iodoacetamide in the dark. A trypsin/protein ratio of 1:30 at 37°C was applied for approximately 12 h.

NanoUPLC-MS/MS Analysis

The samples were acquired on UPLC M-class system (Waters Corporation) online coupled to a Synapt G2-si mass spectrometer equipped with a T-WAVE-IMS device (Waters Corporation). The peptides were first on-line preconcentrated and desalted using a UPLC M-Class Symmetry C18 trap column (100 Å, 180 µm × 20 mm, 5 µm particle size) at a flow rate of 15 µl/min (0.1% aqueous formic acid) and then eluted onto a ACQUITY UPLC HSS T3 analytical column (100 Å, 75 µm X 200, 1.8 µm particle size) at a flow rate of 350 nl/min with the following gradient: 1–9% B over 10 min, 9–19% B over 10 min, 19–32% B over 10 min, 32–48% B over 10 min, 48–58% over 5 min, 70–95% over 5 min, isocratic at 95% B for 4 min, and a return to 1% B over 1 min (phases A and B composed of 0.1% FA and 100% acetonitrile in 0.1% FA, respectively). The analytical column was re-equilibrated for 9 min prior to the next injection. The eluted peptides were transferred into the mass spectrometer operated in V-mode with a FWHM resolving power of at least 20000. All analyses were performed in a positive ESI mode. A 100 fmol/µl human Glu-Fibrinopeptide B in 0.1% formic acid/acetonitrile (1:1 v/v) was infused at a flow rate of 1 µl/min through the reference sprayer every 45 s to compensate for mass shifts in MS and MS/MS fragmentation mode.

During $HDMS^E$ analysis, a wave height of 40 V was applied in IMS past of TriWave, and the traveling wave velocity was ramped from 1000 m/s to 600 m/s. Wave velocities in the trap and transfer cell were set to 311 m/s and 175 m/s and wave heights to 4 V and 4 V, respectively. For fragmentation, the collision energy was linearly ramped in the transfer region of TriWave from 20 to 45 V. The acquisition time in each mode was 0.5 s with a 0.05 s interscan delay. $HDMS^E$ data were collected using MassLynx v4.1 software (Waters Corporation).

Processing of LC-MS Data

Data analysis was performed using ProteinLynx Global Server (PLGS) version 2.5.2 (Waters Corporation). The thresholds for low/high energy scan ions and peptide intensity were set at 300, 30 and 750 counts, respectively. The processed data were searched against the *S. commune* protein database obtained from the Joint Genome Institute, and combined with a subdatabase containing common contaminants (human keratins and trypsin). The database searching was performed at a False Discovery Rate (FDR) of 2%, following searching parameters were applied for the minimum numbers of: fragments per peptide (1), peptides per protein (1), fragments per protein (3), and maximum number of missed tryptic cleavage sites (1). Searches were restricted to tryptic peptides with a fixed carbamidomethyl modification for Cys residues. For functional description of proteins, the Functional Catalog (FunCat) was used as classification system (Ruepp et al., 2004).

Laccase Activity Assays

Extracellular laccase activity was determined from the culture fluid of liquid medium in presence and absence of black slate 7 days after inoculation (dpi, Sánchez et al., 2004), the point in time at which *S. commune* has been shown to release organic carbon from black slate (Wengel et al., 2006). Black slate powder was removed by centrifugation and extracellular enzymes were concentrated using membrane filters (Amicon Ultra-15 Centrifugal Filter Units, 10 kDa cutoff, Merck Millipore, Germany). Laccase activity was observed as increase in absorbance at 420 nm and expressed as units per liter (1 U = 1 µmol 2,2′-azino-bis (3-ethylbenzothiazoline-6-sulphonic acid), ABTS, oxidized per minute) with 1 mM ABTS in 100 mM sodium acetate buffer at pH 4.5 (Linke et al., 2005). Protein concentration was determined (Bradford, 1976). All tests were performed with three biological and three technical

replicates and statistically analyzed using paired, two-tailed *t*-test.

Expression Analyses

Approximately 100 mg of 7-day-old mycelium from monokaryotic or dikaryotic strains were harvested from the liquid black slate culture and washed properly. After grinding in liquid nitrogen, total RNA was isolated (Qiagen RNeasy Plant Mini Kit, Qiagen, Germany). For quantitative real-time PCR (qRT-PCR), the laccases *lcc1* (DOE JGI protein ID 2509814), *lcc2* (protein ID 1194451), laccase-like *mco1* (protein ID 2621035), *mco2* (protein ID 2634619), *mco3* (protein ID 2516955), *mco4* (protein ID 2483752) and reference genes *act1* (protein ID 1194206), *tef1* (protein ID 1037126), and *ubi* (protein ID 71656) were analyzed. Primers were used after Madhavan et al. (2014), and efficiencies were calculated from calibration curves (cDNA concentrations from 0.001 to 200 ng cDNA were used per 25 µl of PCR mixture). The qRT-PCR was performed using the Miniopticon Real Time PCR System (BioRad, Germany) and Maxima SYBR Green qPCR (Fisher Scientific, Germany) with initial denaturation at 94°C for 10 min, followed by 35 cycles of 94°C for 20s, 65°C for 20s (*lcc2* and *mco3*) or 60°C (for all other genes), and 72°C for 20 s. A melting curve analysis was performed for every run and each reaction was conducted with at least three biological and three technical replicates including negative controls, one without template and one without reverse transcription. PCR products were sequenced to verify the gene identity. The C_t values of target genes were normalized with respect to the reference genes, and calculated for relative and normalized fold change compared to treatments without black slate by the term $2^{-\Delta\Delta CT}$ (Pfaffl, 2001; Vandesompele et al., 2002).

RESULTS

Fungal Growth With Black Slate

To test the impact of black slate on fungal growth, *S. commune* was grown with and without powdered rock supplemented to the minimal medium. Both mono- and dikaryons of *S. commune* were able to grow in liquid media with powdered black slate. The growth of the monokaryon was promoted by the addition of rock material during the first 21 days (with a peak in biomass production after 14 days, **Figure 1**). After that point, growth promotion of black slate decreased and a reverse effect, where black slate reduced the biomass production, was observed at 28 days. The dikaryon consistently exhibited a better growth in absence of the rock material, and no black slate induced change in growth was observed between 7 to 28 dpi.

During growth in liquid medium, the mycelium of *S. commune* grew in mycelial balls which enclosed black slate particles (**Figure 2**). Most rock grains and mainly larger particles were located in the center of the grown mycelium, while smaller particles were found at lower incidence at the rim. A closer examination of exterior hyphae indicated the attachment and slight adherence of very small particles with an average size of 0.7 µm (**Figure 2C**).

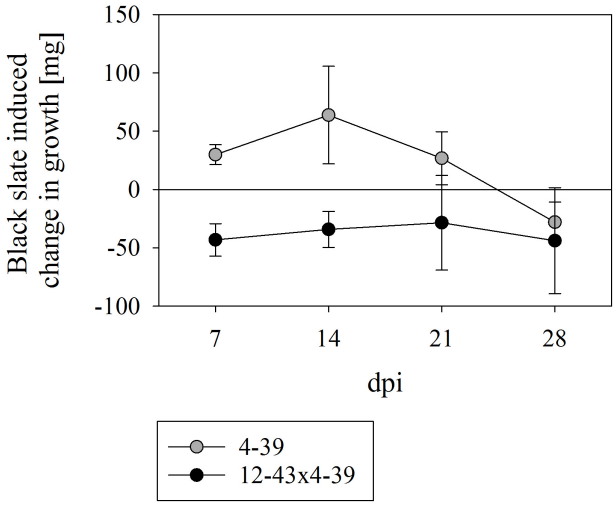

FIGURE 1 | Growth rate of *Schizophyllum commune* strains 4–39 and 12–43 × 4–39 in presence of black slate normalized to the corresponding control without black slate supplement. Positive values indicate a black slate induced burst of growth and negative values reveal a black slate induced inhibition of growth; *dpi* days after inoculation. Error bars represent standard deviation of three biological replicates.

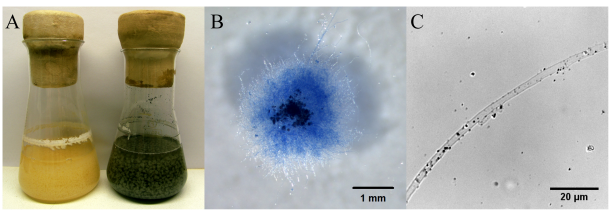

FIGURE 2 | *S. commune* growing in half diluted minimal medium without and with fractionized black slate **(A)**, hyphal ball stained with Lactophenol Cotton Blue with inclusions of black slate **(B)**, and hypha of monokaryon 4–39 with attached small black slate particles **(C)** 14 dpi.

Metal Release

The ability of *S. commune* to release metals from black slate was confirmed with a significantly higher release of Al, Fe, and U and a slight release of Pb in presence of the fungus (**Figure 3**). A reverse effect, at which the monokaryon caused lower metal concentrations in the medium, was seen for Cu. Especially in presence of the fungus, increasing element concentrations were detected for all metals over time.

Black Slate Degradation

The effect on rock degradation was verified by investigating the supernatants of liquid culture media with black slate. Bioweathering of black slate by *S. commune* cracked the rock into smaller pieces and caused the elevated release of dark-colored organic substances that may dissolve in the medium and

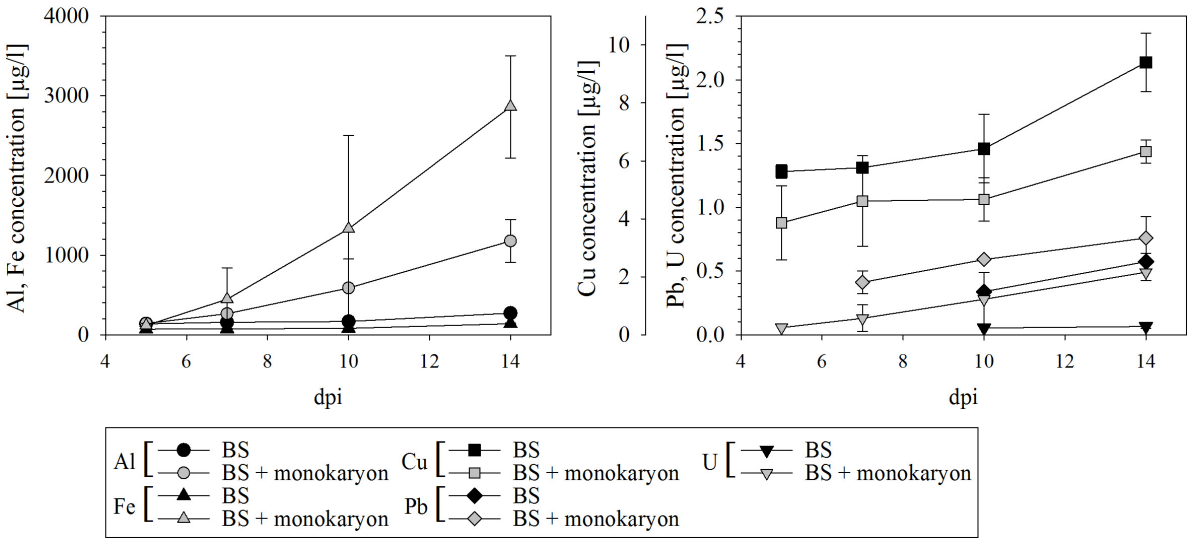

FIGURE 3 | Metal release from black slate into culture medium of black slate containing medium (BS) serving as control and black slate containing medium with fungal inoculum (BS + monokaryon); *dpi* days after inoculation. Missing data points are below the detection limit. Error bars represent standard deviation of three biological replicates.

can be spectrophotometrically measured. Both monokaryon and dikaryon caused a significantly higher absorbance at 450 nm due to organic substances and suspended black slate particles (**Figure 4**). The dikaryon *S. commune* 12–43 × 4–39 caused the highest turbidity of medium and the highest increase in absorbance 5–7 dpi; a less rapid but still escalating effect was seen up to 21 dpi, followed by a constant absorbance to 28 dpi. The monokaryon *S. commune* 4–39 showed a weaker, but similarly increasing absorbance pattern with a sharp rise in absorbance 5 dpi, and a slight increase in absorbance until 28 dpi.

Microscopic analyses demonstrated that both fungal strains caused a decomposition of black slate grains into smaller particles with an average size of 0.7 to 0.8 µm after 14 dpi. In presence of *S. commune*, these particles were present in the supernatant to a larger extent as compared to samples not inoculated with the fungus.

Secretome Analysis

The secreted proteins of *S. commune* monokaryon 4–39 and dikaryon 12–43 × 4–39 were analyzed during cultivation with and without black slate. Both strains revealed the occurrence of 269 proteins, about 60% showed secretion motifs. For functional annotation, 157 proteins could be annotated. With 887 functions within 17 FunCat main categories, multiple function of most proteins was assigned.

For the monokaryon *S. commune* 4–39, 38 of the 241 proteins were exclusively detected in presence of black slate (**Supplementary Table S1**). Their assigned functions mainly belonged to metabolism, to proteins with binding function or cofactor requirement, or to cellular transport, transport facilitation and transport routes (**Figure 5A**). Seventy proteins were detected in absence of black slate and exhibited functions in transport facilitation and transport routes, metabolism, protein fate, and protein with binding function or cofactor requirement (**Figure 5B** and **Supplementary Table S2**).

The analysis of the dikaryon *S. commune* 12–43 × 4–39 revealed 142 proteins, 37 of them were solely present with black slate (**Supplementary Table S3**). They mainly belonged to metabolism and proteins with binding

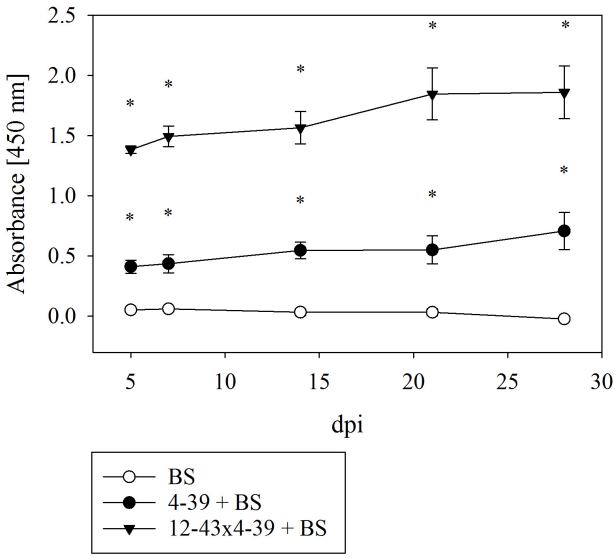

FIGURE 4 | Spectrophotometric analysis for measuring the degradation of black slate (BS) by *S. commune*; *dpi* days after inoculation. Error bars represent standard deviation of three biological replicates; $*p < 0.01$, paired, two-tailed *t*-test.

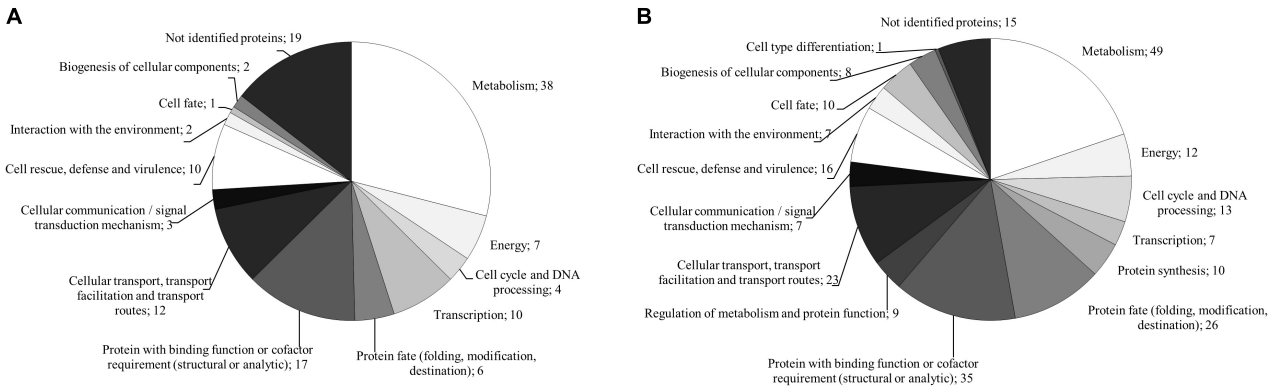

FIGURE 5 | FunCat annotated functions of proteins exclusively produced in presence **(A)** and absence **(B)** of black slate of *S. commune* strain 4–39.

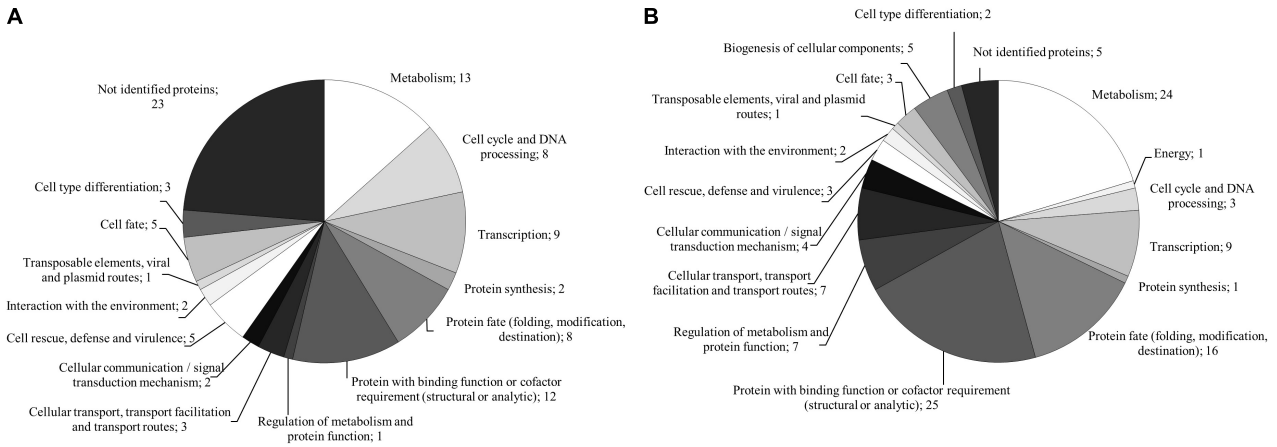

FIGURE 6 | FunCat annotated functions of proteins exclusively produced in presence **(A)** and absence **(B)** of black slate of *S. commune* strain 12–43 × 4–39.

function or cofactor requirement. The 25 proteins exclusively identified without black slate were associated to metabolism, protein fate and protein with binding function or cofactor requirement (**Figure 6** and **Supplementary Table S4**).

Between both life stages, 79 identical proteins were detected. Of these, 12 were exclusively produced in presence of black slate. When considering only predicted secreted proteins, they showed assigned functions in metabolism and cell rescue, defense and virulence. In absence of black slate, ten proteins matched for both strains, and the predicted secreted proteins possessed functions in metabolism or proteins with binding function or cofactor requirement.

From the assigned functions, insights into biological processes during fungal growth with black slate could be gained. To achieve the identification of proteins involved in the process, only proteins exclusively produced during black slate degradation in monokaryon, dikaryon or both were considered. From these, proteins involved in biomass degradation, C-compound metabolism, and stress response were characterized. Many peptidases and glycoside hydrolases (GH) including proteins of GH family 92 and 93, which are generally participating in plant biomass degradation, were secreted. Furthermore, enzymes specifically involved in the degradation of polysaccharides (GH families 5 and 61) or lignin (multicopper oxidases) were secreted. Aside from an intracellular aconitase A/isopropylmalate dehydratase involved in the tricarboxylic acid cycle, proteins associated with carbohydrate metabolism (GH families 5 and 6), polysaccharide metabolism, as well as sugar, glucoside, polyol and carboxylate catabolism (GH family 43, carbohydrate esterase family 4) were detected. Besides these extracellular enzymes, proteome analysis also revealed proteins which are usually intracellularly located and involved in sugar, glucoside, polyol and carboxylate anabolism (phosphoglucose isomerase, aldo/keto reductase, aconitase A/isopropylmalate dehydratase).

Furthermore, proteins involved in stress response (heat shock proteins, peptidyl-prolyl *cis-trans* isomerase) including detoxification processes by export (ABC transporter) and degradation (multicopper oxidase), or thioredoxin, glutaredoxin and glutathione metabolism (gamma-glutamyltranspeptidase) were proven as well as the

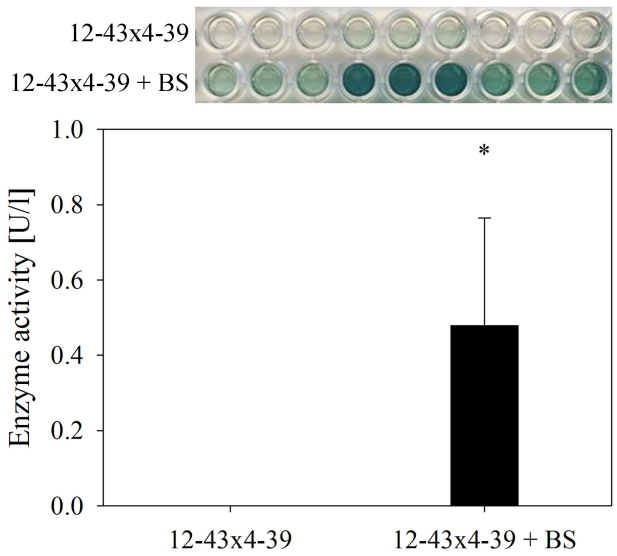

FIGURE 7 | Extracellular laccase activity in *S. commune* 12–43 × 4–39 growing without and with black slate (BS). Error bars represent standard deviation of three biological replicates; *$p < 0.05$, paired, two-tailed *t*-test.

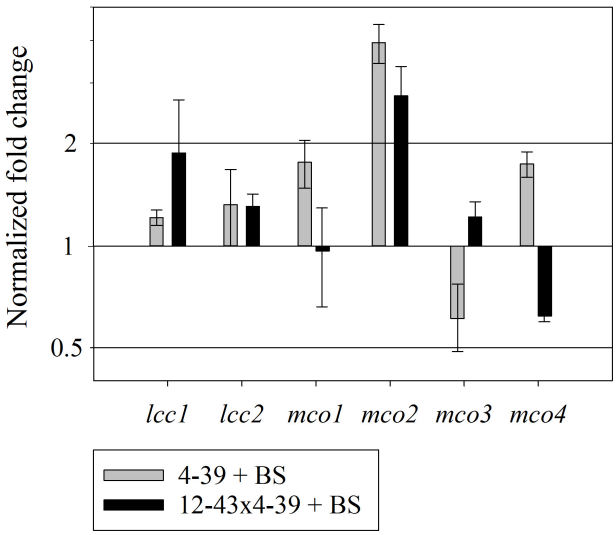

FIGURE 8 | Relative expression of multicopper oxidases in *S. commune* 4–39 and 12–43 × 4–39 during black slate (BS) degradation, normalized by expression for treatments without black slate. Error bars represent standard deviation of three biological replicates.

occurrence of a defense-related protein (osmotin; thaumatin-like protein).

Differential Regulation of Multicopper Oxidases During Black Slate Utilization

At the level of enzyme activity, laccases from culture supernatant was measured 7 dpi with an extracellular activity of 0.48 U/l when the dikaryotic strain was grown with black slate (**Figure 7**). In contrast, no laccase activity was detected in dikaryotic cultures without black slate, or for the monokaryon, neither in absence nor in presence of black slate.

The expression of all laccase and laccase-like multicopper oxidase genes of *S. commune* was tested for regulation on mRNA level. After growth in half diluted minimal medium with black slate powder, up-regulation of multicopper oxidase *mco2* was found in both life-stages (**Figure 8**). The other laccase and multicopper oxidase genes did not show changes in expression during treatment with black slate.

DISCUSSION

S. commune Causes Degradation of Black Slate

The influence of *S. commune* on black slate degradation was tested over a period of 4 weeks. A previous study had suggested the involvement of *S. commune* in release of heavy metals and organic carbon from black slate, when the rock is enzymatically attacked as a substrate (Wengel et al., 2006). Etch pits formed by *S. commune* on the surface of black slate supported the hypothesis of bioweathering (Kirtzel et al., 2017). Here, we could show that both life-stages of the fungus, the haploid monokaryon and the mated dikaryon, caused a decay of rock particles, resulting in a significantly higher turbidity and discoloration of the medium measurable at an absorbance at 450 nm. The dikaryon showed a stronger effect as compared to the monokaryon.

When fungi or bacteria are inoculated with rock samples, an elevated turbidity due to rock compounds like humic substances has been described (Fakoussa, 1988; Hofrichter et al., 1999). Black slates contain high amounts of organic matter which can be, according to their solubility, divided into bitumen or kerogen. They might be rich in humic substances and cause the dark color of the rock. During fungal attack, such organic fractions within the black slate undergo degradation, might dissolve in the medium, and cause its dark colorization. Furthermore, fungal bioweathering might crack solid bitumen or kerogen grains to an average size of 0.7–0.8 μm. Those grains either stick to the hyphae and might be more susceptible to biochemical weathering or remain in the supernatant, are unaffected by centrifugation and thus lead to a further increase in absorbance. Thus, absorbance measurements could be correlated with intensities of fungal-induced black slate degradation.

Black Slate Influences Fungal Metabolism

During growth of *S. commune* in liquid medium supplemented with black slate, rock grains were attached to the hyphae. Like many organisms, fungi are known to produce extracellular polymeric substances which facilitate the attachment to solid surfaces (Warscheid and Braams, 2000; Gadd, 2007). *S. commune* is a well-known producer of several exopolysaccharides

including the glucan schizophyllan (Hao et al., 2010). Therefore, small black slate particles can attach to the mycelial surfaces *via* interaction with the oligo- or polyglucans. Moreover, extracellular polymeric substances frequently contain complex-forming agents and acidic metabolites which in turn can cause an additional accelerated dissolution of black slate (Hoffland et al., 2004; Gorbushina, 2006; Gadd, 2007). Proteome analyses revealed that black slate influenced the tricarboxylic acid cycle where several organic acids like citric, succinic, fumaric and malic acid are produced. They are hypothesized to be deeply involved in rock weathering and could therefore promote black slate degradation (Palmer et al., 1991; Landeweert et al., 2001; Scheerer et al., 2009).

The growth of *S. commune* monokaryon 4–39 was accelerated by black slate. By access to organic materials and released essential nutrients, energy metabolism and biosynthesis are increased allowing for faster growth (Hochella, 2002; Gadd, 2007). However, after 21–28 days, a growth inhibition was scored, likely due to exceeding (heavy) metal concentrations caused by bioweathering of the stone (Gadd, 1993; Baldrian, 2003). Indeed, we could demonstrate that *S. commune* released Pb, U, and exceedingly high concentrations of Al and Fe from black slate. Wengel et al. (2006) have shown an increase in Fe concentrations from 220 μg/l to 330 μg/l and Mn concentrations from 1300 μg/l to 2430 μg/l by different strains of *S. commune* over a period of 84 days. Due to high Al and Fe contents in the black slate used in our study, the release of Fe by *S. commune* is much higher and increases from 140 μg/l to 1180 μg/l within 14 days. Based on these results, *S. commune* might be of interest for industrial bioleaching when addressing the extraction of metals from carbonaceous rocks.

Wood-Degrading Enzymes Are Responsible for Black Slate Degradation

As a wood-rotting fungus, *S. commune* secretes a broad range of enzymes crucial for degrading complex biomolecules (Ohm et al., 2010). The black slate-specific proteome included proteins involved in C-compound and carbohydrate metabolism, as well as extracellular polysaccharide and lignin degradation. Our results thus link wood-degrading proteins to bioweathering of black slate. In particular, several glycoside hydrolase family proteins and a multicopper oxidase seemed to be involved in degradation of the organic carbon fraction of the rock material. Specifically, *mco2* was up-regulated, which may also be explained by a large number of xenobiotic response elements in the *mco2* promoter (Madhavan et al., 2014). Extracellular enzymes have previously been suggested to participate in fungal rock degradation (Willmann and Fakoussa, 1997; Hofrichter et al., 1999; Silva-Stenico et al., 2007). During the formation of sedimentary organic matter, lignin and lipids were presumed to withstood degradation processes (Durand, 1980) and lignin could be converted into aromatic hydrocarbons (Shen et al., 2016). The organic matter fraction of black slate mainly consists of aromatic hydrocarbons and might thus be susceptible to degradation by ligninolytic enzymes such as laccases (Seifert et al., 2011). Since lignin does not provide a primary source of carbon and energy for fungal growth, it had to be derived from other sources such as cellulose and hemicellulose which provide glucose and other sugars, respectively (Fritsche and Hofrichter, 2005). Black slate organic matter could contain, besides lignin, cellulose and other plant residues (Swanson, 1960), thus explaining the detection of proteins able to degrade plant constituents other than lignin.

Rock Degradation Causes Stress in *S. commune*

Bioweathering of black slate by *S. commune* was accompanied by a release of metals which might cause stress in fungi. Stress response was visible in significant changes of the proteome, including the multicopper oxidase gene regulation. This enzyme has been shown to be involved in heavy metal stress and could consequently be involved in stress response (Baldrian and Gabriel, 2002; Lorenzo et al., 2006). Since laccases and multicopper oxidases contain four Cu atoms in the active center, the specific sequestration of Cu may be associated with the increased production of laccases/multicopper oxidases. This assumption could also be supported by the metal analysis of the culture medium. Here, the Cu concentrations released from black slate were lower in presence of the fungus. Released Cu was probably accumulated and used for synthesis of the laccase protein.

As a defense mechanism to metal and oxidative stress, fungi are known to produce antioxidants like glutathione or superoxide dismutase (Bellion et al., 2006; Jozefczak et al., 2012). During growth on black slate, the proteome as well as microarray data of *S. commune* showed an up-regulation of antioxidants like thioredoxin, glutaredoxin and glutathione which could protect the fungus from oxidative stress induced by the released (heavy) metals (Carmel-Harel and Storz, 2000; Belozerskaya and Gessler, 2007; Jozefczak et al., 2012; Kirtzel et al., 2017). Furthermore, these extracellular antioxidants could quench the ABTS reaction and prevent a color development during the enzyme assay (Re et al., 1999). This would also explain the low laccase activity in the dikaryon in presence of black slate as well as the inhibition of the ABTS reaction in the monokaryon although proteomics revealed the presence of multicopper oxidase in this strain under black slate treatment.

The complexity and variation in the organic carbon content as well as the presence of high levels of metals in black slate certainly impact bioweathering through *S. commune*. The investigation could show a diverse pattern of secreted proteins and an altered expression for a multicopper oxidase, encoded by the gene *mco2*, which could explain bioweathering and substrate utilization. This proof-of-principle allows a better understanding of the degradation of recalcitrant organic matter through fungal metabolism.

AUTHOR CONTRIBUTIONS

JK, KK, and EK conceived and designed the study. SM performed laccase assay and gene expression analyses. JK and YH conducted the protein extraction. NW and AS performed MS analyses and data processing. AB cross-referenced protein data with JGI online databases and JL functionally described the proteins according to the Functional Catalog. JK conducted the rest of the experiments, analyzed and interpreted the data, and wrote the manuscript. EK participated in the critical review of the manuscript.

FUNDING

JL was supported by the Deutsche Forschungsgemeinschaft CRC/Transregio "Pathogenic fungi and their human host: Networks of interaction" sub-project INF and the Free State of Thuringia and the European Regional Development Fund. We acknowledge the German Research Foundation support through GRK 1257 and JSMC.

ACKNOWLEDGMENTS

We would like to thank Dirk Merten and Georg Büchel for ICP-MS analysis.

SUPPLEMENTARY MATERIAL

The Supplementary Material for this article can be found online at: https://www.frontiersin.org/articles/10.3389/fmicb.2018.02545/full#supplementary-material

REFERENCES

Baldrian, P. (2003). Interactions of heavy metals with white-rot fungi. *Enzyme Microb. Technol.* 32, 87–91. doi: 10.1016/S0141-0229(02)00245-4

Baldrian, P., and Gabriel, J. (2002). Copper and cadmium increase laccase activity in *Pleurotus ostreatus*. *FEMS Microbiol. Lett.* 206, 69–74. doi: 10.1111/j.1574-6968.2002.tb10988.x

Bellion, M., Courbot, M., Jacob, C., Blaudez, D., and Chalot, M. (2006). Extracellular and cellular mechanisms sustaining metal tolerance in ectomycorrhizal fungi. *FEMS Microbiol. Lett.* 254, 173–181. doi: 10.1111/j.1574-6968.2005.00044.x

Belozerskaya, T., and Gessler, N. (2007). Reactive oxygen species and the strategy of antioxidant defense in fungi: a review. *Appl. Biochem. Microbiol.* 43, 506–515. doi: 10.1134/S0003683807050031

Bradford, M. M. (1976). A rapid and sensitive method for the quantitation of microgram quantities of protein utilizing the principle of protein-dye binding. *Anal. Biochem.* 72, 248–254. doi: 10.1016/0003-2697(76)90527-3

Burford, E. P., Fomina, M., and Gadd, G. M. (2003). Fungal involvement in bioweathering and biotransformation of rocks and minerals. *Mineral Mag.* 67, 1127–1155. doi: 10.1180/0026461036760154

Carmel-Harel, O., and Storz, G. (2000). Roles of the glutathione-and thioredoxin-dependent reduction systems in the *Escherichia coli* and *Saccharomyces cerevisiae* responses to oxidative stress. *Annu. Rev. Microbiol.* 54, 439–461. doi: 10.1146/annurev.micro.54.1.439

Catcheside, D., and Mallett, K. (1991). Solubilization of Australian lignites by fungi and other microorganisms. *Energy Fuels* 5, 141–145. doi: 10.1021/ef00025a025

Durand, B. (1980). "Sedimentary organic matter and kerogen. Definition and quantitative importance of kerogen," in *Kerogen – Insoluble Organic Matter from Sedimentary Rocks*, ed. B. Durand (Paris: Editions Technip), 13–34.

Fakoussa, R. (1988). Production of water-soluble coal-substances by partial microbial liquefaction of untreated hard coal. *Resour. Conserv. Recycl.* 1, 251–260. doi: 10.1016/0921-3449(88)90020-1

Fischer, C., and Gaupp, R. (2004). Multi-scale rock surface area quantification - a systematic method to evaluate the reactive surface area of rocks. *Chem. Erde* 64, 241–256. doi: 10.1016/j.chemer.2003.12.002

Fischer, C., and Gaupp, R. (2005). Change of black shale organic material surface area during oxidative weathering: implications for rock-water surface evolution. *Geochim. Cosmochim. Acta* 69, 1213–1224. doi: 10.1016/j.gca.2004.09.021

Fischer, C., Karius, V., and Thiel, V. (2007). Organic matter in black slate shows oxidative degradation within only a few decades. *J. Sediment. Res.* 77, 355–365. doi: 10.2110/jsr.2007.041

Freihorst, D., Fowler, T. J., Bartholomew, K., Raudaskoski, M., Horton, J. S., and Kothe, E. (2016). "The mating-type genes of the basidiomycetes," in *The Mycota: Growth, Differentiation and Sexuality*, ed. K. Esser (Heidelberg: Springer), 329–349.

Fritsche, W., and Hofrichter, M. (2005). "Aerobic degradation of recalcitrant organic compounds by microorganisms," in *Environmental Biotechnology - Concepts and Applications*, eds H.-J. Jördening and J. Winter (Weinheim: Wiley-VCH), 203–227.

Gadd, G. M. (1993). Interactions of fungi with toxic metals. *New Phytol.* 124, 25–60. doi: 10.1111/j.1469-8137.1993.tb03796.x

Gadd, G. M. (2007). Geomycology: biogeochemical transformations of rocks, minerals, metals and radionuclides by fungi, bioweathering and bioremediation. *Mycol. Res.* 111, 3–49. doi: 10.1016/j.mycres.2006.12.001

Gorbushina, A. A. (2006). "Fungal activities in subaerial rock-inhabiting microbial communities," in *Fungi in Biogeochemical Cycles*, ed. G. M. Gadd (New York, NY: Cambridge University Press), 267–288.

Hao, L.-M., Xing, X.-H., Li, Z., Zhang, J.-C., Sun, J.-X., Jia, S.-R., et al. (2010). Optimization of effect factors for mycelial growth and exopolysaccharide production by *Schizophyllum commune*. *Appl. Biochem. Biotechnol.* 160, 621–631. doi: 10.1007/s12010-008-8507-6

Hochella, M. (2002). Sustaining earth: Thoughts on the present and future roles of mineralogy in environmental science. *Mineral Mag.* 66, 627–652. doi: 10.1180/0026461026650053

Hoffland, E., Kuyper, T. W., Wallander, H., Plassard, C., Gorbushina, A. A., Haselwandter, K., et al. (2004). The role of fungi in weathering. *Front. Ecol. Environ.* 2:258–264. doi: 10.2307/3868266

Hofrichter, M., Bublitz, F., and Fritsche, W. (1997a). Fungal attack on coal: I. Modification of hard coal by fungi. *Fuel Process. Technol.* 52, 43–53.

Hofrichter, M., Bublitz, F., and Fritsche, W. (1997b). Fungal attack on coal II. Solubilization of low-rank coal by filamentous fungi. *Fuel Process. Technol.* 52, 55–64. doi: 10.1016/S0378-3820(97)00015-5

Hofrichter, M., Ziegenhagen, D., Sorge, S., Ullrich, R., Bublitz, F., and Fritsche, W. (1999). Degradation of lignite (low-rank coal) by ligninolytic basidiomycetes and their manganese peroxidase system. *Appl. Microbiol. Biotechnol.* 52, 78–84. doi: 10.1007/s002530051490

Jozefczak, M., Remans, T., Vangronsveld, J., and Cuypers, A. (2012). Glutathione is a key player in metal-induced oxidative stress defenses. *Int. J. Mol. Sci.* 13, 3145–3175. doi: 10.3390/ijms13033145

Kirtzel, J., Siegel, D., Krause, K., and Kothe, E. (2017). Stone-eating fungi: mechanisms in bioweathering and the potential role of laccases in black slate degradation with the basidiomycete *Schizophyllum commune*. *Adv. Appl. Microbiol.* 99, 83–101. doi: 10.1016/bs.aambs.2017.01.002

Konhauser, K. O., Lalonde, S. V., Planavsky, N. J., Pecoits, E., Lyons, T. W., Mojzsis, S. J., et al. (2011). Aerobic bacterial pyrite oxidation and acid rock drainage during the Great Oxidation Event. *Nature* 478, 369–373. doi: 10.1038/nature10511

Kothe, E. (1997). Solving a puzzle piece by piece: sexual development in the basidiomycetous fungus *Schizophyllum commune*. *Plant Biol.* 110, 208–213.

Landeweert, R., Hoffland, E., Finlay, R. D., Kuyper, T. W., and van Breemen, N. (2001). Linking plants to rocks: ectomycorrhizal fungi mobilize nutrients from minerals. *Trends Ecol. Evol.* 16, 248–254. doi: 10.1016/S0169-5347(01)02122-X

Levasseur, A., Piumi, F., Coutinho, P. M., Rancurel, C., Asther, M., Delattre, M., et al. (2008). FOLy: an integrated database for the classification and functional annotation of fungal oxidoreductases potentially involved in the degradation of lignin and related aromatic compounds. *Fungal Genet. Biol.* 45, 638–645. doi: 10.1016/j.fgb.2008.01.004

Linke, D., Bouws, H., Peters, T., Nimtz, M., Berger, R. G., and Zorn, H. (2005). Laccases of *Pleurotus sapidus*: characterization and cloning. *J. Agric. Food Chem.* 53, 9498–9505. doi: 10.1021/jf052012f

Lorenzo, M., Moldes, D., and Sanromán, M. Á (2006). Effect of heavy metals on the production of several laccase isoenzymes by *Trametes versicolor* and on their ability to decolourise dyes. *Chemosphere* 63, 912–917. doi: 10.1016/j.chemosphere.2005.09.046

Madhavan, S., Krause, K., Jung, E.-M., and Kothe, E. (2014). Differential regulation of multi-copper oxidases in *Schizophyllum commune* during sexual development. *Mycol. Prog.* 13, 1199–1206. doi: 10.1007/s11557-014-1009-8

Mustin, C., Berthelin, J., Marion, P., and De Donato, P. (1992). Corrosion and electrochemical oxidation of a pyrite by *Thiobacillus ferrooxidans*. *Appl. Environ. Microbiol.* 58, 1175–1182.

Ohm, R. A., De Jong, J. F., Lugones, L. G., Aerts, A., Kothe, E., Stajich, J. E., et al. (2010). Genome sequence of the model mushroom *Schizophyllum commune*. *Nat. Biotechnol.* 28, 957–963. doi: 10.1038/nbt.1643

Palmer, R. J., Siebert, J., and Hirsch, P. (1991). Biomass and organic acids in sandstone of a weathering building: production by bacterial and fungal isolates. *Microb. Ecol.* 21, 253–266. doi: 10.1007/BF02539157

Petsch, S., Eglinton, T., and Edwards, K. (2001). 14C-dead living biomass: evidence for microbial assimilation of ancient organic carbon during shale weathering. *Science* 292, 1127–1131. doi: 10.1126/science.1058332

Pfaffl, M. W. (2001). A new mathematical model for relative quantification in real-time RT–PCR. *Nucleic Acids Res.* 29, 2002–2007. doi: 10.1093/nar/29.9.e45

Raper, J. R., and Hoffman, R. M. (1974). "*Schizophyllum commune*," in *Bacteria, Bacteriophages, and Fungi*, ed. R. C. King (Boston: Springer), 597–626. doi: 10.1007/978-1-4899-1710-2_32

Raper, J. R., and Miles, P. G. (1958). The genetics of *Schizophyllum commune*. *Genetics* 43, 530–546.

Re, R., Pellegrini, N., Proteggente, A., Pannala, A., Yang, M., and Rice-Evans, C. (1999). Antioxidant activity applying an improved ABTS radical cation decolorization assay. *Free Radical Biol. Med.* 26, 1231–1237. doi: 10.1016/S0891-5849(98)00315-3

Ruepp, A., Zollner, A., Maier, D., Albermann, K., Hani, J., Mokrejs, M., et al. (2004). The FunCat, a functional annotation scheme for systematic classification of proteins from whole genomes. *Nucleic Acids Res.* 32, 5539–5545. doi: 10.1093/nar/gkh894

Sánchez, C., Téllez-Téllez, M., Díaz-Godínez, G., and Moore, D. (2004). Simple staining detects ultrastructural and biochemical differentiation of vegetative hyphae and fruit body initials in colonies of *Pleurotus pulmonarius*. *Lett. Appl. Microbiol.* 38, 483–487. doi: 10.1111/j.1472-765X.2004.01517.x

Scheerer, S., Ortega-Morales, O., and Gaylarde, C. (2009). Microbial deterioration of stone monuments - an updated overview. *Adv. Appl. Microbiol.* 66, 97–139. doi: 10.1016/S0065-2164(08)00805-8

Seifert, A.-G., Trumbore, S., Xu, X., Zhang, D., Kothe, E., and Gleixner, G. (2011). Variable effects of labile carbon on the carbon use of different microbial groups in black slate degradation. *Geochim. Cosmochim. Acta* 75, 2557–2570. doi: 10.1016/j.gca.2011.02.037

Shen, D., Zhao, J., and Xiao, R. (2016). Catalytic transformation of lignin to aromatic hydrocarbons over solid-acid catalyst: effect of lignin sources and catalyst species. *Energy Convers. Manage.* 124, 61–72. doi: 10.1016/j.enconman.2016.06.067

Silva-Stenico, M. E., Vengadajellum, C. J., Janjua, H. A., Harrison, S. T., Burton, S. G., and Cowan, D. A. (2007). Degradation of low rank coal by *Trichoderma atroviride* ES11. *J. Ind. Microbiol. Biotechnol.* 34, 625–631. doi: 10.1007/s10295-007-0223-7

Swanson, V. E. (1960). Oil yield and uranium content of black shales. *U.S. Geol. Surv. Prof. Pap.* 1, 1–44.

Uroz, S., Calvaruso, C., Turpault, M.-P., and Frey-Klett, P. (2009). Mineral weathering by bacteria: ecology, actors and mechanisms. *Trends Microbiol.* 17, 378–387. doi: 10.1016/j.tim.2009.05.004

Vandesompele, J., De Preter, K., Pattyn, F., Poppe, B., Van Roy, N., De Paepe, A., et al. (2002). Accurate normalization of real-time quantitative RT-PCR data by geometric averaging of multiple internal control genes. *Genome Biol.* 3, 1–12. doi: 10.1186/gb-2002-3-7-research0034

Warscheid, T., and Braams, J. (2000). Biodeterioration of stone: a review. *Int. Biodeterior. Biodegrad.* 46, 343–368. doi: 10.1016/S0964-8305(00)00109-8

Wengel, M., Kothe, E., Schmidt, C. M., Heide, K., and Gleixner, G. (2006). Degradation of organic matter from black shales and charcoal by the wood-rotting fungus *Schizophyllum commune* and release of DOC and heavy metals in the aqueous phase. *Sci. Total Environ.* 367, 383–393. doi: 10.1016/j.scitotenv.2005.12.012

Willmann, G., and Fakoussa, R. M. (1997). Extracellular oxidative enzymes of coal-attacking fungi. *Fuel Process. Technol.* 52, 27–41. doi: 10.1016/S0378-3820(97)00013-1

Conflict of Interest Statement: The authors declare that the research was conducted in the absence of any commercial or financial relationships that could be construed as a potential conflict of interest.

frontiers in Microbiology

MINI REVIEW
published: 01 June 2018
doi: 10.3389/fmicb.2018.01191

Extremophilic Microfactories: Applications in Metal and Radionuclide Bioremediation

*Catarina R. Marques**

Departamento de Biologia and Centro de Estudos do Ambiente e do Mar, Universidade de Aveiro, Aveiro, Portugal

Metals and radionuclides (M&Rs) are a worldwide concern claiming for resilient, efficient, and sustainable clean-up measures aligned with environmental protection goals and global change constraints. The unique defense mechanisms of extremophilic bacteria and archaea have been proving usefulness toward M&Rs bioremediation. Hence, extremophiles can be viewed as microfactories capable of providing specific and controlled services (i.e., genetic/metabolic mechanisms) and/or products (e.g., biomolecules) for that purpose. However, the natural physiological plasticity of such extremophilic microfactories can be further explored to nourish different hallmarks of M&R bioremediation, which are scantly approached in the literature and were never integrated. Therefore, this review not only briefly describes major valuable extremophilic pathways for M&R bioremediation, as it highlights the advances, challenges and gaps from the interplay of 'omics' and biological engineering to improve extremophilic microfactories performance for M&R clean-up. Microfactories' potentialities are also envisaged to close the M&R bioremediation processes and shift the classical idea of never 'getting rid' of M&Rs into making them 'the belle of the ball' through bio-recycling and bio-recovering techniques.

Keywords: extremophilic bacteria and archaea, meta-'omics', genetic engineering, synthetic biology, mine wastes, metal-radionuclide recycling/recovering

OPEN ACCESS

Edited by:
Kian Mau Goh,
University of Technology, Malaysia

Reviewed by:
M. Oves,
King Abdulaziz University, Saudi Arabia
Navanietha Krishnaraj,
National Institute of Technology, Durgapur, India

***Correspondence:**
Catarina R. Marques
crmarques@ua.pt

Specialty section:
This article was submitted to Extreme Microbiology, a section of the journal Frontiers in Microbiology

Received: *28 January 2018*
Accepted: *16 May 2018*
Published: *01 June 2018*

Citation:
Marques CR (2018) Extremophilic Microfactories: Applications in Metal and Radionuclide Bioremediation. Front. Microbiol. 9:1191. doi: 10.3389/fmicb.2018.01191

INTRODUCTION

Metals and radionuclides (M&Rs) are problematic pollutants sourced from different industrial sectors, nuclear power plants, electronic waste and, especially, from mining activities. Undoubtedly, mining industry nurtures a plethora of human needs (Carvalho, 2017), but past and ongoing mining activities represent a huge footprint of environmental (Marques et al., 2014) and health injuries (Pereira et al., 2014; Venkateswarlu et al., 2016). Still, future societal demands will force industrial growth, thus making M&R pollution a never-ending threat, mainly due to their persistence and non-biodegradability (Gupta and Diwan, 2017).

Bioremediation, though being often viewed as an 'old fashion' and slow-acting technology, it has been thriving for M&R reclamation. Its sustainability, low-cost and efficiency totally rival conventional remediation techniques (Li and Zhang, 2012). In particular, microbially-based bioremediation relies on microbes abilities, biogenic products and/or components to scavange, transform or immobilize M&Rs (Lloyd and Lovley, 2001; Voica et al., 2016). Despite the interesting nature-based self-healing character of this approach, the tolerance of microbes to high M&R

levels, extreme physical (e.g., radiation), chemical (e.g., acidic pH) and climate changing conditions may constrain (*in situ*) bioremediation efficiencies (Ramos et al., 2011). Extremophilic microbes, though, have attractive skills as bioremediation tiny factories (microfactories), which performance can even be improved and customized for M&R clean-up. This review will hence focus: (1) the peculiar mechanisms of extremophilic bacteria and archaea exploitable as 'microfactories' for M&R bioremediation, (2) the groundbreaking opportunities leveraged from nature and science ('omics' plus biological engineering) interplay to enhance extremophilic-microfactories-based bioremediation, (3) M&R recovery and recycling conducted by extremophilic microfactories as a sustainable and value-added management of M&R-bioremediation-resulting wastes. Overall, this is an innovative overview on the potentialities of extremophilic bacteria/archaea in three M&R bioremediation hallmarks: application, optimization, end-waste management (**Figure 1**).

EXTREMOPHILES AS MICROFACTORIES FOR M&R BIOREMEDIATION

Extremophilic bacteria and archaea evolved specialized mechanisms to endure physical and/or geochemical extreme environments (Rothschild and Mancinelli, 2001). Acidophilic and/or metalophilic microorganisms are especially appealing agents for bioremediation, given their defense mechanisms against M&Rs and acidity. They synthesize extremophilic enzymes (extremozymes) (Elleuche et al., 2014) and biomolecules (Raddadi et al., 2015) that keep active and/or stable under harsh conditions. The stability of thermophilic enzymes, like the esterase EstATII (Mohamed et al., 2013), helps facing acidity and metal stress, thanks to stiff folds sustained by ion-pair networks, to compact hydrophobic cores and aminoacid arrangements/packing (Elleuche et al., 2014). Additionally, extremophiles evolved sharpened metal detoxification pathways (Voica et al., 2016) due to fast-adapting transcriptional and translational mechanisms that activate and/or inhibit many anti-oxidative stress, metal-binding, metal-transport, and membrane-permeability responses (Mukherjee et al., 2012; Dekker et al., 2016). Their membranes exhibit a specific structure (Singh and Singh, 2017), composition and a positively-charged inner layer that promote metal-transporters functioning (Dekker et al., 2016) and minimize metals and protons entrance, thereby controlling acidity and M&R toxicity (Slonczewski et al., 2009; Krulwich et al., 2011; Navarro et al., 2013; Zhang et al., 2016). Notwithstanding, since extremophiles can express defense mechanisms active against multiple extremes simultaneously (Rothschild and Mancinelli, 2001), thermophilic, halophilic, radiophilic, and polyextremophilic bacteria/archaea are additional M&R clean-up agents (Amoozegar et al., 2012; Wheaton et al., 2015). Either as whole-cells or providers of economically-valuable bio-services and/or biomolecules (**Figure 2**), extremophiles can be explored as tiny factories (microfactories) for M&R remediation.

M&R Sensing

Sensing M&Rs presence is the alarm button to trigger the activation/repression of specific regulatory proteins and downstream cascades that control the expression of resistance genes/operons encoding enzymes and biomolecules for M&R detoxification (Das et al., 2016). Along this, the uptake/efflux of M&Rs across extremophiles cell wall and membranes may occur through energy-dependent P-type ATPases ($copA1_{Af}$, $copA2_{Af}$, and $copB_{Af}$), resistance nodulation cell division carriers ($cusA_{Af}$, $cusB_{Af}$, and $cusC_{Af}$) and/or chaperones ($cusF_{Af}$ and $copC_{Af}$) as in the copper-resistant *Acidithiobacillus ferrooxidans* (Navarro et al., 2009). A comprehensive description of the genetic characteristics and functioning of regulatory and M&R uptake/efflux systems was performed namely for thermoacidophilic, acidophilic, and metalophilic bacteria and/or archaea (Nies, 2000; Orell et al., 2010, 2013; Navarro et al., 2013; Wheaton et al., 2015).

Biomolecules for M&R Biosorption

Extremophiles-derived cell wall/capsule, S-layer proteins, extracellular polymer substances (EPS) and siderophores present unusual structural and functional properties for M&Rs biosorption under severe stress. Llorens et al. (2012) suggested uranium sorption by S-layer proteins on the metalophilic *Cupriavidus metallidurans* at pH1; while acidophilic (Masaki et al., 2015) and moderate halophilic bacteria/archaea adsorbed M&Rs onto cell surface (Amoozegar et al., 2007, 2008, 2012). EPS are the most relevant structures for M&R biosorption with proved efficiency namely on psychrotolerant (*Pseudoalteromonas* sp.; Qin et al., 2007) and acidophilic (*A. ferroxidans*; Sand and Gehrke, 2006) bacteria. Either attached on the cell surface or extracellularly released, extremophilic EPS promote cell adhesion, biofilm formation, and M&Rs biosorption (Poli et al., 2011) due to a greater abundance of negatively-charged metal-binding sites of its components (e.g., polysaccharides, proteins, nucleic acids, and lipids) (Nies, 2000; Navarro et al., 2013; Shukla et al., 2017). An improved structure/composition favors enzyme stabilization and protein anchoring, hence boosting bacteria/archaea proliferation (Qin et al., 2007). Some halophilic archae can synthesize EPS with specialized jellifying properties due to abundant glucuronic acids and sulfates that stabilize EPS matrix and enhances M&R sorption (Singh and Singh, 2017). Siderophores are small biomolecules released to the environment for metal scavaging. De Serrano et al. (2016) reviewed regulatory mechanisms and chemical features of siderophores synthesized by extremophiles, evidencing their potential as bioremediation agents for metal chelation.

Biocatalysts for M&R Biotransformation and Bioprecipitation/Bioaccumulation

Extremophiles mediate the chemical transformation of M&R through the biosynthesis of enzymes that intracellularly or extracellularly catalyze M&Rs oxidation (solubilization) or reduction (precipitation) (Das et al., 2016). Overall, the redox reactions may occur through direct or indirect activity of extremophiles (e.g., sulfur-/iron-oxidizing or sulfate-reducing), under aerobiosis and/or anaerobiosis (Zhang et al., 2016;

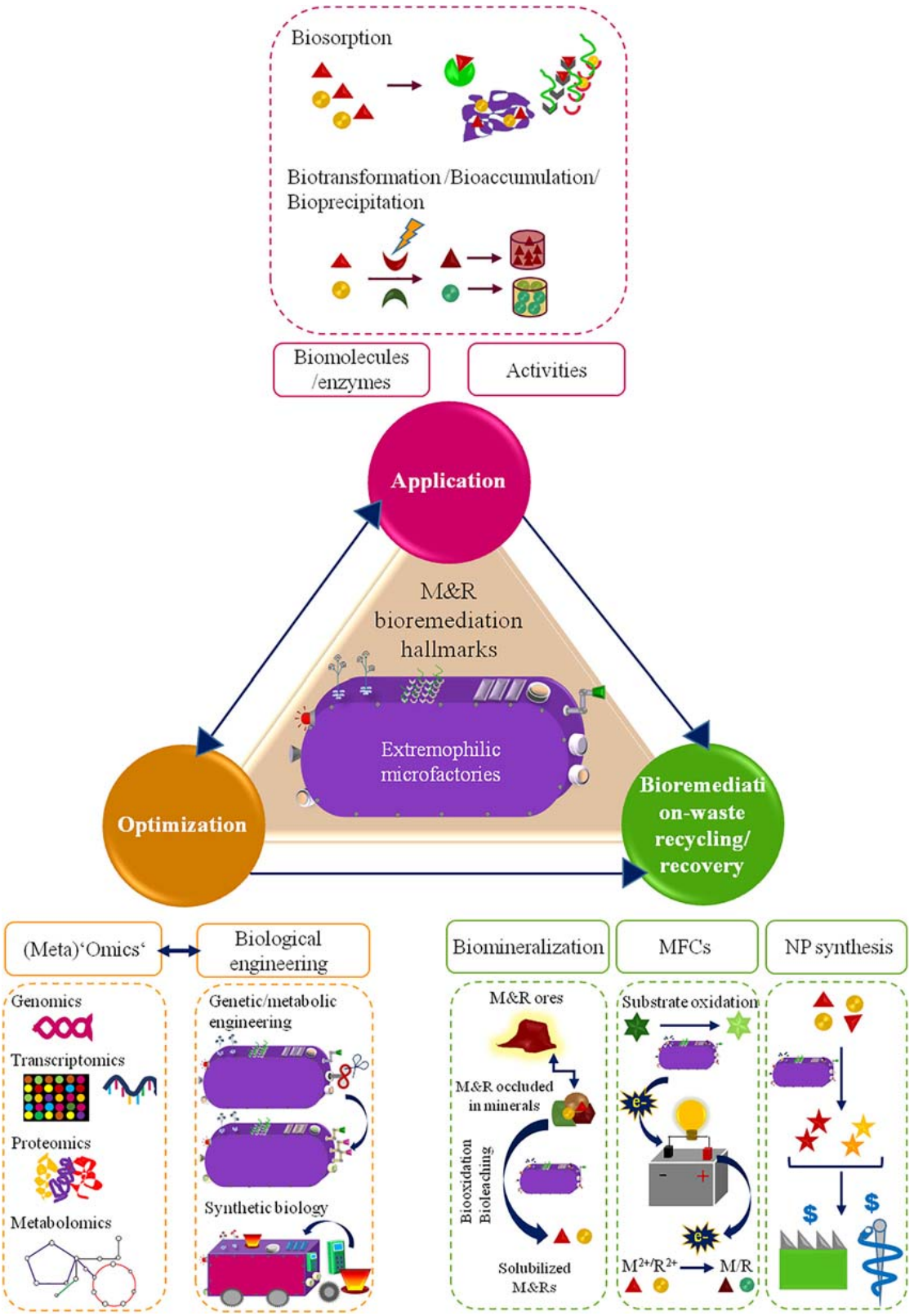

FIGURE 1 | Schematic diagram of the M&R bioremediation hallmarks approached in this review.

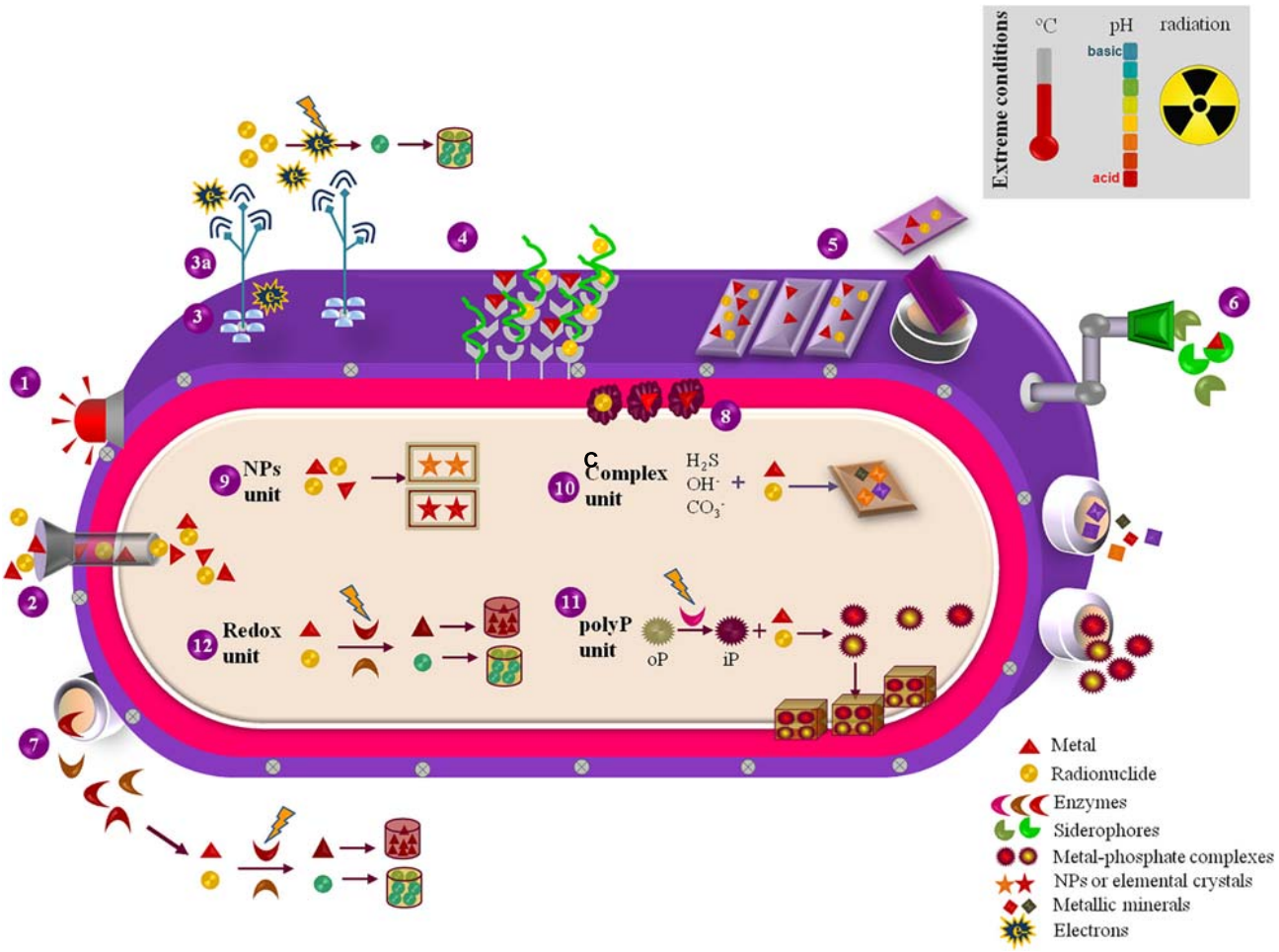

FIGURE 2 | Representation of the exploitable biosynthetic and metabolic features of extremophilic microfactories with relevance for M&R bioremediation purposes. (1) M&R sensing by regulatory proteins that trigger downstream genetic and metabolic pathways coping with M&R exposure. (2) M&R uptake through energy-dependant transporters as resistance nodulation cell division carriers. (3) Surface *c*-cytochromes that promote electron transference to pili (3a), which electron-conductive ability promotes the extracellular reduction and precipitation of M&Rs. (4) M&R binding sites at the cell-surface cationic and anionic functional groups and S-layer proteins. (5) Extracellular polymeric substances (EPS) that function as panels for M&R capture and sorption, either attached to the cell surface or released to the extracellular environment. (6) Biosynthetic siderophores extracellularly excreted for M&R sorption. (7) Redox enzymes liberated for catalyzing the reduction/oxidation of M&Rs that, if reduced, may precipitate and accumulate in the outer environment. (8) Metallic chaperones located in the periplasm space that promote M&Rs quenching and mobilization. (9) M&R-based nanoparticles (NPs) or nanocrystals formed and accumulated in the cytoplasm. (10) M&R biotransformation through complexation with hydroxides, carbonates, sulfides, hence forming M&R-oxides, M&R-carbonates and M&R-sulfides complexes either intracellularly accumulated or released to the exterior environment. (11) Enzymatic hydrolysis of organic poly-phosphates into inorganic phosphates for M&R precipitation and accumulation as metal-phosphate granules in the inner space or expelled to the exterior. (12) Reduction/oxidation of M&Rs in the cytoplasm driven by biosynthesized redox enzymes.

Shukla et al., 2017). Normally, M&R reduction leads to the bioprecipitation/bioaccumulation of organic- and mineral-M&R complexes, and M&R-based nanocrystals. Halophilic (Amoozegar et al., 2012; Srivastava et al., 2013), thermo-tolerant (Özdemir et al., 2017a,b), thermophilic (Kashefi and Lovley, 2000), metalophilic (Lovley et al., 1991), radiophilic (Appukuttan et al., 2011) and acidophilic bacteria and archaea (Orell et al., 2012; Masaki et al., 2015), proved to precipitate tellurite, uranium, iron, silver, chromium, or copper as elemental nanocrystals, carbonate complexes, magnetite and metal-sulfides. Inorganic polyphosphate granules enzymatically-transformed by acidophilic and metalophilic bacteria (e.g., *Caulobacter crescentus*, *Acidithiobacillus* sp.) and archaea (e.g., *Sulfolobus metallicus*) can intracellularly and extracellularly accumulate M&Rs (Hu et al., 2005; Navarro et al., 2009; Orell et al., 2012). M&R bioaccumulation/bioprecipitation was indeed favored by highly reductive pili (Cologgi et al., 2011) and *c*-cytochromes (Marshall et al., 2006; Shelobolina et al., 2007) that increase electron transport, which attached to *Geobacter* sp. or *Shewanella oneidensis* outer membranes, promote the extracellular reduction of U(VI) into the precipitable U(IV) along with cell viability and growth. These strategies are excellent towards *in situ*

bioremediation, as already applied for uranium clean-up in groundwater (Coates and Anderson, 2000).

Despite the great biotechnological potential of extremophilic microfactories, remediation efficiency, biomass productivity, and economic profitability may be challenging, especially for *in situ* applications due to extreme optima, interspecies competition and interaction/communication inhibiting bioremediation, and limited proliferation (Ramos et al., 2011; Johnson et al., 2015). Consequently, extremophiles-based M&R bioremediation may become less attractive considering mining industry demands, hence requiring function-directed improvements.

UPGRADING EXTREMOPHILIC MICROFACTORIES FOR ENHANCED M&R BIOREMEDIATION

'Omics' and biological engineering are leading the achievement of more proficient extremophilic microfactories for M&R bioremediation to keep pace with current economical, technological, social, and climate change defiance.

'Omics' Package: Unraveling New Genes and Functions of Extremophiles

A fundamental step is to untie the genomic and metabolic complexity governing extremophiles-M&R interactions. Therefore, genomic approaches involving amplicon and whole-genome sequencing, comparative genomics and *in silico* genome mining have been employed to target essential genes encoding regulatory proteins, promoters, metal-binding proteins, enzymes, and biomolecules involved in radionuclides (e.g., Makarova et al., 2001; Methé et al., 2003; Zivanovic et al., 2009) and metals (e.g., Nies, 2000; Osorio et al., 2008; Cárdenas et al., 2010; Guo et al., 2014; Kernan et al., 2017) detoxification in extremophilic bacteria (e.g., *Geobacter sulfurreducens*, *Acidithiobacillus* spp., *Deinococcus radiodurans*, *Sulfobacillus thermosulfidooxidans*) and archaea (e.g., *Thermococcus gammatolerans*, *Metallosphaera sedula*).

Despite the relevance of this knowledge, the study of M&R-constrained gene expression and regulation through transcriptomics assumes a pivotal role for bioremediation purposes. DNA microarrays applied to the As-resistant *Thiomonas* spp. evidenced genomic rearrangements and horizontal gene transfer (Arsène-Ploetze et al., 2010), which can be exploited to transfer M&R resistance. Other studies observed overexpression of metallochaperones and enzymes mediating metal-phosphate granules formation in acidophilic bacteria (*A. ferooxidans*) (Navarro et al., 2009) and (thermo)acidophilic archaea (*Sulfolobus metallicus, Metallosphaera sedula*) challenged with M&Rs (Orell et al., 2013; Wheaton et al., 2016).

Nevertheless, many transcripts keep with unassigned functions or activities. Proteomics, through 2-DE gel coupled with mass spectroscopy (e.g., LC–MS, MALDI-ToF, and ICPL) tools and protein libraries, is thereby elucidating the type and abundance of proteins synthesized under M&R stress (Desai et al., 2010). Among them, those associated with EPS and biofilm production, oxidative stress responses, regulation of RND-type Cus system and metal uptake/efflux pumps (Zivanovic et al., 2009; Almárcegui et al., 2014; Martínez-Bussenius et al., 2016) are hugely relevant.

Additionally, metabolomics enlightens the metabolic fingerprinting of M&R-induced responses on extremophiles (Mosier et al., 2013). A diverse toolbox of chromatographic (GC and HPLC) and spectroscopic (FTIR and NMR) techniques have hence been employed to harness the genetic, transcriptional and translational processes sustaining the cellular biomolecules/metabolite fluxes (i.e., fluxomics) (Hold et al., 2009; Desai et al., 2010) leading to M&R sequestration. *In silico* reconstruction of unknown metabolic networks relevant for M&R bioremediation based on sequenced genomes (Sun et al., 2009), robust bioinformatics and libraries, is becoming a powerful fine-tuning approach, though requiring a cautious analysis of metal-microbe interactions to prevent misinterpretations (Johnson et al., 2015). In this context, community-level meta-omics (metagenomics, metatranscriptomics, and metaproteomics) offer great avenues by avoiding extremophiles culturing hurdles, while uncovering pools of novel biomolecules/enzymes for M&R bioremediation without previous sequence data (Mohamed et al., 2013), and providing ecologically-relevant analysis of community shifts and functions (Cowan et al., 2015; Garris et al., 2016; Mirete et al., 2016) along the bioremediation processes. Multi-'omics' integration, either at individual or community levels, constitutes another robust approach to unravel new M&R-bioremediation agents or monitoring bio-devices. Indeed, Wilkins et al. (2011) used a proteogenomic analysis to develop a biomarker of *G. sulfurreducens* activity during uranium bioremediation.

Engineering Extremophic Microfactories for M&R Bioremediation

The advent of DNA recombinant techniques for tailoring existent abilities or to create synthetic ones, in natural or newly designed extremophiles, is a doorway to boost M&R bioremediation.

Genetic/Metabolic Engineering of Whole-Microbes and Communities

The peculiar mechanisms of extremophiles can be customized through the insertion of genes or gene clusters, as to enhance their skills and robustness for M&R attenuation (Cárdenas et al., 2010). Metal-resistant (*Cupriavidus metallidurans*; Rojas et al., 2011), radiophilic (*D. radiodurans*; Brim et al., 2000) and thermoacidophilic (*D. geothermalis*; Brim et al., 2003) bacteria were transformed with genes/clusters encoding enzymes involved in individual- or multi-M&Rs reduction/oxidation. This is biotechnologically worthy given the mixture of M&Rs in mine/nuclear wastes. In order to enhance M&R bioprecipitation, *D. radiodurans* was indeed manipulated to express a Cd(II)-binding synthetic phytochelatin (*EC20*) and metallothionein (*smtA*) (Chaturvedi and Archana, 2014), and a periplasmic acid phosphatase (PhoN), which hydrolysed organic into inorganic phosphates to precipitate uranium (Appukuttan et al., 2006, 2011). However, some extremophiles are more resistant to transformation due to their robust protective mechanisms (Chen

et al., 2011; Liu et al., 2011), hence forcing the construction of adapted vectors (Meng et al., 2013).

Recently, the innovative project NANOBINDERS (PTDC/AAG-REC/3004/2014) is enrolled in the creation of biogenic nanopolymers functionalized to bind M&Rs (the NANOBINDERS) from uranium mine effluents. These M&R-binding nanopolymers are self-assembled inside a host transformed with new constructs harboring nanopolymer- and metal-binding-peptides-encoding genes, originally obtained from microbes isolated in a uranium mine. Such functional nanobeads are a revolutionary option to engineered microbes, which *in situ* release still raises regulatory concerns, besides genetic instability and limited efficiency under real scenarios (de Lorenzo, 2009). Alternatively, manipulated extremophiles may house suicidal genes (Paul et al., 2005) activated upon undetectable M&R levels, for future *in situ* application.

Native microbial communities have been used to rehabilitate M&R-contaminated areas by natural attenuation (Shukla et al., 2017), which can be engineered through biostimulation (i.e., supplementation of compounds/substrates enhancing microbial proliferation and activities) and/or bioaugmentation measures (i.e., addition of microbes endowed with particular functional mechanisms). In mesocosms, Ñancucheo and Johnson (2011) reduced acid mine drainage production when consortia of metabolically-cooperating microalgae, acidophilic and/or acid-tolerant bacteria were added to promote iron- and/or sulfate-reduction of tailings. The biostimulation of *Geobacter* sp. activity by acetate enrichment had enhanced uranium reduction, thereby proving successful *in situ* bioremediation (Anderson et al., 2003). However, metabolic fluxes modeling (Hold et al., 2009) should be applied in the future to design novel extremophilic consortia with tailored co-activities for M&R clean-up.

Synthetic Biology

Synthetic biology (SynBio) moves beyond the simple transformation of genes or operons to the insertion of newly designed and constructed synthetic biological parts and circuits to create robust, profitable, programmable and customized microfactories (Martínez-Garcia and de Lorenzo, 2016). The genetic instability and limited performance of engineered microbes for M&R bioremediation, can be overcome by DNA *de novo* synthesis and genome editing tools [e.g., Clustered Regularly Interspaced Short Palindromic Repeats (CRISPRs)- and protein Cas; Mougiakos et al., 2016, 2017]. Hence, extremophiles can be engineered as novel platforms (or *chassis*) housing stable and multiple designed functions together with the transcriptional and translational machinery to be active from laboratory- to field-scale extreme scenarios (Adams, 2016). Likewise, Gerber et al. (2015) took advantage of *Deinococcus* genetic plasticity and robustness to construct a *chassis* towards different applications. *Deinococcus* spp. was also successfully engineered with metal-resistance genes, demonstrating their genetic flexibility for heterologous and co-expression of different metal-resistance determinants under extreme temperature and radiation (Brim et al., 2000, 2003). Thus, constructing extremophilic-microfactories *chassis* is an appealing new wave for enhanced M&R bioremediation, especially if universal genetic toolkits could be created (Adams, 2016).

The joint endeavor of SynBio and metabolic engineering of communities is indeed enabling the design and building of synthetic consortia (Shong et al., 2012) for M&R remediation. Developing synthetic consortia demands the engineering of cell–cell communication, i.e., quorum-sensing (QS) systems (Brenner et al., 2008). QS modulates behavioral, metabolic and structural dynamics in microbial communities through signaling molecules [e.g., acyl homoserine lactones family (AHL)] (Shong et al., 2012). QS is pivotal namely in EPS synthesis and biofilm formation (Farah et al., 2005; McDougald et al., 2012), as well as AHLs can mediate copper resistance in *A. ferrooxidans* (Wenbin et al., 2011). Thus, putting effort on the modulation or creation of new QS systems and signaling molecules biosynthesis can fine-tune the pool of relevant functions in extremophilic consortia for M&R removal (e.g., biomass production and EPS synthesis) (Brune and Bayer, 2012; Shong et al., 2012).

GENERATING RICHNESS FROM BIOREMEDIATED M&Rs

A discouraging issue in M&R bioremediation is the disposal of final wastes. Nevertheless, extremophilic microfactories can be successfully explored for M&Rs recycling and/or recovery after being remediated, thereby sustainably closing M&R bioremediation processes.

Biomining

Biomining is usually conducted by extremophilic bacteria and archaea for the recovery of M&R from ores and mine/metal-rich/nuclear wastes, through biooxidation (minerals oxidation for metal release) and/or bioleaching (metal solubilization) (Brune and Bayer, 2012; Johnson, 2014). These bioprocesses take advantage of the anaerobic metabolism, redox pathways, intercellular communication, biofilm formation (Vera et al., 2013), and resistance to heat, acid and metals of (thermo)acidophiles consortia (e.g., *Leptospirillum* spp., *Acidithiobacillus* spp., *Sulfobacillus* spp., *Ferroplasma* spp., *Acidiplasma* spp.) (Orell et al., 2010, 2013). Insoluble metal sulfides are converted into soluble metal sulfates by iron- and sulfur-oxidizing extremophiles, thereby facilitating the recovery of economically-relevant metals (e.g., Cu, Fe, Au, Ni, and Zn) (Watling et al., 2015; Wheaton et al., 2015).

Microbial Fuel Cells (MFCs)

Microbial fuel cells (MFCs) can be a valuable recovery method since it uses the catalytic activity of microbes to generate electrical energy from the oxidation of organic substrates (Mathuriya and Yakhmi, 2014). They are composed by an anode that captures electrons from substrate oxidation, a cathode and an intermediate cation-specific membrane. Since M&Rs have a high redox potential, they can be reduced and precipitated by receiving electrons from the

cathode. *Geobacter sulfurreducens* biofilms possessing electron-conductive nanowires (pili) have been exploited for increased electricity generation into MFCs (Reguera et al., 2006). The generated electrons can be further used to reduce U(VI) into removable U(IV), hence synergizing *Geobacter* sp. skills for bioremediation-derived-waste recycling. An anoxic sludge containing *Geobacter* spp. recovered the noble metal silver, while generating electrical energy in a MFC (Ho et al., 2017). Other extremophiles have indeed been used in MFCs (Shrestha et al., 2018), especially towards metal recovery (Dopson et al., 2015).

Recycling Through Nanoparticles (NPs) Production

Extremophiles biosynthesize economically-lucrative inorganic NPs through intracellular or extracellular transformation/precipitation of M&Rs (Ulloa et al., 2016), hence providing another profitable M&R recycling strategy. The metal-tolerant *Cupriavidus metallidurans* CH34 mineralized Au and precipitated it as nanoparticulate Au^0 in the periplasm (Reith et al., 2009), whilst the alkalotolerant *Rhodococcus* sp. accumulated Au-NPs in the cytoplasm and cell wall (Ahmad et al., 2003). Spherical Ag-NPs were also extracellularly synthesized at 80°C by the thermophilic *Ureibacillus thermosphaericus* (Juibari et al., 2011). CdS-NPs with enhanced stability under acidic conditions were produced by *Acidithiobacillus* spp., being a gainful option for Cd turnover (Ulloa et al., 2016). Uraninite, which is a worthy biogenic NP for uranium *in situ* remediation (Bargar et al., 2008), was synthesized by *Geobacter metallireducens* upon extracellular U(VI) reduction (Gorby and Lovley, 1992). The precious metal Pd(II) used in many industrial sectors was precipitated in *G. sulfurreducens* biofilms as Pd(0)-NPs and easily extracted by centrifugation (Yates et al., 2013).

CONCLUDING REMARKS

Extremophiles enclose a pool of genetic and metabolic opportunities that can be harnessed as microfactories for multiple M&R-bioremediation hallmarks. Nevertheless, the complexity of extremophiles' cellular mechanisms, interspecies relationships and M&R interplay under real scenarios of co-occurring extreme conditions may rise some challenges. Multi-'omics' applied side-by-side with genetic engineering techniques are covering knowledge gaps, allowing gene expression and metabolic pathways customization for improved bioremediation. Synthetic biology, however, through an iterative design-build-test-analyze framework is further revolutionizing M&R bioremediation and opening new perspectives on the creation of robust extremophilic recombinants or *chassis* with *de novo*-designed biologically-, energetically-, and economically-viable traits for specific M&R removal processes. Future trends will hence target adaptation or construction of multi-skilled extremophilic microfactories to sustainably empower M&R bioremediation and end-waste recycling, while keeping up with global changes, natural resources availability, and cost-efficiency requirements.

AUTHOR CONTRIBUTIONS

CM was responsible for doing all the tasks concerning the development of the work: conceptualized the idea and goals of the mini-review, performed literature search and revision, and wrote the manuscript.

FUNDING

This work was funded by the Portuguese Foundation for Science and Technology (FCT) and by the European Regional Development Fund (ERDF) through the Portugal 2020 Partnership Agreement between Portugal and the European Union, the Competitiveness and Internationalization Operational Program (COMPETE 2020) and the Regional Operational Program Lisboa (POR-Lisboa), under the project NANOBINDERS (PTDC/AAG-REC/3004/2014). CM was granted as an Invited Scientist within the project NANOBINDERS (ref. BCC/UI88/5626/2016). Thanks are due for the financial support to CESAM (UID/AMB/50017 – POCI-01-0145-FEDER-007638), to FCT/MCTES through national funds (PIDDAC), and the co-funding by the FEDER, within the PT2020 Partnership Agreement and Compete 2020.

REFERENCES

Adams, B. L. (2016). The next generation of synthetic biology chassis: moving synthetic biology from the laboratory to the field. *ACS Synth. Biol.* 5, 1328–1330. doi: 10.1021/acssynbio.6b00256

Ahmad, A., Senapati, S., Khan, M. I., Kumar, R., Ramani, R., Srinivas, V., et al. (2003). Intracellular synthesis of gold nanoparticles by a novel alkalotolerant actinomycete, *Rhodococcus* species. *Nanotechnology* 14, 824–828. doi: 10.1088/0957-4484/14/7/323

Almárcegui, R. J., Navarro, C. A., Paradela, A., Albar, J. P., von Bernath, D., and Jere, C. A. (2014). New copper resistance determinants in the extremophile *Acidithiobacillus ferrooxidans*: a quantitative proteomic analysis. *J. Proteome Res.* 13, 946–960. doi: 10.1021/pr4009833

Amoozegar, M. A., Ashengroph, M., Malekzadeh, F., Reza, R. M., Naddaf, S., and Kabiri, M. (2008). Isolation and initial characterization of the tellurite reducing moderately halophilic bacterium, *Salinicoccus* sp. strain QW6. *Microbiol. Res.* 163, 456–465. doi: 10.1016/j.micres.2006.07.010

Amoozegar, M. A., Ghasemi, A., Razavi, M. R., and Naddaf, S. (2007). Evaluation of hexavalent chromium reduction by chromate-resistant moderately halophile, *Nesterenkonia* sp. strain MF2. *Process. Biochem.* 42, 1475–1479. doi: 10.1016/j.procbio.2007.07.001

Amoozegar, M. A., Khoshnoodi, M., Didari, M., Hamedi, J., Ventosa, A., and Baldwin, S. A. (2012). Tellurite removal by a tellurium-tolerant halophilic bacterial strain, *Thermoactinomyces* sp. QS-2006. *Ann. Microbiol.* 62, 1031–1037. doi: 10.1007/s13213-011-0343-1

Anderson, R. T., Vrionis, H. A., Ortiz-Bernad, I., Resch, C. T., Long, P. E., Dayvault, R., et al. (2003). Stimulating the in situ activity of *Geobacter* species to remove uranium from the groundwater of a uranium-contaminated aquifer. *Appl. Environ. Microbiol.* 69, 5884–5891. doi: 10.1128/AEM.69.10.5884-5891.2003

Appukuttan, D., Rao, A. S., and Apte, S. K. (2006). Engineering of *Deinococcus radiodurans* R1 for bioprecipitation of uranium from diluted nuclear waste. *Appl. Environ. Microbiol.* 72, 7873–7878. doi: 10.1128/AEM.01362-06

Appukuttan, D., Seetharam, C., Padma, N., Rao, A. S., and Apte, S. K. (2011). PhoN-expressing, lyophilized, recombinant *Deinococcus radiodurans* cells for uranium bioprecipitation. *J. Biotechnol.* 154, 285–290. doi: 10.1016/j.jbiotec.2011.05.002

Arsène-Ploetze, F., Koechler, S., Marchal, M., Coppée, J. Y., Chandler, M., Bonnefoy, V., et al. (2010). Structure, function, and evolution of the *Thiomonas* spp. genome. *PLoS Genet.* 6:e1000859. doi: 10.1371/journal.pgen.1000859

Bargar, J. R., Bernier-Latmani, R., Giammar, D. E., and Tebo, B. M. (2008). Biogenic uraninite nanoparticles and their importance for uranium remediation. *Elements* 4, 407–412. doi: 10.2113/gselements.4.6.407

Brenner, K., You, L., and Arnold, F. H. (2008). Engineering microbial consortia: a new frontier in synthetic biology. *Trends Biotechnol.* 26, 483–489. doi: 10.1016/j.tibtech.2008.05.004

Brim, H., McFarlan, S. C., Fredrickson, J. K., Minton, K. W., Zhai, M., Wackett, L. P., et al. (2000). Engineering *Deinococcus radiodurans* for metal remediation in radioactive mixed waste environments. *Nat. Biotechnol.* 18, 85–90. doi: 10.1038/71986

Brim, H., Venkateswaran, A., Kostandarithes, H. M., Fredrickson, J. K., and Daly, M. J. (2003). Engineering *Deinococcus geothermalis* for bioremediation of high-temperature radioactive waste environments. *Appl. Environ. Microbiol.* 69, 4575–4582. doi: 10.1128/AEM.69.8.4575-4582.2003

Brune, K. D., and Bayer, T. S. (2012). Engineering microbial consortia to enhance biomining and bioremediation. *Front. Microbiol.* 3:203. doi: 10.3389/fmicb.2012.00203

Cárdenas, J. P., Valdés, J., Quatrini, R., Duarte, F., and Holmes, D. S. (2010). Lessons from the genomes of extremely acidophilic bacteria and archaea with special emphasis on bioleaching microorganisms. *Appl. Microbiol. Biotechnol.* 88, 605–620. doi: 10.1007/s00253-010-2795-9

Carvalho, F. P. (2017). Mining industry and sustainable development time for change. *Food Energy Sec.* 6, 61–77. doi: 10.1002/fes3.109

Chaturvedi, R., and Archana, G. (2014). Cytosolic expression of synthetic phytochelatin and bacterial metallothionein genes in *Deinococcus radiodurans* R1 for enhanced tolerance and bioaccumulation of cadmium. *Biometals* 27, 471–482. doi: 10.1007/s10534-014-9721-z

Chen, D., Lin, J., Che, Y., Liu, X., and Lin, J. (2011). Construction of recombinant mercury resistant *Acidithiobacillus caldus*. *Microbiol. Res.* 166, 515–520. doi: 10.1016/j.micres.2010.10.003

Coates, J. D., and Anderson, R. T. (2000). Emerging techniques for anaerobic bioremediation of contaminated environments. *Trends Biotechnol.* 18, 408–412. doi: 10.1016/S0167-7799(00)01478-5

Cologgi, D. L., Lampa-Pastirk, S., Speers, A. M., Kelly, S. D., and Reguera, G. (2011). Extracellular reduction of uranium via *Geobacter* conductive pili as a protective cellular mechanism. *Proc. Natl. Acad. Sci. U.S.A.* 108, 15248–15252. doi: 10.1073/pnas.1108616108

Cowan, D. A., Ramond, J. B., Makhalanyane, T. P., and De Maayer, P. (2015). Metagenomics of extreme environments. *Curr. Opin. Microbiol.* 25, 97–102. doi: 10.1016/j.mib.2015.05.005

Das, S., Dash, H. R., and Chakraborty, J. (2016). Genetic basis and importance of metal resistant genes in bacteria for bioremediation of contaminated environments with toxic metal pollutants. *Appl. Microbiol. Biotechnol.* 100, 2967–2984. doi: 10.1007/s00253-016-7364-4

de Lorenzo, V. (2009). Recombinant bacteria for environmental release: what went wrong and what we have learnt from it. *Clin. Microbiol. Infect.* 1, 63–65. doi: 10.1111/j.1469-0691.2008.02683.x

De Serrano, L. O., Camper, A. K., and Richards, A. M. (2016). An overview of siderophores for iron acquisition in microorganisms living in the extreme. *Biometals* 29, 551–571. doi: 10.1007/s10534-016-9949-x

Dekker, L., Arsène-Ploetze, F., and Santini, J. M. (2016). Comparative proteomics of *Acidithiobacillus ferrooxidans* grown in the presence and absence of uranium. *Res. Microbiol.* 167, 234–239. doi: 10.1016/j.resmic.2016.01.007

Desai, C., Pathak, H., and Madamwar, D. (2010). Advances in molecular and "-omics" to gauge microbial communities and bioremediation at xenobiotic/anthropogen contaminated sites. *Bioresour. Technol.* 101, 1558–1569. doi: 10.1016/j.biortech.2009.10.080

Dopson, M., Ni, G., and Sleutels, T. H. (2015). Possibilities for extremophilic microorganisms in microbial electrochemical systems. *FEMS Microbiol. Rev.* 40, 164–181. doi: 10.1093/femsre/fuv044

Elleuche, S., Schröder, C., Sahm, K., and Antranikian, G. (2014). Extremozymes — biocatalysts with unique properties from extremophilic microorganisms. *Curr. Opin. Biotechnol.* 29, 116–123. doi: 10.1016/j.copbio.2014.04.003

Farah, C., Vera, M., Morin, D., Haras, D., Jerez, C. A., and Guiliani, N. (2005). Evidence for a functional quorum-sensing type AI-1 system in the extremophilic bacterium *Acidithiobacillus ferrooxidans*. *Appl. Environ. Microbiol.* 71, 7033–7040. doi: 10.1128/AEM.71.11.7033-7040.2005

Garris, H. W., Baldwin, S. A., van Hamme, J. D., Gardner, W. C., and Fraser, L. H. (2016). Genomics to assist mine reclamation: a review. *Restor. Ecol.* 24, 165–173. doi: 10.1111/rec.12322

Gerber, E., Bernard, R., Castang, S., Chabot, N., Coze, F., Dreux-Zigha, A., et al. (2015). *Deinococcus* as new chassis for industrial biotechnology: biology, physiology and tools. *J. Appl. Microbiol.* 119, 1–10. doi: 10.1111/jam.12808

Gorby, Y. A., and Lovley, D. R. (1992). Enzymatic uranium precipitation. *Environ. Sci. Technol.* 26, 205–207. doi: 10.1021/es00025a026

Guo, X., Yin, H., Liang, Y., Hu, Q., Zhou, X., Xiao, Y., et al. (2014). Comparative genome analysis reveals metabolic versatility and environmental adaptations of *Sulfobacillus thermosulfidooxidans* strain ST. *PLoS One* 9:e99417. doi: 10.1371/journal.pone.0099417

Gupta, P., and Diwan, B. (2017). Bacterial exopolysaccharide mediated heavy metal removal: a review on biosynthesis, mechanism and remediation strategies. *Biotechnol. Rep.* 13, 58–71. doi: 10.1016/j.btre.2016.12.006

Ho, N. A. D., Babel, S., and Kurisu, F. (2017). Bio-electrochemical reactors using AMI-7001S and CMI-7000S membranes as separators for silver recovery and power generation. *Bioresour. Technol.* 244, 1006–1014. doi: 10.1016/j.biortech.2017.08.086

Hold, C., Andrews, B. A., and Asenjo, J. A. (2009). A stoichiometric model of *Acidithiobacillus ferrooxidans* ATCC 23270 for metabolic flux analysis. *Biotechnol. Bioeng.* 102, 1448–1459. doi: 10.1002/bit.22183

Hu, P., Brodie, E. L., Suzuki, Y., McAdams, H. H., and Andersen, G. L. (2005). Whole-genome transcriptional analysis of heavy metal stresses in *Caulobacter crescentus*. *J. Bacteriol.* 187, 8437–8449. doi: 10.1128/JB.187.24.8437-8449.2005

Johnson, D. B. (2014). Biomining-biotechnologies for extracting and recovering metals from ores and waste materials. *Curr. Opin. Biotechnol.* 30, 24–31. doi: 10.1016/j.copbio.2014.04.008

Johnson, D. R., Helbling, D. E., Men, Y., and Fenner, K. (2015). Can meta-omics help to establish causality between contaminant biotransformations and genes or gene products? *Environ. Sci.* 1, 272–278. doi: 10.1039/C5EW00016E

Juibari, M. M., Abbasalizadeh, S., Jouzani, G. S., and Noruzi, M. (2011). Intensified biosynthesis of silver nanoparticles using a native extremophilic *Ureibacillus thermosphaericus* strain. *Mater. Lett.* 65, 1014–1017. doi: 10.1016/j.matlet.2010.12.056

Kashefi, K., and Lovley, D. R. (2000). Reduction of Fe(III), Mn(IV), and toxic metals at 100°C by *Pyrobaculum islandicum*. *Appl. Environ. Microbiol.* 66, 1050–1056. doi: 10.1128/AEM.66.3.1050-1056.2000

Kernan, T., West, A. C., and Banta, S. (2017). Characterization of endogenous promoters for control of recombinant gene expression in *Acidithiobacillus ferrooxidans*. *Biotechnol. Appl. Biochem.* 64, 793–802. doi: 10.1002/bab.1546

Krulwich, T. A., Sachs, G., and Padan, E. (2011). Molecular aspects of bacterial pH sensing and homeostasis. *Nat. Rev. Microbiol.* 9, 330–343. doi: 10.1038/nrmicro2549

Li, J., and Zhang, Y. (2012). Remediation technology for the uranium contaminated environment: a review. *Procedia Environ. Sci.* 13, 1609–1615. doi: 10.1016/j.proenv.2012.01.153

Liu, W., Lin, J., Pang, X., Cui, S., Mi, S., and Lin, J. (2011). Overexpression of rusticyanin in *Acidithiobacillus ferrooxidans* ATCC19859 increased Fe(II) oxidation activity. *Curr. Microbiol.* 62, 320–324. doi: 10.1007/s00284-010-9708-0

Llorens, I., Untereiner, G., Jaillard, D., Gouget, B., Chapon, V., and Carriere, M. (2012). Uranium interaction with two multi-resistant environmental bacteria: *Cupriavidus metallidurans* CH34 and *Rhodopseudomonas palustris*. *PLoS One* 7:e51783. doi: 10.1371/journal.pone.0051783

Lloyd, J. R., and Lovley, D. R. (2001). Microbial detoxification of metals and radionuclides. *Curr. Opin. Biotechnol.* 12, 248–253. doi: 10.1016/S0958-1669(00)00207-X

Lovley, D. R., Phillips, E. J. P., Gorby, Y. A., and Landa, E. R. (1991). Microbial reduction of uranium. *Nature* 350, 413–416. doi: 10.1038/350413a0

Makarova, K. S., Aravind, L., Wolf, Y. I., Tatusov, R. L., Minton, K. W., Koonin, E. V., et al. (2001). Genome of the extremely radiation-resistant bacterium *Deinococcus radiodurans* viewed from the perspective of comparative genomics. *Microbiol. Mol. Biol. Rev.* 65, 44–79. doi: 10.1128/MMBR.65.1.44-79.2001

Marques, C. R., Caetano, A. L., Haller, A., Goncalves, F., Pereira, R., and Rombke, J. (2014). Toxicity screening of soils from different mine areas - A contribution to track the sensitivity and variability of *Arthrobacter globiformis* assay. *J. Hazard. Mater.* 274, 331–341. doi: 10.1016/j.jhazmat.2014.03.066

Marshall, M. J., Beliaev, A. S., Dohnalkova, A. C., Kennedy, D. W., Shi, L., and Wang, Z. (2006). c-Type cytochrome-dependent formation of U(IV) nanoparticles by Shewanella oneidensis. *PLoS Biol.* 4:e268. doi: 10.1371/journal.pbio.0040268

Martínez-Bussenius, C., Navarro, C. A., Orellana, L., Paradela, A., and Jerez, C. A. (2016). Global response of *Acidithiobacillus ferrooxidans* ATCC 53993 to high concentrations of copper: a quantitative proteomics approach. *J. Proteomics* 145, 37–45. doi: 10.1016/j.jprot.2016.03.039

Martínez-Garcia, E., and de Lorenzo, V. (2016). The quest for the minimal bacterial genome. *Curr. Opin. Biotechnol.* 42, 216–224. doi: 10.1016/j.copbio.2016.09.001

Masaki, Y., Hirajima, T., Sasaki, K., and Okibe, N. (2015). Bioreduction and immobilization of hexavalent chromium by the extremely acidophilic Fe(III)-reducing bacterium *Acidocella aromatica* strain PFBC. *Extremophiles* 19, 495–503. doi: 10.1007/s00792-015-0733-6

Mathuriya, A. S., and Yakhmi, J. V. (2014). Microbial fuel cells to recover heavy metals. *Environ. Chem. Lett.* 12, 483–494. doi: 10.1007/s10311-014-0474-2

McDougald, D., Rice, S. A., Barraud, N., Steinberg, P. D., and Kjelleberg, S. (2012). Should we stay or should we go: mechanisms and ecological consequences for biofilm dispersal. *Nat. Rev. Microbiol.* 10, 39–50. doi: 10.1038/nrmicro2695

Meng, J., Wang, H., Liu, X., Lin, J., Pang, X., and Lin, J. (2013). Construction of small plasmid vectors for use in genetic improvement of the extremely acidophilic *Acidithiobacillus caldus*. *Microbiol. Res.* 168, 469–476. doi: 10.1016/j.micres.2013.04.003

Methé, B. A., Nelson, K. E., Eisen, J. A., Paulsen, I. T., Nelson, W., Heidelberg, J. F., et al. (2003). Genome of *Geobacter sulfurreducens*: metal reduction in subsurface environments. *Science* 302, 1967–1969. doi: 10.1126/science.1088727

Mirete, S., Morgante, V., and González-Pastor, J. E. (2016). Functional metagenomics of extreme environments. *Curr. Opin. Biotechnol.* 38, 143–149. doi: 10.1016/j.copbio.2016.01.017

Mohamed, Y. M., Ghazy, M. A., Sayed, A., Ouf, A., El-Dorry, H., and Siam, R. (2013). Isolation and characterization of a heavy metal-resistant, thermophilic esterase from a Red Sea brine pool. *Sci. Rep.* 3:3358. doi: 10.1038/srep03358

Mosier, A. C., Justice, N. B., Bowen, B. P., Baran, R., Thomas, B. C., Northen, T. R., et al. (2013). Metabolites associated with adaptation of microorganisms to an acidophilic, metal-rich environment identified by stable-isotope-enabled metabolomics. *mBio* 4:e00484-12. doi: 10.1128/mBio.00484-12

Mougiakos, I., Bosma, E. F., de Vos, W. M., van Kranenburg, R., and van der Oost, J. (2016). Next generation prokaryotic engineering: the crispr-cas toolkit. *Trends Biotechnol.* 34, 575–587. doi: 10.1016/j.tibtech.2016.02.004

Mougiakos, I., Mohanraju, P., Bosma, E. F., Vrouwe, V., Finger Bou, M., Naduthodi, M. I. S., et al. (2017). Characterizing a thermostable Cas9 for bacterial genome editing and silencing. *Nat. Commun.* 8:1647. doi: 10.1038/s41467-017-01591-4

Mukherjee, A., Wheaton, G. H., Blum, P. H., and Kelly, R. M. (2012). Uranium extremophily is an adaptive, rather than intrinsic, feature for extremely thermoacidophilic *Metallosphaera* species. *Proc. Natl. Acad. Sci. U.S.A.* 109, 16702–16707. doi: 10.1073/pnas.1210904109

Ñancucheo, I., and Johnson, D. B. (2011). Significance of microbial communities and interactions in safeguarding reactive mine tailings by ecological engineering. *Appl. Environ Microbiol.* 77, 8201–8208. doi: 10.1128/AEM.06155-11

Navarro, C. A., Orellana, L. H., Mauriaca, C., and Jerez, C. A. (2009). Transcriptional and functional studies of *Acidithiobacillus ferrooxidans* genes related to survival in the presence of copper. *Appl. Environ. Microbiol.* 75, 6102–6109. doi: 10.1128/AEM.00308-09

Navarro, C. A., von Bernath, D., and Jerez, C. A. (2013). Heavy metal resistance strategies of acidophilic bacteria and their acquisition: importance for biomining and bioremediation. *Biol. Res.* 46, 363–371. doi: 10.4067/S0716-97602013000400008

Nies, D. H. (2000). Significance of microbial communities and interactions in safeguarding reactive mine tailings by ecological engineering. *Appl. Environ. Microbiol.* 77, 8201–8208. doi: 10.1128/AEM.06155-11

Orell, A., Navarro, C. A., Arancibia, R., Mobarec, J. C., and Jerez, C. A. (2010). Life in blue: copper resistance mechanisms of bacteria and archaea used in industrial biomining of minerals. *Biotechnol. Adv.* 28, 839–848. doi: 10.1016/j.biotechadv.2010.07.003

Orell, A., Navarro, C. A., Rivero, M., Aguilar, J. S., and Jerez, C. A. (2012). Inorganic polyphosphates in extremophiles and their possible functions. *Extremophiles* 16, 573–583. doi: 10.1007/s00792-012-0457-9

Orell, A., Remonsellez, F., Arancibia, R., and Jerez, C. A. (2013). Molecular characterization of copper and cadmium resistance determinants in the biomining thermoacidophilic archaeon *Sulfolobus metallicus*. *Archaea* 2013:289236. doi: 10.1155/2013/289236

Osorio, H., Martínez, V., Nieto, P. A., Holmes, D. S., and Quatrini, R. (2008). Microbial iron management mechanisms in extremely acidic environments: comparative genomics evidence for diversity and versatility. *BMC Microbiol.* 8:203. doi: 10.1186/1471-2180-8-203

Özdemir, S., Oduncu, M. K., Kilinc, E., and Soylak, M. (2017a). Resistance, bioaccumulation and solid phase extraction of uranium (VI) by *Bacillus vallismortis* and its UV-vis spectrophotometric determination. *J. Environ. Radioact.* 171, 217–225. doi: 10.1016/j.jenvrad.2017.02.021

Özdemir, S., Oduncu, M. K., Kilinc, E., and Soylak, M. (2017b). Tolerance and bioaccumulation of U(VI) by *Bacillus mojavensis* and its solid phase preconcentration by *Bacillus mojavensis* immobilized multiwalled carbon nanotube. *J. Environ. Manage.* 187, 490–496. doi: 10.1016/j.jenvman.2016.11.004

Paul, D., Pandey, G., Pandey, J., and Jain, R. K. (2005). Accessing microbial diversity for bioremediation and environmental restoration. *Trends Biotechnol.* 23, 135–142. doi: 10.1016/j.tibtech.2005.01.001

Pereira, R., Barbosa, S., and Carvalho, F. P. (2014). Uranium mining in Portugal: a review of the environmental legacies of the largest mines and environmental and human health impacts. *Environ. Geochem. Health* 36, 285–301. doi: 10.1007/s10653-013-9563-6

Poli, A., Di Donato, P., Abbamondi, G. R., and Nicolaus, B. (2011). Synthesis, production, and biotechnological applications of exopolysaccharides and polyhydroxyalkanoates by archaea. *Archaea* 2011:693253. doi: 10.1155/2011/693253

Qin, G., Zhu, L., Chen, X., Wang, P. G., and Zhang, Y. (2007). Structural characterization and ecological roles of a novel exopolysaccharide from the deep-sea psychrotolerant bacterium *Pseudoalteromonas* sp. SM9913. *Microbiology* 153, 1566–1572. doi: 10.1099/mic.0.2006/003327-0

Raddadi, N., Cherif, A., Daffonchio, D., Neifar, M., and Fava, F. (2015). Biotechnological applications of extremophiles, extremozymes and extremolytes. *Appl. Microbiol. Biotechnol.* 99, 7907–7913. doi: 10.1007/s00253-015-6874-9

Ramos, J. L., Marqués, S., van Dillewijn, P., Espinosa-Urgel, M., Segura, A., Duque, E., et al. (2011). Laboratory research aimed at closing the gaps in microbial bioremediation. *Trends Biotechnol.* 29, 641–647. doi: 10.1016/j.tibtech.2011.06.007

Reguera, G., Nevin, K. P., Nicoll, J. S., Covalla, S. F., Woodard, T. L., and Lovley, D. R. (2006). Biofilm and nanowire production leads to increased current in *Geobacter sulfurreducens* fuel cells. *Appl. Environ. Microbiol.* 72, 7345–7348. doi: 10.1128/AEM.01444-06

Reith, F., Etschmann, B., Grosse, C., Moors, H., Benotmane, M. A., Monsieurs, P., et al. (2009). Mechanisms of gold biomineralization in the bacterium *Cupriavidus metallidurans*. *Proc. Natl. Acad. Sci. U.S.A.* 106, 17757–17762. doi: 10.1073/pnas.0904583106

Rojas, L. A., Yáñez, C., González, M., Lobos, S., Smalla, K., and Seeger, M. (2011). Characterization of the metabolically modified heavy metal-resistant *Cupriavidus metallidurans* strain MSR33 generated for mercury bioremediation. *PLoS One* 6:e17555. doi: 10.1371/journal.pone.0017555

Rothschild, L. J., and Mancinelli, R. L. (2001). Life in extreme environments. *Nature* 409, 1092–1101. doi: 10.1038/35059215

Sand, W., and Gehrke, T. (2006). Extracellular polymeric substances mediate bioleaching/biocorrosion via interfacial processes involving iron(III) ions and

acidophilic bacteria. *Res. Microbiol.* 157, 49–56. doi: 10.1016/j.resmic.2005.07.012

Shelobolina, E. S., Coppi, M. V., Korenevsky, A. A., DiDonato, L. N., Sullivan, S. A., Konishi, H., et al. (2007). Importance of c-type cytochromes for U(VI) reduction by Geobacter sulfurreducens. *BMC Microbiol.* 7:16. doi: 10.1186/1471-2180-7-16

Shong, J., Diaz, M. R. J., and Collins, C. H. (2012). Towards synthetic microbial consortia for bioprocessing. *Curr. Opin. Biotechnol.* 23, 798–802. doi: 10.1016/j.copbio.2012.02.001

Shrestha, N., Chilkoor, G., Vemuri, B., Rathinam, N., Sani, R. K., and Gadhamshetty, V. (2018). Extremophiles for microbial-electrochemistry applications: a critical review. *Bioresour. Technol.* 255, 318–330. doi: 10.1016/j.biortech.2018.01.151

Shukla, A., Parmar, P., and Saraf, M. (2017). Radiation, radionuclides and bacteria: an in-perspective review. *J. Environ. Radioact.* 180, 27–35. doi: 10.1016/j.jenvrad.2017.09.013

Singh, A., and Singh, A. K. (2017). Haloarchaea: worth exploring for their biotechnological potential. *Biotechnol. Lett.* 39, 1793–1800. doi: 10.1007/s10529-017-2434-y

Slonczewski, J. L., Fujisawa, M., Dopson, M., and Krulwich, T. A. (2009). Cytoplasmic pH measurement and homeostasis in bacteria and archaea. *Adv. Microb. Physiol.* 55, 1–79. doi: 10.1016/S0065-2911(09)05501-5

Srivastava, P., Bragança, J., Ramanan, S. R., and Kowshik, M. (2013). Synthesis of silver nanoparticles using haloarchaeal isolate *Halococcus salifodinae* BK3. *Extremophiles* 17, 821–831. doi: 10.1007/s00792-013-0563-3

Sun, J., Sayyar, B., Butler, J. E., Pharkya, P., Fahland, T. R., Famili, I., et al. (2009). Genome-scale constraint-based modeling of *Geobacter metallireducens*. *BMC Syst. Biol.* 3:15. doi: 10.1186/1752-0509-3-15

Ulloa, G., Collao, B., Araneda, M., Escobar, B., Álvarez, S., and Bravo, D. (2016). Use of acidophilic bacteria of the genus Acidithiobacillus to biosynthesize CdS fluorescent nanoparticles (quantum dots) with high tolerance to acidic pH. *Enzyme Microb. Technol.* 95, 217–224. doi: 10.1016/j.enzmictec.2016.09.005

Venkateswarlu, K., Nirola, R., Kuppusamy, S., Thavamani, P., Naidu, R., and Megharaj, M. (2016). Abandoned metalliferous mines: ecological impacts and potential approaches for reclamation. *Rev. Environ. Sci. Biotechnol.* 15, 327–354. doi: 10.1007/s11157-016-9398-6

Vera, M., Krok, B., Bellenberg, S., Sand, W., and Poetsch, A. (2013). Shotgun proteomics study of early biofilm formation process of *Acidithiobacillus ferrooxidans* ATCC 23270 on pyrite. *Proteomics* 13, 1133–1144. doi: 10.1002/pmic.201200386

Voica, D. M., Bartha, L., Banciu, H. L., and Oren, A. (2016). Heavy metal resistance in halophilic Bacteria and Archaea. *FEMS Microbiol. Lett.* 363, 1–9. doi: 10.1093/femsle/fnw146

Watling, H. R., Shiers, D. W., and Collinson, D. M. (2015). Extremophiles in mineral sulphide heaps: some bacterial responses to variable temperature, acidity and solution composition. *Microorganisms* 3, 364–390. doi: 10.3390/microorganisms3030364

Wenbin, N., Dejuan, Z., Feifan, L., Lei, Y., Peng, C., Xiaoxuan, Y., et al. (2011). Quorum-sensing system in *Acidithiobacillus ferrooxidans* involved in its resistance to Cu^{2+}. *Lett. Appl. Microbiol.* 53, 84–91. doi: 10.1111/j.1472-765X.2011.03066.x

Wheaton, G., Counts, J., Mukherjee, A., Kruh, J., and Kelly, R. (2015). The confluence of heavy metal biooxidation and heavy metal resistance: implications for bioleaching by extreme thermoacidophiles. *Minerals* 5, 397–451. doi: 10.3390/min5030397

Wheaton, G. H., Mukherjee, A., and Kelly, R. M. (2016). Transcriptomes of the extremely thermoacidophilic archaeon *Metallosphaera sedula* exposed to metal "shock" reveal generic and specific metal responses. *Appl. Environ. Microbiol.* 82, 4613–4627. doi: 10.1128/AEM.01176-16

Wilkins, M. J., Callister, S. J., Miletto, M., Williams, K. H., Nicora, C. D., Lovley, D. R., et al. (2011). Development of a biomarker for Geobacter activity and strain composition; proteogenomic analysis of the citrate synthase protein during bioremediation of U(VI). *Microb. Biotechnol.* 4, 55–63. doi: 10.1111/j.1751-7915.2010.00194.x

Yates, M. D., Cusick, R. D., and Logan, B. E. (2013). Extracellular palladium nanoparticle production using Geobacter sulfurreducens. *ACS Sustainable Chem. Eng.* 1, 1165–1171. doi: 10.1021/sc4000785

Zhang, X., Liu, X., Liang, Y., Fan, F., Zhang, X., and Yin, H. (2016). Metabolic diversity and adaptive mechanisms of iron- and/or sulfur-oxidizing autotrophic acidophiles in extremely acidic environments. *Environ. Microbiol. Rep.* 8, 738–751. doi: 10.1111/1758-2229.12435

Zivanovic, Y., Armengaud, J., Lagorce, A., Leplat, C., Guérin, P., Dutertre, M., et al. (2009). Genome analysis and genome-wide proteomics of *Thermococcus gammatolerans*, the most radioresistant organism known amongst the Archaea. *Genome Biol.* 10:R70. doi: 10.1186/gb-2009-10-6-r70

Conflict of Interest Statement: The author declares that the research was conducted in the absence of any commercial or financial relationships that could be construed as a potential conflict of interest.

frontiers in Microbiology

REVIEW
published: 25 May 2018
doi: 10.3389/fmicb.2018.01081

Survival and Energy Producing Strategies of Alkane Degraders Under Extreme Conditions and Their Biotechnological Potential

*Chulwoo Park and Woojun Park**

Laboratory of Molecular Environmental Microbiology, Department of Environmental Science and Ecological Engineering, Korea University, Seoul, South Korea

Many petroleum-polluted areas are considered as extreme environments because of co-occurrence of low and high temperatures, high salt, and acidic and anaerobic conditions. Alkanes, which are major constituents of crude oils, can be degraded under extreme conditions, both aerobically and anaerobically by bacteria and archaea of different phyla. Alkane degraders possess exclusive metabolic pathways and survival strategies, which involve the use of protein and RNA chaperones, compatible solutes, biosurfactants, and exopolysaccharide production for self-protection during harsh environmental conditions such as oxidative and osmotic stress, and ionic nutrient-shortage. Recent findings suggest that the thermophilic sulfate-reducing archaeon *Archaeoglobus fulgidus* uses a novel alkylsuccinate synthase for long-chain alkane degradation, and the thermophilic *Candidatus Syntrophoarchaeum butanivorans* anaerobically oxidizes butane via alkyl-coenzyme M formation. In addition, gene expression data suggest that extremophiles produce energy via the glyoxylate shunt and the Pta-AckA pathway when grown on a diverse range of alkanes under stress conditions. Alkane degraders possess biotechnological potential for bioremediation because of their unusual characteristics. This review will provide genomic and molecular insights on alkane degraders under extreme conditions.

Keywords: extremophiles, alkane oxidizer, survival strategies, energy production, bioremediation

OPEN ACCESS

Edited by:
Kian Mau Goh, Universiti Teknologi Malaysia, Malaysia

Reviewed by:
Rachel Narehood Austin, Columbia University, United States
Natsuko Hamamura, Kyushu University, Japan

***Correspondence:**
Woojun Park
wpark@korea.ac.kr

Specialty section:
This article was submitted to Microbiotechnology, Ecotoxicology and Bioremediation, a section of the journal Frontiers in Microbiology

Received: *30 December 2017*
Accepted: *07 May 2018*
Published: *25 May 2018*

Citation:
Park C and Park W (2018) Survival and Energy Producing Strategies of Alkane Degraders Under Extreme Conditions and Their Biotechnological Potential. Front. Microbiol. 9:1081. doi: 10.3389/fmicb.2018.01081

BACKGROUND

Extremophiles are microorganisms that can not only survive but also prefer to grow under extremely harsh conditions (Rampelotto, 2013). Based on their habitat, extremophiles are classified as acidophiles (pH 0.5–5), alkaliphiles (pH 9–12), barophiles (approximately 0.1 MPa), psychrophiles (0°C–20°C), thermophiles (50°C–70°C), halophiles (5–20% salt). Extremophiles have evolved to possess special features for adapting to extreme conditions. For example, psychrophilic bacteria synthesize cold-shock proteins, which function as transcriptional enhancers and RNA-binding proteins, to protect RNA from numerous stressors (Wouters et al., 1999). In addition, many oligotrophs increase their surface area by synthesizing appendages for easy nutrient absorption and utilization of a wide range of substrates (Huyop and Cooper, 2012). Halophilic bacteria assimilate glycine betaine from the environment and produce osmoprotectants, such as trehalose or *N*-acetylglutaminylglutamine amide (Sagot et al., 2010).

n-alkanes, the major components of petroleum, can be metabolized aerobically or anaerobically by numerous microorganisms. Several alkane oxidation mechanisms have been documented

till date, namely, terminal oxidation, subterminal oxidation, biterminal oxidation, and the Finnerty pathway. Alkane oxidation by aerobic bacteria produces fatty acids, which are subsequently metabolized via β-oxidation to generate acetyl-CoA (**Figure 1**). On the contrary, anaerobic alkane degradation is initiated by the addition of fumarate onto the terminal or subterminal carbon of alkane molecules, yielding alkylsuccinate derivatives as intermediates (**Figure 1**). Anaerobic alkane degradation was first proposed by So and Young, who demonstrated anaerobic alkane metabolism by fumarate-addition in the sulfate-reducing *Desulfatibacillum alkenivorans* AK-01 (So and Young, 1999; Rojo, 2009). Furthermore, recent studies also suggested that initial hydrocarbon activation by fumarate-addition occurs in syntrophic bacteria which produces acetate, CO_2, and/or H_2 that are utilized by methanogens (Berdugo-Clavijo and Gieg, 2014). Anaerobic hydrocarbon-degrading syntrophic bacteria possess genes encoding an alkylsuccinate (*assA*) or a benzylsuccinate synthase (*bssA*) as well as genes for syntrophic processes, such as H_2 and acetate production (Washer and Edwards, 2007; Kato S. et al., 2009; Walker et al., 2009; Fowler et al., 2012; Aitken et al., 2013; Cheng et al., 2013). However, several questions regarding the mechanism underlying anaerobic alkane degradation persist, such as the nature of all key enzymes and metabolic pathways for methanogenic alkane degradation by syntrophic bacteria and methanogen (Tan et al., 2015a).

Alkane monooxygenases have unique substrate ranges, which are classified into three categories based on the alkane chain length (van Beilen and Funhoff, 2007). Methane (C_1) to butane (C_4) conversion is catalyzed by methane monooxygenase (MMO)-like enzymes such as soluble MMO, particulate MMO, propane monooxygenase (PMO), and butane monooxygenase (BMO). In addition, integral membrane non-heme iron (AlkB) or cytochrome P450 enzymes (CYP153) oxidize pentane (C_5) to hexadecane (C_{16}), and alkanes longer than heptadecane are metabolized by a novel alkane dioxygenase, putative flavin-binding monooxygenase (AlmA), or long-chain alkane monooxygenase (LadA) (Maeng et al., 1996; Feng et al., 2007; Throne-Holst et al., 2007). However, a recent study showed that a novel Rieske-type alkane monooxygenase degrades pentane (C_5) to tetracosane (C_{24}) using NADH as a cofactor (Li et al., 2013). In addition, many bacteria possess multiple alkane hydroxylases (AH), and therefore, it is possible that a wide range of alkanes can be degraded by one microorganism (Whyte et al., 1998; Rozhkova-Novosad et al., 2007; Amouric et al., 2010; Liu et al., 2011; Park et al., 2017).

Biodegradation (transformation or mineralization) of a wide range of hydrocarbons, including aliphatic, aromatic, halogenated, and nitrated compounds, occurs in various extreme habitats. In addition, biodegradation of petroleum hydrocarbons by extremophiles has also been demonstrated under several conditions. For example, *Rhodococcus* sp. strain Q15, a psychrophile, showed short- and medium-alkane (C_{10} to C_{21}) degradation at 5 °C. In addition, solid-phase microextraction–gas chromatography-mass spectrometry showed the co-appearance of 1-hexadecanol and 2-hexadecanol when strain Q15 utilized hexadecane, suggesting that Q15 assimilate alkanes via both the terminal and subterminal oxidation pathways (Whyte et al., 1998). A novel halophilic species, *Amycolicicoccus subflavus*, retains defensive genes against high salinity, osmotic stress, and poor nutrient availability, resulting in growth in the presence of 1–12% NaCl. Furthermore, genome analysis revealed that *Amycolicicoccus subflavus* possesses four AH (AlkB, CYP153, LadA, and PMO), which allows growth on C_{10} to C_{36} alkanes and propane (Nie et al., 2013). Thermophilic *Geobacillus* and *Aeribacillus* species, isolated from petroleum reservoirs and a hot spring, respectively, grew from 38°C to 68–70°Ñ, with maximum growth at 60°Ñ, and utilized C_{10}–C_{30} alkanes as carbon source. Both strains are proven to have an *alkB*-type alkane monooxygenase. Two other *Geobacillus* strains (*G. toebii* B-1024 and 1017) also possess genes homologous to *lad*A and show activity similar to that of *G. toebii* B-1027 during long-chain alkane metabolism (Tourova et al., 2016).

Alkane-degrading extremophiles can be used in bioremediation of diverse oil-contaminated environments because of their special capabilities under extreme conditions. Cold-adapted hydrocarbon degraders have been applied to oil-polluted cold soil (Margesin et al., 2003; Aislabie et al., 2004; Wang J. et al., 2015) and wastewater (Margesin and Schinner, 1998; Gratia et al., 2009). In addition, psychrophiles from alpine habitats showed the highest degradation rate at 10°C within 8 days (40–60%) and at 4°C after 8 days (20–40%), showing high biodegradation efficiency (Margesin et al., 2000; Das and Chandran, 2011). Another well-studied example of bioremediation is the utilization of halophiles. Hydrocarbon biodegradation in the presence of high salinity is substantially valuable, not only from the economical aspect, but also in ecological and scientific studies. Recently, four *Pseudomonas aeruginosa* strains isolated from oil-contaminated saline soil were used to treat 10 g kg^{-1} of crude oil with more than 40% biodegradation efficiency in the presence of 300 mM NaCl after 120 days (Ebadi et al., 2017). *Marinobacter hydrocarbonoclasticus* showed high biodegradation activities of *n*-alkanes such as hexadecane (100%), eicosane (91%), and heneicosane (84%) in the presence of 4.6–20% NaCl (Gauthier et al., 1992). In another study, artificially weathered crude oil was proven to be degraded by microorganisms in a sandy salt marsh with a nitrogen–phosphorus–potassium (NPK) fertilizer (Lin et al., 1999). Several studies have demonstrated the feasibility of applying extremophiles to bioremediation and provided useful information for optimization of biodegradation efficiency.

However, despite the versatile potential of extremophiles in biodegradation, the molecular mechanisms and biological characteristics of these microorganisms have not been well-studied. This review discusses recent studies on alkane monooxygenase and 16S rRNA-based phylogenetic analysis of extremophiles, genotypic and phenotypic characteristics of pollutant-degrading extremophiles, and the ecological/advanced aspects of bioremediation. Overall, this review presents an updated overview of petroleum hydrocarbon degradation by microorganisms in different ecosystems.

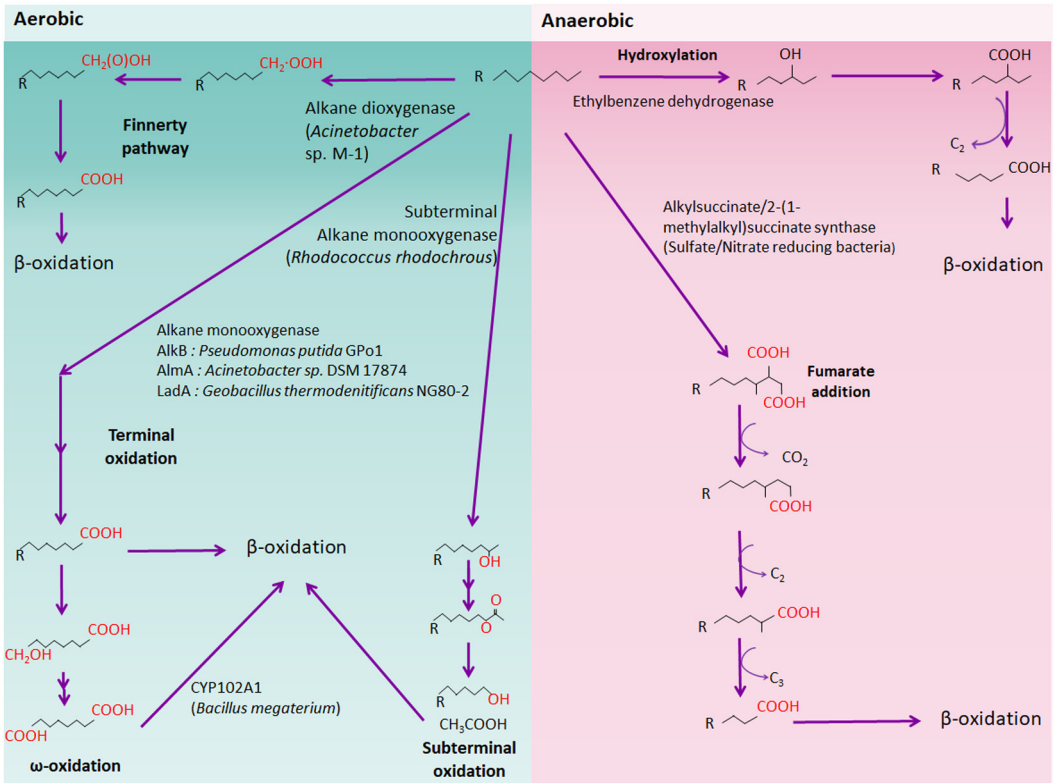

FIGURE 1 | Schematic aerobic and anaerobic alkane degradation pathway. Aerobic (green background) and anaerobic (red background) alkane degradation pathways are shown. Each alkane oxidizer (e.g., alkane monooxygenase) is shown and representative bacteria are written in brackets.

PHYLOGENETIC AFFILIATION AND DISTRIBUTION OF ALKANE-UTILIZING EXTREMOPHILES

Extremophiles Possessing AlkB and CYP153 Family Alkane Hydroxylases

The genetic diversity of alkane hydroxylases has been extensively investigated under several conditions, including various oil-polluted and non-polluted environments. In particular, AlkB and members of the CYP153 family are widely distributed and have been extensively investigated in soil, marine environments, and groundwater (Sotsky et al., 1994; Knaebel and Crawford, 1995; Stapleton and Sayler, 1998; Luz et al., 2004; Kuhn et al., 2009).

Psychrophiles

Biodegradation of several petroleum components by indigenous cold-adapted microbial populations has been observed at low temperatures in hydrocarbon-contaminated Arctic and Antarctic soils. A large population of *Pseudomonas* species was observed in Arctic soil after diesel contamination. Furthermore, gene expression analysis confirmed that *Pseudomonas* and *Rhodococcus* species induce hydrocarbon degradation genes in Arctic biopile soils during bioremediation, indicating the importance of both species in oil-contaminated Arctic soil (Yergeau et al., 2012). DNA-based study showed that rhodococcal *alkB* genotypes (Rh *alkB*) are generally distributed in both contaminated and pristine Antarctic soils, whereas *alkB* from *Pseudomonas putida* (Pp *alkB*) was detected more in contaminated soils than in non-contaminated soils, implying that *Rhodococcus* spp. may be the predominant alkane-degradative bacteria in both polar soils, but *Pseudomonas* spp. may be enriched after contamination (Whyte et al., 2002). Populations of γ-proteobacteria such as *Colwellia*, *Marinomonas*, and *Glaciecola* appeared to be predominated in oil-contaminated Arctic fjord ice cores, (Brakstad et al., 2008). The 16S rRNA gene libraries of both non-contaminated and crude oil-contaminated seawater from sub-Antarctic areas showed the predominance of *Roseobacter*, *Sulfitobacter*, *Staleya*, *Glaciecola*, *Colwellia*, *Marinomonas*, *Cytophaga*, and *Cellulophaga*. However, non α- and γ- proteobacteria (ε-proteobacteria and Bacteroidetes) such as *Arcobacter*, *Polaribacter*, *Ulvibacter*, and *Tenacibaculum* started to appear when seawater was contaminated with hydrocarbons (Prabagaran et al., 2007). Therefore, α-, and γ-proteobacteria contribute maximally to alkane degradation in cold marine environments, whereas non α- and γ- proteobacteria have minor contribution.

Halophiles

The metagenomic database of a seawater sample from the Sargasso Sea (Venter et al., 2004) revealed the presence of *alkB* and *cyp153* (van Beilen and Funhoff, 2007), implying wide

distribution of halophilic and halotolerant alkane degraders in the ocean environment. Other PCR-based study examining the Atlantic Ocean surface seawater revealed that both *alkB* and *cyp153* genes coexist in *Alcanivorax* and *Salinisphaera* species, whereas all *Parvibaculum* species possess only *cyp153* and discovered new culturable alkane-degraders belonging to *Brachybacterium*, *Idiomarina*, *Leifsonia*, *Martelella*, *Kordiimonas*, *Parvibaculum*, and *Tistrella* (Wang W. et al., 2010; Supplementary Table S1). Characterization of culturable *Alcanivorax* strains, *Marinobacter*, *Nocardioides*, *Parvibaculum* strains, originating from deep-sea hydrothermal vents, also revealed that only *Parvibaculum* strain possesses an alkane-oxidizing cytochrome P450 (CYP)-like protein to degrade alkanes (Bertrand et al., 2013). In subtropical seawater, *alkB* was detected in *Gallaecimonas*, *Castellaniella*, *Paracoccus*, and *Leucobacter* species, which shows a completely different bacterial community compared to the pelagic area (Wang L. et al., 2010), indicating that the distribution of alkane degraders varies with ocean conditions and geographical location. The number of α- and γ-proteobacteria (dominated by *Sphingomonadaceae*, *Rhodobacteraceae*, and *Chromatiales*) increased when crude oil was spilled in the supratidal and intertidal zones, on the other hand, γ- and δ-proteobacteria were more abundant in subtidal zones. The phylum Actinobacteria, particularly the genus *Rhodococcus*, was a key player in microbial response to the spillage especially in the supratidal sediment (Acosta-González et al., 2015). Likewise, no *alkB* sequence from Actinobacteria was detected in the marine metagenome despite a high proportion of *alkB* sequences from Actinobacteria in terrestrial and freshwater metagenomes (Nie et al., 2014).

Acidophiles

Although information on acidophilic alkane degraders is limited, some studies on alkane degradation at low pH have indicated the existence of hydrocarbon-degrading acidophiles. 16S rRNA library analysis of acidic soil from natural hydrocarbon seeps (pH 2.8–3.8) showed that majority of sequences were from heterotrophic acidophilic bacteria, including *Acidisphaera* and *Acidiphilium* species of α-proteobacteria, as well as the iron-and sulfur-oxidizing chemolithotroph *Acidithiobacillus* strain. A novel *Acidisphaera*-related strain C197 possesses *alkB* homologs (92.5% similarity with an *alkB* fragment from *Xanthobacter flavus*) and performs hexadecane metabolism (Hamamura et al., 2005). *Mycobacterium* is also a predominant bacterial genus found in extreme acidic sulfur block environments and alkane degradation of strain AG_{S10}, an acidophilic *Mycobacterium*, was demonstrated. Interestingly strain AG_{S10} has both *alkB* and *cyp153* genes, implying the possibility of two alkane hydroxylase families in many acidophilic *Mycobacteria* strains (Ivanova et al., 2014).

Extremophiles Possessing AlmA and LadA Family Alkane Hydroxylases

Flavin-binding family alkane hydroxylase (AlmA) and long-chain alkane monooxygenase (LadA) have recently been investigated; however, little is known about the distribution of either gene in the environment. Studies on functional diversity of alkane hydroxylase genes, including *almA* and *ladA* homologs, provided evidence that some psychrophiles possess AH for long-chain alkane degradation. Alignments with combined Pfam data sets showed the presence of *almA* homologs in *Paraglaciecola psychrophila* 170 (five copies) and *Psychrobacter cryohalolentis* K5 (one copy). On the contrary, a *ladA* candidate appears in the genomes of *Octadecabacter antarcticus* 307, *Octadecabacter arcticus* 238, and *Terriglobus saanensis* SP1PR4 (Bowman and Deming, 2014). These results hint at the occurrence of long-chain alkane metabolism at low temperatures, although the functionality of *almA* and *ladA* genes has not been shown experimentally. The diversity of *almA* in marine bacteria and oil-enrichment bacterial communities was investigated in three surface seawater samples from the South China Sea, Indian Ocean, and Atlantic Ocean (Wang and Shao, 2012). The acquired DNA sequences suggested two clades of *almA* gene. Class I *almA* contained a few sequences represented by the *Salinisphaera* and *Parvibaculum* genera, whereas class II was larger and more diverse and had many proteobacteria-related sequences, mainly from *Alcanivorax* and *Marinobacter*. However, metagenomic studies for detecting *ladA* in marine or saline conditions have not been conducted so far, although several marine hydrocarbonoclastic bacteria and halophilic hydrocarbon-utilizing bacteria harboring either AlmA- or LadA-type homologs, or both, have been reported (Liu et al., 2011; Nie et al., 2013; Meier et al., 2016). Thus, further investigation of long-chain alkane metabolism, especially the involvement of *almA* and *ladA*, under conditions of high salinity, are warranted.

Plasmid-born *ladA* gene was first investigated in *Geobacillus thermodenitrificans* NG80-2, indicating high possibility of horizontal gene transfer (HGT) of the *ladA* gene (Feng et al., 2007; Li et al., 2008). However, other member of *Geobacillus, G. thermoleovorans* B23 harbors three genes encoding LadA-type alkane hydroxylases ($ladA\alpha_{B23}$, $ladA\beta_{B23}$, and $ladB_{B23}$, collectively named the *ladAB* region) on its chromosome. Comparative genome analysis of relevant *Geobacillus* strains confirmed the absence of the *ladA* gene on the chromosome of *G. thermodenitrificans* NG80-2, but the presence of the *ladAB* gene island in many other *Geobacillus* strains (Boonmak et al., 2014).

We retrieved whole genome data of extremophiles from the National Center for Bio-technology Information (NCBI)[1] and Integrated Microbial Genomes (IMG)[2] databases. Total 66 identified genomes were aligned and analyzed (Supplementary Table S1). *alkB* genes are widely distributed in aerobic alkane-degrading extremophiles (psychrophiles, halophiles, acidophiles, and thermophiles), although their association with HGT was not clear; nonetheless, the different evolution patterns of *cyp* and 16S rRNA, shown in **Figure 2**, indicate the occurrence of HGT. Interestingly, *alkB*, *cyp*, and *almA* were mostly detected in psychrophiles, whereas halophiles and thermophiles possess *ladA* (**Figure 3**). In addition, acidophilic alkane degraders possess only

[1]https://www.ncbi.nlm.nih.gov/

[2]https://img.jgi.doe.gov/

alkB, which is not present in the genome of thermophilic alkane degraders (**Figure 2** and Supplementary Table S1).

Methanotrophic and Anaerobic Extremophiles

Anaerobic methane oxidation (AOM) via reverse methanogenesis commonly occurs in anaerobic methane-oxidizing archaea (ANME) under anoxic environments, and was first identified in marine sediments where AOM was coupled to sulfate reduction. Therefore, ANME usually formed a community with sulfate-reducing bacteria (SRB) of δ-proteobacteria. ANME are generally classified into three categories: ANME-1 (sub-clusters a, and b) related to *Methanomicrobiales* and *Methanosarcinales,* ANME-2 (sub-clusters a, b, and c) related to cultivated members of *Methanosarcinales*, and ANME-3 related to *Methanococcoides* spp. (Timmers et al., 2017). However, all *mcr* genes (encoding methyl-coenzyme M reductase) in the class Methanomicrobia, such as *Methanoculleus, Methanoregula,* and *Methanosaeta* showed over 60% identity each other, which is indicative of its high conservation (**Figure 4**). Compared to samples containing only methane, samples from natural freshwater gas sources containing methane and sulfate, harbored ANME-2a/b such as *Methanolobus*, and AOM-associated archaea such as *Candidatus Methanoperedens nitroreducens*, as determined by archaeal 16S rDNA analysis (Timmers et al., 2016).

Methanogenic hydrocarbon-degrading δ-proteobacteria (*Syntrophus*/*Smithella*, *Desulfosarcina*/*Desulfococcus*), Firmicutes (*Desulfotomaculum*, *Desulfosporosinus*, and *Pelotomaculum*), and relatively few bacteria belonging to Spirochaetes, Bacteroidetes, Chloroflexi, and β-proteobacteria have been identified in hydrocarbon-contaminated aquifers (Tan et al., 2015a). In addition, previous reports showed that the γ-proteobacterial genus *Marinobacter,* and δ-proteobacterial genera *Syntrophus* and *Smithella*, are the predominant hydrocarbon degraders in samples from estuarine sand and oil sand tailings under methanogenic conditions (Gray et al., 2011; Siddique et al., 2012). Hydrocarbon degradation in marine environments is predominantly conducted by SRB, and on-site stable isotope probing revealed that *Desulfosarcina*/*Desulfococcus* (DSS) of δ-proteobacteria actively oxidize short- (butane) and long-chain (dodecane) alkanes. Although few SRB alkane degraders have been identified, several culture-dependent and independent studies at oil-contaminated seeps have indicated the presence of more diverse species than the currently known SRB (Kleindienst et al., 2014). In experimental condition, cultures enriched from oil sands tailings ponds included predominant δ-proteobacteria, such as *Desulfoglaeba*, *Desulfobacteraceae*, and *Geobacter* when short-chain alkane-degrading culture with a mixture of C_6, C_7,

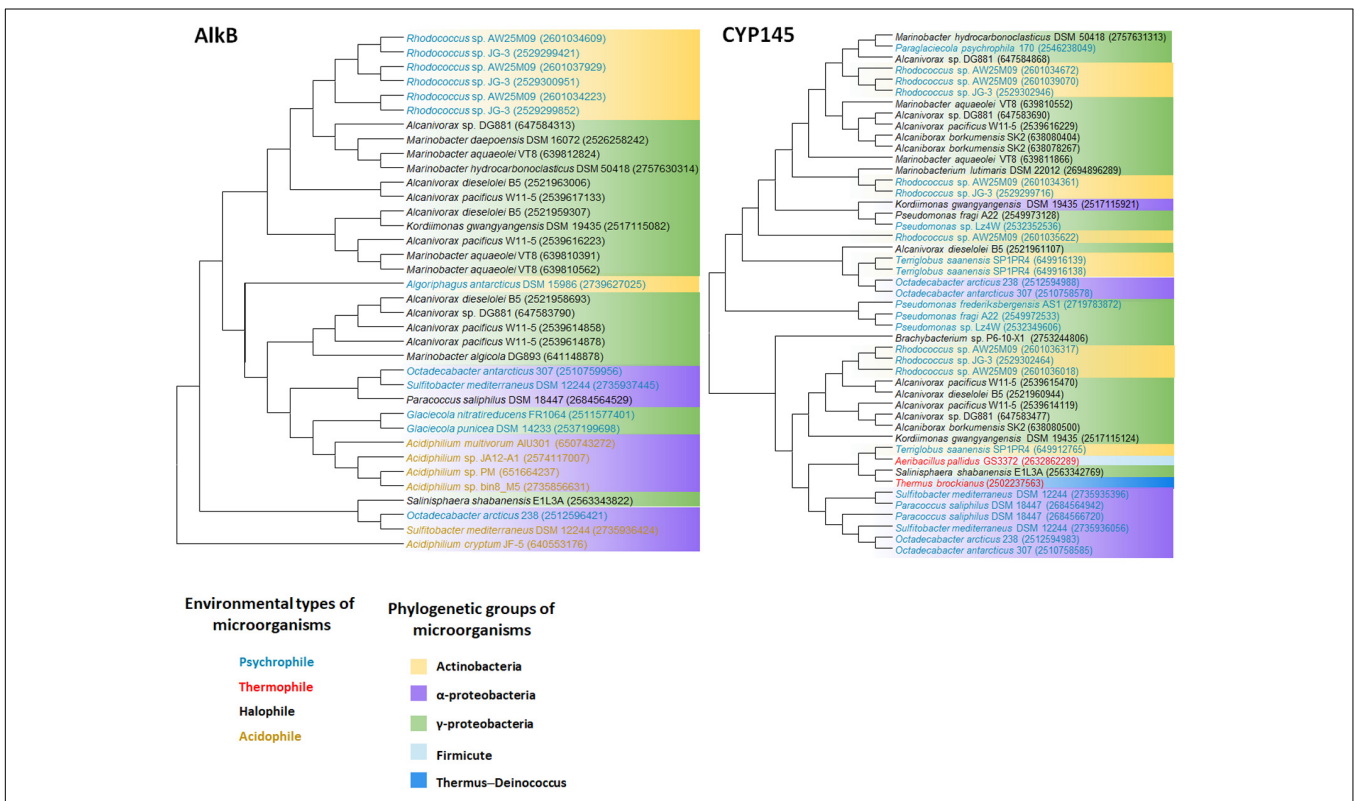

FIGURE 2 | AlkB and Cytochrome P450 (CYP145) phylogenetic tree of extremophiles. Collected sequences were aligned and phylogenetic tree was drawn using the MEGA 6 program. Colored words indicate the following environmental types of microorganisms: blue, psychrophile; red, thermophile; black, halophile; yellow, acidophile. Colored backgrounds indicate the following phylogenetic groups: yellow, Actinobacteria; purple, Alphaproteobacteria; green, Gammaproteobacteria; light blue, Firmicute; dark blue, Thermus–Deinococcus.

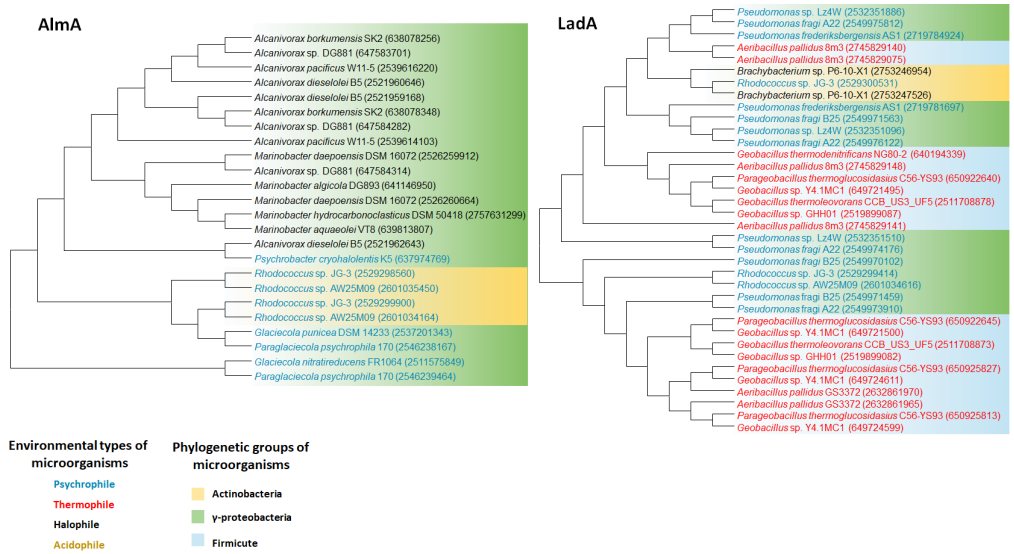

FIGURE 3 | AlmA and LadA phylogenetic tree of extremophiles. Collected sequences were aligned and phylogenetic tree was drawn using the MEGA 6 program. Colored words indicate the following environmental types of microorganisms: blue, psychrophile; red, thermophile; black, halophile; yellow, acidophile. Colored backgrounds indicate the following phylogenetic groups: yellow, Actinobacteria; purple, Alphaproteobacteria; green, Gammaproteobacteria.

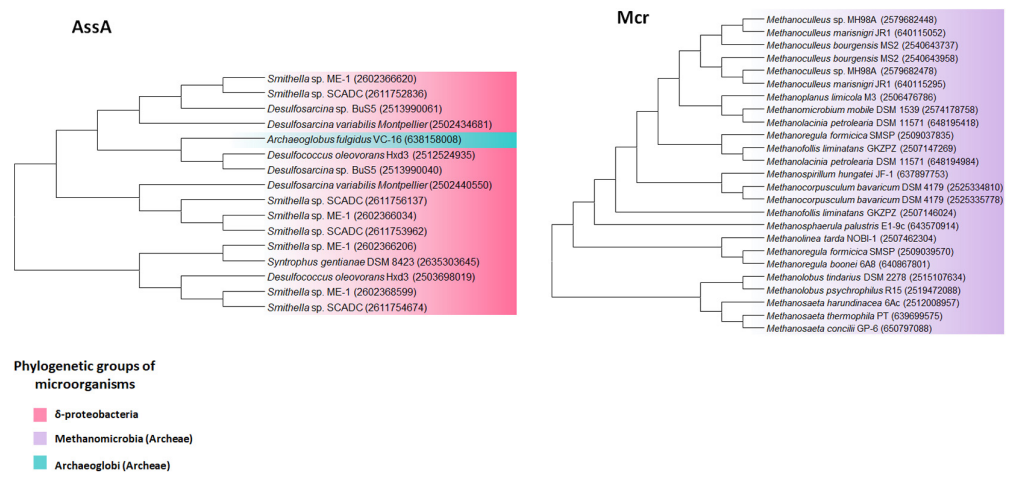

FIGURE 4 | AssA and Mcr phylogenetic tree of extremophiles. Collected sequences were aligned and phylogenetic tree was drawn using the MEGA 6 program. Colored backgrounds indicate the following phylogenetic groups: pink, Deltaproteobacteria; purple, Metanomicrobia (archaea); green, Archaeoglobi (archaea).

C_8, and C_{10} *n*-alkanes as predominant organic carbon sources was transferred into sulfate-supplemented medium (Tan et al., 2015b).

SURVIVAL STRATEGIES OF EXTREMOPHILES UNDER HARSH CONDITION

Psychrophiles

Many DNA-binding proteins are present in extremophiles such as psychrophiles. For example, cold-shock proteins (Csp) play essential roles in DNA or RNA stabilization and membrane rigidity by regulating unsaturated fatty-acid synthesis (D'Amico et al., 2006). Interestingly, *Methanogenium frigidum*, a stenopsychrophilic archaea, possesses *csp* family of genes, which are generally not detected in archaeal (such as thermophilic and hyperthermophilic) genomes (Giaquinto et al., 2007). The Csp sequences of *M. frigidum* and *Escherichia coli*, are highly similar, and complementation of *csp*-knockout *E. coli* strain with *csp* gene from *M. frigidum*, results in growth recovery at low temperature, showing compatibility between archaeal and bacterial Csps. We observed that *Pseudomonas fragi* strains A22 and B25 (Supplementary Table S1) have the most abundant *csp* genes (6 genes) among putative alkane-degrading psychrophiles. However, six *csp* genes were also present in the genome of the

mesophilic alkane degrader *Acinetobacter oleivorans* DR1. Thus, it is assumed that other strategies facilitate cold adaptation in psychrophiles regardless of the number of *csp* genes.

Most cold-adapted proteins in psychrophiles also show other characteristics, including high structure flexibility, low proportion of acyl chains in the cell membrane, and increased protein volume (Siddiqui and Cavicchioli, 2006). Chemical and biological reactions are slower at low temperatures, and therefore, the synthesis of cold-active enzymes with higher activity than mesophilic enzymes are required for maintaining an appropriate rate for essential metabolic reactions. To achieve high enzyme activity in cold conditions, the catalytic center must be flexible and unstable. Therefore, cold-adapted enzymes are heat labile and possess lower Gibbs free energy (ΔG) than mesophilic or thermophilic enzymes (Feller and Gerday, 2003; Siddiqui and Cavicchioli, 2006). Comparative sequence alignments of putative alkane hydroxylases from mesophiles and psychrophiles revealed that substitution by specific amino acids, such as alanine or glycine, contributes to increased flexibility of loops, bends, and α-helical structures of psychrophilic alkane hydroxylases. Furthermore, reports show that the flexible loops, bends, and helical regions of P450 from *Glaciecola psychrophila* are located in the center of three methionine residues, which is known to act as an alternative heme-binding site at low-temperatures (Bowman and Deming, 2014).

Trehalose production plays significant roles in resistance to freezing in cold environments. Observations from neutron diffraction, Raman spectroscopy, and inelastic neutron scattering revealed that trehalose disrupts the tetrahedral intermolecular network of water formed at low temperatures and thereby protects from ice damage. Image analysis based on field-emission transmission electron microscopy showed that trehalose was better than sucrose in preventing ice formation (Magazù et al., 2012). Currently, only psychrophilic *Rhodococcus* is known to produce trehalose lipid as a biosurfactant during alkane degradation (Rapp and Gabriel-Jürgens, 2003). However, there is a high possibility of trehalose lipid production by psychrophilic alkane degraders as trehalose synthesis can be induced by low temperature (Phadtare, 2004). Taken together, trehalose can be utilized as a cryoprotectant or biosurfactant by psychrophiles under cold conditions.

Halophiles

Many halophilic microorganisms develop strategies for surviving in highly saline environments, such as transportation of inorganic ions (mainly potassium) for stabilizing external osmotic pressure or synthesis of metabolism-compatible osmolytes. Genome and expression analyses of the moderately halophilic alkane degrader, *Amycolicicoccus subflavus* DQS3-9A1^T showed upregulation of the KdpD/KdpE two component system (high-affinity K^+ uptake system), Trk-type K^+ transporter and Na^+/K^+ antiporter, MtrA/MtrB two component system (BetP regulator), and glycine/betaine transporter (BetP) in response to high salt stress (Nie et al., 2013). Trk-type K^+ transporter, one of main K^+ transporters, requires three genes for cellular K^+ uptake, namely, *trkA* (1,374 bp, encoding cytoplasmic NAD^+/NADH binding protein), *trkH* (1,449 bp, encoding Trk transporter), and *trkI* (1,479 bp, encoding Trk transporter). Genome data show that several halophilic alkane degraders, such as *Paracoccus saliphilus*, *Marinobacterium lutimaris, Salinisphaera,* and *Marinobacter hydrocarbonoclasticus,* possess multiple Trk potassium uptake proteins, implying that Trk transporter provides osmolarity balance to halophiles during alkane degradation under high salinity conditions.

Several classes of organic compatible solutes, such as amino acids, alcohols, sugars, and derivatives act as organic osmoprotectants, which can be classified into three chemical categories: zwitterionic, non-polar, and anionic solutes (Roberts, 2005). These organic osmoprotectants are regulated by extracellular salt concentration. The synthesis rate of trehalose in *Haladaptatus paucihalophilus* decreases with increase in salinity; on the contrary, the intracellular concentration of glycine betaine increases due to import at high salinities, suggesting dynamic regulation of two compatible solutes for osmoadaptation (Youssef et al., 2014). The obligate hydrocarbon bacterium, *Alcanivorax borkumensis* SK2, synthesizes and accumulates ectoine to maintain osmolality under hyperosmosis, which promotes active metabolism and maintains cell integrity albeit low hydrocarbon degrading performance, thereby protecting cells from damage due to hyperosmosis (Scoma and Boon, 2016).

Undesirable interactions that destroy internal microbial proteins by dehydration can be avoided by controlling net charge. Compared to non-halophilic proteins, halophilic proteins contain several glutamate and aspartate residues on their surfaces, which provides high water solubility in the presence of salinity (Edbeib et al., 2016). Although comparative sequence alignment and structural studies of halophilic alkane hydroxylases have not been performed so far, we speculate that large numbers of glutamate and aspartate on their surfaces distributed to the stabilization of alkane hydroxylases.

Acidophiles

Specific adaptation to and metabolism of alkane degradation have not been extensively studied in acidophiles. Acidophiles possess several systems for surviving in highly acidic conditions (Baker-Austin and Dopson, 2007), such as a cytoplasmic buffering, DNA protection and repair, blocking of extracellular proton uptake, and organic acid utilization (Babu et al., 2015). Buffer capacity in the cytoplasm is determined mainly by amino acids, such as glutamate and arginine, which sequester protons. An acid-resistant *E. coli* strain showed that decarboxylated amino acids which require intracellular proton consumption enhanced internal pH, resulting in maintenance of pH homeostasis. However, the buffering capacities of acidophilic bacteria *Bacillus acidocaldarius* and other neutrophilic bacilli were not significantly different, suggesting that the survival mechanism encompasses several ways via which acidophilic bacteria adapt to low pH (Richard and Foster, 2004).

A large number of DNA and protein repair genes in acidophiles contribute to preservation of pH homeostasis (Dopson et al., 2005). A DNA-binding protein in starved cells (Dps), which protects DNA from reactive oxygen species (ROS) generated by the Fenton reaction, plays a significant role when cells are exposed to oxidative and nutritional stress. Studies

showed that the *E. coli* O157:H7 wild-type strain survives better than *dps*::*nptI* mutants in the initial 1 h of exposure to acidic conditions. Furthermore, complementation of wild type *dps* gene to *dps*::*nptI* mutants restored survival (Choi et al., 2000). However, available genome data showed that Dps is not present in *Acidiphilium*, suggesting that Dps synthesis does not occur by all alkane-degrading acidophiles for surviving under acidic conditions.

Upregulation of an outer membrane porin (Omp40) in *Acidithiobacillus ferrooxidans* was observed when pH was shifted from 3.5 to 1.5 (Amaro et al., 1991). Further studies illustrated that the positively charged L3 loop of the porin protein controls pore size and ion selectivity at pH 2.5 (Guiliani and Jerez, 2000). In addition, the decrease in membrane fluidity of *E. coli* O157:H7 may confer resistance to protons under acidic conditions (Yuk and Marshall, 2004). When lipids of acidophilic strains were adapted to acidic condition, palmitic acid ($C_{16:0}$) concentrations increased, whereas that of *cis*-vaccenic acid (C_{18}:1ω7c) decreased, resulting in reduced membrane fluidity, which regulated porin pore size. Low membrane fluidity confers resistance to toxicity from hydrocarbons and acidic condition, but compromises alkane uptake.

Thermophiles

Most proteins with catalytic and regulatory functions in thermophiles are thermostable and are structurally more compact than their mesophilic counterparts. Hyperthermostable proteins in *Thermococcus onnurineus* NA1, hydperthermophilic archaea, incubated at 100°C include intracellular protease I, thioredoxin reductase, triosephosphate isomerase, putative hydroperoxide reductase, proteasome, and translation initiation factors (Yun et al., 2011). Furthermore, transcriptomic and proteomic analyses of thermophiles revealed that many thermostable proteins of certain categories [heat stable proteins, chaperonin, metalloenzyme, putative ribosomal associated proteins, and superoxide dismutase (SOD)] are translated at high temperatures, implying that they are essential for thermophile survival at those temperatures (Li et al., 2010; Shih and Pan, 2011; Wang W. et al., 2014). These proteins have large numbers of disulfide bonds and positively charged amino acids, such as lysine and arginine, which are critical for their stability (Brocchieri, 2004; Beeby et al., 2005; Ma et al., 2010). Additionally, *in silico* studies illustrated that disulfide bonds are ubiquitous among thermophiles. BLAST revealed the presence of nine genes encoding FAD-dependent pyridine nucleotide-disulfide oxidoreductase, a potential key enzyme in thermophilic intracellular disulfide-bond formation, in the thermophilic alkane degrader *Geobacillus* sp. Y4.1MC1 (Beeby et al., 2005). Increase in the number of small residues such as Gly, Ala, Ser, and Val, and decrease in the number of Cys and polar residues (Asp, Asn, Glu, Gln, and Arg) were observed in membrane proteins of many thermophiles, which increases stringent membrane hydrophobicity at high temperatures (Meruelo et al., 2012). The amino acid preference might occur in membrane proteins of thermophilic alkane degraders.

Proteome analyses in most thermophiles has demonstrated the presence of genes encoding highly thermostable proteins such as antioxidants, antitoxins, heat-shock proteins (Hsps), and enzymes involved in carbon metabolism pathways, including glycolysis (Wang Q. et al., 2015). Several antioxidants and antitoxins, such as the VapBC complex, are translated in response to high-temperature stress (Shih and Pan, 2011). Global transcriptomic analysis demonstrated that VapBC proteins, the virulence-associated proteins in the hyperthermophilic crenarchaeon *Sulfolobus solfataricus*, are induced at elevated temperatures ranging from 80–90°C. Furthermore, a Δ*vapBC S. solfataricus* knockout strain showed a highly altered transcriptomic profile and susceptibility to heat shock (Cooper et al., 2009). However, *S. solfataricus* VapBC homologues do not exist in any thermophilic alkane degrading bacteria (*Geobacillus* species, *Thermus brockianus*, and *Aeribacillus pallidus*) and archaea (*Archaeoglobus fulgidus* DSM 4304), indicating that the VapBC system is not a ubiquitous heat-shock defense mechanism. Small Hsps (sHSPs) bind to proteins and confer protection from denaturation under high temperatures (Li et al., 2012). Unlike Csp proteins, Hsp proteins are abundant in many thermophilic alkane degraders. Five Hsp-encoding genes are present in the *Geobacillus thermodenitrificans* NG 80-2 genome, and most *Geobacillus* species possess more than four genes. Thus, Hsp proteins in alkane-degrading thermophiles may play an important role in survival at high temperatures.

ENERGY PRODUCTION OF EXTREMOPHILES DURING ALKANE METABOLISM

Most alkane-degrading extremophiles have ubiquitous aerobic or anaerobic alkane oxidation pathways represented by ω-oxidation or fumarate addition, respectively (**Figure 1**). It is assumed that most aerobic psychrophiles, halophiles, acidophiles, and thermophiles degrade alkanes through general alkane oxidation pathways, as demonstrated by the possession of AlkB, CYP, AlmA, and LadA-type alkane hydroxylases (Bertrand et al., 2013; Nie et al., 2013; Ivanova et al., 2014). However, some extremophiles oxidize alkanes via a unique pathway and produce energy via alternative pathways to avoid stress under harsh conditions.

Novel Aerobic Alkane Degradation Systems in Extremophiles

The aerobic alkane degrader, *Dietzia* DQ12-45-1b, grown at 4–45°C, pH 6.0–12.0, and 0–20% (w/v) NaCl (Wang et al., 2011), possesses an *alkW1-alkX* system, which is co-expressed and induced by fatty acids (Liang et al., 2016). The proposed mechanism is that *alkX*, a TetR family regulator, competes with DNA polymerase at the *alkW1* promoter region and represses the expression of *alkW1*, an *alkB*-type alkane hydroxylase-rubredoxin fusion gene, in the absence of alkanes. However, fatty acids produced by alkane oxidation directly bind to AlkX, removing it from the *alkW1* promoter when alkanes are present, indicating that this system is energy-cost effective. Furthermore,

phylogenetic and gene alignment analyses showed that *alkW1-alkX* may be ubiquitous in Actinobacteria such as *Rhodococcus* and *Mycobacterium*. Thus, *alkW-alkX* system confer benefits to Actinobacteria living in harsh conditions characterized by high pH, osmotic stress, and lack of nutrients (Liang et al., 2016).

Recent genome sequencing analysis revealed that the moderate halophile, *Amycolicicoccus subflavus* DQS3-9A1^T possesses four different alkane hydroxylation systems (propane monooxygenase, AlkB, CYP, and LadA) (Nie et al., 2013). A previously described halophile, *Alcanivorax dieselolei* B-5, harbors multiple copies of alkane hydroxylases (two AlkB-, one CYP153-, and AlmA-type alkane hydroxylase) and showed broad range of alkane-degrading capability (C_5–C_{36}) (Liu et al., 2011). Furthermore, the available complete genome sequence of *Marinobacter aquaeolei* VT8 shows the existence of three AlkB-, two CYP153-, and one AlmA-like alkane hydroxylase enzymes in the VT8 genome. Although the evolutionary reasons for possession of multiple alkane hydroxylase systems are not yet clear, it probably facilitates utilization of diverse hydrocarbon sources by halophilic bacteria under high saline environments. Illumination and addition of casamino acid as an organic fertilizer were tested to measure biodegradation efficiency of the extremely halophilic archaeal strains, *Haloferax*, *Halobacterium*, and *Halococcus* in highly saline soil (>22% salinity) and pond water (>16% salinity), which resulted in significantly enhanced biodegradation by halophilic archaea in the presence of casamino acid and illumination (Al-Mailem et al., 2012). It was hypothesized that archaea in hypersaline environment can synthesize ATP using a red pigment, perhaps a bacteriorhodopsin-like system, under low oxygen tension. Casamino acid also confers better growth and degradation of halophilic archaea, indicating promotion of biodegradation efficiency by addition of organic nitrogen source. Further studies are required to understand enhanced hydrocarbon degradation by haloarchaea in the presence of light and N source.

Alternative Pathways Producing Energy in Extremophiles

The glyoxylate shunt in the mesophilic alkane-degrading bacteria, *Acinetobacter oleivorans* DR1, is activated to generate energy during triacontane metabolism (Park et al., 2017). The glyoxylate shunt requires isocitrate lyase (encoded by *aceA*) and malate synthase (encoded by *aceB* or *glcB*), which are activated under oxidative stress or in the presence of C_2 carbon sources (Ahn et al., 2016). Among psychrophiles, upregulation of glyoxylate cycle-related genes in *Nesterenkonia* sp. AN1, isolated from Antarctic soil, was observed at 5°C. Furthermore, a large number of glyoxylate shunt-related genes belonging to the psychrophilic bacteria *Colwellia* and *Neptuniibacter* were observed in samples from the area surrounding the Deepwater Horizon oil spill (Rivers et al., 2013). In *Colwellia maris*, the expression level of *icl* was higher at 0°C than at 15°C (Watanabe et al., 2002), implying that *Colwellia* possess the advantage of surviving in cold environment by activating the glyoxylate shunt during alkane degradation.

Little is known about complete energy producing metabolism of alkane-degrading psychrophiles. The presence of methylglyoxal synthase in psychrophilic bacteria, *Exiguobacterium sibiricum,* was proposed as an important alternative catabolic pathway for glyceraldehyde phosphate (Rodrigues et al., 2008). In addition, the glyoxalase family proteins in *Planococcus halocryophilus* Or1 have been emphasized as key enzymes for utilization of carbon sources under cold environments. In addition, repression of energy metabolism at low temperature (−15°C) in *Planococcus halocryophilus* Or1, but increased expression of succinic semialdehyde dehydrogenase, alcohol dehydrogenase, and several oxidoreductases indicate maintenance of energy metabolism and ATP levels (Mykytczuk et al., 2013). Similarly, transcriptomic analysis of *Pseudomonas extremaustralis* showed activation of the ethanol oxidation pathway, involving a pyrroloquinoline quinone (PQQ)-dependent ethanol dehydrogenase, cytochrome c550, and an aldehyde dehydrogenase (encoded by *exaA*, *exaB*, and *exaC*, respectively) although genes associated with tricarboxylic acid (TCA) and cytochrome synthesis are repressed under cold conditions (Tribelli et al., 2018). Proteomics study suggested that enzymes participating in the fatty acid degradation pathway (β-oxidation) were more abundant at low temperatures (4–10°C) in cold adapting marine bacterium, *Sphingopyxis alaskensis* under artificial seawater medium (Ting et al., 2010). Cold adaptation strategy which uses fatty acid metabolism was also observed in *Pseudomonas putida* KT2440 at 10°C in Luria-Bertani (LB) medium. Analyses of proteomics and RNA sequencing data in KT2440 strain showed upregulation of the 2-methylcitrate and branched amino acid degradation pathways under cold temperature, implying conversion of propionate or propionyl-CoA to succinate and pyruvate via 2-methyl citrate under cold condition (Fonseca et al., 2011).

Proteomic analysis of the halophilic bacteria, *Alcanivorax borkumensis* SK2, also showed upregulation of AceA (ABO_2741) and GlcB (ABO_1267) and downregulation of TCA cycle enzymes, including isocitrate dehydrogenase (*icd*, ABO_1281) and 2-oxoglutarate dehydrogenase (*lpdG*, ABO_1494), when bacteria were grown in hexadecane-supplemented media, suggesting that the glyoxylate shunt is the main pathway for hexadecane metabolism (Sabirova et al., 2006). Similarly, another strategy for adapting to high temperatures involves a shift in the carbohydrate metabolism pathways. Transcriptomic and proteomic analysis of *Thermus filiformis* at 63°C, 70°C, or 77°C revealed that oxidative stress generated by high temperature induced genes related to the pentose phosphate (PP) pathway, whereas genes participating in glycolysis and the TCA cycle were downregulated (Mandelli et al., 2017), indicating evasion of ROS generation. In addition, metabolomic analysis revealed accumulation of ROS scavengers such as oxaloacetate and α-ketoglutarate, indicating preservation of ROS homeostasis. It has been reported that the PP pathway, glyoxylate cycle, and ROS defense systems are essential for detoxifying petroleum hydrocarbons (Feng et al., 2007; Kato T. et al., 2009; Shih and Pan, 2011). Thus, exposure to heat shock probably assists the growth of thermophilic alkane degraders at high temperatures in the presence of alkanes. The same pattern was observed in

the genomic and proteomic analysis of thermophilic bacteria *Geobacillus thermodenitrificans* NG80-2, which showed activated glyoxylate shunt instead of the TCA cycle in the presence of hexadecane (Feng et al., 2007).

The interface between alkane degraders and hydrocarbon compounds may form microoxic or anoxic niches because of hydrophobicity (Suter et al., 2017). In addition, alkane oxidation generates excessive acetyl-CoA (Sabirova et al., 2006; Schönfeld and Wojtczak, 2016; Park et al., 2017), creating appropriate conditions for aerobic fermentation, which is also called the Crabtree effect (Zhou et al., 2017). Acetate assimilation via the Pta-AckA pathway occurs in the presence of long-chain alkanes (triacontane), producing ATP (Park et al., 2017). Although studies on the Pta-Ack pathway during alkane metabolism are limited, evidence shows that extremophiles can synthesize ATP via the Pta-AckA pathway. Phenotypic analysis of *Psychrobacter arcticus* 273-4 shows that acetic acid can be diffused into cells without energy consumption, whereas energy-consuming glucose could not be utilized at low temperatures (Bergholz et al., 2009). In addition, transcriptomic and proteomic analysis of *Psychrobacter* sp. PAMC 21119, which was grown under cold conditions, revealed upregulation of acetyl-CoA metabolism, although the central energy production and conversion pathways were downregulated (Koh et al., 2017). *Geobacillus thermodenitrificans* NG80-2 harbors *pta* and *ackA*, which are indicative of possible methods of ATP synthesis during alkane assimilation (Feng et al., 2007). Methanogenic archaea and bacteria also possess *pta* and *ackA* genes. Furthermore, methanogenic and halophilic archaea have the same ancestral Pta lineage (Barnhart et al., 2015), implying the possibility of acetate production via the Pta-AckA pathway during alkane metabolism at high salinity.

Novel Alkane Degradation Pathways Under Anaerobic Conditions

Although many alkane hydroxylase genes involved in aerobic alkane degradation were detected in extremophiles, anaerobic alkane metabolism may have advantages, particularly because extreme environments confer oxidative stress on bacteria. The thermophilic sulfate-reducing archaeon, *Archaeoglobus fulgidus* strain VC-16, which degrades C_{10}–C_{21} alkanes with thiosulfate or sulfate as a terminal electron acceptor, possess pyruvate formate lyase (encoded by *pflD*), which is homologous to alkylsuccinate synthase (encoded by *assA*). Phylogenetic analysis showed that homologs of PflD and PflC mainly belong to bacteria such as Firmicutes, δ-proteobacteria, γ-proteobacteria, and Actinobacteria, indicating that these genes are acquired from bacteria via HGT. Furthermore, three-dimensional simulation suggested that PflD might be a potential alkylsuccinate synthase, which is supported by the upregulation of *pflD* gene expression in the presence of hexadecane but not fatty acid (Khelifi et al., 2014). An anaerobic hyperthermophile, *Geoglobus acetivorans*, isolated from deep-sea hydrothermal vents, requires ferric iron (Fe (III)) as an electron acceptor during alkane degradation. Genome analysis revealed that this archaeon also harbors close homologs of *Archaeoglobus fulgidus* PflC and PflD (69 and 57% identity, respectively). However, Gace_0240 (homolog to PflC in *Archaeoglobus fulgidus*) shares features with alkyl and benzylsuccinate synthases, rather than with pyruvate formate lyase-activating enzymes (Mardanov et al., 2014).

A methanogenic culture, enriched from freshwater hydrocarbon-contaminated aquifer sediments, consumed octacosane (C_{28}) and generated methane. *Smithella* was predominant and *assA* was abundant in the presence of octacosane, furthermore, phylogenetic analysis showed that *assA* copies in the culture were closely related to *assA* of *Smithella*, indicating that fumarate addition in octacosane is mainly performed by *Smithella.* Interestingly, the detection of α,ω-dicarboxylic acids in the octacosane-only media implies simultaneous activation by fumarate addition, although the mechanism remains unclear (Oberding and Gieg, 2017). Another alkane degradation pathway has been suggested in *Verrucomicrobia* methylotrophs, which grow optimally at pH 2.0–2.5 and consume methane. Interestingly, analysis of the draft *Verrucomicrobia* genome detected genes encoding pMMO, which is homologous to the pMMO in methanotrophic proteobacteria. However, genes for subsequent methanol and formaldehyde oxidation were incomplete or missing, suggesting that the bacterium uses novel methylotrophic pathways (Dunfield et al., 2007). Further analysis showed that three *pmoA* genes in *Verrucomicrobia* were located in a different clade of proteobacterial *pmo* homologs, indicating divergent evolution with proteobacterial methanotrophs. Recent metatranscriptome, metaproteome, and metagenome analyses of *Candidatus Syntrophoarchaeum butanivorans* showed that genes encoding β-oxidation enzymes, carbon monoxide dehydrogenase, and reversible C_1 methanogenesis enzymes [reverse methyl coenzyme M (Mcr)] are also expressed, indicating that enzymes for complete butane metabolism exist in *Ca. Syntrophoarchaeum butanivorans.* Furthermore, ultra-high resolution mass spectrometry data showed that *Ca. Syntrophoarchaeum butanivorans* generates alkyl-coenzyme M. Phylogenetic analysis showed that MCR was present in the draft genomes of *Bathyarchaeota* and pan-genome of uncultivated *Hadesarchaea*, indicating that uncultivated alkane degraders may perform non-methane alkane degradation (Laso-Pérez et al., 2016).

BIOTECHNOLOGICAL APPLICATION OF EXTREMOPHILES IN BIOREMEDIATION

In situ bioremediation of petroleum, mainly applied to soil and groundwater, includes biostimulation and bioventing. Biostimulation was recently performed in desert soil near the Arabian Gulf region (Al-Mailem et al., 2015). Community analysis revealed that 19 thermophilic hydrocarbonoclastic bacterial taxa were present in the soil sample. Furthermore, predominant species belonged to *Amycolatopsis*, *Chelativorans*, *Isoptericola*, *Nocardia*, *Aeribacillus*, *Aneurinibacillus*, *Brevibacillus*, *Geobacillus*, *Kocuria*, *Marinobacter*, and *Paenibacillus,* which showed better growth and hydrocarbon consumption rate at 50°C than at 30°C. However, enhanced

growth and hydrocarbon consumption were observed after supplementation with Ca^{2+} (∼2.5 M $CaSO_4$) or addition of 8% w/v dipicolinic acid (DPA), implying that Ca^{2+} and DPA-mediated increased heat resistance of alkane degraders may stimulate biodegradation at high temperatures (Radwan et al., 2017). A bioelectrochemical system was recently applied to marine sediments for hydrocarbon biodegradation, wherein a graphite rod (snorkel) is placed between the anoxic contaminated sediment and the O_2-containing water. The snorkel acts as an electron acceptor and shuttles electrons generated by anaerobic hydrocarbon oxidation using reducing elements, such as S^2 and Fe^{2+}. Electrons move to the water phase along the graphite and fuse with oxygen and protons to form water (Viggi et al., 2015). This device serves as a sustainable respiratory electron acceptor in anaerobic oxidation of hydrocarbons, and can stimulate hydrocarbon degradation by SRB by scavenging toxic sulfide (Mapelli et al., 2017). Psychrophilic bacteria can potentially be used to degrade organic pollutants from soil and water at low temperatures, mainly, psychrophilic petroleum degraders such as *Acinetobacter, Arthrobacter, Colwellia, Cytophaga, Halomonas, Marinobacter, Marinomonas, Pseudoalteromonas, Oleispira, Rhodococcus*, and *Shewanella* (Brakstad et al., 2008). *Acinetobacter* spp. isolated from oil-polluted soils of King George Island were inoculated into a microcosm of contaminated soil, resulting in reduction of contaminant concentration by 75% after 50 days, compared to NP addition, which had no significant influence (Ruberto et al., 2003). Rhoder, composed of hydrocarbon-degrading bacteria *Rhodococcus ruber* and *R. erythrococcus,* oil, and gas, was used for removing oil pollution (Murygina et al., 2000). Over 99% bioremediation rate was obtained in open aquatic surfaces with light contamination (<20 g L^{-1}); however, primary mechanical collection of oil and triple Rhoder treatment resulted in a 94% bioremediation rate in heavily polluted aquatic systems (thickness of oil film $>$ 3 mm) and wetland (2,000 m^2) in Urai, indicating that complex bioremediation strategies for effective oil-degradation are required.

Biopile bioremediation involves excavation of polluted soil, followed by supply of nutrients and air for increasing microbial hydrocarbon degradation and promoting bioremediation. Biopile remediation has recently been applied to polluted extreme environments such as cold regions (Gomez and Sartaj, 2014; Dias et al., 2015; Whelan et al., 2015; Martínez Álvarez et al., 2017). In a recent study, a previously suggested nutrient ratio (C:N:P ratio of 100:17.6:1.73) for biological activity (as FDA levels) was used to treat 0.4-ton geomembrane-covered biopiles from diesel fuel storage tanks of Antarctic expedition (Martínez Álvarez et al., 2017). Results showed a higher hydrocarbon removal rate (75.9%) in biostimulated soil within 40 days than in the control biopile (49.5%). In another study, an optimized biopile condition was obtained using surface response methodology (RSM) − a combination of 3 mL m^{-3} microbial consortia and 5% mature compost. After 94 days, 90.7% petroleum hydrocarbon reduction was observed, whereas hydrocarbon was reduced by only 56% in control soil (excavated from Val-des-Bois, in the Outaouais region of Quebec, Canada) between 1 and 8°C, indicating synergistic interaction between bioaugmentation and biostimulation for bioremediation enhancement. Additionally, biostimulation of Antarctic soils with fishmeal reduced 71% of total hydrocarbon and facilitated a bacterial community shift, increasing Actinobacteria over the 50-day study period (Dias et al., 2015). Landfarming has also been demonstrated as an effective bioremediation method in polar regions, which involves aggressive soil tilling and selective fertilization with a mixture of fertilizers (ammonium phosphate and urea) over a span of 70 days (McCarthy et al., 2004). However, soil concentrations of diesel range organics in northeast (380 mg kg^{-1}) and southwest soil (430 mg kg^{-1}) were already reduced to the target concentrations (500 mg kg^{-1}) at 31 and 55 days, respectively.

CONCLUDING REMARKS

Although many alkane degraders living in extreme environment has been isolated and characterized, there is a great number of uncharacterized extremophiles that appear to be alkane-degraders, such as *Brachybacterium*, *Idiomarina*, and *Leifsonia*. Thus, further investigation of such novel alkane-degrading extremophiles will provide new metabolic pathways and survival strategies under harsh environments. Recent studies on discovery of new alkane metabolic systems in aerobic-, anaerobic extremophiles, such as AlkW1-AlkX system, Pfl homologues, and alkyl-coenzyme M indicate that there are several questions to be solved regarding alkane degradation metabolism. The evidences demonstrated the activation of several alternative pathways, such as glyoxylate shunt, Pta-AckA, or alcohol/fatty acid metabolism, instead of TCA cycle when extremophiles survive under extreme condition, implying that they are beneficial during alkane degradation. Because of high adaptability, strong stress resistance, and unique biodegradation capability, extremophiles are promising bioremediation-reagents to clean up polluted environments with low cost and high efficiency.

AUTHOR CONTRIBUTIONS

CP and WP designed and coordinated the study. CP collected the data. CP wrote the first complete draft of the manuscript. WP provided substantial modifications. All authors contributed to and approved the final version of the manuscript.

FUNDING

This work was supported by a National Research Foundation of Korea (NRF) grant to WP, funded by the Korea Government (MSIP) (No. NRF-2017R1A2B4005838).

SUPPLEMENTARY MATERIAL

The Supplementary Material for this article can be found online at: https://www.frontiersin.org/articles/10.3389/fmicb.2018.01081/full#supplementary-material

REFERENCES

Acosta-González, A., Martirani-von Abercron, S. M., Rosselló-Móra, R., Wittich, R. M., and Marqués, S. (2015). The effect of oil spills on the bacterial diversity and catabolic function in coastal sediments: a case study on the Prestige oil spill. *Environ. Sci. Pollut. Res. Int.* 22, 15200–15214. doi: 10.1007/s11356-015-4458-y

Ahn, S., Jung, J., Jang, I. A., Madsen, E. L., and Park, W. (2016). Role of glyoxylate shunt in oxidative stress response. *J. Biol. Chem.* 291, 11928–11938. doi: 10.1074/jbc.M115.708149

Aislabie, J. M., Balks, M. R., Foght, J. M., and Waterhouse, E. J. (2004). Hydrocarbon spills on Antarctic soils: effects and management. *Environ. Sci. Technol.* 38, 1265–1274. doi: 10.1021/es0305149

Aitken, C. M., Jones, D. M., Maguire, M. J., Gray, N. D., Sherry, A., and Bowler, B. F. J. (2013). Evidence that crude oil alkane activation proceeds by different mechanisms under sulfate-reducing and methanogenic conditions. *Geochim. Cosmochim. Acta* 109, 162–174. doi: 10.1016/j.gca.2013.01.031

Al-Mailem, D. M., Eliyas, M., and Radwan, S. S. (2012). Enhanced haloarchaeal oil removal in hypersaline environments via organic nitrogen fertilization and illumination. *Extremophiles* 16, 751–758. doi: 10.1007/s00792-012-0471-y

Al-Mailem, D. M., Kansour, M. K., and Radwan, S. S. (2015). Moderately thermophilic, hydrocarbonoclastic bacterial communities in Kuwaiti desert soil: enhanced activity via Ca^{2+} and dipicolinic acid amendment. *Extremophiles* 19, 573–583. doi: 10.1007/s00792-015-0739-0

Amaro, A. M., Chamorro, D., Seeger, M., Arredondo, R., Pierano, I., and Jerez, C. A. (1991). Effect of external pH perturbations on in vivo protein synthesis by the acidophilic bacterium *Thiobacillus ferrooxidans*. *J. Bacteriol.* 173, 910–915. doi: 10.1128/jb.173.2.910-915.1991

Amouric, A., Quéméneur, M., Grossi, V., Liebgott, P. P., Auria, R., and Casalot, L. (2010). Identification of different alkane hydroxylase systems in *Rhodococcus ruber* strain SP2B, a hexane-degrading actinomycete. *J. Appl. Microbiol.* 108, 1903–1916. doi: 10.1111/j.1365-2672.2009.04592.x

Babu, P., Chandel, A. K., and Singh, O. V. (2015). *Extremophiles and their Applications in Medical Processes*. New York, NY: Springer International Publishing. doi: 10.1007/978-3-319-12808-5

Baker-Austin, C., and Dopson, M. (2007). Life in acid: pH homeostasis in acidophiles. *Trends Microbiol.* 15, 165–171. doi: 10.1016/j.tim.2007.02.005

Barnhart, E. P., McClure, M. A., Johnson, K., Cleveland, S., Hunt, K. A., and Fields, M. W. (2015). Potential role of acetyl-coa synthetase (*acs*) and malate dehydrogenase (*mae*) in the evolution of the acetate switch in bacteria and archaea. *Sci. Rep.* 5:12498. doi: 10.1038/srep12498

Beeby, M., O'Connor, B. D., Ryttersgaard, C., Boutz, D. R., Perry, L. J., and Yeates, T. O. (2005). The genomics of disulfide bonding and protein stabilization in thermophiles. *PLoS Biol.* 3:e309. doi: 10.1371/journal.pbio.0030309

Berdugo-Clavijo, C., and Gieg, L. M. (2014). Conversion of crude oil to methane by a microbial consortium enriched from oil reservoir production waters. *Front. Microbiol.* 5:197. doi: 10.3389/fmicb.2014.00197

Bergholz, P. W., Bakermans, C., and Tiedje, J. M. (2009). *Psychrobacter arcticus* 273-4 uses resource efficiency and molecular motion adaptations for subzero temperature growth. *J. Bacteriol.* 191, 2340–2352. doi: 10.1128/JB.01377-08

Bertrand, E. M., Keddis, R., Groves, J. T., Vetriani, C., and Austin, R. N. (2013). Identity and mechanisms of alkane-oxidizing metalloenzymes from deep-sea hydrothermal vents. *Front. Microbiol.* 4:109. doi: 10.3389/fmicb.2013.00109

Boonmak, C., Takahashi, Y., and Morikawa, M. (2014). Cloning and expression of three *ladA*-type alkane monooxygenase genes from an extremely thermophilic alkane-degrading bacterium *Geobacillus thermoleovorans* B23. *Extremophiles* 18, 515–523. doi: 10.1007/s00792-014-0636-y

Bowman, J. S., and Deming, J. W. (2014). Alkane hydroxylase genes in psychrophile genomes and the potential for cold active catalysis. *BMC Genomics* 15:1120. doi: 10.1186/1471-2164-15-1120

Brakstad, O. G., Nonstad, I., Faksness, L. G., and Brandvik, P. J. (2008). Responses of microbial communities in Arctic sea ice after contamination by crude petroleum oil. *Microb. Ecol.* 55, 540–552. doi: 10.1007/s00248-007-9299-x

Brocchieri, L. (2004). Environmental signatures in proteome properties. *Proc. Natl. Acad. Sci. U.S.A.* 101, 8257–8258. doi: 10.1073/pnas.0402797101

Cheng, L., Ding, C., Li, Q., He, Q., Dai, L. R., and Zhang, H. (2013). DNA-SIP reveals that *Syntrophaceae* play an important role in methanogenic hexadecane degradation. *PLoS One* 8:e66784. doi: 10.1371/journal.pone.0066784

Choi, S. H., Baumler, D. J., and Kasper, C. W. (2000). Contribution of *dps* to acid stress tolerance and oxidative stress tolerance in *Escherichia coli* O157:H7. *Appl. Environ. Microbiol.* 66, 3911–3916. doi: 10.1128/AEM.66.9.3911-3916.2000

Cooper, C. R., Daugherty, A. J., Tachdjian, S., Blum, P. H., and Kelly, R. M. (2009). Role of *vapBC* toxin-antitoxin loci in the thermal stress response of *Sulfolobus solfataricus*. *Biochem. Soc. Trans.* 37, 123–126. doi: 10.1042/BST0370123

D'Amico, S., Collins, T., Marx, J. C., Feller, G., and Gerday, C. (2006). Psychrophilic microorganisms: challenges for life. *EMBO Rep.* 7, 385–389. doi: 10.1038/sj.embor.7400662

Das, N., and Chandran, P. (2011). Microbial degradation of petroleum hydrocarbon contaminants: an overview. *Biotechnol. Res. Int.* 2011:941810. doi: 10.4061/2011/941810

Dias, R. L., Ruberto, L., Calabró, A., Balbo, A. L., Del Panno, M. T., and Mac Cormack, W. P. (2015). Hydrocarbon removal and bacterial community structure in on-site biostimulated biopile systems designed for bioremediation of diesel-contaminated Antarctic soil. *Polar Biol.* 5, 677–687. doi: 10.1007/s00300-014-1630-7

Dopson, M., Baker-Austin, C., and Bond, P. L. (2005). Analysis of differential protein expression during growth states of *Ferroplasma* strains and insights into electron transport for iron oxidation. *Microbiology* 151, 4127–4137. doi: 10.1099/mic.0.28362-0

Dunfield, P. F., Yuryev, A., Senin, P., Smirnova, A. V., Stott, M. B., Hou, S., et al. (2007). Methane oxidation by an extremely acidophilic bacterium of the phylum *Verrucomicrobia*. *Nature* 450, 879–882. doi: 10.1038/nature06411

Ebadi, A., Khoshkholgh Sima, N. A., Olamaee, M., Hashemi, M., and Ghorbani Nasrabadi, R. (2017). Effective bioremediation of a petroleum-polluted saline soil by a surfactant-producing *Pseudomonas aeruginosa* consortium. *J. Adv. Res.* 8, 627–633. doi: 10.1016/j.jare.2017.06.008

Edbeib, M. F., Wahab, R. A., and Huyop, F. (2016). Halophiles: biology, adaptation, and their role in decontamination of hypersaline environments. *World J. Microbiol. Biotechnol.* 32:135. doi: 10.1007/s11274-016-2081-9

Feller, G., and Gerday, C. (2003). Psychrophilic enzymes: hot topics in cold adaptation. *Nat. Rev. Microbiol.* 1, 200–208. doi: 10.1038/nrmicro773

Feng, L., Wang, W., Cheng, J., Ren, Y., Zhao, G., Gao, C., et al. (2007). Genome and proteome of long-chain alkane degrading *Geobacillus thermodenitrificans* NG80-2 isolated from a deep-subsurface oil reservoir. *Proc. Natl. Acad. Sci. U.S.A.* 104, 5602–5607. doi: 10.1073/pnas.0609650104

Fonseca, P., Moreno, R., and Rojo, F. (2011). Growth of *Pseudomonas putida* at low temperature: global transcriptomic and proteomic analyses. *Environ. Microbiol. Rep.* 3, 329–339. doi: 10.1111/j.1758-2229.2010.00229.x

Fowler, S. J., Dong, X. L., Sensen, C. W., Suflita, J. M., and Gieg, L. M. (2012). Methanogenic toluene metabolism: community structure and intermediates. *Environ. Microbiol.* 14, 754–764. doi: 10.1111/j.1462-2920.2011.02631.x

Gauthier, M. J., Lafay, B., Christen, R., Fernandez, L., Acquaviva, M., Bonin, P., et al. (1992). *Marinobacter hydrocarbonoclasticus* gen. nov., sp. nov., a new, extremely halotolerant, hydrocarbon-degrading marine bacterium. *Int. J. Syst. Bacteriol.* 42, 568–576. doi: 10.1099/00207713-42-4-568

Giaquinto, L., Curmi, P. M., Siddiqui, K. S., Poljak, A., DeLong, E., DasSarma, S., et al. (2007). Structure and function of cold shock proteins in archaea. *J. Bacteriol.* 189, 5738–5748. doi: 10.1128/JB.00395-07

Gomez, F., and Sartaj, M. (2014). Optimization of field scale biopiles for bioremediation of petroleum hydrocarbon contaminated soil at low temperature conditions by response surface methodology (RSM). *Int. Biodeterior. Biodegradation* 89, 103–109. doi: 10.1016/j.ibiod.2014.01.010

Gratia, E., Weekers, F., Margesin, R., D'Amico, S., Thonart, P., and Feller, G. (2009). Selection of a cold-adapted bacterium for bioremediation of wastewater at low temperatures. *Extremophiles* 13, 763–768. doi: 10.1007/s00792-009-0264-0

Gray, N. D., Sherry, A., Grant, R. J., Rowan, A. K., Hubert, C. R., Callbeck, C. M., et al. (2011). The quantitative significance of *Syntrophaceae* and syntrophic partnerships in methanogenic degradation of crude oil alkanes. *Environ. Microbiol.* 13, 2957–2975. doi: 10.1111/j.1462-2920.2011.02570.x

Guiliani, N., and Jerez, C. A. (2000). Molecular cloning, sequencing, and expression of Omp-40, the gene coding for the major outer membrane protein from the acidophilic bacterium *Thiobacillus ferrooxidans*. *Appl. Environ. Microbiol.* 66, 2318–2324. doi: 10.1128/AEM.66.6.2318-2324.2000

Hamamura, N., Olson, S. H., Ward, D. M., and Inskeep, W. P. (2005). Diversity and functional analysis of bacterial community associated with natural hydrocarbon seeps in acidic soils at Rainbow Springs, Yellowstone

National Park. *Appl. Environ. Microbiol.* 71, 5943–5950. doi: 10.1128/AEM.71.10.5943-5950.2005

Huyop, F., and Cooper, R. (2012). Degradation of millimolar concentration of the herbicide dalapon (2,2-dichloropropionic Acid) by *Rhizobium* sp. isolated from soil. *Biotechnol. Biotechnol. Equip.* 26, 3106–3112. doi: 10.5504/BBEQ.2012.0058

Ivanova, A. E., Sukhacheva, M. V., Kanat'eva, A. Y., Kravchenko, I. K., and Kurganov, A. A. (2014). Hydrocarbon-oxidizing potential and the genes for n-alkane biodegradation in a new acidophilic mycobacterial association from sulfur blocks. *Microbiology* 83, 764–772. doi: 10.1134/S0026261714060095

Kato, S., Kosaka, T., and Watanabe, K. (2009). Substrate-dependent transcriptomic shifts in *Pelotomaculum thermopropionicum* grown in syntrophic co-culture with *Methanothermobacter thermautotrophicus*. *Microb. Biotechnol.* 2, 575–584. doi: 10.1111/j.1751-7915.2009.00102.x

Kato, T., Miyanaga, A., Kanaya, S., and Morikawa, M. (2009). Alkane inducible proteins in *Geobacillus thermoleovorans* B23. *BMC Microbiol.* 9:60. doi: 10.1186/1471-2180-9-60

Khelifi, N., Amin Ali, O., Roche, P., Grossi, V., Brochier-Armanet, C., Valette, O., et al. (2014). Anaerobic oxidation of long-chain n-alkanes by the hyperthermophilic sulfate-reducing archaeon, *Archaeoglobus fulgidus*. *ISME J.* 8, 2153–2166. doi: 10.1038/ismej.2014.58

Kleindienst, S., Herbst, F. A., Stagars, M., Von Netzer, F., Von Bergen, M., Seifert, J., et al. (2014). Diverse sulfate-reducing bacteria of the *Desulfosarcina*/*Desulfococcus* clade are the key alkane degraders at marine seeps. *ISME J.* 8, 2029–2044. doi: 10.1038/ismej.2014.51

Knaebel, D. B., and Crawford, R. L. (1995). Extraction and purification of microbial DNA from petroleum-contaminated soils and detection of low numbers of toluene, octane and pesticide degraders by multiplex polymerase chain reaction and Southern analysis. *Mol. Ecol.* 4, 579–591. doi: 10.1111/j.1365-294X.1995.tb00258.x

Koh, H. Y., Park, H., Lee, J. H., Han, S. J., Sohn, Y. C., and Lee, S. G. (2017). Proteomic and transcriptomic investigations on cold-responsive properties of the psychrophilic Antarctic bacterium *Psychrobacter* sp. PAMC 21119 at subzero temperatures. *Environ. Microbiol.* 19, 628–644. doi: 10.1111/1462-2920.13578

Kuhn, E., Bellicanta, G. S., and Pellizari, V. H. (2009). New *alk* genes detected in Antarctic marine sediments. *Environ. Microbiol.* 11, 669–673. doi: 10.1111/j.1462-2920.2008.01843.x

Laso-Pérez, R., Wegener, G., Knittel, K., Widdel, F., Harding, K. J., Krukenberg, V., et al. (2016). Thermophilic archaea activate butane via alkyl-coenzyme M formation. *Nature* 539, 396–401. doi: 10.1038/nature20152

Li, D. C., Yang, F., Lu, B., Chen, D. F., and Yang, W. J. (2012). Thermotolerance and molecular chaperone function of the small heat shock protein HSP20 from hyperthermophilic archaeon, *Sulfolobus solfataricus* P2. *Cell Stress Chaperones* 17, 103–108. doi: 10.1007/s12192-011-0289-z

Li, H., Ji, X., Zhou, Z., Wang, Y., and Zhang, X. (2010). *Thermus thermophilus* proteins that are differentially expressed in response to growth temperature and their implication in thermoadaptation. *J. Proteome Res.* 9, 855–864. doi: 10.1021/pr900754y

Li, L., Liu, X., Yang, W., Xu, F., Wang, W., Feng, L., et al. (2008). Crystal structure of long-chain alkane monooxygenase (LadA) in complex with coenzyme FMN: unveiling the long-chain alkane hydroxylase. *J. Mol. Biol.* 376, 453–465. doi: 10.1016/j.jmb.2007.11.069

Li, P., Wang, L., and Feng, L. (2013). Characterization of a novel Rieske-type alkane monooxygenase system in *Pusillimonas* sp. strain T7-7. *J. Bacteriol.* 195, 1892–1901. doi: 10.1128/JB.02107-12

Liang, J. L., Nie, Y., Wang, M., Xiong, G., Wang, Y. P., Maser, E., et al. (2016). Regulation of alkane degradation pathway by a TetR family repressor via an autoregulation positive feedback mechanism in a Gram-positive *Dietzia* bacterium. *Mol. Microbiol.* 99, 338–359. doi: 10.1111/mmi.13232

Lin, Q., Mendelssohn, I. A., Henry, C. B., Roberts, P. O., Walsh, M. M., Overton, E. B., et al. (1999). Effects of bioremediation agents on oil degradation in mineral and sandy salt marsh sediments. *Environ. Technol.* 20, 825–837. doi: 10.1080/09593332008616878

Liu, C., Wang, W., Wu, Y., Zhou, Z., Lai, Q., and Shao, Z. (2011). Multiple alkane hydroxylase systems in a marine alkane degrader, *Alcanivorax dieselolei* B-5. *Environ. Microbiol.* 13, 1168–1178. doi: 10.1111/j.1462-2920.2010.02416.x

Luz, A. P., Pellizari, V. H., Whyte, L. G., and Greer, C. W. (2004). A survey of indigenous microbial hydrocarbon degradation genes in soils from Antarctica and Brazil. *Can. J. Microbiol.* 50, 323–333. doi: 10.1139/w04-008

Ma, B. G., Goncearenco, A., and Berezovsky, I. N. (2010). Thermophilic adaptation of protein complexes inferred from proteomic homology modeling. *Structure* 18, 819–828. doi: 10.1016/j.str.2010.04.004

Maeng, J. H., Sakai, Y., Tani, Y., and Kato, N. (1996). Isolation and characterization of a novel oxygenase that catalyzes the first step of n-alkane oxidation in *Acinetobacter* sp. strain M-1. *J. Bacteriol.* 178, 3695–3700. doi: 10.1128/jb.178.13.3695-3700.1996

Magazù, S., Migliardo, F., Benedetto, A., La Torre, R., and Hennet, L. (2012). Bioprotective effects of homologous disaccharides on biological macromolecules. *Eur. Biophys. J.* 41, 361–367. doi: 10.1007/s00249-011-0760-x

Mandelli, F., Couger, M. B., Paixão, D. A. A., Machado, C. B., Carnielli, C. M., Aricetti, J. A., et al. (2017). Thermal adaptation strategies of the extremophile bacterium *Thermus filiformis* based on multi-omics analysis. *Extremophiles* 21, 775–788. doi: 10.1007/s00792-017-0942-2

Mapelli, F., Scoma, A., Michoud, G., Aulenta, F., Boon, N., Borin, S., et al. (2017). Biotechnologies for marine oil spill cleanup: indissoluble ties with microorganisms. *Trends Biotechnol.* 35, 860–870. doi: 10.1016/j.tibtech.2017.04.003

Mardanov, A. V., Slododkinab, G. B., Slobodkinb, A. I., Beletskya, A. V., Gavrilovb, S. N., Kublanovb, I. V., et al. (2014). The *Geoglobus acetivorans* genome: Fe(III) reduction, acetate utilization, autotrophic growth, and degradation of aromatic compounds in a hyperthermophilic archaeon. *Appl. Environ. Microbiol.* 81, 1003–1012. doi: 10.1128/AEM.02705-14

Margesin, R., Gander, S., Zacke, G., Gounot, A. M., and Schinner, F. (2003). Hydrocarbon degradation and enzyme activities of cold-adapted bacteria and yeasts. *Extremophiles* 7, 451–458. doi: 10.1007/s00792-003-0347-2

Margesin, R., and Schinner, F. (1998). Low-temperature bioremediation of a waste water contaminated with anionic surfactants and fuel oil. *Appl. Microbiol. Biotechnol.* 49, 482–486. doi: 10.1007/s002530051202

Margesin, R., Zimmerbauer, A., and Schinner, F. (2000). Monitoring of bioremediation by soil biological activities. *Chemosphere* 40, 339–346. doi: 10.1016/S0045-6535(99)00218-0

Martínez Álvarez, L. M., Ruberto, L., Lo Balbo, A., and Mac Cormack, W. P. (2017). Bioremediation of hydrocarbon-contaminated soils in cold regions: development of a pre-optimized biostimulation biopile-scale field assay in Antarctica. *Sci. Total Environ.* 590–591, 194–203. doi: 10.1016/j.scitotenv.2017.02.204

McCarthy, K., Walker, L., Vigoren, L., and Bartel, J. (2004). Remediation of spilled petroleum hydrocarbons by in situ landfarming at an arctic site. *Cold Reg. Sci. Technol.* 40, 31–39. doi: 10.1016/j.coldregions.2004.05.001

Meier, D. V., Bach, W., Girguis, P. R., Gruber-Vodicka, H. R., Reeves, E. P., Richter, M., et al. (2016). Heterotrophic *Proteobacteria* in the vicinity of diffuse hydrothermal venting. *Environ. Microbiol.* 18, 4348–4368. doi: 10.1111/1462-2920.13304

Meruelo, A. D., Han, S. K., Kim, S., and Bowie, J. U. (2012). Structural differences between thermophilic and mesophilic membrane proteins. *Protein Sci.* 21, 1746–1753. doi: 10.1002/pro.2157

Murygina, V., Arinbasarov, M., and Kalyuzhnyi, S. (2000). Bioremediation of oil polluted aquatic systems and soils with novel preparation 'Rhoder'. *Biodegradation* 11, 385–389. doi: 10.1023/A:1011680703911

Mykytczuk, N. C., Foote, S. J., Omelon, C. R., Southam, G., Greer, C. W., and Whyte, L. G. (2013). Bacterial growth at -15°C; molecular insights from the permafrost bacterium *Planococcus halocryophilus* Or1. *ISME J.* 7, 1211–1226. doi: 10.1038/ismej.2013.8

Nie, Y., Chi, C. Q., Fang, H., Liang, J. L., Lu, S. L., Lai, G. L., et al. (2014). Diverse alkane hydroxylase genes in microorganisms and environments. *Sci. Rep.* 4:4968. doi: 10.1038/srep04968

Nie, Y., Fang, H., Li, Y., Chi, C. Q., Tang, Y. Q., and Wu, X. L. (2013). The genome of the moderate halophile *Amycolicicoccus subflavus* DQS3-9A1(T) reveals four alkane hydroxylation systems and provides some clues on the genetic basis for its adaptation to a petroleum environment. *PLoS One* 8:e70986. doi: 10.1371/journal.pone.0070986

Oberding, L. K., and Gieg, L. M. (2017). Methanogenic paraffin biodegradation: alkylsuccinate synthase gene quantification and dicarboxylic acid production. *Appl. Environ. Microbiol.* 84:e01773-17. doi: 10.1128/AEM.01773-17

Park, C., Shin, B., Jung, J., Lee, Y., and Park, W. (2017). Metabolic and stress responses of *Acinetobacter oleivorans* DR1 during long-chain alkane degradation. *Microb. Biotechnol.* 10, 1809–1823. doi: 10.1111/1751-7915.12852

Phadtare, S. (2004). Recent developments in bacterial cold-shock response. *Curr. Issues Mol. Biol.* 6, 125–136.

Prabagaran, S. R., Manorama, R., Delille, D., and Shivaji, S. (2007). Predominance of *Roseobacter*, *Sulfitobacter*, *Glaciecola* and *Psychrobacter* in seawater collected off Ushuaia, Argentina, Sub-Antarctica. *FEMS Microbiol. Ecol.* 59, 342–355. doi: 10.1111/j.1574-6941.2006.00213.x

Radwan, S. R., Al-Mailem, D. M., and Kansour, M. K. (2017). Calcium (II) - and dipicolinic acid mediated-biostimulation of oil-bioremediation under multiple stresses by heat, oil and heavy metals. *Sci. Rep.* 7:9534. doi: 10.1038/s41598-017-10121-7

Rampelotto, P. H. (2013). Extremophiles and extreme environments. *Life* 3, 482–485. doi: 10.3390/life3030482

Rapp, P., and Gabriel-Jürgens, L. H. (2003). Degradation of alkanes and highly chlorinated benzenes, and production of biosurfactants, by a psychrophilic *Rhodococcus* sp. and genetic characterization of its chlorobenzene dioxygenase. *Microbiology* 149, 2879–2890. doi: 10.1099/mic.0.26188-0

Richard, H., and Foster, J. W. (2004). *Escherichia coli* glutamate- and arginine-dependent acid resistance systems increase internal pH and reverse transmembrane potential. *J. Bacteriol.* 186, 6032–6041. doi: 10.1128/JB.186.18.6032-6041.2004

Rivers, A. R., Sharma, S., Tringe, S. G., Martin, J., Joye, S. B., and Moran, M. A. (2013). Transcriptional response of bathypelagic marine bacterioplankton to the Deepwater Horizon oil spill. *ISME J.* 7, 2315–2329. doi: 10.1038/ismej.2013.129

Roberts, M. F. (2005). Organic compatible solutes of halotolerant and halophilic microorganisms. *Saline Systems* 1:5. doi: 10.1186/1746-1448-1-5

Rodrigues, D. F., Ivanova, N., He, Z., Huebner, M., Zhou, J., and Tiedje, J. M. (2008). Architecture of thermal adaptation in an *Exiguobacterium sibiricum* strain isolated from 3 million year old permafrost: a genome and transcriptome approach. *BMC Genomics* 9:547. doi: 10.1186/1471-2164-9-547

Rojo, F. (2009). Degradation of alkanes by bacteria. *Environ. Microbiol.* 11, 2477–2490. doi: 10.1111/j.1462-2920.2009.01948.x

Rozhkova-Novosad, E. A., Chae, J. C., Zylstra, G. J., Bertrand, E. M., Alexander-Ozinskas, M., Deng, D., et al. (2007). Profiling mechanisms of alkane hydroxylase activity in vivo using the diagnostic substrate norcarane. *Chem. Biol.* 14, 165–172. doi: 10.1016/j.chembiol.2006.12.007

Ruberto, L., Vazquez, S. C., and Mac Cormack, W. P. (2003). Effectiveness of the natural bacterial flora, biostimulation and bioaugmentation on the bioremediation of a hydrocarbon contaminated Antarctic soil. *Int. Biodeterior. Biodegradation* 52, 115–125. doi: 10.1016/S0964-8305(03)00048-9

Sabirova, J. S., Ferrer, M., Regenhardt, D., Timmis, K. N., and Golyshin, P. N. (2006). Proteomic insights into metabolic adaptations in *Alcanivorax borkumensis* induced by alkane utilization. *J. Bacteriol.* 188, 3763–3773. doi: 10.1128/JB.00072-06

Sagot, B., Gaysinski, M., Mehiri, M., Guigonis, J. M., Le Rudulier, D., and Alloing, G. (2010). Osmotically induced synthesis of the dipeptide N-acetylglutaminylglutamine amide is mediated by a new pathway conserved among bacteria. *Proc. Natl. Acad. Sci. U.S.A.* 107, 12652–12657. doi: 10.1073/pnas.1003063107

Schönfeld, P., and Wojtczak, L. (2016). Short- and medium-chain fatty acids in the energy metabolism–the cellular perspective. *J. Lipid Res.* 57, 943–954. doi: 10.1194/jlr.R067629

Scoma, A., and Boon, N. (2016). Osmotic stress confers enhanced cell integrity to hydrostatic pressure but impairs growth in *Alcanivorax borkumensis* SK2. *Front. Microbiol.* 7:729. doi: 10.3389/fmicb.2016.00729

Shih, T. W., and Pan, T. M. (2011). Stress responses of thermophilic *Geobacillus* sp. NTU 03 caused by heat and heat-induced stress. *Microbiol. Res.* 166, 346–359. doi: 10.1016/j.micres.2010.08.001

Siddique, T., Penner, T., Klassen, J., Nesbø, C., and Foght, J. M. (2012). Microbial communities involved in methane production from hydrocarbons in oil sands tailings. *Environ. Sci. Technol.* 46, 9802–9810. doi: 10.1021/es302202c

Siddiqui, K. S., and Cavicchioli, R. (2006). Cold-adapted enzymes. *Annu. Rev. Biochem.* 75, 403–433. doi: 10.1146/annurev.biochem.75.103004.142723

So, C. M., and Young, L. Y. (1999). Initial reactions in anaerobic alkane degradation by a sulfate reducer, strain AK-01. *Appl. Environ. Microbiol.* 65, 5532–5540.

Sotsky, J. B., Greer, C. W., and Atlas, R. M. (1994). Frequency of genes in aromatic and aliphatic hydrocarbon biodegradation pathways within bacterial populations from Alaskan sediments. *Can. J. Microbiol.* 40, 981–985. doi: 10.1139/m94-157

Stapleton, R. D., and Sayler, G. S. (1998). Assessment of the microbiological potential for the natural attenuation of petroleum hydrocarbons in a shallow aquifer system. *Microb. Ecol.* 36, 349–361. doi: 10.1007/s002489900121

Suter, E. A., Pachiadaki, M., Taylor, G. T., Astor, Y., and Edgcomb, V. P. (2017). Free-living chemoautotrophic and particle-attached heterotrophic prokaryotes dominate microbial assemblages along a pelagic redox gradient. *Environ. Microbiol.* 20, 693–712. doi: 10.1111/1462-2920.13997

Tan, B., Fowler, S. J., Abu Laban, N., Dong, X., Sensen, C. W., Foght, J., et al. (2015a). Comparative analysis of metagenomes from three methanogenic hydrocarbon-degrading enrichment cultures with 41 environmental samples. *ISME J.* 9, 2028–2045. doi: 10.1038/ismej.2015.22

Tan, B., Semple, K., and Foght, J. (2015b). Anaerobic alkane biodegradation by cultures enriched from oil sands tailings ponds involves multiple species capable of fumarate addition. *FEMS Microbiol. Ecol.* 91:fiv042. doi: 10.1093/femsec/fiv042

Throne-Holst, M., Wentzel, A., Ellingsen, T. E., Kotlar, H. K., and Zotchev, S. B. (2007). Identification of novel genes involved in long-chain n-alkane degradation by *Acinetobacter* sp. strain DSM 17874. *Appl. Environ. Microbiol.* 73, 3327–3332. doi: 10.1128/AEM.00064-07

Timmers, P. H. A., Suarez-Zuluaga, D. A., van Rossem, M., Diender, M., Stams, A. J., and Plugge, C. M. (2016). Anaerobic oxidation of methane associated with sulfate reduction in a natural freshwater gas source. *ISME J.* 10, 1400–1412. doi: 10.1038/ismej.2015.213

Timmers, P. H. A., Welte, C. U., Koehorst, J. J., Plugge, C. M., Jetten, M. S. M., and Stams, A. J. M. (2017). Reverse methanogenesis and respiration in methanotrophic archaea. *Archaea* 2017:1654237. doi: 10.1155/2017/1654237

Ting, L., Williams, T. J., Cowley, M. J., Lauro, F. M., Guilhaus, M., Raftery, M. J., et al. (2010). Cold adaptation in the marine bacterium, *Sphingopyxis alaskensis*, assessed using quantitative proteomics. *Environ. Microbiol.* 12, 2658–2676. doi: 10.1111/j.1462-2920.2010.02235.x

Tourova, T. P., Sokolova, D. S., Semenova, E. M., Shumkova, E. S., Korshunova, A. V., Babich, T. L., et al. (2016). Detection of n-alkane biodegradation genes *alkB* and *ladA* in thermophilic hydrocarbon-oxidizing bacteria of the genera *Aeribacillus* and *Geobacillus*. *Microbiology* 85, 693–707. doi: 10.1134/S0026261716060199

Tribelli, P. M., Rossi, L., Ricardi, M. M., Gomez-Lozano, M., Molin, S., Raiger Iustman, L. J., et al. (2018). Microaerophilic alkane degradation in *Pseudomonas extremaustralis*: a transcriptomic and physiological approach. *J. Ind. Microbiol. Biotechnol.* 45, 15–23. doi: 10.1007/s10295-017-1987-z

van Beilen, J. B., and Funhoff, E. G. (2007). Alkane hydroxylases involved in microbial alkane degradation. *Appl. Microbiol. Biotechnol.* 74, 13–21. doi: 10.1007/s00253-006-0748-0

Venter, J. C., Remington, K., Heidelberg, J. F., Halpern, A. L., Rusch, D., and Eisen, J. A. (2004). Environmental genome shotgun sequencing of the Sargasso Sea. *Science* 304, 66–74. doi: 10.1126/science.1093857

Viggi, C. C., Presta, E., Bellagamba, M., Kaciulis, S., Balijepalli, S. K., Zanaroli, G., et al. (2015). The "Oil-Spill Snorkel": an innovative bioelectrochemical approach to accelerate hydrocarbons biodegradation in marine sediments. *Front. Microbiol.* 6:881. doi: 10.3389/fmicb.2015.00881

Walker, C. B., He, Z. L., Yang, Z. K., Ringbauer, J. A., He, Q., and Zhou, J. H. (2009). The electron transfer system of syntrophically grown *Desulfovibrio vulgaris*. *J. Bacteriol.* 191, 5793–5801. doi: 10.1128/JB.00356-09

Wang, J., Wang, J., Zhang, Z., Li, Y., Zhang, B., Zhang, Z., et al. (2015). Cold-adapted bacteria for bioremediation of crude oil-contaminated soil. *J. Chem. Technol. Biotechnol.* 91, 2286–2297. doi: 10.1002/jctb.4814

Wang, L., Wang, W., Lai, Q., and Shao, Z. (2010). Gene diversity of CYP153A and AlkB alkane hydroxylases in oil-degrading bacteria isolated from the Atlantic Ocean. *Environ. Microbiol.* 12, 1230–1242. doi: 10.1111/j.1462-2920.2010.02165.x

Wang, Q., Cen, Z., and Zhao, J. (2015). The survival mechanisms of thermophiles at high temperatures: an angle of omics. *Physiology* 30, 97–106. doi: 10.1152/physiol.00066.2013

Wang, W., Ma, T., Zhang, B., Yao, N., Li, M., Cui, L., et al. (2014). Novel mechanism of protein thermostability: a unique N-terminal domain confers heat resistance to Fe/Mn-SODs. *Sci. Rep.* 4:7284. doi: 10.1038/srep07284

Wang, W., Wang, L., and Shao, Z. (2010). Diversity and abundance of oil-degrading bacteria and alkane hydroxylase (*alkB*) genes in the subtropical seawater of Xiamen Island. *Microb. Ecol.* 60, 429–439. doi: 10.1007/s00248-010-9724-4

Wang, W., and Shao, Z. (2012). Diversity of flavin-binding monooxygenase genes (almA) in marine bacteria capable of degradation long-chain alkanes. *FEMS Microbiol. Ecol.* 80, 523–533. doi: 10.1111/j.1574-6941.2012.01322.x

Wang, X. B., Chi, C. Q., Nie, Y., Tang, Y. Q., Tan, Y., Wu, G., et al. (2011). Degradation of petroleum hydrocarbons (C6–C40) and crude oil by a novel *Dietzia* strain. *Bioresour. Technol.* 17, 7755–7761. doi: 10.1016/j.biortech.2011.06.009

Washer, C. E., and Edwards, E. A. (2007). Identification and expression of benzylsuccinate synthase genes in a toluene-degrading methanogenic consortium. *Appl. Environ. Microbiol.* 73, 1367–1369. doi: 10.1128/AEM.01904-06

Watanabe, S., Yamaoka, N., Takada, Y., and Fukunaga, N. (2002). The cold-inducible *icl* gene encoding thermolabile isocitrate lyase of a psychrophilic bacterium, *Colwellia maris*. *Microbiology* 148, 2579–2589. doi: 10.1099/00221287-148-8-2579

Whelan, M. J., Coulon, F., Hince, G., Rayner, J., McWatters, R., Spedding, T., et al. (2015). Fate and transport of petroleum hydrocarbons in engineered biopiles in polar regions. *Chemosphere* 131, 232–240. doi: 10.1016/j.chemosphere.2014.10.088

Whyte, L. G., Hawari, J., Zhou, E., Bourbonnière, L., Inniss, W. E., and Greer, C. W. (1998). Biodegradation of variable-chain-length alkanes at low temperatures by a psychrotrophic *Rhodococcus* sp. *Appl. Environ. Microbiol.* 64, 2578–2584.

Whyte, L. G., Schultz, A., Beilen, J. B., Luz, A. P., Pellizari, V., Labbé, D., et al. (2002). Prevalence of alkane monooxygenase genes in Arctic and Antarctic hydrocarbon-contaminated and pristine soils. *FEMS Microbiol. Ecol.* 41, 141–150. doi: 10.1111/j.1574-6941.2002.tb00975.x

Wouters, J. A., Rombouts, F. M., de Vos, W. M., Kuipers, O. P., and Abee, T. (1999). Cold shock proteins and low-temperature response of *Streptococcus thermophilus* CNRZ302. *Appl. Environ. Microbiol.* 65, 4436–4442.

Yergeau, E., Sanschagrin, S., Beaumier, D., and Greer, C. W. (2012). Metagenomic analysis of the bioremediation of diesel-contaminated Canadian high arctic soils. *PLoS One* 7:e30058. doi: 10.1371/journal.pone.0030058

Youssef, N. H., Savage-Ashlock, K. N., McCully, A. L., Luedtke, B., Shaw, E. I., Hoff, W. D., et al. (2014). Trehalose/2-sulfotrehalose biosynthesis and glycine-betaine uptake are widely spread mechanisms for osmoadaptation in the *Halobacteriales*. *ISME J.* 8, 636–649. doi: 10.1038/ismej.2013.165

Yuk, H. G., and Marshall, D. L. (2004). Adaptation of *Escherichia coli* O157:H7 to pH alters membrane lipid composition, verotoxin secretion, and resistance to simulated gastric fluid acid. *Appl. Environ. Microbiol.* 70, 3500–3505. doi: 10.1128/AEM.70.6.3500-3505.2004

Yun, S. H., Choi, C. W., Kwon, S. O., Lee, Y. G., Chung, Y. H., Jung, H. J., et al. (2011). Enrichment and proteome analysis of a hyperthermostable protein set of archaeon *Thermococcus onnurineus* NA1. *Extremophiles* 15, 451–461. doi: 10.1007/s00792-011-0376-1

Zhou, N., Swamy, K. B., Leu, J. Y., McDonald, M. J., Galafassi, S., Compagno, C., et al. (2017). Coevolution with bacteria drives the evolution of aerobic fermentation in *Lachancea kluyveri*. *PLoS One* 12:e0173318. doi: 10.1371/journal.pone.0173318

Conflict of Interest Statement: The authors declare that the research was conducted in the absence of any commercial or financial relationships that could be construed as a potential conflict of interest.

frontiers in Microbiology

ORIGINAL RESEARCH
published: 15 May 2018
doi: 10.3389/fmicb.2018.00959

Synthesis and Antibacterial Activity of Metal(loid) Nanostructures by Environmental Multi-Metal(loid) Resistant Bacteria and Metal(loid)-Reducing Flavoproteins

Maximiliano Figueroa[1†], Valentina Fernandez[1†], Mauricio Arenas-Salinas[2], Diego Ahumada[1], Claudia Muñoz-Villagrán[1,3], Fabián Cornejo[1], Esteban Vargas[4], Mauricio Latorre[5,6,7,8], Eduardo Morales[9], Claudio Vásquez[1] and Felipe Arenas[1]*

[1] *Laboratorio Microbiología Molecular, Departamento de Biología, Facultad de Química y Biología, Universidad de Santiago de Chile, Santiago, Chile,* [2] *Centro de Bioinformática y Simulación Molecular, Universidad de Talca, Talca, Chile,* [3] *Departamento de Ciencias Básicas, Facultad de Ciencia, Universidad Santo Tomas, Sede Santiago, Chile,* [4] *Center for the Development of Nanoscience and Nanotechnology, Santiago, Chile,* [5] *Mathomics, Centro de Modelamiento Matemático, Universidad de Chile, Beauchef, Santiago, Chile,* [6] *Fondap-Center of Genome Regulation, Facultad de Ciencias, Universidad de Chile, Santiago, Chile,* [7] *Laboratorio de Bioinformática y Expresión Génica, INTA, Universidad de Chile, Santiago, Chile,* [8] *Instituto de Ciencias de la Ingeniería, Universidad de O'Higgins, Rancagua, Chile,* [9] *uBiome, San Francisco, CA, United States*

OPEN ACCESS

Edited by:
Edgardo Donati, National University of La Plata, Argentina

Reviewed by:
M. Oves, King Abdulaziz University, Saudi Arabia
Ana Isabel Pelaez, Universidad de Oviedo Mieres, Spain

***Correspondence:**
Felipe Arenas
felipe.arenass@usach.cl

[†] *These authors have contributed equally to this work.*

Specialty section:
This article was submitted to Microbiotechnology, Ecotoxicology and Bioremediation, a section of the journal Frontiers in Microbiology

Received: *12 December 2017*
Accepted: *24 April 2018*
Published: *15 May 2018*

Citation:
Figueroa M, Fernandez V, Arenas-Salinas M, Ahumada D, Muñoz-Villagrán C, Cornejo F, Vargas E, Latorre M, Morales E, Vásquez C and Arenas F (2018) Synthesis and Antibacterial Activity of Metal(loid) Nanostructures by Environmental Multi-Metal(loid) Resistant Bacteria and Metal(loid)-Reducing Flavoproteins. Front. Microbiol. 9:959. doi: 10.3389/fmicb.2018.00959

Microbes are suitable candidates to recover and decontaminate different environments from soluble metal ions, either via reduction or precipitation to generate insoluble, non-toxic derivatives. In general, microorganisms reduce toxic metal ions generating nanostructures (NS), which display great applicability in biotechnological processes. Since the molecular bases of bacterial reduction are still unknown, the search for new -environmentally safe and less expensive- methods to synthesize NS have made biological systems attractive candidates. Here, 47 microorganisms isolated from a number of environmental samples were analyzed for their tolerance or sensitivity to 19 metal(loid)s. Ten of them were highly tolerant to some of them and were assessed for their ability to reduce these toxicants *in vitro*. All isolates were analyzed by 16S rRNA gene sequencing, fatty acids composition, biochemical tests and electron microscopy. Results showed that they belong to the *Enterobacter*, *Staphylococcus*, *Acinetobacter*, and *Exiguobacterium* genera. Most strains displayed metal(loid)-reducing activity using either NADH or NADPH as cofactor. While *Acinetobacter schindleri* showed the highest tellurite (TeO_3^{2-}) and tetrachloro aurate ($AuCl_4^-$) reducing activity, *Staphylococcus sciuri* and *Exiguobacterium acetylicum* exhibited selenite (SeO_3^{2-}) and silver (Ag^+) reducing activity, respectively. Based on these results, we used these bacteria to synthetize, *in vivo and in vitro* Te, Se, Au, and Ag-containing nanostructures. On the other hand, we also used purified *E. cloacae* glutathione reductase to synthesize *in vitro* Te-, Ag-, and Se-containing NS, whose morphology, size, composition, and chemical composition were evaluated. Finally, we assessed the putative anti-bacterial activity exhibited by the *in vitro* synthesized NS: Te-containing NS were more effective than Au-NS in inhibiting *Escherichia coli* and *Listeria monocytogenes* growth. Aerobically synthesized

TeNS using MF09 crude extracts showed MICs of 45- and 66- μg/ml for *E. coli* and *L. monocytogenes*, respectively. Similar MIC values (40 and 82 μg/ml, respectively) were observed for TeNS generated using crude extracts from *gorA*-overexpressing *E. coli*. In turn, AuNS MICs for *E. coli* and *L. monocytogenes* were 64- and 68- μg/ml, respectively.

Keywords: metal, metalloid, reduction, resistance, environmental bacteria, flavoprotein, nanostructure, bioremediation

INTRODUCTION

More than half of the elements in the Periodic Table are represented by metals and metalloids. Whereas some of them are essential for different cellular processes, including electron transfer, enzyme catalysis, and stabilization of protein structure, others such as Ag^{+}, Hg^{+}, SeO_4^{2-}, and TeO_4^{2-} are highly toxic even at very low concentrations (Pérez et al., 2007; Zannoni et al., 2008; Lemire et al., 2013). Thus, organisms like bacteria must maintain a strict balance of the intracellular concentration of these metal(loid)s. Under aerobic conditions the toxicity of compounds containing these elements is mainly related to the production of reactive oxygen species (ROS), which can attack key cell components including polyunsaturated fatty acids, proteins, and nucleic acids (Borsetti et al., 2005; Tremaroli et al., 2007; Vrionis et al., 2015). Additionally, protein carbonylation (Contreras and Vásquez, 2010), [4Fe-4S] cluster dismantling of iron-sulfur proteins (Calderón et al., 2009), membrane lipid peroxidation (Lemire et al., 2013; Pradenas et al., 2013), blocking of cysteine and methionine residues (Stolz and Oremland, 1999), increased cell permeability, and the interference of metabolic pathways have also been observed (Carotti et al., 2000).

Given their great biotechnological potential, we focused our interest in characterizing NS containing silver, gold or the metalloids tellurium and selenium. Selenium can be found in the environment as a solid [Se (0), Se^0], forming part of selenium-containing amino acids, and as the selenium oxyanions selenate [Se (VI), SeO_4^{2-}] and the most toxic, selenite [Se (IV), SeO_3^{2-}] (Stolz and Oremland, 1999). Conversely to selenium, tellurium (Te) has no known biological role to date (Ba et al., 2010) and given its metallic characteristics, it is found in various redox states, mainly elemental tellurium [Te (0), Te^0], telluride [Te (II), Te^{2-}], tellurite [Te (IV), TeO_3^{2-}], and tellurate [Te (VI), TeO_4^{2-}], both oxyanions being highly toxic to most organisms (Nies and Silver, 1995; Taylor, 1999). In turn, silver is mainly found in the 1+ oxidation state [Ag (I)], and less commonly as [Ag (II)], [Ag (III)], or metallic silver (Ag^0) (Burriel et al., 2006). Finally, gold is found as metallic gold (Au^0) as well as in six other oxidation states, 1+ [Au (I)] and 3+ [Au (III)] being the most commonly found in nature (Nies and Grass, 2009).

To date, a number of genetic and biochemical mechanisms that microbial systems use to cope with the toxicity of defined metal(loid)s are relatively well known; however, a strategy providing universal resistance to all these toxicants has not been reported so far. In general, one of the most common strategies employed by microbes to tolerate high metal(loid) concentrations, is their chemical modification to less-toxic forms (Silver and Phung, 2005). For instance, this kind of resistance mechanisms have been observed in *Rhodobacter capsulatus* (Turner et al., 2011), *Geobacillus* sp. (Correa-Llantén et al., 2013), and *Shewanella oneidensis* (Klonowska et al., 2005) which reduce Te (IV), Au (III) and Se (IV), respectively.

Metal(loid) reduction by microbial systems could be of great help in decontaminating soluble metal ions from soils, forming insoluble, less-toxic derivatives that often generate metal arrangements at the nanoscale (Narayanan and Sakthivel, 2010; Thakkar et al., 2010), also known as nanostructures (NS) exhibiting one or more dimensions <100 nm. Gold (Correa-Llantén et al., 2013), selenium (Song et al., 2017), silver (Gurunathan et al., 2009), tellurium (Arenas-Salinas et al., 2016), and uranium (Suresh, 2012) NS have been reported, opening a great interest because of their potential application in the field of biotechnology.

A number of flavoproteins able of metal ion reduction to less toxic, insoluble forms have been described, including (i) mercury reductase (MerA) (Silver and Phung, 2005), (ii) glutathione reductase (Au^{3+} and TeO_3^{2-} reduction, Pugin et al., 2014), (iii) fumarate reductase (selenite reduction, Song et al., 2017), (iv) thioredoxin reductase and alkyl hydroperoxide reductase that reduce tellurite (Arenas-Salinas et al., 2016) and (v) nitrate reductase, able to reduce tellurite as well as silver (Kumar et al., 2007).

Because the optical, mechanical, and fluorescent properties of metal(loid)-containing NS are different from those exhibited by matter at larger scales (Suresh, 2012), NS display a wide range of applications in physics, chemistry, electronics, optics, materials science, biomedicine, and agriculture (Thakkar et al., 2010). The fast development of nanotechnology has provided several kinds of materials for biomedical applications, including cancer detection therapies (Rao, 2008), and antibacterial treatments (Amstad et al., 2011; Azam et al., 2012). In fact, the use of metallic NS displaying bactericidal activity has been reported (Sharma et al., 2009; Li et al., 2011; Cui et al., 2012; Xiu et al., 2012; Dizaj et al., 2014; Pugin et al., 2014; Oves et al., 2017). In other studies, gold-, tellurium-, copper -, silver-, zinc-, and titanium-containing NS proved to be effective as antibacterials against *Escherichia coli* (Cioffi and Rai, 2012).

Summarizing, since NS production by chemical methods often involve high temperature, anaerobic conditions and toxic reagents that in the end affect the clinical application of nanostructures, the generation and characterization of new metallic NS by biological systems is important either for basic as well as for applied research. In this general context, the search for new environmentally friendly and inexpensive methods for metal(loid)-containing NS generation has made biological systems desirable candidates for both *in vivo* and *in vitro*

NS production, either using whole microorganisms or purified enzymes.

MATERIALS AND METHODS

Isolation and Selection of Metal(loid)-Resistant Bacteria

Twenty-two samples were collected from two different Chilean regions from which bacterial isolates were obtained: (i) north (Blanca, Chaxa and Céjar lagoons, El Tatío geyser, Death Valley) and (ii) mid-south (Maule lagoon, El Teniente copper mine). A sample from Uyuni Salar, Bolivia, was also included in this study. In turn, isolates MF02 and MF05 were kindly provided by Dr. Juan Carlos Tantaléan, Universidad San Luis Gonzaga, Ica, Perú.

Four different culture media were individually inoculated with each sample and incubated at 25 or 37°C for 24 h: LB (Sambrook and Russell, 2001); R2A (0.5 g/L yeast extract, 0.5 g/L peptone, 0.5 g/L casamino acids, 0.5 g/L glucose, 0.5 g/L soluble starch, 0.3 g/L sodium pyruvate, 0.3 g/L K_2HPO_4, and 0.5 g/L $MgSO_4$ adjusted to pH 7.2); Acidiphilium (2 g/L $(NH_4)_2SO_4$, 0.1 g/L KCl, 0.5 g/L K_2HPO_4, 0.5 g/L $MgSO_4$, 0.3 g/L yeast extract and 1 g/L D-glucose adjusted to pH 3.0); and Aciduric thermophilic *Bacillus* strains (ATB) (0.2 g/L $(NH_4)_2SO_4$, 0.5 g/L $MgSO_4$, 0.25 g/L $CaCl_2$, 3 g/L KH_2PO_4, 1 g/L yeast extract, 1 g/L tryptone, 1 g/L glucose and 1 g/L starch adjusted to pH 4.3). Pure cultures were obtained after sequential dilutions and successive passages using appropriate solid media.

Purified colonies were seeded on LB-agar plates that contained different concentrations of the following compounds: K_2TeO_3 (0.04–0.4 mM), K_2CrO_4 (1–10 mM), $CdCl_2$ (3–5 mM), $CoCl_2$ (3–5 mM), $CuSO_4$ (3–5 mM), $AgNO_3$ (1–5 mM), $Al(SO_4)_3$ (5 mM), $FeCl_3$ (5–10 mM), $PbCl_2$ (3 mM), $UO_2(CH_3COO)_2$ (2–10 mM), $ZnSO_4$ (2–5 mM), $NiSO_4$ (2–5 mM), $MnSO_4$ (10–20 mM), $HgCl_2$ (0.02–0.1 mM), Na_2SeO_3 (10–50 mM), $FeCl_2$ (5–10 mM), $NaAsO_2$ (5–10 mM), Na_2HAsO_4 (10–50 mM), or $HAuCl_4$ (0.02–1 mM). Selection was for bacterial growth at the highest concentrations and when applicable, also by observing metal(loid) reduction. Strains MF01, MF03, MF04, and MF08 were from Maule lagoon, MF06 from Blanca lagoon (Atacama, Chile), MF07 from Death Valley and MF09 from El Teniente copper mine. Isolate MF10 was from Uyuni Salar, Bolivia.

Growth, Identification, and Characterization of the Environmental Strains

Cells were grown in LB medium at 37°C; *E. coli* BL21 carrying the pET 101/*gorA* vector was grown in ampicillin (0.1 mg/ml)-supplemented LB medium. This *gorA*-expressing plasmid was constructed as follows: the *gorA* gene was amplified from the environmental strain MF01 using primers CACCATGACTAAGCATTATGACTACATCGCA (Gforward) and ACGCATGGTGACAAATTCTTCG (Greverse). PCR products were inserted into the vector Champion TM pET101 Directional TOPO Expression (Invitrogen®). Correct gene insertion was checked by PCR using primers pETForward (ATGCGTCCGGCGTAGAGG) and pETReverse (GCTAGTTATTGCTCAGCGGTGG). Their identity was confirmed by DNA sequencing. The expression of the cloned gene was induced with 1 mM IPTG for 16 h. GorA was purified by Ni-affinity chromatography (HisTrap HP, GE Healthcare).

Physiological characterization of the isolates was carried out using standard biochemical assays (API ZYM and API 20E; BioMérieux Inc.), which were conducted according to the manufacturer's instructions. Morphological analyses were initially done by Gram staining and in the case of selected strains, also by scanning electron microscopy (SEM) as described by Arenas et al. (2014a). Briefly, samples were visualized and analyzed by low voltage electron microscopy using a LVEM5 Benchtop equipment (Center for Bioinformatics and Molecular Simulation).

Bacterial identification was accomplished by sequencing the 16S rRNA gene using the universal primer 8F (forward) and 1492R (reverse). GeneBank accession numbers for the 16S rRNA nucleotide sequences are: MG461635 (MF01), MG459178 (MF02), MG461634 (MF03), MG461632 (MF04), MG461629 (MF05), MG461631 (MF06), MG461630 (MF07), MG461633 (MF08), MG461636 (MF09), and MG459165 (MF10).

Phylogenetic trees were constructed using the MEGA 6.06 program applying the *neighbor-joining* method (Saitou and Nei, 1987), while distances were calculated with bootstrapping (100) applying the *Tamura-Nei* method (Tamura et al., 2004). Bacterial identity was also assessed by analyzing the fatty acid composition at the DSMZ Institute (Braunschweig, Germany).

Determination of minimal inhibitory concentrations (MIC) was carried out using serial dilutions (1: 2) of sterile solutions of K_2TeO_3, $AgNO_3$, $HAuCl_4$, K_2CrO_4, $CdCl_2$, $NaAsO_2$, $CuSO_4$ and Na_2SeO_3 in 1 ml of LB medium in 48-well plates. Subsequently, 10 µl of cultures grown in LB medium up to OD_{600} ~0.6 were added to each well and incubation proceeded with constant shaking at the optimal growth temperature of the particular isolate. MICs were determined after 24 h of incubation. For growth curve construction, overnight cultures were diluted 1:100 with fresh LB medium and incubated with shaking up to OD_{600} ~ 0.6. Then, 10 µL were added to 1 mL of fresh LB medium containing 4 µM K_2TeO_3, 15 µM $AgNO_3$ or $HAuCl_4$. Bacterial growth was monitored at 600 nm every 30 min for 14 h in a TECAN Infinite M200 Pro multimode plate reader.

Determination of Enzymatic Activity

Metal(loid)-reducing activity was determined in a final volume of 200 µl which contained 50 mM Tris-HCl buffer pH 8.0 (or 9.0), 50 mM potassium phosphate pH 7.0, 1 mM NADH (or NADPH), 1 mM β-mercaptoethanol and the crude extract; metal(loid)s tested for reduction were TeO_3^{2-} (1 mM), SeO_3^{2-} (1 mM), $AgNO_3$ (0.2 mM) and $HAuCl_4$ (1 mM). Reactions were monitored in a TECAN Infinite M200 Pro multimode plate reader at the wavelength that the metal(loid) absorbs in its elemental state: 500 nm (Te; Pugin et al., 2014), 400 nm (Se; Song et al., 2017), 424 nm (Ag; Kumar et al., 2007), and 540 nm (Au; Correa-Llantén et al., 2013). The optimal buffer and best nicotinamide cofactor were determined for each crude extract; an enzyme unit (U) was defined as the amount of enzyme required to increase the absorbance by 0.001 units/min at the respective

wavelength. Metal(loid)-reducing activity was also assessed by native polyacrylamide gel electrophoresis (native PAGE). Briefly, proteins in crude extracts were fractionated in 10% gels; after the run, activity was revealed by submerging the gel in the appropriate buffer containing the metal(loid) and a mixture of 1 mM NADH/NADPH as electron donor.

In vivo and *in vitro* Synthesis of Nanostructures

The isolates selected for synthesizing NS *in vivo* were grown to exponential phase (OD_{600}∼0.5) and treated with ¼ of the metal(loid) MIC (TeO_3^{2-}, SeO_3^{2-}, Ag^+ or $AuCl_4^-$), incubated for 4 h and then centrifuged for 10 min at 9,000 *g*. The bacterial pellet was sent for thin sectioning and transmission electron microscopy (TEM) analysis (Advanced Microscopy Unit (AMU), at Pontificia Universidad Católica de Chile).

Formation of NS *in vitro* was carried out using 150 μg/ml of purified recombinant glutathione reductase (GorA) from *E. cloacae* (isolate MF01). Additionally, crude extracts that contained GorA overexpressed for 2 h were used with reduction buffer (50 mM potassium phosphate pH 7.0, 1 mM NADPH, 1 mM β-mercaptoethanol and 0.15 mM TeO_3^{2-} or 1 mM SeO_3^{2-}). In addition, crude extracts (200 μg/ml of protein per reaction) from strains of interest were used for the production of NS by incubation with 1 mM Ag^+, $AuCl_4$, TeO_3^{2-} or 10 mM SeO_3^{2-} for 16 h in reduction buffer under optimal pH conditions and the preferred nicotinamide cofactor.

NS Characterization

A drop containing *in vitro* generated NS was placed on a copper grid and NS morphology was analyzed by TEM using a Hitachi Transmission Electron Microscope HT7700. Their chemical composition was determined through X-ray energy dispersion spectroscopy (EDS) using a SEM Zeiss EVO MA 10, EDS Penta FET Precision X-act Oxford Instruments. Both studies were conducted at the Center for the Development of Nanoscience and Nanotechnology–CEDENNA, USACH. In turn, the hydrodynamic diameter of the metallic nanostructures was assessed by dynamic light scattering (DLS) using a Marlvern Zetasizer Nano ZS equipment at room temperature (25°C) as described by Arenas-Salinas et al. (2016). Final values were calculated based on three independent measurements of twenty repetitions. Furthermore, metal(loid)s were quantified using total reflection X-ray fluorescence spectrophotometry (TXRF). Briefly, *in vitro*-synthesized NS were centrifuged at 13,000 × *g* for 90 min and the sediment was suspended in 200 μl of 65% HNO_3. Samples were heated at 60°C ∼2 h and analyzed in a TXRF Bruker S2 PICOFOX Spectrometer at Bioinformatics and Gene Expression laboratory of the Institute of Nutrition and Food Technology (INTA, University of Chile).

NS Antibacterial Activity

A suspension of *in vitro* synthesized NS was used to challenge *Escherichia coli* and *Listeria monocytogenes*. The NS were dialyzed against 50 mM Tris-HCl buffer (pH 8.0 or 9.0) or 50 mM potassium phosphate (pH 7.0), accordingly to the buffer used to generate them. Dialysis was for 4 h at room temperature with constant shaking. The dialyzed material was maintained at 4°C until further analysis. Concentrations of these metallic NS were calculated by determining the dry weight which was expressed in μg/ml. MIC determinations of the dialyzed NS and growth curves of *E. coli* BW25113 and *L. monocytogenes* were carried out as described in section Growth, Identification, and Characterization of the Environmental Strains.

Data Analysis

Plots and statistical analyses were carried out using the GraphPad Prism 6.0 (GraphPad Software, Inc.). Analysis of variance (ANOVA) and *t*-test were used considering $p < 0.05$. The statistical significance was indicated as follows: *, for values where $p < 0.05$, **, for values where $p < 0.01$, ***, for values where $p < 0.001$ and ****, for values where $p < 0.000$; ns, no significant difference.

RESULTS

Isolation, Identification, and Characterization of Metal(loid) Resistant Bacteria

A total of 47 bacterial strains isolated from environmental samples were assessed for metal(loid) resistance. Cells were routinely grown in LB or LB-agar plates at 37°C and exposed to different concentrations of 19 different, defined metal(loid)s. None of them grew in Cd^{2+}-, Al^{3+}-, or Mn^{2+}-containing LB medium nor in R2A, Acidiphilium, or ATB culture media. **Table S1** shows the ability to grow in the presence of the indicated metal(loid)s; when reduced, some of them (e.g., Te, Se, Au, and Ag) showed a characteristic color that was monitored spectrophotometrically. In turn, while strain MF47 was the most sensitive to all metal(loid)s tested, strains MF45 and MF46 tolerated only Pb^{2+} and Te^{4+}, respectively.

Ten strains (MF01-MF10), including cocci, bacilli and short-bacilli, from which 21 and 26 were Gram negative and Gram positive, respectively (**Table S2**), were selected for further studies because of their ability to grow in the presence of 15, 12, 11, 11, 11, 9, 13, 9, 13, and 9 different metal(loid)s and/or to reduce them (**Table S1**). They belong to the *Enterobacter* (MF01 and MF04), *Staphylococcus* (MF02, MF07, and MF10), *Acinetobacter* (MF05 and MF09), and *Exiguobacterium* (MF03, MF06, and MF08) genera, as determined by 16S rRNA gene sequencing (**Figure S1**, **Table S2**). Their fine morphology was analyzed by scanning electron microscopy (**Figure 1**): MF02, MF07, and MF10 were coccoid, MF01, MF03, MF04, MF06, and MF08 showed bacillar forms and MF09 and MF05 were cocobacilli. Their physiological characteristics, as determined by biochemical tests, are listed in **Table 1**. Excepting MF03, all strains used citrate as carbon source, but none produced indole or hydrogen sulfide. All strains were oxidase negative and catalase positive and while MF05, MF06, MF07, MF08, MF09, and MF10 did not oxidize sugars at all, MF01 oxidized almost all sugars assayed but inositol.

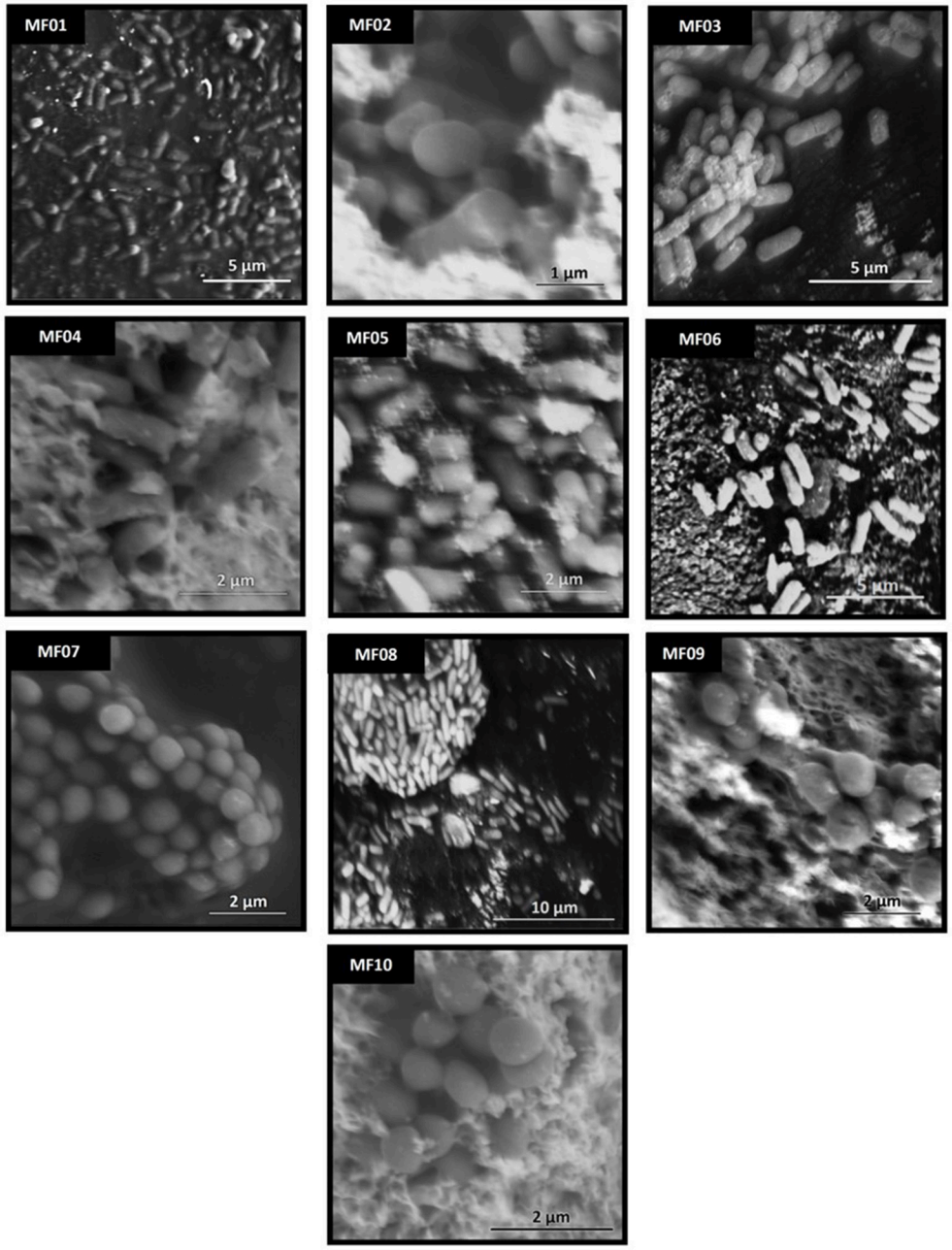

FIGURE 1 | Scanning electron microscopy of the environmental multi-metal(loid) resistant bacterial strains. Cells were prepared for SEM as described in Methods. Each image represents a different strain (indicated in the black box).

Metal(loid) Resistance and Reduction by the Environmental Strains

Minimal inhibitory concentrations of K_2TeO_3, $AgNO_3$, $HAuCl_4$, K_2CrO_4, $CdCl_2$, $NaAsO_2$, $CuSO_4$, and Na_2SeO_3 were determined under aerobic growth conditions for the strains listed in **Table S2**. MF02 and MF04 were the most resistant and sensitive to tellurite, respectively. All strains exhibited similar resistance levels to $HAuCl_4$, $CdCl_2$, $AgNO_3$, and $CuSO_4$, while MF01 and MF03 were the most sensitive to $NaAsO_2$. Differences up to 500-fold in the MIC of K_2CrO_4 were observed, MF02 and MF08 tolerating the highest concentration (400 mM). Finally, while MF01 and MF02 grew in the presence of Na_2SeO_3 up to 500 mM, MF10 was the most sensitive isolate (3.125 mM). Then, the effect of sublethal concentrations of TeO_3^{2-}, $AuCl_4^-$ and Ag^+ on bacterial growth was assessed (**Figure 2**). Although an extended lag phase was observed, cells regained growth between ∼4 and ∼7 h after

TABLE 1 | Physiological characterization of metal(loid)-resistant strains.

Strain	1	2	3	4	5	6	7	8	9	10
UTILIZATION OF										
Citrate	+	+	−	+	+	+	+	+	+	+
PRODUCTION OF										
H_2S	−	−	−	−	−	−	−	−	−	−
Indole	−	−	−	−	−	−	−	−	−	−
Acetoin	−	−	+	−	+	+	+	+	+	+
NO_2	+	+	−	+	−	+	−	+	−	−
N_2	−	−	+	−	+	−	+	−	+	+
TEST										
Oxidase	−	−	−	−	−	−	−	−	−	−
Catalase	+	+	+	+	+	+	+	+	+	+
PRESENCE OF										
Arginine dihydrolase	+	−	−	+	−	+	+	+	+	+
Lysine decarboxylase	−	−	−	−	−	−	−	−	−	−
Ornithine decarboxylase	+	−	−	+	−	−	−	−	−	−
Urease	−	−	−	−	−	−	+	−	−	+
Tryptophane deaminase	−	−	−	−	−	−	−	−	−	−
Gelatinase	−	−	+	−	+	+	+	+	+	+
Alkaline phosphatase	+	+	+	+	−	+	−	+	−	−
Esterase (C4)	−	+	+	+	+	+	+	+	+	+
Esterase lipase (C8)	−	−	+	+	+	+	+	+	+	+
Lipase (C14)	−	−	−	−	−	−	−	−	−	−
Leucine arylamidase	+	−	−	+	+	+	−	−	+	−
Valine arylamidase	−	−	−	−	−	+	+	−	−	+
Cysteine arylamidase	−	−	−	+	+	−	−	−	+	−
Trypsin	−	−	−	−	−	−	+	−	−	−
α-chymotrypsin	−	−	−	−	−	+	−	−	−	−
Acid phosphatase	+	+	+	+	+	−	+	+	+	+
Naphthol-AS-BI-phosphohydrolase	+	+	+	+	+	+	+	+	+	+
α-galactosidase	−	−	−	−	−	−	−	−	−	−
β-galactosidase	+	−	−	+	−	−	−	−	−	−
β-glucuronidase	−	−	−	−	−	−	−	−	−	−
α-glucosidase	+	+	+	−	−	+	−	+	−	−
β-glucosidase	−	+	+	−	−	−	−	+	−	−
N-acetyl-β-glucosaminidase	−	−	−	−	−	−	−	−	−	−
α-mannosidase	−	−	−	−	−	−	−	−	−	−
α-fucosidase	−	−	−	−	−	−	−	−	−	−
OXIDATION OF										
D-glucose	+	+	−	+	−	−	−	−	−	−
D-mannitol	+	+	+	+	−	−	−	−	−	−
Inositol	−	−	−	−	−	−	−	−	−	−
D-sorbitol	+	−	−	+	−	−	−	−	−	−
L-rhamnose	+	−	−	−	−	−	−	−	−	−
D-saccharose	+	+	−	−	−	−	−	−	−	−
D-melibiose	+	−	−	−	−	−	−	−	−	−
Amygdaline	+	+	−	−	−	−	−	−	−	−
L-arabinose	+	−	−	−	−	−	−	−	−	−

+, positive; −, negative. Strains: (1) MF01, (2) MF02, (3) MF03, (4) MF04, (5) MF05, (6) MF06, (7) MF07, (8) MF08, (9) MF09, and (10) MF10.

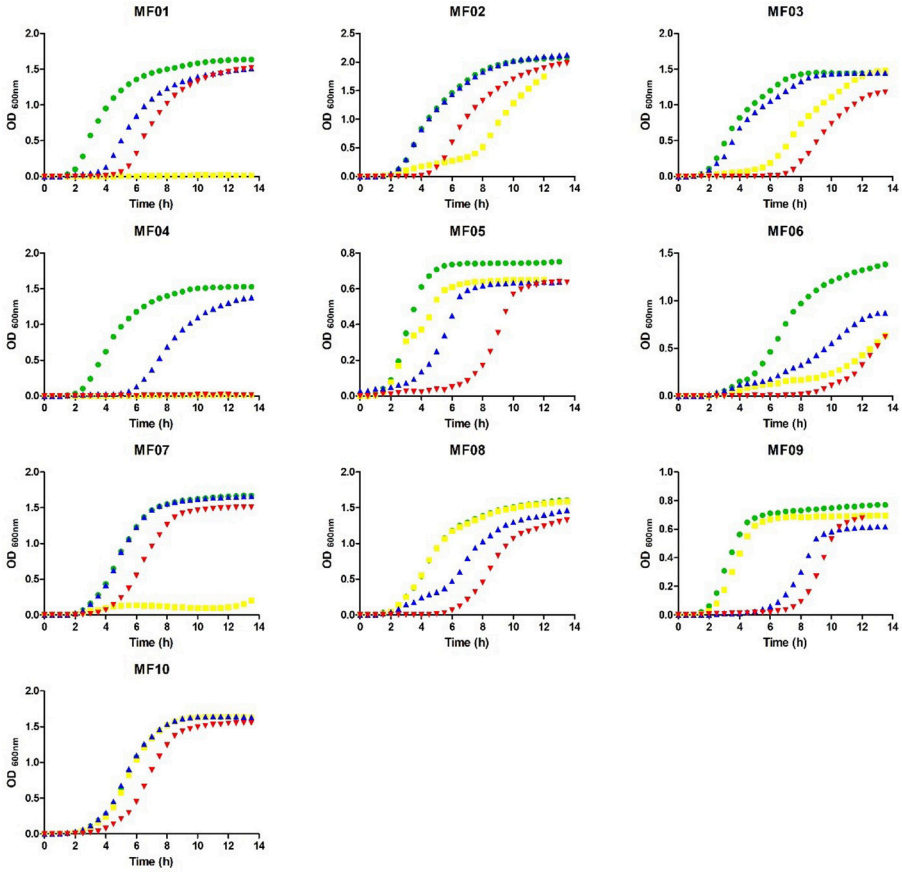

FIGURE 2 | Growth curves of the environmental multi-metal(loid) resistant bacteria exposed to TeO_3^{2-}, $AuCl_4^-$, and Ag^+. Cells were grown in LB medium in the absence (green) or presence of 4 μM TeO_3^{2-} (yellow), 15 μM $AuCl_4^-$ (blue), or 15 μM Ag^+ (red).

exposure to the metalloid. Growth of MF01, MF04, and MF07 was completely abolished in the presence of tellurite.

On the other hand, crude cell extracts were assayed to assess tellurium (IV)-, selenium (IV)-, gold (III)-, and silver (I)-reducing activity in the presence of NADH or NADPH and in the pH range 7–9 (**Figure 3** and **Figure S2**). The reduction of three metal(loid)s generated a change of the solution's color: black, purple and yellow-orange in the case of tellurite (**Figure S2A**), $AuCl_4^-$ (**Figure S2B**) and Ag^+ (**Figure S2C**), respectively. While MF09 was the best tellurium (IV) reducer (pH 8-9 with NADH as cofactor, **Figure 3A**), selenium (IV) was better reduced by MF02 at pH 7.0 using NADPH as cofactor (**Figure 3B**). In turn, MF03 exhibited the best Ag (I)-reducing activity at pH 7.0 in the presence of NADH (**Figure 3C**). Finally, a robust gold-reducing activity was observed in MF09 at pH 8.0 with NADH as the enzyme cofactor (**Figure 3D**).

To look for proteins which could be responsible of metal(loid) reduction, tellurite- and gold- reducing activities were assessed *in situ* by polyacrylamide gel electrophoresis under non-denaturing conditions (**Figures S3A,B**). Reduction bands generated by MF01 extracts were excised from the gel and fractionated by SDS-PAGE (**Figure S3C**). Twelve bands were identified by MALDI-TOF (**Figure S3D**) which included the enzyme glutathione reductase (GorA), belonging to the flavoprotein family. The ability of GorA from the Antarctic strain *Pseudomonas sp.* BNF22 to reduce TeO_3^{2-} had been observed previously in our laboratory (Pugin et al., 2014). However, its ability to reduce other metal(loid)s and/or its efficiency has not yet been determined, which prompted us to focus on this phenomenon. The *gorA* gene was amplified from the *E. cloacae* genome and cloned into the pET/101 expression vector to generate the pET/*gorA* recombinant plasmid (**Figures S3E,F**). A kinetic induction assay showed a ∼50 kDa protein band that accumulated over time (**Figure S3G**). The enzyme was purified and assayed for tellurium (IV), selenium (IV), gold (III), silver (I), and copper (II) reduction, measured in the presence of NADH or NADPH and in the pH range 6–9. GorA reduced optimally TeO_3^{2-}, SeO_3^{2-} and Ag^+ at pH 8.0, 6–7 and 7, respectively (**Figure S3H**).

Synthesis and Characterization of Nanostructures

Ultrathin sections of selected strains that were exposed to sublethal concentrations (¼ of the MIC) of defined metal(loid)s were analyzed by transmission electron microscopy (**Figure 4**). Intracellular, evenly distributed long electron-dense

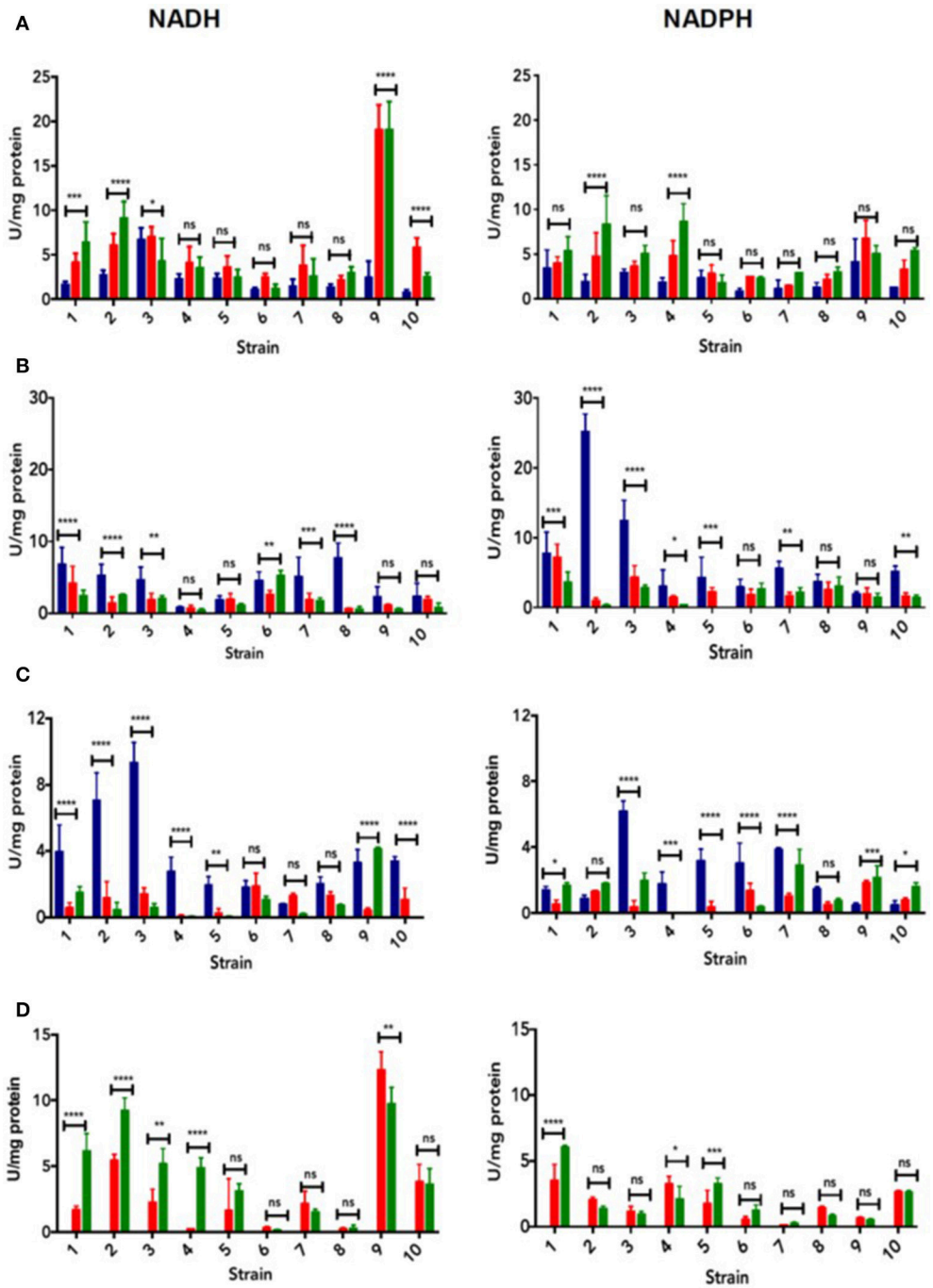

FIGURE 3 | Metal(loid)-reducing activity**.** Reduction of tellurium (IV) **(A)**, selenium (IV) **(B)**, silver (I) **(C)**, and gold (III) **(D)**, in the presence of NADH (left) or NADPH (right). Colored bars indicate different pH values tested: 7.0 (blue), 8.0 (red), and 9.0 (green). Horizontal bars indicate the statistical analysis within the group. Data represent the average of 3 independent assays ± SD. Statistical significance was according to section Data analysis.

rods, representing most probably tellurium nanostructures (TeNS) were observed in tellurite-exposed MF09 (**Figure 4A**). In turn, SeNS generated by MF02 appeared as spherical particles located near the cell membrane (**Figure 4B**). In both cases, alterations in size, morphology and cell division were observed (not shown). No silver-containing particles were generated by MF03 under the same conditions (**Figure 4C**). Finally, small, circular and evenly distributed gold particles were seen when MF09 was treated with sub lethal gold concentrations (**Figure 4D**).

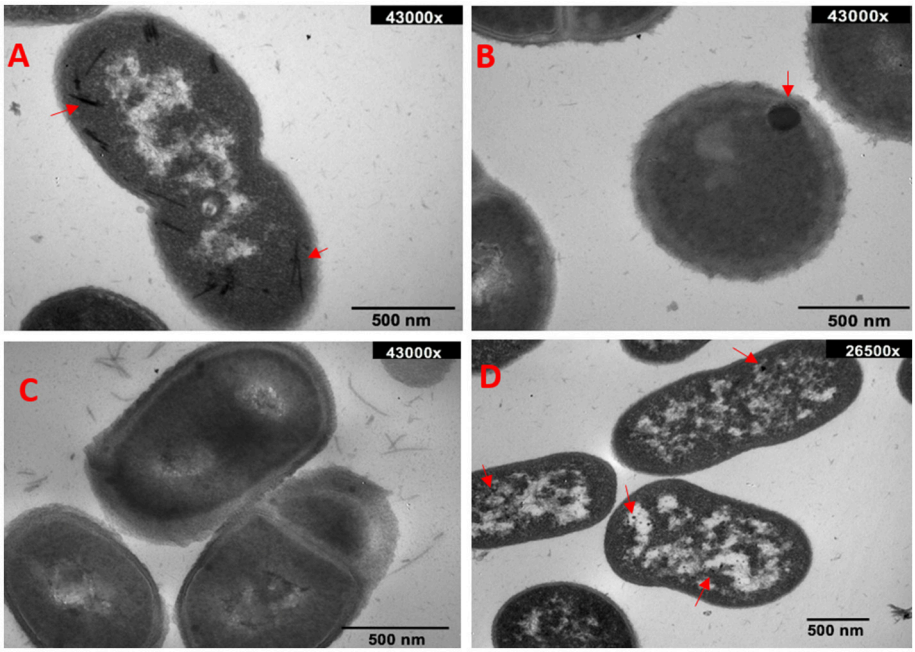

FIGURE 4 | Electron micrographs of *in vivo* synthesized NS. TeNS, SeNS, AgNS, and AuNS synthesized *in vivo* by MF09 **(A)**, MF02 **(B)**, MF03 **(C)**, and MF09 **(D)**, respectively.

On the other hand, *in vitro* generation of NS by bacterial crude extracts lasted ∼16 h, irrespective of the strain or metal(loid) tested. NS morphology, size and chemical composition were determined by transmission electron microscopy (TEM), dynamic light scattering (DLS) and total reflection X-ray fluorescence spectrophotometry (TRXF), respectively. TeNS synthetized using MF09 extracts showed heterogeneous morphology with an average diameter ∼10 nm (**Figure 5A**, left panel) and a hydrodynamic diameter ∼9.36 nm (polydispersity index PDI 0.446), in agreement with TEM results (**Figure 5A**, middle panel). The chemical composition was 23.2% tellurium, 55.8% carbon and low amounts of chlorine, potassium, and phosphorus (**Figure 5A**, right panel). Moreover, TXRF analysis indicated that the tellurium concentration in TeNS was 78.66 ± 7.51 μg/ml. In the case of the SeNS generated with crude extracts from MF02, nanoparticles showed a spherical morphology with regular edges—nanospheres—and a size of ∼100 nm (**Figure 5B**, middle panel); they showed a gaussian distribution (DLS) with a maximum at 105.1 nm (PDI 0.124) (**Figure 5B**, middle panel). Selenium content in SeNS was 83.9%, while TRXF showed that Se concentration was 158.98 ± 16,4 μg/ml (**Figure 5B**, right panel). On the other hand, AgNS generated using crude extracts from MF03 showed a size of ∼10 nm, spherical-like shape with irregular edges and an electron-dense core (**Figure 5C**, left panel). These AgNS also showed a gaussian distribution with a maximum centered at 68.46 nm (PDI 0.43) (**Figure 5B**, middle panel), a size larger than that assessed by TEM; AgNS contained mostly carbon and to a lesser extent silver (9.84 ± 1.05 μg/ml, representing 20.7%) (**Figure 5C**, right panel). The same MF09 crude extract used to prepare TeNS was utilized to generate AuNS, whose morphology was not easy to determine because of the presence of organic material surrounding the particles (**Figure 5D**, left panel). Nevertheless, these NS were rather spherical with a size ∼50 nm. AuNS showed a size distribution with a maximum at 82.35 nm (**Figure 5D,** middle panel). These nanoparticles contained 21.2% gold and other elements in lower amounts such as calcium, magnesium, chlorine, sulfur, and phosphorus (**Figure 5A**, right panel). TXRF analysis indicated that AuNS exhibited a gold concentration of 77.23 ± 12.61 μg/ml.

Finally, crude extracts from GorA-overproducing *E. coli* as well as purified GorA were used to synthesize *in vitro* SeNS and TeNS (**Figure 6**): (i) both, crude extracts and purified protein were able to generate spherical SeNS with a size of ∼50 nm and irregular edges (TEM). DLS analysis indicated that GorA-synthesized NS are prone to aggregation with a size distribution of 74.75 nm (PDI 0.159) (**Figure 6A**); conversely NS obtained using crude extracts did not aggregate and showed a size of 39.09 nm (PDI 0.456) (**Figure 6C**). SeNS from crude extracts showed a higher amount of selenium (131.65 ± 16.46 μg/ml, representing 29.9%) than GorA-SeNS (164.93 ± 24.7 μg/ml, representing 26.6%) (**Figures 6A,C**); (ii) in turn, GorA-TeNS showed a rather stick-like morphology (**Figure 6B**), while nanoparticles synthetized using crude extracts exhibited irregular, non-homogenous morphology, with some of them showing triangular shapes (**Figure 6D**). Size distribution (DLS) of GorA- and crude extract-TeNS was 35.11 nm (PDI 0.32) and 31 nm (PDI 0.63), respectively (**Figures 6B,D**). TeNS from crude extracts showed a higher amount of tellurium (127.36 ± 15.26 μg/ml, representing 10%) than GorA-TeNS

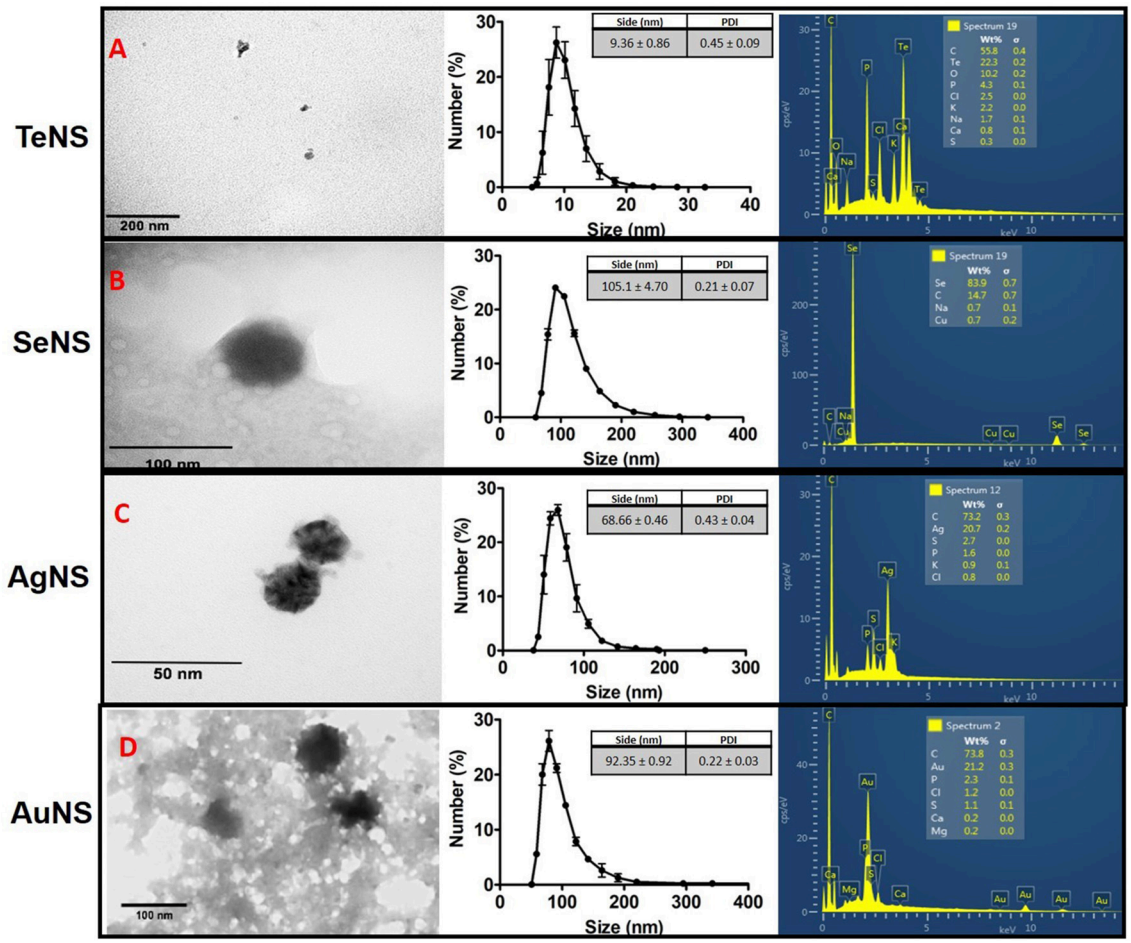

FIGURE 5 | Characterization of *in vitro* synthesized NSs. Electron micrographs (left), dynamic light scattering (middle), and EDS (right) of NS synthetized by: MF09–TeNS– **(A)**; MF02–SeNS– **(B)**; MF03–AgNS– **(C)**; MF09–AuNS– **(D)**. Data represent the average of 3 independent trials ± SD.

(157.6 ± 25.3 μg/ml, representing 8.2%) (**Figure 6B,D**). Both crude extracts and purified protein showed the presence of other elements (more abundant in the GorA solution) such as potassium, sodium, sulfur, and phosphorus, among others.

NS Antibacterial Activity

The minimal inhibitory concentration of *in vitro* synthesized NS was determined and along with the construction of growth curves, were used to assess their putative antibacterial effects. Aerobically synthesized TeNS using MF09 crude extracts showed MICs of 45- and 66- μg/ml for *E. coli* and *L. monocytogenes*, respectively. Similar MIC values (40 and 82 μg/ml, respectively) were observed for TeNS generated using GorA-overproducing *E. coli* crude extracts. In turn, AuNS MICs for *E. coli* and *L. monocytogenes* were 64- and 68- μg/ml, respectively. At the tested concentrations, both SeNS and AgNS did not inhibit *E. coli* or *L. monocytogenes* growth. However, Te- and Au-containing NS inhibited completely the growth of *E. coli* and *L. monocytogenes* (**Figure S4**).

DISCUSSION

Environmental bacteria survive in the presence of toxic agents such as metal(loid)s because they have evolved specific mechanism to cope with them (Summers and Silver, 1978; Bollag et al., 1994). Specifically, bacterial metal(loid)-reduction has gained attention among researchers since naturally reducing- or genetically modified- bacteria are widely used in the field of bioremediation (Stephen and Macnaughtont, 1999; Das et al., 2016) and biotechnology to generate nano-scaled structures exhibiting biomedical, electronic and pharmacological applications, among others (Suresh, 2012).

In this line, environmental bacteria from different Chilean regions were isolated, identified and characterized. Such regions exhibit a combination of many extreme factors like high salinity, desiccation, high and low temperatures, volcanic intervention, etc., most of them responsible for generating oxidative stress in organisms. Since metal(loid)s are also able to induce oxidative stress (Nies, 1999; Imlay, 2003), it was inferred that those places from where the samples were taken could host metal(loid)-resistant bacteria. The 10 most resistant to- and

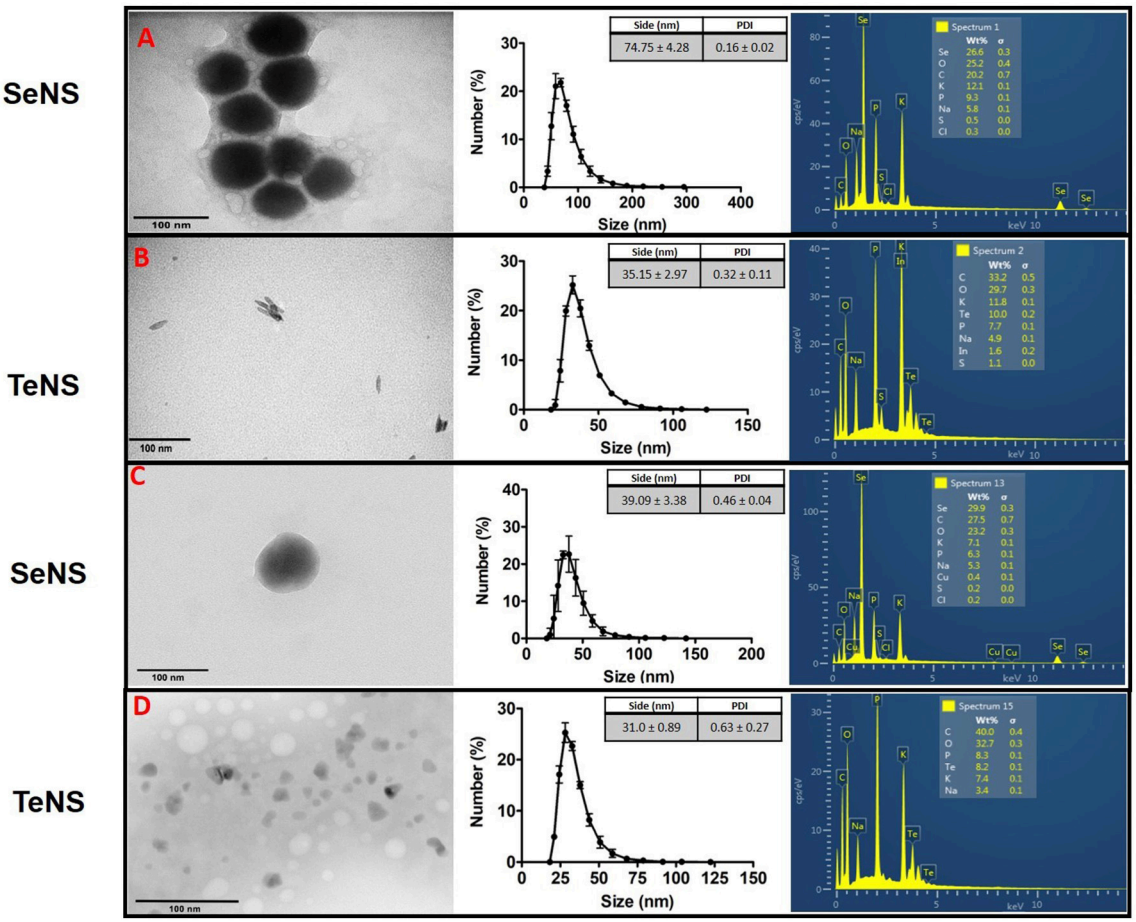

FIGURE 6 | Characterization of GorA-synthesized NS. Electron micrographs (left), dynamic light scattering (middle), and EDS (right). Whereas the SeNS **(A)** and TeNS **(B)** were generated using purified GorA, SeNS **(C)** and TeNS **(D)** were generated using crude extracts of *E. coli* overexpressing the *gorA* gene. Numbers are the average of 3 independent trials ± SD.

able of metal(loid)s reduction bacteria were chosen for further analyses because of their potential biotechnological applicability.

Their resistance level to 8 metal(loid)s was evaluated under aerobic conditions (**Table S2**). In this situation, most of these toxicants exert -at least in part- toxicity because of ROS production (mainly superoxide), causing the inactivation of certain enzymes and metabolic pathways, modification of nucleic acids and lipid peroxidation of the cell membrane (Ahearn et al., 1995; Calderón et al., 2009; Contreras and Vásquez, 2010; Lemire et al., 2013). High levels of tellurite resistance (4 mM) were observed for some isolates, while tellurite MIC did not exceed 0.004 mM for sensitive bacteria such as *E. coli* (Taylor, 1999). In the case of chromate and selenite, resistance levels observed for some isolates were up to ∼500- (MF02 and MF08) and ∼160-fold (MF01 and MF02) higher than that of other isolates, respectively. Interestingly, phylogenetically related strains (MF01 and MF04, MF09 and MF05, MF07 and MF10) exhibited different levels of resistance, probably because of the different environmental conditions where they thrive. Growth curves also showed that the isolates are differentially affected by these toxicants (**Figure 3**).

When reduced to their elemental state, tellurite, selenite, auric tetrachloride and silver generate colored, insoluble NS (**Figure S2**), which could serve as markers for putative biotechnological applications including medicine, electronics, pharmacy and engineering, among others (Ba et al., 2010; Suresh, 2012; Oves et al., 2013). Most strains exhibited metal(loid)-reducing ability (**Figure 3**, **Figure S2**), whose optimal reduction condition -pH range and enzyme cofactor among others- was determined. MF09 showed maximal tellurite reduction at pH 8 and 9 using NADH as electron donor (**Figure 3A**). This could be explained because, in general, redox centers of proteins exhibiting tellurite reductase activity contain reactive vicinal cysteines that are very sensitive to pH (Arenas et al., 2014b). Deprotonation of thiol groups of these cysteines generates the thiolate anion ($-S^-$, pKa ∼8.0) which is highly reactive (Vlamis-Gardikas, 2008). This high pKa implies that most cysteine thiols are protonated at pH 7.0 and hence, inactive.

Similar results were observed during $AuCl_4^-$ reduction by MF09 at pH 8.0 in the presence of NADH (**Figure 3D**). In turn, optimal selenite and silver reduction by MF03 and MF02,

respectively, occurred at pH 7.0. Particularly, while Se^0 is slowly oxidized to SeO_4^{2-} in alkaline conditions (Kamal, 1994), SeO_3^{2-} is reduced at more acidic pH values, thus favoring the formation elemental Se. On the other hand, pH influences metal(loid) speciation thus causing the formation of complexes and the deprotonation/protonation of functional groups that may participate in the catalytic process (Panda and Deepa, 2011). Also, pH can result in precipitation of defined ions (Atkins and Jones, 2006). For instance, Ag^+ precipitates as silver hydroxide in alkaline conditions and is spontaneously transformed into the more stable, insoluble, silver oxide (Ag_2O) (Burriel et al., 2006).

Next, the *in vivo* generation of tellurium-, selenium-, silver-, and gold-containing NS was evaluated using three of the environmental strains under study (**Figure 4**). TeNS generated by MF09 exhibited an elongated morphology, a situation that has been previously reported in *Rhodobacter capsulatus* (Turner et al., 2011). On the other hand, MF02-generated SeNS showed spherical morphology and a size >100 nm (**Figure 4B**). Actually, SeNS produced by most microorganisms exhibit spherical morphology and in some cases, transformation from spheres to nanowires do occur (Mane et al., 2015). In turn, MF03 did not form AgNS (**Figure 4C**), probably because Ag^+ interacts with- and precipitate with a large number of intra- or extracellular anions (thus decreasing its availability to form NS) (Atkins and Jones, 2006); such is the case when PO_4^{3-} present in the culture medium form stable compounds such as Ag_3PO_4 (Xiu et al., 2011). MF09- generated AuNS were observed as small intracellular deposits evenly distributed in the cell (**Figure 4D**). It general, AuNS synthesis is directly dependent on the microorganism and pH of the medium. In this line, marine yeasts form large-sized AuNPs at acidic pH values, while it reduced at alkaline pHs; conversely, fungi belonging to the *Verticillium* genus form larger AuNPs at alkaline pH values (Dhillon et al., 2012).

It should be noted that the molecular basis of the *in vivo* metal(loid)-reducing activity is very hard to determine accurately since a large number of factors that are present in the cell context may affect and/or influence this activity; this makes almost impossible to correlate directly *in vitro* activity and the generation of metal(loid) deposits *in vivo* and variables such as culture medium, toxicant exposure time, temperature, oxygen availability, among others, should be explored further.

The ability of crude extracts to generate metal(loid)-containing NS was used to characterize NS synthesis *in vitro*, including their morphology, size, composition and metal(loid)concentration (**Figure 5**). All the formed structures exhibited sizes <100 nm and hence, fall in the definition of nanostructures, i.e., at least one dimension does not exceed 100 nm (Suresh, 2012). MF09 crude extracts formed TeNS that were smaller in size than AuNS (**Figures 5A,D**). An important factor that affects NS morphology and size is related to the formation of the NS itself, where NS nucleation and growth are limiting steps for these NS characteristics (Xiong and Lu, 2015). Both TeNS and AuNS contain a high proportion of the respective metal(loid), 22.3 and 21.2%, respectively, in addition to other elements such as carbon. In particular, TeNS exhibited small sizes and poorly defined morphologies. Unfortunately, the presence of organic material hampered the correct visualization of AuNS. This did not affect SeNS observation, which showed a rather spherical morphology with poorly defined edges, and contained as much as 83.9% Se (**Figure 5B**). This result is consistent with the high Se concentration determined by TXRF ($158.98 \pm 16.4\,\mu g/ml$). Different was the case of AgNS, which contained lower metal abundance (**Figure 5C**) and is probably due to the presence of phosphate in the reaction buffer (see above).

Lastly, NS were also generated using purified GorA from *E. cloacae* (>92% pure) as well as crude extracts of a recombinant *E. coli* overexpressing the *E. cloacae gorA* gene (**Figure 6**). Given that it is a relatively new procedure, not much information is available in the literature. This flavoprotein, which was identified and characterized in this work, exhibits the ability to efficiently reduce SeO_3^{2-} and TeO_3^{2-} (**Figure S3H**). TeNS synthesized using crude extracts showed a rather triangular shape, while those generated by the purified protein were slightly larger size, irregular and exhibited a more spherical morphology (**Figures 6B,D**). As mentioned, difference in size and morphology could be attributed to the influence of the cellular environment on the metal(loid)-reducing efficiency.

Intracellular tellurite reduction could occur also because the participation of reductants such as gluthatione (GSH) and other cytosolic thiols (painter-type reactions) whose reducing ability would promote Te^0 formation (Chasteen et al., 2009). Given that GorA is responsible for appropriate GSH levels, it is tempting to speculate that TeNS could be formed more efficiently when it is overproduced. This situation could explain why TeNS generated by crude extracts of GorA-overproducing *E. coli* are larger than those generated by the purified protein. No differences were observed regarding the Te content in TeNS. Actually, elemental analyses showed that Te was present in lower amount regarding other elements such as carbon, oxygen and phosphorus. Based on the stoichiometry of Te and O (oxygen percent is at least twice that of Te) in TeNS generated under aerobic conditions either by GorA or crude extracts, it could be inferred that in NS tellurium is present as tellurium dioxide (TeO_2). Nevertheless, additional experimental evidence is required to state it definitely. It has been observed lately that GorA-generated TeNS remain attached to the enzyme, probably through covalent bonding with the active site catalytic cysteine residues (Pugin et al., 2014). Unlike TeNS, SeNS generated using crude extracts of GorA-overproducing cells were smaller than those produced by purified GorA (**Figures 6A,C**). This could be explained by some kind of electron leak, thus making selenite reduction less efficient (Zare et al., 2013; Mane et al., 2015). However, Se concentration was about the same in SeNS synthesized in both conditions.

Given that antibiotic-resistant, pathogenic bacteria have increased almost exponentially worldwide, the development of tools from biotechnological origin for biomedical applications is mandatory (Yacoby and Benhar, 2008). In this work, the antibacterial activity of the *in vitro*-generated NS was tested against *E. coli* and *L. monocytogenes*. TeNS made by crude extracts of GorA-overproducing *E. coli* were the most toxic for *E. coli* and *L. monocytogenes*. Similar results were observed with MF09-generated AuNS and TeNS (**Figure S4**). The effect of NS on *E. coli* and *L. monocytogenes* growth was also assessed by

constructing growth curves. Results from **Figure S4** show that in general all NS inhibited completely the bacterial growth.

Toxic effects of NS are generally related to the specific particle. Thus, AuNS have been widely used in therapeutic as well as diagnostic procedures, and exhibit antibacterial activity against *Salmonella* sp., *Bacillus subtilis*, *E. coli* and *Pseudomonas aeruginosa* (Das et al., 2009). In particular, chemically-generated AuNS seem to exert their toxicity in two ways: (i) changing membrane potential and inhibiting ATP synthase activity, which results in a general turn down of metabolism and (ii) inhibiting the binding of tRNAs to the ribosome, thus generating a global collapse of biological processes. Other NS are toxic because the release of metal ions, as in the case of some AgNS; in fact, Ag^+ release causes damage to the cell membrane, inactivates proteins and inhibits DNA replication (Chaloupka et al., 2010; Xiu et al., 2012).

Our results show that in general all tested NS were more toxic for *E. coli* as compared to *L. monocytogenes*, which, as a Gram positive organism, possess a cell wall that probably retards or prevents the entry of NS. In this context, no information on the mechanism of NS uptake is available in the literature. Unlike TeNS and AuNS, *in vitro*-synthesized SeNS and AgNS did not inhibit bacterial growth (not shown). Results with SeNS could be explained because selenium is an essential element for microorganisms (Lemire et al., 2013), and probably higher Se amounts in NS would be needed to generate toxicity. It has been also shown that SeNS inhibits both growth and proliferation of cancer cells in culture (Selenius et al., 2010). On the other hand and although AgNS have been reported as the most toxic NS (Rai et al., 2009; Lin et al., 2012), they did not exhibit toxicity for the tested bacteria.

Finally, it seems very interesting that the same enzyme can reduce two metalloids possessing different chemical characteristics, as for instance, their reactivity with certain enzymes (Rigobello et al., 2011). We trust that the results of this work will help to define the molecular basis governing the biological synthesis of many potentially useful nanostructures.

CONCLUSION

Ten bacteria exhibiting resistance to various metals and metalloids were isolated and characterized from environmental samples. Whole cells as well as crude extracts derived from them were successfully used for the biological synthesis of TeNS, SeNS, AuNS, and AgNS, which exhibited different, specific characteristics. In particular, *E. cloacae* was used as model to look for toxicant-reducing enzymes. In this context, it was found that purified *E. cloacae* GorA reduced efficiently TeO_3^{2-} and SeO_3^{2-}. Finally, especially interesting were TeNS and AuNS, which exhibited antibacterial properties and inhibited *E. coli* and *L. monocytogenes* growth.

AUTHOR CONTRIBUTIONS

MF, VF, MA-S, CM-V, FC, EM, DA, CV, and FA: Conceived and designed the experiments; MF, VF, EV, ML, DA, FC, MA-S, and CM-V: Performed the experiments; MF, VF, DA, MA-S, EM, ML, EV CM-V, CV, and FA: Analyzed the data; MA-S, CV, ML, and FA: Contributed reagents, materials, analysis tools; CV and FA: Wrote the paper.

FUNDING

This work received financial support from FONDECYT (Fondo Nacional de Ciencia y Tecnología) Iniciación en la Investigación #11140334 (FA), #11150679 (ML), and Regular #1160051 (CV), Support from DICYT (Dirección de Investigación en Ciencia y Tecnología, Universidad de Santiago de Chile), Basal FB0807 (CEDENNA) (EV) and Universidad de Talca (Fondo De Proyectos De Investigación Para Investigadores Iniciales) (MA-S) is also acknowledged.

ACKNOWLEDGMENTS

We would like to thank Natalia Valdes from the Universidad de Santiago de Chile, Facultad de Química y Biología for her support in bioinformatics analysis. Also Yerko Argandoña from the Universidad de Talca, for support in electron microscopy. In addition, to Dr. Rivas-Pardo and Mrs. Paulina Ramirez of Columbia University for his critical review of the manuscript. This paper is dedicated in memory of my daughter María Ignacia Arenas Monterey, our little angel.

SUPPLEMENTARY MATERIAL

The Supplementary Material for this article can be found online at: https://www.frontiersin.org/articles/10.3389/fmicb.2018.00959/full#supplementary-material

Figure S1 | Phylogenetic trees based on the 16S rRNA gene sequence. Trees were constructed using the *neighbor-joining* method as described in Methods. **(A)** *Exiguobacterium*, **(B)** *Enterobacter*, **(C)** *Acinetobacter*, and **(D)** *Staphylococcus*. The numbers on the nodes represent the percentage of bootstrap (1,000 repetitions).

Figure S2 | *in vitro* metal(loid)- reduction by crude extracts of the indicated strains. The reduction of TeO_3^{2-} **(A)**, $AuCl_4^-$ **(B)**, and Ag^+ **(C)** was performed as described in Methods. The activity was measured at different pH values and monitored for 24 h. Strains analyzed: (1) MF01, (2) MF02, (3) MF03, (4) MF04, (5) MF05, (6) MF06, (7) MF07, (8) MF08, (9) MF09, (10) MF10.

Figure S3 | Identification, cloning, and purification of GorA. Tellurite **(A)** and gold **(B)** reductase activity *in situ*. Crude extracts from each strain [MF01 (1), MF02 (2), MF03 (3), MF04 (4), MF05 (5), MF06 (6), MF07 (7), MF08 (8), MF09 (9), MF10(10)] were fractionated by NATIVE-PAGE and revealed as TeO_3^{2-} or $AuCl_4^-$ activity as described in Methods. **(C)** SDS-PAGE of the reduction bands of TeO_3^{2-} and $AuCl_4^-$ from MF01 extracts; Lanes 1, 2, and 5: molecular weight standards (BioRad, #1610305). Lanes 3 and 4: fractionation of proteins present in the reduction band of TeO_3^{2-} and $AuCl_4^-$, respectively. **(D)** Identification of protein bands by MALDI-TOF. **(E)** Agarose gel electrophoresis of PCR-amplified *gorA*; Lane 1, molecular size standards (1 kb DNA ladder, Promega). Lane 2, amplification of *gorA*. **(F)** Agarose gel electrophoresis of *gorA* amplification by PCR. Lane 1, molecular size standards (1 kb DNA ladder, Invitrogen); lane 2, colony PCR amplification of *gorA*; lane 3, directional cloning of *gorA* assessed by PCR using the primers Gforward and pETReverse described in section Growth, identification and characterization of the environmental strains; **(G)** Induction kinetics and purification of GorA; SDS-PAGE of crude extracts of *E. coli* overexpressing *gorA* and the purified enzyme; ST, SDS-PAGE molecular weight standards (low range). Lanes 1-6, induction kinetics for GorA at 0, 1, 2, 3, 4, and 16 h, respectively. Lane 7, purified recombinant GorA. **(H)** GorA

metal(loid)-reductase activity (U/mg protein), showing the dependence on the pH and cofactor.

Figure S4 | Growth curves of *E. coli* and *L. monocytogenes* exposed to NS. Effect of TeNS synthesized by crude extracts of cells overexpressing the *E. cloacae gorA* gene in *E. coli* **(A)** and *L. monocytogenes* **(B)**. Effect of TeNS synthesized using crude extracts of MF09 in *E. coli* **(C)** and *L. monocytogenes* **(D)**. Effect of AuNS synthesized by crude extracts of MF09 in *E. coli* **(E)** and *L. monocytogenes* **(F)**. Black and blue lines represent the growth of control and NS-treated cells, respectively.

Table S1 | Metal(loid)-resistant strains.

Table S2 | MICs for the metal(loid)-resistant strains.

REFERENCES

Ahearn, D. G., May, M. M., and Gabriel, M. M. (1995). Adherence of organisms to silver-coated surfaces. *J. Ind. Microbiol.* 15, 372–376. doi: 10.1007/BF01569993

Amstad, E., Textor, M., and Reimhult, E. (2011). Stabilization and functionalization of iron oxide nanoparticles for biomedical applications. *Nanoscale* 3, 2819–2843. doi: 10.1039/c1nr10173k

Arenas, F. A., Leal, C. A., Pinto, C. A., Arenas-Salinas, M. A., Morales, W. A., Cornejo, F. A., et al. (2014b). On the mechanism underlying tellurite reduction by *Aeromonas caviae* ST dihydrolipoamide dehydrogenase. *Biochimie* 102, 174–182. doi: 10.1016/j.biochi.2014.03.008

Arenas, F. A., Pugin, B., Henríquez, N. A., Arenas-Salinas, M. A., Díaz-Vásquez, W. A., Pozo, M. F., et al. (2014a). Isolation, identification and characterization of tellurite hyper-resistant, tellurite-reducing bacteria from Antarctica. *Polar Sci.* 8, 40–52. doi: 10.1016/j.polar.2014.01.001

Arenas-Salinas, M., Vargas, J. I., Morales, W., Pinto, C., Muñoz, P., Cornejo, F. A., et al. (2016). Flavoprotein-mediated tellurite reduction: structural basis and applications to the synthesis of tellurium-containing nanostructures. *Front. Microbiol.* 7:1160. doi: 10.3389/fmicb.2016.01160

Atkins, P., and Jones, L. (2006). Principles of Chemistry. *The* Ways *of* Discovery. Madrid: Panamericana.

Azam, A., Ahmed, A. S., Oves, M., Khan, M. S., Habib, S. S., and Memic, A. (2012). Antimicrobial activity of metal oxide nanoparticles against Gram-positive and Gram-negative bacteria: a comparative study. *Int. J. Nanomed.* 7, 6003–6009. doi: 10.2147/IJN.S35347

Ba, L. A., Döring, M., Jamier, J., and Jacob, C. (2010). Tellurite: an element with great biological potency and potential. *Org. Biomol. Chem.* 8, 4203–4216. doi: 10.1039/c0ob00086h

Bollag, J. M., Mertz, T., and Otjen, L. (1994). "Role of microorganisms in soil bioremediation," in *Bioremediation Through Rhizosphere Technology, ACS Symposium Series*, eds T. Anderson and J. Coats (Washington, DC: American Chemical Society), 2–10.

Borsetti, F., Tremaroli, V., Michelacci, F., Borghese, R., Winterstein, C., Dalda, F., et al. (2005). Tellurite effects on *Rhodobacter capsulatus* cell viability and superoxide dismutase activity under oxidative stress conditions. *Res. Microbiol.* 156, 7–13. doi: 10.1016/j.resmic.2005.03.011

Burriel, F., Lucena, F., Arribas, S., and Hernández, F. (2006). "Analytical chemistry of the cations: Silver," in *Qualitative Analytical Chemistry,* ed Carmen de la Fuente (Madrid: Thomson), 419–426.

Calderón, I. L., Elías, A. O., Fuentes, E. L., Pradenas, G. A., Castro, M. E., Arenas, F. A., et al. (2009). Tellurite-mediated disabling of [4Fe-4S] clusters of *Escherichia coli* dehydratases. *Microbiology* 155, 40–46. doi: 10.1099/mic.0.026260-0

Carotti, S., Marcon, M., Marussich, M., Mazzei, T., Messori, L., Mini, E., et al. (2000). Cytotoxicity and DNA binding properties of a chloro glycythistidinate gold (III) complex (GHAu). *Chem. Biol. Interact.* 125, 29–38. doi: 10.1016/S0009-2797(99)00160-X

Chaloupka, K., Malam, Y., and Seifalian, A. M. (2010). Nanosilver as a new generation of nanoproduct in biomedical applications. *Trends Biotechnol.* 28, 580–588. doi: 10.1016/j.tibtech.2010.07.006

Chasteen, T. G., Fuentes, D. E., Tantaleán, J. C., and Vásquez, C. C. (2009). Tellurite: history, oxidative stress, and molecular mechanisms of resistance. *FEMS Microbiol. Rev.* 33, 1–13. doi: 10.1111/j.1574-6976.2009.00177.x

Cioffi, N., and Rai, M. (eds). (2012). *Nano-Antimicrobials: Progress and Prospects.* Berlin: Springer Science & Business Media.

Contreras, N. P., and Vásquez, C. C. (2010). Tellurite-induced carbonylation of the *Escherichia coli* pyruvate dehydrogenase multienzyme complex. *Arch. Microbiol.* 192, 969–973. doi: 10.1007/s00203-010-0624-2

Correa-Llantén, D., Muñoz-Ibacache, S., Castro, M., Muñoz, P., and Blamey, J. (2013). Gold nanoparticles synthesized by *Geobacillus* sp. strain ID17 a thermophilic bacterium isolated from deception Island, Antarctica. *Microb. Cell Fact.* 12:75. doi: 10.1186/1475-2859-12-75

Cui, Y., Zhao, Y., Tian, Y., Zhang, W., Lu, X., and Jiang, X. (2012). The molecular mechanism of action of bacterial gold nanoparticles on *E. coli. Biomaterials* 33, 2327–2333. doi: 10.1016/j.biomaterials.2011.11.057

Das, S., Dash, H., and Chakraborty, J. (2016). Genetic basis and importance of metal resistant genes in bacteria for bioremediation of contaminated environments with toxic metal pollutants. *Appl. Microbiol. Biotechnol.* 100, 2967–2984. doi: 10.1007/s00253-016-7364-4

Das, S. K., Das, A. R., and Guha, A. K. (2009). Gold nanoparticles: microbial synthesis and application in water hygiene management. *Langmuir* 25, 8192–8199. doi: 10.1021/la900585p

Dhillon, G. S., Brar, S. K., Kaur, S., and Verma, M. (2012). Green approach for nanoparticle biosynthesis by fungi: current trends and applications. *Crit. Rev. Biotechnol.* 32, 49–73. doi: 10.3109/07388551.2010.550568

Dizaj, S. M., Lotfipour, F., Barzegar-Jalali, M., Zarrintan, M. H., and Adibkia, H. (2014). Antimicrobial activity of the metals and metal oxides nanoparticles. *Mater. Sci. Eng. C* 44, 278–284. doi: 10.1016/j.msec.2014.08.031

Gurunathan, S., Kalishwaralal, K., Vaidyanathan, R., Deepak, V., Pandian, S., Muniyandi, J., et al. (2009). Biosynthesis, purification and characterization of silver nanoparticles using *Escherichia coli. Colloids Surf.* 50, 328–335. doi: 10.1016/j.colsurfb.2009.07.048

Imlay, J. A. (2003). Pathways of oxidative damage. *Annu. Rev. Microbiol.* 57, 395–418. doi: 10.1146/annurev.micro.57.030502.090938

Kamal, M. A. (1994). Sodium selenate and sodium selenite. *Natl. Toxicol. Progr.* 48, 2–70.

Klonowska, A., Heulin, T., and Vermeglio, A. (2005). Selenite and tellurite reduction by *Shewanella oneidensis*. *Appl. Environ. Microbiol.* 71, 5607–5609. doi: 10.1128/AEM.71.9.5607-5609.2005

Kumar, S. A., Abyaneh, M. K., Gosavl, S. W., Kulkarni, S. K., Pasricha, R., Ahmad, A., et al. (2007). Nitrate reductase-mediated synthesis of silver nanoparticles from $AgNO_3$. *Biotechnol. Lett.* 29, 439–445. doi: 10.1007/s10529-006-9256-7

Lemire, J. A., Harrison, J. J., and Turner, R. J. (2013). Antimicrobial activity of metals: mechanisms, molecular targets and applications. *Nat. Rev. Microbiol.* 11, 371–384. doi: 10.1038/nrmicro3028

Li, W. R., Xie, X. B., Shi, Q. S., Duan, S. S., Ouyang, Y. S., and Chen, Y. B. (2011). Antibacterial effect of silver nanoparticles on *Staphylococcus aureus*. *Biometals* 24, 135–141. doi: 10.1007/s10534-010-9381-6

Lin, Z. N., Lee, C. H., Chang, H. Y., and Chang, H. T. (2012). Antibacterial activities of tellurium nanomaterials. *Chem. Asian J.* 7, 930–934. doi: 10.1002/asia.201101006

Mane, R. S., Naushad, M., Shirsat, S., and Kadam, A. S. (2015). Selenium nanostructures: microbial synthesis and applications. *RSC Adv.* 112, 1–9. doi:10.1039/C5RA17921A

Narayanan, K. B., and Sakthivel, N. (2010). Biological synthesis of metal nanoparticles by microbes. *Adv. Colloid Interface Sci.* 156, 1–13. doi: 10.1016/j.cis.2010.02.001

Nies, D. H. (1999). Microbial heavy-metal resistance. *Appl. Microbiol. Biotechnol.* 51, 730–750. doi: 10.1007/s002530051457

Nies, D. H., and Grass, G. (2009). Transition metal homeostasis. *EcoSal Plus* 3, 730–750. doi: 10.1128/ecosalplus.5.4.4.3

Nies, D. H., and Silver, S. (1995). Ion efflux systems involved in bacterial metal resistance. *J. Ind. Microbiol.* 14, 186–199. doi: 10.1007/BF01569902

Oves, M., Khan, M. S., Zaidi, A., Ahmed, A. S., Ahmed, F., Ahmad, E., et al. (2013). Antibacterial and cytotoxic efficacy of extracellular silver nanoparticles

biofabricated from chromium reducing novel OS4 strain of Stenotrophomonas maltophilia. *PLoS ONE* 8:e59140. doi: 10.1371/journal.pone.0059140

Oves, M., Qari, H. A., Felemban, N. M., Khan, M. Z., Rehan, Z. A., and Ismail, I. M. I. (2017). Marinobacter lipolyticus from Red Sea for lipase production and modulation of silver nanomaterials for anti-candidal activities. *IET Nanobiotechnol.* 11, 403–410. doi: 10.1049/iet-nbt.2016.0104

Panda, T., and Deepa, K. (2011). Biosynthesis of gold nanoparticles. *J. Nanosci. Nanotechnol.* 11, 10279–10294. doi: 10.1166/jnn.2011.5021

Pérez, J. M., Calderón, I. L., Arenas, F. A., Fuentes, D. E., Pradenas, G. A., Fuentes, E. L., et al. (2007). Bacterial toxicity of potassium tellurite: unveiling an ancient enigma. *PLoS ONE* 2:e211. doi: 10.1371/journal.pone.0000211

Pradenas, G. A., Díaz-Vásquez, W. A., Pérez-Donoso, J. M., and Vásquez, C. C. (2013). Monounsaturated fatty acids are substrates for aldehyde generation in tellurite-exposed *Escherichia coli*. *Biomed Res. Int*. 2013:563756. doi: 10.1155/2013/563756

Pugin, B., Cornejo, F., Muñoz, P., Muñoz, C., Vargas, J., Arenas, F., et al. (2014). Glutathione reductase-mediated synthesis of tellurium-containing nanostructures exhibiting antibacterial properties. *Appl. Environ. Microbiol.* 80, 7061–7070. doi: 10.1128/AEM.02207-14

Rai, M., Yadav, A., and Gade, A. (2009). Silver nanoparticles as a new generation of antimicrobials. *Biotechnol. Adv.* 27, 76–83. doi: 10.1016/j.biotechadv.2008.09.002

Rao, J. (2008). Shedding light on tumors using nanoparticles. *ACS Nano* 2, 1984–1986. doi: 10.1021/nn800669n

Rigobello, M., Folda, A., Citta, A., Scutari, G., Gandin, V., Fernandes, A., et al. (2011). Interaction of selenite and tellurite with thiol-dependent redox enzymes: kinetics and mitochondrial implications. *Free Radical Biol. Med.* 50, 1620–1629. doi: 10.1016/j.freeradbiomed.2011.03.006

Saitou, N., and Nei, M. (1987). The neighbor-joining method: a new method for reconstructing phylogenetic trees. *Mol. Biol. Evol.* 4, 406–425.

Sambrook, J., and Russell, D. (2001). *Molecular Cloning. A Laboratory Manual, 3rd Edn*. Cold Spring Harbor, NY: Cold Spring Harbor Laboratory Press.

Selenius, M., Rundlöf, A., Olm, E., Fernandes, A., and Björnstedt, M. (2010). Selenium and the selenoprotein thioredoxin reductase in the prevention, treatment and diagnostics of cancer. *Antioxid. Redox Signal.* 12, 867–880. doi: 10.1089/ars.2009.2884

Sharma, V. K., Yngard, R. A., and Lin, Y. (2009). Silver nanoparticles: green synthesis and their antimicrobial activities. *Adv. Colloid Interface Sci.* 145, 83–96. doi: 10.1016/j.cis.2008.09.002

Silver, S., and Phung, T. (2005). A bacterial view of the periodic table: genes and proteins for toxic ions. *J. Ind. Microbiol. Biotechnol.* 32, 587–605. doi: 10.1007/s10295-005-0019-6

Song, D., Li, X., Cheng, Y., Xiao, X., Lu, Z., Wang, Y., et al. (2017). Aerobic biogenesis of selenium nanoparticles by *Enterobacter cloacae* Z0206 as a consequence of fumarate reductase mediated selenite reduction. *Sci. Rep.* 7, 1–10. doi: 10.1038/s41598-017-03558-3

Stephen, J. R., and Macnaughtont, S. J. (1999). Developments in terrestrial bacterial remediation of metals. *Curr. Opin. Biotechnol.* 10, 230–233. doi: 10.1016/S0958-1669(99)80040-8

Stolz, J. F., and Oremland, R. S. (1999). Bacterial respiration of arsenic and selenium. *FEMS Microbiol. Rev.* 23, 615–627. doi: 10.1111/j.1574-6976.1999.tb00416.x

Summers, A., and Silver, S. (1978). Microbial transformations of metals. *Annu. Rev. Microbiol.* 32, 637–672. doi: 10.1146/annurev.mi.32.100178.003225

Suresh, A. K. (2012). *Metallic Nanocrystallites and Their Interaction with Microbial Systems. Springer Briefs in Molecular Science Biometals*. Dordrecht; Heidelberg; New York, NY; London: Springer.

Tamura, K., Nei, M., and Kumar, S. (2004). Prospects for inferring very large phylogenies by using the neighbor-joining method. *Proc. Natl. Acad. Sci. U.S.A.* 101, 11030–11035. doi: 10.1073/pnas.0404206101

Taylor, D. E. (1999). Bacterial tellurite resistance. *Trends Microbiol.* 7, 111–115. doi: 10.1016/S0966-842X(99)01454-7

Thakkar, K., Mhatre, S., and Parikh, R. (2010). Biological synthesis of metallic nanoparticles. *Nanomedicine* 23, 257–262. doi: 10.1016/j.nano.2009.07.002

Tremaroli, V., Fedi, S., and Zannoni, D. (2007). Evidence for a tellurite-dependent generation of reactive oxygen species and absence of a tellurite-mediated adaptive response to oxidative stress in cells of *Pseudomonas pseudoalcaligenes* KF707. *Arch. Microbiol.* 187, 127–135. doi: 10.1007/s00203-006-0179-4

Turner, R. J., Borghese, R., and Zannoni, D. (2011). Microbial reduction of tellurium metalloids as a tool in biotechnology. *Biotechnol. Adv.* 30, 954–963. doi: 10.1016/j.biotechadv.2011.08.018

Vlamis-Gardikas, A. (2008). The multiple functions of the thiol-based electron flow pathways of *Escherichia coli*: eternal concepts revisited. *Biochim. Biophys. Acta* 1780, 1170–1200. doi: 10.1016/j.bbagen.2008.03.013

Vrionis, H. A., Wang, S., Haslam, B., and Turner, R. J. (2015). Selenite protection of tellurite toxicity toward *Escherichia coli*. *Front. Mol. Biosci.* 69, 1–10. doi: 10.3389/fmolb.2015.00069

Xiong, Y., and Lu, X. (2015). *Metallic Nanoestructures: From Controlled Synthesis to Applications*. Cham: Springer International publishing.

Xiu, Z. M., Ma, J., and Alvarez, P. J. (2011). Differential effect of common ligands and molecular oxygen on antimicrobial activity of silver nanoparticles versus silver ions. *Environ. Sci. Technol.* 45, 9003–9008. doi: 10.1021/es201918f

Xiu, Z. M., Zhang, Q. B., Puppala, H. L., Colvin, V. L., and Alvarez, P. J. (2012). Negligible particle-specific antibacterial activity of silver nanoparticles. *Nano Lett.* 12, 4271–4275. doi: 10.1021/nl301934w

Yacoby, I., and Benhar, I. (2008). Antibacterial nanomedicine. *Nanomedicine* 3, 329–341. doi: 10.2217/17435889.3.3.329

Zannoni, D., Borsetti, F., Harrison, J. J., and Turner, R. J. (2008). The bacterial response to the chalcogen metalloids Se and Te. *Adv. Microb. Ecol.* 53, 1–72. doi: 10.1016/S0065-2911(07)53001-8

Zare, B., Babaie, S., Setayesh, N., and Shahverdi, A. R. (2013). Isolation and characterization of a fungus for extracellular synthesis of small selenium nanoparticles. *Nanomedicine* 1, 13–19. doi: 10.7508/nmj.2013.01.002

Conflict of Interest Statement: The authors declare that the research was conducted in the absence of any commercial or financial relationships that could be construed as a potential conflict of interest.

frontiers in Microbiology

ORIGINAL RESEARCH
published: 22 March 2018
doi: 10.3389/fmicb.2018.00506

Transcriptional Regulation of the Peripheral Pathway for the Anaerobic Catabolism of Toluene and *m*-Xylene in *Azoarcus* sp. CIB

*Blas Blázquez†, Manuel Carmona and Eduardo Díaz**

Department of Microbial and Plant Biotechnology, Centro de Investigaciones Biológicas–Consejo Superior de Investigaciones Científicas, Madrid, Spain

OPEN ACCESS

Edited by:
Kian Mau Goh, Universiti Teknologi Malaysia, Malaysia

Reviewed by:
Maximino Manzanera, University of Granada, Spain
Victor Ladero, Instituto de Productos Lácteos de Asturias (CSIC), Spain

****Correspondence:***
Eduardo Díaz
ediaz@cib.csic.es

†Present address:
Blas Blázquez, Systems Biology Programme, Centro Nacional de Biotecnología–Consejo Superior de Investigaciones Científicas, Madrid, Spain

Specialty section:
This article was submitted to Microbiotechnology, Ecotoxicology and Bioremediation, a section of the journal Frontiers in Microbiology

Received: *08 January 2018*
Accepted: *06 March 2018*
Published: *22 March 2018*

Citation:
Blázquez B, Carmona M and Díaz E (2018) Transcriptional Regulation of the Peripheral Pathway for the Anaerobic Catabolism of Toluene and m-Xylene in Azoarcus sp. CIB. Front. Microbiol. 9:506. doi: 10.3389/fmicb.2018.00506

Alkylbenzenes, such as toluene and *m*-xylene, are an important class of contaminant hydrocarbons that are widespread and tend to accumulate in subsurface anoxic environments. The peripheral pathway for the anaerobic oxidation of toluene in bacteria consists of an initial activation catalyzed by a benzylsuccinate synthase (encoded by *bss* genes), and a subsequent modified β-oxidation of benzylsuccinate to benzoyl-CoA and succinyl-CoA (encoded by *bbs* genes). We have shown here that the *bss* and *bbs* genes, which are located within an integrative and conjugative element, are essential for anaerobic degradation of toluene but also for *m*-xylene oxidation in the denitrifying beta-proteobacterium *Azoarcus* sp. CIB. New insights into the transcriptional organization and regulation of a complete gene cluster for anaerobic catabolism of toluene/*m*-xylene in a single bacterial strain are presented. The *bss* and *bbs* genes are transcriptionally coupled into two large convergent catabolic operons driven by the *PbssD* and *PbbsA* promoters, respectively, whose expression is inducible when cells grow anaerobically in toluene or *m*-xylene. An adjacent *tdiSR* operon driven by the *PtdiS* promoter encodes a putative two-component regulatory system. TdiR behaves as a transcriptional activator of the *PbssD*, *PbbsA*, and *PtdiS* promoters, being benzylsuccinate/(3-methyl)benzylsuccinate, rather than toluene/*m*-xylene, the inducers that may trigger the TdiS-mediated activation of TdiR. In addition to the TdiSR-based specific control, the expression of the *bss* and *bbs* genes in *Azoarcus* sp. CIB is under an overimposed regulation that depends on certain environmental factors, such as the presence/absence of oxygen or the availability of preferred carbon sources (catabolite repression). This work paves the way for future strategies toward the reliable assessment of microbial activity in toluene/*m*-xylene contaminated environments.

Keywords: toluene, *m*-xylene, *Azoarcus*, anaerobic degradation, *tdiSR*, catabolite repression, biomarker

INTRODUCTION

Aromatic compounds such as alkylbenzenes, e.g., toluene, xylenes, ethylbenzene and benzene, are an important class of contaminants that are prominently placed amongst the US Agency for Toxic Substances and Disease Registry's list of priority pollutants because of their carcinogenic and/or neurotoxic effects to humans. Since alkylbenzenes are relatively soluble and mobile in water, they are widespread and tend to accumulate in hostile environments, e.g., subsurface

anoxic environments, where they are of major concern to groundwater quality and ecosystem health. Therefore, the anaerobic degradation of alkylbenzenes is an important practical aspect of bioremediation and becomes crucial for the biogeochemical cycles (Kummel et al., 2013; Rabus et al., 2016; Lueders, 2017). Despite the aerobic degradation of alkylbenzenes has been extensively studied, the microbial catabolism of these aromatic hydrocarbons under anaerobic conditions is much less known, and novel pathways and enzymes have been recently described, some of which are of potential biotechnological interest (Rabus et al., 2016; Lueders, 2017). Toluene has been used widely as a model compound for studying anaerobic alkylbenzene degradation. Toluene can be degraded coupled to anaerobic respiration with nitrate, sulfate, iron (III), manganese (IV) or carbonate serving as terminal electron acceptors (Foght, 2008; Carmona et al., 2009; Rabus et al., 2016). *Geobacter metallireducens* GS-15 was the first pure bacterial culture described to be able to degrade toluene in anaerobic conditions (Lovley et al., 1989). Several isolates capable of anaerobic toluene degradation have been described since then, including both facultative anaerobes, e.g., beta-proteobacteria of the *Azoarcus*, "*Aromatoleum,*" *Thauera, Georgfuchsia, Herminiimonas* genera, and alpha-proteobacteria of the *Magnetospirillum* genus, and obligate anaerobes, e.g., delta-proteobacteria of the *Geobacter, Desulfobacula* and *Desulfobacterium* genera, and some clostridial strains (Wöhlbrand et al., 2013; Bozinovski et al., 2014; Kim et al., 2014; Strijkstra et al., 2014; Rabus et al., 2016; Lueders, 2017; Meyer-Cifuentes et al., 2017). Most of the studies on anaerobic toluene degradation have been made on the denitrifying bacteria *Thauera aromatica* K172 and T1 strains, *Azoarcus* sp. strain T and "*Aromatoleum aromaticum*" EbN1 strain (Coschigano and Young, 1997; Leuthner et al., 1998; Krieger et al., 1999; Achong et al., 2001; Hermuth et al., 2002; Leutwein and Heider, 2002; Chakraborty and Coates, 2004; Coschigano and Bishop, 2004; Kube et al., 2004; Kühner et al., 2005).

The first step in the anaerobic catabolism of toluene is the addition of the methyl group of toluene to fumarate to form (*R*)-benzylsuccinate by the strictly anoxic benzylsuccinate synthase (BSS), a glycyl radical enzyme (**Figure 1A**). The genes *bssA*, *bssB* and *bssC* code for the α (BssA), β (BssB) and γ (BssC) subunits of the heterohexameric $(\alpha\beta\gamma)_2$ BSS (Leuthner et al., 1998; Krieger et al., 2001; Bhandare et al., 2006; Funk et al., 2014; Heider et al., 2016). Conversion to the active, radical-containing form of BSS depends on an activating enzyme (BssD) that belongs to the family of *S*-adenosyl-methionine radical enzymes and that is encoded by a gene (*bssD*) which is closely associated with the *bssABC* genes constituting the *bssDCAB* operon of toluene-degrading bacteria (**Figure 2**) (Selmer et al., 2005; Heider et al., 2016). The *bss* operons contain two additional conserved genes, *bssE* and *bssF* (**Figure 2**), whose functions are still unknown. Whereas BssE is an essential protein for toluene degradation (Bhandare et al., 2006), the role of BssF in the anaerobic oxidation of toluene has not yet been explored. Moreover, in beta-proteobacteria the *bss* cluster contains a set of additional genes, i.e., the *bssGIJKL* genes (**Figure 2**), whose function is so far unknown. Despite the primary structure of the gene products is conserved in the *bss* clusters from different denitrifying bacteria, the transcriptional organization of the *bss* clusters differs between species and even between strains of the same species (Coschigano, 2000; Achong et al., 2001; Kube et al., 2004).

Further anaerobic degradation of toluene consists of a modified beta-oxidation of (*R*)-benzylsuccinate to benzoyl-CoA and succinyl-CoA (**Figure 1A**). All enzymes of this pathway are encoded by the *bbs* gene cluster (**Figure 2**) (Leuthner and Heider, 2000; Leutwein and Heider, 2001, 2002; Kube et al., 2004). Like in the *bss* gene cluster, the *bbs* cluster contains genes, e.g., *bbsI* and *bbsJ*, of unknown function (Carmona et al., 2009). Although the gene organization of the *bbsABCDEFJGH* cluster is usually conserved except in some delta-proteobacteria (**Figure 2**) (Kube et al., 2004; Butler et al., 2007; Chaurasia et al., 2015), the transcriptional organization of a *bbs* cluster has not been studied so far in any bacteria.

Upstream of the *bss* cluster in most denitrifying bacteria there are two genes, *tdiS* and *tdiR* (toluene-degradation inducer) (**Figure 2**) that were proposed to encode the sensor histidine kinase and the cognate response regulator, respectively, of a two-component regulatory system likely involved in the transcriptional control of the catabolic *bss* and *bbs* genes (Coschigano, 2000; Achong et al., 2001; Hermuth et al., 2002; Kube et al., 2004; Kühner et al., 2005). Extracts of *Escherichia coli* cells that expressed the *tdiR* gene from *T. aromatica* K172 were able to retard the migration of a DNA probe that contained the *bssD* promoter, supporting the notion that TdiR likely behaves as a transcriptional regulator of the *bss* genes (Leuthner and Heider, 1998). Nevertheless, a clear experimental demonstration that TdiS and TdiR control the expression of both *bss* and *bbs* genes in beta-proteobacteria is still missing.

Unlike toluene degradation, anaerobic degradation of xylenes (*meta*-, *ortho*-, and *para*-xylene) has been much less studied. The first reaction of the *m*-xylene degradation pathway is performed by the BSS enzyme that catalyzes the addition of fumarate to the methyl group to form (3-methyl)benzylsuccinate (**Figure 1A**) (Krieger et al., 1999; Verfürth et al., 2004). The (3-methyl)benzylsuccinate was also detected as a key intermediate of the fumarate addition pathway in xylene-degrading sulfate-reducing cultures (Morasch et al., 2004; Herrmann et al., 2009). On the other hand, it has been proposed that the *bbs* gene products might be responsible of the β-oxidation of (3-methyl)benzylsuccinate to 3-methylbenzoyl-CoA and succinyl-CoA in a similar way than in the catabolism of toluene (**Figure 1A**) (Krieger et al., 1999; Bozinovski et al., 2014), although there is not yet a genetic demonstration that *bbs* genes are responsible for anaerobic *m*-xylene degradation.

Azoarcus sp. CIB is facultative anaerobic bacterium able to grow aerobically in toluene and anaerobically (nitrate-reducing) in toluene and *m*-xylene (López-Barragán et al., 2004). Moreover, *Azoarcus* sp. CIB also shows an endophitic lifestyle (Fernández et al., 2014) and is able to resist some metals and metalloids (Fernández-Llamosas et al., 2016). The strain CIB has been used previously to decipher the transcriptional organization and regulation of several gene clusters involved in the anaerobic degradation of aromatic compounds and in the resistance strategies to survive in the presence of high concentrations of these contaminants (López-Barragán et al., 2004; Blázquez et al.,

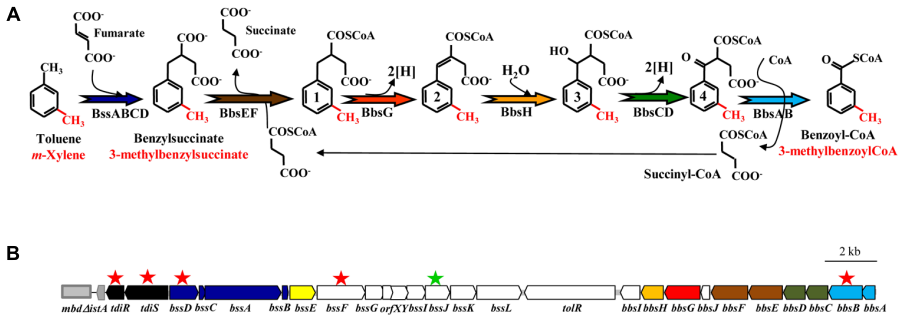

FIGURE 1 | Proposed toluene and *m*-xylene anaerobic peripheral degradation pathway in *Azoarcus* sp. CIB: **(A)** Scheme of the proposed peripheral pathway of anaerobic degradation of toluene and *m*-xylene. The enzymes are indicated following the color code indicated in **(B)**. Toluene and *m*-xylene derivatives are shown in black and red color, respectively. Intermediates 1 correspond to benzylsuccinyl-CoA (black) and (3-methyl)benzylsuccinyl-CoA (red). Intermediates 2 correspond to phenylitaconyl-CoA (black) and (3-methyl)phenylitaconyl-CoA (red). Intermediates 3 correspond to 2-[hydroxyphenyl]-succinyl-CoA (black) and 2-[hydroxyphenyl(methyl)]-succinyl-CoA (red). Intermediates 4 correspond to benzoylsuccinyl-CoA (black) and (3-methyl)benzoylsuccinyl-CoA (red). Modified from Carmona et al. (2009). **(B)** Scheme of the gene cluster encoding the anaerobic peripheral pathway of toluene and *m*-xylene in *Azoarcus* sp. CIB. Genes are represented by arrows and their predicted function is annotated as follows: black, regulatory genes; dark blue, genes encoding the (3-methyl)benzylsuccinate synthase (BSS); yellow, gene encoding a putative BSS chaperone; orange, gene encoding the (3-methyl)phenylitaconyl-CoA hydratase; red, gene encoding the (3-methyl)benzylsuccinyl-CoA dehydrogenase; brown, genes encoding the succinyl-CoA:(3-methyl)benzylsuccinate CoA transferase; green, genes encoding a 2-[hydroxyphenyl(methyl)]-succinyl-CoA dehydrogenase; light blue, genes encoding the (3-methyl)benzoylsuccinyl-CoA thiolase; white, genes of unknown function. A truncated IS*21* transposase *istA* gene (Δ*istA*) is shown by a gray arrow. The gray rectangle indicates the *mbd* cluster responsible for the 3-methylbenzoyl-CoA central pathway. Genes that have been inactivated in this work and avoid the use of toluene and *m*-xylene as sole carbon and energy source by the corresponding mutant strains (*Azoarcus* sp. CIBd*tidR*, *Azoarcus* sp. CIBd*tidS*, *Azoarcus* sp. CIBd*bssD*, *Azoarcus* sp. CIBd*bssF*, *Azoarcus* sp. CIBd*bbsB*) are indicated with a red star. The gene that has been inactivated and does not avoid the use of toluene and *m*-xylene as sole carbon and energy source in the corresponding mutant strain (*Azoarcus* sp. CIBd*bssJ*) is indicated with a green star.

2008; Carmona et al., 2009; Valderrama et al., 2012, 2014; Juárez et al., 2013; Juárez et al., 2015; Martín-Moldes et al., 2016; Zamarro et al., 2016). An *in silico* analysis of the *Azoarcus* sp. CIB genome sequence revealed the presence of a chromosomal region within the integrative and conjugative ICE_{XTD} element coding for proteins with significant amino acid sequence identity with Bss and Bbs proteins in closely related bacteria from the *Azoarcus*, "*Aromatoleum*" and *Thauera* genera (Martín-Moldes et al., 2015; Zamarro et al., 2016). This sequence comparison analysis allowed us to propose a similar biochemical pathway for the anaerobic conversion of toluene and *m*-xylene to benzoyl-CoA and 3-methylbenzoyl-CoA, respectively, in strain CIB (**Figure 1**). Further degradation of benzoyl-CoA and 3-methylbenzoyl-CoA in *Azoarcus* sp. CIB proceeds via the central bzd (stands for benzoate degradation) and mbd (stands for methylbenzoate degradation) pathways, respectively (López-Barragán et al., 2004; Juárez et al., 2013). In this work we have used *Azoarcus* sp. CIB to study for the first time the transcriptional organization and regulation of the complete *bss-bbs* cluster in a facultative anaerobe. Our results reveal that both the *bss* and *bbs* genes are essential for the anaerobic degradation of toluene and *m*-xylene.

MATERIALS AND METHODS

Bacterial Strains, Plasmids and Growth Conditions

The *E. coli* and *Azoarcus* strains, as well as the plasmids used in this study, are detailed in **Table 1**. *E. coli* strains were grown at 37°C in Lysogeny Broth (LB) mediun (Bertani, 1951). *Azoarcus* sp. strain CIB and its derivatives were grown anaerobically under nitrate reducing conditions (10 mM nitrate) at 30°C in MC medium as previously described (López-Barragán et al., 2004). Aromatic hydrocarbons such as toluene, xylenes, styrene were supplied at 250 mM in an inert carrier phase of 2,2,4,4,6,8,8-heptamethylnonan (HMN). Benzylsuccinate was added at 4 mM to the culture medium as inducer. Organic acids such as succinate or pyruvate were added at 0.2% (w/v). *Azoarcus* sp. CIB cells were also cultivated aerobically in MC medium in the absence of nitrate. When using toluene aerobically as sole carbon source, it was added directly to the culture medium at 1 mM. Where appropriate, antibiotics were added to the culture medium at the following concentrations: ampicillin, 100 μg/ml; gentamicin, 10 μg/ml; kanamycin, 50 μg/ml. Growth was determined by measuring the optical density at 600 nm (OD_{600}) in a Shimadzu UV-260 spectrophotometer.

Molecular Biology Techniques

Standard molecular biology techniques were performed as previously described (Sambrook and Russell, 2001). DNA fragments were purified with Gene-Clean Turbo (BIO101 Systems); plasmids and PCR products were purified with a High Pure Plasmid and PCR Product Purifications kits (Roche), respectively. Oligonucleotides were supplied by Sigma Co. All cloned inserts and DNA fragments were confirmed by DNA sequencing with fluorescently labeled dideoxynucleotide terminators (Sanger et al., 1977) and AmpliTaq FS DNA polymerase (Applied Biosystems) in an ABI Prism 377 automated DNA sequencer (Applied Biosystems). Transformation of *E. coli* cells was carried out by using the RbCl method or by

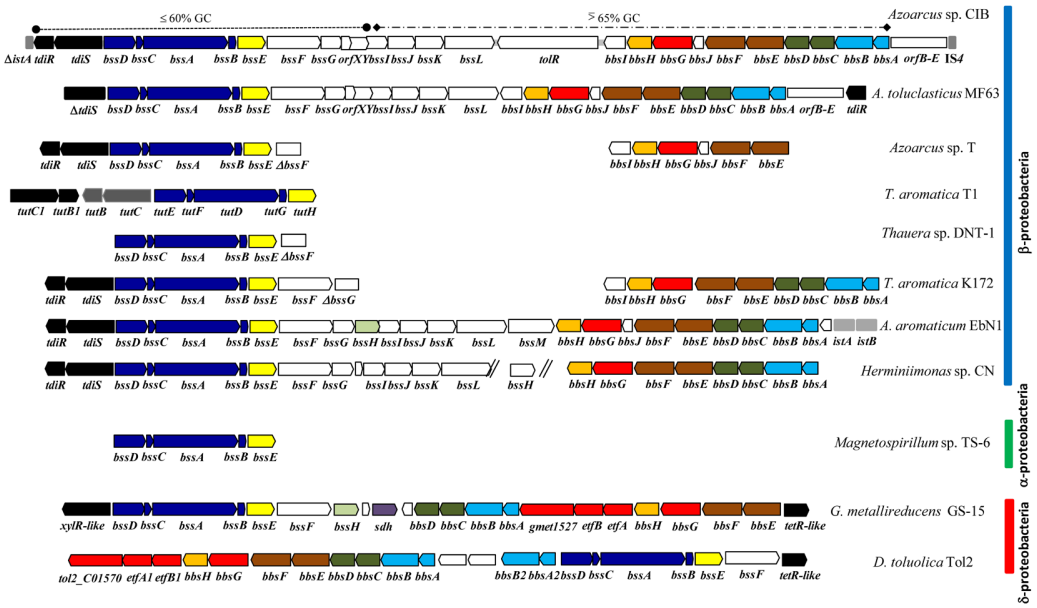

FIGURE 2 | Scheme of the genetic organization of the *tdi-bss-bbs* cluster in different bacteria. The *tdi-bss-bss* clusters from *Azoarcus* sp. CIB, *Azoarcus toluclasticus* MF63 (Acc. No. NZ_ARJX00000000.1), *Azoarcus* sp. strain T (Ac. No. AY032676), *T. aromatica* T1 (Ac. No. U57900 and AF113168), *Thauera* sp. strain DNT-1 (Ac. No. AB066263), *T. aromatica* K172 (Ac. No. AJ001848 and AF173961), "*Aromatoleum aromaticum*" EbN1 (Ac. No. NC_006513), *Herminiimonas* sp. CN (Ac. No. AVCC01000000), *Magnetospirillum* sp. strain TS-6 (Ac. No. AB167725), *Geobacter metallireducens* GS-15 (Ac. No. NC_007517) and *Desulfobacula toluolica* Tol2 (Ac. No. NC_018645) are represented here. Genes are represented by arrows following the color code indicated in **Figure 1**: black, regulatory genes; gray, putative regulatory genes of an aerobic toluene degradation pathway; dark blue, genes encoding the (3-methyl)benzylsuccinate synthase (BSS); yellow, genes encoding a putative BSS chaperone; orange, genes encoding the (3-methyl)phenylitaconyl-CoA hydratase; red, genes encoding the (3-methyl)benzylsuccinyl-CoA dehydrogenase and its predicted associated electron-transfer system; brown, genes encoding the succinyl-CoA:(3-methyl)benzylsuccinate CoA transferase; green, genes encoding a 2-[hydroxyphenyl(methyl)]-succinyl-CoA dehydrogenase; light blue, genes encoding the (3-methyl)benzoylsuccinyl-CoA thiolase; light green, genes encoding a putative toluene transport system; violet, gene encoding a putative succinate-dehydrogenase flavoprotein; white, genes of unknown function. Insertion sequences are indicated by gray rectangles. The white rectangle next to the *bbs* operon in *Azoarcus* sp. CIB represents *orfB* (AzCIB_4527), *orfC* (AzCIB_4528), *orfD* (AzCIB_4529) and *orfE* (AzCIB_4530) genes, that are also present in *A. toluclasticus* MF63. In the *bss-bbs* cluster of *Azoarcus* sp. CIB, the DNA fragment harboring the *bssDCABEFG* genes and whose average GC content is 58% is indicated by a disontinuous line flanked by circles. The DNA fragment containing the rest of the *bss* (*bssIJKL*) and *bbs* genes, whose average GC content is 65%, is indicated by a discontinuous line flanked by diamonds.

electroporation (Gene Pulser, Bio-Rad) (Sambrook and Russell, 2001). Plasmids were transferred from *E. coli* S17-1λpir (donor strain) into *Azoarcus* sp. recipient strains by biparental filter mating as described previously (López-Barragán et al., 2004).

Construction of *Azoarcus* sp. CIBd*tdiR*, *Azoarcus* sp. CIBd*tdiS*, *Azoarcus* sp. CIBd*bssD*, *Azoarcus* sp. CIBd*bssF*, *Azoarcus* sp. CIBd*bssJ*, and *Azoarcus* sp. CIBd*bbsB* Strains

For insertional disruption of the genes through single homologous recombination, an internal region of each gene was PCR-amplified, cloned into plasmid pGEM-T Easy, and subcloned into the pK18*mob* suicide vector (**Table 1**). For gene disruption of the *tdiR* gene, a 0.4-kb internal fragment was PCR-amplified using primers tdiRint5 and tdiR131.5 (Supplementary Table S1), and cloned in plasmid pGEM-tdiR (**Table 1**). The pGEM-tdiR plasmid was XbaI/PstI double-digested and the 0.4-kb fragment was then subcloned giving rise to the suicide plasmid pK18*mobtdiR* (**Table 1**). For gene disruption of the *tdiS* gene, a 0.6-kb internal fragment was PCR amplified using primers 5TdiS and 3TdiS (Supplementary Table S1), and cloned in plasmid pGEM-tdiS (**Table 1**). The pGEM-tdiS plasmid was EcoRI digested and the 623-bp fragment was then subcloned producing plasmid pK18*mobtdiS* (**Table 1**). The *tdiS* mutant allows expression of the downstream *tdiR* gene by transcription from the promoter of the kanamycin resistance gene present in the suicide plasmid. For gene disruption of the *bssD* gene, a 0.6-kb internal fragment was PCR amplified using primers 5BssD and 3BssD (Supplementary Table S1), and cloned in plasmid pGEM-bssD (**Table 1**). The pGEM-bssD plasmid was PstI/BamHI double-digested and the 593-bp fragment was then subcloned into pK18*mob* producing plasmid pK18*mobbssD* (**Table 1**). For gene disruption of the *bssF* gene, a 0.4-kb internal fragment was PCR-amplified using primers 5BssF and 3BssF (Supplementary Table S1) and cloned in plasmid pGEM-bssF (**Table 1**). The pGEM-bssF plasmid was HindIII/XbaI double-digested and the 451-bp fragment was then subcloned giving rise to the suicide plasmid pK18*mobbssF* (**Table 1**). For gene disruption of the *bssJ* gene, a 0.3-kb internal fragment was PCR amplified using primers 5BssJ and 3BssJ (Supplementary Table S1) and cloned in plasmid pGEM-bssJ (**Table 1**). The

TABLE 1 | Bacterial strains and plasmids used in this work.

Strains and plasmids	Description[a]	Reference or source
Strains		
E. coli		
DH10B	F', *mcrA*, D(*mrr*, *hsdRMS-mcrBC*), f80d*lac*DM15, D*lacX74*, *deoR*, *recA1*, *araD139*, D(*ara-leu*)*7697*, *galU*, *galK* l, *rpsL*, *endA1*, *nupG*	Life Technologies
S17-1λpir	*recA, thi, hsdRM*+, RP4::2-Tc::Mu::Km, Tn*7*, λpir phage lysogen; Tp^r, Sm^r	de Lorenzo and Timmis, 1994
Azoarcus sp. CIB	Wild-type strain; T^+ X^+	López-Barragán et al., 2004
Azoarcus sp. CIBd*tdiR*	CIB mutant strain with a disruption of the *tdiR* gene; Km^r, T^- X^-	This study
Azoarcus sp. CIBd*tdiS*	CIB mutant strain with a disruption of the *tdiS* gene; Km^r, T^- X^-	This study
Azoarcus sp. CIBd*bssD*	CIB mutant strain with a disruption of the *bssD* gene; Km^r, T^- X^-	This study
Azoarcus sp. CIBd*bssF*	CIB mutant strain with a disruption of the *bssF* gene; Km^r, T^- X^-	This study
Azoarcus sp. CIBd*bssJ*	CIB mutant strain with a disruption of the *bssJ* gene; Km^r, T^+ X^+	This study
Azoarcus sp. CIBd*bbsB*	CIB mutant strain with a disruption of the *bbsB* gene; Km^r, T^- X^-	This study
Plasmids		
pGEM-T Easy	Ap^r, *ori*ColE1, *lacZ*α, used for cloning PCR products	Promega
pGEM-tdiR	Ap^r, pGEM-T Easy containing a 400 bp XbaI/PstI *tdiR* internal fragment	This study
pGEM-tdiS	Ap^r, pGEM-T Easy containing a 623 bp EcoRI *tdiS* internal fragment	This study
pGEM-bssD	Ap^r, pGEM-T Easy containing a 593 bp PstI/BamHI *bssD* internal fragment	This study
pGEM-bssF	Ap^r, pGEM-T Easy containing a 458 bp HindIII/XbaI *bssF* internal fragment	This study
pGEM-bssJ	Ap^r, pGEM-T Easy containing a 353 bp PstI/SalI *bssJ* internal fragment	This study
pGEM-bbsB	Ap^r, pGEM-T Easy containing a 512 bp PstI/BamHI *bbsB* internal fragment	This study
pK18*mob*	Km^r, *ori*ColE1, Mob^+, *lacZ*α, used for directed insertional disruption	Schäfer et al., 1994
pK18*mobtdiR*	Km^r, pK18*mob* containing a 400 bp XbaI/PstI *tdiR* internal fragment	This study
pK18*mobtdiS*	Kmr, pK18*mob* containing a 623 bp EcoRI *tdiS* internal fragment	This study
pK18*mobbssD*	Km^r, pK18*mob* containing a 593 bp PstI/BamHI *bssD* internal fragment	This study
pK18*mobbssF*	Km^r, pK18*mob* containing a 458 bp HindIII/XbaI *bssF* internal fragment	This study
pK18*mobbssJ*	Km^r, pK18*mob* containing a 353 bp PstI/SalI *bssJ* internal fragment	This study
pK18*mobbbsB*	Km^r, pK18*mob* containing a 512 bp PstI/BamHI *bbsB* internal fragment	This study
pSJ3	Ap^r, *ori*ColE1, '*lacZ* promoter probe vector	Ferrández et al., 1998
pSJPbbsA	Ap^r, pSJ3 derivative carrying the *PbbsA::lacZ* fusion	This study
pSJPtdiS	Ap^r, pSJ3 derivative carrying the *PtdiS::lacZ* fusion	This study
pBBR5T	Gm^r, pBBR1MCS-5 derivative with a T7 transcriptional terminator upstream of the '*lacZ* gene	Blázquez et al., 2008
pBBRPbbsA	Gm^r, pBBR5T derivative carrying the *PbbsA::lacZ* fusion	This study
pBBRPbssD	Gm^r, pBBR5T derivative carrying the *PbssD::lacZ* fusion	This study
pBBRPtdiS	Gm^r, pBBR5T derivative carrying the *PtdiS::lacZ* fusion	This study

[a] *The abbreviations used are: T^+, anaerobic growth in toluene; X^+, anaerobic growth in m-xylene; T^-, lack of anaerobic growth in toluene; X^-, lack of anaerobic growth in m-xylene; Ap^r, ampicillin-resistant; Gm^r, gentamicin-resistant; Km^r, kanamycin-resistant; Sm^r, streptomycin-resistant.*

pGEM-bssJ plasmid was PstI/SalI double-digested and the 347-bp fragment was then subcloned producing plasmid pK18*mobbssJ* (**Table 1**). For gene disruption of the *bbsB* gene, a 0.5-kb internal fragment was PCR amplified using primers 5BbsB and 3BbsB, and cloned in plasmid pGEM-bbsB (**Table 1**). The pGEM-bbsB plasmid was *Pst*I/*Bam*HI double-digested and the 512-bp fragment was then subcloned producing plasmid pK18*mobbbsB* (**Table 1**). The derivative pK18*mob* plasmids were then transferred from *E. coli* S17-1λpir (donor strain) into *Azoarcus* sp. CIB (recipient strain) by biparental filter mating as previously described (de Lorenzo and Timmis, 1994; López-Barragán et al., 2004). Exconjugant *Azoarcus* sp. CIB mutant strains harboring the disrupted genes by insertion of the corresponding suicide plasmids, were isolated aerobically on kanamycin-containing MC medium lacking nitrate and containing 0.2% citrate as the sole carbon source for counter-selection of donor cells. The mutant strains were analyzed by PCR to confirm the disruption of the target genes.

Construction of *lacZ* Translational Fusions

To construct plasmid pSJPbbsA that harbors the *PbbsA::lacZ* translational fusion, a 356-bp *Xba*I/*Pst*I DNA fragment containing the *bbsA* (AzCIB_4526)-*orfB* (AzCIB_4527) intergenic region was PCR-amplified from *Azoarcus* sp. CIB chromosomal DNA by using oligonucleotides 5PbbsA and 3PbbsA (5′-AACTGCAGGACATGACGCCTCCGCAGCATTTG-3′ (Supplementary Table S1), and then cloned into the XbaI/PstI double-digested pSJ3 plasmid (**Table 1**). Plasmid pBBRPbbsA was constructed by subcloning a 3.5-kb EcoRI/HindIII fragment harboring the *PbbsA::lacZ* translational fusion from pSJPbbsA into the EcoRI/HindIII double-digested broad-host range plasmid pBBR5T (**Table 1**). To construct plasmid pBBRPbssD that

carries the *PbssD::lacZ* fusion, a 335-bp SpeI/BamHI DNA fragment containing the *tdiS-bssD* intergenic region was PCR-amplified from *Azoarcus* sp. CIB chromosomal DNA by using oligonucleotides 5PtdiS and 3PbssD (Supplementary Table S1), and then cloned into the SpeI/BamHI double-digested pBBRPbbsA (**Table 1**). To construct plasmid pSJ3PtdiS that carries the *PtdiS::lacZ* translational fusion, a 314-bp BamHI fragment containing the *bssD-tdiS* intergenic region was PCR-amplified from *Azoarcus* sp. CIB chromosomal DNA by using oligonucleotides 3PbssD and PtdiS3'(Supplementary Table S1), and then cloned into the BamHI digested pSJ3 plasmid (**Table 1**). Plasmid pBBRPtdiS was constructed by subcloning a 3.5-kb EcoRI/HindIII DNA fragment harboring the *PtdiS::lacZ* fusion from pSJ3PtdiS into the EcoRI/HindIII double-digested broad-host range plasmid pBBR5T (**Table 1**).

RNA Extraction and Reverse Transcription-PCR Experiments

Azoarcus sp. CIB cells grown in MC medium containing the appropriate carbon sources were harvested at the mid-exponential phase of growth and stored at −80°C. *Azoarcus* sp. CIBd*bbsB* and CIBd*bssD* strains grown in kanamycin-containing MC medium with pyruvate plus toluene were harvested at the stationary phase of growth and stored at −80°C. Pellets were thawed, and cells were lysed in TE buffer (10 mM Tris-HCl, pH 7.5, 1 mM EDTA) containing 50 mg ml^{-1} lysozyme. Total RNA was extracted using the RNeasy mini kit (Qiagen), including a DNase treatment according to the manufacturer instructions (Ambion), precipitated with ethanol, washed, and resuspended in RNase-free water. The concentration and purity of the RNA samples were measured by using a ND1000 Spectrophotometer (Nanodrop Technologies) according to the manufacturer's protocols. Synthesis of total cDNA was carried out with 20 μl of reverse transcription reactions containing 400 ng of RNA, 0.5 mM concentrations of each dNTP, 200 U of SuperScript II reverse transcriptase (Invitrogen), and 5 μM concentrations of random hexamers as primers in the buffer recommended by the manufacturer. Samples were initially heated at 65°C for 5 min then incubated at 42°C for 2 h, and the reactions were terminated by incubation at 70°C for 15 min. In standard RT-PCR reactions, the cDNA was amplified with 1 U of AmpliTaq DNA polymerase (Biotools) and 0.5 μM concentrations of the corresponding primer pairs (oligonucleotides 1–20; Supplementary Table S1). Samples were initially denatured by heating at 94°C for 3 min. A 30-cycle amplification program was followed (94°C for 40 s, 60°C for 40 s and 72°C for 60 s). Control reactions in which reverse transcriptase was omitted from the reaction mixture ensured that DNA products resulted from the amplification of cDNA rather than from DNA contamination. The *dnaE* gene encoding the α-subunit of DNA polymerase III was used to provide an internal control cDNA that was amplified with oligonucleotides 5′POLIIIHK/3′POLIIIHK (Supplementary Table S1). The expression of the internal control was shown to be constant across all samples analyzed.

β-Galactosidase Assays

The β-galactosidase activities from promoter-*lacZ* reporter fusions were measured with permeabilized cells when cultures reached mid-exponential or stationary phase of growth, as described (Miller, 1972).

Sequence Data Analyses

Nucleotide sequence analyses were done at the National Center for Biotechnology Information (NCBI) server[1]. The amino acid sequences of the open reading frames were compared with those present in databases using the TBLASTN algorithm (Altschul et al., 1990) at the NCBI server[2]. Pairwise and multiple protein sequence alignments were made with the ClustalW program (Thompson et al., 1994) at the EMBL-EBI server[3]. Phylogenetic analysis of the different proteins was carried out according to the Kimura two-parameter method (Kimura, 1980), and a tree was reconstructed using the neighbor-joining method (Saitou and Nei, 1987) of the PHYLIP program (Felsenstein, 1993) at the TreeTop-GeneBee server[4] and represented using TreeView X 0.5.1 (Glasgow University).

RESULTS AND DISCUSSION

The *bss-bbs* Cluster Is Involved in the Anaerobic Degradation of Toluene and *m*-Xylene in *Azoarcus* sp. CIB

As indicated in the Introduction, the *in silico* analysis of the genome sequence of *Azoarcus* sp. CIB revealed a gene cluster of 26 open reading frames most of which encode orthologous of the Bss and Bbs proteins involved in the peripheral pathway for the anaerobic degradation of toluene in several bacteria. This cluster is located in the close vicinity of the *mbd* genes encoding the 3-methylbenzoyl-CoA anaerobic central pathway (Juárez et al., 2013), strongly suggesting that it constitutes the *bss-bbs* cluster for the anaerobic degradation of toluene and *m*-xylene in strain CIB (Zamarro et al., 2016) (**Figure 1B**).

Since the toluene peripheral pathway was shown to be inducible when bacteria grow in the presence of toluene (Coschigano, 2000; Achong et al., 2001; Hermuth et al., 2002; Kube et al., 2004; Kühner et al., 2005), we checked whether the expression of the *bss-bbs* genes was inducible when *Azoarcus* sp. CIB cells were grown anaerobically on toluene or *m*-xylene with respect to the use of succinate or benzoate as sole carbon source. The analysis of the RT-PCR amplification products revealed that the expression of the *bssA* and *bbsA* genes is induced when the cells grow in the presence of toluene or *m*-xylene as sole carbon sources (**Figures 3A,B**), suggesting their participation in the anaerobic degradation of both aromatic hydrocarbons.

Usually the transcription of anaerobic degradation pathways is regulated by the presence of oxygen in the culture medium

[1]http://www.ncbi.nlm.nih.gov

[2]http://blast.ncbi.nlm.nih.gov

[3]http://www.ebi.ac.uk/Tools/msa/clustalw2/

[4]http://www.genebee.msu.su/services/phtree_reduced.html

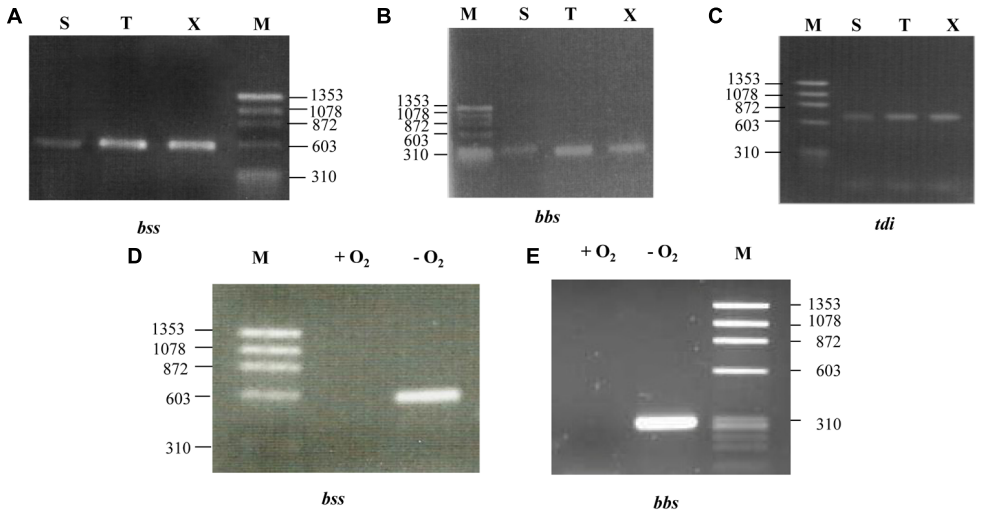

FIGURE 3 | The expression of the *bss, bbs* and *tdi* genes is inducible in *Azoarcus* sp. CIB. Agarose gel electrophoresis of the RT-PCR products. Gene expression was monitored by RT-PCR as described in Section "Materials and Methods" with the primer pairs bssA5new/bssA3new, bbsA331.3/bbsA5new and tdiRint5/tdiSF.3 (Supplementary Table S1) that amplify a *bssA* gene fragment **(A,D)**, a *bbsA* gene fragment **(B,E)**, or the *tdiS-tdiR* intergenic region **(C)**, respectively. **(A–C)** *Azoarcus* sp. CIB cells were grown anaerobically until mid-exponential phase by using 0.2% succinate (S), 250 mM of toluene (T) or 250 mM *m*-xylene (X) as sole carbon source. **(D,E)** *Azoarcus* sp. CIB cells were grown under anaerobic ($-O_2$) or aerobic ($+O_2$) conditions using toluene as only carbon source. Lanes M, molecular size markers (HaeIII-digested ΦX174 DNA); numbers indicate the sizes of the markers (in bp).

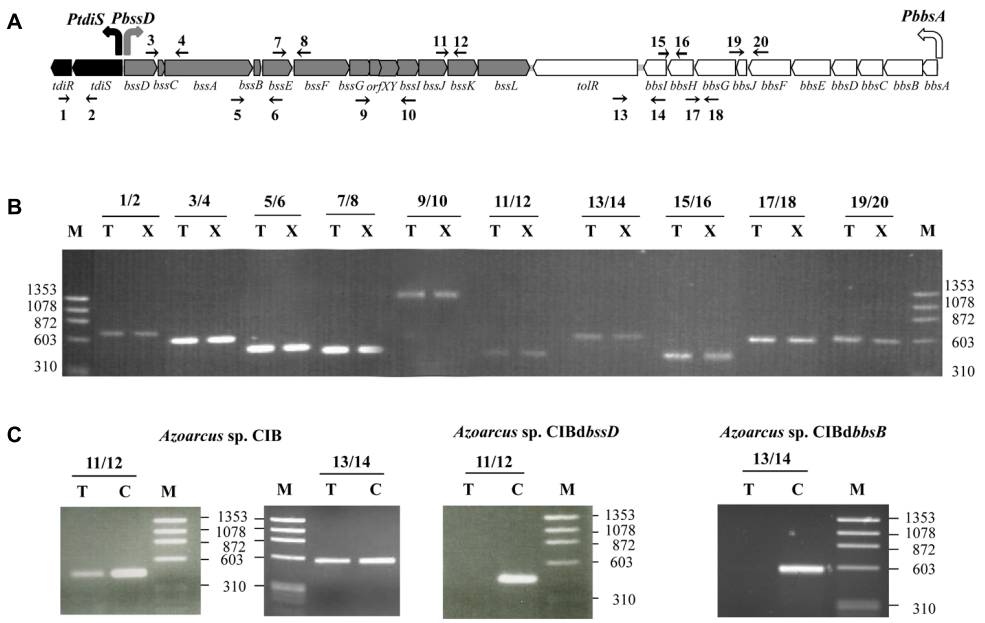

FIGURE 4 | Transcriptional organization of the *tdi-bss-bbs* genes: **(A)** Schematic representation of the *tdi-bss-bbs* gene cluster from *Azoarcus* sp. CIB. The regulatory *tdi* genes are indicated by black arrows; the catabolic *bss* and *bbs* genes are indicated by gray and white arrows, respectively. The *PtdiS*, *PbssD* and *PbbsA* promoters are represented by bent arrows. The intergenic regions whose expression was checked by RT-PCR are marked by the oligonucleotides (thin arrows) used in the analysis (1–20; see Supplementary Table S1). **(B)** Agarose gel electrophoresis of RT-PCR products. RT-PCRs from *Azoarcus* sp. CIB cells grown under denitrifying conditions on 250 mM toluene (lanes T) or 250 mM *m*-xylene (lanes X) were performed as described in Section "Materials and Methods." The numbers correspond to each primer pair that amplifies each of the intergenic regions indicated in **(A)**. Lanes M, molecular size markers (HaeIII-digested ΦX174 DNA); numbers indicate the sizes of the markers (in bp). **(C)** RT-PCRs from *Azoarcus* sp. CIB, *Azoarcus* sp. CIBd*bssD* and *Azoarcus* sp. CIBd*bbsB* cells anaerobically grown until stationary phase in 0.2% pyruvate plus 250 mM toluene (lanes T) by using the oligonucleotide pairs 11/12 and 13/14 (Supplementary Table S1). Lanes C, PCRs performed with the same primer pairs and with genomic DNA as a positive control. Lanes M, molecular size markers (HaeIII-digested ΦX174 DNA); numbers indicate the sizes of the markers (in bp).

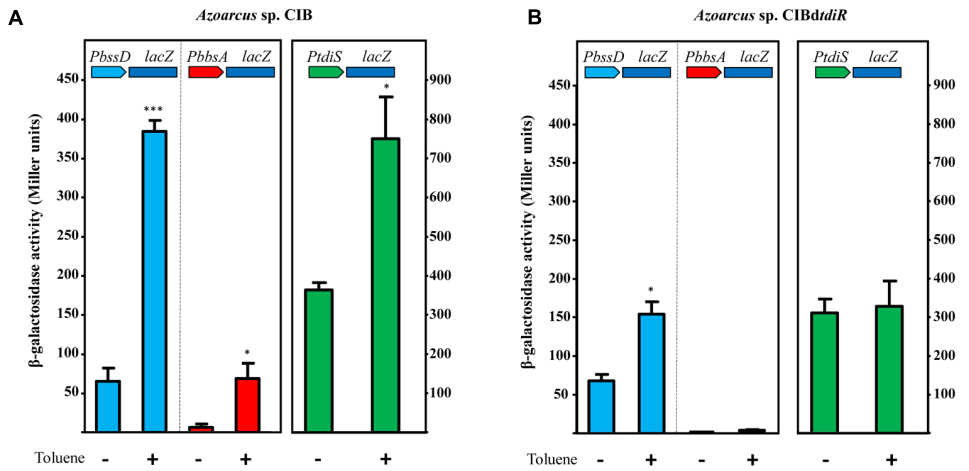

FIGURE 5 | TdiR is a transcriptional activator of the *PbssD*, *PbbsA* and *PtdiS* promoters. Cells of *Azoarcus* sp. CIB **(A)** or *Azoarcus* sp. CIBd*tdiR* **(B)** containing plasmids pBBRPbssD, pBBRPbbsA, or pBBRPtdiS that express the *PbssD::lacZ*, *PbbsA::lacZ,* or *PtdiS::lacZ* translational fusions, respectively, were grown anaerobically on 0.2% pyruvate (–) or 0.2% pyruvate plus toluene (+) until stationary growth phase. β-galactosidase activity values were determined as detailed in Section "Materials and Methods." Error bars represent standard deviation of three different experiments, and asterisks mark the results that are statistically significant (unpaired *t*-test; ***P-value < 0.001, *P-value 0.01–0.05).

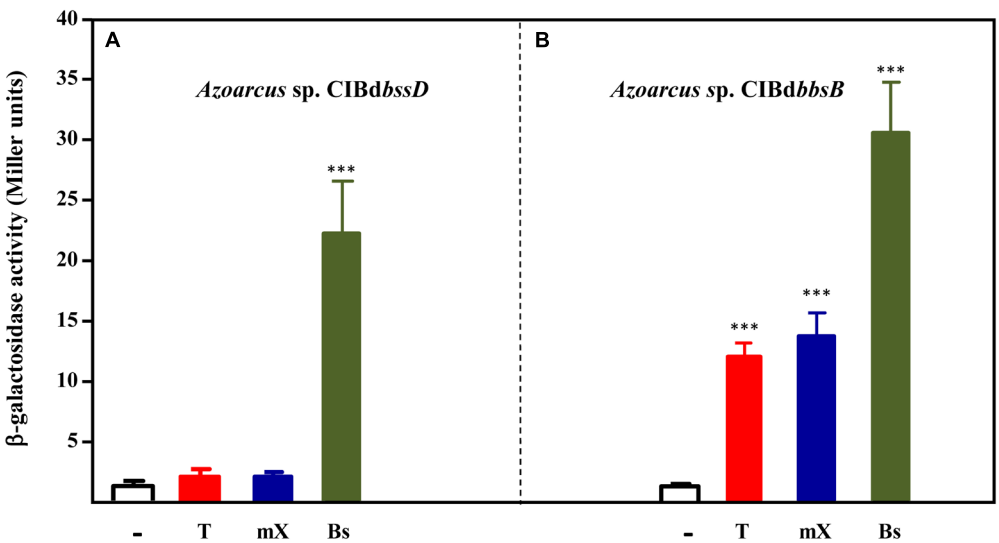

FIGURE 6 | Analysis of the inducers of the *PbbsA* promoter. Cells of *Azoarcus* sp. CIBd*bssD* **(A)** or *Azoarcus* sp. CIBd*bbsB* **(B)** containing plasmid pBBRPbbsA that expresses the *PbbsA::lacZ* translational fusion, were grown anaerobically until stationary growth phase in 0.2% pyruvate (–) or in 0.2% pyruvate plus toluene (T), *m*-xylene (mX), or benzylsuccinate (Bs). β-galactosidase activity values were determined as detailed in Section "Materials and Methods." Error bars represent standard deviation of three different experiments, and asterisks mark the results that are statistically significant (unpaired *t*-test; ***P-value < 0.001).

(Durante-Rodríguez et al., 2006; Carmona et al., 2009; Juárez et al., 2013). To determine if the *bss-bbs* cluster from *Azoarcus* sp. CIB is under oxygen control, gene expression studies were performed with cells grown with toluene as sole carbon source under aerobic or anaerobic conditions. RT-PCR experiments showed that the *bssA* and *bbsA* genes are expressed only under anoxic conditions (**Figures 3D,E**). A similar oxygen-dependent expression of the *bss* genes was reported in *Magnetospirillum* sp. TS-6 (Shinoda et al., 2005), and it appears to be consistent with the fact that BSS is a strictly anaerobic enzyme (Beller and Spormann, 1998; Leuthner et al., 1998; Heider et al., 2016). Nevertheless, the oxygen-dependent regulation of the anaerobic toluene degradation pathway may differ from one strain to another since the *bss* genes from *Thauera* sp. DNT-1 were shown to be transcribed both in aerobic and anaerobic conditions (Shinoda et al., 2004).

To confirm that the *bss-bbs* cluster described above was responsible for the anaerobic degradation of toluene and *m*-xylene in *Azoarcus* sp. CIB, we constructed CIB mutant strains with insertional disruptions within some of the *bss* and *bbs* genes

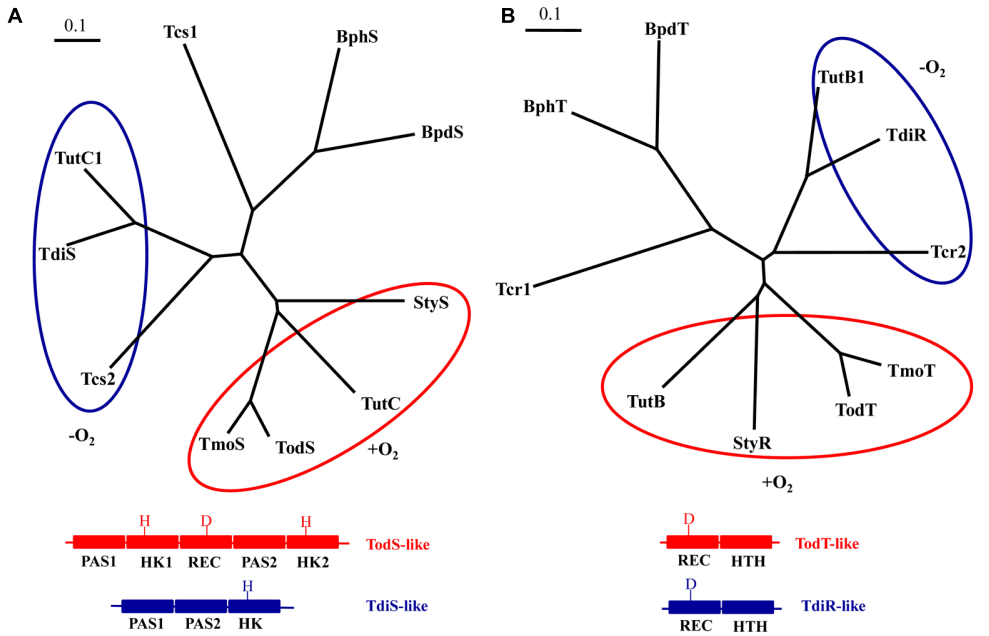

FIGURE 7 | Phylogenetic relationships of the two-component regulatory systems involved in the regulation of aromatic hydrocarbon catabolic pathways: **(A)** Phylogenetic tree built from the multiple amino acid sequence alignment of the sensor histidine kinases TdiS from *Azoarcus* sp. CIB (ABK15651), TutC1 from *T. aromatica* T1 (AAD12187), Tcs2 from "*A. aromaticum*" sp. EbN1 (YP_158339), StyS from *Pseudomonas* sp. Y2 (CAA03998), TutC from *P. mendocina* (AAL13332), TodS from *P. putida* DOT-T1 (AAC45438), TmoS from *P. mendocina* (AAL13333), Tcs1 from *A. aromaticum* sp. EbN1 (YP_158337), BphS from *Rhodococcus* sp. RHA1 (BAC75411) and BpdS from *Rhodococcus* sp. M5 (AAB52543) using the program CLUSTALW and visualized with the TreeView software application. The aerobic TodS-like and anaerobic TdiS-like families are circled by red and blue lines, respectively, and a scheme of their different domain architecture and primary structure is shown at the bottom. PAS, HK, and REC correspond to the PAS sensor, autokinase and receiver domains, respectively. H and D indicate the presence of key phosphorylatable histidine and aspartic acid residues at the HK and REC domains, respectively. **(B)** Phylogenetic tree built from the multiple amino acid sequence alignment of the regulatory protein TdiR from *Azoarcus* sp. CIB (ABK15650), TutB1 from *T. aromatica* T1 (AAD12186), Tcr2 from "*A. aromaticum*" sp. EbN1 (YP_158340), TutB from *T. aromatica* T1 (AAD12186), StyR from *Pseudomonas* sp. Y2 (CAA03999), TodT from *P. putida* DOT-T1 (CAB43736), TmoT from *P. mendocina* (AAL13333), Tcr1 from *A. aromaticum* sp. EbN1 (YP_158338), BphT from *Rhodococcus* sp. RHA1 (BAC75412) and BpdT from *Rhodococcus* sp. M5 (AAB52544) using the program CLUSTALW and visualized with the TreeView software application. The aerobic TodT-like and anaerobic TdiR-like families are circled by red and blue lines, respectively, and a scheme of their similar domain architecture but different primary structure is shown at the bottom. REC and HTH correspond to the receiver and helix-turn-helix DNA-binding domains, respectively. D indicates the presence of key phosphorylatable aspartic acid residue at the REC domain. The bars represent one inferred amino acid substitution per ten amino acids.

that are orthologous to those that have been reported or suggested to be essential for toluene degradation in other bacteria. Thus, we constructed the *Azoarcus* sp. CIBd*bssD*, and CIBd*bbsB* mutant strains harboring the *bssD* and *bbsB* disrupted genes, respectively (**Table 1**). As expected, none of the two mutant strains was able to use toluene as the sole carbon and energy source under anaerobic conditions (**Table 1**). Interestingly, none of the mutant strains was also able to use anaerobically *m*-xylene as carbon source (**Table 1**). Although inactivation of the *bssA* gene in *Azoarcus* sp. strain T was shown previously to prevent anaerobic growth on *m*-xylene (Achong et al., 2001), and (3-methyl)benzylsuccinate was proposed to be converted into 3-methylbenzoyl-CoA via a modified β-oxidation pathway (**Figure 1A**) (Krieger et al., 1999), a genetic demonstration that the *bbs* genes were indeed needed for the anaerobic growth on *m*-xylene was still lacking. In fact, some studies had suggested the existence of separate Bbs isoenzymes in toluene and *m*-xylene catabolism (Leutwein and Heider, 2002). However, our results reveal that both the *bss* and *bbs* genes are essential for the anaerobic degradation of toluene and *m*-xylene in *Azoarcus* sp. CIB.

So far, only the *bssDCABE* genes have been shown to be essential for the anaerobic conversion of toluene to benzylsuccinate (Leuthner et al., 1998; Krieger et al., 2001; Bhandare et al., 2006; Funk et al., 2014; Heider et al., 2016). However, the *bss* cluster contains additional genes of unknown function that are conserved in all toluene degraders, e.g., the *bssF* gene, or that are restricted to *bss* clusters from beta-proteobacteria, e.g., the *bssGIJKL* genes (**Figure 2**) (Kube et al., 2004; Carmona et al., 2009; Kim et al., 2014). To gain further knowledge on whether these additional *bss* genes might be essential for the initial reaction of the toluene/*m*-xylene degradation pathway, we constructed *Azoarcus* sp. CIB mutant strains with disruptional insertions within the *bssF* and *bssJ* genes. Whereas the strain *Azoarcus* sp. CIBd*bssF* was unable to grow anaerobically in toluene or *m*-xylene as sole carbon sources, the strain *Azoarcus* sp. CIBd*bssJ* could use these two aromatic hydrocarbons as growth substrates (**Table 1**). Therefore, these results reveal that inactivation of *bssF* prevents the anaerobic growth on toluene and *m*-xylene, and suggest that this gene and/or any of the downstream co-transcribed genes, i.e., *bssG,*

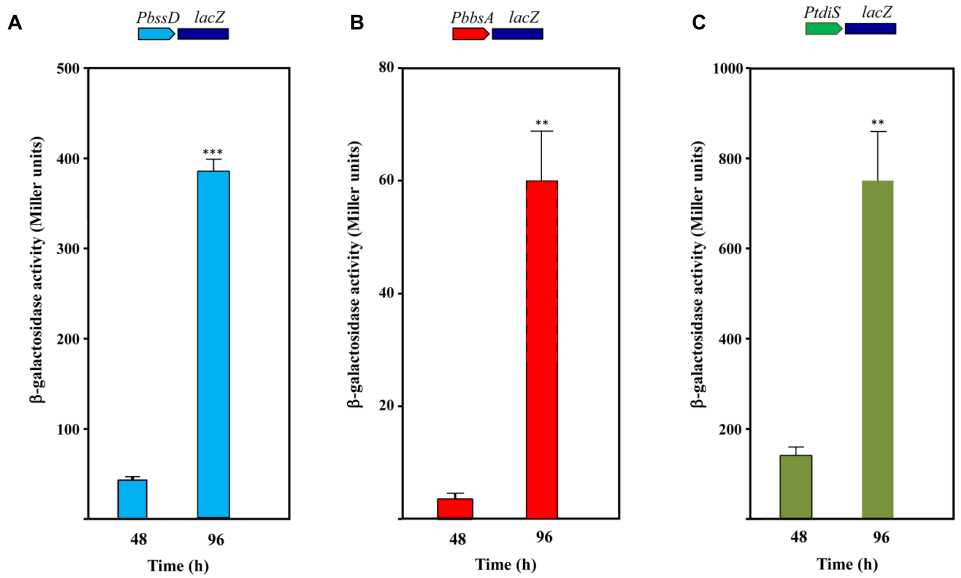

FIGURE 8 | Carbon catabolite control of the *PbbsA*, *PbssD* and *PtdiS* promoters in *Azoarcus* sp. CIB. *Azoarcus* sp. CIB cells containing plasmid pBBRPbssD (*PbssD::lacZ* fusion) **(A)**, pBBRPbbsA (*PbbsA::lacZ* fusion) **(B)** or pBBRPtdiS (*PtdiS::lacZ* fusion) **(C)** were grown anaerobically in 0.2% pyruvate plus 250 mM toluene, and after 72 h they were supplemented with an additional amount of 10 mM nitrate. Culture samples were collected at mid-exponential phase (48 h) or at stationary phase (96 h). β-galactosidase activity values were determined as detailed in Section "Materials and Methods." Error bars represent standard deviation of three different experiments, and asterisks mark the results that are statistically significant (unpaired *t*-test; ***P-value < 0.001, **P-value 0.001–0.01).

orfXY, bssI (see below), are needed for the synthesis of a functional BSS enzyme. The BssF protein (580 amino acids) does not show significant similarity to other proteins of known function, which precludes so far any prediction of its functional role in the BSS activity. On the other hand, although the BssJ protein (307 amino acids) appears to be not essential for the BSS activity, we cannot rule out its involvement in toluene degradation by, for instance, mediating in the stress response caused by toxic aromatic hydrocarbons (Trautwein et al., 2008).

Transcriptional Organization of the *bss-bbs* Gene Cluster

The organization of the genes within the *bss-bbs* cluster in *Azoarcus* sp. CIB is very similar to that observed in other beta-proteobacteria (**Figure 2**). The *bss* and *bbs* genes are arranged in two opposite orientations and most of the genes are separated by very short distances suggesting that they constitute two convergent operons (Zamarro et al., 2016) (**Figure 4A**). The existence of the *bssDCABEFGH* catabolic operon has been described in "*A. aromaticum*" EbN1 (Kube et al., 2004), but it is not known whether these genes are cotranscribed with the *bssIJKLM* genes. On the contrary, whereas the *bss* cluster from *Azoarcus* sp. strain T contains a *bssDCABE* operon and a transcriptional initiation site upstream of *bssF* (Achong et al., 2001), the *tutE* (*bssD*) gene of *T. aromatica* T1 constitutes an operon different to that formed by *tutFDGH* (*bssCABE*) (Coschigano, 2000). On the other hand, the transcriptional organization of the *bbs* cluster has not been elucidated so far in any bacteria.

Since a transcriptional analysis of the whole gene cluster for anaerobic toluene and *m*-xylene degradation in bacteria has not been reported so far, we aimed to validate the presumed transcriptional organization of the *bss-bbs* genes in strain CIB. To this end, we performed RT-PCR experiments using total RNA harvested from *Azoarcus* sp. CIB cells grown anaerobically in toluene or *m*-xylene as sole carbon sources, and different primer sets that amplify *bssD-bssC* (3/4), *bssB-bssE* (5/6), *bssE-bssF* (7/8), *bssG-orfX-orfY-bssI* (9/10), *bssJ-bssK* (11/12), *tolR-bbsI* (13/14), *bbsI-bbsH* (15/16), *bbsH-bbsG* (17/18) and *bbsJ-bbsF* (19/20) gene fragments (**Figure 4A**). The results obtained (**Figure 4B**) strongly suggest that the *bssD-L* and *bbsA-tol* genes are co-transcribed and, therefore, constitute two separate convergent operons. To confirm that the *bss* and *bbs* genes constitute two separate operons, we performed gene expression studies in the *Azoarcus* sp. CIBd*bssD* and CIBd*bbsB* mutant strains that harbor insertional disruptions within the *bssD* and *bbsB* genes, respectively (**Table 1**). To this end, the two mutant strains were grown anaerobically in the presence of toluene, and RT-PCR analyses revealed the lack of expression of the *bss* and *bbs* genes (**Figure 4C**), hence suggesting that the mutations caused polar effects on the expression of the genes located dowsntream of the insertion site and, therefore, that these genes are co-transcribed. Therefore, all these data taken together suggest that in *Azoarcus* sp. CIB the *bssD-L* and *bbsA-tol* genes are arranged as two separate convergent operons. A comparative analysis of the upstream regions of the *bssD* and *bbsA* genes in different *Azoarcus, Aromatoleum, Thauera,* and *Herminiimonas* strains confirmed the existence of the previously proposed *PbssD* and *PbbsA* promoters, respectively (Supplementary Figure S1). *PbssD*

and *PbbsA* contain potential −10/−35 sequences recognized by the RNA polymerase as well as the transcription initiation sites which have been mapped for *bssD* in *T. aromatica* (Coschigano, 2000; Hermuth et al., 2002; Kube et al., 2004) and *Azoarcus* sp. strain T (Achong et al., 2001), and for *bbsA* in *T. aromatica* K172 (Leuthner and Heider, 2000). Similar *PbssD* and *PbbsA* promoter regions driving the expression of the *bss* and *bbs* operons were identified in *Azoarcus* sp. CIB (**Figure 4A** and Supplementary Figure S1). Although an internal promoter or RNA processing event was reported upstream of *bssC* in some *Thauera* strains (Coschigano, 2000; Hermuth et al., 2002), the predicted stem-loop structure resembling a RNase processing site (Hermuth et al., 2002) is not observed in the *bss* operon of *Azoarcus* sp. CIB.

A couple of conserved genes, i.e., *tdiS* (*tutC1*) and *tdiR* (*tutB1*), are located upstream of the *bss* genes in most anaerobic toluene degraders from the beta-proteobacteria group (**Figure 2**). These two genes were proposed to code for a two-component regulatory system that regulates transcription of the catabolic *bss* genes (Coschigano, 2000; Achong et al., 2001; Hermuth et al., 2002; Kube et al., 2004; Kühner et al., 2005). A couple of orthologous *tdiSR* genes are also divergently transcribed with respect to the *bss* genes in *Azoarcus* sp. CIB (**Figures 1B**, **2**, **4A**). RT-PCR studies revealed that *tdiS* and *tdiR* are co-transcribed (**Figure 4B**) and, therefore, constitute an operon controlled by the *PtdiS* promoter in *Azoarcus* sp. CIB (**Figure 4A**). Moreover, the *tdiSR* operon appears to be slightly inducible when the cells grow anaerobically in toluene or *m*-xylene (**Figure 3C**), thus suggesting a common regulatory mechanism for the catabolic (*bss, bbs*) and predicted regulatory (*tdiSR*) genes in strain CIB.

All these results taken together constitute the first transcriptional analysis of the whole gene cluster responsible for the anaerobic peripheral pathway for toluene and *m*-xylene degradation in a single bacterial strain. In *Azoarcus* sp. CIB these genes are organized in two catabolic operons, *bssDCABEFGIJJKL* and *bbsABCDEFJGHtol,* and a putative regulatory operon, *tdiSR*, that are inducible when cells grow in toluene and *m*-xylene.

tdiSR Control the Expression of the *bss-bbs* Genes in *Azoarcus* sp. CIB

To confirm the implication of the *tdiSR* genes in the anaerobic degradation of toluene and *m*-xylene in *Azoarcus* sp. CIB, we constructed two mutant strains, *Azoarcus* sp. CIBd*tdiS* and *Azoarcus* sp. CIBd*tdiR*, that harbor disruptional insertions within the *tdiS* (allows expression of *tdiR* from the kanamycin resistance gene, see Supplementary Figure S2) and *tdiR* genes, respectively. The two mutant strains were unable to grow using toluene or *m*-xylene as sole carbon sources (**Table 1**), thus suggesting that the *tdiSR* genes are involved in the anoxic degradation of toluene/*m*-xylene and they are likely behaving as an activator system of the *PbssD* and/or *PbbsA* promoters.

To study further the role of TdiSR in the activation of the *PbssD* and *PbbsA* promoters in *Azoarcus* sp. CIB, we constructed plasmids pBBRPbssD and pBBRPbbsA that contain the *PbssD::lacZ* and *PbbsA::lacZ* translational fusions, respectively (**Table 1**). The *Azoarcus* sp. CIB strains containing plasmid pBBRPbssD or pBBRPbbsA were grown anaerobically in the absence or presence of toluene or *m*-xylene, and β-galactosidase assays were performed at the end of the growth curve. As shown in **Figure 5A**, the presence of toluene increased the activity of the *PbssD* and *PbbsA* promoters by more than fivefold with respect to the activity observed in the absence of toluene (similar results were obtained with *m*-xylene, data not shown). These results are in agreement with the observed induction of the *bss* and *bbs* genes when *Azoarcus* sp. CIB grows anaerobically in toluene (**Figures 3A,B**). Moreover, the activity of the *PbssD* promoter appears to be significantly higher than that of the *PbbsA* promoter both in the absence or presence of toluene (**Figure 5A**). We then analyzed the activity of the *PbssD* and *PbbsA* promoters in the *Azoarcus* sp. CIBd*tdiR* mutant strain harboring the pBBRPbssD or pBBRPbbsA plasmids. In contrast to the wild-type strain, the *Azoarcus* sp. CIBd*tdiR* (pBBRPbbsA) strain did not show β-galactosidase activity even in the presence of toluene (**Figure 5B**), which strongly suggests that TdiR acts as an essential activator of the *PbbsA* promoter. On the other hand, the *Azoarcus* sp. CIBd*tdiR* (pBBRPbssD) strain revealed that the activity of the *PbssD* promoter region in the absence of toluene did not increase as much as in the wild-type strain in the presence of toluene (**Figure 5B**), suggesting that although TdiR is needed for a full induction of *bss* genes, there is some TdiR-independent activation of *PbssD* when the cells are in the presence of toluene.

Since the expression of the *tdiSR* genes is also induced when *Azoarcus* sp. CIB grows in the presence of toluene (**Figure 3C**), we checked whether the *tdiR* gene product could also act as a transcriptional activator of its own *PtdiS* promoter. To accomplish this, we constructed plasmid pBBRPtdiS, that contains the *PtdiS::lacZ* translational fusion (**Table 1**), and monitored the β-galactosidase activity in *Azoarcus* sp. CIB (pBBRPtdiS) and *Azoarcus* sp. CIBd*tdiR* (pBBRPtdiS) strains grown anaerobically in the absence or presence of toluene. Toluene increased the activity of the *PtdiS* promoter by more than twofold with respect to the activity observed in the absence of toluene in the wild-type but not in the *tdiR* mutant strain (**Figure 5**).

All these results taken together reveal for the first time that the *tdiSR* genes, which are highly conserved in the anaerobic toluene degradation clusters of beta-proteobacteria, encode an activator system of the promoters that drive expression of the *bss* and *bbs* catabolic genes and of that controlling transcription of the *tdi* regulatory genes in the presence of toluene. Whereas the expression of the *bbs* genes is strictly dependent on TdiR, the induction of the *bss* genes appears to be controlled by TdiR and some additional factors that respond to the presence of toluene in *Azoarcus* sp. CIB, and whose characterization requires further research.

Benzylsuccinate Might Be the Inducer Molecule of the TdiSR-Mediated Control

As described above, the expression of the *tdi-bss-bbs* genes is inducible in *Azoarcus* sp. CIB cells growing in the presence of toluene and *m*-xylene (**Figures 3**, **4**). In *T. aromatica* T1, benzylsuccinate or any other further intermediate in the toluene peripheral pathway (**Figure 1A**), was suggested

to be the inducer of the *tut*(*bss*) genes (Coschigano and Bishop, 2004). To determine if toluene and/or *m*-xylene, or an intermediate metabolite derived from the anaerobic degradation of the former, are the true inducers of the TdiSR-mediated control of the peripheral pathway in *Azoarcus* sp. CIB, we analyzed the expression of the *PbbsA::lacZ* fusion in different CIB strains. We selected CIB mutants strains that lack: (i) the first enzymatic step for the conversion of toluene/*m*-xylene to benzylsuccinate/(3-methyl)benzylsuccinate, i.e., *Azoarcus* sp. CIBd*bssD,* which does not express the *bss* operon (**Figure 4C**); (ii) the modified β-oxidation pathway that converts benzylsuccinate/(3-methyl)benzylsuccinate to the central intermediates benzoyl-CoA/3-methylbenzoyl-CoA (**Figure 1**), i.e., *Azoarcus* sp. CIBd*bbsB*, which does not express the *bbs* operon (**Figure 4C**). *Azoarcus* sp. CIBd*bssD* (pBBRPbbsA) cells grown anaerobically on pyruvate or pyruvate supplemented with toluene or *m*-xylene as inducers showed very low β-galactosidase activity in all the tested conditions, thus suggesting that none of the two aromatic hydrocarbons is the real inducer of the *bbs* operon (**Figure 6A**). On the contrary, *Azoarcus* sp. CIBd*bbsB* (pBBRPbbsA) cells, which retain a functional *bss* operon and should be capable to transform toluene and *m*-xylene accumulating benzylsuccinate and (3-methyl)benzylsuccinate, respectively, presented β-galactosidase activity when they were cultivated anaerobically in the presence of toluene or *m*-xylene (**Figure 6B**). Therefore, all these data suggest that benzylsuccinate and (3-methyl)benzylsuccinate, rather than toluene and *m*-xylene, are the real inducers of the *bbs* genes. In agreement with this hypothesis, the two *Azoarcus* sp. CIB mutant strains grown anaerobically in the presence of benzylsuccinate showed activation of the *PbbsA* promoter (**Figure 6**). Interestingly, none of *Azoarcus* strains could use benzylsuccinate as sole carbon and energy source, suggesting a poor uptake of this compound inside the cells.

Taken together all these results reveal that benzylsuccinate is the inducer compound of the TdiSR-mediated control of the toluene peripheral pathway in *Azoarcus* sp. CIB. Although a similar regulatory scenario can be predicted in other toluene degrader denitrifying bacteria, such as in *Thauera* strains (Coschigano and Bishop, 2004), benzylsuccinate may not always behave as the inducer molecule. Thus, it was reported that "*A. aromaticum*" EbN1 strain grown in a mixture of pyruvate and benzylsuccinate did not induce the expression of *bssA* or the formation of Bss/Bbs proteins (Kühner et al., 2005). Nevertheless, the lack of induction of benzylsuccinate in strain EbN1 could be due to unefficient transport of this molecule or to putative pyruvate-dependent catabolite repression of the *bss-bbs* genes, as it was shown in strain CIB (see below), and therefore further studies should be carried out to confirm whether benzylsuccinate behaves also as an inducer molecule in "*A. aromaticum*" EbN1.

Two-component regulatory systems that consist of a sensor histidine kinase and its cognate transcriptional regulator have been shown to be involved in the control of the catabolism of aromatic hydrocarbons in several bacteria (Carmona et al., 2008). According to their primary structure and molecular architecture, the sensor histidine kinases of these two-component regulatory systems can be classified in at least three different phylogenetic groups, i.e., the TodS, TdiS and BphS groups (**Figure 7A**). Hybrid histidine kinases of the TodS family are complex enzymes that contain two sensor PAS domains, i.e., PAS1, that recognizes aromatic hydrocarbons (Busch et al., 2007), and PAS2, involved in dimerization (Koh et al., 2016), two transmitter (autokinase) domains, and a response regulator receiver domain (**Figure 7A**) (Busch et al., 2009). They are involved in the control of the genes for the aerobic degradation of toluene in *Pseudomonas putida* (TodS) (Busch et al., 2007), *P. mendocina* (TmoS) (Silva-Jiménez et al., 2012) and, probably, in *T. aromatica* (TutC) (Leuthner and Heider, 1998), and styrene in some *Pseudomonas* strains (StyS) (Velasco et al., 1998; Leoni et al., 2003). Histidine kinases of the TdiS group are shorter than TodS-like kinases. They contain two tandem PAS domains, PAS1 and PAS2, and a single transmitter domain (**Figure 7A**), and are encoded in the clusters for the anaerobic degradation of toluene in some strains of the genera *Azoarcus*/"*Aromatoleum*" (TdiS) (Achong et al., 2001); *Thauera* (TdiS/TutC1) (Leuthner and Heider, 1998) and *Herminiimonas* (**Figure 2**), as well as in the cluster for the anaerobic degradation of ethylbenzene in "*A. aromaticum*" sp. EbN1 (Tcs2) (Kühner et al., 2005). On the other hand, the large histidine-kinases BphS and BpdS from *Rhodococcus* sp. RHA1 and *Rhodococcus* sp. M5, respectively, are involved in the aerobic degradation of biphenyls and they harbor a N-terminal domain similar to that of serine/threonine kinases and a C-terminal histidine-kinase domain (Takeda et al., 2010). It is worth noting that the amino acid residues shown to be involved in the binding to the inducer in the PAS1 domain of TodS, i.e., Phe46, Ile74, Phe79 and Ile114, are conserved in PAS1 domains of other TodS family members but not in any of the PAS domains of TdiS-like proteins. This observation is in agreement with the fact that TodS family members recognize aromatic hydrocarbons as inducers (Busch et al., 2007; Busch et al., 2009; Koh et al., 2016) but TdiS-like histidine kinases may respond to an intermediate, i.e., a benzylsuccinate derivative, rather than to the precursor aromatic hydrocarbon.

The response regulators of the two component regulatory systems that control the catabolism of aromatic hydrocarbons show a similar modular architecture with a N-terminal receiver domain that contains the phosphoaccepting Asp residue (putative Asp58 in TdiR) and a C-terminal helix-turn-helix (HTH) DNA-binding domain of the NarL/FixJ family separated by a glutamine-rich Q linker (**Figure 7B**) (Milani et al., 2005). As with the sensor histidine kinases, three different phylogenetic groups can be identified when comparing their cognate response regulator partners, i.e., the TodT, TdiR and BphT groups (**Figure 7B**). The 3D-structure of the HTH domain of StyR shows four α helices, one of them responsible of DNA recognition with three residues (Lys175, Val176 and His179) putatively involved in the interaction with the operator region of the cognate promoter (Milani et al., 2005). The same amino acid residues are conserved in other StyR-like regulators, such as TodT, TutB and TmoT, all of which may recognize the consensus ATAAACN$_4$GTTTAT sequence at their corresponding operator regions (Lacal et al., 2006; Silva-Jiménez et al., 2012). Interestingly, these residues are not conserved in the HTH

domains of the anaerobic TdiR-like response regulators, which were proposed to recognize a different palindromic region, GGTGTTCGCACC, that is conserved upstream of the −35 regions at the *PbssD* and *PbbsA* promoters of different anaerobic toluene degraders (Supplementary Figure S1) (Kube et al., 2004).

In *T. aromatica* T1 the genes *tutC1* (*tdiS*) and *tutB1* (*tdiR*) are separated from the *tutEFDGH (bssDCABE)* catabolic genes by *tutB* and *tutC* (**Figure 2**). The products of the *tutB* and *tutC* genes show high identity with TodS and TodT regulators, respectively, rather than with TdiS and TdiR regulators (**Figure 7**), thus strongly suggesting that TutBC are involved in the aerobic catabolism of toluene in *T. aromatica* T1 (Leuthner and Heider, 1998). However, the observation that a mutation in the *tutB* gene disabled the capacity to grow anaerobically in toluene (Coschigano and Young, 1997) and reduced significantly the expression of the *bss* genes (Coschigano and Bishop, 2004), might suggest the existence of some cross-talk in the regulation of the aerobic and anaerobic toluene degradation pathways in *T. aromatica* T1.

Carbon Catabolite Repression of the Toluene/*m*-Xylene Peripheral Pathway in *Azoarcus* sp. CIB

The expression of the genes responsible of the catabolism of aromatic compounds is usually under carbon catabolite control when the cells grow in the presence of preferred carbon sources. This catabolite repression phenomenon has been extensively studied in the aerobic catabolism of aromatic compounds (Marqués et al., 1994; Cases et al., 1996; Carmona et al., 2008; Rojo, 2010), and it has also been described for the central pathways involved in the anaerobic catabolism of aromatic compounds in *T. aromatica* (Heider et al., 1998) and *Azoarcus* sp. CIB (López-Barragán et al., 2004; Carmona et al., 2009; Juárez et al., 2013; Valderrama et al., 2014). However, there were no reports about the expression of the peripheral pathways for anaerobic degradation of aromatic hydrocarbons when bacteria grow in the presence of alternative carbon sources.

To determine if the expression of the toluene/*m*-xylene anaerobic peripheral pathway in *Azoarcus* sp. CIB is under catabolite repression, we checked the activation of the *PbbsA* and *PbssD* promoters in *Azoarcus* sp. CIB (pBBRPbbsA) and *Azoarcus* sp. CIB (pBBRPbssD) cells, respectively, grown in minimal medium containing toluene plus an additional carbon source, e.g, pyruvate, glutamate, glutarate or benzoate. All the carbon sources tested produced an inhibitory effect on the induction of *PbbsA* and *PbssD* promoters, but this inhibition disappeared when the cells reached the stationary phase of growth and consumed the preferred carbon source (**Figures 8A,B**). In contrast, the induction of these promoters was observed at the exponential and stationary growth phases when the cells were grown in toluene as sole carbon source (Supplementary Figure S3). These results suggest that the *bss* and *bbs* genes are under carbon catabolite repression, but induction of these genes can be observed at the stationary growth phase as reported above (**Figures 5**, **6**). Interestingly, we also observed a pyruvate-dependent catabolite repression of the *PtdiS* promoter when *Azoarcus* sp. CIB (pBBRPtdiS) cells were grown in minimal medium containing toluene plus pyruvate, and this repression was alleviated at the stationary phase of growth (**Figure 8C**). Thus, catabolite repression of the *tdiST* regulatory operon might be a major reason of the observed repression by organic acids of the TdiSR-dependent expression of the *bss-bbs*-genes in *Azoarcus* sp. CIB. Although carbon catabolite repression by organic acids had been reported in the aerobic catabolism of toluene in some bacteria (Duetz et al., 1996; Ruíz et al., 2004; Busch et al., 2010), catabolite repression of the peripheral pathway for the anaerobic degradation of toluene has not been shown before.

Evolutionary Considerations on the Toluene Peripheral Pathway

A detailed sequence comparison analysis of the organization of the *bss-bbs* genes in different beta-proteobacteria revealed the existence of a region that shows a high variability among strains. Thus, the *bssG-bssI* intergenic region contains a *bssH* gene encoding a putative transporter in "*A. aromaticum*" EbN1, but this gene is lacking in *Herminiimonas* sp. CN, and is substituted by *orfX-orfY*, two genes of unknown function, in *Azoarcus* sp. CIB and *A. toluclasticus* MF63 strains (**Figure 2**). Interestingly, this region divides the *bss-bbs* cluster of the CIB and MF63 strains into two different DNA fragments according to their GC content, i.e., a fragment containing the *bssDCABEFG* genes and whose GC content (58%) is lower that than of the fragment containing the rest of the *bss* (*bssIJKL*) and *bbs* genes, whose GC content (65%) matches the average GC content of the *Azoarcus* genome. It is worth noting that the *bssDCABE* genes from *Azoarcus* sp. T, *T. aromatica* T1 and *Thauera* sp. DNT-1 have also a GC content (<57%) lower than the average GC content (65%) described for *Azoarcus/Thauera* strains (Liu et al., 2013; Martín-Moldes et al., 2015). On the contrary, the GC content of the *bssDCABE* genes from "*A. aromaticum*" EbN1, *T. aromatica* K172 and *Magnetospirillum* sp. TS-6 is close to the average GC content of the corresponding species. These observations suggest that the *bssDCABEFG* genes from *Azoarcus* sp. CIB, *Azoarcus* sp. T, *T. aromatica* T1 and *Thauera* sp. DNT-1 have an evolutionary origin different than that of their orthologous from *Magnetospirillum* sp. TS-6, "*A. aromaticum*" EbN1 and T. *aromatica* K172, and most probably they come from a microorganism, such as a *Hermimiimonas*-related strain, with a GC content lower than that of *Thauera* or *Azoarcus* strains. Interestingly, this subgrouping of Bss orthologs has also a reflect in the subtle differences observed in their reaction mechanism when using stable isotope tools (Kummel et al., 2013).

Analysis of the flanking regions of the *tdi-bss-bbs* cluster in *Azoarcus* sp. CIB revealed the presence of full or truncated mobile genetic elements (**Figure 2**). Thus, next to the *tdiSR* genes there is a sequence (Δ*istA*) encoding the first amino acids of a truncated IS*21* transposase. *istA/istB* genes encoding the two subunits of a IS*21* transposase are located adjacent to the *bbs* genes in "*A. aromaticum*" EbN1 (**Figure 2**) (Kube et al., 2004). On the other hand, next to the *bbs* operon of strain CIB there is a set of genes (*orfB-E*) (**Figure 2**) that are orthologous to *c1A68*, *c1A87*, *c1A90,* and *c1A92* genes that encode proteins of unknown function and are located

within the cluster for anaerobic degradation of ethylbenzene in "*A. aromaticum*" EbN1 strain (Rabus et al., 2002). These genes are also present in a similar organization next to the *bbs* genes in *A. toluclasticus* MF63 (**Figure 2**). Downstream of the *orfB-E* genes in strain CIB there are three additional genes encoding two complete and one truncated IS*4* transposase (**Figure 2**). All these observations strongly suggest that the *bss-bbs* genes in *Azoarcus* sp. CIB and some closely related bacteria have been acquired by horizontal gene transfer events as a result of different genetic rearrangements. A different genetic organization is observed in the *bss-bbs* clusters from phylogenetically distant delta-proteobacteria toluene-degrading obligate anaerobes, e.g., *Geobacter* or *Desulfobacula* (**Figure 2**) (Carmona et al., 2009; Wöhlbrand et al., 2013). The different genetic organization of the toluene peripheral pathway in facultative and obligate anaerobes correlates also with the significant differences found both in the predicted regulatory genes, e.g., TetR-like and XylR-like regulators are present in obligate anaerobes versus TdiSR-like regulators present in facultative anaerobes (**Figure 2**), and in the catabolic genes, e.g., *bss* and genes involved in auxiliary functions for Bss and Bbs enzymes are also distinct in facultative and strict anaerobes (**Figure 2**) (Wöhlbrand et al., 2013; Bozinovski et al., 2014). In summary, despite the biochemical strategy to convert toluene into benzoyl-CoA via benzylsuccinate appears to be shared by most anaerobic toluene-degraders, the complete set of genetic determinants involved in this peripheral pathway may have arisen through different evolutionary events in facultative and obligate anaerobes.

CONCLUSION

Toluene and *m*-xylene are important contaminant hydrocarbons that tend to accumulate in subsurface anoxic environments. We have shown here that the *bss* and *bbs* genes are essential for the anaerobic degradation of toluene and *m*-xylene in *Azoarcus* sp. CIB. Moreover, we have characterized for the first time the transcriptional organization and regulation of a complete cluster encoding the peripheral pathway for the anaerobic degradation of toluene and *m*-xylene in bacteria. Benzylsuccinate and (3-methyl)benzylsuccinate were shown to be the inducer molecules recognized by the TdiSR two-component regulatory system that specifically controls the activation of the *bss*, *bbs* and *tdi* operons in *Azoarcus* sp. CIB. In addition to the TdiSR-mediated specific control, the expression of the *bss* and *bbs* genes in *Azoarcus* sp. CIB is under an overimposed regulation that depends on certain environmental factors, such as the presence/absence of oxygen or the availability of preferred carbon sources (catabolite repression). Interestingly, our results indicate that the *bss* and *bbs* operons from *Azoarcus* sp. CIB display differential regulation in the presence of toluene. Whereas the activity of the *PbbsA* promoter is strictly dependent on TdiR, the activation of the *PbssD* promoter is also under control of unknown factor(s) triggered by the presence of the aromatic hydrocarbons. Moreover, it is worth noting that the *PbssD* promoter shows a significant basal activity when the cells grow in the absence of toluene/*m*-xylene. This basal activity and the TdiR-independent activation of *PbssD* by toluene could be a strategy to increase the organism's capacity to react quickly to transient toluene availability. Thus, the presence of basal levels of BSS enzyme in the cell will facilitate the formation of some inducer intermediate (benzylsuccinate) and, therefore, the subsequent full induction of all regulatory and catabolic genes when the cells face the presence of the aromatic hydrocarbons. Our results are in agreement with recent reports which suggest that *bssA* transcription may occur at a basal level even in the absence of toluene, supporting the idea that detection of *bssA* gene transcripts alone is not sufficient to indicate toluene degradation activity in contaminated environments (Brow et al., 2013; Lünsmann et al., 2016). In this context, and for a reliable assessment of microbial activity in toluene-contaminated samples, we propose here to monitor the expression of the tightly regulated *bbs* genes as an alternative or complementary approach to the current methods based only on the study of *bssA* expression. In this sense, highly conserved nucleotide sequence regions within the *bbsAB* genes of different bacteria could be used to design degenerate oligonucleotides primers for amplification of a *bbs* gene probe. Finally, the TdiSR-*PbbsA* regulatory couple identified in this work might constitute also an interesting genetic tool to develop whole cell biosensors for detecting benzylsuccinate, a widely used metabolic biomarker of *in situ* anaerobic bioremediation of toluene-contaminated sites (Young and Phelps, 2005).

AUTHOR CONTRIBUTIONS

BB carried out the practical work. BB, MC, and ED designed the experiments, analyzed the results, and wrote the manuscript.

FUNDING

This work was supported by grants BIO2012-39501, BIO2016-79736-R, and PCIN-2014-113 from the Ministry of Economy and Competitiveness of Spain and by a grant of Fundación Ramón Areces XVII CN. We acknowledge support of the publication fee by the CSIC Open Access Publication Support Initiative through its Unit of Information Resources for Research (URICI).

ACKNOWLEDGMENTS

We thank A. Valencia for technical assistance and Secugen S. L. for DNA sequencing.

SUPPLEMENTARY MATERIAL

The Supplementary Material for this article can be found online at: https://www.frontiersin.org/articles/10.3389/fmicb.2018.00506/full#supplementary-material

REFERENCES

Achong, G. R., Rodriguez, A. M., and Spormann, A. M. (2001). Benzylsuccinate synthase of *Azoarcus* sp. strain T: cloning, sequencing, transcriptional organization, and its role in anaerobic toluene and *m*-xylene mineralization. *J. Bacteriol.* 183, 6763–6770. doi: 10.1128/JB.183.23.6763-6770.2001

Altschul, S., Gish, W., Miller, W., Myers, E., and Lipman, D. (1990). Basic local alignment search tool. *J. Mol. Biol.* 215, 403–410. doi: 10.1016/S0022-2836(05)80360-2

Beller, H. R., and Spormann, A. M. (1998). Analysis of the novel benzylsuccinate synthase reaction for anaerobic toluene activation based on structural studies of the product. *J. Bacteriol.* 180, 5454–5457.

Bertani, G. (1951). Studies on lysogenesis. I. The mode of phage liberation by lysogenic *Escherichia coli*. *J. Bacteriol.* 62, 293–300.

Bhandare, R., Calabroa, M., and Coschigano, P. W. (2006). Site-directed mutagenesis of the *Thauera aromatica* strain T1 *tutE tutFDGH* gene cluster. *Biochem. Biophys. Res. Commun.* 346, 992–998. doi: 10.1016/j.bbrc.2006.05.199

Blázquez, B., Carmona, M., García, J. L., and Díaz, E. (2008). Identification and analysis of a glutaryl-CoA dehydrogenase-encoding gene and its cognate transcriptional regulator from *Azoarcus* sp. CIB. *Environ. Microbiol.* 10, 474–482. doi: 10.1111/j.1462-2920.2007.01468.x

Bozinovski, D., Taubert, M., Kleinsteuber, S., Richnow, H. H., von Bergen, M., Vogt, C., et al. (2014). Metaproteogenomic analysis of a sulfate-reducing enrichment culture reveals genomic organization of key enzymes in the *m*-xylene degradation pathway and metabolic activity of proteobacteria. *Syst. Appl. Microbiol.* 37, 488–501. doi: 10.1016/j.syapm.2014.07.005

Brow, C. N., O'Brien Johnson, R., Johnson, R. L., and Simon, H. M. (2013). Assessment of anaerobic toluene biodegradation activity by *bssA* transcript/gene ratios. *Appl. Environ. Microbiol.* 79, 5338–5344. doi: 10.1128/AEM.01031-13

Busch, A., Guazzaroni, M. E., Lacal, J., Ramos, J. L., and Krell, T. (2009). The sensor kinase TodS operates by a multiple step phosphorelay mechanism involving two autokinase domains. *J. Biol. Chem.* 284, 10353–10360. doi: 10.1074/jbc.M900521200

Busch, A., Lacal, J., Martos, A., Ramos, J. L., and Krell, T. (2007). Bacterial sensor kinase TodS interacts with agonistic and antagonistic signals. *Proc. Natl. Acad. Sci. U.S.A.* 104, 13774–13779. doi: 10.1073/pnas.0701547104

Busch, A., Lacal, J., Silva-Jímenez, H., Krell, T., and Ramos, J. L. (2010). Catabolite repression of the TodS/TodT two-component system and effector-dependent transphosphorylation of TodT as the basis for toluene dioxygenase catabolic pathway control. *J. Bacteriol.* 192, 4246–4250. doi: 10.1128/JB.00379-10

Butler, J. E., He, Q., Nevin, K. P., He, Z., Zhou, J., and Lovley, D. R. (2007). Genomic and microarray analysis of aromatics degradation in *Geobacter metallireducens* and comparison to a *Geobacter* isolate from a contaminated field site. *BMC Genomics* 8:180. doi: 10.1186/1471-2164-8-180

Carmona, M., Prieto, M. A., Galán, B., García, J. L., and Díaz, E. (2008). "Signaling networks and design of pollutants biosensors," in *Microbial Biodegradation: Genomics and Molecular Biology*, ed. E. Díaz (Norfolk, VA: Caister Academic Press), 97–143.

Carmona, M., Zamarro, M. T., Blázquez, B., Durante-Rodríguez, G., Juárez, J. F., Valderrama, J. A., et al. (2009). Anaerobic catabolism of aromatic compounds: a genetic and genomic view. *Microbiol. Mol. Biol. Rev.* 73, 71–133. doi: 10.1128/MMBR.00021-08

Cases, I., de Lorenzo, V., and Pérez-Martín, J. (1996). Involvement of sigma 54 in exponential silencing of the *Pseudomonas putida* TOL plasmid *Pu* promoter. *Mol. Microbiol.* 19, 7–17. doi: 10.1046/j.1365-2958.1996.345873.x

Chakraborty, R., and Coates, J. D. (2004). Anaerobic degradation of monoaromatic hydrocarbons. *Appl. Microbiol. Biotechnol.* 64, 437–446. doi: 10.1007/s00253-003-1526-x

Chaurasia, A. K., Tremblay, P. L., Holmes, D. E., and Zhang, T. (2015). Genetic evidence that the degradation of para-cresol by *Geobacter metallireducens* is catalyzed by the periplasmic *para*-cresol methylhydroxylase. *FEMS Microbiol. Lett.* 362:fnv145. doi: 10.1093/femsle/fnv145

Coschigano, P. W. (2000). Transcriptional analysis of the *tutE tutFDGH* gene cluster from *Thauera aromatica* strain T1. *Appl. Environ. Microbiol.* 66, 1147–1151. doi: 10.1128/AEM.66.3.1147-1151.2000

Coschigano, P. W., and Bishop, B. J. (2004). Role of benzylsuccinate in the induction of the *tutE tutFDGH* gene complex of *T. aromatica* strain T1. *FEMS Microbiol. Lett.* 231, 261–266. doi: 10.1016/S0378-1097(04)00005-9

Coschigano, P. W., and Young, L. Y. (1997). Identification and sequence analysis of two regulatory genes involved in anaerobic toluene metabolism by strain T1. *Appl. Environ. Microbiol.* 63, 652–660.

de Lorenzo, V., and Timmis, K. N. (1994). Analysis and construction of stable phenotypes in gram-negative bacteria with Tn*5*- and Tn*10*-derived minitransposons. *Methods Enzymol.* 235, 386–405. doi: 10.1016/0076-6879(94)35157-0

Duetz, W. A., Marqués, S., Wind, B., Ramos, J. L., and van Andel, J. G. (1996). Catabolite repression of the toluene degradation pathway in *Pseudomonas putida* harboring pWW0 under various conditions of nutrient limitation in chemostat culture. *Appl. Environ. Microbiol.* 62, 601–606.

Durante-Rodríguez, G., Zamarro, M. T., García, J. L., Díaz, E., and Carmona, M. (2006). Oxygen-dependent regulation of the central pathway for the anaerobic catabolism of aromatic compounds in *Azoarcus* sp. strain CIB. *J. Bacteriol.* 188, 2343–2354. doi: 10.1128/JB.188.7.2343-2354.2006

Felsenstein, J. (1993). *PHYLIP (Phylogenetic Inference Package) Version 3.5.1*. Seattle, WA: University of Washington.

Fernández, H., Prandoni, N., Fernández-Pascual, M., Fajardo, S., Morcillo, C., Díaz, E., et al. (2014). *Azoarcus* sp. CIB, an anaerobic biodegrader of aromatic compounds shows an endophytic lifestyle. *PLoS One* 9:e110771. doi: 10.1371/journal.pone.0110771

Fernández-Llamosas, H., Castro, L., Blázquez, M. L., Díaz, E., and Carmona, M. (2016). Biosynthesis of selenium nanoparticles by *Azoarcus* sp. CIB. *Microb. Cell Fact.* 15:109. doi: 10.1186/s12934-016-0510-y

Ferrández, A., Miñambres, B., García, B., Olivera, E. R., Luengo, J. M., García, J. L., et al. (1998). Catabolism of phenylacetic acid in *Escherichia coli*. Characterization of a new aerobic hybrid pathway. *J. Biol. Chem.* 273, 25974–25986. doi: 10.1074/jbc.273.40.25974

Foght, J. (2008). Anaerobic biodegradation of aromatic hydrocarbons: pathways and prospects. *J. Mol. Microbiol. Biotechnol.* 15, 93–120. doi: 10.1159/000121324

Funk, M. A., Judd, E. T., Marsh, E. N., Elliott, S. J., and Drennan, C. L. (2014). Structures of benzylsuccinate synthase elucidate roles of accessory subunits in glycyl radical enzyme activation and activity. *Proc. Natl. Acad. Sci. U.S.A.* 111, 10161–10166. doi: 10.1073/pnas.1405983111

Heider, J., Boll, M., Breese, K., Breinig, S., Ebenau-Jehle, C., Feil, U., et al. (1998). Differential induction of enzymes involved in anaerobic metabolism of aromatic compounds in the denitrifying bacterium *Thauera aromatica*. *Arch. Microbiol.* 170, 120–131. doi: 10.1007/s002030050623

Heider, J., Szaleniec, M., Martins, B. M., Seyhan, D., Buckel, W., and Golding, B. T. (2016). Structure and function of benzylsuccinate synthase and related fumarate-adding glycyl radical enzymes. *J. Mol. Microbiol. Biotechnol.* 26, 29–44. doi: 10.1159/000441656

Hermuth, K., Leuthner, B., and Heider, J. (2002). Operon structure and expression of the genes for benzylsuccinate synthase in *Thauera aromatica* strain K172. *Arch. Microbiol.* 177, 132–138. doi: 10.1007/s00203-001-0375-1

Herrmann, S., Vogt, C., Fischer, A., Kuppardt, A., and Richnow, H. H. (2009). Characterization of anaerobic xylene biodegradation by two-dimensional isotope fractionation analysis. *Environ. Microbiol. Rep.* 1, 535–544. doi: 10.1111/j.1758-2229.2009.00076.x

Juárez, J. F., Liu, H., Zamarro, M. T., McMahon, S., Liu, H., Naismith, J. H., et al. (2015). Unraveling the specific regulation of the central pathway for anaerobic degradation of 3-methylbenzoate. *J. Biol. Chem.* 290, 12165–12183. doi: 10.1074/jbc.M115.637074

Juárez, J. F., Zamarro, M. T., Eberlein, C., Boll, M., Carmona, M., and Díaz, E. (2013). Characterization of the *mbd* cluster encoding the anaerobic 3-methylbenzoyl-CoA central pathway. *Environ. Microbiol.* 15, 148–166. doi: 10.1111/j.1462-2920.2012.02818.x

Kim, S. J., Park, S. J., Jung, M. Y., Kim, J. G., Madsen, E. L., and Rhee, S. K. (2014). An uncultivated nitrate-reducing member of the genus *Herminiimonas* degrades toluene. *Appl. Environ. Microbiol.* 80, 3233–3243. doi: 10.1128/AEM.03975-13

Kimura, M. (1980). A simple method for estimating evolutionary rates of base substitutions through comparative studies of nucleotide sequences. *J. Mol. Evol.* 16, 111–120. doi: 10.1007/BF01731581

Koh, S., Hwang, J., Guchhait, K., Lee, E. G., Kim, S. Y., Kim, S., et al. (2016). Molecular insights into toluene sensing in the TodS/TodT signal transduction system. *J. Biol. Chem.* 291, 8575–8590. doi: 10.1074/jbc.M116.718841

Krieger, C. J., Beller, H. R., Reinhard, M., and Spormann, A. M. (1999). Initial reactions in anaerobic oxidation of *m*-xylene by the denitrifying bacterium *Azoarcus* sp. strain T. *J. Bacteriol.* 181, 6403–6410.

Krieger, C. J., Roseboom, W., Albracht, S. P., and Spormann, A. M. (2001). A stable organic free radical in anaerobic benzylsuccinate synthase of *Azoarcus* sp. strain T. *J. Biol. Chem.* 276, 12924–12927. doi: 10.1074/jbc.M009453200

Kube, M., Heider, J., Amann, J., Hufnagel, P., Kühner, S., Beck, A., et al. (2004). Genes involved in the anaerobic degradation of toluene in a denitrifying bacterium, strain EbN1. *Arch. Microbiol.* 181, 182–194. doi: 10.1007/s00203-003-0627-3

Kühner, S., Wöhlbrand, L., Fritz, I., Wruck, W., Hultschig, C., Hufnagel, P., et al. (2005). Substrate-dependent regulation of anaerobic degradation pathways for toluene and ethylbenzene in a denitrifying bacterium, strain EbN1. *J. Bacteriol.* 187, 1493–1503. doi: 10.1128/JB.187.4.1493-1503.2005

Kummel, S., Kuntze, K., Vogt, C., Boll, M., Heider, J., and Richnow, H. H. (2013). Evidence for benzylsuccinate synthase subtypes obtained by using stable isotope tools. *J. Bacteriol.* 195, 4660–4667. doi: 10.1128/JB.00477-13

Lacal, J., Busch, A., Guazzaroni, M. E., Krell, T., and Ramos, J. L. (2006). The TodS-TodT two-component regulatory system recognizes a wide range of effectors and works with DNA-bending proteins. *Proc. Natl. Acad. Sci. U.S.A.* 103, 8191–8196. doi: 10.1073/pnas.0602902103

Leoni, L., Ascenzi, P., Bocedi, A., Rampioni, G., Castellini, L., and Zennaro, E. (2003). Styrene-catabolism regulation in *Pseudomonas fluorescens* ST: phosphorylation of StyR induces dimerization and cooperative DNA-binding. *Biochem. Biophys. Res. Commun.* 303, 926–931. doi: 10.1016/S0006-291X(03)00450-9

Leuthner, B., and Heider, J. (1998). A two-component system involved in regulation of anaerobic toluene metabolism in *Thauera aromatica*. *FEMS Microbiol. Lett.* 166, 35–41. doi: 10.1111/j.1574-6968.1998.tb13180.x

Leuthner, B., and Heider, J. (2000). Anaerobic toluene catabolism of *Thauera aromatica:* the *bbs* operon codes for enzymes of β oxidation of the intermediate benzylsuccinate. *J. Bacteriol.* 182, 272–277. doi: 10.1128/JB.182.2.272-277.2000

Leuthner, B., Leutwein, C., Schulz, H., Hörth, P., Haehnel, W., Schiltz, E., et al. (1998). Biochemical and genetic characterization of benzylsuccinate synthase from *Thauera aromatica*: a new glycyl radical enzyme catalysing the first step in anaerobic toluene metabolism. *Mol. Microbiol.* 28, 615–628. doi: 10.1046/j.1365-2958.1998.00826.x

Leutwein, C., and Heider, J. (2001). Succinyl-CoA:(R)-benzylsuccinate CoA-transferase: an enzyme of the anaerobic toluene catabolic pathway in denitrifying bacteria. *J. Bacteriol.* 183, 4288–4295. doi: 10.1128/JB.183.14.4288-4295.2001

Leutwein, C., and Heider, J. (2002). (R)-Benzylsuccinyl-CoA dehydrogenase of *Thauera aromatica*, an enzyme of the anaerobic toluene catabolic pathway. *Arch. Microbiol.* 178, 517–524. doi: 10.1007/s00203-002-0484-5

Liu, B., Frostegård, A., and Shapleigh, J. P. (2013). Draft genome sequences of five strains in the genus *Thauera*. *Genome Announc.* 1:e00052-12. doi: 10.1128/genomeA.00052-12

López-Barragán, M. J., Carmona, M., Zamarro, M. T., Thiele, B., Boll, M., Fuchs, G., et al. (2004). The bzd gene cluster, coding for anaerobic benzoate catabolism, in *Azoarcus* sp. strain CIB. *J. Bacteriol.* 186, 5762–5774. doi: 10.1128/JB.186.17.5762-5774.2004

Lovley, D. R., Baedecker, M. J., Lonergan, D. J., Cozzarelli, I. M., Phillips, E. J. P., and Siegel, D. I. (1989). Oxidation of aromatic contaminants coupled to microbial iron reduction. *Nature* 339, 297–300. doi: 10.1038/339297a0

Lueders, T. (2017). The ecology of anaerobic degraders of BTEX hydrocarbons in aquifers. *FEMS Microbiol. Ecol.* 93:fiw220. doi: 10.1093/femsec/fiw220

Lünsmann, V., Kappelmeyer, U., Taubert, A., Nijenhuis, I., von Bergen, M., Heipieper, H. J., et al. (2016). Aerobic toluene degraders in the rhizosphere of a constructed wetland model show diurnal polyhydroxyalkanoate metabolism. *Appl. Environ. Microbiol.* 82, 4126–4132. doi: 10.1128/AEM.00493-16

Marqués, S., Holtel, A., Timmis, K. N., and Ramos, J. L. (1994). Transcriptional induction kinetics from the promoters of the catabolic pathways of TOL plasmid pWW0 of *Pseudomonas putida* for metabolism of aromatics. *J. Bacteriol.* 176, 2517–2524. doi: 10.1128/jb.176.9.2517-2524.1994

Martín-Moldes, Z., Blázquez, B., Baraquet, C., Harwood, C. S., Zamarro, M. T., and Díaz, E. (2016). Degradation of cyclic diguanosine monophosphate by a hybrid two-component protein protects *Azoarcus* sp. strain CIB from toluene toxicity. *Proc. Natl. Acad. Sci. U.S.A.* 113, 13174–13179. doi: 10.1073/pnas.1615981113

Martín-Moldes, Z., Zamarro, M. T., del Cerro, C., Valencia, A., Gómez, M. J., Arcas, A., et al. (2015). Whole-genome analysis of *Azoarcus* sp. strain CIB provides genetic insights to its different lifestyles and predicts novel metabolic features. *Syst. Appl. Microbiol.* 38, 462–471. doi: 10.1016/j.syapm.2015.07.002

Meyer-Cifuentes, I., Martinez-Lavanchy, P. M., Marin-Cevada, V., Böhnke, S., Harms, H., Müller, J. A., et al. (2017). Isolation and characterization of *Magnetospirillum* sp. strain 15-1 as a representative anaerobic toluene-degrader from a constructed wetland model. *PLoS One* 12:e0174750. doi: 10.1371/journal.pone.0174750

Milani, M., Leoni, L., Rampioni, G., Zennaro, E., Ascenzi, P., and Bolognesi, M. (2005). An active-like structure in the unphosphorylated StyR response regulator suggests a phosphorylation- dependent allosteric activation mechanism. *Structure* 13, 1289–1297. doi: 10.1016/j.str.2005.05.014

Miller, J. H. (1972). *Experiments in Molecular Genetics*. New York, NY: Cold Spring Harbord Laboratory.

Morasch, B., Schink, B., Tebbe, C. C., and Meckenstock, R. U. (2004). Degradation of o-xylene and m-xylene by a novel sulfate-reducer belonging to the genus *Desulfotomaculum*. *Arch. Microbiol.* 181, 407–417. doi: 10.1007/s00203-004-0672-6

Rabus, R., Boll, M., Heider, J., Meckenstock, R. U., Buckel, W., Einsle, O., et al. (2016). Anaerobic microbial degradation of hydrocarbons: from enzymatic reactions to the environment. *J. Mol. Microbiol. Biotechnol.* 26, 5–28. doi: 10.1159/000443997

Rabus, R., Kube, M., Beck, A., Widdel, F., and Reinhardt, R. (2002). Genes involved in the anaerobic degradation of ethylbenzene in a denitrifying bacterium, strain EbN1. *Arch. Microbiol.* 178, 506–516. doi: 10.1007/s00203-002-0487-2

Rojo, F. (2010). Carbon catabolite repression in *Pseudomonas*: optimizing metabolic versatility and interactions with the environment. *FEMS Microbiol. Rev.* 34, 658–684. doi: 10.1111/j.1574-6976.2010.00218.x

Ruíz, R., Aranda-Olmedo, M. I., Domínguez-Cuevas, P., Ramos-González, M. I., and Marqués, S. (2004). "Transcriptional regulation of the toluene catabolic pathways," in *Pseudomonas Virulence and Gene Regulation*, Vol. 2, ed. J. L. Ramos (New York, NY: Kluwer Academic), 509–537.

Saitou, N., and Nei, M. (1987). The neighbor-joining method: a new method for reconstructing phylogenetic trees. *Mol. Biol. Evol.* 4, 406–425.

Sambrook, J., and Russell, D. W. (2001). *Molecular Cloning: A Laboratory Manual*. New York, NY: Cold Spring Harbor.

Sanger, F., Nicklen, S., and Coulson, A. R. (1977). DNA sequencing with chain-terminating inhibitors. *Proc. Natl. Acad. Sci. U.S.A.* 74, 5463–5467. doi: 10.1073/pnas.74.12.5463

Schäfer, A., Tauch, A., Jäger, W., Kalinowski, J., Thierbach, G., and Pühler, A. (1994). Small mobilizable multi-purpose cloning vectors derived from the *Escherichia coli* plasmids pK18 and pK19: selection of defined deletions in the chromosome of *Corynebacterium glutamicum*. *Gene* 145, 69–73. doi: 10.1016/0378-1119(94)90324-7

Selmer, T., Pierik, A. J., and Heider, J. (2005). New glycyl radical enzymes catalysing key metabolic steps in anaerobic bacteria. *Biol. Chem.* 386, 981–988. doi: 10.1515/BC.2005.114

Shinoda, Y., Akagi, J., Uchihashi, Y., Hiraishi, A., Yukawa, H., Yurimoto, H., et al. (2005). Anaerobic degradation of aromatic compounds by *Magnetospirillum* strains: isolation and degradation genes. *Biosci. Biotechnol. Biochem.* 69, 1483–1491. doi: 10.1271/bbb.69.1483

Shinoda, Y., Sakai, Y., Uenishi, H., Uchihashi, Y., Hiraishi, A., Yukawa, H., et al. (2004). Aerobic and anaerobic toluene degradation by a newly isolated denitrifying bacterium, *Thauera* sp. strain DNT-1. *Appl. Environ. Microbiol.* 70, 1385–1392. doi: 10.1128/AEM.70.3.1385-1392.2004

Silva-Jiménez, H., García-Fontana, C., Cadirci, B. H., Ramos-González, M. I., Ramos, J. L., and Krell, T. (2012). Study of the TmoS/TmoT two-component system: towards the functional characterization of the family of TodS/TodT like systems. *Microb. Biotechnol.* 5, 489–500. doi: 10.1111/j.1751-7915.2011.00322.x

Strijkstra, A., Trautwein, K., Jarling, R., Wöhlbrand, L., Dörries, M., Reinhardt, R., et al. (2014). Anaerobic activation of *p*-cymene in denitrifying betaproteobacteria: methyl group hydroxylation versus addition to fumarate. *Appl. Environ. Microbiol.* 80, 7592–7603. doi: 10.1128/AEM.02385-14

Takeda, H., Shimodaira, J., Yukawa, K., Hara, N., Kasai, D., Miyauchi, K., et al. (2010). Dual two-component regulatory systems are involved in aromatic compound degradation in a polychlorinated-biphenyl degrader, *Rhodococcus jostii* RHA1. *J. Bacteriol.* 192, 4741–4751. doi: 10.1128/JB.00429-10

Thompson, J. D., Higgins, D. G., and Gibson, T. J. (1994). CLUSTAL W: improving the sensitivity of progressive multiple sequence alignment through sequence weighting, position-specific gap penalties and weight matrix choice. *Nucleic Acids Res.* 22, 4673–4680. doi: 10.1093/nar/22.22.4673

Trautwein, K., Kühner, S., Wöhlbrand, L., Halder, T., Kuchta, K., Steinbüchel, A., et al. (2008). Solvent stress response of the denitrifying bacterium "*Aromatoleum aromaticum*" strain EbN1. *Appl. Environ. Microbiol.* 74, 2267–2274. doi: 10.1128/AEM.02381-07

Valderrama, J. A., Durante-Rodríguez, G., Blázquez, B., García, J. L., Carmona, M., and Díaz, E. (2012). Bacterial degradation of benzoate: cross-regulation between aerobic and anaerobic pathways. *J. Biol. Chem.* 287, 10494–10508. doi: 10.1074/jbc.M111.309005

Valderrama, J. A., Shingler, V., Carmona, M., and Díaz, E. (2014). AccR is a master regulator involved in carbon catabolite repression of the anaerobic catabolism of aromatic compounds in *Azoarcus* sp. CIB. *J. Biol. Chem.* 289, 1892–1894. doi: 10.1074/jbc.M113.517714

Velasco, A., Alonso, S., García, J. L., Perera, J., and Díaz, E. (1998). Genetic and functional analysis of the styrene catabolic cluster of *Pseudomonas* sp. Strain Y2. *J. Bacteriol.* 180, 1063–1071.

Verfürth, K., Pierik, A. J., Leutwein, C., Zorn, S., and Heider, J. (2004). Substrate specificities and electron paramagnetic resonance properties of benzylsuccinate synthases in anaerobic toluene and m-xylene metabolism. *Arch. Microbiol.* 181, 155–162. doi: 10.1007/s00203-003-0642-4

Wöhlbrand, L., Jacob, J. H., Kube, M., Mussmann, M., Jarling, R., Beck, A., et al. (2013). Complete genome, catabolic sub-proteomes and key-metabolites of *Desulfobacula toluolica* Tol2, a marine, aromatic compound-degrading, sulfate-reducing bacterium. *Environ. Microbiol.* 15, 1334–1355. doi: 10.1111/j.1462-2920.2012.02885.x

Young, L. Y., and Phelps, C. D. (2005). Metabolic biomarkers for monitoring in situ anaerobic hydrocarbon degradation. *Environ. Health Perspect.* 113, 62–67. doi: 10.1289/ehp.6940

Zamarro, M. T., Martín-Moldes, Z., and Díaz, E. (2016). The ICEXTD of *Azoarcus* sp. CIB, an integrative and conjugative element with aerobic and anaerobic catabolic properties. *Environ. Microbiol.* 18, 5018–5031. doi: 10.1111/1462-2920.13465

Conflict of Interest Statement: The authors declare that the research was conducted in the absence of any commercial or financial relationships that could be construed as a potential conflict of interest.

frontiers in Microbiology

ORIGINAL RESEARCH
published: 15 February 2018
doi: 10.3389/fmicb.2018.00231

Structural and Biochemical Characterization of BdsA from *Bacillus subtilis* WU-S2B, a Key Enzyme in the "4S" Desulfurization Pathway

Tiantian Su[1†], Jing Su[1,2†], Shiheng Liu[1], Conggang Zhang[1], Jing He[1], Yan Huang[1], Sujuan Xu[1] and Lichuan Gu[1]**

[1] State Key Laboratory of Microbial Technology, School of Life Sciences, Shandong University, Jinan, China, [2] Faculty of Light Industry, Province Key Laboratory of Microbial Engineering, Qilu University of Technology (Shandong Academy of Sciences), Jinan, China

OPEN ACCESS

Edited by:
Edgardo Donati, National University of La Plata, Argentina

Reviewed by:
Willem J. H. Van Berkel, Wageningen University & Research, Netherlands
John Joseph Kilbane, Illinois Institute of Technology, United States

***Correspondence:**
Sujuan Xu
xu_sujuan@sdu.edu.cn
Lichuan Gu
lcgu@sdu.edu.cn

† These authors have contributed equally to this work.

Specialty section:
This article was submitted to Microbiotechnology, Ecotoxicology and Bioremediation, a section of the journal Frontiers in Microbiology

Received: *12 September 2017*
Accepted: *30 January 2018*
Published: *15 February 2018*

Citation:
Su T, Su J, Liu S, Zhang C, He J, Huang Y, Xu S and Gu L (2018) Structural and Biochemical Characterization of BdsA from Bacillus subtilis WU-S2B, a Key Enzyme in the "4S" Desulfurization Pathway. Front. Microbiol. 9:231. doi: 10.3389/fmicb.2018.00231

Dibenzothiophene (DBT) and their derivatives, accounting for the major part of the sulfur components in crude oil, make one of the most significant pollution sources. The DBT sulfone monooxygenase BdsA, one of the key enzymes in the "4S" desulfurization pathway, catalyzes the oxidation of DBT sulfone to 2′-hydroxybiphenyl 2-sulfonic acid (HBPSi). Here, we determined the crystal structure of BdsA from *Bacillus subtilis* WU-S2B, at the resolution of 2.2 Å, and the structure of the BdsA-FMN complex at 2.4 Å. BdsA and the BdsA-FMN complex exist as tetramers. DBT sulfone was placed into the active site by molecular docking. Seven residues (Phe12, His20, Phe56, Phe246, Val248, His316, and Val372) are found to be involved in the binding of DBT sulfone. The importance of these residues is supported by the study of the catalytic activity of the active site variants. Structural analysis and enzyme activity assay confirmed the importance of the right position and orientation of FMN and DBT sulfone, as well as the involvement of Ser139 as a nucleophile in catalysis. This work combined with our previous structure of DszC provides a systematic structural basis for the development of engineered desulfurization enzymes with higher efficiency and stability.

Keywords: FMN-binding, dibenzothiophene, desulfurization, monooxygenase, "4S" pathway

INTRODUCTION

The burning of fossil fuels causes worldwide environmental pollution because of the sulfur compounds present in fossil fuels. Hydrodesulfurization (HDS) can remove sulfur from petroleum, but heterocyclic sulfur compounds are difficult to remove completely. Thus, reducing the presence of heterocyclic sulfur compounds, such as dibenzothiophene (DBT) and alkylated DBTs, has become increasingly important. Physical and chemical methods of desulfurization are not economically viable and may cause additional environmental pollution. Therefore, biological desulfurization (BDS) for the treatment of recalcitrant organic sulfur compounds has gained attention (Monticello et al., 1985; Gray et al., 2003).

Numerous efforts have been focused on investigating biodesulfurization systems, using DBT or its alkylated derivatives as model compounds. The pathway specifically cleaving the C-S bond during metabolic desulfurization has been termed the "4S" pathway (**Figure 1**).

The genes, involved in the metabolic desulfurization of the "4S" pathway (*dszABCD*), were first reported in *Rhodococcus* sp. IGTS8 (Denome et al., 1993; Kayser et al., 1993). In the initial step of the desulfurization process, DBT is oxidized into DBT sulfone by DBT monooxygenase DszC. Then, DBT sulfone monooxygenase DszA catalyzes the oxidation of DBT sulfone into 2′-hydroxybiphenyl 2-sulfonic acid (HBPSi). Finally, HBPSi is desulfurized by the HBPSi desulfinase DszB to 2-hydroxybiphenyl (2-HBP) and sulfite (Denome et al., 1994; Gray et al., 1998). Some thermophilic desulfurizing bacteria, such as *Bacillus subtilis* WU-S2B, *Paenibacillus,* and *Pseudomonas*, can grow in the presence of DBT, utilizing DBT as their sole source of sulfur (Konishi et al., 1997; Ishii et al., 2000a; Kahnert and Kertesz, 2000). The DBT desulfurization enzymes, TszABCD, have been isolated from *Paenibacillus* (Ishii et al., 2000b). TszABCD have higher heat stability than DszABCD, but the enzymatic activities of TszABCD are lower than those of DszABCD. The corresponding genes from *Bacillus subtilis* WU-S2B have been identified and the enzymes (BdsABCD) characterized (Kirimura et al., 2001). Additionally, recombinant *Escherichia coli* cells harboring the *bdsABCD* genes exhibit DBT desulfurizing activity at 50°C, and purified BdsA and BdsB have higher enzymatic activities than those of DszA and DszB (Kirimura et al., 2004; Ohshiro et al., 2005). The DNA sequences of BdsABC share high identities (52–73%) with those of DszABC and TdsABC. Multiple conserved proteins motifs have also been identified (Kilbane and Robbins, 2007). These most highly conserved regions could be used to construct improved universal primers for the PCR detection/cloning of bdsA/dszA genes in uncharacterized biodesulfurization-competent microbial cultures, which may help identify possible biodesulfurization genes in genomic data and provide an aid to the annotation of genes in the desulfurization pathway.

The reactions, catalyzed by DBT desulfurization enzymes, have been characterized (Gallagher et al., 1993; Yan et al., 2000; Gray et al., 2003; Kilane, 2006). DszA and DszC belong to Group C of the family of flavin-dependent monooxygenases which contain a TIM-barrel fold and receive reduced flavin from a NAD(P)H-dependent reductase (Montersino et al., 2011; Huijbers et al., 2014). The oxidoreductase DszD supplies the NADH necessary for the activity of monooxygenases DszA and DszC. DszB is a hydrolase that participates in the last desulfurization step and hydrolyzes 2′-hydroxybiphenyl-2-sulfinic acid into 2-hydroxybiphenyl and sulfite. During preliminary characterization research of these enzymes, the results showed that DszB is the rate-limiting enzyme (Abin-Fuentes et al., 2014; Kilbane, 2016). Biological desulfurization can make greater contributions in future, but there exist some issues regarding the catalytic mechanism of key enzymes in the "4S" pathway that need to be resolved.

The structures of these key enzymes, involved in the "4S" pathway, have been studied extensively. The structure of DszB was first reported in 2006, and the reaction mechanism was further illustrated (Lee et al., 2006). The crystal structures of DszC and its complex with FMN have also been reported (Liu et al., 2014; Zhang et al., 2014; Guan et al., 2015), and the homology TdsC has also been reported (Hino et al., 2017). Recently, a liquid chromatography–mass spectrometry analysis showed that the C2 hydroperoxide of the DBT sulfone reacts with reduced flavin to form a flavin-N5-oxide intermediate in DszA, which is involved in subsequent protonation (Adak and Begley, 2016). However, without the structure of BdsA, it is unknown how this process

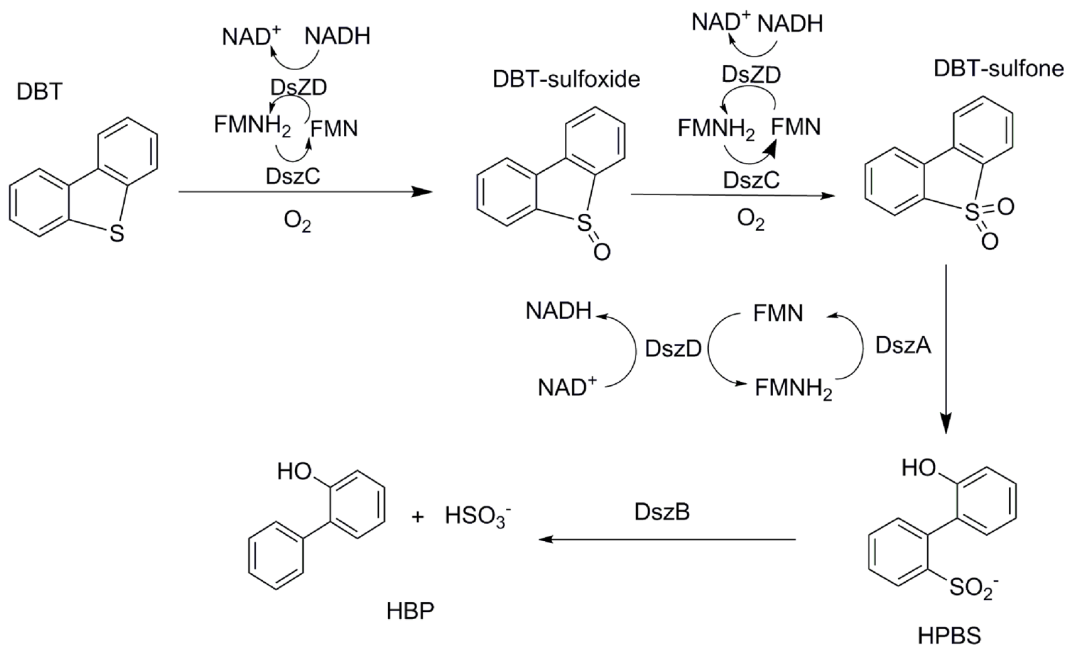

FIGURE 1 | Primary four-step 4S biodesulfurization pathway as adapted from Oldfield et al. (1997).

happens in the active site of BdsA and how the protein enzyme facilitates the reaction.

To further understand the catalytic mechanism of DBT sulfone monooxygenation, we determined the crystal structure of BdsA from *Bacillus subtilis* WU-S2B at the resolution of 2.2 Å, and the structure of the BdsA-FMN complex at 2.4 Å. Site-directed mutagenesis showed that mutations in the residues involved in catalysis or in flavin substrate-binding result in a significant loss of enzymatic activity, which provides valuable clues for elucidating the catalytic mechanism of DBT sulfone monooxygenase.

MATERIALS AND METHODS

Cloning, Protein Expression, and Purification

The *bdsA* gene, from *Bacillus subtilis* WU-S2B, was synthesized and used as the template for PCR amplification. The amplified *bdsA* was inserted into the NdeI and XhoI sites of a pET-15b vector (Novagen) in frame with an N-terminal His-tag; the resulting plasmid was transformed into *E. coli* BL21 (DE3) cells for BdsA overexpression.

Escherichia coli BL21 (DE3) cells, harboring the *bdsA* overexpression plasmid, were grown in Luria-Bertani (LB) medium supplemented with 100 μg/mL ampicillin. The cells were induced by 0.12 mM isopropyl β-D-1-thiogalactopyranoside (IPTG) when the OD_{600} reached 0.9, and were incubated overnight at 22°C. Cells were subsequently harvested by centrifugation (8400 *g* for 15 min) and lysed by ultrasonication in lysis buffer [25 mM Tris-HCl, pH 8.0; 200 mM NaCl; 0.4 mM phenylmethylsulfonyl fluoride (PMSF)]. After centrifugation at 28,000 *g* for 45 min at 4°C, the supernatant was applied to a Ni-NTA affinity column (GE Healthcare) equilibrated in the lysis buffer. The 6× His-tagged BdsA was eluted with elution buffer (25 mM Tris-HCl, pH 8.0; 100 mM NaCl; 250 mM imidazole), followed by further purification by anion exchange on a 16/10 HR Source-15Q column (GE Healthcare) with gradient buffer (Buffer A: 25 mM Tris-HCl, pH 8.0; Buffer B : 25 mM Tris-HCl, pH 8.0, 1 M NaCl), and then by size-exclusion chromatography using a gel-filtration column (Superdex 200 10/300 GL, GE Healthcare) in 10 mM Tris-HCl pH 8.0, 100 mM NaCl. Purified BdsA was analyzed by SDS-PAGE followed by Coomassie brilliant blue staining (R250). The concentrations of purified proteins were determined using Nanodrop (A-280 nm) (Thermo Scientific).

Site-Directed Mutagenesis of BdsA

Site-directed mutagenesis of BdsA was conducted by two-step PCR using the wild-type pET-15b/*bdsA* plasmid as template. The mutant clones were confirmed by DNA sequencing (Invitrogen). The expression and purification processes were the same as that for the wild-type BdsA protein.

Crystallization and Data Collection

For crystallization, the purified BdsA proteins were concentrated to 10–20 mg/mL measured by Nanodrop (A-280nM). Crystals were first screened by sitting drop vapor diffusion using crystallization screen kits (Hampton Research) at 20°C. After optimization, native crystals were obtained from the hanging drops by mixing equal volumes of the protein solution and reservoir solution [0.1 M sodium citrate (pH 5.5) and 35% PEG 200]. To obtain crystals of the BdsA-FMN complex, native crystals were soaked in the solution, containing 0.1 M sodium citrate (pH 5.5), 35% PEG 200 and 1 mM FMN, for 30 min. We also tried to obtain the crystals of the BdsA-FMN-substrate complex by the same means. Unfortunately, the efforts failed.

For data collection, crystals were flash-frozen in liquid nitrogen, with 15–20% (v/v) ethylene glycol used as cryoprotectant. The X-ray diffraction data sets were collected at 100K on a beam line BL17U at the Shanghai Synchrotron Radiation Facility (Shanghai, China) equipped with an ADSC Q315r CCD-detector.

TABLE 1 | X-ray data collection and refinement statistics.

Data collection	Apo	FMN-bound
Space group	P21212	P21212
Unit-cell parameters		
a, b, c (Å)	132.494, 174.574, 85.345	131.616, 175.890, 84.934
α, β, γ (°)	90.00, 90.00, 90.00	90.00, 90.00, 90.00
Wavelength (Å)	0.9870	0.9870
Resolution (Å)	50.00-2.20 (2.28-2.20)	50-2.40 (2.49-2.40)
Unique reflections	98498 (9746)	78295 (7724)
Completeness (%)	99.9 (100)	99.9 (99.9)
Redundancy	6.7 (6.5)	6.8 (6.6)
$I/\sigma(I)$	33.89 (4.72)	29.07 (4.21)
R_{merge} (%)[a]	9.4 (57.0)	10.5 (56.9)
Refinement		
$R_{working}$ (%)	17.47	18.11
R_{free} (%)	21.30	22.11
No. of		
Protein residues	1784 (homotetramer)	1784 (homotetramer)
FMN		4
solvent	446	250
R.m.s.d. from ideal geometry		
Bond length (Å)	0.007	0.010
Bond angles (°)	1.030	1.440
Wilson *B*-value (Å^2)	33.48	36.17
Average *B*-factors (Å^2)		
Protein	41.27	48.79
FMN		47.44
Solvent	40.10	45.04
Ramachandran plot (%)		
Favored	96.85	97.40
Allowed	2.98	2.54
Outliers	0.17	0.06

[a] $R_{merge} = \Sigma_{hkl}\Sigma_i|I_i(hkl) - \langle I(hkl)\rangle|/\Sigma_{hkl}\Sigma_i I_i(hkl)$. *where* $\langle I(hkl)\rangle$ *is the mean intensity of multiply recorded reflections.*

The coordinates and structure factors have been deposited in the Protein Data Bank with the accession code 5XKC (apo-BdsA) and 5XKD (FMN-bound).

Structure Determination and Refinement

The X-ray diffraction data were integrated and scaled using the HKL-2000 program suite (Otwinowski and Minor, 1997). The native BdsA structure was resolved by molecular replacement using Phaser from the CCP4 suit of programs (Winn et al., 2011) with LadA (PDB entry 3B9N) as the search model. Refinement was performed using the PHENIX crystallography suite (Adams et al., 2002) and the COOT interactive model-building program (Emsley and Cowtan, 2004). The final R-values were R_{work} = 17.47% and R_{free} = 21.30% based on a subset of 5% of the reflections. The cofactor FMN was added to the complex model, based on the F*o*–F*c* density map of the ligand structure, and refinement was conducted in the same manner as that for apo-BdsA. The final model had a R_{work} = 18.11% and R_{free} = 22.11% based on a subset of 5% of the reflections.

Diffraction data collection and refinement statistics are listed in **Table 1**. The final models were checked and validated using PROCHECK (Laskowski et al., 1993), QMEAN (Benkert et al., 2008), and ProQ (Cristobal et al., 2001) model quality assessment tools, which indicated that the models were of good quality. Structure graphics were illustrated with the PyMOL molecular visualization system (Lill and Danielson, 2011). The atomic coordinates and structure factors of BdsA and the BdsA-FMN complex were deposited in the Protein Data Bank with accession codes 5XKC and 5XKD, respectively.

Calculations of Enzyme-Substrate Molecular Docking

AutoDock 4.2 was used for the molecular docking calculations (Morris et al., 2009). The substrate coordinates were designed using the Dundee PROGRG server (Schuttelkopf and van Aalten, 2004). The DBT sulfone docking was based on the BdsA-FMN complex structure. The ligands and BdsA were prepared using AutoDockTools, and the BdsA was designed to be rigid. Polar hydrogens and Kollman United Atom charges were added to the enzyme; Gasteiger charges were assigned; and non-polar hydrogen atoms were merged for the ligands. Docking calculations were performed using the default settings for the genetic algorithm parameters with 25,000,000 energy evaluations per run. A composite file of all possible conformers was analyzed by AutoDock Tools. The chemical reasonableness of best results was evaluated by examining the interactions between the BdsA and best-docked conformer.

Enzymatic Activity Assays

The activity of BdsA was determined by measuring the amount of HBPSi using high-performance liquid chromatography (HPLC) according to a method described previously (Ohshiro et al., 1997, 1999). The enzyme reaction system for measuring the activity of BdsA contained 100 mM potassium phosphate buffer (pH 7.0), 0.25 mM DBT sulfone, 6 mM NADH,

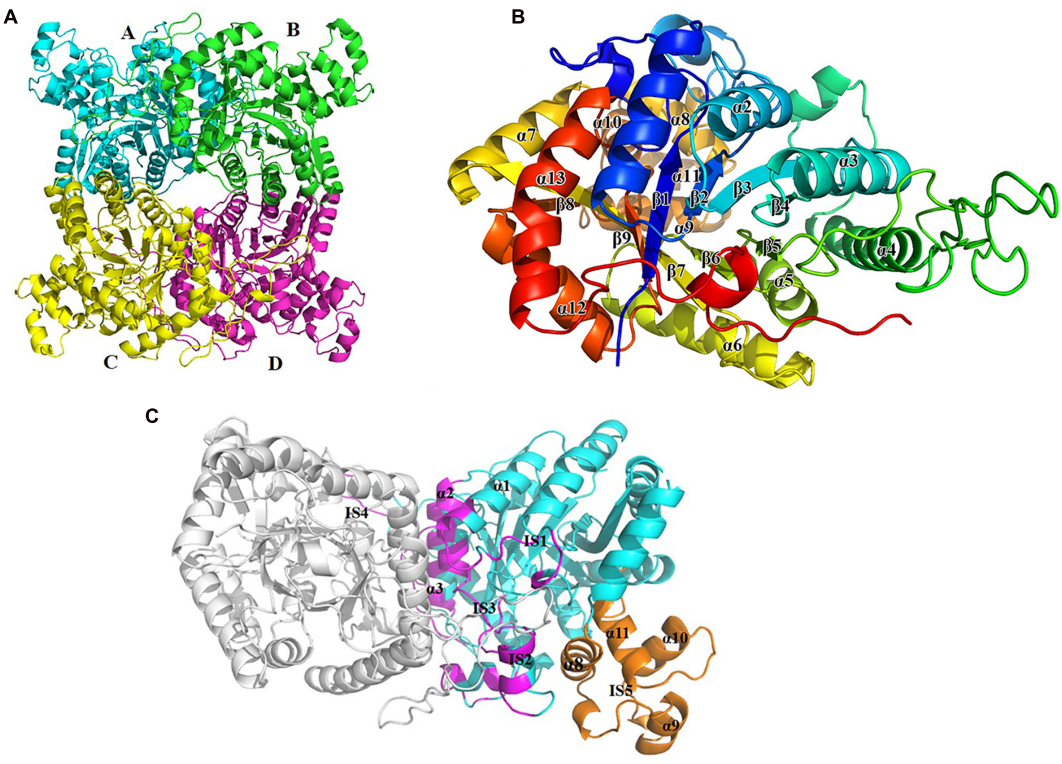

FIGURE 2 | Overall structure of BdsA. **(A)** The four BdsA monomers (A, B, C, and D) forming two homodimers are designated with cartoon in different colors. **(B)** The secondary structures (13 α-helices and 9 β-strands) of BdsA monomer are depicted in rainbow colored cartoon. **(C)** Structure of BdsA dimer. The dimer is shown in cartoon model. Molecule A is in gray color and molecule B is in blue color. The dimer interface consists of α1, IS1, IS2, α2, α3, IS3, and IS4. IS5 separated from the protein core is located between α7 and β8, which contains four small helices (α8, α9, α10, and α11).

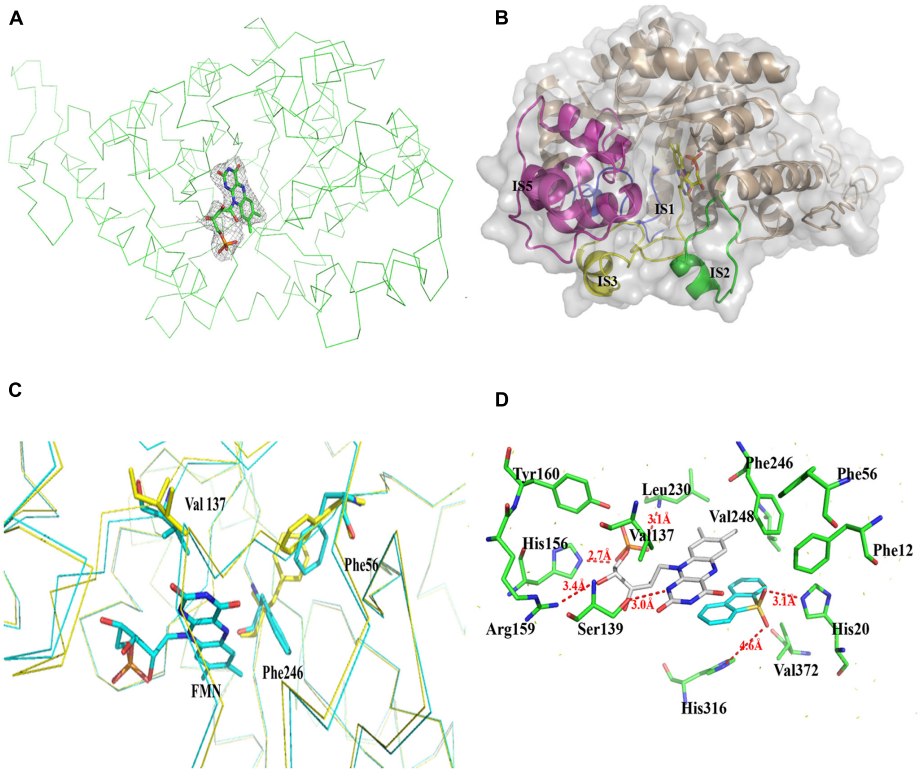

FIGURE 3 | Structure of BdsA-FMN complex. **(A)** The electron density map (contoured at 2.0σ) reveals the existence of FMN within BdsA active pocket. **(B)** The pocket constituting of IS1, IS2, IS3, and IS5 forms the active site of FMN and substrate binding. **(C)** Structure comparison of the apo and FMN bound BdsA. Yellow ribbon represents the apo-BdsA structure and cyan ribbon stands for the FMN bound structure. The FMN is depicted in color sticks. Distinct structural rearrangements occur at residues Phe56, Val137, and Phe246. **(D)** The docking result of the BdsA-FMN-DBT sulfone complex. Residues constituting the binding pocket are shown as green sticks. The cofactor FMN is shown as gray sticks. DBT sulfone is shown as cyan sticks. V137, S139, H156, R159, Y160, and L230 play significant roles in FMN binding. F12, F56, F246, V248, H316, and V372 play directional roles in substrate binding.

10 μM FMN, 20 nM Fre (flavin reductase from *E. coli* O157), and 2 μM BdsA, in a total volume of 1 mL. The reaction was performed with rotary shaking (2000 rpm) at 35°C for 20 min, and stopped by the addition of 100 μL of 12 M HCl. The mixture was extracted with ethyl acetate, centrifuged at 15,000 *g* for 5 min, and then the supernatant was injected into an HPLC system using 20 mM KH_2PO_4 (pH 2.5) and methanol as the mobile phase, at a ratio of 2:3.

The reaction mixture was loaded onto a C18 reversed-phase column (Venusil XBP-C18, Agela Technologies) attached to an HPLC system (LC-10AT pump, SPD-10A UV/VIS detector). An increase in absorbance at 280 nm, which indicates the amount of HBPSi, was observed. The enzymatic assays for all mutants were performed in the same manner as that for the wild-type BdsA protein.

RESULTS

Overall Structure of apo-BdsA

The crystal structure of apo-BdsA (unbound structure) from *Bacillus subtilis* belongs to the P21212 space group with the cell dimension a = 132.494 Å, b = 174.574 Å, and c = 85.345 Å. The asymmetric unit contains four peptide chains, designated A, B, C, and D, which form two homodimers, AB and CD (**Figure 2A**). Each BdsA monomer is composed of 453 amino acids. In the structure of BdsA, the electron densities for the N-terminus to Gln4 and Ser451 to the C-terminus are not visible, likely because these regions are flexible and disordered. In the final model of apo-BdsA, more than 96.85% of the residues were located in the favored regions of the Ramachandran plot and only 2.98% in the generous and allowed regions.

The BdsA monomer contains nine β-strands (β1–β9) and 13 α-helices (α1–α13), which fold into a triosephosphate isomerase (TIM)-barrel with five extended insertion regions (**Figure 2B**). These extended insertion regions are located in the connecting regions between β-strands and α-helices, designated as insertion segments IS1 to IS5 (**Figure 2C**). IS1 is located between β1 and α1, IS2 between β2 and α2, IS3 between β3 and α3, and IS4 between α4 and β5. According to the structure, IS1 to IS4 play important roles in the formation of the BdsA homodimer (**Figure 2C**). IS5 is located between α7 and β8, which contain four small helices (α8, α9, α10, and α11). IS5, the largest insertion region, is separated from the protein core and forms a deep groove with the protein core (**Figures 2B,C**). The deep groove is important in

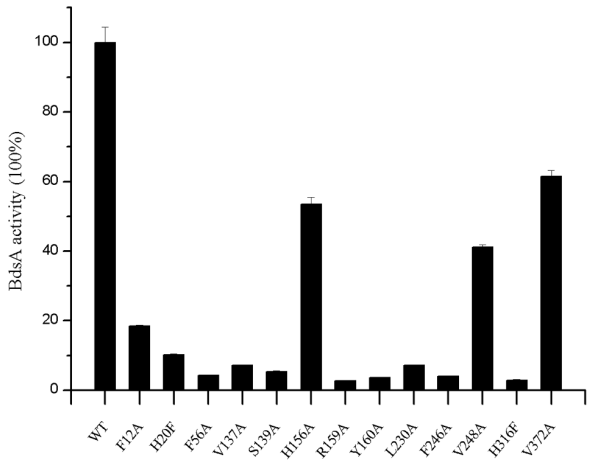

FIGURE 4 | Effects of active site residue mutants on enzyme activity of BdsA. Activity is defined as the number of nmol of HBPSi produced min^{-1} $nmol^{-1}$ in the presence of BdsA. Enzyme assays for all mutants were performed in the same way that the wild-type BdsA protein was tested. Error bars indicate the standard deviation of four repeats. The result figure was generated by origin pro 8.

FMN-binding and substrate catalysis. IS5 forms the entrance for FMN and the substrate.

Tetramer Structure of BdsA

The crystal structure of BdsA shows that there are four molecules in an asymmetric unit (**Figure 2A**). To determine its oligomeric state in solution, we performed gel-filtration experiments using a Superdex-200 column (GE Healthcare) running in 10 mM Tris-HCl (pH 8.0) and 100 mM NaCl. The elution volume of BdsA indicated a molecular mass of ∼220 kDa, indicating that BdsA exists as a tetramer in the solution.

Structure comparison showed that the two homodimers, AB and CD, have a high structural similarity. The root-mean-square deviation (RMSD) value for C_α is 0.165 Å. As predicted by PISA (Krissinel and Henrick, 2005), the AB dimer has a surface area of approximately 3,177 $Å^2$, and CD has a surface area of approximately 3,217 $Å^2$. The dimer interface is extensive and consists predominantly of hydrophobic residues, which are derived from α1, IS1, IS2, α2, α3, IS3, and IS4 (**Figure 2C**).

Structure of the BdsA–FMN Complex

The structure of the tetrameric BdsA–FMN complex contains four FMN molecules, with each subunit binding one FMN (**Figure 3A**). The TIM-barrel structure confirms that BdsA belongs to the group C flavin-dependent monooxygenases. The binding pocket is mainly formed by IS1, IS2, IS3, and IS5 (**Figure 3B**). The overall C_α RMSD between apo-BdsA and the BdsA-FMN complex is only 0.240 Å. The most substantial structural discriminations were observed at the side chains of residues Phe56, Val137, and Phe246 (**Figure 3C**), which may facilitate the binding of FMN.

The binding of FMN to BdsA is maintained through hydrogen bonds and hydrophobic interactions. The flavin ring of FMN lies in the barrel, with its plane nearly parallel with the staves of the barrel, and its si-face exposed to the solvent. There are several hydrogen bonding interactions between BdsA and FMN: the NE2 atom of His 156 with the O3 atom of the flavin phosphate groups (2.7 Å); the OG atom of Ser139 with the N1 atom of the flavin ring (2.8 Å); backbone nitrogen of Leu230 with the phosphate group (3.1 Å); and the Arg159 with the O4 atom of the flavin ring (3.4 Å). Two residues, Tyr160 and Val137, form van der Waals contacts with FMN (**Figure 3D**).

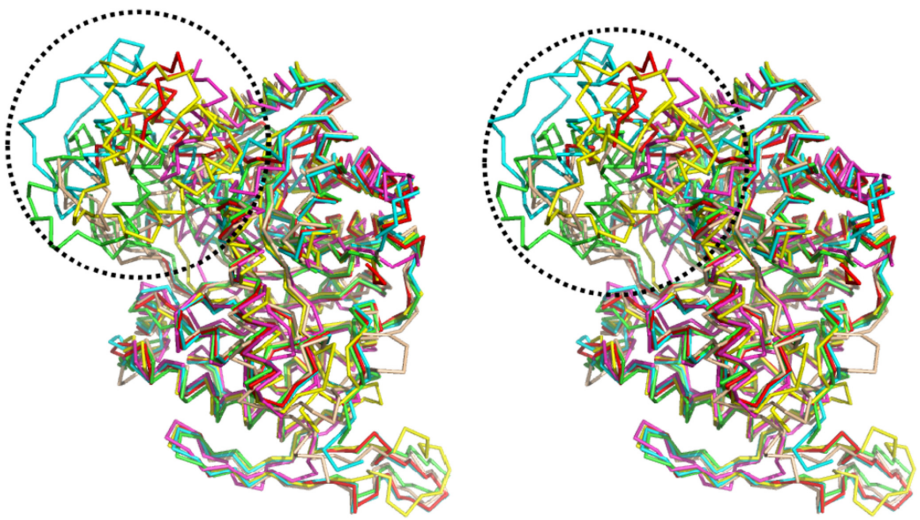

FIGURE 5 | Structure comparison of BdsA with homology structures by the DALI program against Protein Data Bank. BdsA, Ytnj, Lada, Emoa, and Luciferase-like Monooxygenase are illustrated in green, cyan, red, yellow, and magenta, respectively. The most difference in the structure of BdsA range from Val304–Val375 (circled by black dashed line), including α8, α9, α10, and α11. It is the key component of the active pocket, which controls the size of the pocket accompanied with IS1, IS2, and IS3.

Based on the structural analysis, six single-point mutations of BdsA were constructed: V137A, S139A, H156A, R159A, Y160A, and L230A. The secondary structures of mutant BdsA proteins were in good agreement with the wild type protein when examined by circular dichroism spectroscopy (**Supplementary Figure S1**). The results of enzymatic activity showed that mutant proteins V137A, S139A, R159A, Y160A, and L230A completely lost their activity (**Figure 4**). The activity of H156A was decreased by approximately 50% (**Figure 4**). We also showed the superposition of the wild type and variant amino acids, which indicated that all the point mutations significantly disrupt the interactions between the side chains of the active site residues and FMN (**Supplementary Figure S2**). These results indicate that these residues play significant roles in the binding of FMN, which was consistent with the results of the structural analysis.

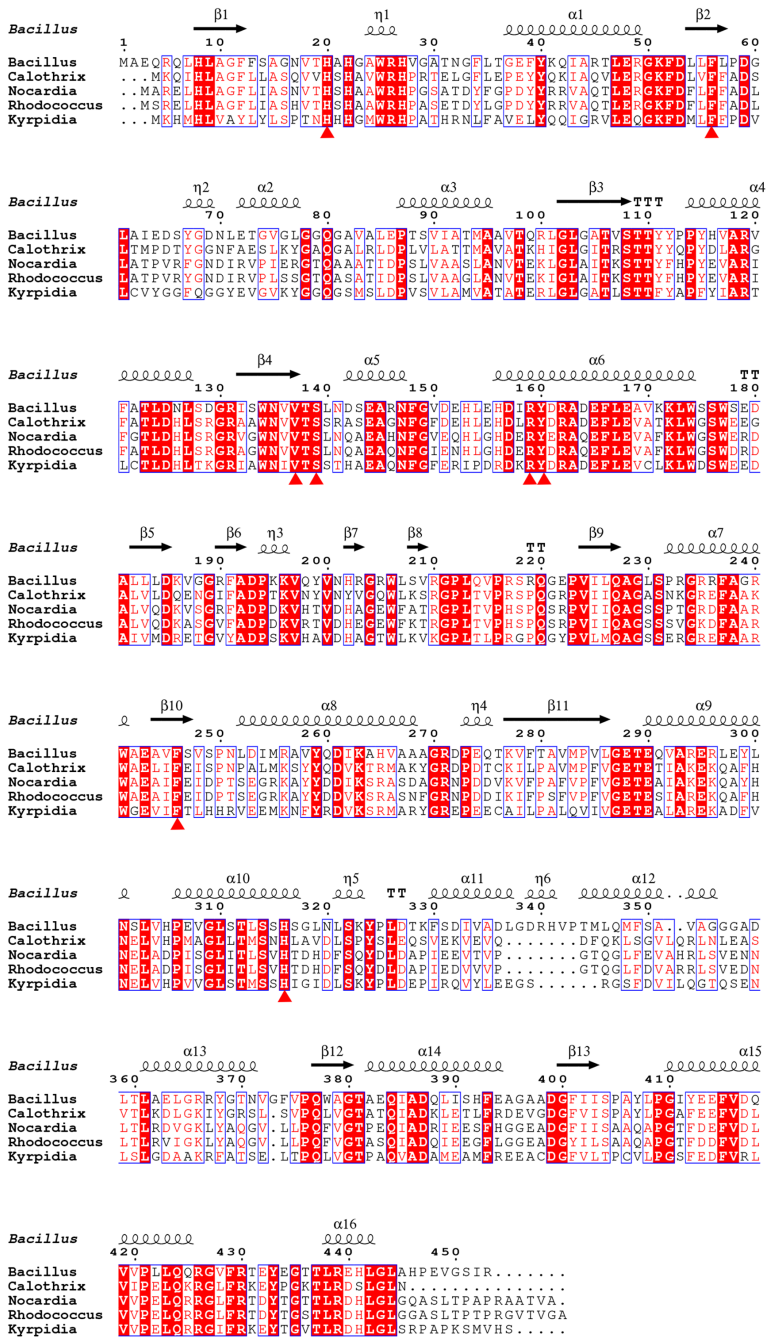

FIGURE 6 | Sequence alignment of BdsA with homologs from different species sharing identities from 48 to 72%. H20, F56, V137, S139, R159, Y160, F246, and H316 are all conserved in BdsA from different species and are denoted by red triangles.

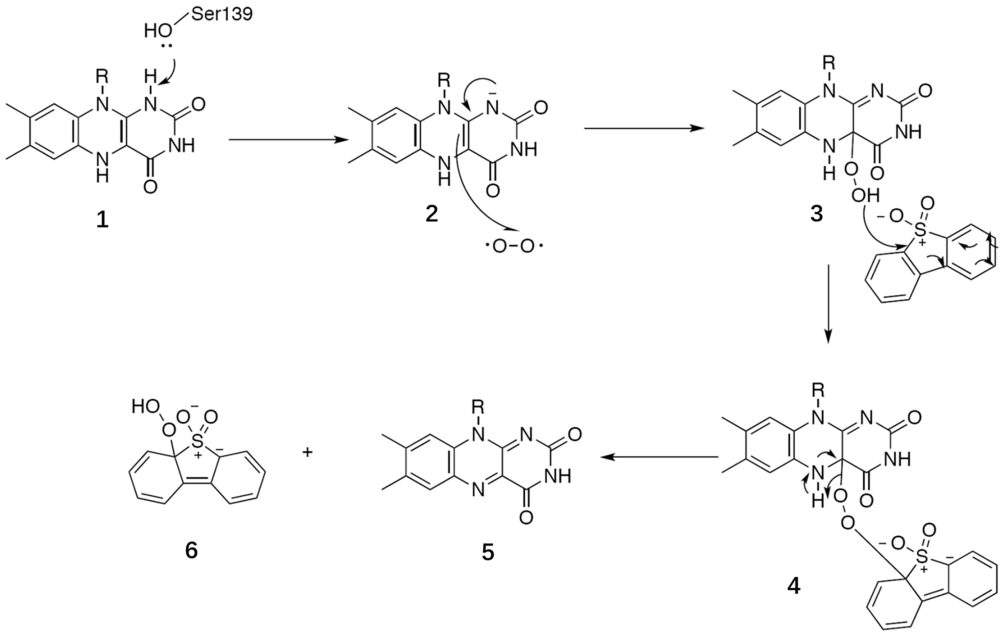

FIGURE 7 | General catalytic mechanism proposed for BdsA.

Substrate Docking and Analysis of Mutagenesis

The substrate DBT sulfone is the intermediate product of DBT desulfurization. It is difficult to crystallize the BdsA-FMN-substrate complex because DBT sulfone binds poorly to the oxidized form of the enzyme. To examine the binding and catalytic mechanism of DBT sulfone, we used flexible docking (Autodock 4.2) to build three-dimensional models of the BdsA-FMN-DBT sulfone complex. The docking result is illustrated in **Figure 3D**. As shown, the DBT sulfone substrate is located in the active site, on the si-face of the FMN isoalloxazine ring (**Supplementary Figure S3**). According to the results of the molecular docking analysis, seven residues (Phe12, His20, Phe56, Phe246, Val248, His316, and Val372) are involved in the binding of DBT sulfone (**Figure 3D**). The distance between flavin C4a and the carbon atom of the DBT sulfone attacked by the flavin hydroperoxide is 4.5 Å. The structure suggests that there is space between flavin C4a and the attacked atom of DBT sulfone for the formation of a (hydro) peroxyflavin intermediate (Li et al., 2008).

To illustrate the function of the substrate-binding residues, seven single-point mutants of BdsA were constructed: F12A, H20F, F56A, F246A, V248A, H316F, and V372A. The enzyme activities of these proteins were analyzed by measuring the formation of HBPSi on HPLC, and each assay was repeated four times (**Figure 4**). The results showed that mutant proteins H20F, F56A, F246A, and H316F lost more than 90% activity compared with wild-type BdsA. The activity of F12A was decreased by approximately 80%, and those of V248A and V372A were decreased by approximately 50%. These results were consistent with the results of the molecular docking calculations. Taken together, our results indicate that residues F12, H20, F56, F246, V248, H316, and V372 may play vital roles in substrate binding.

DISCUSSION

The Overall Structure and Active Site of BdsA Are Highly Conserved

A structure-based alignment was conducted, using the DALI program (Holm and Rosenström, 2010), against the Protein Data Bank (PDB). The similarity results showed that the scaffold of BdsA is highly conserved among all the group C flavoprotein monooxygenase superfamily. The nitrilotriacetate monooxygenase (PDB: 3sdo Z-score 48.8) is most similar to BdsA, followed by Ytnj (PDB: 1ywl, Z-score 47.6), alkane monooxygenase (Lada, PDB: 3b9n, Z-score 46.9) (Li et al., 2008), ethylenediaminetetra acetic acid (EDTA) monooxygenase (Emoa, PDB: 5dqa, Z-score 44.2) (Macdonald et al., 2016), and luciferase-like monooxygenase (PDB: 3rao, Z-score 32.9). The C_α superposition of BdsA with Ytnj, Lada, Emoa, and luciferase-like monooxygenase yielded the RMSD values of 1.178, 1.322, 1.316, and 2.364 Å, respectively. The homologs fold as TIM-barrels and are highly conserved in structural folding. However, the structural identities of the insertion segment IS5 were very low (**Figure 5**). In BdsA, IS5 ranges from Val304 to Val375, including α8, α9, α10, and α11. It is the key component of the active pocket, which, along with IS1, IS2, and IS3, controls the size of the pocket. The volume of the active pocket of BdsA, and those of homologous proteins, are calculated using CASTp server (Dundas et al., 2006). The volume of the BdsA activity

pocket is 5134.9 Å^3. Nitrilotriacetate monooxygenase catalyzes the degradation of the nitrilotriacetate substrate, with the active pocket volume of 5288.4 Å^3. Ytnj has an active pocket with the volume of 5030.2 Å^3, but its function remains unknown. Alkane monooxygenase catalyzes the terminal hydroxylation of long-chain *n*-alkanes (C15–C36), and its active pocket volume is 4118.7 Å^3. The luciferase-like monooxygenase-active pocket volume is 2611.1 Å^3. The maximum cavity, 8158.3 Å^3, is that of the EDTA monooxygenase. The figure highlighting the different binding modes of substrate are shown in **Supplementary Figure S4**. We interpreted that the structural variations may be related to the specificities of substrate-binding.

In this study, we have determined the putative residues participating in substrate binding of BdsA through molecular docking and enzyme activity assays. According to the molecular docking result, the substrate-binding site of BdsA may be located on the si-face of the isoalloxazine ring of FMN. As shown in **Figure 3D**, the DBT sulfone is in its stable form and fits well with the active pocket. According to the structure, 13 mutations (six mutations related to FMN-binding and seven mutations related to DBT-sulfone-binding) were constructed. Single mutations in these residues caused near-complete loss in the activity of BdsA. To illustrate the putative substrate-binding site, a sequence conservation analysis was performed, using BdsA homologs from different species with sequence identities from 48 to 72% (**Figure 6**). H20, F56, V137, S139, R159, Y160, F246, and H316 are all conserved in BdsA from different species. As shown in **Figure 3D**, these residues constitute a hydrophobic pocket, which fits well with the substrate DBT sulfone and can stabilize the conformation of the substrate, contributing to the formation of a C4a-(hydro) peroxyflavin intermediate on the si-face of the flavin isoalloxazine ring.

Mechanism of BdsA

The three-dimensional structure of BdsA is essential for elucidating the catalytic mechanism of the DBT sulfone monooxygenation. Recently, the crystal structure of BdsA was reported by Masahiko at a resolution of 2.8 Å (Okai et al., 2017), which provides architectural information and comparison with the homologous proteins of BdsA. However, the study by Masahiko did not give the structure of the complex with FMN or the substrate. In our study, we determined the crystal structure of BdsA from *Bacillus subtilis* WU-S2B, at a resolution of 2.2 Å, and the structure of the BdsA-FMN complex at 2.4 Å. In addition, we have also constructed a three-dimensional model of the BdsA-FMN-DBT sulfone complex by using flexible molecular docking. These structures may help in the future design of experiments aimed at elucidating the catalytic mechanism in further detail.

BdsA is a DBT sulfone monooxygenase that shares a 79% sequence identity with DszA from *Rhodococcus* sp. IGTS8. We reason that the catalysis of BdsA most probably exploits the same mechanism as DszA. Based on the structures we have resolved and previous works on homologous proteins, we propose a general catalytic mechanism for BdsA in sulfinic acid formation (**Figure 7**). The first step is Ser139 as an electron donor accepting the hydride from the N1 atom of the reduced flavin ring to activate FMNH2 (Massey et al., 1969; Bruice, 1984); and the second step of the reaction was a radical combination of 2 (activate FMNH2) to oxygen resulting in flavin hydroperoxide 3, which is the nucleophilicity reagent established in the flavoenzyme-mediated Baeyer–Villiger oxidation of ketones (Walsh and Chen, 1988) and the RutA-catalyzed uracil ring opening reaction (Mukherjee et al., 2010). Then, the addition of compound 3 to DBT sulfone forms the sulfone-stabilized carbanion 4. Succeedent forms 5 (FMN) and hydroperoxide 6.

BdsA play two roles in this process. First, the protein provides an environment that keeps the DBT sulfone and FMN in the correct positions with right orientation (**Figure 3D**). Second, the amino acid Ser139 functions as a nucleophile, activating $FMNH_2$. According to the suggested mechanism of DszA (Adak and Begley, 2016), the catalytic cycle is then completed by the conversion of 6 to benzenesulfinic acid and flavin-N5-oxide intermediate to FMN. In the process, the protein only supplies the reaction environment and may not catalyze directly.

AUTHOR CONTRIBUTIONS

LG, SX, TS, JS, and SL designed the research. TS, JS, SL, CZ, and JH performed the experiments. TS, JS, SL, YH, SX, and LG analyzed the data and wrote the paper. All authors contributed to the editing of the manuscript.

FUNDING

This work was supported by National Natural Science Foundation of China (Grant No. 30800167).

ACKNOWLEDGMENTS

We thank Professor Minyong Li at School of Pharmaceutical Sciences, Shandong University for assistance with mechanism discussion. We also thank the staff at the Beamline BL17U1 of the Shanghai Synchrotron Radiation Facility for assistance with data collection.

SUPPLEMENTARY MATERIAL

The Supplementary Material for this article can be found online at: https://www.frontiersin.org/articles/10.3389/fmicb.2018.00231/full#supplementary-material

FIGURE S1 | The binding modes of FMN in these homology proteins.

FIGURE S2 | The CD spectra result. The wild-type and mutant proteins are shown in different colors.

FIGURE S3 | Superposition of the wild and variants amino acids of the active site. The cofactor FMN is shown as yellow sticks. Wild amino acids are shown as cyan sticks, and mutant amino acids are shown as magenta sticks.

FIGURE S4 | BdsA, 1yw1, and 3b9o are illustrated in cyan, magentas, and wheat cartoon, respectively.

REFERENCES

Abin-Fuentes, A., Leung, J. C., Mohamed, M. E., Wang, D. I. C., and Prather, K. L. J. (2014). Rate-limiting step analysis of the microbial desulfurization of dibenzothiophene in a model oil system. *Biotechnol. Bioeng.* 111, 876–884. doi: 10.1002/bit.25148

Adak, S., and Begley, T. P. (2016). Dibenzothiophene catabolism proceeds via a Flavin-N5-oxide intermediate. *J. Am. Chem. Soc.* 138, 6424–6426. doi: 10.1021/jacs.6b00583

Adams, P. D., Grossekunstleve, R. W., Hung, L. W., Ioerger, T. R., Mccoy, A. J., and Moriarty, N. W. et al. (2002). PHENIX: building new software for automated crystallographic structure determination. *Acta Crystallogr.* 58(Pt 11), 1948–1954. doi: 10.1107/S0907444902016657

Benkert, P., Tosatto, S. C. E., and Schomburg, D. (2008). QMEAN: a comprehensive scoring function for model quality assessment. *Proteins* 71, 261–277. doi: 10.1002/prot.21715

Bruice, T. C. (1984). Chemlnform abstract: flavin oxygen chemistry brought to date. *Isr. J. Chem*. 24, 54–61. doi: 10.1002/ijch.198400008

Cristobal, S., Zemla, A., Fischer, D., Rychlewski, L., and Elofsson, A. (2001). A study of quality measures for protein threading models. *BMC Bioinformatics* 2:5. doi: 10.1186/1471-2105-2-5

Denome, S., Oldfield, C., Nash, L., and Young, K. (1994). Characterization of the desulfurization genes from Rhodococcus sp. strain IGTS8. *J. Bacteriol.* 176, 6707–6716. doi: 10.1128/jb.176.21.6707-6716.1994

Denome, S. A., Olson, E. S., and Young, K. D. (1993). Identification and cloning of genes involved in specific desulfurization of dibenzothiophene by Rhodococcus sp. strain IGTS8. *Appl. Environ. Microbiol*. 59, 2837–2843.

Dundas, J., Ouyang, Z., Tseng, J., Binkowski, A., Turpaz, Y., and Liang, J. (2006). CASTp: computed atlas of surface topography of proteins with structural and topographical mapping of functionally annotated residues. *Nucleic Acids Res.* 34, W116–W118. doi: 10.1093/nar/gkl282

Emsley, P., and Cowtan, K. (2004). Coot: model-building tools for molecular graphics. *Acta Crystallogr.* 60, 2126–2132. doi: 10.1107/S0907444904019158

Gallagher, J. R., Olson, E. S., and Stanley, D. C. (1993). Microbial desulfurization of dibenzothiophene: a sulfur-specific pathway. *FEMS Microbiol. Lett.* 107, 31–35. doi: 10.1111/j.1574-6968.1993.tb05999.x

Gray, K. A., Mrachko, G. T., and Squires, C. H. (2003). Biodesulfurization of fossil fuels. *Curr. Opin. Microbiol.* 6, 229–235. doi: 10.1016/S1369-5274(03)00065-1

Gray, K. A., Squires, C. H., and Monticello, D. J. (1998). DszD utilization in desulfurization of DBT by Rhodococcus sp. IGTS8. U.S. patent No. 5,811,285.

Guan, L. J., Lee, W. C., Wang, S., Ohshiro, T., Izumi, Y., Ohtsuka, J., et al. (2015). Crystal structures of apo-DszC and FMN-bound DszC from *Rhodococcus erythropolis* D-1. *FEBS J.* 282, 3126–3135. doi: 10.1111/febs.13216

Hino, T., Hamamoto, H., Suzuki, H., Yagi, H., Ohshiro, T., and Nagano, S. (2017). Crystal structures of TdsC, a dibenzothiophene monooxygenase from the thermophile *Paenibacillus* sp. A11-2, reveal potential for expanding its substrate selectivity. *J. Biol. Chem*. 292, 15804–15813. doi: 10.1074/jbc.M117.788513

Holm, L., and Rosenström, P. (2010). Dali server: conservation mapping in 3D. *Nucleic Acids Res.* 38, W545–W549. doi: 10.1093/nar/gkq366

Huijbers, M. M., Montersino, S., Westphal A. H., Tischler, D., and Van Berkel, W. J. (2014). Flavin dependent monooxygenases. *Arch. Biochem. Biophys*. 544, 2–17. doi: 10.1016/j.abb.2013.12.005

Ishii, Y., Konishi, J., Okada, H., Hirasawa, K., Onaka, T., and Suzuki, M. (2000a). Operon structure and functional analysis of the genes encoding thermophilic desulfurizing enzymes of *Paenibacillus* sp. A11-2. *Biochem. Biophys. Res. Commun*. 270, 81–88.

Ishii, Y., Konishi, J., Suzuki, M., and Maruhashi, K. (2000b). Cloning and expression of the gene encoding the thermophilic NAD(P)H-FMN oxidoreductase coupling with the desulfurization enzymes from *Paenibacillus* sp. A11-2. *J. Biosci. Bioeng*. 90, 591–599.

Kahnert, A., and Kertesz, M. A. (2000). Characterization of a sulfur-regulated oxygenative alkylsulfatase from *Pseudomonas putida* S-313. *J. Biol. Chem.* 275, 31661–31667. doi: 10.1074/jbc.M005820200

Kayser, J. K., Barbara, A. B., Kathy, J., Opeoluwa, O., and John, J. K. (1993). Utilization of organosulphur compounds by axenic and mixed cultures of *Rhodococcus rhodochrous* IGTS8. *J. Gen. Microbiol.* 139, 3123–3129. doi: 10.1099/00221287-139-12-3123

Kilane, J. J. II (2006). Microbial biocatalyst developments to upgrade fossil fuels. *Curr. Opin. Biotechnol.* 17, 305–314. doi: 10.1016/j.copbio.2006.04.005

Kilbane, J., and Robbins, J. (2007). Characterization of the *dszABC* gene of *Gordonia amicalis* F.5.25.8 and identification of conserved protein an DNA sequences. *Appl. Microbiol. Biotechnol*. 75, 843–851

Kilbane, J. J. (2016). Biodesulfurization: how to make it work? *Arab. J. Sci. Eng.* 42, 1–9 doi: 10.1007/s13369-016-2269-1.

Kirimura, K., Furuya, T., Nishii, Y., Ishii, Y., Kino, K., and Usami, S. (2001). Biodesulfurization of dibenzothiophene and its derivatives through the selective cleavage of carbon-sulfur bonds by a moderately thermophilic bacterium *Bacillus subtilis* WU-S2B. *J. Biosci. Bioeng.* 91, 262–266. doi: 10.1016/S1389-1723(01)80131-6

Kirimura, K., Harada, K., Iwasawa, H. T., Iwasaki, Y., Furuya, T., Ishii, Y., et al. (2004). Identification and functional analysis of the genes encoding dibenzothiophene-desulfurizing enzymes from thermophilic bacteria. *Appl. Microbiol. Biotechnol.* 65, 703–713. doi: 10.1007/s00253-004-1652-0

Konishi, J., Ishii, Y., Onaka, T., Okumura, K., and Suzuki, M. (1997). Thermophilic carbon-sulfur-bond-targeted biodesulfurization. *Appl. Environ. Microbiol.* 63, 3164–3169.

Krissinel, E., and Henrick, K. (2005). "Detection of protein assemblies in crystals," in *Proceedings of the International Conference on Computational Life Sciences*, Konstanz, 163–174. doi: 10.1007/11560500_15

Laskowski, R. A., Macarthur, M. W., Moss, D. S., and Thornton, J. M. (1993). PROCHECK: a program to check the stereochemical quality of protein structures. *J. Appl Crystallogr.* 26, 283–291. doi: 10.1107/S0021889892009944

Lee, W. C., Ohshiro, T., Matsubara, T., Izumi, Y., and Tanokura, M. (2006). Crystal structure and desulfurization mechanism of 2'-hydroxybiphenyl-2-sulfinic acid desulfinase. *J. Biol. Chem.* 281, 32534–32539. doi: 10.1074/jbc.M602974200

Li, L., Liu, X., Yang, W., Xu, F., Wang, W., and Feng, L. (2008). Crystal structure of long-chain alkane monooxygenase (LadA) in complex with coenzyme FMN: unveiling the long-chain alkane hydroxylase. *J. Mol. Biol.* 376, 453–465. doi: 10.1016/j.jmb.2007.11.069

Lill, M. A., and Danielson, M. L. (2011). Computer-aided drug design platform using PyMOL. *J. Comput. Aided Mol. Des.* 25, 13–19. doi: 10.1007/s10822-010-9395-8

Liu, S., Zhang, C., Su, T., Wei, T., Zhu, D., and Wang, K. et al. (2014). Crystal structure of DszC from *Rhodococcus* sp. XP at 1.79 Å. *Proteins* 82, 1708–1720. doi: 10.1002/prot.24525

Macdonald, J. T., Kabasakal, B. V., Godding, D., Kraatz, S., Henderson, L., and Barber, J. (2016). Synthetic beta-solenoid proteins with the fragment-free computational design of a beta-hairpin extension. *Proc. Natl. Acad. Sci. U.S.A.* 113, 10346–10351. doi: 10.1073/pnas.1525308113

Massey, V., Müller, F., Feldberg, R., Schuman, M., Sullivan, P. A., Howell, L. G., et al. (1969). The reactivity of flavoproteins with sulfite. Possible relevance to the problem of oxygen reactivity. *J. Biol. Chem.* 244, 3999–4006.

Montersino, S., Tischler, D., Gassner, G. T., and van Berkel, W. J. H. (2011). Catalytic and structural features of flavoprotein hydroxylases and epoxidases. *Adv. Synth. Catal.* 353, 2301–2319. doi: 10.1002/adsc.201100384

Monticello, D. J., Bakker, D., and Finnerty, W. R. (1985). Plasmid-mediated degradation of dibenzothiophene by *Pseudomonas* species. *Appl. Environ. Microbiol.* 49, 756–760.

Morris, G. M., Huey, R., Lindstrom, W., Sanner, M. F., Belew, R. K., Goodsell, D. S., et al. (2009). AutoDock4 and autoDockTools4: automated docking with selective receptor flexibility. *J. Comput. Chem.* 30, 2785–2791. doi: 10.1002/jcc.21256

Mukherjee, T., Zhang, Y., Abdelwahed, S., Ealick, S. E., and Begley, T. P. (2010). Catalysis of a flavoenzyme-mediated amide hydrolysis. *J. Am. Chem. Soc.* 132, 5550–5551. doi: 10.1021/ja9107676

Ohshiro, T., Ishii, Y., Matsubara, T., Ueda, K., Izumi, Y., Kino, K., et al. (2005). Dibenzothiophene desulfurizing enzymes from moderately thermophilic bacterium *Bacillus subtilis* WU-S2B: purification, characterization and overexpression. *J. Biosci. Bioeng.* 100, 266–273. doi: 10.1263/jbb.100.266

Ohshiro, T., Kojima, T., Torii, K., Kawasoe, H., and Izumi, Y. (1999). Purification and characterization of dibenzothiophene (DBT) sulfone monooxygenase, an enzyme involved in DBT desulfurization, from *Rhodococcus erythropolis* D-1. *J. Biosci. Bioeng.* 88, 610–616. doi: 10.1016/S1389-1723(00)87088-7

Ohshiro, T., Suzuki, K., and Izumi, Y. (1997). Dibenzothiophene (DBT) degrading enzyme responsible for the first step of DBT desulfurization by *Rhodococcus*

erythropolis D-1: purification and characterization. *J. Ferment. Bioeng.* 83, 233–237. doi: 10.1016/S0922-338X(97)80985-3

Okai, M., Lee, W. C., Guan, L. J., Ohshiro, T., Izumi, Y., and Tanokura, M. (2017). Crystal structure of dibenzothiophene sulfone monooxygenase BdsA from *Bacillus subtilis* WU-S2B. *Proteins* 85, 1171–1177. doi: 10.1002/prot.25267

Oldfield, C., Pogrebinsky, O., Simmonds, J., Olson, E. S., and Kulpa, C. F. (1997). Elucidation of the metabolic pathway for dibenzothiophene desulphurization by *Rhodococcus* sp. strain IGTS8 (ATCC 53968). *Microbiology* 143, 2961–2973. doi: 10.1099/00221287-143-9-2961

Otwinowski, Z., and Minor, W. (1997). Processing of X-ray diffraction data collected in oscillation mode. *Methods Enzymol.* 276, 307–326. doi: 10.1016/S0076-6879(97)76066-X

Schuttelkopf, A. W., and van Aalten, D. M. F. (2004). PRODRG: a tool for high-throughput crystallography of protein-ligand complexes. *Acta Crystallogr.* 60, 1355–1363. doi: 10.1107/S0907444904011679

Walsh, C. T., and Chen, Y. C. J. (1988). Enzymic Baeyer–Villiger oxidations by flavin-dependent monooxygenases. *Angew. Chem. Int. Ed.* 27, 333–343. doi: 10.1002/anie.198803331

Winn, M. D., Ballard, C. C., Cowtan, K. D., Dodson, E. J., Emsley, P., and Evans, P. R. et al. (2011). Overview of the CCP4 suite and current developments. *Acta Crystallogr.* 67(Pt 4), 235–242. doi: 10.1107/S0907444910045749

Yan, H., Kishimoto, M., Omasa, T., Katakura, Y., Suga, K., Okumura, K., et al. (2000). Increase in desulfurization activity of *Rhodococcus erythropolis* KA2-5-1 using ethanol feeding. *J. Biosci. Bioeng.* 89, 361–366. doi: 10.1016/S1389-1723(00)88959-8

Zhang, X., Liu, C., Nepal, S., Yang, C., Dou, W., and Chen, J. (2014). A hybrid approach for scalable sub-tree anonymization over big data using MapReduce on cloud. *J. Comput. Syst. Sci.* 80, 1008–1020. doi: 10.1016/j.jcss.2014.02.007

Conflict of Interest Statement: The authors declare that the research was conducted in the absence of any commercial or financial relationships that could be construed as a potential conflict of interest.

frontiers in Microbiology

ORIGINAL RESEARCH
published: 15 September 2017
doi: 10.3389/fmicb.2017.01777

Agdc1p – a Gallic Acid Decarboxylase Involved in the Degradation of Tannic Acid in the Yeast *Blastobotrys (Arxula) adeninivorans*

*Anna K. Meier[1], Sebastian Worch[1], Erik Böer[1], Anja Hartmann[1], Martin Mascher[1], Marek Marzec[1,2], Uwe Scholz[1], Jan Riechen[1], Kim Baronian[3], Frieder Schauer[4], Rüdiger Bode[4] and Gotthard Kunze[1]**

[1] Leibniz Institute of Plant Genetics and Crop Plant Research, Gatersleben, Germany, [2] Department of Genetics, Faculty of Biology and Environmental Protection, University of Silesia, Katowice, Poland, [3] Department of Microbiology, School of Biological Sciences, University of Canterbury, Christchurch, New Zealand, [4] Institute of Microbiology, University of Greifswald, Greifswald, Germany

OPEN ACCESS

Edited by:
Rajesh K. Sani, South Dakota School of Mines and Technology, United States

Reviewed by:
Willem J. H. Van Berkel, Wageningen University & Research, Netherlands
Maria Fátima Carvalho, Centro Interdisciplinar de Pesquisa Marine e Ambiental (CIIMAR), Portugal

***Correspondence:**
Gotthard Kunze
kunzeg@ipk-gatersleben.de

Specialty section:
This article was submitted to Microbiotechnology, Ecotoxicology and Bioremediation, a section of the journal Frontiers in Microbiology

Received: *22 May 2017*
Accepted: *31 August 2017*
Published: *15 September 2017*

Citation:
Meier AK, Worch S, Böer E, Hartmann A, Mascher M, Marzec M, Scholz U, Riechen J, Baronian K, Schauer F, Bode R and Kunze G (2017) Agdc1p – a Gallic Acid Decarboxylase Involved in the Degradation of Tannic Acid in the Yeast Blastobotrys (Arxula) adeninivorans. Front. Microbiol. 8:1777. doi: 10.3389/fmicb.2017.01777

Tannins and hydroxylated aromatic acids, such as gallic acid (3,4,5-trihydroxybenzoic acid), are plant secondary metabolites which protect plants against herbivores and plant-associated microorganisms. Some microbes, such as the yeast *Arxula adeninivorans* are resistant to these antimicrobial substances and are able to use tannins and gallic acid as carbon sources. In this study, the *Arxula* gallic acid decarboxylase (Agdc1p) which degrades gallic acid to pyrogallol was characterized and its function in tannin catabolism analyzed. The enzyme has a higher affinity for gallic acid (K_m −0.7 ± 0.2 mM, k_{cat} −42.0 ± 8.2 s^{-1}) than to protocatechuic acid (3,4-dihydroxybenzoic acid) (K_m −3.2 ± 0.2 mM, k_{cat} −44.0 ± 3.2 s^{-1}). Other hydroxylated aromatic acids, such as 3-hydroxybenzoic acid, 4-hydroxybenzoic acid, 2,3-dihydroxybenzoic acid, 2,4-dihydroxybenzoic acid and 2,5-dihydroxybenzoic acid are not gallic acid decarboxylase substrates. *A. adeninivorans* G1212/YRC102-AYNI1-AGDC1, which expresses the *AGDC1* gene under the control of the strong nitrate inducible *AYNI1* promoter achieved a maximum gallic acid decarboxylase activity of 1064.4 U/l and 97.5 U/g of dry cell weight in yeast grown in minimal medium with nitrate as nitrogen source and glucose as carbon source. In the same medium, gallic acid decarboxylase activity was not detected for the control strain G1212/YRC102 with *AGDC1* expression under the control of the endogenous promoter. Gene expression analysis showed that *AGDC1* is induced by gallic acid and protocatechuic acid. In contrast to G1212/YRC102-AYNI1-AGDC1 and G1212/YRC102, *A. adeninivorans* G1234 [Δ*agdc1*] is not able to grow on medium with gallic acid as carbon source but can grow in presence of protocatechuic acid. This confirms that Agdc1p plays an essential role in the tannic acid catabolism and could be useful in the production of catechol and *cis,cis*-muconic acid. However, the protocatechuic acid catabolism via Agdc1p to catechol seems to be not the only degradation pathway.

Keywords: biodegradation, aromatic acids, gallic acid, antimicrobial plant substances, fungi

INTRODUCTION

The non-conventional, non-pathogenic, imperfect, dimorphic yeast *Arxula adeninivorans* (syn. *Blastobotrys adeninivorans*) is a fungal organism with great biotechnological potential due to its wide substrate spectrum and robustness against osmotic, salt and temperature stresses (Middelhoven et al., 1984; Wartmann et al., 1995; Malak et al., 2016). It grows in harsh environments, tolerates up to 20% NaCl in the medium, endures temperatures of ≤48°C. It is also able to use a variety of tannins including tannic acid and hydroxylated aromatic acids as carbon sources (Wartmann et al., 1995; Tag et al., 1998; Yang et al., 2000; Böer et al., 2009a). To date, this research has focused on the wildtype strain, *A. adeninivorans* LS3 that was isolated from wood hydrolysate in Siberia (Gienow et al., 1990). In 2014, the complete genome of *A. adeninivorans* LS3 was sequenced and genome analysis revealed the presence of two potential tannin acyl hydrolases (Atan1p, Atan2p) as well as gallic acid decarboxylase (Agdc1p) (Kunze et al., 2014).

Tannins are part of almost all types of plant tissues and their hydrolysis releases glucose and gallic acid. Gallic acid belongs to the hydroxylated aromatic acid compounds, which share primarily antifungal and bacteriostatic properties and are toxic for most microbes at very low concentrations (Sikkema et al., 1995). Gallic acid recently became a useful compound in pharmaceutical and chemical industries because of its antifungal, bacteriostatic, anticancer, antimelanogenic, and antioxidant properties (Badhani et al., 2015).

A large amount of gallic acid is produced in the food and agriculture industries, which has contributed to a remarkable increase of phenolic compounds, mostly toxic agents, in the environment. Unfortunately, di- and trihydroxylated aromatic acids such as gallic acid and protocatechuic acid are difficult to degrade and often accumulate in water and soil, which is resulting in additional environmental pollution (Zhang et al., 2014). Before there can be an attempt to increase the efficiency of bioremediation processes, the microorganisms and the enzymes that degrade these pollutants need to be investigated.

Many bacteria and filamentous fungi have been characterized as organisms able to degrade hydroxylated aromatic acids by enzymatic degradation. These microorganisms developed several different ways to degrade these aromatic compounds. One option is the decarboxylation of a carboxyl group attached to the aromatic ring, which is catalyzed by enzymes from the decarboxylase family (Grant and Patel, 1969; Yoshida et al., 1982; Wright, 1993; O'Donovan and Brooker, 2001; Hashidoko et al., 2002; Mukherjee and Banerjee, 2004). In most cases, these decarboxylases are encoded by inducible genes, which ensure that the synthesis of the enzymes only occurs in the presence of their substrates. However, only a few of these enzymes have been characterized to date because they exhibit high oxygen sensitivities and are relatively unstable (Yoshida et al., 1982; Nakajima et al., 1992; Zeida et al., 1998; Jiménez et al., 2013).

The general strategy of aerobic degradation of aromatic compounds is the cleavage of the aromatic ring with the degradation products being channeled into the central metabolism. Usually the compounds go through *ortho* or *meta* pathways and are completely utilized (Williams and Sayers, 1994). However, there are microorganisms which can non-oxidatively decarboxylate gallic acid but the pathway results in death of the cell because of a lack in further degradative enzymes (Nakajima et al., 1992; Zeida et al., 1998; Rodríguez et al., 2008).

The decarboxylation of gallic acid results in the production of pyrogallol. This phenol derivate is very sensitive to oxygen and is used in many industrial applications, for example as a developing agent in photography and in cosmetic products, such as in hair dying agents.

The tannin acyl hydrolase 1 (Atan1p) has been already characterized and described as the enzyme which catalyzes the first reaction step in tannin degradation by *A. adeninivorans* LS3 (Böer et al., 2009a). It was described as extracellular enzyme, induced by tannins or gallic acid. The transformation of gallic acid and protocatechuic acid by *A. adeninivorans* LS3 wildtype strain have also been investigated (Sietmann et al., 2010). However, it is still not known if the degradation pathway is common for all hydroxylated aromatic acids and the role of gallic acid decarboxylase is currently unclear.

In this study, the *Arxula* gallic acid decarboxylase gene, *AGDC1*, was identified, isolated and expressed using a strong promoter in *A. adeninivorans*. The recombinant enzyme was purified, characterized and in addition, its function in the yeast cell determined. Growth of the *AGDC1* expression yeast strain and a *Δagdc1* gene disruption mutant on different aromatic acids was studied to elucidate the role of the gene product in *A. adeninivorans*.

MATERIALS AND METHODS

Strains and Culture Conditions

Escherichia coli strains XL1 blue [r*ecA1, endA1, gyrA96, thi-1, hsdR17, supE44, relA1, lac* [F'proABlacl q Z DM15 Tn10 (Tetr)], from Invitrogen (Grand Island, NY, USA) or DH5α [F– Φ80d*lac*ZΔM15 Δ(*lac*ZYA-*arg*F) U169, deoR, *rec*A1, *end*A1, *hsd*R17 (r_K-, m_K+) *pho*A *sup*E44, λ^-, *thi*-1, *gyr*A96 *rel*A1] were used as host strains for bacterial transformation and plasmid isolation. Both strains were cultured in Luria Bertani medium (LB - Sigma, USA) supplemented with 50 mg/l ampicillin (AppliChem, Germany) or 50 mg/l kanamycin (Roth, Germany).

Arxula adeninivorans G1212 (*aleu2 ALEU2::atrp1*) (Steinborn et al., 2007) and the wildtype strain *A. adeninivorans* LS3 (Kunze and Kunze, 1994), originally isolated from wood hydrolysate in Siberia (Russia), were used as experimental strains. Both strains are deposited in the yeast collection of the Department of Biology of the University of Greifswald (SBUG, Germany). They were cultivated in shaking flasks at 30°C, 180 rpm either under non-selective conditions in complex medium (YEPD-yeast

Abbreviations: GDC, gallic acid decarboxylases; *AGDC* gene, *gallic acid decarboxylase 1* gene from *A. adeninivorans*; Agdc1p, gallic acid decarboxylase 1 protein from *A. adeninivorans*; dcw, dry cell weight; YRC, yeast rDNA integrative expression cassette; YIC, yeast integrative expression cassette; YEPD, complex medium; YMM: yeast minimal medium; U, unit; GA, gallic acid; PA, protocatechuic acid; 3-HBA, 3-hydroxybenzoic acid; 4-HBA, 4-hydroxybenzoic acid; 2,3-DHBA, 2,3-dihydroxybenzoic acid; 2,4-DHBA, 2,4-dihydroxybenzoic acid; 2,5-DHBA, 2,5-dihydroxybenzoic acid; ORF, open reading frame.

extracts-peptone-dextrose) or in yeast minimal medium (YMM) supplemented with 43.5 mM $NaNO_3$ as nitrogen source and 20 g/l glucose as carbon source (YMM-glucose-$NaNO_3$) (Tanaka et al., 1967; Rose et al., 1990).

Transformation Procedures and Isolation of Nucleic Acids

Transformations of *E. coli* and *A. adeninivorans* were performed according to Böer et al. (2009a). Plasmid DNA isolation and DNA restriction were carried out as described by Wartmann et al. (2002).

Construction of *AGDC1* Expression Plasmids and Generation of Transgenic *A. adeninivorans* Strains

For *AGDC1* overexpression, the *AGDC1* ORF (PRJEB19393) with a HisTag encoding region at the 3′-end (*AGDC1-6H*) was amplified from genomic DNA of *A. adeninivorans* LS3 in a PCR reaction using primers that incorporated flanking *Eco*RI and *Not*I cleavage sites: primer AGDC1-1-6H-5′-**GAA TTC** ATG ACT ACT TCC TAC GAG CCC TGG-3′ (primer nucleotide positions 1-20, *Eco*RI restriction site is in bold type and underlined); primer AGDC1-2-6H 5′-**GCG GCC GC**T TAG TGG TGG TGA TGA TGG TGC CAG TGG AGG TCA ATC TCC T-3′ (primer nucleotide positions 674–693, HisTag encoding region underlined, *Not*I restriction site is in bold type and underlined). The resulting *Eco*RI-*Not*I flanked AGDC1-6H ORF was inserted into the plasmid pBS-AYNI1-PHO5-SS between the *A. adeninivorans* derived *AYNI1* promoter and the *S. cerevisiae PHO5* terminator (Böer et al., 2009c). The *AYNI1* promoter - *AGDC1-6H* gene - *PHO5* terminator flanked by *Spe*I–*Sac*II restriction sites expression modules were inserted into the plasmid Xplor2.2 to generate Xplor2.2-AYNI1-AGDC1-6H-PHO5 (Böer et al., 2009b). The resulting plasmids contained fragments of 25S rDNA, which are interrupted by the selection marker module (*ALEU2* promoter-*ATRP1m* gene-*ATRP1* terminator), the AGCD1 expression module and an *E. coli* resistance marker and replicator. To prepare the cassettes for yeast transformation, Xplor2.2-AYNI1-AGDC1-6H-PHO5 and the control plasmid Xplor2.2 lacking AGDC1 expression module were digested with *Asc*I (YRC) or *Sbf*I (YIC) to remove the *E. coli* sequences including the resistance marker. The resulting restriction products YRC102-AYNI1-AGDC1-6H, YIC102-AYNI1-AGDC1-6H and YRC102 (control) were used to transform *A. adeninivorans* G1212.

Yeast transformants were selected by tryptophan auxotrophy in YMM-glucose-$NaNO_3$. The cells were stabilized by passaging on selective (YMM-glucose-$NaNO_3$) and non-selective (YEPD) agar medium, to attain a high level of protein production (Klabunde et al., 2003).

Construction of Δ*agdc1* Gene Disruption Mutant

To create disruption mutants, the gene disruption cassette contained 1,019 bp up and 1,032 bp down the ORF of *AGDC1* as well as the ATRP1m selection marker module was constructed. All fragments were amplified by PCR (up and down ORF overlapped fragments using chromosomal DNA of *A. adeninivorans* LS3 as the template and ATRP1m selection marker module using plasmid pBS-ALEU2-TRP1m as the template-Steinborn et al., 2007). Primers used for fragment amplification were created with additional 15 bp overlapping sides (**Table 1A**). This strategy allowed ligation of fragments in one step by using an In-Fusion Cloning Kit (TaKaRa Clontech, USA Inc.). The resulting construct was amplified in *E. coli* DH5α. Finally, the complete construct covering 1019 bp in front of the *AGDC1* gene, the ATRP1m selection marker module and 1032 bp behind the *AGDC1* was amplified using the primers 5′-AAATTCTTCTACAGGAAGTCAGG-3′ and 5′-ATTGTTATGCACTATTCGTTAACGG-3′. The resulting 3,548 bp PCR-product was used to transform *A. adeninivorans* G1212 (Böer et al., 2009a).

Microscopic Analysis

The phenotype of *A. adeninivorans* G1212/YRC102, G1212/YRC102-AYNI1-AGDC1-6H and G1234 [Δ*agdc1*] was investigated. For this purpose, strains were cultivated on agar plates containing YMM-glucose-$NaNO_3$ at 30°C for 48 h. Colony morphology was investigated using a VHX-5000 Digital Microscope (KEYENCE Deutschland GmbH, Neu-Isenburg, Germany). For detailed analysis, a FESEM S 4100 device (Hitachi High-Technologies Europe GmbH, Krefeld, Germany) was used. Fragments of agar plates containing colonies were dried in 30°C, attached to carbon-coated aluminum sample blocks and gold-coated in an Edwards S150B sputter coater (Edwards High Vacuum Inc., Clevedon, United Kingdom).

Assay for Determination of Gallic Acid Decarboxylase Activity

Gallic acid decarboxylase activity was assayed by following gallic acid or protocatechuic acid biotransformation during the enzymatic reaction in 50 mM potassium phosphate buffer pH 6.2. The reactions were carried out in 96-well UV-transparent microtiter plates (Greiner Bio-One GmbH) in triplicates, in a total volume of 100 µl. Reaction was started by adding 0.5 mM substrate solution to the enzyme and monitored 15 min at 40°C, 259 nm (ε = 7100 [1/M/cm]) and 288 nm (ε = 1,570 [1/M/cm]) for gallic acic and protocatechuic acid respectively (Krumholz et al., 1987). Blank values were established by assaying using water instead of the enzyme. One Unit (1 U) of enzyme activity was defined as the amount of enzyme required to decarboxylate 1 µmol gallic acid to pyrogallol or 1 µmol protocatechuic acid to catechol per min at 40°C, pH 6.2.

Gallic acid decarboxylase activity with 3-hydroxybenzoic acid, 4-hydroxybenzoic acid, 2,3-dihydroxybenzoic acid, 2,4-dihydroxybenzoic acid, 2,5-dihydroxybenzoic acid as substrates were measured by GC-MS. 470 µl 1 mg/ml substrate in 50 mM potassium phosphate buffer pH 6.2 and 30 µl purified Agdc1p were incubated at 40°C for 0, 5, 15, 25, and 35 min. The blank for the reaction was assayed using boiled enzyme (15 min, 95°C). The reactions were stopped by increasing the temperature for 95°C for 15 min. The pH of the samples was adjusted to 2 with HCl and the compounds extracted using

TABLE 1 | (A) Primers used for construction of deletion mutant strain G1234 [Δ*agdc1*]. **(B)** Primers used for analysis of *AGDC1* expression levels.

(A) Primers for construction of *A. adeninivorans* G1234 [Δ*agdc1*]

Primer	Sequence (5′ → 3′)
01. 1000bp ΔAGDC left	GTTTTAATTACAAAAAGCTAAATTCTTCTACAGGAAGTCAGG
02. Primer right 1 ΔAGDC	TGTACAATGTTTCTTTCTTGTCTG
03. Marker left ΔAGDC	AAGAAACATTGTACATTTCAATCGACGATTGCAATTGAC
04. Marker right 1 ΔAGDC	GAGTCTGTATTGAAGCTTAGCTTG
05. Primer left 1 ΔAGDC	CTTCAATACAGACTCACAGAACTAGAATATATAACAATGTTATTAAA
06. 1000bp ΔAGDC right	TTAGTTAAAAGCACTCCATTGTTATGCACTATTCGTTAACGG

(B) Primers for nested quantitative RT PCR

Reaction step	Primer	Sequence (5′ → 3′)
Step1 cDNA synthesis	(dT) 15V-RTA	TGA CAG GAT ACC ATA CAG ACA CTA TTT TTT TTT TTT TTT V
Step 2 Second PCR synthesis	RTA-1 rv	TGA CAG GAT ACC ATA CAG ACA C
	AGDC1-V fw	TGC TGT GGC TCA GGC TAA TC
	TFC1-3 fw	TGA AGA AGA GCA CCA AGC A
	ALG9-7	TGGTATCGGTCGCATTCT
Step 3 Second PCR synthesis	RTA rv	TGA CAG GAT ACC ATA CAG ACA CTA
	AGDC1-III fw	ATG TAC GAC GCC ATG AAG GA
	TFC1-1 fw	ACA ACA AGA TGA AAA CGC
	ALG9-8	TCAATTGCAGTGGACTGACTA

organic solvent MTBS (Sigma-Aldrich, USA). Extracts were lyophilized and resuspended in 400 µl pyridine and 100 µl BSTFA (Sigma-Aldrich, USA) and incubated overnight at 60°C. GC/MS measurements were done according to method described in "Analysis of supernatant from strains growing on YMM-$NaNO_3$ supplemented with different carbon sources."

Agdc1-6hp Analysis

Agdc1-6hp was purified by column chromatography on HisTrap FF (1 ml) Novagen, USA) in 20 mM Tris, 0.5 mM NaCl pH 7.9, and 5 mM imidazole as binding buffer and 20 mM Tris, 0.5 mM NaCl pH 7.9, and 1 M imidazole as elution buffer. Finally, the purified protein was desalted with PD10 columns (GE Health Care Europe GmbH, Germany).

The indicative molecular mass determination of native Agdc1-6hp was done by gel filtration using Superdex^{TM} 200 (Amersham Biosciences, UK). The flow rate was 1 ml/min and fractions of about 1 ml were collected for 182 min (buffer: 50 mM Tris pH 8 + 0.15 M NaCl). A calibration curve was constructed using blue dextran, ferritin, catalase, bovine albumin, RNAse A and vitamin B12 as standards.

The K_m value for gallic acid and protocatechuic acid were determined as described in "Assay for determination of gallic acid activity." All measurements were done in triplicate and Michaelis-Menten and Hanes plots were constructed.

The Agdc1p concentration was determined using a Coomassie stained SDS-PAGE for the calculation of k_{cat} (Kunze et al., 1998).

Protein Analysis

SDS-PAGE and Western blot analysis were performed as described by Kunze et al. (1998). The antibodies used for Western blot analysis were anti-His-tag specific primary antibody produced in rabbit (Sigma-Aldrich, USA) and secondary antibody anti-mouse IgG alkaline phosphatase conjugate produced in goat (Sigma-Aldrich, USA). The staining procedure was done by membrane incubation with NBT/BCIP substrate (Roche Diagnostics, Switzerland).

The dye-binding method of Bradford was used for protein quantification (BIO-RAD, USA), using bovine serum albumin as the standard (Bradford, 1976).

Quantitative Reverse Transcriptase PCR Analysis (qRT PCR)

Arxula adeninivorans G1212/YRC102 cells were grown in YMM-glucose-$NaNO_3$ for 24 h at 30°C and 180 rpm. Afterwards cells were harvested (3,220 × g at 4°C), washed with YMM-$NaNO_3$ and resuspended in YMM-$NaNO_3$ containing 0.2% glucose or hydroxylated aromatic acids. 2 ml of culture samples were collected after 0, 4, 8, 24, and 48 h. Cells were pelleted (2,300 × g, 4°C), and disrupted mechanically using silica beads and a Mixer Mill MM400 (RETSCH, Germany) operating for 3 min, vibrational frequency of 30/s. Total RNA was isolated using RNeasy Mini Kit (Qiagen, Germany) as described by the manufacturer. RNA concentration was analyzed using NanoDrop2000c spectrophotometer (Thermo Fisher, Germany). cDNA was synthesized using RevertAid H Minus First Strand cDNA Synthesis Kit (Fermentas, Germany) with an Oligo(dT)15V-RTA primer. For the analysis of temporal gene expression patterns a nested qRT-PCR assay was applied (Worch and Lemke, 2017). The first PCR synthesis was made with cDNA-template (10 cycles) using gene-specific primers and RTA1 primer (**Table 1B**). The PCR

product was diluted 1:500 and amplified in the presence of SYBR Green fluorescent dye (Power SYBR® Green PCR Master Mix, Applied Biosystems, Foster City, CA, USA) using ABI 7900HT Fast Sequence Detection System (Applied Biosystems) with gene-specific primers 2 or 4 and RTA primer (**Table 1B**). *TFCI* and *ALG9* were used as reference (housekeeping) genes (Rösel and Kunze, 1995; Teste et al., 2009). The calculations were done using $\Delta\Delta c_t$-method (Livak and Schmittgen, 2001).

Microarray Design and Hybridization for Gene Expression Analysis

The gene expression profiling was performed using a microarray produced by Agilent Technologies in 8 × 60 k format. The microarray was based on 6,025 annotated chromosomal sequences and 36 putative mitochondrial gene oligos and was designed using Agilent Technologies eArray software (https://earray.chem.agilent.com; design number 035454). Depending on the sequence length of the genes, up to 10 60-mers per gene were created, resulting in a total of 56,312 *A. adeninivorans* specific oligos.

A. adeninivorans LS3 was cultivated overnight in YMM-glucose-$NaNO_3$. Cells were then pelleted (3,220 × g at 20°C), and shifted to YMM-$NaNO_3$ containing a mixture of 0.5% gallic acid plus 1% glucose or 1% glucose only. After 15 min, 30 min, 2 and 5 h of cultivation at 30°C and 180 rpm, cells were harvested and total RNA was isolated using RNeasy Mini Kit (Qiagen, Germany). The samples were labeled and the microarray hybridized according to the Agilent Technologies "One-Color Microarray-Based Gene Expression Analysis (v6.5)" instructions. The R package limma was used for microarray data analysis (Smyth, 2005). The background of raw expression data was corrected by "normexp" and normalized between arrays using "quantile." Differentially expressed genes were detected by fitting a linear model to $\log_2$-transformed data by an empirical Bayes method (Smyth, 2004). The Bonferroni method was used to correct for multiple testing.

Analysis of Supernatant from Strains Growing on YMM-$NaNO_3$ Supplemented With Different Carbon Sources

Quantities of glucose, hydroxylated aromatic acids, as well as various phenol derivatives were measured by GC-MS (Clarus SQ 8 GC Mass Spectrometers). Samples were previously extracted and derivatized. For this purpose, 2 ml cultures were centrifuged for 10 min, 16,000 × g, 4°C, 500 µl supernatant was adjusted to pH 2 with HCl and compounds were extracted with 1 ml MTBS (Sigma-Aldrich, USA). Extracts were lyophilized in a Freeze Dryer, Alpha 1-4 LSC plus (Christ), resuspended in 400 µl pyridine, 100 µl BSTFA (Sigma-Aldrich, USA) was added and samples were incubated overnight at 60°C. 1 µl sample was injected into an Elite-5MS column, Length 30 m, I.D 0.25 mm, 25 µm (Elite, USA). The injection was performed with a split speed 10 ml/min. The temperature was held at 60°C for 1 min and was then ramped up to 230°C at 15°C/min and held at this temperature for 11.33 min. The peak areas (triplicates) were calculated by TurboMass 6.1 using data from external quantification standards assayed four times.

RESULTS

Identification of the *A. adeninivorans AGDC1* Gene Encoding Gallic Acid Decarboxylase (Agdc1p)

A putative *gallic acid decarboxylase* gene (ARAD1C45804g) was annotated in the genome of *A. adeninivorans* LS3. The gene, *Arxula gallic acid decarboxylase 1* (*AGDC1*), is localized on chromosome *Arad1C*. The open reading frame is a 696 bp encoding a protein with 232 amino acids. The predicted subunit molecular mass of Agdc1p is 27.3 kDa. Protein analysis according to the SignalP (version 4.1) program (http://www.cbs.dtu.dk/services/SignalP/) predicted the absence of a secretion signal sequence, which was corroborated by cytoplasmic localization in cell fractionation experiments (data not shown).

In *Lactobacillus plantarum* WCFS1 the enzyme comprises three subunits. There are several conserved domains that are fundamental for enzyme catalytic activity and structure were found in the Agdc1p sequence such as subunit B which is homologous with *Lactobacillus plantarum* WCFS1 gallic acid decarboxylase and putative gallic acid decarboxylase protein sequences from other lactic bacteria described by Jiménez et al. (2013) (**Figure 1A**).

A phylogenetic tree between Agdc1p and gallic acid decarboxylase from *L. plantarum* as well as the putative gallic acid decarboxylase protein sequences from lactic bacteria was developed using the Neighbor-Joining method. It demonstrated that the *Lactobacillus sakei* and *Pediococcus pentosaceus* putative enzymes originated from the same ancestral node, which shares a common ancestor with Agdc1p, whereas *Enterococcus faecium*, *Streptococcus gallolyticus*, *Oenococcus oeni*, *Lactobacillus plantarum, Lactobacillus pentosus* and *Lactobacillus brevis* form other branches with common ancestors (**Figure 1B**).

Generation of an Agdc1-6hp Producing Yeast Strain

Arxula adeninivorans G1212 [Δ*trp1*] served as a host strain for overexpression of *AGDC1* gene with a HisTag encoding sequence fused to the 3′-end of the ORF under control of the nitrate inducible *AYNI1* promoter (*A. adeninivorans* nitrate reductase promoter). Cassettes with the AGDC expression module (YRC102-AYNI1-AGDC1-6H, YIC102-AYNI1-AGDC1-6H-**Figure 2A**) and control (YRC102) were prepared as described in "Material and Methods." After genome integration of the cassettes, a number of selected clones (YICs and YRCs) were passaged to establish high plasmid stability. The transformants were then cultivated in YMM-glucose-$NaNO_3$ at 30°C for 48 h. The yeast cells were harvested, disrupted and screened for gallic acid decarboxylase activity. This activity was detected in all stabilized *A. adeninivorans* G1212/YRC102-AYNI1-AGDC1-6H and G1212/YIC102-AYNI1-AGDC1-6H strains. However transgenic yeast strains with genome integrated YRCs achieved approximately 2.2-fold higher enzyme activity

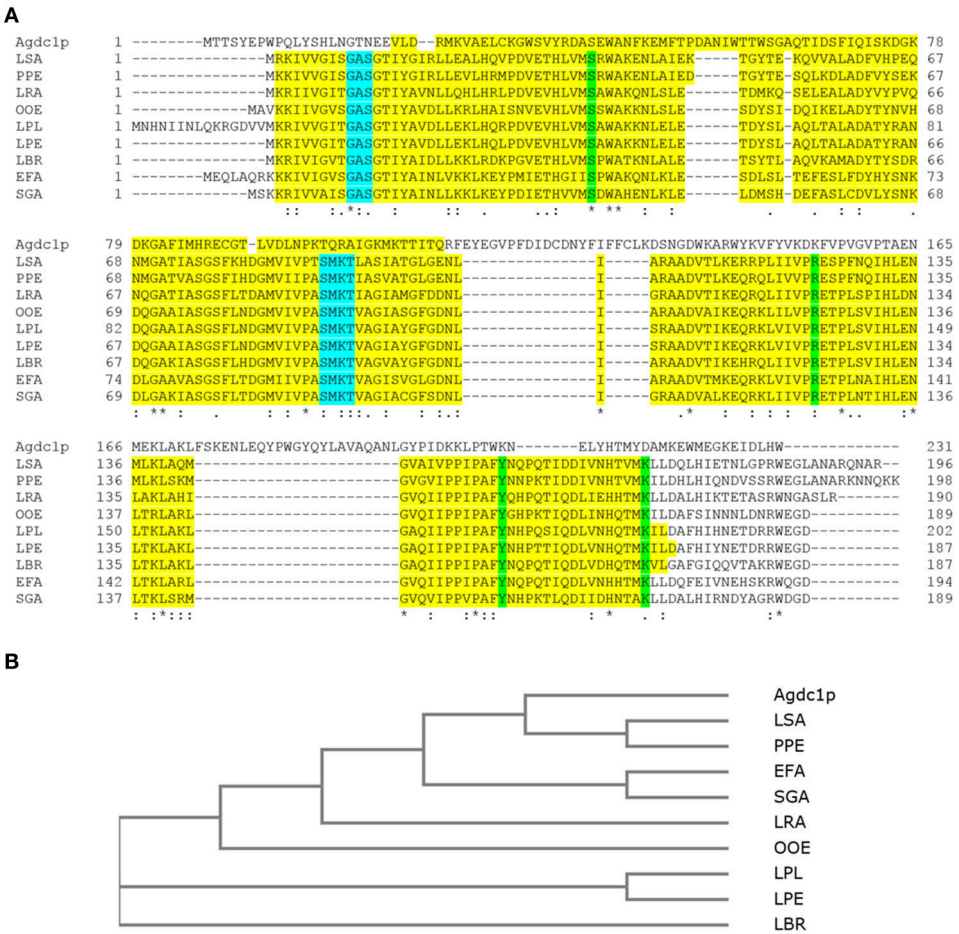

FIGURE 1 | (A) Multiple alignment of Agdc1p sequence to subunit B from *Lactobacillus plantarum* ATCC 14917^T (LPL) (D7V849) and other putative gallic acid decarboxylases from lactic acid bacteria *Lactobacillus pentosus* KCA1 (LPE) (I9L531), *Lactobacillus brevis* ATCC 367 (LBR) (Q03P27), *Lactobacillus rhamnosus* HN001 (LRA) (B5QPH7), *Lactobacillus sakei* 23K (LSA) (Q38Y44), *Enterococcus faecium* DO (EFA) (Q3Y2U4), *Oenococcus oeni* PSU-1 (OOE) (A0NKP0), *Pediococcus pentosaceus* ATCC 25745 (PPE) (Q03HH4), and *Streptococcus gallolyticus* UCN34 (SGA) (D3HEZ0). Alignment was done using ClustalOmega. The domains are highlighted in yellow; binding sites in green and nucleotide binding sites in blue. **(B)** The phylogenetic tree was constructed by the neighbor joining method of Agdc1p to subunit B of selected lactic bacteria without distance corrections. An asterisk (*) indicates positions which have a single, fully conserved residue, a colon (:) indicates conservation between groups of strongly similar properties, and a period (·) indicates conservation between groups of weakly similar properties.

than YIC transformants. In contrast, gallic acid decarboxylase activity was not detectable in the control strain *A. adeninivorans* G1212/YRC102 using glucose as carbon source. *A. adeninivorans* G1212/YRC102-AYNI1-AGDC1-6H with the highest gallic acid decarboxylase activity was used in further investigations.

AGDC1 expression and control strains *A. adeninivorans* G1212/YRC102-AYNI1-AGDC1-6H and G1212/YRC102 were cultivated in YMM-glucose-$NaNO_3$ at 30°C and 180 rpm for 120 h and dry cell weight (dcw), gallic acid decarboxylase activity with gallic acid as substrate and yield [Y(P/X)] were determined each 24 h. The experiment was performed in triplicate.

All yeast strains reached a maximum dcw after 24 h of cultivation and then remained constant until the end of the experiment. In contrast gallic acid decarboxylase activity was detected in *A. adeninivorans* G1212/YRC102-AYNI1-AGDC1-6H only. This strain achieved its maximum enzyme activity of 972 U/l with 94 U/g dcw after 96 h (**Figure 2B**).

Phenotype of Transgenic *A. adeninivorans* Strains

The deletion of gallic acid decarboxylase gene results in change of cells shape and through this, changes in morphology of colonies. The difference was visible already on the agar plate (YMM-$NaNO_3$ supplemented with 2% glucose as sole source of carbon) without magnification. The microscopic analysis showed that the deletion mutant strains were growing as mycelia at 30°C; this phenomenon was not observed in the case of G1212/YRC102 control strain and G1212/YRC102-AYNI1-AGDC1-6H overexpression strain (**Figure 3**).

Purification and Characterization of Agdc1-6hp

Arxula adeninivorans G1212/YRC102-AYNI1-AGDC1-6H with HisTag encoding sequence at the 3′-end of the *AGDC1* ORF was

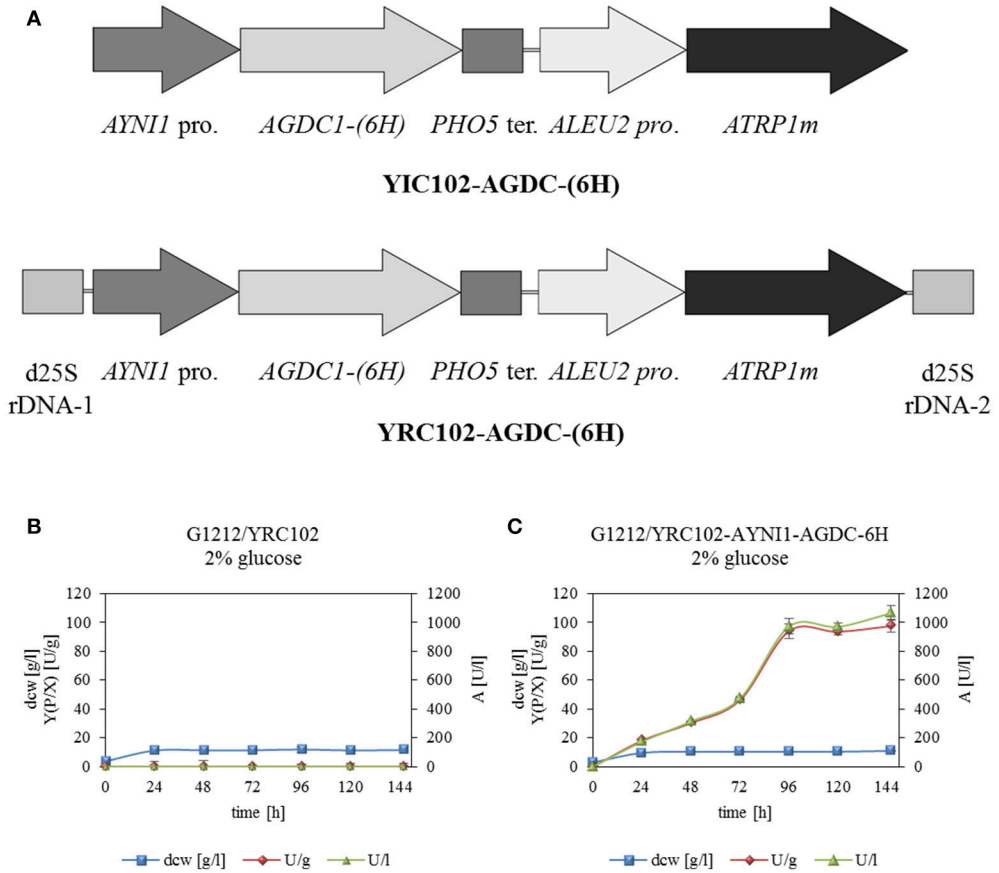

FIGURE 2 | (A) Physical maps of YRC102-AYNI1-AGDC1-6H, YIC102-AYNI1-AGDC1-6H transformed into *A. adeninivorans* G1212. Both cassettes contained the selection marker module with *ATRP1m* gene fused to the *ALEU2* promoter and the expression module with *AYNI1* promoter—*AGDC1-6H* gene—*PHO5* terminator. In addition, YRC (*Asc*I fragment) is flanked by 25S rDNA sequences for targeting the cassette into genomic 25S rDNA. YIC (*Sbf*I fragment) contain the selection marker and expression module and was integrated randomly into the genome. **(B)** Time-course traces of *A. adeninivorans* G1212/YRC102 and **(C)** G1212/YRC102-AYNI1-AGDC1-6H grown on YMM-glucose-$NaNO_3$ in shake flasks at 30°C for 146 h. Intracellular Agdc1-6hp activity (triangles) detected with gallic acid as substrate, calculated yield [Y(P/X)] (circles) and dry cell weight (squares). Measurements were done in triplicate.

selected for synthesis of recombinant Agdc1-6hp. Purification was by Immobilized Metal Affinity Chromatography (IMAC). Crude extract and a fraction containing purified Agdc1-6hp were analyzed on Coomassie-stained SDS-PAGE and Western blot.

Predicted molecular mass of Agdc1-6hp is 27.3 kDa. The denatured protein was visible at around the 25 kDa position on SDS-PAGE and Western blot in both the crude extract and the purified protein fraction (**Figure 4A**). Gallic acid decarboxylase activity was measured for crude extract and purified Agdc1-6hp. Total activity in crude extract was 1 U/mg whereas it was 5.9 U/mg in the purified fraction, corresponding to 77% of yield. The specific activity was 1 and 5.9 U/mg in crude extract and the purified Agdc1-6hp fraction respectively (**Figure 4**).

The indicative molecular mass of native Agdc1-6hp was estimated by gel filtration on a Superdex^{TM} 200 column (as described in "Material and methods"). The calculated molecular mass of the native enzyme was 27.1 kDa, whereas predicted molecular mass of the His-tagged Agdc1-6hp was 28.1 kDa. This data indicates that Agdc1-6hp is a monomeric protein.

In vitro study of Agdc1-6hp established the optimal conditions for enzymatic activity. The reaction mixture contained 0.5 mM gallic acid as substrate. The optimum pH was determined using the following buffers: 50 mM citrate-phosphate (pH 2.6–8), 50 mM sodium acetate (pH 3–6), 50 mM sodium citrate (pH 3.5–6.5), 50 mM potassium phosphate buffer (pH 5.8–6.8), 50 mM sodium phosphate (pH 5.5–8), and 50 mM TRIS-HCl (pH 7–9). Agdc1-6hp was most active when reaction was carried out in 50 mM potassium phosphate buffer pH 6.2 at 40°C. Enzyme activity of 80% was observed between pH 5.6–7.1 and at temperatures between 25 and 45°C. Some buffer systems reduced the activity of Agdc1-6hp, for example citrate-phosphate buffer exhibited 52% activity whereas sodium-citrate buffer had only 15% of activity in comparison to potassium phosphate buffer when the reaction was carried out under optimal conditions.

A study of thermostability demonstrated that Agdc1-6hp is stable between 4 and 30°C. After 24 h 100% of the initial activity was detected, however incubation at 35°C resulted in loss of 60% of initial activity after 24 h. Incubation at optimum

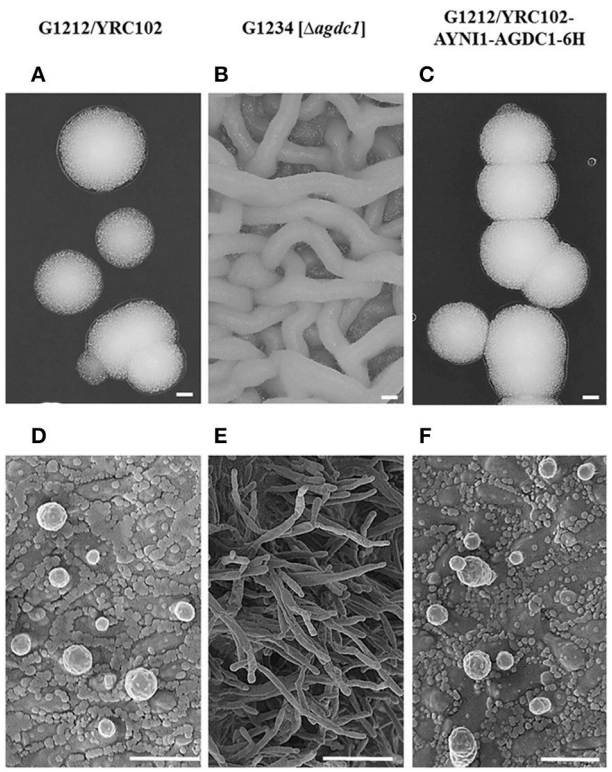

FIGURE 3 | Microscopic analysis of *A. adeninivorans* G1212/YRC102, G1212/YRC102-AYNI1-AGDC1-6H and G1234 [*Δagdc1*] cultivated on agar plates containing YMM-glucose-$NaNO_3$ at 30°C for 48 h using a VHX-5000 Digital Microscope (Scale bar: **A–C**-200 μm) and a SEM FESEM S 4100 device (Scale bar: **D**-3 μm, **E**-9 μm, **F**-4 μm).

temperature (40°C) resulted 100% gallic acid decarboxylase activity after only 7 h of incubation, however activity decreased drastically thereafter. Temperatures above 40°C led to a complete loss of activity after 4 h. Enzyme stored at −80°C exhibited no loss of activity even after 1 month of storage in these conditions.

A number of metal ions and reagents were tested to determine which acted as inhibitors and/or cofactors. When 1 mM Ni^{2+}, Fe^{2+}, Fe^{3+}, Co^{2+}, or Cu^{2+} were present in a reaction mixture, the enzyme was almost completely inhibited (relative activity <30%). In contrast addition of 1 mM Mg^{2+}, Mn^{2+}, Ca^{2+} K^{+} $Na_2S_2O_3$, PEG4000, PEG6000, or PEG8000 to the reaction mixture had no significant influence on gallic acid decarboxylase activity. In all cases activities were >80% of activity in control reaction mixture. The slight positive effect was detected when 1 mM EDTA, ascorbic acid or DTT were present in reaction mixture (**Table 2**).

The kinetic parameters of purified Agdc1-6hp were determined photometrically for gallic acid and protocatechuic acid. The K_m of Agdc1-6hp for gallic acid is 4 times lower than for protocatechuic acid (0.7 ± 0.2 mM and 3.2 ± 0.2 mM respectively). Turnover, k_{cat}, is 42.0 ± 8.2 s^{-1} for gallic acid and 44.0 ± 3.4 s^{-1} for protocatechuic acid. However, the catalytic efficiency is much lower for protocatechuic acid (14.0 ± 2.0 [mM^{-1} s^{-1}]) than for gallic acid (57.8 ± 7.6 [mM^{-1} s^{-1}]) (Supplementary Table S1).

TABLE 2 | Relative Agdc1-6hp activity [%] assayed for 0.5 mM gallic acid as substrate and presence of different additives in the reaction mixture.

1 [mM]	Relative activity [%]	1 [mM]	Relative activity [%]	1 [mM]	Relative activity [%]
Control (H_2O)	100	$ZnSO_4$	52	$Na_2S_2O_3$	85
$NiSO_4$	0	$ZnCl_2$	60	PEG4000	91
$NiCl_2$	0	$AlCl_3$	73	PEG6000	95
$FeSO_4$	0	$MgSO_4$	84	PEG8000	95
$FeCl_3$	24	$MgCl_2$	84	Ascorbic acid	107
$CoSO_4$	4	$MnSO_4$	86	DTT	116
$CoCl_2$	27	$MnCl_2$	94	EDTA	146
$CuSO_4$	4	$CaSO_4$	84		
$CuCl_2$	39	$CaCl_2$	97		

Five additional hydroxylated aromatic acids (3-hydroxybenzoic acid, 4-hydroxybenzoic acid, 2,3-dihydroxybenzoic acid, 2,4-dihydroxybenzoic acid, 2,5-dihydroxybenzoic acid) with different numbers and positions of hydroxyl groups were tested to determine the *in vitro* substrate specificity of Agdc1-6h. The enzyme, incubated in optimal conditions for 35 min, did not catalyze the decarboxylation of these compounds.

Expression Analysis of *AGDC1* on Various Carbon Sources

The expression level of *AGDC1* relative to the housekeeping genes *TFCI* and *ALG9* was analyzed by nested quantitative RT-PCR. *A. adeninivorans* G1212/YRC102 was cultivated on YMM-$NaNO_3$ supplemented with 0.2% (w/v) of glucose or different hydroxylated aromatic acids as sole source of carbon. Samples were collected at different times and total RNA was isolated. An increase of gene transcription of *AGDC1* was observed when cells were cultivated on gallic acid and protocatechuic acid. None of the other carbon sources (glucose, 3-hydroxybenzoic acid, 4-hydroxybenzoic acid, 2,4-dihydroxybenzoic acid, 2,3-dihydroxybenzoic acid, 2,5-dihydroxybenzoic acid) induced the expression of *AGDC1*. The highest expression level was detected after 8 h of cultivation (**Figure 5**).

In order to get information on whole transcriptome variations upon incubation of *A. adeninivorans* with gallic acid, microarray expression analysis was performed. The changes in genes expression of wildtype strain, *A. adeninivorans* LS3, cultivated in YMM-$NaNO_3$ supplemented with 1% glucose and YMM-$NaNO_3$ supplemented with 1% glucose plus 0.5% gallic acid were analyzed. Cells were harvested after 15 min, 30 min, 5 h, and 12.5 h of incubation in shaking flasks at 30°C and 180 rpm. Total RNA was isolated and analysis of microarray data allowed recognition of the candidate genes involved in tannic acid degradation pathway (**Figure 6**). Significant upregulation was observed for *gallic acid decarboxylase 1* (*AGDC1*) and *tannase 1* (*ATAN1*) genes, as well as for genes annotated as putative *tannase 2* (*ATAN2*), *catechol-1,2-dioxygenase*, *oxalocrotonate*

A

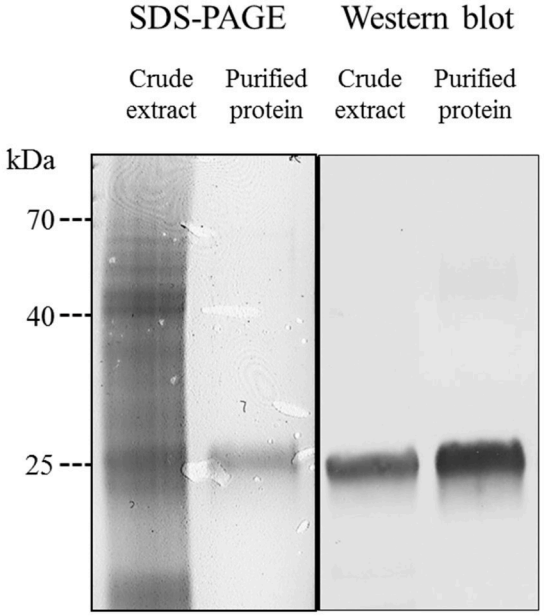

B

Purification efficiency:

Step	Protein [mg]	A_{total} [U]	$A_{specific}$ [U/mg]	Yield [%]	Purification fold
Crude extract	1.95 ± 0.08	2 ± 0.1	1 ± 0.05	100	1
Purified protein	0.26 ± 0.13	1.55 ± 0.03	5.9 ± 0.12	77	6

FIGURE 4 | Purification of Agdc1-6hp on Ni Sepharose. **(A)** Crude extract and purified Agdc1-6hp visualized on Coomassie-stained SDS-PAGE (12%) and Western blot, using primary antibodies anti-polyhistidine from rabbit and secondary antibodies anti-rabbit from goat. **(B)** Summary of the Agdc1-6hp purification.

decarboxylase, *2-oxopent-4-dienoate hydratase*, *4-hydroxy-2-oxovalerate aldolase*. These data suggest that additional enzymes are involved in tannic acid degradation. These enzymes convert the pyrogallol into pyruvate and acetaldehyde and make them available to the central metabolism (**Figure 6**). In addition, microarray data showed the upregulation of genes involved in β-oxidation process but not in the glyoxylate cycle, methyl citrate cycle and in the catabolism of the branched-chain amino acids valine, leucine and isoleucine (Supplementary Figures S1–S4).

Gallic Acid Tolerance by *A. adeninivorans*

The growth behavior of *A. adeninivorans* G1212/YRC102 on different gallic acid concentrations was investigated. The cells were cultivated at 30°C, 180 rpm on YMM-$NaNO_3$ supplemented with 0.05–2% (w/v) gallic acid as sole source of carbon. Growth occurred in all concentrations and the growth profile at all concentrations was characterized by long adaptation phase. Cell growth required 48 h of cultivation (Supplementary Figure S5) to start to increase in rate. The $OD_{600\ nm}$ values were strongly correlated to the amount of carbon sources in medium. Despite the long adaptation phase, no growth inhibition was observed. Additionally, the final optical densities, reached during cultivation on gallic acid were lower than those seen in growth on medium supplemented with an equal concentration of glucose.

Role of Agdc1p in *A. adeninivorans* on Metabolizing Gallic Acid

Previous investigations indicated that Agdc1p is an enzyme expressed by a gallic acid inducible gene. To analyse its *in vivo* role, three *A. adeninivorans* strains G1212/YRC102, G1212/YRC102-AYNI1-AGDC1-6H, and G1234 [*Δagdc1*] were studied. All strains were cultivated at 30°C up to 146 h on YMM-$NaNO_3$ supplemented with 2% (w/v) glucose, 2% (w/v) gallic acid, or 1% (w/v) gallic acid plus 1% (w/v) glucose. Dcw, gallic acid decarboxylase activity and its yield [Y(P/X)] were determined. Deletion of *AGDC1* contributed to cells death or growth inhibition when gallic acid was present in culture medium (**Figure 7**). No gallic acid decarboxylase activity was detected in crude extract of *A. adeninivorans* G1234 [*Δagdc1*] in all cultivation conditions. Additional metabolite analysis showed that gallic acid remains in the culture medium during the entire cultivation. This was not detected when *A. adeninivorans* G1234 [*Δagdc1*] was cultivated in a medium with protocatechuic acid as the carbon source

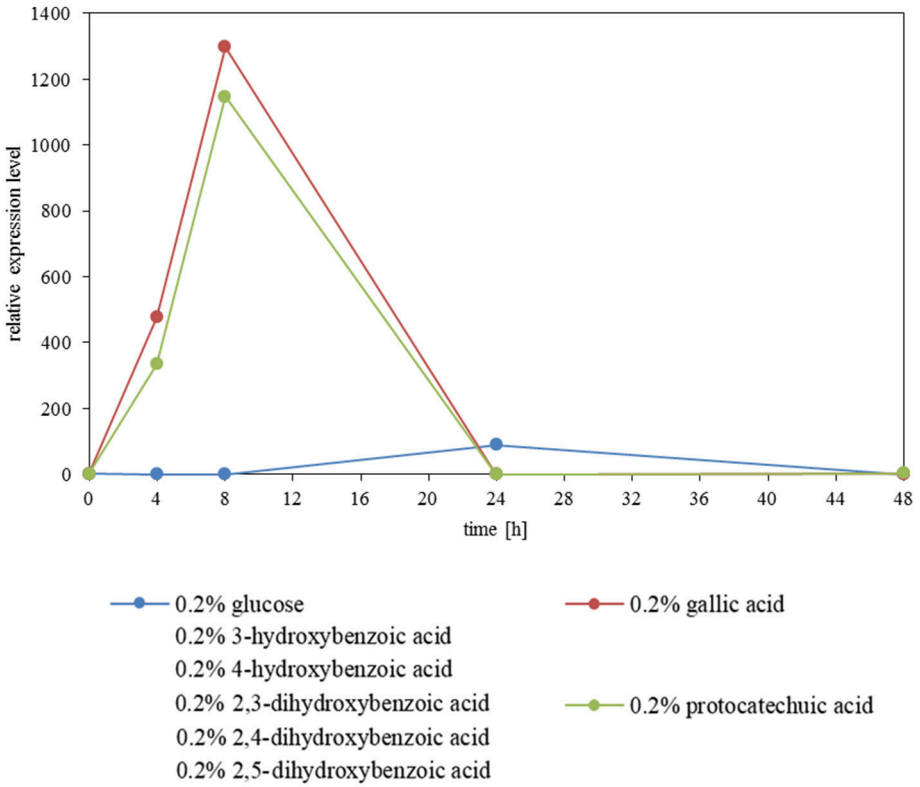

FIGURE 5 | Influence of carbon sources on the gene expression level of *AGDC1* in *A. adeninivorans* G1212/YRC102 cultivated on YMM-$NaNO_3$ supplemented with each 0.2% glucose, gallic acid, protocatechuic acid, 3-hydroxybenzoic acid, 4-hydroxybenzoic acid, 2,3-dihydroxybenzoic acid, 2,4-dihydroxybenzoic acid and 2,5-dihydroxybenzoic acid. Expression analysis was performed by nested quantitative real time PCR.

(**Figure 8**). In contrast gallic acid decarboxylase was synthesized and accumulated in the control strain *A. adeninivorans* G1212/YRC102 when gallic acid was present in the medium. On the other hand, the overexpression strain *A. adeninivorans* G1212/YRC102-AYNI1-AGDC1-6H exhibited activity during cultivation on glucose and reached 1,064 U/l and 97.5 U/g between 96–146 h of cultivation. The highest enzyme activity of 1,617 U/l and 148 U/g was detected in the crude extract of *A. adeninivorans* G1212/YRC102-AYNI1-AGDC1-6H after cultivation on a mixture of gallic acid and glucose. In comparison, the cultivation of G1212/YRC102 in the same conditions exhibited maximal 446.7 U/l and 37.5 U/g. However, the overexpression of *AGDC1* did not significantly improve the cells growth on gallic acid (**Figure 7**).

To demonstrate that the main role of gallic acid decarboxylase in *A. adeninivorans* is to degrade gallic acid, *A. adeninivorans* G1212/YRC102 and G1234 [*Δagdc1*] were cultivated for 48 h on YMM-$NaNO_3$ supplemented with 0.2% (w/v) of different hydroxylated aromatic acids as sole source of carbon. Samples were collected at 0, 30, and 48 h of cultivation for metabolite analysis. This investigation demonstrated that *A. adeninivorans* G1212/YRC102 is unable to grow on 2.3-dihydroxybenzoic acid. However, this strain was able to grow on all other carbon sources (gallic acid, protocatechuic acid, 3-hydroxybenzoic acid, 4-hydroxybenzoic acid, 2,4-dihydroxybenzoic acid and 2,5-dihydroxybenzoic acid) with different adaptation times. The deletion mutant was unable to grow on gallic acid and 2.3-dihydroxybenzoic acid as carbon source. In all other cases, the adaptation phase of *A. adeninivorans* G1234 [*Δagdc1*] was shorter and cells grew faster compared to the control strain. Interestingly, the best growth of both strains was observed for 3-hydroxybenzoic acid and the slowest growth was with 4-hydroxybenzoic acid (**Figure 9**).

In vivo transformation of gallic acid to pyrogallol by *A. adeninivorans* was investigated. *A. adeninivorans* G1212/YRC102 and G1212/YRC102-AYNI1-AGDC1-6H were cultivated on YMM-$NaNO_3$ supplemented with 0.25% gallic acid plus 0.5% glucose as the carbon source. The metabolites were analyzed by GS-MS. Complete consumption of gallic acid occurred after 48 h cultivation of the control strain and after 96 h of the G1212/YRC102-AYNI1-AGDC1-6H strain. The maximum extracellular pyrogallol production was detected after 24 h incubation. The yield, calculated as the % of substrate converted into the product detected in the culture medium, was similar for both strains; approximately 2.7% for control strain and 2.2% for overexpression strain (**Figure 10**). Pyrogallol was only product detected during degradation of gallic acid by *A. adeninivorans*.

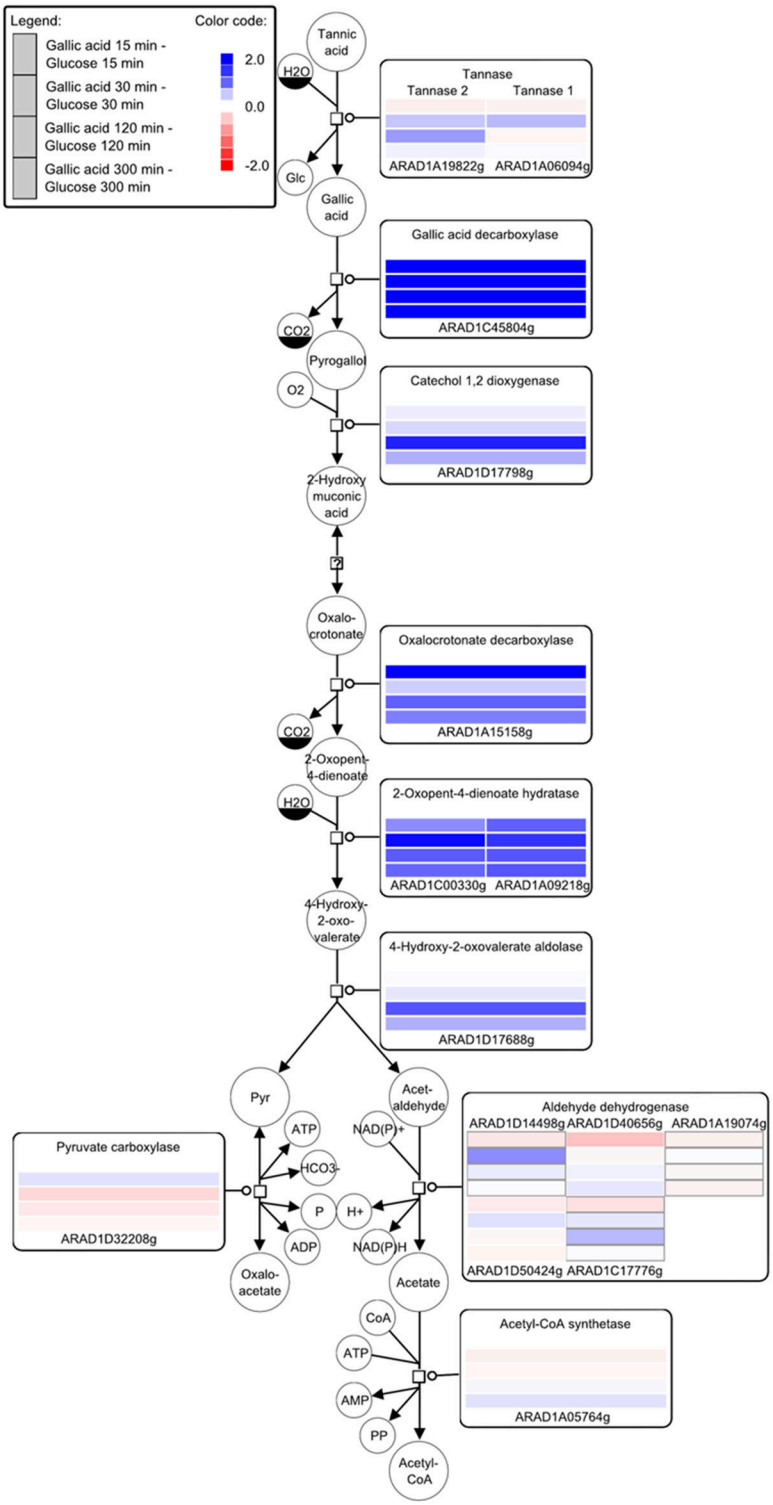

FIGURE 6 | Key compounds of the tannin catabolism - microarray studies. The SBGN style metabolic network depicts reactions catalyzed by the corresponding enzymes (rectangular square). Enzymes are enriched with color-coded fold change values of time resolved expression data of the respective genes. The colors represent upregulation (blue) and downregulation (red) of genes in cells shifted to a medium containing gallic acid as the carbon source compared to cells grown with glucose. Metabolites or enzymes occurring multiple times in the metabolic network are decorated with a clone marker (e.g., NAD^+) [produced using VANTED–(Junker et al., 2012; Rohn et al., 2012)].

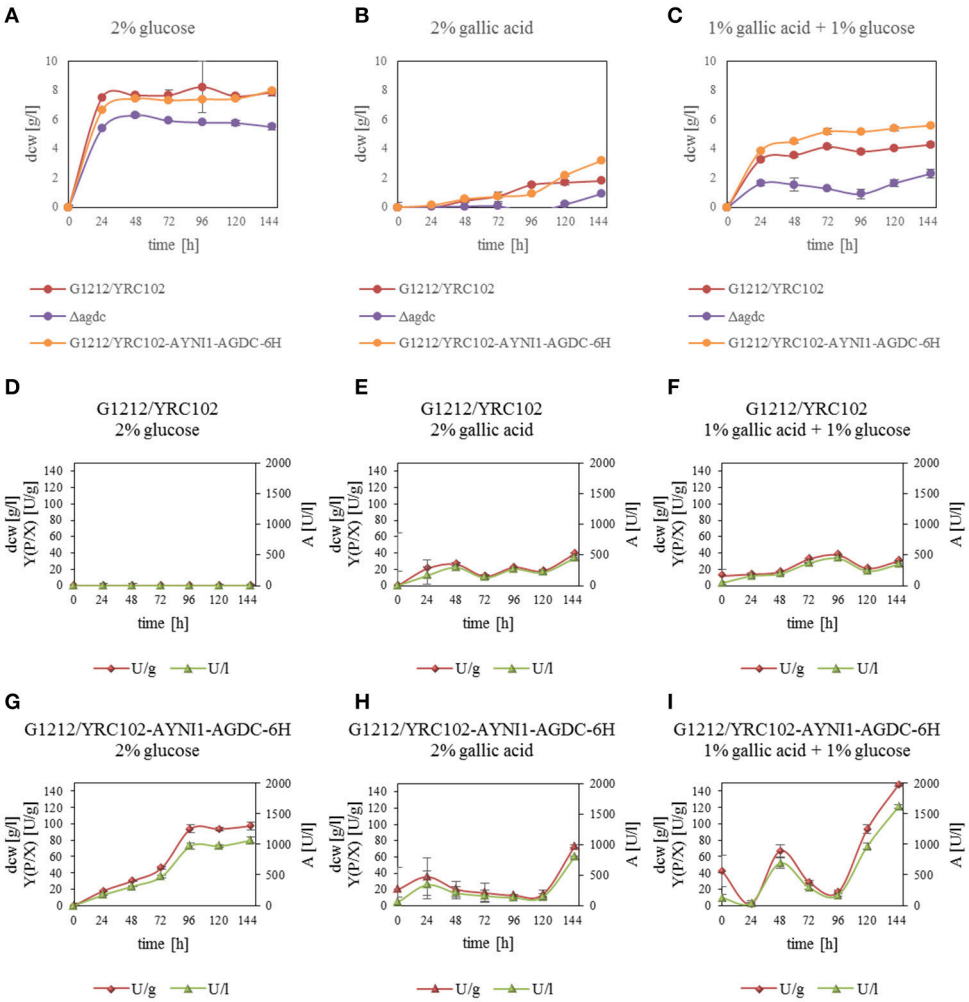

FIGURE 7 | (A–C) Influence of carbon source on the dry cell weight of *A. adeninivorans* G1212/YRC102, G1212/YRC102-AYNI1-AGDC1-6H and G1234 [Δ*agdc1*] as well as **(D–I)** Agdc1-6hp activity and yield [Y(P/X)] with cultivation in YMM-$NaNO_3$ with 2% glucose, 2% gallic acid or 1% glucose plus 1% gallic acid as carbon sources.

Degradation of protocatechuic acid in *A. adeninivorans* was also studied and the products produced during the degradation of protocatechuic acid by G1212/YRC102 and G1212/YRC102-AYNI1-AGDC1-6H were analyzed. The products detected in the culture medium during cultivation were catechol, *cis,cis*-muconic acid and trace amounts of 3-hydroxybenzoic acid, 4-hydroxybenzoic acid, 1,4-dihydroxybenzene and 1,3,4-benzentriol (**Figures 11A,B**).

In addition, a time course analysis of protocatechuic acid consumption (**Figures 11A,B**) by the overexpression strain *A. adeninivorans* G1212/YRC102-AYNI1-AGDC1-6H was conducted. The protocatechuic acid was completely degraded after 48 h and the maximum catechol concentration was detected after 24 h of cultivation. *Cis,cis*-muconic acid appeared even later, and the highest concentration was observed at 48 h of cultivation of G1212/YRC102 strain and after 72 h in G1212/YRC102-AYNI1-AGDC1-6H. The yield, calculated as the % of protocatechuic acid converted into the product (*cis,cis*-muconic acid) detected in the culture medium, was 42.5% for G1212/YRC102 and 71.2% for G1212/YRC102-AYNI1-AGDC1-6H (**Figure 11B**).

DISCUSSION

Decarboxylation of hydroxylated aromatic acids has been reported in bacteria and fungi. A well-known example is the non-oxidative decarboxylation of gallic acid, which leads to the synthesis of pyrogallol (Grant and Patel, 1969; Yoshida et al., 1982; Li and Wang, 2015). The yeast *A. adeninivorans* LS3 has been described as a microorganism able to utilize some hydroxylated aromatic acids such as tannic acid, gallic acid, protocatechuic acid, as a sole source of carbon and energy (Sietmann et al., 2010). The authors described the pathways for the degradation of gallic acid, protocatechuic acid and 4-hydroxybenzoic acid in the LS3 wildtype strain. However, the enzymes involved in the degradation of these compounds have

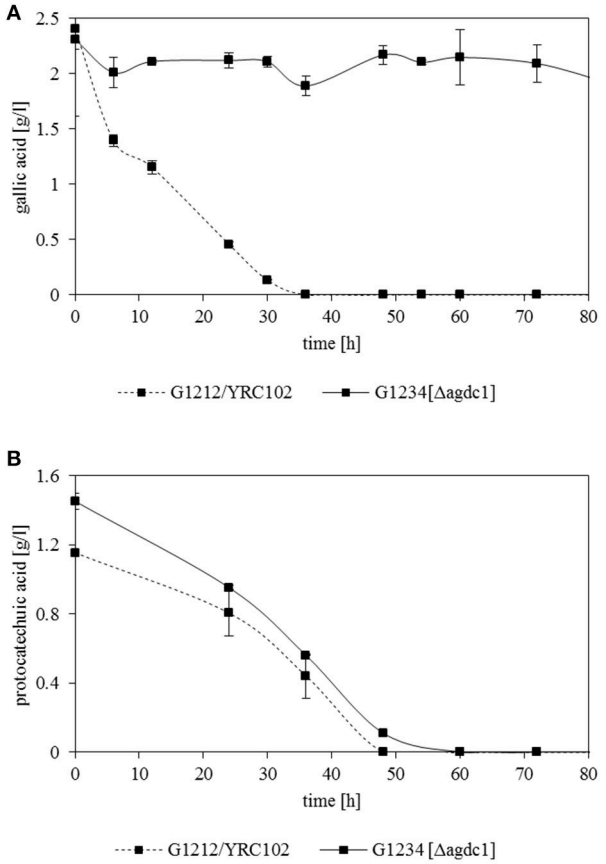

FIGURE 8 | Degradation of **(A)** gallic acid and **(B)** protocatechuic acid by *A. adeninivorans* G1212/YRC102 and G1234 [Δ*agdc1*] cultured in YMM-$NaNO_3$ with 0.25% (w/v) gallic acid or protocatechuic acid as sole carbon source. The metabolites accumulated in the supernatant were analyzed by GC-MS.

not been identified and characterized. The complete genome data of *A. adeninivorans* has been available since 2014 (Kunze et al., 2014), which has allowed detailed studies of the tannic acid degradation pathway.

For the first time, it has been demonstrated that deletion of the gene encoding gallic acid decarboxylase causes changes in the morphology of *A. adeninivorans* cells. This organism is a dimorphic microorganism but the exact physiological regulation of dimorphism is still unknown. The only factor known to initiate a change of cell shape from budding cells to mycelia is a temperature above 42°C. It is not clear why the lack of this enzyme causes the change in morphology and it is not known if deletion of further enzymes involved in this pathway will have a similar effect. Gallic acid decarboxylase plays very important role in the metabolism of tannins and phenol derivatives, which are toxic for cells and the lack of this enzyme may cause cell stress and possible changes in shape. It is also possible that the enzyme is somehow connected with a signaling pathway which is controlled by temperature allowing mycelia to form at 30°C. Finally, it is possible that the enzyme plays some other important roles which are still not known and further study is required to explain the enzymes role in the dimorphism of *A. adeninivorans*.

Gallic acid decarboxylase is one enzyme of this pathway that transforms gallic acid to pyrogallol. Gallic acid decarboxylases described so far are known for their instability due to a high oxygen sensitivity, and only a few have been successful purified (Zeida et al., 1998; Jiménez et al., 2013). Some gallic acid decarboxylases have been partially characterized, whereas the rest of them remain uncharacterized due to their complete loss of activity after purification (Grant and Patel, 1969; Brune and Schink, 1992; Yoshida et al., 2010). In this study gallic acid decarboxylase from *A. adeninivorans* fused with C-terminal HisTag region (Agdc1-6hp) has been successfully purified and characterized for the first time. Selection of the appropriate buffer and pH seems to be crucial for the storage of purified Agdc1-6hp. The enzyme stored in crude extract at 4°C for 5 days led to 42% loss of activity which is similar to the results obtained by Zeida et al. (1998). In 50 mM potassium phosphate buffer (pH 6) the purified enzyme retained 60% activity after 9 days at 4°C. A decrease in enzyme activity was not observed after one-month storage at −80°C. This suggests the possibility for long-term storage of Agdc1-6hp. The native molecular mass is approximately 27 kDa which indicates a monomeric enzyme. This is uncommon in comparison to known bacterial gallic acid decarboxylases, some of which consist of six subunits (Zeida et al., 1998; Jiménez et al., 2013) and decarboxylases from *Bacillus megaterium* and *Clostridium hydroxybenzoicum* possess a minimum two enzyme subunits (He and Wiegel, 1995, 1996; Omura et al., 1998).

Several metal ions were tested as potential cofactors for Agdc1p. Almost all metal ions had negative influence and some like Fe^{2+} or Ni^{2+} completely inhibited the activity. $Na_2S_2O_3$ used as stabilizer for gallic acid decarboxylases from *Pantotea agglomerans* T71 or *Lactobacillus plantarum* WCFS1 did not show any stabilization effect on Agdc1p. Instead, it resulted in decrease of activity up to 85% (Zeida et al., 1998; Jiménez et al., 2013). Addition of DTT and ascorbic acid to the reaction mixture exhibited 107 and 116% of relative activity respectively, compared to the control. Addition of EDTA alone led to 146% relative activity which is in contrast to the inhibitory effect of EDTA on gallic acid decarboxylase observed in *P. agglomerans* T71 (Zeida et al., 1998). Because the purification procedure was carried out on Ni Sepharose column, it is possible that the EDTA does not directly affect the enzyme but acts by chelating the nickel residues after purification, which could have inhibitory effects on the enzyme activity. However, it is also possible that EDTA positively affects the enzyme. *In vitro* investigation of kinetic and substrate specificity of Agdc1-6hp indicated that the enzyme has four times higher affinity for gallic acid than for protocatechuic acid. The K_m value for gallic acid is 0.7 ± 0.2 mM and 3.2 ± 0.2 mM for protocatechuic acid. In comparison, the K_m for gallic acid is 0.96 mM for gallic acid decarboxylase from *P. agglomerans* T71 which is unable to decarboxylate other gallic acid analogs (Zeida et al., 1998). The ability of Agdc1-6hp to decarboxylate other hydroxylated aromatic acids *in vitro* has not been confirmed. Most of the gallic acid decarboxylases, which have been characterized have a limited substrate spectrum (He and Wiegel, 1995, 1996; Zeida

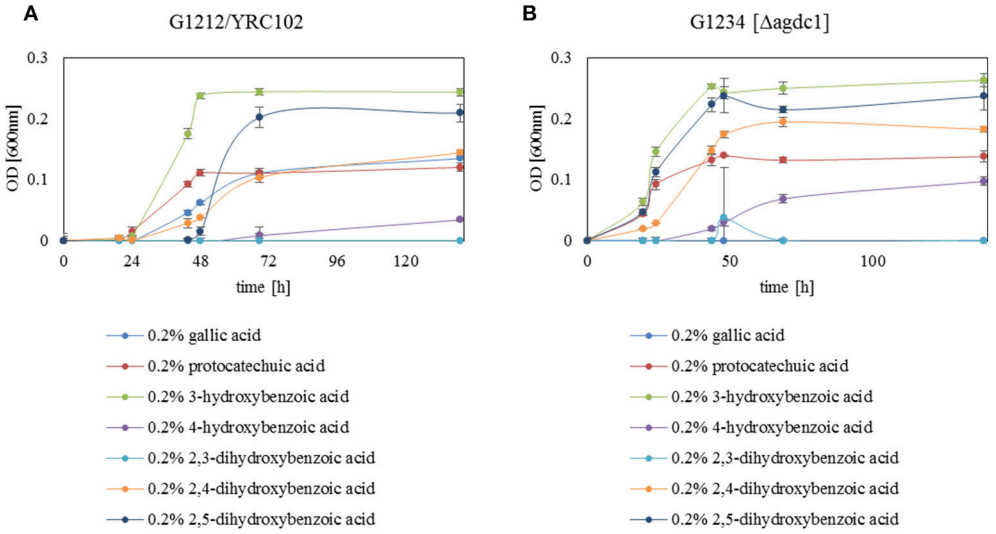

C

	Cells growth	
Carbon source (0.2%)	G1212/YIC102	G1234 [Δ*agdc1*]
gallic acid	yes	**no**
protocatechuic acid	yes	yes
3-hydroxybenzoic acid	yes	yes
4-hydroxybenzoic acid	yes	yes
2,3-dihydroxybenzoic acid	**no**	**no**
2,4-dihydroxybenzoic acid	yes	yes
2,5-dihydroxybenzoic acid	yes	yes

FIGURE 9 | Growth behavior of **(A)** *A. adeninivorans* G1212/YRC102 and **(B)** G1234 [Δ*agdc1*] on YMM-$NaNO_3$ with different hydroxylated aromatic acids (each 0.2% gallic acid, protocatechuic acid, 3-hydroxybenzoic acid, 4-hydroxybenzoic acid, 2,3-dihydroxybenzoic acid, 2,4-dihydroxybenzoic acid and 2,5-dihydroxybenzoic acid) as carbon source. Measurements were made in triplicate. **(C)** Summarize of growth behavior of *A. adeninivorans* on different hydroxylated aromatic acids as sole source of carbon.

et al., 1998). The 3,4-dihydroxybenzoate decarboxylase from *Enterobacter cloacae* P can decarboxylate protocatechuic acid, but not gallic acid (Yoshida et al., 2010).

The cultivation of the control strain, *A. adeninivorans* G1212/YRC102, on YMM-glucose-$NaNO_3$ did not reveal gallic acid decarboxylase activity during the cultivation. This suggests that Agdc1p is an enzyme encoded by an inducible gene. Nested qRT-PCR assays confirmed the inducibility of the *AGDC1* gene in presence of gallic acid and also protocatechuic acid. In contrast, glucose and the other selected hydroxybenzoic acid compounds were not able to induce the *AGDC1* gene. The most vigorous gallic acid degrading microorganisms contain inducible *GDC* genes (Yoshida and Yamada, 1985; O'Donovan and Brooker, 2001; Gauri et al., 2013; Jiménez et al., 2013; Li and Wang, 2015; Reverón et al., 2015). An exception is *Klebsiella aerogenes* where decarboxylation of gallic acid, protocatechuic acid and 2.5-dihydroxybenzoic acid were shown to be constitutive (Grant and Patel, 1969).

A. adeninivorans tolerates as much as 2% (w/v) gallic acid however, regardless of the gallic acid concentration, the growth curves exhibit long lag phases. Since gallic acid is a weak acid, its presence results in the lowering of the pH value of the culture medium a moderate amount e.g. supplementation with 1% (w/v) gallic acid lowered the pH value to approximately 3.8. At this pH, gallic acid is undissociated and can go across the yeast cell membrane. Inside the cell, the higher pH causes the gallic acid to dissociate, which reduces the pH_i to below the physiological range of the cell and thus interferes homeostasis. Both factors generate antimicrobial properties of hydroxylated aromatic acids, generating cell stress, extending the lag phase and inhibiting cell growth (Noda et al., 1982; Restaino et al., 1982; Beales, 2003; Ibraheem and Ndimba, 2013). An experiment which cultivated *A. adeninivorans* on a medium with a constant pH 6 (optimal for growth of *A. adeninivorans*) showed that cells were unable to degrade gallic acid resulting in cell death (data not showed). The overexpression of *AGDC1* did not shorten the

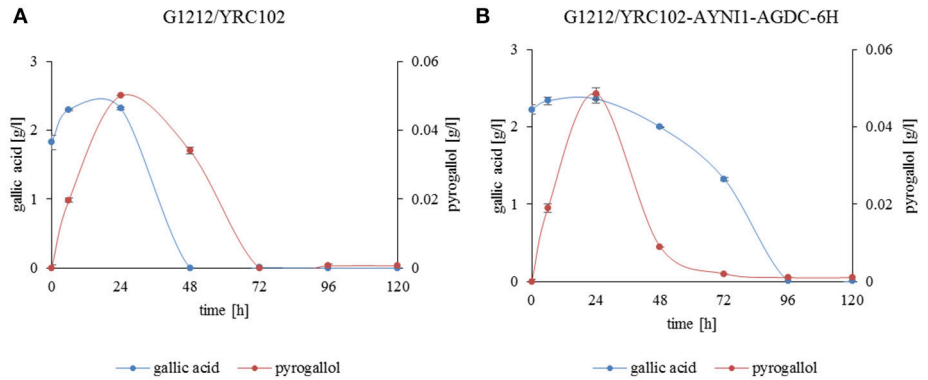

FIGURE 10 | Gallic acid degradation (blue line) and pyrogallol production (red line) by **(A)** *A. adeninivorans* G1212/YRC102 and **(B)** G1212/YRC102-AYNI1-AGDC1-6H cultivated on YMM-$NaNO_3$ with 0.25% gallic acid plus 0.5% glucose.

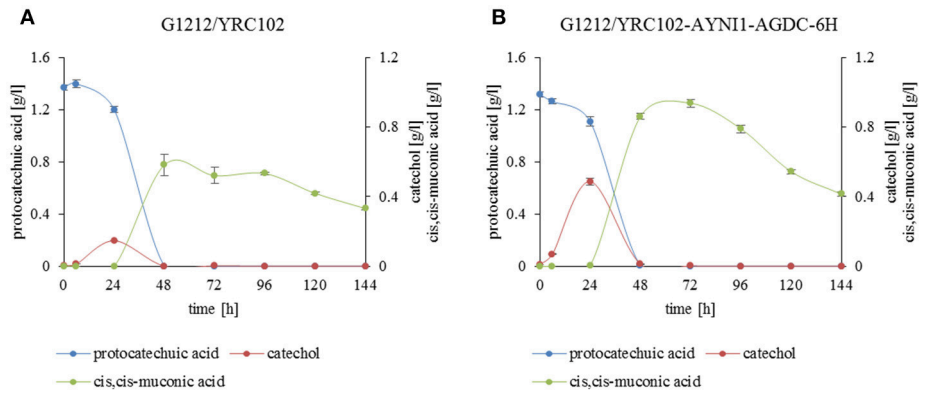

FIGURE 11 | Substrate and product accumulation during the degradation of protocatechuic acid by *A. adeninivorans* **(A)** G1212/YRC102 and **(B)** G1212/YRC102-AYNI1-AGDC1-6H. Cells were cultivated on YMM-$NaNO_3$ with 0.25% protocatechuic acid plus 0.5% glucose. Compounds present in culture medium were detected via GC-MS.

lag phase or increase the cell growth period significantly over 120 h (**Figure 7**). Also, the activity of Agdc1p was lower and appeared later in comparison to cultivation on glucose. These results suggest a stress response at the level of gene expression generated by gallic acid. A longer log phase was also observed when *A. adeninivorans* was cultivated on other hydroxylated aromatic acids as sole source of carbon which indicates a similar effect on the cells (**Figure 9**).

The deletion of *AGDC1* in *A. adeninivorans* genome results in cell death when cells were cultivated on gallic acid (**Figure 8**). This suggests that there is no other pathway able to degrade gallic acid which is supported by extracellular metabolite analysis of the control strain, *A. adeninivorans* G1212/YRC102, which showed only the production of pyrogallol. In the previous study Sietmann et al. (2010) reported that in *A. adeninivorans,* oxidative and non-oxidative decarboxylation of protocatechuic acid occur simultaneously; indeed the G1234 [Δ*agdc1*] was still able to grow and degrade protocatechuic acid. Analysis of the metabolites in culture medium showed that control strain and the overexpression strain produced catechol and *cis,cis*-muconic acid. Trace amounts of 3-hydroxybenzoic acid, 4-hydroxybenzoic acid, 1,4-dihydroxybenzene and 1,3,4-benzentriol were also detected. Our investigations have confirmed that the degradation of protocatechuic acid involves gallic acid decarboxylase and other enzymes.

To confirm which compounds are produced during the cultivation of *A. adeninivorans* on protocatechuic acid, further investigations are required. Cultivation of *A. adeninivorans* G1234 [Δ*agdc1*] on media containing different hydroxylated aromatic acids as sole source of carbon revealed that only cultivation on gallic acid led to cell death (**Figure 9**). This indicates that gallic acid decarboxylase is the key enzyme in the degradation of gallic acid by *A. adeninivorans*. Furthermore, we determined that all of the tested aromatic acids except 2,3-dihydroxybenzoic acid can serve as sole source of carbon for *A. adeninivorans*. However, the first step of degradation is not carried out by gallic acid decarboxylase. Considering all aspects of growth and gene expression analysis, it seems that the tannic acid degradation pathway is used exclusively for tannins and gallic acid. Protocatechuic acid can be degraded also by this pathway,

but the other aromatic acids are degraded through a separate pathway(s).

Interestingly the overexpression of *AGDC1* did not increase the accumulation of extracellular pyrogallol when cells were cultivated on glucose and gallic acid. The yield was approximately the same for both the control and the overexpression strain. The reason could be that most extracellular pyrogallol is accumulated in the first 24 h of cultivation. At this time, the cells are under strong stress conditions created by gallic acid. This results in low gene expression and low recombinant enzyme content. Probably the pre-adaptation of cells on low gallic acid concentration increases the yield of pyrogallol in the strain with overexpression of *AGDC1*. To obtain a higher yield of extracellular pyrogallol, further engineering of *A. adeninivorans* and optimization of the cultivation conditions are necessary.

Unexpectedly, the overexpression of gallic acid decarboxylase contributed to the accumulation of *cis,cis*-muconic acid. The yield increased almost by 71.2% over the control which suggests that *A. adeninivorans* could be an efficient synthesizer of this difficult to produce molecule. Nevertheless, further investigation and optimization are necessary to demonstrate this possibility.

The microarray data revealed the genes involved in the degradation of gallic acid. The *AGDC1* and *catechol-1,2-dioxyenase* genes encode the first two enzymes involved in the degradation of gallic acid which cleave the aromatic ring, resulting in the production of pyruvate and acetaldehyde. This is similar to the situation in *Eubacterium oxidoreducens* and *Pelobacter acidigallici* (Krumholz et al., 1987; Brune and Schink, 1992). The highest upregulation of genes in the presence of gallic acid are found in the ß-oxidation pathway. It is still an open question whether or not transporters are involved in the transport of gallic acid into *A. adeninivorans* cells. Microarray data did not exhibit any potential genes which could be recognized as gallic acid transporter(s) and there is little in the literature concerning the transport of hydroxylated aromatic acids in microorganisms. Two possibilities exist, either *A. adeninivorans* does not have transporters, and therefore gallic acid couldn't enter the cells at pH 6 because it is in the dissociated form or there exist pH dependent transporter(s), which are not yet annotated in the genome.

In this study, physiological and transcriptome analysis was used to understand the catabolism of hydroxylated aromatic acids in *A. adeninivorans*. We confirmed that the genes encoding enzymes involved catabolic pathway of gallic acid are induced and aromatic acid substrates are the inducers. The construction of gallic acid decarboxylase disruption mutants revealed that gallic acid decarboxylase Agdc1p is the only enzyme responsible for transformation of gallic acid. However, other enzymes were demonstrated to be responsible for the transformation of other hydroxylated aromatic acids.

Gallic acid decarboxylase affinity for gallic acid, its substrate specificity and the possibility of long-term storage of the Agdc1p will be advantageous if the enzyme were to be commercialized. The enzyme may have useful industrial applications e.g. in bioremediation processes or in chemical synthesis. Further culture optimization as well as strain engineering could also contribute to more efficient conversion of protocatechuic acid to *cis,cis*-muconic acid which may also have industrial application.

AUTHOR CONTRIBUTIONS

AM and EB carried out the construction of the *E. coli* and *A. adeninivorans* strains, enzyme activities determination and Agdc1p analysis. AM prepared the quantitative reverse transcriptase PCR analysis. AM, AH, MM, US, and SW participated in microarray design, hybridization, gene annotation and gene expression analysis as well as visualization, AM and JR in GC–MS analysis. MM and AM prepared the microscopic analysis. RB and FS gave several useful suggestions. AM, KB, and GK drafted the manuscript. All authors read and approved the final manuscript.

ACKNOWLEDGMENTS

The research work was supported by grant from the Marie Curie Actions–Initial Training Networks (Grant No. FP7-PEOPLE-2013-ITN).

SUPPLEMENTARY MATERIAL

The Supplementary Material for this article can be found online at: http://journal.frontiersin.org/article/10.3389/fmicb.2017.01777/full#supplementary-material

REFERENCES

Badhani, B., Sharma, N., and Kakkar, R. (2015). Gallic acid: a versatile antioxidant with promising therapeutic and industrial applications. *RSC Adv.* 5, 27540–27557. doi: 10.1039/C5RA01911G

Beales, N. (2003). Adaptation of microorganisms to cold temperatures, weak acid preservatives, low pH, and osmotic stress: a review. *Compr. Rev. Food Sci. Food Saf.* 3, 1–20. doi: 10.1111/j.1541-4337.2004.tb00057.x

Böer, E., Bode, R., Mock, H. P., Piontek, M., and Kunze, G. (2009a). Atan1p-an extracellular tannase from the dimorphic yeast *Arxula adeninivorans*: molecular cloning of the *ATAN1* gene and characterization of the recombinant enzyme. *Yeast* 26, 323–337. doi: 10.1002/yea.1669

Böer, E., Piontek, M., and Kunze, G. (2009b). Xplor 2 - an optimized transformation/expression system for recombinant protein production in the yeast *Arxula adeninivorans*. *Appl. Microbiol. Biotechnol.* 84, 583–594. doi: 10.1007/s00253-009-2167-5

Böer, E., Schröter, A., Bode, R., Piontek, M., and Kunze, G. (2009c). Characterization and expression analysis of a gene cluster for nitrate assimilation from the yeast *Arxula adeninivorans*. *Yeast* 26, 83–93. doi: 10.1002/yea.1653

Bradford, M. (1976). A rapid and sensitive method for the quantitation of microgram quantities of protein utilizing the principle of protein-dye binding. *Anal. Biochem.* 72, 248–254. doi: 10.1016/0003-2697(76)90527-3

Brune, A., and Schink, B. (1992). Phloroglucinol pathway in the strictly anaerobic *Pelobacter acidigallici*: fermentation of trihydroxybenzenes to acetate via triacetic acid. *Arch. Microbiol.* 5, 157–417. doi: 10.1007/BF00249098

Gauri, S. S., Mandal, S. M., Atta, S., Dey, S., and Pati, B. R. (2013). Novel route of tannic acid biotransformation and their effect on major biopolymer synthesis

in *Azotobacter* sp. SSB81. *J. Appl. Microbiol.* 114, 84-95. doi: 10.1111/jam.12030

Gienow, U., Kunze, G., Schauer, F., Bode, R., and Hofemeister, J. (1990). The yeast genus *Trichosporon* spec. LS3; molecular characterization of genomic complexity. *Zbl. Mikrobiol.* 145, 3–12.

Grant, D. J. W., and Patel, J. C. (1969). The non-oxidative decarboxylation of *p*-hydroxybenzoic acid, gentisic acid, protocatechuic acid and gallic acid by *Klebsiella aerogenes (Aerobacter aerogenes). Antonie Van Leeuwenhoek* 35, 325–343. doi: 10.1007/BF02219153

Hashidoko, Y., Itoh, E., Yokota, K., Yoshida, T., and Tahara, S. (2002). Characterization of five phyllosphere bacteria isolated from *Rosa rugosa* leaves, and their phenotypic and metabolic properties. *Biosci. Biotechnol. Biochem.* 66, 2474–2478. doi: 10.1271/bbb.66.2474

He, Z., and Wiegel, J. (1995). Purification and characterization of an oxygen-sensitive reversible 4-hydroxybenzoate decarboxylase from *Clostridium hydroxybenzoicum*. *Eur. J. Biochem.* 229, 77–82. doi: 10.1111/j.1432-1033.1995.0077l.x

He, Z., and Wiegel, J. (1996). Purification and characterization of an oxygen-sensitive, reversible 3,4-dihydroxybenzoate decarboxylase from *Clostridium hydroxybenzoicum*. *J. Bacteriol.* 178, 3539–3543. doi: 10.1128/jb.178.12.3539-3543.1996

Ibraheem, O., and Ndimba, B. K. (2013). Molecular adaptation mechanisms employed by ethanologenic bacteria in response to lignocellulose-derived inhibitory compounds. *Int. J. Biol. Sci.* 9, 598–612. doi: 10.7150/ijbs.6091

Jiménez, N., Curiel, J. A., Reverón, I., de Las Rivas, B., and Muñoz, R. (2013). Uncovering the *Lactobacillus plantarum* WCFS1 gallate decarboxylase involved in tannin degradation. *Appl. Environ. Microbiol.* 79, 4253–4263. doi: 10.1128/AEM.00840-13

Junker, A., Rohn, H., Czauderna, T., Klukas, C., Hartmann, A., and Schreiber, F. (2012). Creating interactive, web-based and data-enriched maps using the systems biology graphical notation. *Nat. Protoc.* 7, 579–593 doi: 10.1038/nprot.2012.002

Klabunde, J., Kunze, G., Gellissen, G., and Hollenberg, C. P. (2003). Integration of heterologous genes in several yeast species using vectors containing a *Hansenula polymorpha*-derived rDNA-targeting element. *FEMS Yeast Res.* 4, 185–193. doi: 10.1016/S1567-1356(03)00148-X

Krumholz, L. R., Crawford, R. L., Hemling, M. E., and Bryant, M. P. (1987). Metabolism of gallate and phloroglucinol in *Eubacterium oxidoreducens* via 3-hydroxy-5-oxohexanoate. *J. Bacteriol.* 169, 1886–1890. doi: 10.1128/jb.169.5.1886-1890.1987

Kunze, G., Gaillardin, C., Czernicka, M., Durrens, P., Martin, T., Böer, E., et al. (2014). The complete genome of *Blastobotrys* (*Arxula*) *adeninivorans* LS3: a yeast of biotechnological interest. *Biotechnol. Biofuels* 7:66. doi: 10.1186/1754-6834-7-66

Kunze, G., and Kunze, I. (1994). Characterization of *Arxula adeninivorans* strains from different habitats. *Antonie Van Leeuwenhoek* 65, 607–614. doi: 10.1007/BF00878276

Kunze, I., Nilsson, C., Adler, K., Manteuffel, R., Horstmann, C., Bröker, M., et al. (1998). Correct targeting of a vacuolar tobacco chitinase in *Saccharomyces cerevisiae* - post-translational modifications are dependent on the host strain. *Biochim. Biophys. Acta* 1395, 329–344. doi: 10.1016/S0167-4781(97)00163-2

Li, W., and Wang, C. (2015). Biodegradation of gallic acid to prepare pyrogallol by *Enterobacter aerogenes* through substrate induction. *Bioresources* 10, 3027–3044. doi: 10.15376/biores.10.2.3027-3044

Livak, K. J., and Schmittgen, T. D. (2001). Analysis of relative gene expression data using real-time quantitative PCR and the $2-\Delta\Delta C_T$. method. *Methods* 25, 402–408. doi: 10.1006/meth.2001.1262

Malak, A., Baronian, K., and Kunze, G. (2016). *Blastobotrys* (*Arxula*) *adeninivorans*: a promising alternative yeast for biotechnology and basic research. *Yeast* 33, 535–547. doi: 10.1002/yea.3180

Middelhoven, W. J., Hoogkamer-Te Niet, M. V., and Kreger-Van Rij, N. J. W. (1984). *Trichosporon adeninovorans* sp. nov., a yeast species utilizing adenine, xanthine, uric acid, putrescine and primary n-alkylamines as the sole source of carbon, nitrogen and energy. *Antonie van Leeuwenhoek* 50, 369–378. doi: 10.1007/BF00394651

Mukherjee, G., and Banerjee, R. (2004). Biosynthesis of tannase and gallic acid from tannin rich substrates by *Rhizopus oryzae* and *Aspergillus foetidus*. *J. Basic Microbiol.* 44, 42–48. doi: 10.1002/jobm.200310317

Nakajima, H., Otani, C., and Niimura, T. (1992). Decarboxylation of gallate by cell-free extracts of *Streptococcus faecalis* and *Klebsiella pneumoniae* isolated from rat feces. *J. Food Hyg. Soc. Jpn.* 33, 371–376. doi: 10.3358/shokueishi.33.371

Noda, F., Hayaski, K., and Mizunuma, T. (1982). Influence of pH on inhibitory activity of acetic acid on osmophilic yeasts used in brine fermentation of soy sauce. *Appl. Environ. Microbiol.* 43, 245–246.

O'Donovan, L., and Brooker, J. D. (2001). Effect of hydrolysable and condensed tannins on growth, morphology and metabolism of *Streptococcus gallolyticus* (*S. caprinus*) and *Streptococcus bovis*. *Microbiology* 147, 1025–1033. doi: 10.1099/00221287-147-4-1025

Omura, H., Wieser, M., and Nagasawa, T. (1998). Pyrrole-2-carboxylate decarboxylase from *Bacillus megaterium* PYR2910, an organic-acid-requiring enzyme. *Eur. J. Biochem.* 253, 480–484. doi: 10.1046/j.1432-1327.1998.2530480.x

Restaino, L., Lenovich, L. M., and Bills, S. (1982). Effect of acids and sorbate combinations on the growth of four osmophilic yeasts. *J. Food Protection* 45, l38–l42. doi: 10.4315/0362-028X-45.12.1138

Reverón, I., de las Rivas, B., Matesanz, R., Muñoz, R., and López de Felipe, F. (2015). Molecular adaptation of *Lactobacillus plantarum* WCFS1 to gallic acid revealed by genome-scale transcriptomic signature and physiological analysis. *Microb. Cell Fact.* 14:160. doi: 10.1186/s12934-015-0345-y

Rodríguez, H., Landete, J. M., de las Rivas, B., and Muñoz, R. (2008). Metabolism of food phenolic acids by *Lactobacillus plantarum* CECT 748^T. *Food Chem.* 107, 1393–1398. doi: 10.1016/j.foodchem.2007.09.067

Rohn, H., Junker, A., Czauderna, T., Hartmann, A., Klapperstück, M., Treutler, H., et al. (2012). VANTED v2: a framework for systems biology applications. *BMC Systems Biol.* 6:139. doi: 10.1186/1752-0509-6-139

Rösel, H., and Kunze, G. (1995). Cloning and characterization of a *TEF* gene for elongation factor 1 alpha from the yeast *Arxula adeninivorans*. *Curr. Genet.* 28, 360–366. doi: 10.1007/BF00326434

Rose, M. D., Winston, F., and Hieter, P. (1990). *Methods in Yeast Genetics. A Laboratory Manual*. Cold Spring Harbor, NY: Cold Spring Harbor Laboratory.

Sietmann, R., Uebe, R., Böer, E., Bode, R., Kunze, G., and Schauer, F. (2010). Novel metabolic routes during the oxidation of hydroxylated aromatic acids by the yeast *Arxula adeninivorans*. *J. Appl. Microbiol.* 108, 789–799. doi: 10.1111/j.1365-2672.2009.04474.x

Sikkema, J., de Bont, J. A., and Poolman, B. (1995). Mechanisms of membrane toxicity of hydrocarbons. *Microbiol. Rev.* 59, 201–222.

Smyth, G. K. (2004). Linear models and empirical Bayes methods for assessing differential expression in microarray experiments. *Stat. Appl. Genet. Mol. Biol.* 3, 3. doi: 10.2202/1544-6115.1027

Smyth, G. K. (2005). "Limma: linear models for microarry data," in *Bioinformatics and Computational Biology Solutions Using R and Bioconductor,* eds R. Gentleman,V. Carey, S. I. Dudoit, and W. Huber (New York, NY: Springer), 397–420.

Steinborn, G., Gellissen, G., and Kunze, G. (2007). A novel vector element providing multicopy vector integration in *Arxula adeninivorans*. *FEMS Yeast Res.* 7, 1197–1205. doi: 10.1111/j.1567-1364.2007.00280.x

Tag, K., Lehmann, M., Chan, C., Renneberg, R., Riedel, K., and Kunze, G. (1998). *Arxula adeninivorans* LS3 as suitable biosensor for measurements of biodegradable substances in salt water. *J. Chem. Technol. Biotechnol.* 73, 385–388.

Tanaka, A., Ohnishi, N., and Fukui, S. (1967). Studies on the formation of vitamins and their function in hydrocarbon fermentation. production of vitamins and their function in hydrocarbon medium. *J. Ferment. Technol.* 45, 617–623.

Teste, M. A., Duquenne, M., François, J. M., and Parrou, J. L. (2009). Validation of reference genes for quantitative expression analysis by real-time RT-PCR in *Saccharomyces cerevisiae*. *BMC Mol. Biol.* 10, 99–113. doi: 10.1186/1471-2199-10-99

Wartmann, T., Böer, E., Pico, A. H., Sieber, H., Bartelsen, O., Gellissen, G., et al. (2002). High-level production and secretion of recombinant proteins by the dimorphic yeast *Arxula adeninivorans*. *FEMS Yeast Res.* 2, 363–369. doi: 10.1111/j.1567-1364.2002.tb00105.x

Wartmann, T., Krüger, A., Adler, K., Duc, B., Kunze, I., and Kunze, K. (1995). Temperature-dependent dimorphism of the yeast *Arxula adeninivorans* LS3. *Antonie Van Leeuwenhoek* 68, 215–223. doi: 10.1007/BF00871818

Williams, P. A., and Sayers, J. R. (1994). The evolution of pathways for aromatic hydrocarbon oxidation in *Pseudomonas*. *Biodegradation* 5, 195–217. doi: 10.1007/BF00696460

Worch, S., and Lemke, I. (2017). "Gene expression analysis in *Arxula adeninivorans*: a nested quantitative real time PCR approach," in *Yeast Diversity in Human Welfare,* eds T. Satyanarayana and G. Kunze (Singapore: Springer Science + Business Media), 251–256.

Wright, J. D. (1993). Fungal degradation of benzoic acid and related compounds. *World J. Microbiol. Biotechnol.* 9, 9–16. doi: 10.1007/BF00656508

Yang, X., Wartmann, T., Stoltenburg, R., and Kunze, G. (2000). Halotolerance of the yeast *Arxula adeninivorans* LS3. *Antonie Van Leeuwenhoek* 77, 303–311. doi: 10.1023/A:1002636606282

Yoshida, H., Tani, Y., and Yamada, H. (1982). Isolation and identification of a pyrogallol producing bacterium from soil. *Agric. Biol. Chem.* 46, 2539–2546.

Yoshida, H., and Yamada, H. (1985). Microbial production of pyrogallol through decarboxylation of gallic acid. *Agric. Biol. Chem.* 49, 659–663.

Yoshida, T., Inami, Y., Matsui, T., and Nagasawa, T. (2010). Regioselective carboxylation of catechol by 3,4-dihydroxybenzoate decarboxylase of *Enterobacter cloacae* P. *Biotechnol. Lett.* 32, 701–705. doi: 10.1007/s10529-010-0210-3

Zeida, M., Wieser, M., Yoshida, T., Sugio, T., and Nagasawa, T. (1998). Purification and characterization of gallic acid decarboxylase from *Pantoea agglomerans* T71. Appl. Environ. *Microbiol.* 64, 4743–4747.

Zhang, Z., Pang, Q., Li, M., Zheng, H., Chen, H., and Chen, K. (2014). Optimization of the condition for adsorption of gallic acid by *Aspergillus oryzae* mycelia using Box-Behnken design. *Environ. Sci. Pollut. Res.* 22, 1085–1094. doi: 10.1007/s11356-014-3409-3

Conflict of Interest Statement: The authors declare that the research was conducted in the absence of any commercial or financial relationships that could be construed as a potential conflict of interest.

frontiers in Microbiology

REVIEW
published: 25 August 2017
doi: 10.3389/fmicb.2017.01615

Microbial Carbonic Anhydrases in Biomimetic Carbon Sequestration for Mitigating Global Warming: Prospects and Perspectives

Himadri Bose and Tulasi Satyanarayana **

Department of Microbiology, University of Delhi, New Delhi, India

All the leading cities in the world are slowly becoming inhospitable for human life with global warming playing havoc with the living conditions. Biomineralization of carbon dioxide using carbonic anhydrase (CA) is one of the most economical methods for mitigating global warming. The burning of fossil fuels results in the emission of large quantities of flue gas. The temperature of flue gas is quite high. Alkaline conditions are necessary for $CaCO_3$ precipitation in the mineralization process. In order to use CAs for biomimetic carbon sequestration, thermo-alkali-stable CAs are, therefore, essential. CAs must be stable in the presence of various flue gas contaminants too. The extreme environments on earth harbor a variety of polyextremophilic microbes that are rich sources of thermo-alkali-stable CAs. CAs are the fastest among the known enzymes, which are of six basic types with no apparent sequence homology, thus represent an elegant example of convergent evolution. The current review focuses on the utility of thermo-alkali-stable CAs in biomineralization based strategies. A variety of roles that CAs play in various living organisms, the use of CA inhibitors as drug targets and strategies for overproduction of CAs to meet the demand are also briefly discussed.

Keywords: global warming, polyextremophilic microbes, thermo-alkali-stable, carbonic anhydrase, biomineralization, CA inhibitors

OPEN ACCESS

Edited by:
Rajesh K. Sani,
South Dakota School of Mines and Technology, United States

Reviewed by:
Navanietha Krishnaraj Rathinam, National Institute of Technology, Durgapur, India
Saurabh Dhiman, South Dakota School of Mines and Technology, United States

***Correspondence:**
Tulasi Satyanarayana
tsnarayana@gmail.com

Specialty section:
This article was submitted to Microbiotechnology, Ecotoxicology and Bioremediation, a section of the journal Frontiers in Microbiology

Received: *28 April 2017*
Accepted: *08 August 2017*
Published: *25 August 2017*

Citation:
Bose H and Satyanarayana T (2017) Microbial Carbonic Anhydrases in Biomimetic Carbon Sequestration for Mitigating Global Warming: Prospects and Perspectives. Front. Microbiol. 8:1615. doi: 10.3389/fmicb.2017.01615

INTRODUCTION

In the early Eighteenth century, industrial revolution took the world by storm. This led to large scale manufacture, which at that time proved to be a major economic boost world over. In the last 300 years, there has been a marked transformation in human life. Due to improved farming practices, food production increased. This along with technological advances in health, communication and transport sectors paved the way toward modern age for human civilization. This modernization led to a heavy toll on "mother nature" (Shakun et al., 2012).

The concentrations of greenhouse gases are increasing day by day mainly due to anthropogenic activities, of them about two-thirds is contributed by fossil fuels. The burning of fossil fuels results in the emission of large quantities of flue gas that contains ~ 71% N_2, 14% CO_2, 1–2% hydrocarbons, carbon monoxide, NO_x, and minor amounts of SO_x (Perry and Gee, 1995). According to IPCC, among all the greenhouse gases, CO_2 is emitted most (65% from fossil fuels and 11% from forestry). Other gases such as methane (16%), nitrous oxide (6%), and fluorinated gases (2%) are emitted in smaller amounts by anthropogenic activities (IPCC, 2014). Cumulative carbon emissions from different sectors have increased by

about 40% since 1970s. The concentrations of hazardous gases such as NOx, SOx and methane are well beyond their threshold in many cities all over the world, thus, the Air Quality Index (AQI) is declining (IPCC, 2000). CO_2 levels in the atmosphere have surged past the threshold of 400 ppm and it may not climb down for generations. This 400 ppm benchmark was broken first time in the recorded history last year. According to World Meteorological Organization (WMO), 2016 would be the first full year to exceed the mark (NOAA, 2016). As per the latest measurement by NOAA in April 2017, the concentration of CO_2 at present is 406.17 ppm (NOAA, 2017). Some of the isolated places (Arctic regions) have already breached this mark in the past few years as recorded in Mouna Loa Observatory in 2013 (IPCC, 2013). Emission Database for Global Atmospheric Research stated that global emission of CO_2 has increased by 48% in the last two decades (http://edgar.jrc.ec.europa.eu/ overview.php?v)[1]. The increase in GHG emissions has led to increase in earth's surface temperature by about 2°C from pre-industrial times (IPCC, 2000). These conditions have also led to widespread natural calamities and affected the environment adversely. An increase in warm temperature extremes and decrease in cold temperature extremes have been noted in the past few years. This has also led to an impact on the precipitation patterns around the world and disturbed the water cycle. Agricultural production has been affected due to adverse climatic changes. There has been a reduction in crop yields leading to increase in food prices, food shortage and insecurity (Adams et al., 1998). These climatic hazards are affecting the lives of people round the world particularly those who are living below the poverty line. Many freshwater, marine and terrestrial species are already on the verge of extinction. A change in the distribution and interaction pattern has been observed in many freshwater and marine phytoplanktons. According to IPCC, the period from 1983 to 2012 were the warmest years (IPCC, 2014).

Air pollution causes various respiratory and cardiac diseases. Tiny particles produced by vehicular engines and industry worsen heart and brain related disorders and increase the risk of stroke. Global warming is taking the earth toward peril and it is essential to tackle this catastrophe for our survival. It is next to impossible for developing and under developed nations to control large scale CO_2 emissions. Nevertheless, global warming has to be mitigated. Scientific and global consensus on global warming and climate change has brought the world powers together in order to hunt for new technologies for mitigating the global warming (Kheshgi et al., 2012).

The year 2015 ushered in an era of optimism and action with Paris climate change agreement. It also marks a new era of climate change reality with record levels of high greenhouse gases. In order to tackle increasing carbon emissions, carbon trading and taxation have been implemented by various countries (Princiotta, 2007). The progress made in developing carbon capture technologies has been reviewed from time to time (Boone et al., 2013; Frost and McKenna, 2013). IPCC has also published a wholesome review on different CCS technologies providing a precious input for policy makers and researchers in developing schemes for reducing GHG emissions (IPCC, 2000, 2013, 2014). Some reviews have also outlined various holistic approaches for carbon capture and also described methods for mitigating global warming. This review discusses biomimetic approach for mitigation of global warming with a special focus on utilizing nature's own catalyst, carbonic anhydrase (CA), as the biomimetic carbon sequestering agent.

APPROACHES FOR MITIGATING GLOBAL WARMING

Countries round the world have initiated a number of measures to counter the alarming rise of CO_2 in the environment which includes use of low carbon fuels (nuclear power, natural gas etc.), increasing the use of renewal energy and applying geo-engineering approaches [afforestation and reforestation, and CO_2 capture, storage and utilization (CCSU)]. All these approaches have their own set of merits and demerits. It is impossible to curtail the carbon emissions by using only one of the measures. The major drawback of these measures is very high capital investments as non-conventional energy sources are associated with high cost and at times they are not user friendly as well (Faridi and Satyanarayana, 2015). Among them, CCSU can reduce the carbon emissions by 80–85% by capturing CO_2 directly from power plants and energy intensive processes such as cement industries, which are described in detail (Boot-Handford et al., 2014; Leung et al., 2014) in the following sections.

CARBON CAPTURE AND STORAGE (CCS)

CO_2 Capture

CO_2 emissions are captured and separated from flue gas, transported via huge pipelines and stored permanently deep underground or reutilized for various applications. Various approaches have been designed for efficient CO_2 capture. These approaches are basically divided into three phases:

- Pre-combustion CO_2 capture
- Post-combustion CO_2 capture
- Oxyfuel combustion

In pre-combustion CO_2 capture, the fuel is treated initially before combustion as in the case of coal or natural gas. Coal undergoes gasification process resulting in the formation of syngas ($CO + H_2$). The reaction takes place in low O_2 environment. Further, this syngas (which is free from pollutants) undergoes water gas shift reaction to form CO_2 and H_2O. This technique can be applied in power plants using coal as a fuel source, but it incurs an efficiency loss of 7–8%. Natural gas containing mainly methane (CH_4) can be converted to syngas and rest of the procedure is same like that of coal (Olajire, 2010). In post-combustion CO_2 capture, carbon is captured from flue gas generated after combustion. This technique has been considered useful for the existing power plants and approved in small scale with a CO_2 recovery rate of 800 t/day (Wall, 2007). Oxyfuel combustion uses oxygen in place of air for combustion. This substantially reduces the NOx load in the exhaust gas. Hence

[1]Emission database for global atmospheric research EDGAR, European Commission. Available online at: http://edgar.jrc.ec.europa.eu/ (Accessed February 27, 2017).

the remaining gas only contains SO_2, water and CO_2. SO_2 can be easily removed by precipitation or desulphurization leading to about 80–98% recovery of CO_2. This process requires large quantities of pure O_2 that increases overall cost of the process. The presence of a large amount of SO_2 in flue gas would cause corrosion problems (Buhre et al., 2005; Pfaff and Kather, 2009).

CO_2 separation from flue gas is carried out by various ways such as absorption [liquid sorbents such as monoethanolamine (MEA), diethanolamine (DEA) used to separate CO_2], adsorption (solid adsorbent such as zeolite, activated carbon are used to bind CO_2 on its surface), chemical looping combustion (metal oxide is used as oxygen carrier for combustion), membrane separation (allows only CO_2 to pass through while trapping other components), hydrate based separation (flue gas exposed to high pressure of water, leading to formation of hydrates and CO_2 gets trapped within them) and cryogenic distillation (distillation at low temperature and high pressure), thereby separating the solidified CO_2 (Aaron and Tsouris, 2005; Knudsen et al., 2009; Bhown and Freeman, 2011).

CO_2 Transport

Large pipelines are used in transport of CO_2 to storage sites or to facilities where it can be reutilized. Pipelines are the most efficient and viable method of CO_2 transport to long distances. Various factors have to be considered for the proper transport of CO_2. Mass/volume ratio is optimized by transporting the CO_2 in supercritical conditions (i.e., pressure is maintained at 72.1 atm and temperature around 32°C; Svensson et al., 2004). Impurities in the CO_2 stream leads to alteration in pressure and temperature, thus, impurities must be taken care of. The formation of carbonic acid due to the presence of water leads to corrosion of the pipelines, which are mostly made of carbon steel. Large integrated network of pipelines are needed for a commercial CCS project (Aspelund et al., 2006). These large networks will help in decreasing overall length of the pipeline by 25%, thereby reducing the associated cost. The cost of transport also depends on the regional and economic conditions of a country. A cost analysis in China showed that for a mass flow of 4,000 t CO_2/day, the use of ship tankers will cost 7.48 USD/tonne CO_2 as compared to 12.64 USD/tonne CO_2 for railway tankers and 7.05 USD/tonne CO_2 for 300 km pipelines. Periodical monitoring and assessment of the pipelines is needed for efficient and regular transport (Gao et al., 2014).

CO_2 Storage: Geological Storage

Carbon dioxide can be stored into rock pores 800 m below the surface in abandoned deep saline aquifers and oil or gas reservoirs. This is called geological carbon sequestration (Orr, 2009). The choice of a good sequestering site is always useful for long term carbon storage. Porous and permeable surfaces having non-potable ground water or the sites having sedimentary rock formations made of such chemicals (e.g., calcium) can react with CO_2 leading to more stable formations, which are preferable sites for storage (Benson et al., 2005). The first large scale CO_2 sequestration project which started in 1996 was called Sleipner, located in the North Sea where Norway's Statoil Hydro strips carbon dioxide from natural gas with amine solvents and disposed of carbon dioxide in a deep saline aquifer. CO_2 can be transported in high pressures into nearly depleted oil/gas wells in order to extract the residual oil and gases, while the injected CO_2 remains stored (enhanced oil recovery). CO_2 can be injected into deep coal beds to release methane which is trapped in porous structure of coal seams (CO_2–enhanced coal bed mehane). Deep aquifers at a depth of 700–1,000 m below ground level contain high salinity brines, which can be used to store injected CO_2 captured from CCS process (Hart and Gnanendran, 2009).

Deep Ocean Storage

Oceans are the natural sinks for CO_2 and it can be injected into the ocean by direct injection and ocean fertilization. Oceans can take up about 2 billion metric tons of CO_2 per annum, the amount of carbon that would double the load in the atmosphere and would increase the concentration in the deep ocean by only 2%. At depths of more than 3 km, CO_2 gets liquefied and can easily sink to the sea floor due to its higher density than the adjoining seawater and can be stored there for a long time. Beside these, three other mechanisms have also been proposed for CO_2 storage. Physical trapping of CO_2 using immobilization in a gaseous or supercritical phase in geological formations causes its immobilization that leads to either static trapping in structural traps or residual gas trapping in porous structure. Chemical trapping in formation fluids (water/hydrocarbon) either by ionic trapping or by dissolution, where CO_2 can react chemically with minerals after dissolution to form mineral trappings or it can get adsorbed on mineral surface (adsorption trapping). Hydrodynamic trapping through the upward migration of CO_2 at very slow speed results in its trapping into the intermediate layers. In this manner, large quantities of CO_2 can be stored (Benson et al., 2005). Polymer microcapsules composed of liquid carbonate cores, which have high surface area for controlled uptake of CO_2, have been utilized for large scale carbon capture process. Higher adsorption of carbon dioxide was achieved and these microcapsules were found to be stable under typical industrial operating conditions (Vericella et al., 2015).

Demerits of CCS Technology

Although, CCS approaches are quite efficient, they still have certain implications. First of all the cost of the overall process is quite high. It has been estimated that CCS will lead to a rise in power tariff by about 10% in US alone. It also requires a large amount of energy as it consumes 25 percent of the power plant's output capacity. The use of MEA in capture methods may lead to corrosion, evaporative losses, generation of toxic degradation products, and may require significant energy to remove CO_2 during sorbent regeneration (Nielsen et al., 2012; Reynolds et al., 2012; Da Silva and Booth, 2013). There are some other disadvantages associated with the post-combustion amine capture method. The equipment will be very large as compared to the small size of a coal-fired power plant. Large volumes of solvents are needed. Regeneration of solvent by heating produces toxic byproducts, which should be scrubbed and eliminated. This

process also utilizes large volumes of water (Herzog, 1998). In this approach, the energy utilization increases by about 15–25%. During transport and storage of CO_2, there is a risk of leakage. Direct injection of CO_2 will lead to the acidification of deep ocean (Dutreuil et al., 2009) which may cause disastrous effects on marine ecosystem. That's why only geological storage of CO_2 into deep saline aquifers and unused mines is somewhat acceptable (Shahbazi and Nasab, 2016). The CCS technology is still in pilot scale and a large scale commercialization is yet to be undertaken. Way back in 2010, Tsouris et al. (2010) pointed high costs associated with CCS technology and urged the world to direct its energies on alternative energy technology. It is also true that in near future it will be very difficult to move away from fossil fuels as energy source. Biomineralization of CO_2 using metal oxides (MgO and CaO) with the help of ubiquitous biocatalyst carbonic anhydrase (CA) provides a cost effective and environmentally benign solution for mitigation of global warming, which will be discussed in detail in the ensuing sections.

Mineralization of Atmospheric Carbon

This process mimics the mineralization process occurring in nature which is responsible for the presence of huge amounts of limestone on the surface of Earth. This is called silicate weathering. It traps the atmospheric carbon by reacting with large limestone rocks such as wollastonite ($CaSiO_3$), serpentine ($Mg_3Si_2O_5(OH)_4$) and olivine (Mg_2SiO_4) (Huijgen et al., 2007; Santos et al., 2007). This process occurs in both salt and fresh waters as CO_2 gets dissolved in water easily and there exists equilibrium between CO_2, HCO_3^-, and CO_3^{2-}. The set of reactions involved in CO_2 mineralization is outlined below (Farrell, 2011):

Gaseous CO_2 dissolves quickly in water and produces a loosely hydrated aqueous form (1).

$$CO_2\,(g) \rightarrow CO_2\,(aq) \quad (1)$$

Then carbonic acid is formed when aqueous CO_2 reacts with water (2).

$$CO_2\,(aq) + OH^- \rightarrow H_2CO_3 \quad (2)$$

In the 2nd step, carbonic acid breaks down into carbonate and bicarbonate ions [(3), (4)]

$$H_2CO_3 \rightarrow wHCO_3^- + H^+ \quad (3)$$

$$HCO_3^- + OH^- \rightarrow CO_3^{2-} + H_2O \quad (4)$$

The presence of metal ions such as Ca^{2+}, Mg^{2+}, and F^{e2+} drives the precipitation of carbonate into mineral carbonates as depicted below (5):

$CO_3^{2-} + Ca^{2+} \rightarrow CaCO_3 \downarrow$ (calcite)

$CO_3^{2-} + Mg^{2+} \rightarrow MgCO_3 \downarrow$ (magnesite)

$CO_3^{2-} + Ca^{2+} + Mg^{2+} \rightarrow CaMg(CO_3)_2 \downarrow$ (dolomite)

$CO_3^{2-} + Fe^{2+} \rightarrow FeCO_3 \downarrow$ (siderite)

This process is pH dependent. At pH below 8.0, reaction 2 becomes insignificant as OH^- ions are absent. Between pH 8.0 and 10.0, both the reactions (2 and 3) occur, and above pH 10, reaction 2 occurs mainly. Due to abundant supply of OH^- at alkaline pH, mainly HCO_3^- (bicarbonate) and CO_3^- form leading to $CaCO_3$ precipitation. Also at acidic pH, the solubility of carbonate increases. In order to increase carbonate precipitation, it is necessary to make the environment alkaline. Mineral carbonation is being studied at length for its utility in biomineralization of CO_2 from flue gas. Some pilot scale studies have already been undertaken to demonstrate the viability of the process (Reddy et al., 2010).

This technique has several advantages over other sequestration based approaches:

1. This process is an environmentally benign and one of the most effective techniques of carbon sequestration, and carbonates produced naturally via mineralization of CO_2 can remain stable for centuries. This process is free from complexities and many researchers have already outlined this process in minute details, hence, easily adaptable (Seifritz, 1990; Druckenmiller and Maroto-Valer, 2005; Liu et al., 2005; Stolaroff et al., 2005; Mirjafari et al., 2007; Favre et al., 2009).
2. Raw materials for mineralization of CO_2 are in abundance. These minerals comprise a huge CO_2 reservoir having carbon equivalent to about 150,000 × 10 metric tons of CO_2. Metal oxides such as MgO and CaO are emitted from the industries as hazardous wastes in the form of fly ash (Soong et al., 2006). Mineral carbonation using such wastes will allow their re-utilization in sequestering CO_2 (Stolaroff et al., 2005). Fly ash was used for mineral carbonation in USA and concentration of CO_2 reduced from 13.0 to 9.6% and SO_2 concentration drastically decreased from 107.8 ppm to 15.1 ppm within 2 min (Reddy et al., 2010).
3. Mineral carbonates formed after sequestration will also provide industrially valuable and useful byproducts such as cements, chemicals, fillers for paper making, white paints, and other construction materials. These mineral carbonates are also used in manufacturing calcium supplements, antacids and tableting the excipient for medical usage as well as remediation of waste feed stocks (Ciullo, 1996). Pure silica with a desirable particle size can be used as a material in the construction, plastics, electronics, and glass industries.
4. The process is economically viable, since it eliminates the large scale and energy-intensive process of solvent capture of CO_2 from industrial wastes. This process does not require the transportation of supercritical CO_2 into deep underground.

Despite being very effective, it has certain limitations. The process is very slow in ambient conditions (Haywood et al., 2001). According to the study of kinetics of calcite precipitation by Dreybodt et al. (1997), except at high pH, the formation of HCO_3^- (bicarbonate) is the rate limiting step. Equilibrium constants for reactions (2) and (3) are 2.6×10^{-3} and 1.7×10^{-4}, respectively (Mirjafari et al., 2007). The rate of reaction (3) and (4) is being virtually diffusion controlled and very rapid. If CO_2 hydration rate could be enhanced in some way or the other, then maximal amount of anthropogenic CO_2 can be converted into mineral carbonates. As it is said that the "Nature has solution to every problem," we are endowed with a natural solution to the climate change problem in the form of carbonic anhydrase (CA). The CAs can speed up the entire mineralization process by catalyzing the hydration of dissolved CO_2 into bicarbonate i.e.,

the reaction 2 at a faster rate (biomineralization). The addition of dolomite and K-feldspar to the soil can further enhance carbon sequestration in soil (Xiao et al., 2016). Use of CA as a potential biocatalyst has caught the attention of many researchers and much work has been done on exploring the possibilities of using this "Nature's own catalyst" for CCS (Farrell, 2011; Alvizo et al., 2014). Zinc(II) cyclen, which is a mimic of the enzyme carbonic anhydrase, was evaluated for its utilization in carbon capture process in rigorous conditions as that in industries and it was shown to be inhibited by bicarbonate accumulation (Floyd et al., 2013). There are some CA variants which can minimize bicarbonate inhibition by protecting the active site with a hydrophobic pocket. Hence, it is worthwhile to search for natural CA enzymes which can circumvent bicarbonate inhibition. Power et al. (2016) have successfully demonstrated the utility and efficiency of bovine carbonic anhydrase (BCA) and CO_2-rich gas streams in the carbonation rate of brucite [$Mg(OH)_2$], which is a highly reactive mineral. Carbonation was affected by decrement in CO_2 supply. In the following sections, the role of CA in CCS has been described in greater detail.

Carbonic Anhydrase: Vital Cog in the Wheel of Life

Carbonic anhydrases catalyze CO_2 hydration and HCO_3^- dehydration, in almost all organisms. It (EC No. 4.2.1.1) is a zinc metalloenzyme which is used as a catalyst in living systems for the conversion of carbon dioxide to bicarbonates and vice-versa. It was the first zinc metalloenzyme to be discovered in living systems (Smith and Ferry, 2000). Zinc ion complex facilitates carbon dioxide hydration activity. In most of the organisms, CAs are required for rapid processes, particularly transport processes. For example, it is required for the removal of CO_2 from lungs and for synthesis of eye secretions. CAs maintain optimum level of CO_2 and HCO_3^- in the body as they are utilized as substrate for many enzymatic reactions. It maintains acid—base balance in blood and helps in maintaining its physiological pH and also actively participates in ion transport and respiration. Mutations in CA genes can lead to osteoporosis and mental retardation. Carbonic anhydrase II (hCAII) is present in relatively high concentrations in red blood cells (Berg et al., 2002).

Initially the presence of the enzyme was found in the animal kingdom but later on CAs showed their signatures in all three living domains (Kaur et al., 2012; Di Fiore et al., 2015). This enzyme is either found intracellularly in cytoplasm or secreted outside (extracellular) associated with the periplasm and an essential component for survival of nearly all life forms. CAs are one of the fastest among the enzymes known having k_{cat} in the order of 10^6 s^{-1} and k_{cat}/K_m in the order of $10^8 M^{-1}s^{-1}$. An "anhydrase" is defined as an enzyme that catalyzes the removal of a water molecule from a compound, and so it is this "reverse" reaction that gives carbonic anhydrase its name, because it removes a water molecule from carbonic acid (Smith et al., 1999). In plants, β—CAs have a role in photosynthesis in chloroplasts by raising the concentration of CO_2 to enhance the carboxylation rate of ribulose 1, 5-bisphosphate carboxylase (RuBisCO) (Smith and Ferry, 2000). It functions in three modes: conversion of CO_2 to bicarbonate (to be utilized by RuBisCO in C_4 plants), conversion of bicarbonate into CO_2 [for fixation by phosphoenol pyruvate carboxylase (PEPC)] and also aids in facilitated diffusion by rapid equilibration between CO_2 and HCO_3^-. It also provides bicarbonate, which is required for the metabolism in plants (Monti et al., 2013). Recently β–CA has been shown to play a role in the perception of salicylic acid in *Arabidopsi thaliana*, suggesting its requirement in defense response (Medina-Puche et al., 2017). Besides higher organisms, CAs are also required in lower organisms. In some of the heterotrophs such as *Propionibacterium*, CAs help in CO_2 reduction during glycerol fermentation that results in the formation of oxaloacetate (Wood et al., 1941). In cyanobacteria and microalgae, CAs are involved in the CO_2 concentrating mechanism (CCM), which helps the cells to photosynthesize in the absence of inorganic carbon and also due to decline in levels of CO_2 in their surrounding environment (Badger and Price, 2003). CCM helps in maintenance of CO_2 levels around the RuBisCo active centers thereby improving the efficiency of Calvin cycle. CAs have also been reported from facultative anaerobes such as *Rhodospirillum rubrum* (Gill et al., 1984). CAs supply the cellular transporters with HCO_3^- by converting CO_2 penetrating the cells into HCO_3^-. Extracellular CA in alkaliphilic cyanobacteria plays a role in their survival in high alkaline conditions in alkaline soda lakes (Soltes-Rak et al., 1997; So et al., 1998; Kupriyanova et al., 2007, 2011). In *Microcoleus* and *Rhabdoderma*, CA doesn't allow CO_2 to leak out from the cell by converting it into bicarbonate, thus preserving the intracellular C_i pool for photoautotrophic assimilation. In *Rhabdoderma*, out of two CAs present, one is bound to photosystem II (PSII) of thylakoid membranes. It participates in the light photosynthetic reactions, regulating operation of the water oxidizing complex via its protection against excess of protons, similar to luminal CA of microalgae and higher plants (Shutova et al., 2008). CA in cyanobacterial thylakoid membranes supplies CO_2 for photosynthesis in cyanobacteria. CA helps in the formation of oxaloacetic acid from carboxylase and phosphoenolpyruvate (PEP) carboxylase by providing bicarbonate which is utilized by pyruvate (Norici et al., 2002). This oxaloacetate is used for the synthesis of aspartate family of amino acids. Lysine production increases in elevated CO_2 conditions owing to the action CA and PEP carboxylase (Puri and Satyanarayana, 2010). CA in carboxysomal shell of chemolithoautotrophic cyanobacterium *Halothiobacillus neapolitanus* (CsoS3) supplies the active sites of RuBisCO with high concentrations of CO_2 necessary for RuBisCO activity and efficient carbon fixation (So et al., 2004). β–CA present in *Escherichia coli* is a major player in the cyanate degradation pathway of the organism. This type of CA has also been shown to play a role in pathogenesis of some bacteria such as *Salmonella typhimurium* (Valdivia and Falkow, 1997). In methanogens, CA plays an active role in acetate metabolism by converting the excess carbon dioxide produced into bicarbonates. It also helps in the conversion of acetate into methane. γ–class homologs of the CamH subclass are found in mitochondria, where it might have a role in the carbon transport system to increase the efficiency of photosynthetic carbon dioxide fixation (Tripp and Ferry, 2000). Hence CA and its classes play an

important role in metabolic functions of all life forms. Life without CA is virtually out of question. CA levels are also correlated with aging (Cabiscol and Levine, 1995). A variety of diseases have been associated with such oxidative damage, which includes Parkinson's disease, diabetes, rheumatoid arthritis and alzheimer's disease. Classes of CA have been briefly described in the next section.

Types of CA and Mechanism of Action

There are basically six types of CAs discovered till now, namely α, β, γ, δ, ζ, and η. They don't have any specific sequence similarity, hence representing a classical case of convergent evolution (Lane and Morel, 2000; Smith and Ferry, 2000; Lapointe et al., 2008; Del Prete et al., 2014). Characteristic features of these classes are briefly described in **Table 1**.

Despite their structural differences, CAs have similar action mechanism. This mechanism has been widely studied in α–CAs. It is a two–step ping-pong reaction that catalyzes the reversible hydration/dehydration of CO_2 into bicarbonate and a proton (Silverman, 1982). A histidine residue present near the water molecule accepts a proton (H^+) which gets released from the water molecule. It leaves only hydroxide ion attached to zinc ion. The active site has specific pockets for binding CO_2, where it gets bound to the hydroxide ion. Further, nucleophilic attack on the carbonyl group by the zinc-bound hydroxide takes place that results in HCO_3^- formation. The enzyme is then regenerated and the bicarbonate ion is released (Lindskog and Coleman, 1973; Silverman and Lindskog, 1988).

$$EZnOH^- + CO_2 + H_2O \longleftrightarrow EZnH_2O + HCO_3^- \quad (1)$$

$$EZnH_2O + PSR \longleftrightarrow EZnOH^- + PSR - H^+ \quad (2a)$$

$$PSR - H^+ + B \longleftrightarrow PSR + B - H^+ \quad (2b)$$

CA Specific Inhibitors and their Biological Relevance

CA abnormality leads to several diseases such as edema, glaucoma, hypertension, epilepsy, and cancer (Supuran, 2008). Pharmaceuticals that suppress the activity of carbonic anhydrase are classified as carbonic anhydrase inhibitors. Their clinical use has been established as diuretics, anti-glaucoma agents and antiepileptics in the management of gastric and duodenal ulcers, mountain sickness, neurological disorders, or osteoporosis (Supuran et al., 2003). Among human CA isoforms, CAIX and CAXII have already been identified as potent drug targets and molecular markers for the treatment of various types of cancer and tumors. Both show upregulated expression in cancerous cells as compared to normal cells. The two isoforms are required for maintaining intracellular pH of tumor cells. The inhibition of these two CAs is, therefore, important for cancer treatment. Several workers and companies have developed several ureido and sulfonamide based pharmaceuticals for cancer treatment which inhibit CAIX and CAXII (Cabiscol and Levine, 1995; Lomelino and McKenna, 2016).

Sulfonamide, Sulfamate, and Sulfamide Inhibitors

Sulfonamides ($R–NH_2SO_2$) constitute an important group of classical drugs which have been known for their pharmaceutical and CA inhibitory properties. The most effective are the heterocyclic sulfonamides (acetazolamide, methazolamide, ethoxzolamide). Acetazolamide is one of the well-known inhibitors of carbonic anhydrase and has rendered its effectiveness for the *in vivo* inhibition of intracellular CAs (Teicher et al., 1992). It is used in the treatment of glaucoma, epilepsy (rarely), idiopathic intracranial hypertension, and altitude sickness. Similarly other sulfanamide inhibitors such as dorzolamide and brinzolamide are used in the treatment

TABLE 1 | Characteristic features of basic six classes of carbonic anhydrases.

Characteristics	α CA	β CA	γ CA	δ CA	ζ CA	η CA
Occurrence	Predominantly in animal kingdom also found in protozoa, algae, green plants, and in some archaea, bacteria and fungi	Reported in all three domains of life	Eubacteria and Archaea *Methanosarcina thermophila*	*Thalassiosira weissfogii*	*Thalassiosira weissfogii* (marine diatom)	*Plasmodium falciparum*
Molecular weight	monomeric (Mw: 26-37 kDa)	dimer, can form various olgomeric structures 45 to 200 kDa	homotrimer 60 kDa (native)	monomer27 kDa	69 kDa	-
Active site amino acids	His – 94, His – 96, His – 119	Cys 38, His 96 and Cys 99	His 81, His 122 and His 117	-	-	His – 94, His – 96, His – 118
Function	pH homeostasis, secretion of HCO_3^-, ion exchange	cyanate degradation (*E.coli*), CO_2 fixation (cyanobacteria), Overexpressed during pathogenesis of some pathogens (*Salmonella*)	acetate metabolism and conversion of acetate to methane (methanogens)	-	-	Overexpressed during pathogenesis
Other features	esterase activity, N – terminal signal peptide for periplasmic localisation or extracellular secretion	Basic component of Carbon Concentrating Mechanism (CCM)	Oldest form of CA	-	cambialistic	

of glaucoma as well. Near about 20 CA inhibitors have been granted FDA approval and they are being put to wide clinical usage (More et al., 1946; Sugrue, 2000; Frost and McKenna, 2013; Wulf and Matuszewski, 2013; Supuran, 2016a). Sulfamic acid (NH_3SO_3) and sulfamide ($NH_2SO_2NH_2$) are the simplest CA inhibitors containing the $-NH_2SO_2$ moiety. However, the sulfonamides are less effective against some of the β–CAs like Cab and also some of the γ–CAs (Zimmerman et al., 2004) and fungal MG-CA where they inhibit in millimolar/micromolar concentrations. Sulfamic acid and sulfamide are the weakest with inhibition constants (K_i) in the millimolar range. Interestingly, a completely different inhibition profile was observed against Zn-Cam and MG-CA, where sulfamic acid and sulfananilamide were shown to be more potent than sulfonamide inhibitors. Over the years various other inhibitors of CAs (benzenesulfonamides, arylbenzenesulfonamides, tetrafluorobenzenesulfonamides, 4-aminoethylbenzenesulfonamide) have been synthesized/discovered and their potential inhibitory properties have been evaluated (Pastoreková and Pastorek, 2004; Pala et al., 2014). Two CAs (LpCA1 and LpCA2) from *Legionella pneumophila*, a pathogenic bacterium, also get inhibited by sulfanamide inhibitors (sulfonylated aromatic sulphonamides, acetazolamide, ethoxzolamide, methazolamide, and dichlorophenamide). They can serve as a promising drug target for this pathogen (Supuran, 2016b). MGM Institute of Health Sciences has developed cerium oxide nanoparticles which are plant based that exhibit CA inhibitory and antioxidant properties (Lomelino and McKenna, 2016). An electrochemical enzyme inhibition biosensor, based on CA entrapped in a carbon paste electrode using carbon black nanoparticles and solid paraffin, was developed that measures sulfanilamide inhibition of CA (Bourais et al., 2017). This biosensor can even detect the sub-micromolar levels of sulfanilamide and the detection limit was 0.4μm (Bourais et al., 2017).

Novel Inhibitors

Coumarins, phenols, polyamines, fullerenes, boronic acid and their substituted derivatives have been effective against animal CAs (Innocenti et al., 2009b; Carta et al., 2012; Supuran, 2013). Their efficacy against microbial CAs, however, must be investigated. Carta et al. (2012) recently introduced dithiocarbamates (DTCs) as a new class of Zn-binding CA inhibitors, which can interact with the nearby amino acid residues for effective binding. Indeed these promising inhibitors have been effective even in sub-nanomolar concentrations. Nitroimidazoles decrease the pH of the hypoxic cancer cells, thereby helping in the uptake of chemotherapeutic agents. Scientists are also developing CA inhibitory antibodies for cancer treatment (Lomelino and McKenna, 2016). Incorporation of sugar moieties into sulfanilamide has resulted in sharp improvement in their solubility and effectiveness. The inhibition constants for ribose and galactose sulfanilamides against bsCA1 were reduced to 8.9 and 9.2 nM as compared to 2,500 nM for the unsubstituted sulfanilamide. In contrast to other sulfonamides and sulfanilamides, glycosylsulfanilamides have a good balance between its hydro- and liposolubility, therefore, it can easily penetrate through membranes to affect the growth of microorganisms (Supuran, 2015). Mete et al. (2016) synthesized a series of new thienyl-substituted pyrazoline benzenesulfonamides and showed their effective inhibition against hCAI and hCAII.

Thermo-Alkalistable Carbonic Anhydrases

Advances in recombinant DNA technology have enabled us to modify/change a protein's structure and function as per the demand. As already stated, utilization of CAs in biomineralization of CO_2 requires the enzyme to be alkalistable as the mineralization is favored at alkaline pH (Farrell, 2011) and the temperature of flue gas is too high (around 140°C), which is cooled to about 60°C for post-combustion CO_2 capture. Hence, the enzymes needed for carbon sequestration must be thermostable. Several efforts have been made to modify the mesophilic CAs in order to make them thermo-alkali-stable. CO_2 Solutions Inc. has developed a thermally optimized CA by genetic engineering which is stable at 90°C for 24 h (CO_2 Solutions Inc., 2012). Fisher et al. (2012) modified the surface amino acid residues of hCAII (which are far away from active site) to increase the thermostability by 6°C. Some of the amino acid residues present at the surface (Tyr7, Leu224, Leu100, Leu240, Asn67, and Asn62) were replaced by Phe, Ser, His, Pro, Gln, and Leu, respectively. Directed evolution technique was utilized in order to develop a thermostable CA from β–CA from *Desulfovibrio vulgaris*. It can even retain activity at 107°C. The enzyme was stable in the presence of primary flue gas contaminats such as NOx and SOx as well as in the presence of 4.2 M concentration of N-methyl-diethanolamine (MDEA) at 50°C for about 14 weeks. The enzyme retains 40% residual activity at alkaline pH (11.8). This highly stable CA has been efficiently used for biomineralization of CO_2 at high temperature (87°C) (Alvizo et al., 2014). A whole cell bacterial catalyst was generated from the CA of *Neisseria gonorrhoeae* (*ng*CA) by engineering it in such a way that it is secreted in the periplasm of *E. coli*. This whole cell catalyst was also found stable at low pH. It might be possible to sequester CO_2 more efficiently using whole cell enzyme systems even at a pH below the pKa of HCO^{3-} or CO_3^{2-}, thereby reducing the cost of maintaining it at elevated pH (Jo et al., 2013). The modified CA thus generated by these strategies can aid in efficiently capturing CO_2, but adds to the cost. It is worthwhile to search for enzymes that are stable at two/more extreme conditions. The use of thermo-alkali-stable CA from polyextrmophiles would simplify the process. Jo et al. (2016) engineered the de-novo sulfide bond of ngCA which resulted in enhancement in both kinetic and thermodynamic stabilities. The major reason for this enhancement is the loss of conformational entropy of the unfolded state, thereby increasing rigidity.

Recent advances in technology have enabled biologists to reach the extreme maxima of earth, sea and sky for exploring their diversity. Extremophiles have been isolated from a wide array of extreme environments like deep sea vents, hot springs, upper troposphere and stratosphere, outer space and others (Wilson and Brimble, 2009). There are also reports on the isolation of polyextremophiles from mines and industries (Onstott et al., 2003; Bhojiya and Joshi, 2012). Their characterization and applications have added new dimension

to applied biology. Polyextremophiles are known to produce a variety of useful products (Coker, 2016). Metagenomics and data mining studies have revealed the presence of α, β, γ CA genes in microbes from stressed environments. β–CA from *Methanobacterium thermoautotrophicum* (CabCA) and γ–CA from *Methanosarcina thermophila* (CamCA) were the first known CAs from extremophiles (Alber and Ferry, 1994; Smith and Ferry, 2000). Two novel and highly thermo-alkali-stable α–CAs (SazCA and Ssp CA) have been discovered from thermophilic archaea *Sulfurihydrogenibium azorense* and *Sulfurihydrogenibium yellowstonense.* YO3AOP1, respectively. The former being one of the fastest known CAs till date (k_{cat}/K_m value of $3.5 \times 10^8 M^{-1}\ s^{-1}$) (De Luca et al., 2013). SSp CA is even active after 3 h incubation at 70°C. SazCA is also highly thermostable having 53 days and 8 days of half-life at 40° and 70°C, respectively. It retains carbon dioxide hydration activity even after incubation at 80 and 90°C for several hours (Russo et al., 2013). Both these enzymes are alkalistable (active at pH 9.6) and stable in the presence of flue gas contaminants such as NO^{2-}, NO^{3-}, and SO_4^{2-} (Vullo et al., 2012; De Luca et al., 2013). Two highly thermophilic bacteria isolated from hydrothermal vent ecosystems *Persephonella marina* EX-H1 (PMCA) and *Thermovibrio ammonificans* produced highly thermostable α–CA. The CA of *T. ammonificans* (TaCA) was more stable than SazCA and SspCA. This enzyme (taCA) showed thermo-stimulating properties (activity of taCA was elevated after the high temperature incubation (Jo et al., 2014). Faridi and Satyanarayana (2016a) reported a moderately thermostable and highly alkalistable α–CA(BhCA) from polyextremophilic bacterium *Bacillus halodurans*. It has a unique property of sulfate stimulation (its activity enhanced in the presence of sulfate ions). This property can be exploited for CCS as the flue gas contains SOx as one of the contaminants. BhCA did not get denatured in the presence of EDTA (Faridi and Satyanarayana, 2016b). Bose and Satyanarayana (2016) reported a moderately thermostable and alkalistable γ–CA from *Aeribacillus pallidus*, a polyextremophilic bacterium. Both ApCA and BhCA were stable in presence presence of bicarbonate (0.1M). *Psychrobacter* sp. SHUES1 isolated from frozen alkaline samples from Shanghai (China) produced carbonic anhydrase and urease which are important in microbially induced carbonate precipitation (MICP; Li et al., 2016). List of some of the thermo-alkali-stable CAs which have been characterized in the last few years have been highlighted in **Table 2** with their characteristics.

Crystal structures of three of the most thermo-alkali-stable CAs were solved and their analysis revealed the reasons of their higher thermostabilities. As per the crystallographic structure, SspCA was found to have increased structural compactness. It contained a large number of charged residues on the protein surface with a greater number of ionic networks. These might be the key factors involved in the higher thermostability of this enzyme with respect to its mesophilic homologs. It has a fold which is characterized by a 10—stranded centrally placed β–sheet, which is surrounded by several helices and β–strands. A deep conical cavity that extends from the center to the protein surface harbors the active site. Several polar and hydrophobic interactions play active role in stabilization of SspCA. SazCA has a similar structure to that of SSpCA with minor differences. SspCA has Glu2 and Gln207 residues which are substituted with His2 and His207 in SazCA. This substitution is responsible for higher SazCA catalytic activity. The crystallographic structures of both SazCA and SspCA confirmed the dimeric nature of the enzymes (Di Fiore et al., 2013; De Simone et al., 2015). Crystallographic structure analysis of TaCA revealed it to be similar to the structure of other previously known bacterial homologs (Huang et al., 1998; Di Fiore et al., 2013; De Simone et al., 2015), but having entirely novel oligomeric pattern. Indeed TaCA forms a tetramer that comprises two dimers, which are structurally similar to that of SazCA and SspCA. The two dimers are joined together by two intermolecular disulfide bridges and by inter-subunit ionic interactions (James et al., 2014). This tetrameric state may be a possible reason for the enhanced thermostability of TaCA. Tahirov et al. (1998) recorded that thermostable enzymes have higher degree of oligomerization than mesophilic enzymes. It is also worthwhile to mention that the two conserved cysteine residues, Cys202 and Cys47, are reduced partially in SspCA and SazCA due to insufficiently oxidative expression conditions. It is suggested that the presence of two cysteine residues in TaCA leads to its increased stability (James et al., 2014). These structural analyses of thermostable CAs not only provide structural insights of the enzymes but also aid in their modification, so that they can be efficiently utilized for biomineralization.

Utilization of Thermo-alkali-stable CAs in Biomineralization

Several strategies are being developed for utilization of thermo-alkali-stable CAs in mitigating global warming. CO_2 Solutions Company has developed a CA based reactor for capturing CO_2 from different CO_2 intensive industries (http://www.co_2solutions.com/en/the-process). This process requires immobilized CA. Utilization of thermo-alkali-stable CAs for carbon capture requires a series of bioreactors which will have direct supply of flue gas. It is directly supplied to a bioreactor containing the immobilized enzyme. This enzyme in aqueous condition will hydrate CO_2 present in flue gas and releases HCO_3^- and H^+. Alvizo et al. (2014) developed a process which utilizes a highly thermostable β–CA engineered from the β–CA of *Desulfovibrio vulgaris*. In this process, the set up consists of absorber column where carbon dioxide gets absorbed into MDEA; CA present in the column generates proton and bicarbonate. The residual flue gas is released and the rest (bicarbonate+amine+CA) is transferred to the next column maintained at 87°C, where CO_2 is again regenerated, accompanied by regeneration of the solvent. Pure CO_2 is later reutilized and the solvent returns back to the initial absorber column for the next cycle. The rate of CO_2 absorption increases by about 25-fold in the catalyzed reaction as compared to the non-catalyzed reaction. Normal conditions for steady-state experiments were 2 l per minute of solvent, 180 l per minute of flue gas at 25°C and absorber and desorber temperature at 87°C. All enzyme–solvent mixtures were made

TABLE 2 | Thermostable CAs and their characteristic features.

Sl. No.	Enzyme	Organism	Class	Characteristic features	References
1.	SspCA	*Sulfurihydrogenibium yellowstonense.* YO3AOP1	α	Dimer, Stable at high temperatures (70°C for 3 h) Optimum working condition–95°C, pH 9.6	Capasso et al., 2012
2.	Saz CA	*Sulfurihydrogenibium azorense*	α	Dimer, Half-life at 70°C is 8 days and 53 days at 50°C. Alkalistable (pH 9.6)	De Luca et al., 2013; Russo et al., 2013
3.	TaCA	*Thermovibrio ammonificans*	α	77 days of half-life at 60°C, tetramer	Jo et al., 2014
4.	PmCA	*Persephonella marina* EX-H1	α	88 days of half-life at 100°C, Dimer	Jo et al., 2014; Kanth et al., 2014
5.	Cab CA	*Methanobacterium thermoautotrophicum*	β	Tetramer Optimal CO_2 hydration activity at 75°C	Smith and Ferry, 2000
6.	MtCam (aerobically purified)	*Methanosarcina thermophila*	γ	Optimally active at 55°C and displayed 15 min of stability at 75°C, Activity doubles when zinc is replaced by cobalt	Alber and Ferry, 1994
7.	MtCam (anaerobicaly purified)	*Methanosarcina thermophila*	γ	NA	Tripp et al., 2004
8.	MtCam (expressed in *M. acetivorans*)	*Methanosarcina thermophila*	γ	Fe^{2+} present at active site enhances its activity	MacAuley et al., 2009
9.	BhCA	*Bacillus halodurans*	α	Thermo-alkali-table (pH 6–11), gets stimulated in the presence of SOx, stable with EDTA	Faridi and Satyanarayana, 2016a
10.	ApCA	*Aeribacillus pallidus*	γ	Thermo-alkali-stable (pH 8–11), stable in the presence of SOx and NOx	Bose and Satyanarayana, 2016

using normal tap water without any further treatment (Alvizo et al., 2014). CAs from *Caminibacter mediatlanticus* (CmCA) and *Sulfurihydrogenibium yellowstonense* YO3AOP1 (SspCA), both belonging to α–class, have been used to capture CO_2 from flue gas (Daigle and Fradette, 2014; Rossi, 2014). SspCA was characterized as prospective biocatalyst for CO_2 capture as it has regenerative absorption ability in alkaline conditions. Its prolonged half life (53 days at 40°C and 8 days at 70°C) making it one of the most suitable candidates for CCS. Ssp CA was, therefore, tested for its biomimetic carbon sequestration (Russo et al., 2013). Ssp CA immobilized in polyurethane foam (PU-SspCA) has been used in designing a bioreactor to mimic CO_2 capture process in industries (Migliardini et al., 2014). The immobilized CA (PU-SspCA) showed exceptional thermostability for very long duration even at 70°C and was highly stable at 100°C even after 48 h (Capasso et al., 2012). Heat stable carbonic anhydrases from *M. thermophila* and *Caminibacter* sp. have been used in bioreactors for efficient CO_2 removal from flue gases. *Pyrococcus horikoshii* and *M. thermophila* secreted γ–CA which was used in developing γ–CA nanoassemblies. These assemblies were developed by joining the single entitites to make multiple linked interactions with the surface of the reactor. Biotinylation sites were created by specifically mutating some of the residues to cysteines. Firm nanostructures were thus created by cross-linking biotinylated-γ–CAs with streptavidin tetramers (Salemme and Weber, 2014).

There are basically three different crystal phases for calcium carbonate ($CaCO_3$), viz. calcite (rhombic), aragonite (needle like) and vaterite (spherical)]. Calcite phase is thermodynamically the most stable phase, while the vaterite is the metastable phase which is more soluble (Favre et al., 2009). When PMCA and TaCA (both α–CAs) were utilized for biomineralization; it resulted in the formation of stable calcite (Jo et al., 2014). α–CA from *Dunaliella* sp. produced 8.9 mg of calcite per 100 μg (172 U/mg) of enzyme in presence of 10 mM Ca^{2+} (Kanth et al., 2012). Another thermo-alkali-stable γ–CA (ApCA) from polyextremophilic bacterium *A. pallidus* was used for biomineralization and well faceted rhombohedral calcite crystals were observed when viewed under scanning electron microscopy (SEM; **Figure 1**). The partially purified enzyme caused precipitation of 42.5 mg CO_3^{2-} mg^{-1} protein (Bose and Satyanarayana, 2016). Optimization of the process parameters led to an increase in carbonate precipitation up to 200 mg CO_3^{2-} mg^{-1} protein (Bose and Satyanarayana, 2017).

When a highly alkalistable and moderately thermostable α–CA (BhCA) from *Bacillus halodurans* was used for biomineralization, well defined calcite crystals were observed (Faridi and Satyanarayana, 2016a). ApCA and BhCA were also utilized for testing their efficacy in CO_2 sequestration from flue gas using vehicular exhaust (**Figure 2**). Vehicular exhaust has a comparable composition as that of flue gas emitted from the thermal power plants (∼71% N_2, 14% CO_2, 1–2%

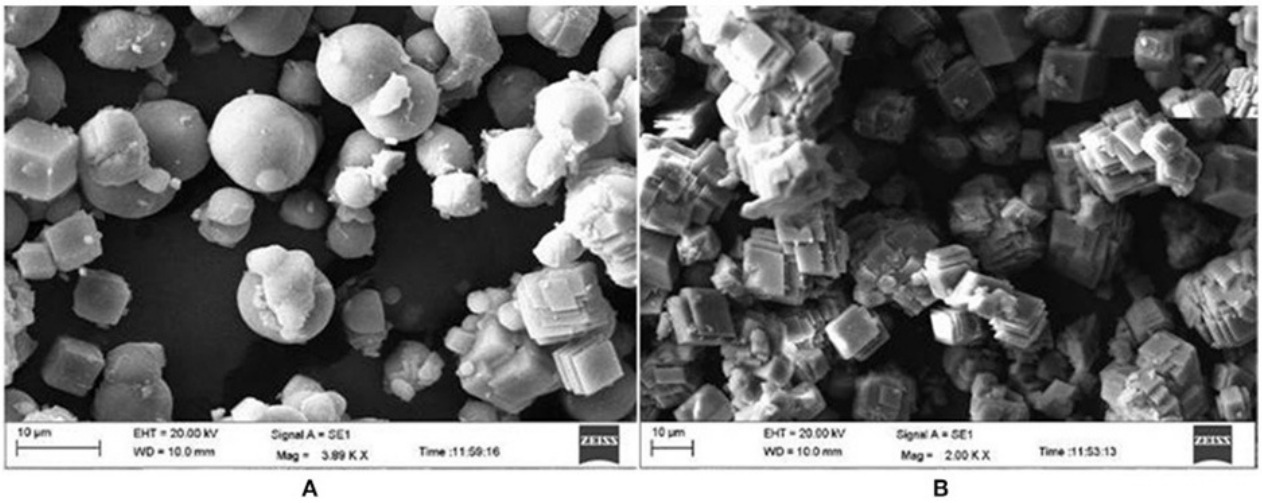

FIGURE 1 | Scanning electron microscopic picture of calcium carbonate crystals in the presence and absence of CA (control). **(A)** Spherical vaterite crystals were formed in the control. **(B)** Rhombohedral and well faceted calcite crystals were formed in the presence of ApCA (adopted from Bose and Satyanarayana, 2016).

hydrocarbons, carbon monoxide, NO_x, and minor amount of SO_2; Perry and Gee, 1995). Both the enzymes were useful in sequestering CO_2 from vehicular exhaust, hence making them efficient candidates for biomineralization (Faridi and Satyanarayana, 2016b; **Figure 3**). Biomineralization process for ApCA and BhCA was performed at 37°C in a 75 mL total reaction volume. CA (0.05 mg) was dispersed in 15 mL Tris buffer containing 0.9 g of $CaCl_2.2H_2O$ in Tris (2.52 g) buffer according to a protocol used by Mirjafari et al. (2007). To initiate the mineralization process, 60 mL of CO_2 solution was added to the enzyme mix. The reaction was performed for 10 min at 37°C. In an interesting study, the effect of CA from *Bacillus mucilaginosus* on carbonate formation and wollastonite dissolution were explored under variable CO_2 conditions. Real time PCR was used to analyze the correlation between CA gene expression, sufficiency or deficiency of calcium and CO_2 concentration. The findings reaffirmed the belief that CO_2 concentration is not related to effects of CA. Further, they also showed that microbial CA has some role in silicate weathering (Xiao et al., 2014). Some of the other alkalistable CAs have also shown efficacy in carbon sequestration. Another α–CA from *Serratia* sp., which was alkalistable in nature, was successful in generating calcite crystals (Srivastava et al., 2015). Some of the mesophilic CAs from some other microorganisms such as *Pseudomonas fragi* (27.33 mg CO_3^{2-}/mg of protein), *Bacillus pumillus* (25.43 CO_3^{2-}/mg of protein), *M. lylae* (24.02 CO_3^{2-}/HCO^{3-}/mg of protein) (Prabhu et al., 2011) and *Citrobacter freundii* SW3 (Ramanan et al., 2009) [225 mg $CO3^{2-}$/mg of protein] also produced calcite crystals. *Rhodobacter sphaeroides* was genetically modified to harbor a surface displayed CA with inducible expression of phosphoenolpyruvate carboxylase led to very high CO_2 reduction efficiency and the production of several organic compounds (carotenoids, polyhydroxybutyrate, malic acid, succinic acid; Park et al., 2017).

Production and Over Expression of Carbonic Anhydrase Genes by Molecular Approaches

One of the key factors that determine the cost effectiveness of any biotechnological application is the availability and cost of the biocatalysts. Microorganisms are well known to produce CAs for use in CCS technologies. Researchers have also displayed the ability of many prokaryotic species such as planktonic *Bacillus mojavensis* cells for microbially enhanced CCS by mineral trapping and solubility trapping (Mitchell et al., 2010). The production levels of CAs are, however, quite low for industrial use. Hence the production parameters must be optimized. Statistical approaches such as Response surface methodology (RSM) and two factorial designs are some of the well-known methods for optimizing production of biocatalysts (Kumar and Satyanarayana, 2014). The production of carbonic anhydrase is growth associated; hence, optimization of growth parameters leads to high enzyme titres. Optimization of growth conditions by mono-factor tests with blank control and orthogonal design methodology resulted in 7-fold increase in CA titres in *B. mucilaginosus* K02 (Zhang et al., 2011). Bose and Satyanarayana (2016) reported about 4-fold increment in enzyme titres on optimization of growth parameters. In both the studies, the CA production was found to be synchronous to that of the growth of the bacterium. The CA production by the wild type strain becomes too cumbersome. The production of CA from thermo-alkaliphilic microorganisms is difficult as it is not easy to provide accurate conditions [anaerobic, high temperature, pH (high/low) etc.] for their growth and enzyme production. Many archaeal life forms producing bioactive compounds need specialized growth conditions (Alber and Ferry, 1994; Mesbah and Wiegel, 2012). The advent of genome mining, metagenomics and bioinformatics approaches have enabled to use molecular biological tools for cloning and over expression of industrially relevant enzymes in prokaryotic (*E. coli, Bacillus subtilis*) and eukaryotic (*Pichia*

FIGURE 2 | Exhaust fumes from the petrol driven car and motorcycle were collected by connecting one end of a plastic pipe to the exhaust of the car and the other to saturate distilled water (DW) kept in ice bath for an hour which served as a source of CO_2 (adopted from Faridi and Satyanarayana, 2016a).

pastoris) hosts. Downstream processing becomes easy as the enzymes have various protein tags (e.g., His, GST) for easy purification of the recombinant proteins (Swartz, 2001). Since late 1990s, the prokaryotic CA genes from different strata have been cloned and the protein was over expressed in *E. coli* for analytical and application purposes. The first CA gene cloned from prokaryotes was α–CA (NCA) from *N. gonorrhoeae*, which encoded a protein of 28 kDa (Chirică et al., 1997). This enzyme was also expressed heterologously in *E. coli* as a periplasmic protein in order to use it as a whole cell biocatalyst (Jo et al., 2013). The yield of ∼106 mg L^{-1} with a specific activity of 3090 U mg^{-1} in the pure protein was achieved (Kim et al., 2012).

Since then many other microbial CAs have been cloned and expressed in prokaryotic hosts. Many researchers have already cloned and over expressed all the CA-encoding genes from *E. coli* (*can*, *cynT*, *cynT2, caiE*, *pay*, and *yrdA*) and studied their expression profiles in response to different growth conditions (Fujita et al., 1994; Cronk et al., 2001; Merlin et al., 2003). CA genes from thermophilic bacteria such as *Thermovibrio ammonificans*, *M. thermobacterium*, *M. thermophila*, *Sulfurihydrogenibium*, *B. halodurans* and others have been cloned and over expressed in *E. coli* to assess their efficacy in biomineralization. These CAs have been shown to be useful in sequestering CO_2 from flue gas (Capasso et al., 2012; Faridi and Satyanarayana, 2016a). The role of CAs in virulence/pathogenesis have been studied. They play an active role in metabolism during pathogenesis in many bacterial and fungal pathogens such as *Vibrio cholerae, Helicobacter pylori*, *Candida albicans, Aspergillus fumigatus,* and others. List of CAs from some of the pathogens have been summarized in **Table 3**.

FIGURE 3 | Mineralization of vehicular exhaust gas CO_2 using BhCA in the presence of Ca^{2+}. Test reaction containing CA showed efficient mineralization of CO_2 as compared to the control (adopted from Faridi and Satyanarayana, 2016a).

One of the major problems with cloning of genes in heterologous hosts is obtaining the active protein in soluble

TABLE 3 | Characteristics of CA from some pathogenic bacteria.

Sl. No.	Organism	Type	Cloning Vector/Host	Molecular weight	Other Features	References
1	*V. cholerae*	α	*E. coli* (pET15b)	26.4 kDa	K_m = 11.7 mM k_{cat} = 8.23 × $10^5 s^{-1}$ k_{cat}/K_M = 7.0 × 10^7 M^{-1} s^{-1}	Del Prete et al., 2012
2	*Brucella suis*	B	*E. coli* (pET15b)	25 kDa	k_{cat} = 1.1 × 10^6, k_{cat}/K_m = 8.9 × 10^7 M^{-1} s^{-1}	Joseph et al., 2010
3	*H. pylori*	α	*E. coli* (pACA1)	28.28 kDA	k_{cat} = 2.4 × $10^5 s^{-1}$ K_M = 17 mM kcat/K_M = 1.4 × 10^7 $M^{-1}s^{-1}$ at pH 8.9 and 25°C	Chirica et al., 2001
4	*Salmonella typhimurium*	β (two stCA1 and stCA2)	*E. coli* (pGEX-4T2)	24.8 kDa (stCA1) 26.6 kDa (stCA2)	k_{cat} = 0.79 × 10^6 s^{-1} and 1.0 × 10^6 s^{-1}, k_{cat}/K_m = 5.2 x$10^7 M^{-1}s^{-1}$ and 8.3 × 10^7 M^{-1} s^{-1}	Vullo et al., 2011
5	*Mycobacterium tuberculosis*	β (mtCA1)	*E. coli* pGEX-4T2	NA	k_{cat} = 3.9 × 10^5 s^{-1} k_{cat}/K_m = 3.7 × 10^7 M^{-1} s^{-1}	Minakuchi et al., 2009
6	*Streptococcus pneumoniae*	β (PCA)	*E. coli*	NA	k_{cat} = 7.4 × 10^5 s^{-1} k_{cat}/K_m = 6.5 × 10^7 M^{-1} s^{-1} at an optimum pH of 8.4	Burghout et al., 2011
7	*Plasmodium falciparum*	η (PfCA)	*E. coli*	NA	k_{cat} = 1.4 × 10^5 $s^{-1}k_{cat}/K_m$ = 5.4 × 10^6 $M^{-1}s^{-1}$	Del Prete et al., 2014
8	*Haemophilus influenzae*	β (HICA)	*E. coli*	105.26 kDA (native molecular weight)	Tetramer, presence of a novel non-catalytic bicarbonate binding site, k_{cat}, k_{cat}/K_m is pH dependent	Cronk et al., 2006
9	*Candida albicans*	β (Nce103)		31.5 Da	k_{cat} = 8.0 × 10^5 $s^{-1}k_{cat}/K_m$ = 9.7 × 10^7 $M^{-1}s^{-1}$	Innocenti et al., 2009a
10	*Malassezia globosa*	β (MG-CA)	*E. coli*	27 kDa	k_{cat} = 8.6 × 10^5 $s^{-1}k_{cat}/K_m$ = 6.9 × 10^7 $M^{-1}s^{-1}$ K_i (acetazolamide) 76000 ± 450 nm	Hewitson et al., 2012
11	*Cryptococcus neoformans*	β (Can2)	*E. coli*	26 kDa	k_{cat} = 3.9 × 10^5 $s^{-1}k_{cat}/K_m$ 4.3 × 10^7 $M^{-1}s^{-1}K_i$ (acetazolamide) 10.5 nm (homodimer)	Mogensen et al., 2006; Innocenti et al., 2009a
12	*Aspergillus fumigatus*	4-βCAs (cafA-cafD)	*Saccharomyces cerevisiae*	–	All four CAs strongly expressed during pathogensis	Han et al., 2010; Tobal and Balieiro, 2014

form, as the recombinant proteins are aggregated as inclusion bodies, which need to be solubilised (Clark, 2001). Generally optimization of IPTG concentration, growth temperature (after induction) and incubation time brings the protein into the soluble form (Prasad et al., 2011). Techniques such as size-exclusion chromatography (Li et al., 2004), dialysis and dilution (Marston, 1986; Tsumoto et al., 2003; Umetsu et al., 2003), zeolite absorbing systems (Nara et al., 2009), reversed micelle systems (Sakono et al., 2004), microfluidic chips (Jahn et al., 2007) and the natural GroEL—GroES chaperone system (Zhi et al., 1992) could be used in soluble expression of recombinant proteins. Other problems include codon bias and lack of post translational machinery in *E. coli* (Gustafsson et al., 2004; Sahdev et al., 2008). The latter can be overcome by cloning the gene of interest in eukaryotic hosts such as *Saccharomyces cerevisiae* and *P. pastoris*. In this case, protein is expressed extracellularly, hence, we are saved from the energy intensive step of breaking the cells in disruptors or sonicators. Codon optimization also results in faster translation rates. α–CA from *Dunaliella* species was codon optimized and effectively expressed in *E. coli*, which was used for biosequestration of CO_2 (Kanth et al., 2012). A synthetic α–CA (*HC-aCA*) from *Hahella chejuensis* was cloned and expressed (Ki et al., 2013). The codon-optimized carbonic anhydrase gene of thermophilic *Persephonella marina* EX-H1 (PMCA) was expressed and characterized. The removal of the signal peptide resulted in 5-fold enhancement of CA (Kanth et al., 2014).

Role of Metagenomics in CCS Technologies

The advent of metagenomics has permitted discovery of numerous microorganisms from extreme environments, which could be of biotechnological interest. Metagenomics analysis has revealed the presence of CA encoding genes in the Indian Ocean viral metagenome (Williamson et al., 2012). Jones et al. (2012) showed the existence of RuBisCo and CA gene clusters in the *Acidithiobacillus*, an extremely acidophilic sulfur-oxidizing biofilm by community genome analysis. Microarray data of a metagenome of acid mine drainage also showed the presence of CA encoding genes along with the RuBisCo gene clusters (Guo et al., 2013). Three gene copies were identified which encoded CA in the metagenome of the marine ammonium oxidizing bacteria (van de Vossenberg et al., 2003). The metagenomes of the serpentinite-hosted Lost City hydrothermal field and Mid-Atlantic Ridge also indicated the presence of CA encoding genes. These metagenomes were found to be similar to the genome of *Thiomicrospira crunogena* XCL-2, an isolate from a basalt-hosted hydrothermal vent in the Pacific Ocean (Brazelton and Baross, 2010). Microorganisms exhibit great potential as bioindicators to detect leakages from CO_2 storage projects and for that metagenomics becomes handy. Metagenomics and high throughput screen (HTS) methods can also be utilized for studying the effect of environmental changes on microbial communities at the CCS sites (Caporaso et al., 2012; Håvelsrud et al., 2012, 2013; Howe et al., 2014). Information about amplicons and metagenomes helps in establishing a CCS monitoring approach, which could even be useful in the detection of CO_2 leaks (Noble et al., 2012). The use of HTS has already been found to be effective in evaluating the response of *in situ* bacterial populations to increased CO_2, and matching community shifts to metabolic potential (Mu et al., 2014). The metagenomic approach along with appropriate bioinformatics tools makes the system competent. Metagenomics can thus be used as a biosensor for monitoring the CCS sites efficiently (Hicks et al., 2017).

Utilization of Immobilized CA in CCSU

Immobilization strategies are necessary so that the enzyme can be recycled number of times. Their stability can be enhanced by various immobilization techniques. Immobilization has long been used as an approach for increasing the stability of mesophilic enzymes. There are several reports of immobilization of mesophilic CAs. These CAs have been proved to be more efficient than the free enzymes for CO_2 capture. CAs from *P. fragi*, *Bacilllus pumilus,* and *Micrococcus lylae* have been immobilized on chitosan and surfactant-modified silylated chitosan beads (Prabhu et al., 2009; Wanjari et al., 2011); these displayed enhanced CO_2 hydration capacity. Chitosan is made of glucosamine and acetyl glucosamine units. The functional groups present on chitosan are amino and hydroxyl groups which are required for enzyme immobilization. The enzyme is adsorbed on the surface of chitosan beads. Immobilization of CAs also improved their thermal stabilities, for e.g., the immobilized CA retained at least 60% of the initial activity after 90 days at 50°C compared to about 30% for their free counterparts under the same conditions. The CAs also exhibit a high stability in the presence of inhibitors upon immobilization (Prabhu et al., 2009; Kanbar and Ozdemir, 2010). $CaCO_3$ precipitation rate doubled in a period of 5 min when pure CA from *P. fragi* was immobilized by adsorption on chitosan beads in comparison with the free enzyme (Wanjari et al., 2012; Yadav et al., 2012). Immobilization of CAs on several other matrices such as ordered mesoporous aluminosilicate, octa(aminophenyl)silsesquioxane-functionalized Fe_3O_4/SiO_2 nanoparticles, silica nanoparticles and by single/multiple attachments to polymers deposited on Fe_3O_4 particles was also attempted (Sharma et al., 2011; Rayalu et al., 2012). CA immobilized on ordered mesoporous aluminosilicate exhibited CO_2 sequestration efficiency of 16.14 mg of $CaCO_3$/mg CA as compared to that of free enzyme which sequesters 33.08 mg of $CaCO_3$/mg CA. Immobilized CA even showed enhanced stability and retained 67% of initial activity even after six cycles (Yadav et al., 2011). Kinetics of the immobilized CAs (immobilized on ordered mesoporous aluminosilicate) were studied and compared with that of the free enzyme by Yadav et al. (2010). The *K*m, *V*max, and k_{cat} values of the immobilized enzyme were 0.158 mM, 2.307 μ mole $min^{-1}ml^{-1}$, and 1.9 s^{-1}, and these for free CA were 0.876 mM, 0.936 μ mole $min^{-1}ml^{-1}$, and 2.3 s^{-1}, respectively (Yadav et al., 2010). A high CO_2 sequestration and improved stability have been achieved when CA was immobilized on core-shell CA-chitosan nanoparticles (SEN-CA; Rayalu et al., 2012). Ssp CA was immobilized on solid matrix made of silica particles (silanized Sipernat® 22 particles). Enzyme-carrier covalent bonding was adopted as immobilization technique and it was observed that the enzyme stability and activity increased on immobilization. Immobilization of this CA in polyutherane foam also exhibited enhanced stability. The immobilized CA (PU-SspCA) showed exceptional thermostability for very long duration even at 70°C. The CO_2 absorption capacity of PU-SspCA was verified in a three phase trickled bed bioreactor which mimics the post-combustion processes in a thermal power plant. The three-phase reactor was filled with shredded foam with PU-SspCA. The gas mixture (CO_2/N_2) was fed from both the sides (i.e., concurrent and countercurrent). Increasing the flow rate of water and decreasing the CO_2 flow rate also greatly improved CO_2 capture in these reactors. SspCA showed good CO_2 capture performance when the PU-SspCA-shredded foam was used in the bioreactor (Migliardini et al., 2014). Concerted efforts are needed to develop CA immobilization techniques that allow reuse of the enzyme 100–500 times with sustained activity. Immobilization can also lead to unwanted release of enzyme on surface of the reactor. In order to overcome this problem, some novel immobilization techniques have been developed using γ–CA from *P. horikoshii* and *M. thermophila* (Salemme and Weber, 2014). The immobilization techniques allowed the development of γ–CA nanoassemblies (Salemme and Weber, 2014). An immobilization sequence was added at amino- or carboxy-terminus which aided in proper and reversible immobilization of γ–CA to the functionalized surface. Gas-liquid membrane contractors are also emerging as potential bio reactors for using CAs for CO_2 capture. Iliuta and Iliuta (2017) has demonstrated a novel, cost effective and environmentally friendly approach for

CO_2 capture by immobilizing CA in a hollow-fiber membrane bioreactor (*HFMB*) by multiscale steady-state model, under partially liquid-filled and gas-filled membrane pores conditions.

Nanoparticles are also widely used for immobilization of enzymes due to their unique size and physical properties. The immobilization of enzymes on nanoparticles (NPs) offers high surface area and may lead to reduction in protein unfolding, improvement in storage stability and performance (Laurent et al., 2008; Xu et al., 2014). Iron mangnetic nanoparticles (MNPs) are being synthesized with various surface modifications in order to use them for immobilizing protein/enzyme. The CA from *B. pumilus* TS1 was immobilized successfully on chitosan stabilized iron MNPs (Yadav et al., 2012). Silanization of iron MNPs is being widely used for surface modifications of iron MNPs. It is also very easy and cost effective technique, which can be carried out simply in aqueous or organic media at moderate temperatures (Xu et al., 2014). Faridi et al. (2017) showed that even after 22 cycles of reuse, recombinant α–CA (rBhCA) from *B. halodurans* TSLV1 immobilized on silanized iron MNPs (rBhCA-Si-MNPs) lost only 50% of activity. Nickel nanoparticles have been successfully used as a direct catalyst for CO_2 hydration reaction for assessing their application in CO_2 mineralization (Bhaduri et al., 2015).

Other Applications of Carbonic Anhydrases

Apart from their utility in CCSU, the CAs have some other applications too as discussed below:

Carbonic Anhydrase in Formation of Bioconcrete

Biomineralization by bacteria facilitates the development of bioconcrete, wherein calcium carbonate is formed by the metabolic activity of microorganisms, which involves a series of complex reactions directed mainly by urease and carbonic anhydrase enzymes (Castro et al., 2016). The activity of urease, CA, concentration of calcium and pH are very important in bioconcrete formation (Achal and Mukherjee, 2015).

Artificial Lungs

This equipment helps to overcome respiratory problems. The major drawback of this technique is the insufficient transfer of CO_2 per square inch through the polymeric hollow fiber membranes (HFM). CAs can be utilized by immobilizing on HFM in order to increase the rate of CO_2 transfer. CAs can, therefore, be used in developing small artificial lungs, which could be efficiently utilized within the human body (Kaar et al., 2007).

Biosensors

HCA II based biosensors have been employed to check the toxic effects of zinc on marine life (Thompson and Jones, 1993; Rout and Das, 2003; Muyssen et al., 2006). Many researchers are attempting to develop biosensor variants for other transition metals (Thompson et al., 2000, 2002; Frederickson et al., 2006; Bozym et al., 2008; Wang et al., 2011; McCranor et al., 2012).

Pharmalogical Considerations

CAs can be incorporated into stimuli-triggered drug delivery systems which utilize CO_2, bicarbonate or pH changes as signaling molecules. This can improve the efficiency of these antidote based delivery systems (Satav et al., 2010).

Blood Substitutes

The current blood substitutes have inadequate CO_2 removal rate, which leads to coma or death. CAs can be utilized along with catalase (CAT) and superoxide dismutase (SOD into the PolySFHb substitute (PolySFHb-SOD-CAT-CA) in order to overcome this limitation (Bian et al., 2011).

CONCLUSIONS AND FUTURE PERSPECTIVES

CAs are a class of enzymes which are essential for the survival of living beings. This enzyme not only helps in our metabolic activities but also aids in the protection of Mother Nature. Due to anthropogenic activities, the nature is getting destroyed day by day. Global warming is having its toll on the climate and weather. Carbonic anhydrase can aid in tackling the future catastrophes due to global warming. Unfortunately the CCS and biomineralization techniques are either in the lab stage or pilot plant stage. Researchers are constantly attempting to address a few of the key issues related to this technology, thus, it has become quite difficult to generate a public consensus on CCS technology. The technology needs to be ameliorated. We are also not able to bring down the carbon emissions as fossil fuels are (also will be in near future) the main energy source which drives today's world. Although much is known about CAs, the current metadata reveals the presence of many CA genes in the extreme realms of earth which are waiting to be discovered. These are mostly from unculturable microbes. Bioinformatics tools have been useful in identifying different CA encoding genes. Once identified, they can be easily cloned and expressed in different microbial hosts for studying their novel properties and utility in CO_2 biomineralization. Currently the unexplored data is so vast that we may discover a few novel classes of CAs in addition to the known six classes in future. CAs from polyextremophilic microbial sources have already been tried for CCS related strategies. Enzyme immobilization techniques permit the repeated use of the enzyme and designing continuously operating reactors. We need to improve the CA immobilization technology so that it becomes cost effective and readily accepted by people. Further research efforts are called for developing highly efficient and robust CAs, efficient immobilization techniques and designing continuously operating reactors for cost effective biomimetic carbon sequestration.

AUTHOR CONTRIBUTIONS

All authors listed have made a substantial, direct and intellectual contribution to the work, and approved it for publication.

ACKNOWLEDGMENTS

We wish to thank University Grants Commission, Govt. of India, New Delhi for awarding Faculty Fellowship to one of us (TS) while writing this review.

REFERENCES

Aaron, D., and Tsouris, C. (2005). Separation of CO_2 from flue gas: a review. *Sep. Sci. Technol.* 40, 321–348. doi: 10.1081/SS-200042244

Achal, V., and Mukherjee, A. (2015). Review of microbial precipitation for sustainable construction. *Constr. Build. Mater.* 93, 1224–1235. doi: 10.1016/j.conbuildmat.2015.04.051

Adams, M. R., Hurd, H. B., Lenhart, S., and Leary, N. (1998). Effects of global climate change on agriculture: an interpretative review. *Clim. Res.* 11, 19–30. doi: 10.3354/cr011019

Alber, B. E., and Ferry, J. G. (1994). A carbonic anhydrase from the archaeon *Methanosarcina thermophila*. *Proc. Nat. Acad. Sci. U.S.A.* 91, 6909–6913. doi: 10.1073/pnas.91.15.6909

Alvizo, O., Nguyen, L. J., Savile, C. K., Bresson, J. A., Lakhapatri, S. L., Solis, E. O., et al. (2014). Directed evolution of an ultrastable carbonic anhydrase for highly efficient carbon capture from flue gas. *Proc. Nat. Acad. Sci. U.S.A.* 111, 16436–16441. doi: 10.1073/pnas.1411461111

Aspelund, A., Molnvik, M. J., and DeKoeijer, G. (2006). Ship transport of CO_2, technical solutions and analysis of costs, energy utilization, energy efficiency and CO_2 emissions. *Chem. Eng. Res. Des.* 84, 847–855. doi: 10.1205/cherd.5147

Badger, M. R., and Price, G. D. (2003). CO_2 concentrating mechanisms in cyanobacteria: molecular components, their diversity and evolution. *J. Exp. Bot.* 54, 609–622. doi: 10.1093/jxb/erg076

Benson, S., Cook, P., Anderson, J., Bachu, S., Nimir, H. B., Basu, B., et al. (2005). "Underground geological storage," in *IPCC Special Report on Carbon Dioxide Capture and Storage*, eds B. Metz, O. Davidson, H. de Coninck, M. Loos, L. Meyer (Cambridge: Cambridge University Press), 195–277.

Berg, J. M., Tymoczko, J. L., and Stryer, L. (2002). *Biochemistry 5th edn.*, New York, NY: W H Freeman.

Bhaduri, G. A., Alamiry, M. A., and Šiller, L. (2015). Nickel nanoparticles for enhancing carbon capture. *J. Nanomater.* 16:376. doi: 10.1155/2015/581785

Bhojiya, A. A., and Joshi, H. (2012). Isolation and characterization of zinc tolerant bacteria from Zawar mines Udaipur, India. *IJEEM.* 3, 239–242.

Bhown, A. S., and Freeman, B. C. (2011). Analysis and status of post-combustion carbon dioxide capture technologies. *Environ. Sci. Technol.* 45, 8624–8632. doi: 10.1021/es104291d

Bian, Y., Rong, Z., and Chang, T. M. S. (2011). Polyhemoglobin-superoxide dismutase-catalase-carbonic anhydrase: a novel biotechnology-based blood substitute that transports both oxygen and carbon dioxide and also acts as an antioxidant. *Artif. Cells. Blood. Substit. Immobil. Biotechnol.* 39, 127–136. doi: 10.3109/10731199.2011.581052

Boone, C. D., Gill, S., Habibzadegan, A., and McKenna, R. (2013). Carbonic anhydrase: an efficient enzyme with possible global implications. *Int. J. Chem. Eng.* 2013, 1–7. doi: 10.1155/2013/813931

Boot-Handford, M. E., Abanades, J. C., Anthony, E. J., Blunt, M. J., Brandani, S., Mac Dowell, N., et al. (2014). Carbon capture and storage update. *Energy Environ. Sci.* 7, 130–189. doi: 10.1039/C3EE42350F

Bose, H., and Satyanarayana, T. (2016). Suitability of the alkalistable carbonic anhydrase from a polyextremophilic bacterium *Aeribacillus pallidus* TSHB1 in biomimetic carbon sequestration. *Bioprocess. Biosyst. Eng.* 39, 1515–1525. doi: 10.1007/s00449-016-1627-4

Bose, H., and Satyanarayana, T. (2017). Utility of thermo-alkali-stable γ-CA from polyextremophilic bacterium *Aeribacillus pallidus* TSHB1 in biomimetic sequestration of CO2 and as a virtual peroxidase. *Environ. Sci. Pollut. Res.* 24, 10869–10884. doi: 10.1007/s11356-017-8739-5

Bourais, I., Maliki, S., Mohammadi, H., and Amine, A. (2017). Investigation of sulfonamides inhibition of carbonic anhydrase enzyme using multiphotometric and electrochemical techniques. *Enzyme Microb. Technol.* 96, 23–29. doi: 10.1016/j.enzmictec.2016.09.007

Bozym, R., Hurst, T. K., Westerberg, N., Stoddard, A., and Fierke, C. A., Frederickson, C. J., et al. (2008). Determination of zinc using carbonic anhydrase-based fluorescence biosensors. *Meth. Enzymol.* 450, 287–309. doi: 10.1016/S0076-6879(08)03414-9

Brazelton, J. W., and Baross, A. J. (2010). Metagenomic comparison of two *Thiomicrospira* lineages inhabiting contrasting deep-sea hydrothermal environments. *PLoS ONE* 5:e13530. doi: 10.1371/journal.pone.0013530

Buhre, B. J. P., Elliott, L. K., Sheng, C. D., Gupta, R. P., and Wall, T. F. (2005). Oxy-fuel combustion technology for coal-fired power generation. *Prog. Energy Combust. Sci.* 31, 283–307. doi: 10.1016/j.pecs.2005.07.001

Burghout, P., Vullo, D., Scozzafava, A., Hermans, P. W., and Supuran, C. T. (2011). Inhibition of the β-carbonic anhydrase from *Streptococcus pneumoniae* by inorganic anions and small molecules: toward innovative drug design of antiinfectives? *Bioorg. Med. Chem.* 19, 243–248. doi: 10.1016/j.bmc.2010.11.031

Cabiscol, E., and Levine, R. L. (1995). Carbonic anhydrase III. Oxidative modification *in vivo* and loss of phosphate activity during aging. *J. Biol. Chem.* 270, 14742–14747. doi: 10.1074/jbc.270.24.14742

Capasso, C., De Luca, V., Carginalea, V., Caramuscioc, P., Cavalheiroc, C. F., Canniod, R., et al. (2012). Characterization and properties of a new thermoactive and thermostable carbonic anhydrase. *Chem. Eng.* 27, 271–276. doi: 10.3303/CET1227046

Caporaso, J. G., Lauber, C. L., Walters, W. A., Berg-Lyons, D., Huntley, J., Fierer, N., et al. (2012). Ultra-high-throughput microbial community analysis on the Illumina HiSeq and MiSeq platforms. *ISME. J.* 6, 1621–1624. doi: 10.1038/ismej.2012.8

Carta, F., Aggarwal, M., Maresca, A., Scozzafava, A., McKenna, R., and Supuran, C. T. (2012). Dithiocarbamates: a new class of carbonic anhydrase inhibitors. Crystallographic and kinetic investigations. *Chem. Commum.* 48, 1868–1870. doi: 10.1039/c2cc16395k

Castro, M. J., and Lopez, C. E., Narayanasamy, R., Marszalek, J. E., Luevanos-Escareno, M. P., Fajardo, G. J., et al. (2016). Potential of enzymes (urease & carbonic anhydrase). *Chim. Oggi. Chem.* 34:4.

Chirica, L. C., Elleby, B., and Lindskog, S. (2001). Cloning, expression and some properties of α-carbonic anhydrase from *Helicobacter pylori*. *Biochim. Biophys. Acta* 1544, 55–63. doi: 10.1016/S0167-4838(00)00204-1

Chirică, L. C., Elleby, B., Jonsson, B. H., and Lindskog, S. (1997). The complete sequence, expression in *Escherichia coli*, purification and some properties of carbonic anhydrase from *Neisseria gonorrhoeae*. *FEBS. J.* 244, 755–760. doi: 10.1111/j.1432-1033.1997.00755.x

Ciullo, P. A. (1996). *Industrial Minerals and their Uses: A Handbook and Formulatory*. New Jersey: William Andrew Publishing/Noyes.

Clark, E. D. B. (2001). Protein refolding for industrial processes. *Curr. Opin. Biotechnol.* 12, 202–207. doi: 10.1016/S0958-1669(00)00200-7

CO_2 Solutions Inc. (2012). Available online at: www.co2solutions.com/en/the-process (Accessed January 11, 2017).

Coker, J. A. (2016). Extremophiles and biotechnology: current uses and prospects. *F1000Research* 5:F1000 Faculty Rev-396. doi: 10.12688/f1000research.7432.1

Cronk, J. D., Endrizzi, J. A., Cronk, M. R., O'neill, J. W., and Zhang, K. Y. (2001). Crystal structure of *E. coli* β–carbonic anhydrase, an enzyme with an unusual pH–dependent activity. *Protein Sci.* 10, 911–922. doi: 10.1110/ps.46301

Cronk, J. D., Rowlett, R. S., Zhang, K. Y. J., Tu, C., Endrizzi, J. A., Lee, J., et al. (2006). Identification of a novel noncatalytic bicarbonate binding site in eubacterial β-carbonic anhydrase. *Biochemistry* 45, 4351–4361. doi: 10.1021/bi052272q

Da Silva, E. F., and Booth, A. M. (2013). Emissions from post-combustion CO_2 capture plants. *Environ. Sci. Technol.* 47, 659–660. doi: 10.1021/es305111u

Daigle, R. M. E., and Fradette, S. (2014). *Techniques for CO_2 Capture Using Sulfurihydrogenibium sp. Carbonic Anhydrase*. Patent WO 2014066999 A1.

De Luca, V., Vullo, D., Scozzafava, A., Carginale, V., Rossi, M., Supuran, C. T., et al. (2013). An α-carbonic anhydrase from the thermophilic bacterium *Sulphurihydrogenibium azorense* is the fastest enzyme known for the CO_2 hydration reaction. *Bioorg. Med. Chem.* 21, 1465–1469. doi: 10.1016/j.bmc.2012.09.047

De Simone, G., Monti, S. M., Alterio, V., Buonanno, M., De Luca, V., Rossi, M., et al. (2015). Crystal structure of the most catalytically effective carbonic anhydrase enzyme known, SazCA from the thermophilic bacterium *Sulfurihydrogenibium azorense*. *Bioorg. Med. Chem. Lett.* 25, 2002–2006. doi: 10.1016/j.bmcl.2015.02.068

Del Prete, S., Isik, S., Vullo, D., De Luca, V., Carginale, V., Scozzafava, A., et al. (2012). DNA cloning, characterization, and inhibition studies of an α-carbonic anhydrase from the pathogenic bacterium *Vibrio cholerae*. *J. Med. Chem.* 55, 10742–10748. doi: 10.1021/jm301611m

Del Prete, S., Vullo, D., Fisher, G. M., Andrews, K. T., Poulsen, S. A., Capasso, C., et al. (2014). Discovery of a new family of carbonic anhydrases in the malaria pathogen *Plasmodium falciparum*—The η-carbonic anhydrases. *Bioorg. Med. Chem. Lett.* 24, 4389–4396. doi: 10.1016/j.bmcl.2014.08.015

Di Fiore, A., Alterio, V., Monti, S. M., De Simone, G., and D'Ambrosio, K. (2015). Thermostable carbonic anhydrases in biotechnological applications. *Int. J. Mol. Sci.* 16, 15456–15480. doi: 10.3390/ijms160715456

Di Fiore, A., Capasso, C., De Luca, V., Monti, S. M., Carginale, V., and Supuran, C. T. (2013). X-ray structure of the firstextremo-α-carbonic anhydrase', a dimeric enzyme from the thermophilic bacterium *Sulfurihydrogenibium yellowstonense* YO3AOP1. *Acta. Crystallogr. Sect. D.* 69, 1150–1159. doi: 10.1107/S0907444913007208

Dreybodt, W., Eisenlohr, L., Madry, B., and Ringer, S. (1997). Precipitation kinetics of calcite in the system $CaCO_3$-H_2O-CO_2. *Geochim. Cosmochim. Acta.* 61, 3987–3904.

Druckenmiller, M. L., and Maroto-Valer, M. M. (2005). Carbon sequestration using brine of adjusted pH to form mineral carbonates. *Fuel Process. Technol.* 86, 1599–1614. doi: 10.1016/j.fuproc.2005.01.007

Dutreuil, S., Bopp, L., and Tagliabue, A. (2009).Impact of enhanced vertical mixing on marine biogeochemistry: lessons for geo-engineering and natural variability. *Biogeosci. Discuss.* 6, 901–912. doi: 10.5194/bg-6-901-2009

Faridi, S., and Satyanarayana, T. (2016b). Characteristics of recombinant α-carbonic anhydrase of polyextremophilic bacterium *Bacillus halodurans* TSLV1. *Int. J. Biol. Macromol.* 89, 659–668. doi: 10.1016/j.ijbiomac.2016.05.026

Faridi, S., and Satyanarayana, T. (2015). "Bioconversion of industrial CO_2 emissions into utilizable products," in *Industrial Waste Management*, ed R. Chandra (New York, NY: CRC Press), 111–156.

Faridi, S., and Satyanarayana, T. (2016a). Novel alkalistable α-carbonic anhydrase from the polyextremophilic bacterium *Bacillus halodurans*: characteristics and applicability in flue gas CO_2 sequestration. *Environ. Sci. Pollut. Res.* 23, 15236–15249. doi: 10.1007/s11356-016-6642-0

Faridi, S., Bose, H., and Satyanarayana, T. (2017). Utility of immobilized recombinant carbonic anhydrase of *Bacillus halodurans* TSLV1 on the surface of modified iron magnetic nanoparticles in carbon sequestration. *Energy Fuels* 31, 3002–3009. doi: 10.1021/acs.energyfuels.6b02777

Farrell, A. (2011). *Carbon Dioxide Storage in Stable Carbonate Minerals.* University of Maryland Geology, Basalt Laboratory Studies of Interest to Carbon Capture and Storage, Advisor MN Evans.

Favre, N., Christ, M. L., and Pierre, A. C. (2009). Biocatalytic capture of $CO_2$with carbonic anhydrase and its transformation to solid carbonate. *J. Mol. Catal. B. Enzym.* 60, 163–170. doi: 10.1016/j.molcatb.2009.04.018

Fisher, Z., Boone, C. D., Biswas, S. M., Venkatakrihnan, B., Aggarwal, M., and Tu, C., et al. (2012). R. Kinetic and structural characterization of thermostabilized mutants of human carbonic anhydrase II. *Protein Eng. Des. Sel.* 25, 347–355. doi: 10.1093/protein/gzs027

Floyd, W. C. III., Baker, S. E., Valdez, C. A., Stolaroff, J. K., Bearinger, J. P., Satcher, J. H. Jr., et al. (2013). Evaluation of a carbonic anhydrase mimic for industrial carbon capture. *Environ. Sci. Technol.* 47, 10049–10055. doi: 10.1021/es401336f

Frederickson, C. J., Giblin, L. J., Krężel, A., McAdoo, D. J., Muelle, R. N., Zeng, Y., et al. (2006). Concentrations of extracellular free zinc (pZn) e in the central nervous system during simple anesthetization, ischemia and reperfusion. *Exp. Neurol.* 198, 285–293. doi: 10.1016/j.expneurol.2005.08.030

Frost, S. C., and McKenna, R. (2013). *Carbonic Anhydrase: Mechanism, Regulation, Links to Disease, and Industrial Applications*. Dordrecht: Springer Science & Business Media.

Fujita, N., Mori, H., Yura, T., and Ishihama, A. (1994). Systematic sequencing of the *Escherichia coli* genome: analysis of the 2.4–4.1 min (110,917–193,643 bp) region. *Nucleic Acids Res.* 22, 1637–1639. doi: 10.1093/nar/22.9.1637

Gao, L., Fang, M., Li, H., and Hetland, J. (2014). Cost analysis of CO_2 transportation: case study in China. *Energy Procedia* 4, 5974–5981. doi: 10.1016/j.egypro.2011.02.600

Gill, S. R., Fedorka-Cray, P. J., Tweten, R. K., and Sleeper, B. P. (1984). Purification and properties of the carbonic anhydrase of *Rhodospirillum rubrum*. *Arch. Microbiol.* 138, 113–118. doi: 10.1007/BF00413010

Guo, X., Yin, H., Cong, J., Dai, Z., Liang, Y., and Liua, X. (2013). RubisCO gene clusters found in a metagenome microarray from acid mine drainage. *Appl. Environ. Microbiol.* 79, 2019–2026. doi: 10.1128/AEM.03400-12

Gustafsson, C., Govindarajan, S., and Minshull, J. (2004). Codon bias and heterologous protein expression. *Trends Biotechnol.* 22, 346–353. doi: 10.1016/j.tibtech.2004.04.006

Han, K. H., Chun, Y. H., De Castro Pimentel Figueiredo, B., Soriani, F. M., Savoldi, M., Almeida, A., et al. (2010). The conserved and divergent roles of carbonic anhydrases in the filamentous fungi *Aspergillus fumigatus* and *Aspergillus nidulans*. *Mol. Microbiol.* 75, 1372–1388. doi: 10.1111/j.1365-2958.2010.07152.x

Hart, A., and Gnanendran, N. (2009). Cryogenic CO_2 capture in natural gas. *Energy Procedia* 1, 697–706. doi: 10.1016/j.egypro.2009.01.092

Håvelsrud, O. E., Haverkamp, T. H., Kristensen, T., Jakobsen, K. S., and Rike, A. G. (2013). Metagenomics in CO_2 monitoring. *Energy Procedia* 37, 4215–4233. doi: 10.1016/j.egypro.2013.06.324

Håvelsrud, O. E., Haverkamp, T. H., Kristensen, T., Jakobsen, K. S., and Rike, A. G. (2012). Metagenomic and geochemical characterization of pockmarked sediments overlaying the troll petroleum reservoir in the North Sea. *BMC Microbiol.* 12:203. doi: 10.1186/1471-2180-12-203

Haywood, H., Eyre, J., and Scholes, H. (2001). Carbon dioxide sequestration as stable carbonate minerals–environmental barriers. *Environ. Geol.* 41, 11–16. doi: 10.1007/s002540100372

Herzog, H. J. (1998). "Ocean sequestration of CO_2 – an overview," in *Fourth International Conference on Greenhouse Gas Control Technologies August 30 - September 2.* (Interlaken), 1–5.

Hewitson, K. S., Vullo, D., Scozzafava, A., Mastrolorenzo, A., and Supuran, C. T. (2012). Molecular cloning, characterization, and inhibition studies of a β-carbonic anhydrase from *Malassezia globosa*, a potential antidandruff target. *J. Med. Chem.* 55, 3513–3520. doi: 10.1021/jm300203r

Hicks, N., Vik, U., Taylor, P., Ladoukakis, E., Park, J., Kolisis, F., et al. (2017). Using prokaryotes for carbon capture storage. *Trends Biotechnol.* 35, 22–32. doi: 10.1016/j.tibtech.2016.06.011

Howe, A. C., Jansson, J. K., Malfatti, S. A., Tringe, S. G., Tiedje, J. M., and Brown, C. T. (2014). Tackling soil diversity with the assembly of large, complex metagenomes. *Proc. Nat. Acad. Sci. U.S.A.* 111, 4904–4909. doi: 10.1073/pnas.1402564111

Huang, S., Xue, Y., Sauer-Eriksson, E., Chirica, L., Lindskog, S., and Jonsson, B. H. (1998). Crystal structure of carbonic anhydrase from *Neisseria gonorrhoeae* and its complex with the inhibitor acetazolamide. *J. Mol. Biol.* 283, 301–310. doi: 10.1006/jmbi.1998.2077

Huijgen, W. J., Comans, R. N., and Witkamp, G. J. (2007). Cost evaluation of CO_2 sequestration by aqueous mineral carbonation. *Energy Convers. Manage.* 48, 1923–1935. doi: 10.1016/j.enconman.2007.01.035

Iliuta, I., and Iliuta, M. C. (2017). Investigation of CO_2 Removal by immobilized carbonic anhydrase enzyme in a hollow-fiber membrane bioreactor. *AIChE J.* 63, 2996–3007. doi: 10.1002/aic.15646

Innocenti, A., Hall, R. A., Schlicker, C., Scozzafava, A., Steegborn, C., Mühlschlegel, F. A., et al. (2009a). Carbonic anhydrase inhibitors. Inhibition and homology modeling studies of the fungal β-carbonic anhydrase from *Candida albicans* with sulfonamides. *Bioorg. Med. Chem. Lett.* 17, 4503–4509. doi: 10.1016/j.bmc.2009.05.002

Innocenti, A., Leewattanapasuk, W., Muhlschlegel, F. A., Mastrolorenzo, A., and Supuran, C. T. (2009b). Carbonic anhydrase inhibitors.Inhibition of the beta-class enzyme from the pathogenic yeast *Candida glabrata* with anions. *Bioorg. Med. Chem. Lett.* 19, 4802–4805. doi: 10.1016/j.bmcl.2009.06.048

IPCC (2000) *Special Report on Emissions Scenarios: A Special Report of Working Group III of the Intergovernmental Panel on Climate Change*. New York, NY: Cambridge University Press.

IPCC (2013) *Fourth assessment report: climate change (AR5) from IPCC*. Available online at: http://ipcc.ch/publications_and_data/publications_and_data_reports.shtml/; (Accessed March 2, 2017).

IPCC (Inter-governmental Panel on Climate Change) (2014) *Climate Change Synthesis Report*. Cambridge: Cambridge University Press.

Jahn, A., Vreeland, W. N., DeVoe, D. L., Locascio, L. E., and Gaitan, M. (2007). Microfluidic directed formation of liposomes of controlled size. *Langmuir* 23, 6289–6293. doi: 10.1021/la070051a

James, P., Isupov, M. N., Sayer, C., Saneei, V., Berg, S., Lioliou, M., et al. (2014). The structure of a tetrameric α-carbonic anhydrase from *Thermovibrio ammonificans* reveals a core formed around intermolecular disulfides that contribute to its thermostability. *Acta Crystallogr. Sect. D.* 70, 2607–2618. doi: 10.1107/S1399004714016526

Jo, B. H., Kim, I. G., Seo, J. H., Kang, D. G., and Cha, H. J. (2013). Engineered *Escherichia coli* with periplasmic carbonic anhydrase as a biocatalyst for CO_2 sequestration. *Appl. Environ. Microbiol.* 79, 6697–6705. doi: 10.1128/AEM.02400-13

Jo, B. H., Park, T. Y., Park, H. J., Yeon, Y. J., Yoo, Y. J., and Cha, H. J. (2016). Enginering de novo disulfide bond in bacterial α-type carbonic anhydrase for thermostable carbon sequestration. *Sci. Rep.* 6, 1–9. doi: 10.1038/srep29322

Jo, B. H., Seo, J. H., and Cha, J. C. (2014). Bacterial extremo- α-carbonic anhydrases from deep-sea hydrothermal vents as potential biocatalysts for CO_2 sequestration. *J. Mol. Catal. B. Enzym.* 109, 31–39. doi: 10.1016/j.molcatb.2014.08.002

Jones, S. D., Albrecht, L. H., and Dawson, S. K. (2012). Community genomic analysis of an extremely acidophilic sulfur-oxidizing biofilm. *ISME J.* 6, 158–117. doi: 10.1038/ismej.2011.75

Joseph, P., Turtaut, F., Ouahrani-Bettache, S., Montero, J. L., Nishimori, I., Minakuchi, T., et al. (2010). Cloning, characterization, and inhibition studies of a β-carbonic anhydrase from *Brucella suis*. *J. Med. Chem.* 53, 2277–2285. doi: 10.1021/jm901855h

Kaar, J. L., Oh, H. I., Russell, A. J., and Federspiel, W. J. (2007). Towards improved artificial lungs through biocatalysis. *Biomaterials* 28, 3131–3139. doi: 10.1016/j.biomaterials.2007.03.021

Kanbar, B., and Ozdemir, E. (2010). Thermal stability of carbonic anhydrase immobilized within polyurethane foam. *Biotechnol. Prog.* 26, 1474—1480. doi: 10.1002/btpr.452

Kanth, B. K., Jun, S. Y., and Kumari, S. (2014). Highly thermostable carbonic anhydrase from *Persephonella marina* EX-H1: its expression and characterization for CO_2 sequestration Applications. *Proc. Biochem.* 49, 2114–2121. doi: 10.1016/j.procbio.2014.10.011

Kanth, B. K., Min, K., Kumari, S., Jeon, H., Jin, E. S., Lee, J., et al. (2012). Expression and characterization of codon-optimized carbonic anhydrase from *Dunaliella* species for CO_2 sequestration application. *Appl. Biochem. Biotechnol.* 167, 2341–2356. doi: 10.1007/s12010-012-9729-1

Kaur, S., Bhattacharya, A., Sharma, A., and Tripathi, A. K. (2012). "Diversity of microbial carbonic anhydrases, their physiological role and applications", in *Microorganisms in Environmental Management: Microbes and Environment* eds T. Satyanarayana, B. N. Johri, A. Prakash (New york, NY: Springer), 151–173.

Kheshgi, H., deConninck, H., and Kessels, J. (2012). Carbon dioxide capture and storage: seven years after the IPCC special report. *Mitig. Adapt. Strat. Glob. Change* 17, 563–567. doi: 10.1007/s11027-012-9391-5

Ki, M. R., Min, K., Kanth, B. K., Lee, J., and Pack, S. P. (2013). Expression, reconstruction and characterization of codon-optimized carbonic anhydrase from *Hahella chejuensis* for CO_2 sequestration application. *Bioprocess. Biosyst. Eng.* 36, 375–381. doi: 10.1007/s00449-012-0788-z

Kim, I. G., Jo, B. H., Kang, D. G., Kim, C. S., Choi, Y. S., and Cha, H. J. (2012). Biomineralization-based conversion of carbon dioxide to calcium carbonate using recombinant carbonic anhydrase. *Chemosphere* 87, 1091–1096. doi: 10.1016/j.chemosphere.2012.02.003

Knudsen, J. N., Jensen, J. N., Vilhelmsen, P. J., and Biede, O. (2009). Experience with CO_2 capture from coal flue gas in pilot-scale: testing of different amine solvents. *Energy Procedia* 1, 783–790. doi: 10.1016/j.egypro.2009.01.104

Kumar, V., and Satyanarayana, T. (2014). Production of thermo-alkali-stable xylanase by a novel polyextremophilic *Bacillus halodurans* TSEV1 in cane molasses medium and its applicability in making whole wheat bread. *Bioprocess. Biosyst. Eng.* 37, 1043–1053. doi: 10.1007/s00449-013-1075-3

Kupriyanova, E. V., Sinetova, M. A., Markelova, A. G., Allakhverdiev, S. I., Los, D. A., and Pronina, N. A. (2011). Extracellular β_class carbonic anhydrase of the alka-liphilic cyanobacterium *Microcoleus chthonoplastes*. *J. Photochem. Photobiol. B.* 103, 78–86. doi: 10.1016/j.jphotobiol.2011.01.021

Kupriyanova, E., Villarejo, A., Markelova, A., Gerasi-menko, L., Zavarzin, G., Samuelsson, G., et al. (2007). Extracellular carbonic anhydrases of the stromatolite_forming cyanobacterium *Microcoleus chthonoplastes*. *Microbiology (SGM)* 153, 1149–1156. doi: 10.1099/mic.0.2006/003905-0

Lane, T. W., and Morel, F. M. M. (2000). A biological function for cadmium in marine diatoms. *Proc. Nat. Acad. Sci.U.S.A.* 97, 4627–4631. doi: 10.1073/pnas.090091397

Lapointe, M., MacKenzie, T. D. B., and Morse, D. (2008). An external δ-carbonic anhydrase in a free-living marine dinoflagellate may circumvent diffusion-limited carbon acquisition. *Plant. Physiol.* 147, 1427–1436. doi: 10.1104/pp.108.117077

Laurent, S., Forge, D., Port, M., Roch, A., Robic, C., Vander Elst, L., et al. (2008). Magnetic iron oxide nanoparticles: synthesis, stabilization, vectorization, physicochemical characterizations, and biological applications. *Chem. Rev.* 108, 2064–2110. doi: 10.1021/cr068445e

Leung, D. Y., Caramanna, G., and Maroto-Valer, M. M. (2014). An overview of current status of carbon dioxide capture and storage technologies. *Renew. Sustainable Energy Rev.* 39, 426–443. doi: 10.1016/j.rser.2014.07.093

Li, M., Su, Z. G., and Janson, J. C. (2004). *In vitro* protein refolding by chromatographic procedures. *Protein. Expr. Purif.* 33, 1–10. doi: 10.1016/j.pep.2003.08.023

Li, M., Zhu, X., Wilkinson, S., Huang, M., and Achal, V. (2016). Complete genome sequence of carbonic anhydrase producing *Psychrobacter* sp. SHUES1. *Front. Microbiol.* 7:1442. doi: 10.3389/fmicb.2016.01442

Lindskog, S., and Coleman, J. E. (1973). The catalytic mechanism of carbonic anhydrase. *Proc. Nat. Acad. Sci. U.S.A.* 70, 2505–2508. doi: 10.1073/pnas.70.9.2505

Liu, N., Bond, G. M., Abel, T. A., McPherson, B. J., and Stringer, J. (2005). Biomimetic sequestration of CO_2 in carbonate form: role of produced waters and other brines. *Fuel Process. Technol.* 86, 1615–1625. doi: 10.1016/J.FUPROC.2005.01.008

Lomelino, C., and McKenna, R. (2016). Carbonic anhydrase inhibitors: a review on the progress of patent literature (2011–2016). *Expert Opin. Ther. Pat.* 26, 947–956. doi: 10.1080/13543776.2016.1203904

MacAuley, S. R., Zimmerman, S. A., Apolinario, E. E., Evilia, C., Hou, Y. M., Ferry, J. G., et al. (2009). The archetype γ-class carbonic anhydrase (cam) contains iron when synthesized *in vivo*. *Biochemistry* 48, 817–819. doi: 10.1021/bi802246s

Marston, F. A. O. (1986). The purification of eukaryotic polypeptides synthesized in *Escherichia coli*. *Biochem. J.* 240, 1–12. doi: 10.1042/bj2400001

McCranor, B. J., Bozym, R. A., Vitolo, M. I., Fierke, C. A., Bambrick, L., Polster, B. M., et al. (2012). Quantitative imaging of mitochondrial and cytosolic free zinc levels in an in vitro model of ischemia/reperfusion. *J. Bioenerg. Biomembr.* 44, 253–263. doi: 10.1007/s10863-012-9427-2

Medina-Puche, L., Castello, M. J., Canet, J. V., Lamilla, J., Colombo, L. M., and Tornero, P. (2017). B-carbonic anhydrases play a role in salicylic acid perception in *Arabidosis*. *PLoS ONE* 12:e0181810. doi: 10.1371/journal.pone.0181820

Merlin, C., Masters, M., McAteer, S., and Coulson, A. (2003). Why is carbonic anhydrase essential to *Escherichia coli*? *J. Bacteriol.* 185, 6415–6424. doi: 10.1128/JB.185.21.6415-6424.2003

Mesbah, N. M., and Wiegel, J. (2012). Life under multiple extreme conditions: diversity and physiology of the halophilic alkalithermophiles. *Appl. Environ. Microbiol.* 78, 4074–4082. doi: 10.1128/AEM.00050-12

Mete, E., Comez, B., Inci Gul, H., Gulcin, I., and Supuran, C. T. (2016). Synthesis and carbonic anhydrase inhibitory activities of new thienyl-substituted pyrazoline benzenesulfonamides. *J. Enzyme Inhib. Med. Chem.* 31, 1–5. doi: 10.1080/14756366.2016.1181627

Migliardini, F., De Luca, V., Carginale, V., Rossi, M., Corbo, P., Supuran, C. T., et al. (2014). Biomimetic CO_2 capture using a highly thermostable bacterial α-carbonic anhydrase immobilized on a polyurethane foam. *J. Enzyme. Inhib. Med. Chem.* 29, 146–150. doi: 10.3109/14756366.2012.761608

Minakuchi, T., Nishimori, I., Vullo, D., Scozzafava, A., and Supuran, C. T. (2009). Molecular cloning, characterization, and inhibition studies of the Rv1284 β-carbonic anhydrase from *Mycobacterium tuberculosis* with sulfonamides and a sulfamate. *J. Med. Chem.* 52, 2226–2232. doi: 10.1021/jm9000488

Mirjafari, P., Asghari, K., and Mahinpey, N. (2007). Investigating the application of enzyme carbonic anhydrase for CO_2 sequestration purposes. *Ind. Eng. Chem. Res.* 46, 921–926. doi: 10.1021/ie060287u

Mitchell, A. C., Dideriksen, K., Spangler, L. H., Cunningham, A. B., and Gerlach, R. (2010). Microbially enhanced carbon capture and storage by mineral-trapping and solubility-trapping. *Environ. Sci. Technol.* 44, 5270–5276. doi: 10.1021/es903270w

Mogensen, E. G., Janbon, G., Chaloupka, J., Steegborn, C., Fu, M. S., Moyrand, F., et al. (2006). *Cryptococcus neoformans* senses CO_2 through the carbonic anhydrase Can2 and the adenylyl cyclase Cac1. *Eukaryot. Cell* 5, 103–111. doi: 10.1128/EC.5.1.103-111.2006

Monti, S. M., De Simone, G., Dathan, N. A., Ludwig, M., Vullo, D., Scozzafava, A., et al. (2013). Kinetic and anion inhibition studies of a β-carbonic anhydrase (FbiCA 1) from the C4 plant *Flaveria bidentis*. *Bioorg. Med. Chem. Lett.* 23, 1626–1630. doi: 10.1016/j.bmcl.2013.01.087

More, R. H., McMillan, G. C., and Duff, G. L. (1946). The pathology of sulphonamide allergy in man. *Am. J. Pathol.* 22, 703–735.

Mu, A., Boreham, C., Leong, H. X., Haese, R., and Moreau, J. W. (2014). Changes in the deep subsurface microbial biosphere resulting from a field-scale CO_2 geosequestration experiment. *Front. Microbiol.* 5:209. doi: 10.3389/fmicb.2014.00209

Muyssen, B. T., De Schamphelaere, K. A., and Janssen, C. R. (2006). Mechanisms of chronic waterborne Zn toxicity in Daphnia magna. *Aquat. Toxicol.* 77, 393–401. doi: 10.1016/j.aquatox.2006.01.006

Nara, T. Y., Togashi, H., Sekikawa, C., Kawakami, M., Yaginuma, N., Sakaguchi, K., et al. (2009). Use of zeolite to refold a disulfide-bonded protein. *Colloids Surf. B.* 68, 68–73. doi: 10.1016/j.colsurfb.2008.09.012

Nielsen, C. J., Herrmann, H., and Weller, C. (2012). Atmospheric chemistry and environmental impact of the use of amines in carbon capture and storage (CCS). *Chem. Soc. Rev.* 41, 6684–6704. doi: 10.1039/c2cs35059a

NOAA (2016) *National Oceanic and Atmospheric Administration*. Available online at: http://www.esrlnoaa.gov/gmd/ccgg/trends. (Accessed March 9, 2017).

NOAA (2017) *National Oceanic and Atmospheric Administration*. Available online at: https://climate.nasa.gov/vital-signs/carbon-dioxide/ (Accessed June 23, 2017).

Noble, R. R., Stalker, L., Wakelin, S. A., Pejcic, B., Leybourne, M. I., Hortle, A. L., et al. (2012). Biological monitoring for carbon capture and storage–A review and potential future developments. *Int. J. Greenh. Gas. Con.* 10, 520–535. doi: 10.1016/j.ijggc.2012.07.022

Norici, A., Dalsass, A., and Giordano, M. (2002). Role of phosphoenolpyruvate carboxylase in anaplerosis in the green microalga *Dunaliella salina* cultured under different nitrogen regimes. *Physiol. Plant.* 116, 186–191. doi: 10.1034/j.1399-3054.2002.1160207.x

Olajire, A. A. (2010). CO_2 capture and separation technologies for end-of-pipe application – a review. *Energy* 35, 2610–2628. doi: 10.1016/j.energy.2010.02.030

Onstott, T. C., Moser, D. P., Pfiffner, S. M., Fredrickson, J. K., Brockman, F. J., Phelps, T. J., et al. (2003). Indigenous and contaminant microbes in ultradeep mines. *Environ. Microbiol.* 5, 1168–1191. doi: 10.1046/j.1462-2920.2003.00512.x

Orr, J. F. M. (2009). CO_2 capture and storage: are we ready? *Energy Environ. Sci.* 2, 449–458. doi: 10.1039/b822107n

Pala, N., Micheletto, L., Sechi, M., Aggarwal, M., Carta, F., McKenna, R., et al. (2014). Carbonic anhydrase inhibition with benzenesulfonamides and tetrafluorobenzenesulfonamides obtained via click chemistry. *ACS Med. Chem. Lett.* 5, 927–930. doi: 10.1021/ml500196t

Park, J. Y., Kim, Y. H., and Min, J. (2017). CO_2 reduction and organic compounds production by photosynthetic bacteria with surface displayed carbonic anhydrase and inducible expression of phosphoenolpyruvate carboxylase. *Enzym. Microb. Technol.* 96, 103–110. doi: 10.1016/j.enzmictec.2016.10.005

Pastoreková, S., and Pastorek, J. (2004). "Cancer-related carbonic anhydrase isozymes and their inhibition" in *Carbonic Anhydrase: Its Inhibitors and Activators*, eds A. Andrea Scozzafava, C. T. Supuran, and J. Conway (Boca Raton: CRC Press), 255–281.

Perry, R., and Gee, I. L. (1995). Vehicle emissions in relation to fuel composition. *Sci. Total Environ.* 169, 149–156. doi: 10.1016/0048-9697(95)04643-F

Pfaff, I., and Kather, A. (2009). Comparative thermodynamic analysis and integration issues of CCS steam powerplants based on oxy-combustion with cryogenic or membrane based air separation. *Energy Procedia* 1, 495–502. doi: 10.1016/j.egypro.2009.01.066

Power, I. M., Harrison, A. L., and Dipple, G. M. (2016). Accelerating mineral carbonation using carbonic anhydrase. *Environ. Sci. Technol.* 50, 2610–2618. doi: 10.1021/acs.est.5b04779

Prabhu, C., Wanjari, S., Gawande, S., Das, S., Labhsetwar, N., Kotwal, S., et al. (2009). Immobilization of carbonic anhydrase enriched microorganism on biopolymer based materials. *J. Mol. Catal. B. Enzym.* 60, 13–21. doi: 10.1016/j.molcatb.2009.02.022

Prabhu, C., Wanjari, S., Puri, A., Bhattacharya, A., Pujari, R., Yadav, R., et al. (2011). Region-specific bacterial carbonic anhydrase for biomimetic sequestration of carbon dioxide. *Energy Fuels* 25, 1327–1332. doi: 10.1021/ef101608r

Prasad, S., Khadatare, P. B., and Roy, I. (2011). Effect of chemical chaperones in improving the solubility of recombinant proteins in *Escherichia coli*. *Appl. Environ. Microbiol.* 77, 4603–4609. doi: 10.1128/AEM.05259-11

Princiotta, F. (2007). "The role of power generation technology in mitigating global climate change," in *Challenges of Power Engineering and Environment,* eds K. Cen, Y. Chi, and F. Wang (Berlin, Heidelberg: Springer), 3–13.

Puri, A. K., and Satyanarayana, T. (2010). "Enzyme and microbe mediated carbon sequestration" in *CO_2 Sequestration Technologies for Clean Energy*, eds S. Z. Qasim and M. Goel (Delhi: Daya Publishing House), 119−129.

Ramanan, R., Kannan, K., Sivanesan, S. D., Mudliar, S., Kaur, S., Tripathi, A. K., et al. (2009). Bio-sequestration of carbon dioxide using carbonic anhydrase enzyme purified from *Citrobacter freundii*. *World J. Microbiol. Biotechnol.* 25, 981–987. doi: 10.1007/s11274-009-9975-8

Rayalu, S., Yadav, R., Wanjari, S., Prabhu, C., Mushnoori, S. C., Labhsetwar, N., et al. (2012). Nanobiocatalysts for carbon capture, sequestration and valorisation. *Top. Catal.* 55, 1217–1230. doi: 10.1007/s11244-012-9896-x

Reddy, K. J., Weber, H., Bhattacharya, P., Morris, A., Taylor, D., Christensen, M., et al. (2010). Instantaneous capture and mineralization of flue gas carbon dioxide: pilot scale study. *Nat. Precedings*. doi: 10.1038/npre.2010.5404.1

Reynolds, A. J., Verheyen, T. V., Adeloju, S. B., Meuleman, E., and Feron, P. (2012). Towards commercial scale post combustion capture of CO_2 with monoethanolamine solvent: key considerations for solvent management and environmental impacts. *Environ. Sci. Technol.* 46, 3643–3654. doi: 10.1021/es204051s

Rossi, M. (2014). *A New Heat-Stable Carbonic Anhydrase and Uses Thereof*. Patent WO 013064195 A1.

Rout, G. R., and Das, P. (2003). Effect of metal toxicity on plant growth and metabolism: I. Zinc. *Agronomie* 23, 3–11. doi: 10.1051/agro:2002073

Russo, M. E., Scialla, S., De Luca, V., Capasso, C., Olivieri, G., and Marzocchella, A. (2013). Immobilization of carbonic anhydrase for biomimetic CO_2 capture. *Chem. Eng. Trans.* 32, 1867–1872. doi: 10.3303/CET1332312

Sahdev, S., Khattar, S. K., and Saini, K. S. (2008). Production of active eukaryotic proteins through bacterial expression systems: a review of the existing biotechnology strategies. *Mol. Cell. Biochem.* 307, 249–264. doi: 10.1007/s11010-007-9603-6

Sakono, M., Kawashima, Y. M., Ichinose, H., Maruyama, T., Kamiya, N., and Goto, M. (2004). Direct refolding of inclusion bodies using reversed micelles. *Biotechnol. Prog.* 20, 1783–1787. doi: 10.1021/bp049887j

Salemme, F. R., and Weber, P. C. (2014). *Engineered Carbonic Anhydrase Proteins for CO_2 Scrubbing Applications*. US 20140178962 A1.

Santos, A., Toledo-Fernandez, J. A., Mendoza-Serna, R., Gago-Duport, L., de la Rosa-Fox, N., Pinero, M., et al. (2007). Chemically active silica aerogel—wollastonite composites for CO2 fixation by carbonation reactions. *Ind. Eng. Chem. Res.* 46, 103–107. doi: 10.1021/ie0609214

Satav, S. S., and Bhat, S., Thayumanavan, S. (2010). Feedback regulated drug delivery vehicles: carbon dioxide responsive cationic hydrogels for antidote release. *Biomacromolecules* 11, 1735–1740. doi: 10.1021/bm1005454

Seifritz, W. (1990). CO_2 disposal by means of silicates. *Nature* 345:486. doi: 10.1038/345486b0

Shahbazi, A., and Nasab, B. R. (2016). Carbon capture and storage (CCS) and its impacts on climate change and global warming. *J. Pet. Environ. Biotechnol.* 7:291. doi: 10.4172/2157-7463.1000291

Shakun, J. D., Clark, P. U., He, F., Marcott, S. A., Mix, A. C., Liu, Z., et al. (2012). Global warming preceded by increasing carbon dioxide concentrations during the last deglaciation. *Nature* 484, 49–54. doi: 10.1038/nature10915

Sharma, A., Bhattacharya, A., and Shrivastava, A. (2011). Biomimetic CO_2 sequestration using purified carbonic anhydrase from indigenous bacterial strains immobilized on biopolymeric materials. *Enzyme Microb. Technol.* 48, 416–426. doi: 10.1016/j.enzmictec.2011.02.001

Shutova, T., Kenneweg, H., Buchta, J., Nikitina, J., Terentyev, V., Chernyshov, S., et al. (2008). The photosystem II_associated Cah3 in *Chlamydomonas* enhances the O_2 evolution rate by proton removal. *EMBO J.* 27, 782–791. doi: 10.1038/emboj.2008.12

Silverman, D. N. (1982). Carbonic anhydrase: oxygen-18 exchange catalyzed by an enzyme with rate-contributing Proton-transfer steps. *Meth. Enzymol.* 87, 732–752. doi: 10.1016/S0076-6879(82)87037-7

Silverman, D. N., and Lindskog, S. (1988). The catalytic mechanism of carbonic anhydrase: implications of a rate-limiting protolysis of water. *Acc. Chem. Res.* 21, 30–36. doi: 10.1021/ar00145a005

Smith, K. S., and Ferry, J. G. (2000). Prokaryotic carbonic anhydrases. *FEMS Microbiol. Rev.* 24, 335–366. doi: 10.1111/j.1574-6976.2000.tb00546.x

Smith, K. S., Jakubzick, C., Whittam, T. S., and Ferry, J. G. (1999). Carbonic anhydrase is an ancient enzyme widespread in prokaryotes. *Proc. Nat. Acad. Sci. U.S.A.* 96, 15184–15189. doi: 10.1073/pnas.96.26.15184

So, A. K. C., Espie, G. S., Williams, E. B., Shively, J. M., Heinhorst, S., and Cannon, G. C. (2004). A novel evolutionary lineage of carbonic anhydrase (ε class) is a component of the carboxysome shell. *J. Bacteriol.* 186, 623–630. doi: 10.1128/JB.186.3.623-630.2004

So, A. K., van Spall, H. G. C., Coleman, J. R., and Espie, G. S. (1998). Catalytic exchange of 18O from 13C18O labelled CO_2 by wild type cells and *ecaA, ecaB*, and *ccaA* mutants of the cyanobacteria *Synechococcus* PCC7942 and *Synechocystis* PCC6803. *Can. J. Bot.* 76, 1153–1160. doi: 10.1139/b98-063

Soltes-Rak, E., Mulligan, M. E., and Coleman, J. R. (1997). Identification and characterization of gene encoding a vertebrate type carbonic anhydrase in cyanobacteria. *J. Bacteriol.* 179, 769–774. doi: 10.1128/jb.179.3.769-774.1997

Soong, Y., Fauth, D. L., and Howard, B. H. (2006). CO_2 sequestration with brine solution and fly ashes. *Energy Convers. Manage.* 47, 1676–1685. doi: 10.1016/j.enconman.2005.10.021

Srivastava, S., Bharti, R. K., Verma, P. K., and Thakur, I. S. (2015). Cloning and expression of gamma carbonic anhydrase from *Serratia* sp. ISTD04 for sequestration of carbon dioxide and formation of calcite. *Biores. Technol.* 188, 209–213. doi: 10.1016/j.biortech.2015.01.108

Stolaroff, J. K., Lowry, G. V., and Keith, D. W. (2005). Using CaO and MgO rich industrial waste streams for carbon sequestration. *Energy Convers. Manage.* 46, 687–699. doi: 10.1016/j.enconman.2004.05.009

Sugrue, M. F. (2000). Pharmacological and ocular hypotensive properties of topical carbonic anhydrase inhibitors. *Prog. Retin. Eye. Res.* 19, 87–112. doi: 10.1016/S1350-9462(99)00006-3

Supuran, C. T. (2008). Carbonic anhydrases: novel therapeutic applications for inhibitors and activators. *Nat. Rev. Drug Disc.* 7, 168–181. doi: 10.1038/nrd2467

Supuran, C. T. (2013). Carbonic anhydrases: from biomedical applications of the inhibitors and activators to biotechnological use for CO_2 capture. *J. Enzyme Inhib. Med. Chem.* 28, 229–230. doi: 10.3109/14756366.2013.761876

Supuran, C. T. (2015). How many carbonic anhydrase inhibition mechanisms exist? *J. Enzyme Inhib. Med. Chem.* 31, 345–360. doi: 10.3109/14756366.2015.1122001

Supuran, C. T. (2016a). Drug interaction considerations in the therapeutic use of carbonic anhydrase inhibitors. *Expert. Opin. Drug. Metab. Toxicol.* 12, 423–431. doi: 10.1517/17425255.2016.1154534

Supuran, C. T. (2016b). *Legionella pneumophila* carbonic anhydrases: underexplored antibacterial drug targets. *Pathogens* 5:44. doi: 10.3390/pathogens5020044

Supuran, C. T., Scozzafava, A., and Casii, A. (2003). Carbonic anhydrase inhibitors. *Med. Res. Rev.* 23, 146–189. doi: 10.1002/med.10025

Svensson, R., Odenberger, M., Johnsson, F., and Stromberg, L. (2004). Transportation systems for CO_2 – application to carbon capture and storage. *Energy Convers. Manage.* 45, 2343–2353. doi: 10.1016/j.enconman.2003.11.022

Swartz, J. R. (2001). Advances in *Escherichia coli* production of therapeutic proteins. *Curr. Opin. Biotechnol.* 12, 195–201. doi: 10.1016/S0958-1669(00)00199-3

Tahirov, T. H., Oki, H., Tsukihara, T., Ogasahara, K., Yutani, K., Ogata, K., et al. (1998). Crystal structure of methionine aminopeptidase from hyperthermophile, *Pyrococcus furiosus*. *J. Mol. Biol.* 284, 101–124. doi: 10.1006/jmbi.1998.2146

Teicher, B. A., Liu, S. D., Liu, J. T., Holden, S. A., and Herman, T. S. (1992). A carbonic anhydrase inhibitor as a potential modulator of cancer therapies. *Anticancer Res.* 13, 1549–1556.

Thompson, R. B., and Jones, E. R. (1993). Enzyme-based fiber optic zinc biosensor. *Anal. Chem.* 65, 730–734. doi: 10.1021/ac00054a013

Thompson, R. B., Peterson, D., Mahoney, W., Cramer, M., Maliwal, B. P., Suh, S. W., et al. (2002). Fluorescent zinc indicators for neurobiology. *J. Neurosci. Methods* 118, 63–75. doi: 10.1016/S0165-0270(02)00144-9

Thompson, R. B., Whetsell, W. O. Jr., Maliwal, B. P., Fierke, C. A., and Frederickson, C. J. (2000). Fluorescence microscopy of stimulated Zn (II) release from organotypic cultures of mammalian hippocampus using a carbonic anhydrase-based biosensor system. *J. Neurosci. Methods* 96, 35–45. doi: 10.1016/S0165-0270(99)00183-1

Tobal, J. M., and Balieiro, M. E. (2014). Role of carbonic anhydrases in pathogenic micro-organisms: a focus on *Aspergillus fumigatus*. *J. Med. Microbiol.* 63, 15–27. doi: 10.1099/jmm.0.064444-0

Tripp, B. C., and Ferry, J. G. (2000). A structure− function study of a proton transport pathway in the γ-class carbonic anhydrase from *Methanosarcina thermophila*. *Biochemistry* 39, 9232–9240. doi: 10.1021/bi0001877

Tripp, B. C., Bell, C. B. III., Cruz, F., Krebs, C., and Ferry, J. G. (2004). A role for iron in an ancient carbonic anhydrase. *J. Biol. Chem.* 279, 6683–6687. doi: 10.1074/jbc.M311648200

Tsouris, C., Aaron, D. S., and Williams, K. A. (2010). Is carbon capture and storage really needed? *Environ. Sci. Technol.* 44, 4042–4045. doi: 10.1021/es903626u

Tsumoto, K., Ejima, D., Kumagai, I., and Arakawa, T. (2003). Practical considerations in refolding proteins from inclusion bodies. *Protein. Expr. Purif.* 28, 1–8. doi: 10.1016/S1046-5928(02)00641-1

Umetsu, M., Tsumoto, K., Hara, M., Ashish, K., Goda, S., Adschiri, T., et al. (2003). How additives influence the refolding of immunoglobulin-folded proteins in a stepwise dialysis system spectroscopic evidence for highly efficient refolding of a single-chain fv fragment. *J. Biol. Chem.* 278, 8979–8987. doi: 10.1074/jbc.M212247200

Valdivia, R. H., and Falkow, S. (1997). Fluorescence-based isolation of bacterial genes expressed within host cells. *Science* 277, 2007–2011. doi: 10.1126/science.277.5334.2007

van de Vossenberg, J., Woebken, D., Maalcke, W. J., Wessels, H. J., Dutilh, B. E., Kartal, B., et al. (2003). The metagenome of the marine anammox bacterium '*Candidatus Scalindua profunda*' illustrates the versatility of this globally important nitrogen cycle bacterium. *Environ. Microbiol.* 15, 1275–1289. doi: 10.1111/j.1462-2920.2012.02774.x

Vericella, J. J., Baker, S. E., Stolaroff, J. K., Duoss, E. B., Hardin, J. O. IV., Lewicki, J., et al. (2015). Encapsulated liquid sorbents for carbon dioxide capture. *Nat. Commun.* 6, 1–7. doi: 10.1038/ncomms7124

Vullo, D., De Luca, V., Scozzafava, A., Carginale, V., Rossi, M., Supuran, C. T., et al. (2012). Anion inhibition studies of the fastest carbonic anhydrase (CA) known, the extremo-CA from the bacterium Sulfurihydrogenibium azorense. *Bioorg. Med. Chem. Lett.* 22, 7142–7145. doi: 10.1016/j.bmcl.2012.09.065

Vullo, D., Nishimori, I., Minakuchi, T., Scozzafava, A., and Supuran, C. T. (2011). Inhibition studies with anions and small molecules of two novel β-carbonic anhydrases from the bacterial pathogen *Salmonella enterica* serovar *typhimurium*. *Bioorg. Med. Chem. Lett.* 21, 3591–3595. doi: 10.1016/j.bmcl.2011.04.105

Wall, T. F. (2007). Combustion processes for carbon capture. *Proc. Combus. Instit.* 31, 31–47. doi: 10.1016/j.proci.2006.08.123

Wang, D., Hurst, T. K., Thompson, R. B., and Fierke, C. A. (2011). Genetically encoded ratiometric biosensors to measure intracellular exchangeable zinc in *Escherichia coli*. *J. Biomed. Opt.* 16, 087011–087011. doi: 10.1117/1.3613926

Wanjari, S., Prabhu, C., Satyanarayana, T., Vinu, A., and Rayalu, S. (2012). Immobilization of carbonic anhydrase on mesoporous aluminosilicate for carbonation reaction. *Micropor. Mesopor. Mat.* 160, 151–158. doi: 10.1016/j.micromeso.2012.04.005

Wanjari, S., Prabhu, C., Yadav, R., Satyanarayana, T., Labhsteswar, N., and Rayalu, S. (2011). Immobilization of carbonic anhydrase on chitosan beads for enhanced carbonation reaction. *Process Biochem.* 46, 1010−1018. doi: 10.1016/j.procbio.2011.01.023

Williamson, S. J., Allen, L. Z., Lorenzi, H. A., Fadrosh, D. W., Brami, D., Thiagarajan, M., et al. (2012). Metagenomic exploration of viruses throughout the Indian Ocean. *PLoS ONE* 7:e42047. doi: 10.1371/journal.pone.0042047

Wilson, Z. E., and Brimble, M. A. (2009). Molecules derived from the extremes of life. *Nat. Prod. Rep.* 26, 44–71. doi: 10.1039/B800164M

Wood, H. G., Werkman, C. H., Hemingway, A., and Nier, A.O. (1941). Heavy carbon as a tracer in heterotrophic carbon dioxide assimilation. *J. Biol. Chem.* 139, 367–375.

Wulf, N. R., and Matuszewski, K. A. (2013). Sulfonamide cross-reactivity: is there evidence to support broad cross-allergenicity? *Am. J. Health-Syst. Pharm.* 70, 1483–1494. doi: 10.2146/ajhp120291

Xiao, L., Hao, J., Wang, W., Lian, B., Shang, G., Yang, Y., et al. (2014). The up-regulation of carbonic anhydrase genes of *Bacillus mucilaginosus* under soluble Ca^{2+} deficiency and the heterologously expressed enzyme promotes calcite dissolution. *Geomicrobiol. J.* 31, 632–641. doi: 10.1080/01490451.2014.884195

Xiao, L., Sun, Q., Yuan, H., Li, X., Chu, Y., Ruan, Y., et al. (2016). A feasible way to increase carbon sequestration by adding dolomite and K-feldspar to soil. *Cogent Geosci.* 2:1205324. doi: 10.1080/23312041.2016.1205324

Xu, J., Sun, J., Wang, Y., Sheng, J., Wang, F., and Sun, M. (2014). Application of iron magnetic nanoparticles in protein immobilization. *Molecules* 19, 11465–11486. doi: 10.3390/molecules190811465

Yadav, R. R., Mudliar, S. N., Shekh, A. Y., Fulke, A. B., Devi, S. S., Krishnamurthi, K., et al. (2012). Immobilization of carbonic anhydrase in alginate and its influence on transformation of CO_2 to calcite. *Process Biochem.* 47, 585–590. doi: 10.1016/j.procbio.2011.12.017

Yadav, R., Satyanarayanan, T., Kotwal, S., and Rayalu, S. (2011). Enhanced carbonation reaction using chitosan-based carbonic anhydrase nanoparticles. *Curr. Sci.* 100, 520–524.

Yadav, R., Wanjari, S., Prabhu, C., Kumar, V., Labhsetwar, N., Satyanarayanan, T., et al. (2010). Immobilized carbonic anhydrase for the biomimetic carbonation reaction. *Energy Fuels* 24, 6198–6207. doi: 10.1021/ef100750y

Zhang, Z., Lian, B., Hou, W., Chen, M., Li, X., Shen, W., et al. (2011). Optimization of nutritional constituents for carbonic anhydrase production by *Bacillus mucilaginosus* K02. *Afr. J. Biotechnol.* 10, 8403–8413. doi: 10.5897/AJB10.1508

Zhi, W., Landry, S. J., Gierasch, L. M., and Srere, P. A. (1992). Renaturation of citrate synthase: influence of denaturant and folding assistants. *Protein Sci.* 1, 522–529. doi: 10.1002/pro.5560010407

Zimmerman, S., Innocenti, A., Casini, A., Ferry, J. G., Scozzafava, A., and Supuran, C. T. (2004). Carbonic anhydrase inhibitors. Inhibition of the prokariotic beta and gamma-class enzymes from Archaea with sulfonamides. *Bioorg. Med. Chem. Lett.* 14, 6001–6006. doi: 10.1016/j.bmcl.2004.09.085

Conflict of Interest Statement: The authors declare that the research was conducted in the absence of any commercial or financial relationships that could be construed as a potential conflict of interest.

The reviewer SD and handling Editor declared their shared affiliation, and the handling Editor states that the process nevertheless met the standards of a fair and objective review.

Advantages of publishing in Frontiers

OPEN ACCESS
Articles are free to read for greatest visibility and readership

FAST PUBLICATION
Around 90 days from submission to decision

HIGH QUALITY PEER-REVIEW
Rigorous, collaborative, and constructive peer-review

TRANSPARENT PEER-REVIEW
Editors and reviewers acknowledged by name on published articles

Frontiers
Avenue du Tribunal-Fédéral 34
1005 Lausanne | Switzerland

Visit us: www.frontiersin.org
Contact us: frontiersin.org/about/contact

REPRODUCIBILITY OF RESEARCH
Support open data and methods to enhance research reproducibility

DIGITAL PUBLISHING
Articles designed for optimal readership across devices

FOLLOW US
@frontiersin

IMPACT METRICS
Advanced article metrics track visibility across digital media

EXTENSIVE PROMOTION
Marketing and promotion of impactful research

LOOP RESEARCH NETWORK
Our network increases your article's readership